Modulation of transglutaminase 2 by pituitary adenylyl cyclase activating polypeptide and nerve growth factor in neuroblastoma cells: A role in cell survival and neurite outgrowth

Alanood S. Algarni

A thesis submitted in partial fulfilment of the requirements of Nottingham Trent University for the degree of
Doctor of Philosophy

June 2018

Copyright Statement:

Declaration

I, Alanood S. Algarni, hereby declare that the work presented in this thesis was conducted by myself. Exceptions to this have been clearly stated in the text.

Abstract

Several studies have reported that the multifunctional enzyme tissue transglutaminase (TG2) play important roles in neurite outgrowth and modulation of neuronal cell survival. Recently, TG2 enzymatic activity has been shown to be regulated by protein kinases such as PKA and PKC, modulating through G-protein coupled receptors (GPCRs). However, the regulation of TG2 following stimulation of GPCRs coupled to PKC and PKA activation are not fully understood. In neuronal cells, the neurotrophic factors; pituitary adenylate cyclase activating polypeptide (PACAP) and nerve growth factor (NGF) promote the differentiation, maturation, neurite outgrowth and survival of neurons via their GPCR's; the pituitary adenylate cyclase type 1 receptor (PAC_1) and the tyrosine kinase receptor (TrKA) Including multiple protein kinase signalling pathways. As some of these kinase pathways are associated with modulation of intracellular TG2 activity, it is conceivable to hypothesised that PACAP and NGF directly regulates TG2 activity. If this was found to be the case, it sought to determine whether the PACAP and/or NGF-induced neurite outgrowth and modulation of neuronal cell survival involved TG2. The main aims of this study were to investigate the molecular mechanisms underlying TG2 modulation by PACAP and NGF and its role in neurite outgrowth and neuroprotection in differentiating mouse N2a and human SH-SY5Y neuroblastoma cells.

In the first part, the regulation of TG2 transamidase activity by PACAP-27 and NGF in differentiating mouse N2a and human SH-SY5Y neuroblastoma cells was assessed. TG2 transamidase activity was determined using an amine incorporation and a peptide cross linking assay. *In situ* TG2 activity was assessed by visualising the incorporation of biotin-X-cadaverine using confocal microscopy. TG2 phosphorylation was monitored via immunoprecipitation and Western blotting. In the second part of this study, the role of TG2 in PACAP-27 and NGF-induced cytoprotection was investigated by monitoring hypoxia-induced cell death and assessing MTT reduction, LDH release, and caspase-3 activity. The neurite outgrowth was assessed using high-throughput analysis of immunofluorescently stained cells.

In differentiating N2a and SH-SY5Y cells, stimulation of PAC_1 and TrKA receptor with PACAP-27 and NGF respectively, resulted in a time- and concentration- dependent activation of TG2 amine incorporation and protein crosslinking activity, which was abolished by TG2 inhibitors Z-DON and R283. Responses to PACAP-27 were attenuated mainly by pharmacological inhibition of protein kinase A (KT 5720 and Rp-cAMPs), MEK1/2 (PD 98059), PKB (Akt inhibitor XI) and by removal of extracellular Ca^{2+}. Responses to NGF were abolished by MEK1/2 (PD 98059), PKB (Akt inhibitor XI) and PKC (Ro 31-8220). Immunoprecipitation technique showed that both PACAP-27 and NGF triggered the levels of TG2-associated phosphoserine and phosphothreonine, which were attenuated by inhibition of MEK1/2 and PKA for PACAP and MEK1/2, PKB, PKC and removal of extracellular Ca^{2+} for NGF. Fluorescence microscopy demonstrated that PACAP-27 and NGF induced *in situ* TG2 activity. TG2 inhibition blocked PACAP-27- and NGF-induced attenuation of hypoxia-induced cell death and neurite outgrowth. Taken together, this study highlights for the first time the importance of TG2 in the cellular functions of PACAP and NGF in neuronal cells and provides initial characterisation of the molecular mechanisms possibly involved.

Publication and scientific communication

Algarni, A. S., Hargreaves, A.J., and Dickenson, J. M. "Activation of Transglutaminase 2 by Nerve Growth Factor in Differentiating Neuroblastoma Cells: A Role in Cell Survival and Neurite Outgrowth." *European Journal of Pharmacology, 820* (2018): 113–129.

Algarni, A. S., Hargreaves, A.J., and Dickenson, J. M. "Role of Transglutaminase 2 in PAC $_1$ Receptor Mediated Protection against Hypoxia-Induced Cell Death and Neurite Outgrowth in Differentiating N2a Neuroblastoma Cells." *Biochemical Pharmacology, 128* (2017): 55-73.

Algarni, A. S., Hargreaves, A.J., and Dickenson, J. M. "Modulation of transglutaminase-2 activity by Pituitary adenylate cyclase activating polypeptide type 1 (PAC_1) receptor by protein kinases in differentiated mouse N2a neuroblastoma cells". 15th Annual East Midlands Proteomics Workshop, Nottingham Trent University (November 2016). Poster presentation, abstract no (06).

Algarni, A. S., Hargreaves, A.J., Bonner, P. L., and Dickenson, J. M. " Modulation of transglutaminase-2 activity by Pituitary adenylate cyclase activating polypeptide type 1 (PAC_1) receptor in differentiated mouse N2a neuroblastoma cells". The 9th Saudi Scientific International Conference (13 -14 February 2016), Birmingham University, United Kingdom, Poster presentation, abstract no (317).

Algarni, A. S., Hargreaves, A.J., Bonner, P. L., and Dickenson, J. M. "Modulation of transglutaminase-2 activity by pituitary adenylate cyclase activating polypeptide type 1 (PAC_1) receptor in differentiated mouse N2a neuroblastoma cells: role of neurite outgrowth". School of Science and Technology 10th Annual Research Conference (STAR conference), Nottingham Trent University (May 2015). Poster and oral presentation abstract no (15).

Acknowledgements

First and foremost, all thanks and praise be to Allah, who gave me the strength to persevere and complete my thesis. In addition, I owe a huge debt of gratitude to many people who have inspired and supported me during my PhD studies at Nottingham Trent University.

In particular, I would like to offer my deepest thanks to my supervisor, Dr John Dickenson, for his counsel, continuous support, motivation, enthusiasm and immense knowledge, as well as encouraging me to perform to the best of my abilities. I am also grateful for his assistance in writing papers and this thesis. Without his help, my work would not have been completed. I am deeply honoured to have been mentored by him.

Additionally, I want to extend my sincerest gratitude to the other members of my supervisory team, Dr Alan Hargreaves and Dr Phillip Bonner, for their help and support. I would like to single out Dr Hargreaves in particular for his constant advice, invaluable inspiration and guidance during my research.

Special thanks also go to all the current and past members of my lab, especially Adeola and Falguni. They are and have always been very nice and helpful, providing a friendly and cooperative atmosphere at work and throughout my studies.

In addition, I would like to acknowledge the academic and technical support I received from Nottingham Trent University.

I also want to express my gratitude for the funding and assistance of Umm Al-Qura University (Faculty of Pharmacy) throughout my studies in the UK, as well as the Royal Embassy of Saudi Arabia Cultural Bureau for all the social, living, legal and academic services provided.

A special thanks to my friends Nada, Intisar, Hayat, Reham and Shatha for their endless emotional support and encouragement throughout my journey.

It is a pleasure to express my deep sense of gratitude, appreciation and love to the greatest parents in the world, Fatimah and Saeed. Since I am so much of what I learned from them, they will always be part of me and dear to my heart. Without their constant love, prayers, understanding, endless patience and belief in me, this would not have been possible.

Heartfelt thanks also go to my brother and sisters, Muhammed, Ola, Sheemah, Dr Bayan, Ala’a and Bara’ah, for their kindness, support, love, patience and inspiration in every moment of my life.

In addition, my love for my sweet daughters, Reetal and Rosa, is beyond words. Looking into their eyes every morning shows me the brightest side of my life, encourages me to carry on and reminds me to enjoy the long days in the lab with my experiments. I missed a lot of their important moments, but I promise that I will make up for it.

Finally, I am forever grateful to my dear husband, my love, Ahmad. I want to thank him for being my partner, my friend, my consultant and my all in countless wonderful adventures. I am indebted to him for his constant love, understanding and support. I appreciate his taking on so many responsibilities during my studies. He bore the pressures of work and life with grace. I am glad he pushed me to have fun and reminded me to enjoy the little things. Therefore, I dedicate this thesis to him.

Table of content

List of Figures

List of Tables

List of Abbreviations

AC	Adenylyl cyclase
AD	Alzheimer's disease
AIDA	Advanced Image Data Analysis software
AIF	Apoptosis inducing factor
ALS	Amyotrophic lateral sclerosis
Apaf-1	Apoptotic-protein activation factor-1
BAD	Bcl-2-associated death promoter
Bax	Bcl-2-associated X protein
BBB	Blood brain barrier
Bcl	B-cell lymphoma
BDNF	Brain-derived neurotrophic factor
BNST	Bed nucleus of the stria terminalis
BSA	Bovine serum albumin
BXC	Biotin X cadaverine
CAD	Caspase-activated DNase
cAMP	Adenosine 3', 5'-cyclic monophosphate
ChAT	Choline acetyltransferase
CNS	Central nervous system
CREB	cAMP response element-binding protein
DAG	Diacylglycerol
DISC	Death-inducing signalling complex
DMEM	Dulbecco's modified eagle medium
DMSO	Dimethyl sulfoxide deoxyribonucleic acid
DNA	Deoxyribonucleotide triphosphate
DNA-PK	DNA-dependent protein kinase
DTT	Dithiothreitol
ECL	Enhanced chemiluminescence
ECM	Extracellular matrix
EDTA	Ethylenediamine tetra-acetic acid
EGF	Epidermal growth factor
ERK1/2	Extracellular signal-regulated kinase 1/2
FBS	Foetal bovine serum
GAPDH	Glyceraldehyde 3-phosphate dehydrogenase
GDP	GDP guanosine 5'-diphosphate
GHRH	Growth hormone–releasing hormone
GPCR	G-protein-coupled receptors
GTP	GTP guanosine 5'-triphosphate
HD	Huntington's disease
HIF1β	Hypoxia inducible factor 1β
IL-8	Interleukin-8
IP_3	Inositol 1,4,5-trisphosphate
JNK	c-Jun N-terminal kinase
LDH	Lactate dehydrogenase
MAPK	Mitogen-activated protein kinase
MTs	Microtubules
mTORC2	Mammalian target of rapamycin complex 2
NFs	Neurofilaments
NF-κB	Nuclear factor kappa-light-chain-enhancer of activated B cells
NGF	Nerve growth factor
NMDA	N-Methyl-D-aspartate
NT-3	Neurotrophin 3
OGD	Oxygen and glucose deprivation
PAC_1	Pituitary adenylate cyclase type 1 receptor
PACAP	Pituitary adenylate cyclase activating polypeptide
PBS	PBS phosphate-buffered saline

PDGF	Platelet-derived growth factor
PDI	Protein disulphide isomerase
PDK	Phosphoinositide dependent protein kinase
PHLPP	PH domain and leucine rich repeat protein phosphatases
PI-3K	Phosphoinositol-3 kinase
PIP_2	phosphatidylinositol 4,5-bisphosphate
PIP_3	Phosphatidylinositol (3,4,5)-trisphosphate
PKA	Protein kinase A
PKB/Akt	Protein kinase B/Akt
PKC	Protein kinase C
PLC	Phospholipase C
PNS	Peripheral nervous system
PP2A	Protein phosphatase 2A
PTEN	Phosphatase and tensin homolog
ROS	Reactive oxygen species
RTKs	Receptor tyrosine kinases
SAPK	Stress-activated protein kinase
SDS	Sodium dodecyl sulphate
TG	Transglutaminase
TG2	Transglutaminase 2
TH	Tyrosine hydroxylase
TNF-α	Tumour necrosis factor α
TrkA	Tyrosine kinase A receptor
VEGF	Vascular endothelial growth factor
VIP	Vasoactive intestinal polypeptide
WHO	World Health Organisation

Chapter 1

1 Introduction

1.1 Overview of the nervous system

The nervous system is the body's control system. The mammalian nervous system is anatomically divided into two main parts, namely the central (CNS) and peripheral nervous system (PNS). The CNS is the integrative and control centre, consisting of the brain and spinal cord. The PNS represents the communication lines between the CNS and the rest of the body, and it is composed of the cranial and spinal nerves. The brain receives/sends impulses from/to the spinal cord to integrate the sensory input and initiate properly coordinated motor output (Barres & Barde, 2000).

Nerve tissue is composed of two common cell types, namely neuronal and glial cells. Neurons are the basic structural unit of the nervous system; they receive, process and respond to stimuli and transmit cellular signals to other neurons and/or effector cells via synaptic transmission. Upon differentiation, neurons produce axons and dendrites (Coleman 2012). Glial cells, including astrocytes, oligodendrocytes, glioblasts and microglia, are generally smaller than neuronal cells, and they lack axons; however, they perform complex processes extending from their cell bodies. They are not involved in signal transmission, but they mainly provide mechanical, structural, nutritional and defensive support to the neurons (Compston et al., 1997; Rice & Barone, 2000). The nervous system undergoes various series of sensitive and complex development processes, extending from early embryonic life to adolescence. These processes include neuronal cell proliferation, migration, differentiation, synapse formation, glial cell development and apoptosis (Barone et al., 2000). All these cellular processes are tightly coordinated and regulated by highly integrated cell signalling. Cell signalling is a complex communication system that transfers information from one molecule to another in the cytoplasm. It ordinarily occurs when a cell receives an external signal, leading to the initiation of a cascade to transfer cellular signals to obtain the proper intracellular process (Bezzi & Volterra, 2001).

Neuronal signalling is the receiving and transferring of signals from one neuron to another. The low-resistance gap junctions connecting neuronal cells can communicate rapidly and directly, either by passing rapid electrical currents or via diffusion of a low-mass second messenger, such as cyclic adenosine 3', 5'-cyclic monophosphate (cAMP) or inositol 1,4,5-trisphosphate (IP_3). This signalling system, known as electrical signal communication, forms mostly between neuroglia (Knight & Verkhratsky, 2010). Another type of communication is chemical communication, which occurs when one cell releases a specific chemical stimulus, such as a neurotransmitter, hormone or growth factor, which passes to the target cells. These have receptors able to translate the incoming signal into a suitable internal cell signalling pathway, thereby causing a change in internal neuronal cell process (Perron and Bixby, 1999).

The development of the healthy mammalian brain requires a functional, coordinated neuronal cell signalling system. It has been suggested that the interruption of such a signalling system may cause damage or death of neuronal cells, resulting in different neurodegenerative diseases (Knight & Verkhratsky, 2010). Neurons have complex molecular and cellular biology systems. Their physiological function is only possible due to their sensitive and precise coordination of extracellular and intracellular signalling pathways. Since the current study has focused on the effects of neurotrophic factors on modulation of transglutaminase 2 mechanisms of cell survival and signalling pathways, a detailed discussion of such events would be worthwhile.

1.1.1 Signalling mechanisms

Cell signalling is the mechanism that occurs in response to an external stimulus, where a message is transmitted through a signal transduction cascade; this amplifies the message, resulting in internal signals performing the appropriate response in the desired effector (Uing & Farrow, 2000; Bezzi & Volterra, 2001). Most cell signals are chemical in nature, where the cells typically recognise the signals by their specific receptors. On activation, the receptor undergoes a conformational change, which provokes the synthesis of the second messenger(s) required to initiate the intracellular signalling pathways of interest (Uings & Farrow, 2000). A cell can receive various signals and produce multiple signal transduction pathways at one time, with many points of intersection. For example, a single second messenger or protein kinase could have different roles in one pathway.

One of the most systematic intracellular signalling pathways is cAMP; discovered in 1957, it was the first second messenger to be identified (Murad, 2011). The cAMP transduction cascade begins when adenylyl cyclase (AC), a membrane-bound enzyme, is activated by G_s protein and

then stimulates the synthesis of cAMP; this activates the enzyme protein kinase A, which then phosphorylates various substrates. Each of these signal amplifications continues to initiate different cell responses, such as the regulation of gene expression, proliferation, survival and differentiation (Uings & Farrow, 2000). Another common pathway controlled by second messengers is the phospholipase C (PLC) pathway. This pathway is initiated by the hydrolysis of phosphatidylinositol 4,5-bisphosphate (PIP_2) by PLC to produce two second messengers, namely diacylglycerol (DAG) and 1,4,5-inositol trisphosphate (IP_3). IP_3, stimulates the release of intracellular Ca^{2+}, which also has a role as a second messenger. DAG and Ca^{2+} jointly regulate protein kinase C (PKC), which modulates via phosphorylation many cellular responses (Putney & Tomita, 2011).

The intracellular responses to cell surface receptors are complicated and poorly understood. This complexity of cell signalling is related to the way in which different pathways intersect and integrate to control diverse cellular processes. This complication may develop because cells do not act in isolation, a specific signalling event in one cell could have impact on other adjacent cells. Also, the activation of one second messenger and/or protein kinase can regulate the activity of a second component, either positively or negatively. Some of these diversities are summarised in the subsections below.

The mitogen-activated protein kinase (MAPK) pathway

The mitogen-activated protein kinases (MAPKs) comprise a family of protein kinases that are considered the central elements in highly conserved intracellular signalling pathways. MAPKs are a specific class of ubiquitous serine/ threonine kinases that participate in the transduction of signals from the surface to the interior of the cell and regulate a variety of cellular process such as cell proliferation, cell differentiation, cell survival and stress response (Johnson & Lapadat, 2002, Korhonen and Moilanen, 2014). The MAPK family mainly consists of extracellular signal-regulated kinase 1/2 (ERK1/2), c-Jun N-terminal kinase 1/2/3 (JNK1/2/3) and p38 MAPKs (p38 MAPK-α/β/γ/δ). Each protein kinase cascade consists of no less than three enzymes – MAPKKK, MAPKK and MAPK – that are activated in sequence (Figure 1.1; Johnson and Lapadat, 2002). Activated MAPKs stimulate the phosphorylation of protein substrates such as transcription factors, protein kinases and phosphatases. A substantial number of reports confirm the central role of MAPKs in neuronal development, neuronal cell survival and neuroprotection (Creedon et al., 1996; Collins et al., 2015).

Extracellular-signal-regulated kinases 1/2

ERK1/2 was the first characterised MAPK cascade. The binding of a ligand, such as epidermal growth factor (EGF), insulin or platelet-derived growth factor (PDGF), to its receptor leads to signalling cascade that activate ERK1/2. This cascade starts with Ras (H-Ras, K-Ras and N-Ras) which is converted from Ras-GDP to Ras-GTP. Ras-GTP then activates Raf (A-Raf, B-Raf, C-Raf; examples of MAPKKK), which initiates the downstream phosphorylation of the kinase MEK1/2. MEK1/2 phosphorylates the Thr^{202} and Tyr^{204} in ERK1 and Thr^{185} and Tyr^{187} in ERK2, which results in activation of the ERK1/2 cascade as shown in Figure 1.1(Wortzel & Seger, 2011). The activated ERKs have widespread cytoplasmic and nuclear substrates, and translocate to the nucleus and activate transcription factors and gene expression to promote cell proliferation and differentiation (Zhang et al., 2002; Roskoski 2012). It has been reported that in pheochromocytoma PC12 cells, transient activation of the Raf signal triggers cell proliferation; in contrast, a sustained activation leads to cell differentiation and results in cell cycle arrest (Zhang et al., 2002). With regard to neuronal damage, activation of the ERK signalling cascade in myelinated Schwann cells has been shown to induce the specific inflammatory responses required for nerve repair (Napoli et al., 2012).

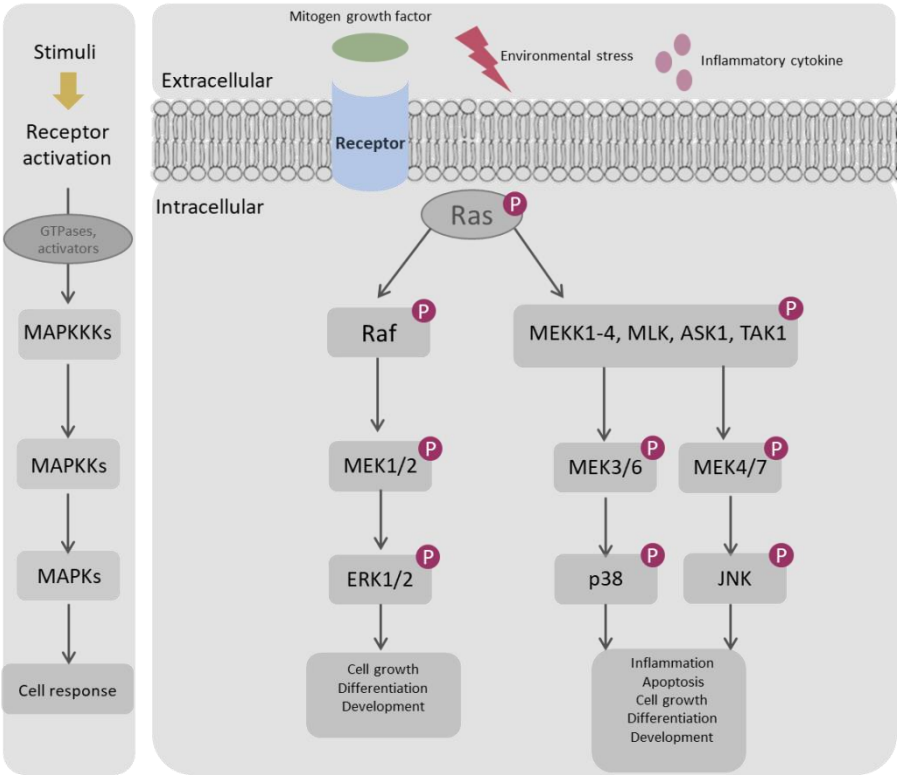

Figure 1.1 Schematic diagram of the general mitogen-activated protein kinase (MAPK) signalling pathways.

The MAPK cascade consists three main signalling modules including the extracellular-signal regulated kinases (ERK1/2), the stress-activated protein kinases p38, and the JUN N-terminal kinases (JNK). Each pathway is initiated by Ras activation, which phosphorylates serine/threonine residues of MAPKKK, which subsequently phosphorylates tyrosine/threonine residues of a MAPKK. This leads to the activation of MAPK, which in turn activates other protein kinases involved in cellular responses.

The p38 MAPK signalling pathway

Evidence shows that the p38 MAPK signalling pathway plays a key role in neuronal process; such as differentiation, proliferation (Morooka & Nishida, 1998), and different neurodegenerative diseases (Corrêa & Eales, 2012). The p38 MAPK enzyme is activated by dual phosphorylation of the Thr^{180} and Tyr^{182} residues either by MAP kinase kinase 3 (MKK3) or MAP kinase kinase 6 (MKK6) (Cuenda & Rousseau, 2007). The p38 MAPK family is composed of p38-α, p38-β, p38-γ and p38-δ isoforms, which are all phosphorylated by MKK6, while MKK3 can activate the α, γ and δ but not β isoforms. In neurons, p38 MAPK is activated in response to inflammatory cytokines (such as interleukin 1 [IL-1] and tumour necrosis factor α [TNF-α]) and cellular stress stimuli such as ultraviolet [UV] radiation, heat shock and osmotic shock (Corrêa & Eales, 2012). The wide range of stimuli integrating p38 MAPK signalling pathways provide the diversity of cellular responses and regulatory mechanisms (extensively reviewed in (Zarubin & Han, 2005; Cuenda & Rousseau, 2007). Previous *in vitro* studies have revealed that p38 MAPK is involved in the production and release of pro-inflammatory cytokines such as IL-6 and IL-8, which are involved in neuroinflammatory processes. Moreover, this activity is blocked by inhibition of p38 MAPK with SB203580 (Li et al. 2003). On the other hand, a substantial body of evidence indicates that the p38 MAPK pathway is involved in neuronal cell differentiation. An important role of the p38 MAPK signalling pathway involves promoting adult neural differentiation by triggering neural transcription factors, such as neurogenin 1 (Oh et al., 2009). Other studies have suggested that nerve growth factor (NGF) induces PC12 cell differentiation, and it has been shown that the p38 MAPK pathway is activated by NGF in PC12 cells, whereas blocking of the p38 MAPK pathway leads to the inhibition of NGF-induced neurite outgrowth (Morooka & Nishida, 1998; Takeda & Ichiijo, 2002).

The c-Jun N-terminal kinase (JNK) signalling pathway

JNK, also called stress-activated protein kinase (SAPK), is composed of three members, namely JNK1, JNK2 and JNK3. Like p38 MAPK, JNK is usually activated by various types of external stress stimuli, MKK4 and MKK7 being its main activation factors. It has been shown that MKK4/7 is mediated by the up-stream kinases apoptosis signal-regulation kinases (ASKs; Derijard et al. 1994). Activation of the JNK downstream pathway results in the phosphorylation of several transcription factors to initiate programmed cell death or apoptosis (Dhanasekaran & Reddy, 2008). The precise mechanisms of JNK-mediated apoptosis and neuronal death remain

to be illustrated. There is strong evidence that the activation of JNKs leads to the phosphorylation of transcription factors that regulate the apoptotic process (Dhanasekaran and Reddy, 2008), thus leading to cell death, which develops in numerous neurodegenerative disorders (Bogoyevitch et al., 2004). The pharmacological inhibition of JNK has been shown to have a neuroprotective role in Alzheimer disease' (AD) models and this could be therapeutically effective in the treatment of AD (Braithwaite et al., 2010). Furthermore, the knockdown of all three JNK isoforms provides substantial protection; however, the knockdown of only one or two JNK isoforms does not show any protective effect (Björkblom et al., 2008). To date evidence for the crucial role of JNK-dependent neuronal death has been mainly pharmacological; further investigation is needed to determine the therapeutic efficiency of JNK inhibition.

The protein kinase B/Akt signalling pathway

Protein kinase B (PKB)/Akt is one of the most widely studied and ubiquitously distributed kinase family, and it plays a major role in the nervous system. It is composed of three isoforms, namely PKBα/Akt1, PKBβ/Akt2 and PKBγ/Akt3. Extracellular signals trigger the PKB/Akt pathway via receptor tyrosine kinases (RTKs), activated monomeric G-protein Ras (Shaw & Cantley, 2006) or GPCRs (Katso et al., 2001). The PKB/Akt pathway has a key role in numerous cellular processes such as cell survival, differentiation, growth and metabolism (Brazil and Hemmings 2001; Dillon et al., 2007; Courtney et al., 2010). The activation of PKB is initiated with the up-stream activation of phosphatidylinositol-4,5-bisphosphate 3-kinase (PI-3K). Activated PI-3K phosphorylates PIP_2 (phosphatidylinositol 4,5-bisphosphate) to PIP3 (phosphatidylinositol 3,4,5-triphosphate), leading to the activation of pyruvate dehydrogenase kinase 1 (PDK1). Activation of PDK1 leads to subsequent phosphorylation of PKB at Thr308, while the other required site Ser^{473} is phosphorylated either by PDK2, integrin-linked kinase ILK, mammalian target of rapamycin complex 2 (mTORC2) or DNA-dependent protein kinase (DNA-PK; Vanhaesebroeck and Alessi 2000; Vanhaesebroeck et al., 2012). However, this PI-3K-dependent signalling cascade is regulated by the lipid phosphatase PTEN (phosphatase and tensin homologue) that dephosphorylates PIP_3 to PIP_2 thereby leading to the termination of the PKB/Akt pathway (Carracedo et al., 2008; Mendoza et al., 2011). Furthermore, PKB activity can also be modulated either by protein phosphatase 2A (PP2A) that dephosphorylates PKB at Thr^{308} or PH domain and leucine rich repeat protein phosphatases (PHLPP) that

dephosphorylate PKB at Ser^{473} (Bayascas & Alessi, 2005; Pozuelo-Rubio et al., 2010) Figure 1.2 summarises the PKB/Akt pathway.

It has been reported that PKB is essential for many neuronal biological and physiological processes, such as metabolism regulation, regulation of cell growth, survival, proliferation, development, neurogenesis and axon establishment (Crowder & Freeman, 1998). Evidence has shown that PKB participates in neuron protection, and it has been reported that treatment of neurons with NGF stimulates the activation of endogenous PKB, while the PI-3K inhibitors LY294002 and wortmannin block this activation (Crowder & Freeman, 1998). It has also been reported that the functional expression of PKB or PI-3K efficiently prevents neuronal cell death following NGF deprivation (Crowder & Freeman, 1998).

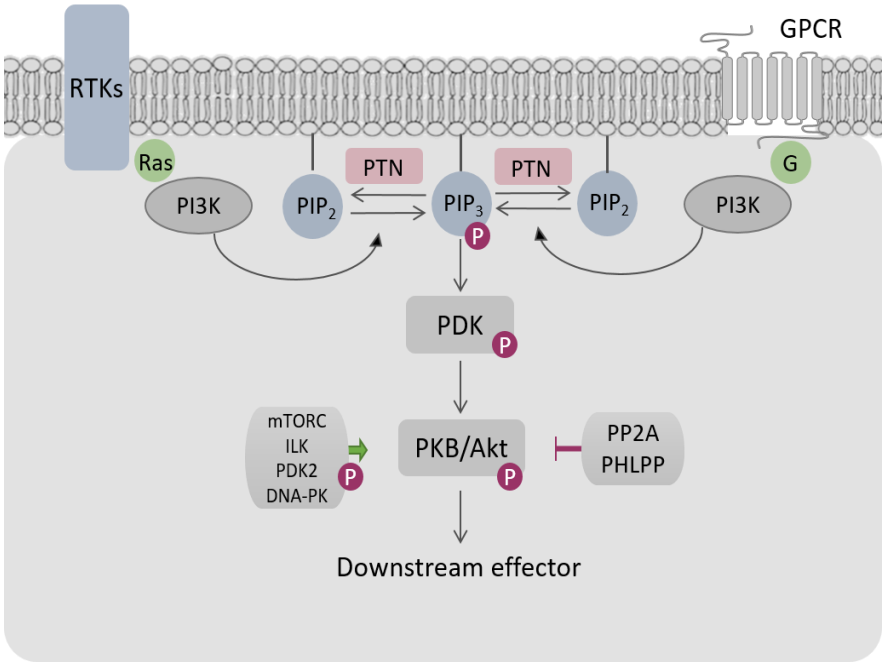

Figure 1.2 Schematic representation of the key steps in the PKB/Akt signalling cascade.

The pathway is mainly activated by both RTKs and GPCRs and initiated by RAS activation, which in turn activates PI3K. PI3-Kinase is activated and generates the second messenger PIP3, which activates the downstream PKB/Akt. PKB/Akt is important for cell growth, survival, and metabolism (Adapted from Courtney et al, 2010).

1.2 Neurodegenerative disease

Neurodegenerative diseases are either acute or chronic illnesses with high morbidity and mortality that are associated with the progressive dysfunction or death of nerve cells. Examples of neurodegenerative diseases include Huntington's disease (HD), Alzheimer's disease (AD), Parkinson's disease and amyotrophic lateral sclerosis (ALS), and associated dysfunction such as stroke or cerebral hypoxia (Friedlander, 2003). Programmed neuronal cell death is one of the pathological characteristics shared by most neurodegenerative diseases (Gorman, 2008). According to the latest update of the World Health Organization (WHO) in January 2017, cerebral stroke has a mortality rate of 30%, and it has been the second leading cause of death globally in the last 15 years (World Health Organization, 2017).

1.3 Cerebral stroke

Cerebral stroke occurs when there is interruption in the oxygen supply to the brain; this happens when an artery to the brain is blocked, resulting in a loss of the neurological function in the affected area (Ter Horst and Korf, 1997). As the brain has a high metabolic rate, it exhibits a high demand for ATP and low affinity for anaerobic energy production; neuronal cells consume a huge amount of oxygen and glucose, of which they require a steady supply. Thus, neuronal cells and brain tissue are extremely sensitive to oxygen deprivation; in such conditions, they can be rapidly damaged and die within 5 minutes (harp & Bernaudin, 2004; Tomaselli et al., 2005; Zhang et al., 2006; Semenza, 2011).

Oxygen deficiency in neuronal cells or tissue causes an impairment of neuronal functions known as cerebral hypoxia (Friedlander, 2003). Long-lasting cerebral hypoxia is associated with symptoms like memory loss, decreased motor coordination, poor judgement and inattentiveness, seizure and coma (Feriche et al., 2007). Currently, the available treatments involve helping to relieve the symptoms; however, an official neuroprotective strategy is lacking (Meloni, 2017). Therefore, it is important to characterise the molecular mechanisms and cellular pathways that lead to neuronal cell death after exposure to hypoxia, which is important for identifying selective and effective therapeutic approaches for cerebral stroke.

The pathophysiology of neuron death after hypoxia

Primary energy failure develops immediately after the brain is exposed to hypoxia/ischaemia, where the levels of high-energy phosphates and ATP decrease. This deprivation is not easy to manage or cure. The second energy failure in the brain reaches its peak at 48 h after the hypoxia incident, after which time the brain restores the energy level to normal (Descloux et al., 2015). It has been shown that in response to ischaemia, adenosine, the final metabolic product of the ATP dephosphorylation, is produced during the energy failure induced by hypoxia/ischaemia; this occurs via different mechanisms and it plays a role as a powerful endogenous neuroprotectant. It decreases the neuronal metabolism process and works as a vasodilator and thus increases blood flow to the affected area (Tomaselli et al., 2005).

The molecular neuronal response to hypoxia/ischaemia is either acute or chronic. Excitotoxicity is a neuronal adaptive mechanism that takes place during the early stage of the insult, and it mainly depends on the modulation of ion channels (Mahura, 2003). This results in ion haemostasis involving the accumulation of extracellular neurotransmitters, mainly glutamate, and over-activation of its receptor, N-Methyl-D-aspartate (NMDA); this leads to massive increase in Ca^{2+} influx (Mahura, 2003). Following this, cell damage occurs due to the formation of reactive oxygen and nitrogen species, membrane destruction, DNA damage and the activation of enzymes, such as neuronal nitric oxide synthase and xanthene and NADPH oxidase. These enzymes are involved in the production of reactive oxygen species (ROS).

These elevated levels of ROS are toxic and their accumulation triggers a different cytotoxic cascade of events, such as membrane destruction, lipid peroxidation, DNA damage, inflammation activation and increased blood brain barrier (BBB) permeability (Descloux et al., 2015). ROS lead to the excessive production of free radicals, such as oxygen free radicals (O_2^-), which have a role as signalling molecules to activate inflammation and apoptosis (Durukan & Tatlisumak, 2007). It has been found that NMDA receptor antagonists, Ca^{2+} channel blockers and antioxidants can provide neuroprotection in experimental models of hypoxia/ischaemia; however, this could also lead to disruption of normal brain function (Mahura, 2003; Durukan & Tatlisumak, 2007; Pun et al., 2009). Understanding the different neuronal cell death mechanisms of apoptosis or necrosis cell death will help in the ultimate targeting of treatment approaches.

Apoptosis is a programmed and delayed cell death that is essential for supporting physiological and pathological processes (Elmore, 2007). It is mainly triggered by either intrinsic or extrinsic intracellular signalling pathways, where the caspase precursor is the main mediator for

controlled apoptosis (Jin & El-Deiry, 2005). Necrosis is the passive, un-programmed cell death characterised by cell swelling followed by cell lysis; it is mainly triggered by ATP deprivation. Necrosis mainly occurs in areas that are severely affected and results in the production of excitotoxins, such as glutamate, cytokines and calcium. In addition, the mitochondria and nuclei swell, followed by the rupture of the cytoplasm and nuclear degeneration of the DNA. This is considered a rapid, irreversible process; therefore, treatment of neuronal cells undergoing necrotic death is a complex problem (Galluzzi & Kroemer, 2008). To determine which mechanism is responsible for neuronal cell death under specific conditions, it is important to understand the entire molecular pathway involved (Nikoletopoulou et al., 2013). Cells cultured under hypoxia condition is a widely used model to study the signalling pathway and the mechanisms underlying apoptosis induced-cell death process.

1.4 Apoptosis signalling pathways

Apoptosis is the delayed cell death mechanism that usually occurs in areas that are not severely affected by hypoxia. It has been reported that apoptosis is the predominant mechanism of neuronal cell death in chronic neurodegenerative diseases (Yuan et al., 2003). In the intrinsic pathway of apoptosis, the B-cell lymphoma 2 (Bcl-2) family is involved in the permeabilisation of the mitochondrial membrane, which results in the release of apoptogenic factors, such as cytochrome c and apoptosis inducing factor (AIF). The release of cytochrome c leads to caspase-9 activation, which activates caspase-3, the executioner caspase; this, in turn, activates caspase-activated DNase (CAD), leading to DNA damage, and mediates neuronal cell death (Jin & El-Deiry, 2005). The release of AIF and endonuclease G from the permeabilised mitochondria results in mediation of the caspase-independent pathway. The extrinsic apoptosis pathway mediated by cell death signalling factors, such as TNF-α, leads to the activation of caspase-8 (Riedl & Shi, 2004). Activated caspase-8 turns on the activation of the effector caspase, caspase-3. Activated caspase-3 cleaves different cell death substrates, such as inhibitor of CAD (ICAD) and lamin, which in turn, induces apoptotic cell death as shown in Figure 1.3 (Riedl & Shi, 2004).

The apoptosis pathways that induce neuronal cell death after hypoxia insult exhibit remarkable potential as therapeutic targets for neuroprotection. A substantial body of research indicates that treatment with caspase inhibitors has a potential role in neuroprotection in adult cerebral ischaemia (Akpan & Troy, 2013) and neonatal hypoxia/ischaemia models (Feng et al., 2003; Carlsson et al. 2011; Chauvier et al. 2011). It has been found that pharmacologically pre-treating

mice with a broad or partially selective caspase 1 and 3 inhibitor leads to brain protection from ischaemic insult (Fink et al., 1998; Hara & Snyder, 2007). However, using caspase inhibition as a neuroprotection treatment approach will be affected by the severity of the hypoxia/ischaemia in the adult model (Li, 2000). One of the limitations of the caspase inhibitor efficiency as a neuroprotective agent is that they remain unspecific and until now, no caspase inhibitor has been tested in a clinical trial (Northington et al., 2011).

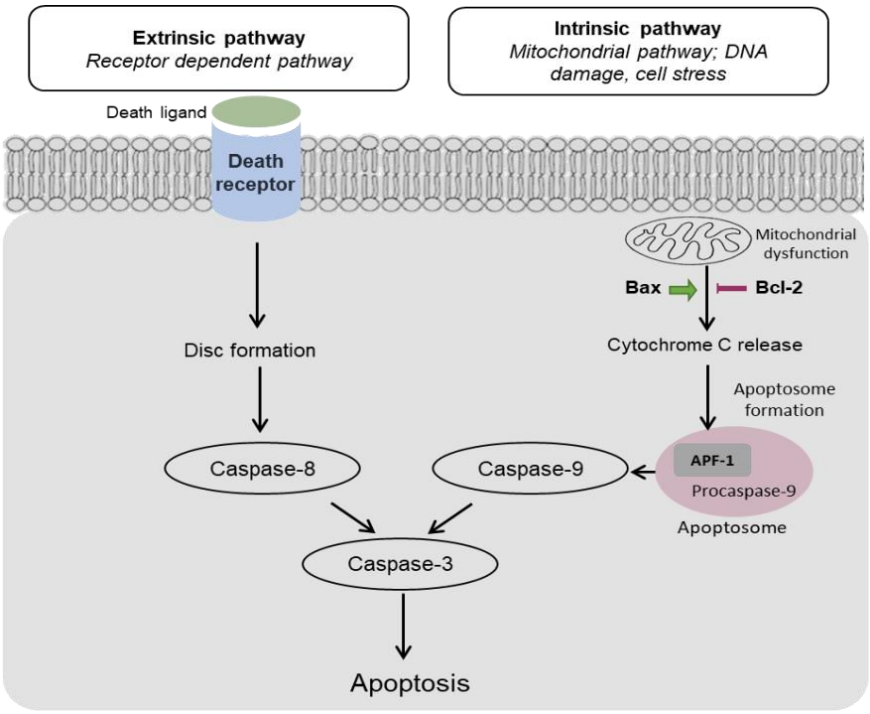

Figure 1.3 Schematic representation of the key steps in the main apoptosis molecular pathways

In the extrinsic pathway death ligands activate their receptors, resulting in the formation of a death-inducing signalling complex (DISC). This trigger the activation of caspase-8. The intrinsic pathway is initiated by cellular stress lead to mitochondrial dysfunction and release of cytochrome c into the cytoplasm, this process is promoted by pro-apoptotic factor such as Bax and prevented by anti-apoptotic factor Bcl-2. Then form the apoptosome; an activation complex with apoptotic-protein activation factor-1 (Apaf-1) and caspase 9. Caspase 8 and 9 then activate downstream executioner caspases such as caspase-3 resulting in apoptotic cell death.

Signalling pathways involved in brain hypoxia/ischaemia

Generally, activation of ERK1/2 and PKB promote cell survival, while activation JNK and p38 MAPK promote cell death (Neary, 2005). Thus, in the brain, the MAPK pathways may be triggered after ischaemia induction (Lee et al., 2000; Sugawara et al., 2004). ERK signalling has been indicated to be involved in the neuroprotection process, either by alleviating apoptosis or mediating the compensation of the oxygen glucose deprivation process (Nozaki et al., 2001). The MAPKs' neuroprotective roles seem to be complicated. Thus, additional studies are needed to illustrate the activated signal transduction upstream and downstream cascades in cerebral ischaemia and define the involved signalling pathways prior to pharmacological manipulation of the MAPK cascades in this context. The neuroprotective role of ERK1/2 has been well established. It has been shown that activation of the ERK1/2 pathway is involved in protection against glutamate-induced-excitotoxicity, ischaemia and brain-derived neurotrophic factor (BDNF)-induced reversal of DNA damage (Alessandrini et al., 1999; Hetman et al., 1999). Also it has been established that in both *in vivo* models of cerebral ischaemia and *in vitro* research, activation of the ERK1/2 pathway results in the inactivation of Bad due to its phosphorylation at the Ser^{112} site (Zhu et al., 2002). Protein kinase A (PKA), is one of the most widely studied in this context. Studies have shown that PKA has a role in regulating Bad activity and its phosphorylation, as intraventricular treatment with H89, a PKA inhibitor, in rodent focal cerebral ischaemia models showed decreased PKA activity and Bad-Bcl2 dimerisation and associated cell death (Kimura et al., 1998; Lizcano et al., 2000; Saito et al., 2003).

Furthermore, the findings indicate that stimulating PI3-kinase and/or a downstream effector, the Akt kinase, could also play a central protection role against apoptosis in different cell types including neuronal cells (Crowder & Freeman, 1998). In 2003, Bijur and his group demonstrated the existence of previously unrecognised Akt signalling inside the mitochondria. It has also been clarified that Akt has a key attenuating role in the intrinsic apoptotic pathway in both the pre- and post-mitochondrial apoptotic cascades (Bijur & Jope, 2003). It has been found that in primary hippocampal neurons exposed to hypoxia Akt blocks Bax apoptosis regulation, conformational change and distribution to the mitochondrial membrane (Yamaguchi & Wang, 2001). In addition to the antiapoptotic capacity of cytosolic Akt, its mitochondrial antiapoptotic activity has been studied in human SH-SY5Y neuroblastoma cells treated with staurosporine, a powerful apoptosis inducer. It has been shown that constitutively active Akt in the mitochondria decreased the level of the released cytochrome c, along with attenuating subsequent consecutive activation of caspase-9 and caspase-3 (Mookherjee et al., 2007).

On the other hand, JNK and p38 MAPK stress kinases, are activated by different cellular stressors and is thought to have a central role participating in neuronal cell death. In an *in vitro* model of AD, cortical neurons treated with JNK inhibitors blocked intracellular JNK activity and protected against neuronal cell death and thus promoted cell survival (Bozyczko-Coyne et al., 2001). The pharmacological inhibition of JNK or p38 MAPK was also reported to protect neurons from cell death induced by lack of survival signal such as Akt or NGF (Kummer et al., 1997; Le-Niculescu et al., 1999; Harding et al., 2001). Similarly, Xia et al. (1995) observed that inhibition of JNK and p38 MAPK attenuated apoptosis in PC12 cells and they proposed that cell survival or cell death could be predicted by the balance between ERK and JNK/p38 MAPK. This cumulative evidence all suggests that the ERK1/2, Akt and PKA pathways promotes cell survival, whilst JNK and p38 MAPK, promote cell death signalling pathways after cerebral hypoxia/ischaemia.

1.5 Neurotrophic factors

It has recently been found that neurotrophic factors contribute to protecting neuronal cells from cell death after cerebral ischaemia. Both NGF and pituitary adenylate cyclase activating polypeptide (PACAP) have neurotrophic effects, which have been extensively studied; they promote the differentiation, maturation, neurite outgrowth and survival of neurons *in vivo* and *in vitro* (Williams et al., 1986; Hatanaka et al., 1988; Takei et al., 2000; Yuhara et al., 2001). In addition, the intracellular transduction pathways involved in their neurotrophic effects are now well established; for a review, see Ravni et al. (2006). Several well established transduction pathways are involved in these effects (Kaplan & Miller, 2000; Ravni et al., 2006), for example, in the PC12 cell line, PACAP prevented cell apoptosis by activating PKA signal cascade (Reglodi et al., 2004) whereas, NGF inhibited apoptosis through the PI-3K/Akt pathway (Shimoke & Chiba, 2001; Salinas et al., 2003; Wu & Wong, 2005). Interestingly, researchers have been studying the possible complementary role of PACAP and NGF. It has been found that their ability to block programmed cell death is a synergistic action of both PACAP and NGF in differentiated PC12 cells (Seaborn et al., 2014). Within this context, additional study elucidated that co-treatment with PACAP and NGF induced choline acetyltransferase (ChAT) enzymatic activity in cultured basal forebrain neurons (Yuhara et al., 2003). This suggests that they may have potential therapeutic value for AD, as this neurodegenerative condition is associated with dysfunction of the basal forebrain cholinergic system. Based on previous observations and current data that the two trophic factors exerted similar effects particularly

neurite outgrowth and neuronal survival, it can be speculated that they may be protecting neuronal cell death via a similar modulator. Hence, this study aims to investigate the possible modulation of the multifunctional enzyme transglutaminase 2 by both neurotrophic factors separately, to induce neuronal cell outgrowth and survival. This will be further discussed in the upcoming sections.

1.5.1 The pituitary adenylate cyclase activating polypeptide

Overview, structure and function

In 1989, the sequence of a novel regulatory peptide known as PACAP was first established to have adenylyl cyclase (AC) activity in pituitary cells (Miyata et al., 1989). PACAP exists as a 27 or 38 amino acid C-terminal-amidated peptide (PACAP-27 and PACAP-38), and it is widely expressed in the brain, so it is also classified as a neuropeptide (Vaudry et al., 2009). Sequencing of PACAP has revealed that there is a high degree of sequence identity with vasoactive intestinal polypeptide (VIP), such that they are both classified as members of the VIP-secretin-growth hormone-releasing hormone GHRH glucagon family (Vaudry et al., 2009). In 1991, it was demonstrated that in the human brain, the mRNA binding sites of PACAP/VIP are mainly localised in the cortex, basal ganglia, hypothalamus, cerebellum and brainstem (Suda et al., 1991). The highest level of expression is found in the hypothalamus. In 1992, Suda and his group further investigated the affinity in these sites in the human brain, reporting that they had 10–20 times greater affinity to PACAP than VIP (Suda et al., 1992). It is well reported that the PAC_1 receptor gene is primarily expressed in neurons, as well as glial cells, including astrocytes (Jaworski, 2000; Suzuki et al., 2003). The PAC_1 receptor is also found in various peripheral tissues, mainly in the pituitary gland, adrenal medulla, lymphocytes and immune system (Table 1.1). PACAP is also present peripherally in the gastrointestinal tract, adrenal gland and testis (Ghatei et al., 1993; Shioda & Arimura, 1995). The PAC_1 receptor has been found to be expressed in the brain areas implicated in the emotional control of behaviour and learning, such as the hypothalamus, amygdala, bed nucleus of the stria terminalis (BNST) and periaqueductal grey matter (Hammack et al., 2010). Studies using the isolated VIP receptor complex from rat liver membrane have shown an association with GTP regulatory protein, and further studies have suggested that the VIP-associated G-protein is $G\alpha_s$ (Couvineau et al., 1986). Studies have shown a direct correlation between VIP, PACAP and their receptors and $G\alpha_s$ subunits, confirming that VIP and PACAP interact with GPCRs to activate intracellular signalling

cascades (Dickson & Finlayson, 2009). Three PACAP–G-protein coupled receptor (GPCRs) have been characterised, namely the PAC_1, $VPAC_1$ and $VPAC_2$ receptors; these all belong to the group II secretin receptor family (Table 1.1). They are further divided into two classes according to the affinity for PACAP and VIP. Class I includes the PAC_1 receptor, which is predominantly expressed in the CNS and specifically binds to PACAP with high affinity. Meanwhile, class II includes the $VPAC_1$ and $VPAC_2$ receptors, which are abundant in various peripheral organs and have comparable affinity to both VIP and PACAP (Dickson & Finlayson, 2009; Harmar et al., 2012). PACAP is coupled primarily to Gs for adenylate cyclase activation, leading to the production of cAMP and subsequent activation of PKA. The PAC_1 receptor also couples to Gq and activates PLC; this leads to increases in intracellular Ca^{2+} and the activation of PKC (Zhou et al., 200; May et al., 2010; Baxter et al., 2011). Stimulation of the PAC_1 receptor results in a variety of intracellular transduction pathways. PAC_1 receptor signalling regulates various cellular and physiological responses, such as cell survival and differentiation, as well as the release of neuroendocrine hormones and neurotransmitters/neurotrophic factors (McCulloch et al., 2001; Lutz et al., 2006; Blechman & Levkowitz, 2013).

As agonists, PACAP-27 and PACAP-38 are 100-fold more potent than VIP to the PAC_1 receptor (Harmar et al., 2012). It has been indicated that there is a limited number of the VIP and PAC receptor selective drugs available, both in terms of agonists and antagonists (Nicole et al., 2000). For example, maxadilan is a peptide isolated from the salivary gland of *Lutzomyia longipalpis* that has no significant homology with PACAP or VIP sequences and has been characterised as a potent selective agonist for the PAC_1 receptor; however, due to its lack of availability, the use of this peptide is limited. In addition, in many studies, PACAP 6-38 has been implicated for use as a PAC_1 receptor antagonist, but it also has affinity to antagonising the $VAPC_2$ receptor (Dickinson et al., 1997). Further studies are required to identify and design more selective ligands for the PAC_1 receptor by elucidating the mechanism of its activation.

Cloning of the PAC_1 receptor gene has shown that there are several variants produced from alternative splicing. The PAC_1 receptor gene exhibits a high level of alternative splicing, and this accounts for the variation in its affinity and selectivity, leading to the modulation of a variety of intracellular signal transduction cascades (Lelièvre et al., 1998). A splice variant denotes the existence of different amino acid sequences; if these are found in the extracellular loops or N-terminus, it may result in altered ligand affinity and selectivity, whereas variance in the internal loops or C-terminus could affect the signal transduction pathways. In the PAC_1 receptor, the splice variants include either the absence or presence of each of the alternative exons called ‘hip’ and ‘hop’. Human PAC_1 receptor shows four variants (null, SV-1, SV-2, SV-3) produced

from alternative splicing (Pisegna and Wanks 1996; Lelièvre et al. 1998). Different splice variants exert different coupling affinities to G-protein and second messengers and their subsequent intracellular signal transduction in neuronal cells. For example, the PAC_1-hip cassette type of splice variant results in eliminating the coupling to the PLC pathway and maintain the AC mediated signalling pathway (May et al. 2010). Alternative splicing of the PAC_1 receptor also alters the ligand binding properties involved in the determination of receptor selectivity for either PACAP-27 or PACAP-38 peptide or its potencies. The diversity of PAC_1 receptor splice variants and the subsequent activated signalling pathways could account for the broad spectrum of physiological functions and biological responses triggered by this peptide. PACAP and its receptors appear to affect various biological and physiological functions, such as circadian rhythm regulation, reproduction, cognitive behaviour, neuromodulation, neuroprotection and neurite outgrowth (Waschek, 2002; Hashimoto et al., 2006; Laburthe et al., 2007). In the nervous system, PACAP peptides act as neurohormones and neurotransmitters. In the hypothalamus, PACAP peptides act as neuromodulators to regulate the neurohormones, such as somatostatin and luteinising hormone (LH). Moreover, PACAP acts as a potent modulator of hypothalamic neurons, triggering the release of oxytocin and vasopressin via stimulation of the cAMP/PKA pathway (Lutz-Bucher et al., 1996).

The roles of the PACAP and PAC_1 receptor in cell survival, neuronal outgrowth and neuronal protection

A substantial body of evidence indicates that PACAP has neurotrophic activities during development and protects the brain from damage associated with different types of injury. Moreover, the PAC_1 receptor is known to be actively expressed during development and proliferation in the CNS (Monaghan et al., 2008; May et al., 2010). It has been found that, following neuronal injury, PACAP expression is increased and neuronal regeneration is promoted (Monaghan et al., 2008). Furthermore, it has also been indicated that PACAP-38 is effective even if it is administered several hours after cerebral ischaemia (Reglodi et al., 2000). In addition, PACAP-38 pre-treatment could reduce the infarct size induced by stroke (Reglodi et al. 2002). PAC_1 receptor stimulation results in PLC activation, leading to PKC translocation and cellular Ca^{2+} influx to facilitate neuronal cell proliferation (May et al., 2010). It has also been shown that PAC_1 receptor activation protects neuronal cells against cytotoxicity from β-amyloid aggregation, a key element in AD, as well as against glutamate-induced cell death (Lee and Seo 2014). Recently, PACAP's neuroprotective potential against hypoxia has been

demonstrated, as it reduces brain damage after ischaemia (Reglodi et al., 2000; Dejda et al., 2005). PACAP has also been revealed to inhibit programmed cell death through the PAC_1 receptor in cultured cells induced to undergo apoptosis (Villalba et al., 1997). Indeed, the literature data indicate that PACAP neurotrophic activity is modulated via two different major pathways, involving either stimulation of the AC or PLC pathway (Vaudry et al., 2000). The mechanism underlying the neuroprotective activities of PAC_1 receptor have been suggested mainly to involve activation of the AC, cAMP, PKA and MAPK pathways; this activation is required for deactivation of caspase-3, a key enzyme in apoptosis (Falluel-Morel et al., 2004; Baxter et al., 2011) and regulation of gene expression changes that promote differentiation of neurons. PACAP activation of PLC leads to the production of IP_3/DAG and activation of PKC signalling pathways and results in deactivation of caspase-3 activity (Dejda et al., 2005; Vaudry et al., 2009; Harmar et al., 2012). It has been investigated that, in vitro, PACAP shows neuroprotective activity against apoptotic cell death induced by oxidative stress in cerebellar neurons via different mechanisms (Vaudry et al., 2000). One of the mechanisms is inhibition of the activation of JNK/stress-activating proteins (Ohnou et al., 2016). Another intracellular mechanism that is likely to be involved in the neuroprotective activities of PACAP is the PKA pathway, which regulates c-fos gene expression, thereby triggering Bcl-2 expression (Aubert et al., 2006; Botia et al., 2007). PACAP mainly regulates this Bcl-2 downstream activity by preventing the release of cytochrome c and inhibiting caspase-9 and the activation of caspase-3 (Figure 1.4 summarises PACAP intracellular mechanisms involved in neurotrophic activities). As described above, previous studies have revealed that stimulation of the PAC_1 receptor by PACAP peptides exerts neuroprotective activity, suggesting that this receptor could be of therapeutic interest for the treatment of hypoxia/ischaemia and stroke. Hence, it is necessary to investigate the signalling pathways involved, specifically those that may lead to the development of novel therapies for the treatment of such neuronal injury.

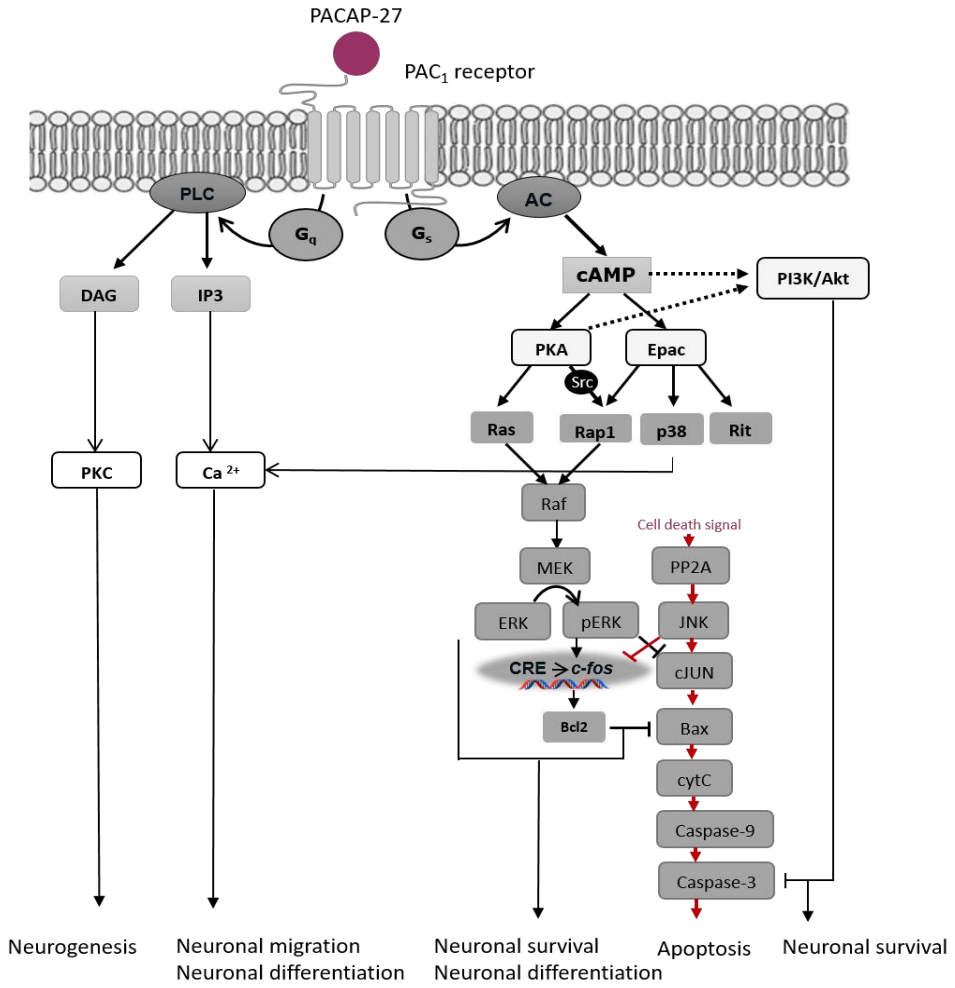

Figure 1.4 Schematic representation of the intracellular mechanisms involved in neurotrophic activities of PACAP on neuronal cells.

Bax, Bcl-2-associated X protein; Bcl-2, B-cell lymphoma 2; caspase, cysteinyl-aspartate-cleaving protease; cFos, Finkel Biskis Jinkins osteosarcoma-related oncogene; cJun, jun oncogene; cytC, cytochrome c; DAG, diacylglycerol; Epac, exchange factor directly activated by cAMP; IP_3, inositol 1,4,5-trisphosphate; G, guanine-nucleotide binding regulatory protein; p38, p38 mitogen-activated protein kinase; PAC_1-R, PACAP-specific receptor; Raf, Raf proto-oncogene serine/threonine-protein kinase; Rap1, small GTPase of the RAS oncogene family; Ras, retrovirus-associated DNA sequences; Rit, Ras-like GTPase without CAAX 1; Shh, sonic hedgehog; Src, sarcoma viral oncogene homolog. Figure adapted from Vaudry (2000).

Table 1.1 Pharmacological characteristics and transduction mechanisms associated with PACAP receptors

Receptor subtypes	Ligand binding affinity K_d	G-protein subunits	Splice variants	Transduction mechanisms			Physiological distribution	References
				Adenylyl Cyclase	PLC	Others		
PAC_1	Agonist Maxadilan ~ 0.05 ηM PACAP-38 ≈ PACAP-27 ≈ 0.5 ηM VIP> 500 mM Antagonist PACAP 6-38	$G_{\alpha s}$ $G_{\alpha q}$	S Hop1 Hop2 Hip-Hop		Stimulates IP turnover	Stimulates calcium mobilization And PLD	CNS; olfactory bulb, hippocampus, cerebral, cerebellar, cingulate and entorhinal cortices, hypothalamic, amygdaloid, thalamic Peripheral organ: Pituitary, adrenal medulla and placenta	Moro and Lerner, 1997; Dickson et al. 2006a; Robberecht et al. 1992b; Vaudry et al. 2009
			Hip	Stimulated cAMP production	-			
			Vs		Stimulates IP turnover	L-type channel		
			TM4		-			
$VAPC_1$	Agonist [$Ala^{11,22,28}$] VIP [$Ala^{2,8,9,11,19,22,24,25,27,28}$]-VIP 0.7 ηM PACAP-38 ≈ PACAP-27 ≈ VIP ≈ 1 ηM Antagonist PG 97-269	$G_{\alpha s}$ $G_{\alpha q}$ $G_{\alpha i}$	-	Stimulated cAMP production	Stimulated PLC	Stimulates calcium mobilization And PLD	Peripheral organ: Lung, intestine, pancreas and adrenal medulla, almost all human epithelial tissues.	Moro and Lerner, 1997; Dickson et al. 2006a; Robberecht et al. 1992b; Vaudry et al. 2009
$VAPC_2$	Agonist Ro 25-1553 ≈ 1 ηM Ro 25-1392 ≈ 5 ηM Bay 55-9837 0.3 ηM PACAP-38 ≈ PACAP-27≈ VIP≈ 1 ηM Antagonist PG 99-465	$G_{\alpha s}$ $G_{\alpha q}$ $G_{\alpha i}$	-	Stimulated cAMP production	-	Stimulates calcium mobilization And PLD	Peripheral organ: hippocampus, thalamus, pituitary, reproductive organ, spleen and adrenal cortex.	Moro and Lerner, 1997; Dickson et al. 2006a; Robberecht et al. 1992b; Vaudry et al. 2009

Affinity data from the IUPHAR Database (Sharman et al., 2011).

1.5.2 Nerve growth factor (NGF)

Overview, structure and function

Nerve growth factor (NGF) was the first neurotrophin to be characterised. It was initially described by Levi-Montalcini after transplantation of a mouse malignant sarcoma into a chick embryo resulted in an increase in size and strength of the root dorsal ganglia and sympathetic ganglia; even the ganglia that did not directly innervate the tumour showed an obvious increase in size (Levi-Montalcini and Hamburger 1951). Further in vitro investigation in 1954 by the same group showed that a signalling protein, later known as NGF, significantly promoted neurite outgrowth of co-cultured sympathetic and dorsal root ganglia. In 1986, Levi-Montalcini was awarded a Nobel Prize for Physiology and Medicine for the first of many growth-regulating signal substances to be discovered and characterized. In the following decades, NGF was considered as one of the most interesting parameters, and it was implicated in several novel findings, especially in the nervous system, as a part of much neuroprotective research.

Several other factors closely related to NGF have been established and classified as neurotrophins. Neurotrophins comprise a group of proteins known as neurotrophic factors that promote neuronal survival during development. These factors include NGF, BDNF, neurotrophin 3 (NT-3) and neurotrophin 4/5 (Cai et al., 2014). NGF is synthesised in the cortex, hippocampus and pituitary gland. NGF generally modulates a wide range of biological functions and signalling events in the nervous system; it regulates cell proliferation, differentiation and survival. Furthermore, NGF has been found to have a function in immune cells; inflammatory mediators induce the synthesis of NGF by different cells to elicit a pain response (Kawamoto and Matsuda 2004; Chao, Rajagopal, and Lee 2006). It has also been found that NGF induces B and T cell proliferation and IL-2 receptor expression on T-lymphocytes (Otten et al., 1989; Thorpe & Perez-Polo, 1987). Therapeutically, it is well documented that NGF is linked to pain treatment, and thus it is a potential target to discover a drug to treat chronic pain. Studies have led to the development of NGF inhibitors in the form of antibodies that have analgesic effects (Lane et al., 2010; Kumar & Mahal, 2012).

In neurons, NGF regulates the expression of enzymes involved in the synthesis of neurotransmitters and neuropeptides, such as tyrosine hydroxylase (TH) and dopamine β-hydroxylase. Furthermore, NGF has a crucial role in the function and survival of the neurons of the basal forebrain complex (BFC) area, which includes memory and motivations; its neurons are those mainly affected in AD (Allen & Dawbarn, 2006; Aloe et al., 2012). Thus, NGF has

been indicated to have a potentially protective role against neurodegenerative disorders affecting this area (Allen & Dawbarn, 2006). An NGF knockout mouse model has been used to demonstrate the neuronal survival role of NGF during development, and it shows a significant loss of sympathetic and sensory neurons (Crowley et al., 1994; Freund et al., 1994; Ruberti et al., 2000). A substantial body of evidence shows that in neurons that depend on NGF for survival, NGF is secreted from the target tissue innervated by the neurons activating a signal by which the axon terminals communicate with the cell bodies to exert survival (Korsching & Thoenen, 1983). This highlights the question of the possible mechanisms by which NGF generates signals that travel to the cell body over long distances to mediate cell survival. NGF has also shown to possess a strong anti-apoptotic effect, and in the absence of NGF neurons display various morphological changes and undergo apoptosis (Lomb et al., 2009).

Neurotrophins, including NGF, develop their biological functions through different signalling pathways by binding to two classes of structurally unrelated receptor, with varying affinities; these are the tyrosine kinase receptor family Trk (TrkA, TrkB and TrkC) and the p75NTR, tumour necrosis factor receptor family (TNFR). p75NTR was the first NGF receptor cloned and it has equal binding affinity for all neurotrophins, including NGF (Chao et al. 1986). Trk family receptors are generally more selective for neurotrophin ligand binding; NGF exerts its biological effects mainly through TrkA, while TrkB binds BDNF and NT4/5, and TrkC binds NT3 (Reichardt, 2006). NGF binds to p75NTR non-selectively and with high-affinity ($K_D = 10^{-9}$ M), leading to either apoptosis via the JNK/c-Jun signalling pathway or cell survival through the nuclear factor kappa-light-chain-enhancer of activated B cells (NF-κB) pathway, according to the cellular context (Bai et al., 2010; Verbeke et al., 2010). A substantial number of studies have suggested that p75NTR promotes apoptosis via the activation of downstream apoptotic signalling pathways, possibly through JNK/c-Jun (Bamji et al., 1998; Kenchappa et al., 2006) as shown in Figure 1.5. It has been found that in sympathetic neurons, treatment with neurotrophins that do not preferentially bind to TrkA, such as BDNF, pro-BDNF, pro-NGF and NT-4, modulates apoptosis (Bamji et al., 1998; Kenchappa et al., 2006; Deppmann et al., 2008). Furthermore, it has been shown that p75NTR-induced neuronal survival can be considered a NGF-dependent response. In contrast, in the absence of TrkA signalling, p75NTR modulates a cytotoxicity response in some cells (Casaccia-Bonnefil et al., 1996; María Frade et al., 1996; Van der Zee et al., 1996; Yeo et al., 1997). Although, positive results have been obtained from the use of NGF in the treatment of classical neurodegenerative diseases (Van der Zee et al., 1996), to date, the specific molecular mechanisms implicated to these opposing responses of p75NTR are not yet fully understood. Although this receptor is expressed during neuron

development, it has been found that binding of NGF to this receptor in the absence of the co-expression of TrkA mainly promotes apoptosis by activating the JNK signalling cascade (Aloe et al., 2012). A p75NTR disrupted mouse model exhibited a considerable delay in the apoptosis of sympathetic and sensory neurons during the normal period of developmental death (Bamji et al., 1998; Agerman et al., 2000). Further studies on the co-expression of both receptors find that this co-expression results in increasing NGF affinity to TrkA. It has been shown that, in the presence of p75NTR, lower concentrations of NGF are required for TrkA to induce neuronal survival (Horton et al., 1997). Figure 1.5 summarises the multiple intracellular signalling of NGF receptors.

Tyrosine kinase receptor A (TrkA)

TrkA is mainly expressed in the central and peripheral nervous system, it is member of transmembrane glycoprotein of tyrosine-kinase receptor family; it is the preferable, high-affinity NGF receptor known to activate signalling cascades that induce neuronal survival, neurite outgrowth and differentiation (Zhang et al. 2000; Reichardt, 2006). NGF exerts most of its biological and cell survival effetcs by binding selectively to TrkA with high affinity ($K_D = 10^{-11}$ M; Hefti et al. 2006). Activation of TrkA by NGF results in the intracellular auto-phosphorylation of TrkA, causing activation of signalling cascades that include Ras/Raf/MEK/ERK1/2, PI-3K/Akt and PLC/PKC signalling pathways, which subsequently lead to the prevention of apoptosis (Hausott et al., 2009; Mendoza et al., 2011). Studies using a TrkA knockout mouse model have shown that it is crucial for promoting the survival of neurons that depend on NGF during development (Wyatt & Davies, 1993, 1995). Altogether, evidence suggests that NGF-induced neuronal cell survival and differentiation are mediated particularly through the high-affinity TrkA receptor; therefore, it is worthwhile to further investigate this protective role as a therapeutic target for neuronal hypoxia. As the current study has focused on the effects of neurotrophic factor NGF, on mechanisms of cell survival and signalling pathways a detailed discussion of such events would be worthwhile.

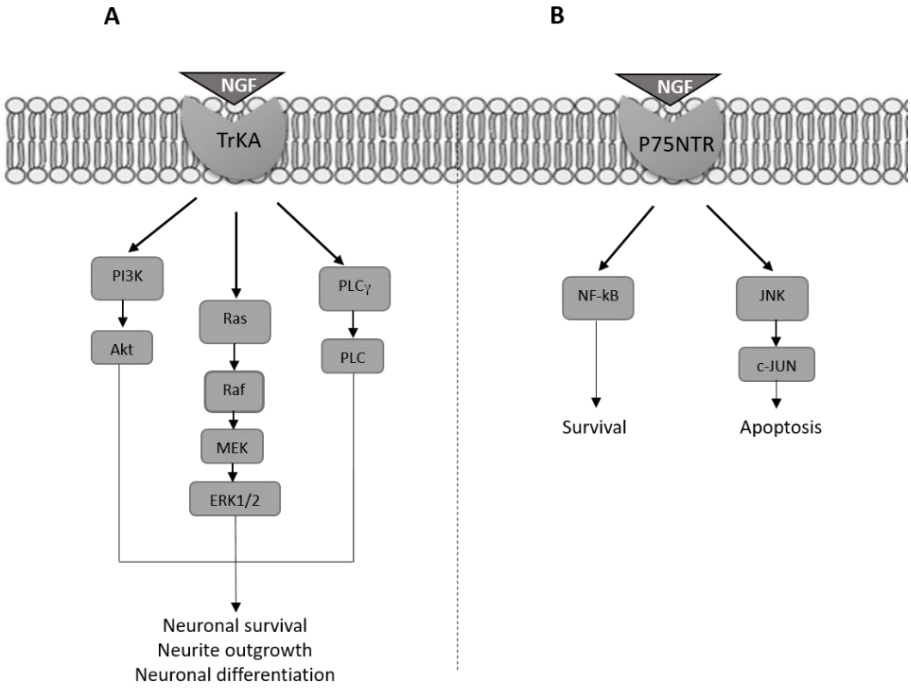

Figure 1.5 Schematic representation of the multiple intracellular signalling of NGF receptors.

A; NGF binding to TrkA receptor activates PI3K/Akt, Ras/MAPK and PLCγ pathways mediates proliferation, differentiation and survival. B; NGF binding to the p75NTR receptor activate NF-κB and c-Jun N-terminal kinase (JNK), mediate opposing effects of survival and apoptosis respectively. PI3K, Phosphatidylinositol-3-kinase; MAPK, Mitogen activated protein kinase; PLCγ, Phospholipase Cγ; NF-κB, Nuclear factor-κB; JNK, c-Jun N-terminal kinase (Wang et al., 2014).

The role of NGF in cell survival, neurite outgrowth and neuronal protection

NGF signalling appears to play crucial neuroprotective roles in response to neurodegeneration associated with brain injury or diseases. Multiple experimental animal studies have illustrated NGF's neuroprotective role in response to hypoxic/ischaemic brain injury, while a few studies have examined the protective mechanism in patients with the same severe incidents (Tanaka et al., 1994; Holtzman et al., 1996; Tabakman et al., 2004; Tabakman et al., 2005). One clinical study was conducted on two cases of children with hypoxic/ischaemic brain injury, and the researchers reported a remarkable improvement in their electroencephalograms (EEGs) after treatment with intraventricular NGF (Fantacci et al., 2013). As discussed earlier, most molecular characterisation studies of the pathways initiated by NGF and associated with cell survival and neuroprotection have been indicated to be through the TrkA receptor. Furthermore, NGF

signalling has been shown to be involved in various neuronal processes associated with survival, neuronal differentiation and axon growth (Bibel & Barde, 2000; Sofroniew et al., 2001). It is important to take into consideration that NGF signalling and the molecular events associated with neuronal protection have not yet been fully characterised. Thus, this thesis focusses on how the NGF signalling cascade may be implicated in the response to specific conditions.

One of the NGF-activated pathways contributing to neuronal cell survival occurs through the activation MAPK signalling. This signalling pathway is initiated by the phosphorylation of Shc, leading to the activation of a membrane-associated monomeric G-protein, Ras; which promotes the activation of Raf. Raf, in turn, activates MAPKK (MEK1/2) and ERK1/2, which facilitate the phosphorylation of ribosomal S6 kinase (RSK), leading to activation of the cAMP response element binding (CREB) protein. This regulates the expression of different genes contributing to neuronal differentiation or neurite outgrowth (Bibel & Barde, 2000).

In addition, the PI-3K/Akt pathway is especially important for neuronal survival induced by NGF, and it is the most studied pathway. Activated PI-3K phosphorylates PIP_2 to PIP_3, which then recruits Akt for activation. The activated Akt induces downstream targets that promote neuronal survival. For example, Akt phosphorylates pro-apoptotic proteins, such as forkhead box-O (FoxO) transcription factors and Bad; this leads to the inhibition of neuronal apoptosis by controlling the expression of genes involved in cell death (Brunet et al., 1999). Various studies examined the requirement of this pathway in NGF-inducing neuronal survival. It has been shown that the pharmacological inhibition of PI-3K using LY294002 leads to the partial blocking of NGF-induced neuronal survival (Atwal et al., 2000). It has been reported that, NGF-activation of PKC via the PLCγ pathway results in the inhibition of gene expression associated with programmed cell death (Cabeza et al., 2012). Much of the research has focussed on how survival is promoted by the cooperation of PKC and PI-3K pathways in NGF-dependent neuron survival. It has been found that the PKC pathway induces inhibition in the expression of genes responsible for neuronal cell death, which takes place in conjunction with the PI-3K pathway (Pierchala et al., 2004; Lallemend et al., 2005).

The implication NF-κB in NGF-dependent neuron survival has also been investigated. NF-κB is a nuclear transcription factor that regulates the expression of genes that play roles in cell survival. It has been found that NF-κB regulates NGF-induced neuronal survival during embryonic development through p75NTR (Hamanoue et al., 1999).

These studies on NGF and those previously discussed on PACAP, have increased the interest in the study of a possible role for the multifunctional enzyme transglutaminase 2 (TG2) in

neuroprotection and neurite outgrowth signalling pathways induced by PACAP- and NGF. Therefore, it is worthwhile to discuss how TG2 could link in to such events.

1.6 Transglutaminases

1.6.1 Family and physiological function

Transglutaminases (TGs) are a family of ubiquitous and related enzymes that were first characterised in 1957, when they were isolated from guinea pig liver (Clarke et al., 1959). They possess the ability to catalyse calcium-dependent post-translational modification of proteins, and they were first described as TGs in 1959 by Clarke et al. (1959). Nine different genes encoding TG isozymes have been identified, and some of them have been studied at the protein level (Grenard et al., 2001). The precise biochemical activity of TGs was first established in blood plasma, where coagulation factor XIII was shown to have the ability to crosslink and stabilise fibrin during the coagulation cascade (Pisano et al., 1969). This brought up the concept that these enzymes can modify proteins and act as a biological glue.

In mammals, there are nine genes encoding isoforms of TGs; eight of the gene products are classified as catalytically active enzymes, named TG1–7 and Factor XIIIa and the ninth one is the catalytically inactive erythrocyte membrane protein band 4.2 (Griffin et al., 2002; Eckert et al., 2014). They are widely distributed among various tissues. All the isoforms shared the same amino acid sequence at the active site except band 4.2 (Eckert et al., 2014). The characterisation of the TG family is summarised in Table 1.2.

The protein structure of the TG family consists of four domains, including an NH_2 terminal–β-sandwich, and α/β catalytic core and two COOH-terminal β-barrel domains. The active site consists of a cysteine, histidine and aspartate residue and tryptophan, which stabilises the transition state. This generates a compact structure (GDP-bound form) in which the active site is enfolded; this is called the catalytically inactive state. Upon activation, in presence of calcium, the structure takes an extended form (GTP-bound), where the active site is exposed (Nurminskaya & Belkin, 2013; Eckert et al., 2014). The TG1 and FXIII isoforms have an additional NH_2 terminal pro-peptide sequence that is cleaved in order to make them active (Iismaa et al., 2009). Active TGs crosslink proteins by catalysing an acyl transfer reaction between γ-carboxamides of glutamines and the ε-amino group of lysine residues, which results in different outcomes. Other TG activities include the incorporation of polyamines into proteins

and deamidation of proteins (Griffin et al., 2002; Iismaa et al., 2009). TGs' actions modulate different activities such as signal transduction, membrane stabilisation and protein polymerisation, and this could modulate a wide range of physiological functions. TG2 is the most widely expressed TG isoform, and it is found in most mammalian tissues (Fesus & Piacentini, 2002) and implicated in a wide range of cellular processes. In the mammalian CNS, TG2 is the most predominantly expressed isoform, but TG1 and 3 have also been identified (shii & Ui, 1994; Bailey et al., 2004; Bailey & Johnson, 2005). Consequently, most studies on the role of TG in neuronal cell function have focussed on TG2. As a ubiquitous and multifunctional protein, it would be anticipated to have a crucial physiological role. The TG2 cellular functions and significant roles in cell physiology are discussed in the following section.

Table 1.2 Members of transglutaminase family: classification and related information about molecular mass, cell or tissue localisation and biological function

Isoform name	Alternative name	Molecular weight KDa	Tissue expression	Main biological functions	References
Factor XIIIA	Plasma transglutaminase	83	Plasma, platelets, chondrocytes, astrocytes, macrophages, heart, eye and dendritic cells in the dermis	Blood clotting, bone growth, ECM stabilization, wound healing	Schroeder and kohler, 2013; Odii and Coussons, 2014; Eckert et al, 2014
TG1	Keratinocyte transglutaminase, type 1 TG	90	Keratinocytes, cytosol, membrane and squamous epithelia	keratinocytes Epidermal differentiation and cell envelope formation	Yamanishi et al., 1992, Odii and Coussons, 2014; Eckert et al., 2014
TG2	Tissue transglutaminase, type 2 TG, Gαh, cytosolic transglutaminase, transglutaminase type II, liver TG, erythrocyte TG, endothelial TG	78	Ubiquitous distribution in different tissues, membrane, cytosol, nucleus and extracellular	cell - ECM adhesion, cell differentiation, matrix stabilisation, cell survival, apoptosis, signalling	Collighan and Griffin, 2009; Eckert et al., 2014; Nurminskaya and Belkin, 2012; Odii and Coussons, 2014
TG3	Epidermal transglutaminase, type 3 TG, TGE	77	Cytosol, hair follicle, brain, epidermis	Keratinocyte differentiation, terminal differentiation of keratinocytes and hair follicle, GTPase activity	Rose et al,2009; Odii and Coussons, 2014; Eckert et al., 2014
TG4	Prostatic transglutaminase, type 4 TG, TGP	77	Prostate gland, prostatic fluids and seminal plasma	Prostate isoform, reproduction and fertility, semen coagulation in rodents	Ablin et al., 2011; Odii and Coussons, 2014; Jiang et al., 2013; Eckert et al., 2014
TG5	Type 5 TG, TGX	81	Epithelial tissues	Keratinocyte differentiation and cornified cell envelope assembly	Thibaut et al., 2005; Odii and Coussons, 2014; Eckert et al., 2014
TG6	Type 6 TG, TGY	78	Skin epidermis	Development and motor function	Thomas et al, 2013; Odii and Coussons, 2014; Eckert et al., 2014
TG7	Type 7 TG, TGZ	81	Ubiquitous	Not characterised	Odii and Coussons, 2014; Eckert et al., 2014
Band 4.2	Erythrocyte membrane protein band 4.2	72	Erythrocyte membranes, spleen, bone marrow, foetal liver	Maintain membrane integrity	Mouro-Chanteloup et al., 2003; Odii and Coussons, 2014; Eckert et al., 2014; Kalfa et al., 2014

1.7 Tissue transglutaminase TG2

1.7.1 The cellular and biological function of transglutaminase 2 (TG2)

Tissue TG2 is a multifunctional enzyme that is found both intracellularly and extracellularly (Eckert et al., 2014). TG2 is the most abundant and widely distributed member of the TG family (Lorand & Graham, 2003). It is mainly cytosolic; however, its presence in the nucleus and other cell components has been documented (Griffin et al., 2002; Filiano et al., 2010). The wide range of TG2 protein substrates accounts for its various biological functions, such as cell adhesion and migration, growth and differentiation, survival and apoptosis and organisation of the extracellular matrix (ECM; Eckert et al., 2014; Odii and Coussons, 2014). TG2 catalyses the Ca^{2+} -dependent transamination of proteins involving the acyl transfer reaction between the γ-carboxamide group of polypeptide-bound glutamine and the primary amino group of either a polypeptide-bound lysine or polyamine (Mhaouty-Kodja, 2004). Moreover, TG2 has Ca^{2+}-independent enzymatic and non-enzymatic functions (Eckert et al., 2014). The Ca^{2+}-independent enzymatic activities are the protein kinase function (Mishra et al., 2007), GTPase activity (Nanda et al., 2001), protein disulphide isomerase (PDI) activity (Hasegawa et al., 2003) and signal transduction G-protein (Gαh). The non-enzymatic functions include roles in cell adhesion and stabilisation of the ECM (Eckert et al., 2014). The TG2 structure is like that of the other TGs, containing in the four domains, as previously discussed (Figure 1.6). The TG2 N-terminus contains a fibronectin binding site, which is involved in the cell adhesion processes (Hang et al., 2005); the catalytic domains, which are required for the transamidating activity with some residues involved in GTP/GDP-binding (Griffin et al., 2002; Ruan et al., 2008). β-barrel-1, mainly contains the GTP/GDP binding site and β-barrel-2 is essential for PLCδ1 activation via Gαh and signal transduction (Nurminskaya & Belkin, 2013).

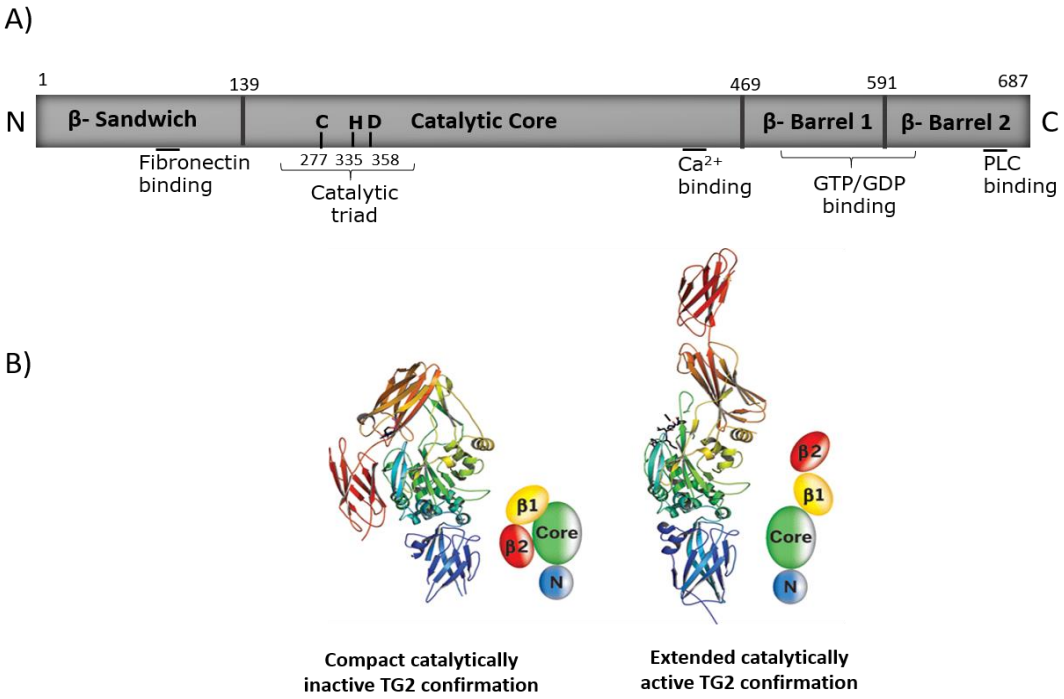

Figure 1.6 Schematic diagram of TG2 protein domain and crystal structure

Protein boundary of TG2 (A); the diagram shows the four TG2 structural domains N terminal, β-sandwich, catalytic core domain that contain essential (cys277, His335, Asp358) residues, β-barrel-1 and 2. Figure adapted from Lai and Greenberg (2012). The crystal structure of TG2 (B); shows compact form, GDP-bound TG2 (left) and extended form, exposed active site. Figure modified from Pinkas et al., (2007).

GTPase and G protein function

TG2's ability to bind and hydrolyse GTP was first established in 1987 (Achyuthan & Greenberg, 1987). In 1994, the correlation between GTP hydrolysis activity and the function of GPCRs was first demonstrated (Nakaoka et al., 1994). This showed that when the high-molecular-weight GTP-binding protein known as $G_{\alpha h}$ was co-isolated with the α_{1B} adrenergic receptor, it was identical to the TG2 sequence from different species (Lee et al., 1989; Im et al., 1993). Another shared functional ability between TG2 and $G_{\alpha h}$ is mediating signalling through different GPCRs, which results in the stimulation of PLCδ1 (Das et al., 1993). TG2/$G_{\alpha h}$ activity is independent of the transamidating activity (Achyuthan & Greenberg, 1987). A substantial number of studies focussing on functional comparisons between TG2 and $G_{\alpha h}$ have shown that $G_{\alpha h}$ displays similar activity to TG2, and this activity is inhibited by guanine nucleotides; it also binds with GTP at a 1:1 ratio and hydrolyses it to GDP (Achyuthan & Greenberg, 1987; Greenberg et al., 1991; Bergamini & Signorini, 1993). Together, these studies confirmed that

TG2 and $G_{\alpha h}$ exert the same cellular functions and pass on a receptor signal to the effector; this is described as TG2-GTPase activity.

It has also been reported that TG2-GTPase activity regulates signalling pathways namely ERK and the regulatory kinase MEK in cardiomyocytes (Lee et al. 2003). Moreover, it triggers AC activity in neuroblastoma cells (Tucholski & Johnson, 2003), but inhibits AC activity in fibroblasts and endothelial cells (Gentile et al., 1997). In fibroblasts, it has been confirmed that via GTP-binding activity, TG2 promotes cell migration (Kang et al., 2004) and regulates cell-cycle progression (Mian et al., 1995). Increasing evidence confirms that the GTPase activity of TG2 plays a definite role in shedding light on the possible kinase activity of TG2, which is discussed in the next section.

Kinase activity

In 2004, evidence was obtained for possible TG2 kinase activity, since it was indicated that in breast cancer cells, TG2 phosphorylates insulin-like growth factor-binding protein-3 (IGFBP-3), thereby reducing its pro-apoptotic activity (Mishra & Murphy, 2004). Furthermore, researchers have reported that TG2 kinase activity is inhibited with increases in intracellular calcium (Mishra & Murphy, 2004). It has also been found that in embryonic fibroblasts, TG2 kinase activity is stimulated by PKA and inhibited by increasing calcium levels (Mishra & Murphy, 2007).

Protein kinases, such as PKA and PKC, have been shown to regulate the activity and expression of TG2. For example, PKA phosphorylates TG2 at serine^{216} which promotes the binding of the adaptor protein 14-3-3 (Mishra & Murphy, 2006). This results in the modulation of various TG2 activities, such as the activation of pro-survival factors, NF-κB and PKB/Akt, and downregulation of tumour suppressor phosphatase and tensin homologue PTEN (Wang et al., 2012). The interaction between TG2 and 14-3-3 protein has been suggested to be an important regulator of TG2 kinase function. It has been also shown that TG2 serine^{212} is also a potential phosphorylation site for kinases such as PKC, RSK; ribosomal S6 kinase and CDK5; cyclin-dependent-like kinase 5 (Rikova et al., 2007). This regulates the interaction of TG2 with Bcl-2, resulting in an attenuated pro-apoptotic function (Wang et al., 2012). It has also been reported that TG2 is involved in activation of various signalling pathways, such as ERK1/2, JNK1/2 and p38 MAPK (Singh et al., 2003), CREB (Tucholski & Johnson, 2002), and PLC (Nakaoka et al., 1994). Further work would benefit from considering the role of TG2 kinase activity in these different pathways and the regulation among signalling events.

Protein disulphide isomerase activity

Protein disulphide isomerase (PDI) is an enzyme member of the thioredoxin family in the endoplasmic reticulum (ER); it catalyses the formation, breakup and exchange of disulphide bonds within proteins to ensure correct protein folding (Hasegawa et al., 2003). It has been found that several PDIs exert transamidating activity involving Cys, His and Asp residues, which TG2 requires in order to initiate the primary amine incorporation into proteins (Blaskó et al., 2003). This finding suggests a possible PDI activity of TG2 in the cytosol, where TG2 is present in higher concentrations. Thus, the PDI function of TG2 was first reported when the inactive RNase A was folded into the active form by TG2. Furthermore, TG2 mediated PDI activity is independent of calcium/GTP and transamidating function (Hasegawa et al., 2003). It has been also found that the PDI activity of TG2 can control the ADP/ATP transportation mechanism in the mitochondria, as researchers have reported that there is low ATP production in TG2 knockout mouse cardiomyocytes and skeletal muscle, and they suggested that this reduction is due to a lack of TG2 mediated formation of disulphide bridges (Krasnikov et al., 2005; Malorni et al., 2009).

Protein scaffolding

Another TG2 function is protein scaffolding. TG2 is mainly present in the cytosol; however, it can also be found in the ECM c and on the cell surface, where it can act as a scaffolding protein. This activity was shown in the interaction of TG2 with fibronectin (Gaudry et al., 1999) and β-integrins (β1, β3 and β5; Akimov et al. 2000). This reaction leads to the stabilising and remodelling of the ECM and produces stronger cell adhesion, migration and differentiation due to the modulation of various signalling pathways (Akimov and Belkin 2001; Wang and Griffin 2011). It has been well documented that the ability of TG2 to enhance cell attachment to the ECM has a supportive effect on cell survival; a lack of this supportive attachment leads to cell death. As cell surface TG2 has a role in enhancing the attachment to ECM, this promotes cell survival and protects cells from the death process (Aeschlimann and Paulsson 1991; Martinez et al. 1994; Belkin 2011). TG2 can also act as a scaffolding protein in the cytosol and nucleus. In the cytosol, it has been reported that TG2 scaffolding activity is required for NF-kB pathway activation (Lee et al. 2004). In the nucleus, the evidence on the existence of TG2 as scaffolding protein is well documented to be implicated in various types of transcriptional regulation (Ahn et al. 2008; Filiano et al. 2008; McConoughey et al. 2010; Jang et al. 2010). It has been shown that in cellular models of Huntington's disease, nuclear TG2 can interact with cytochrome-c

promoters and decrease their transcriptional activity (McConoughey et al., 2010). Later studies have suggested that the nuclear TG2 activity implicated in gene expression depended on its transamidation activity (Tatsukawa et al., 2009). Consequently, in the nucleus, TG2 could possibly act as scaffolding protein or transamidating enzyme, according to the physiological and pathological context.

Transamidase activity

The transamidating activity of TG2 was first identified in 1957. In this activity, TG2 catalyses a calcium-dependent post-translational modification (Sarkar et al., 1957). TG2 was initially considered a transamidating enzyme; however, further studies showed that under normal physiological condition, TG2 is not active in transamidation. The transamidating function of TG2 must be initiated by Ca^{2+} binding; the Ca^{2+} binding site in the TG2 structure is situated in the catalytic domain, and any mutation of one of the Ca^{2+} binding sites result in a reduction in the transamidating activity of TG2 (Király et al., 2009). GTP is also another modulator of this activity, GTP-bound form of TG2 is the catalytically inactive state. Under normal physiological conditions, the cytosolic has high GTP concentration and TG2 is in catalytically inactive (Klöock & Khosla, 2012). Inactive TG2 requires high concentration of Ca^{2+}influx to activate, which may associate with physiological disruption conditions such as apoptosis and this activation is depend on the precise level of Ca^{2+} (Orrenius et al., 2003). Once TG2 is activated by binding to Ca^{2+}, the catalytic domain (containing a cysteine residue) is exposed, leading to transfer of the acyl group between γ-carboxamide of the glutamines and the ε-amino group of lysine residue, as well as the formation of an ϵ-(γ-glutamyl) lysine isopeptide bond. The mechanism of this reaction consists of two main steps. First, the acyl acceptor substrate (glutamine containing) binds to the enzyme catalytic site and forms a thioester bond with the active cysteine site of TG2; this step is associated with the release of ammonia. Second, an amine donor binds to the enzyme by attacking the thioester intermediate bond and reforming the active site of the enzyme. If the amine donor group is a primary amine (free amine), the reaction will result in protein post-translational modification by amine incorporation. In contrast, if the involved group is peptide-bound lysine, the reaction outcome will be crosslinking of the two proteins. Furthermore, the reaction will result in deamidation if the group is a water molecule (Folk et al., 1983). For the purpose of this study, transamidation activity has been used to assess the TG2 activity. A simple summary illustrating the transamidation reaction catalysed by TG2 is shown in Figure 1.7.

The various outcomes of transamidating reactions have been found to be implicated in different biological and pathological processes. For example, it has been found that the transamidation function of TG2 is implicated in the activation of the small G-protein (Rac1) in pancreatic β-cells by incorporating serotonin (5-HT) on glutamine residues of GTPase to form a glutamyl amide bond (Paulmann et al., 2009). In skin, TG2 transamidation activity is essential for the *de novo* formation of functional dermo-epidermal cohesion apparatus required for bone healing (Haroon et al. 1999; Mearns et al. 2002). In contrast, excessive TG2 crosslinking activity has been reported to be involved in pathological processes, such as wound healing or the fibrogenic reactions associated with different diseases (Aeschlimann and Thomazy 2000). The role of TG2 in different diseases or disorders is discussed in the next section.

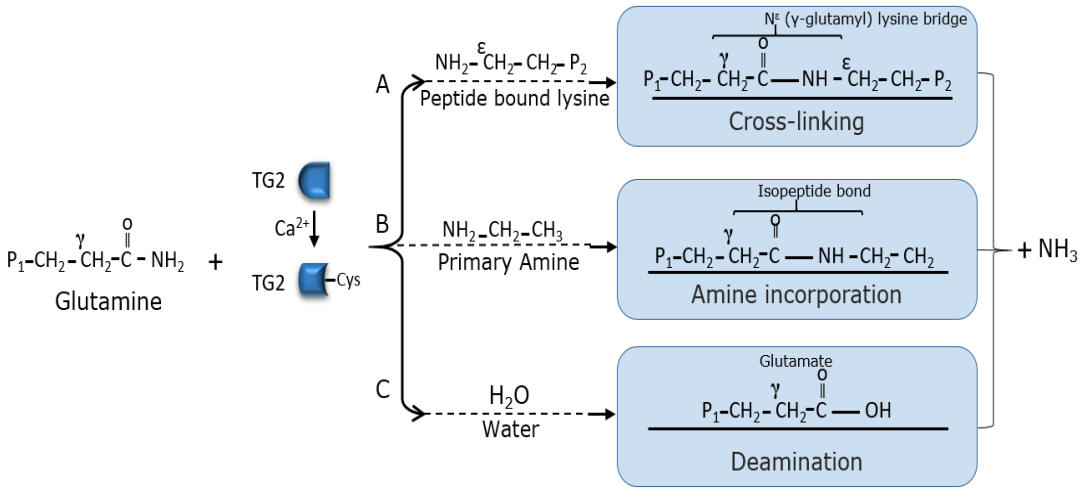

Figure 1.7 TG2 Transamidation reaction

A, Crosslinking reaction between γ-carboxamide group of a peptidyl glutamine and ε-amino group of a peptidyl lysine. B, Transamidation reaction between - γ carboxamide group of a peptidyl glutamine and a free amine. C, deamidation reaction between γ-carboxamide group of glutamine and water molecule (Adapted from Eckert et al., 2014).

1.7.2 TG2's role in diseases and disorders

As discussed previously, TG2 is important in various intracellular signalling processes, where it is either involved in the modulation of cellular process or pathological conditions, such as coeliac disease, fibrosis, inflammation and neurodegenerative disease. TG2 can be activated under pathological conditions in response to immune signals, and it exerts potential cellular protective and stabilising roles. Although any abnormal activation, deactivation or increase in the cellular level of TG2 is associated with various pathological processes, it has been found that autoimmune inflammatory disorders, such as coeliac disease (Briani et al., 2008) liver cirrhosis and fibrosis (Elli et al., 2009) and rheumatoid arthritis (Picarelli et al., 2003), are associated with increased TG2 expression. Furthermore, TG2 has a potential role in neurodegenerative diseases, such as Parkinson's disease (Andringa et al., 2004), AD and HD (Citron et al., 2001), thus making TG2 one of the most important therapeutic targets.

Coeliac disease

A substantial body of evidence suggests the possible role of TG2 in coeliac disease's pathological process. The protein post-translational modification activity of TG2 results in the generation of autoantibodies, such as that produced in the autoimmune disorder of gluten-sensitivity disease/coeliac disease (Siegel & Khosla, 2007; Ciccocioppo et al., 2010; Wanf & Griffin, 2011; Nurminskaya & Belkin, 2013). Coeliac disease is a chronic autoimmune disease caused by a permanent intolerance to ingesting wheat gluten or any related products; it is characterised by innate immune responses to this type of protein in the diet (Di Sabatino & Corazza, 2009). Increasing TG2 expression has been reported in jejunal biopsies from coeliac disease patients, suggesting that TG2 is implicated in this disease pathology (Bruce et al., 1985). In this process, TG2 is involved in the generation of deamidated gluten, thereby triggering inflammatory responses (Matysiak-Budnik et al., 2008). The immune complex is recognised by T cells, leading to the formation of autoantibody immunoglobulin A (IgA) against TG2 (Koning et al., 2005; Ciccocioppo et al., 2010). This is used as a diagnostic marker for this disease, revealing the role of TG2 in modulation of the immune responses in its pathogenesis.

Inflammation and tumour progression

Various inflammatory diseases have been associated with either activation or deactivation of TG2. TG2 has been reported to promote inflammation through the activation of the NF-kB cascade, which is known to be a key switch for inflammation (Lee et al. 2004). TG2 induces activation of the NF-kB cascade via enhancing crosslinking and the subsequent degradation of IkBα, its inhibitory subunit. This TG2 crosslinking activity leads to the dissociation of NF-kB and its translocation to the nucleus, which results in the up-regulation of inflammatory genes, such as TNF-α, and promoting the expression of anti-apoptotic proteins, such as Bcl-xL (Lee et al. 2004; Mann et al. 2006). Conflicting regulation mechanisms with regard to TG2 expression in response to inflammation and injury have been reported, with its upregulation enhanced by cytokines, such as IL-1 and IL-6, that are secreted in response to inflammation (Suto et al., 1993; Johnson et al., 2001). In addition, it has been reported that the pro-inflammatory cytokine transforming growth factor β1 (TGF-β1) enhances TG2 expression; sequentially, TG2 binds to the cell surface, activating the conversion of TGF-β1 to its biologically active form. This has been suggested to be a crucial stabilisation mechanism of inflammation (Quan et al., 2005).

Tumour progression shows high similarity to the inflammatory responses; TG2 shows conflicting integration in tumour progression being either up- or down-regulated (Mehta & Han, 2011). It has been reported that TG2 expression is down-regulated in primary tumours and tumour progression, while it is up-regulated in the metastatic stage of tumours that have developed resistance to chemotherapy (Kotsakis & Griffin, 2007). Increasing the TG2 at the metastatic stage reveals a possible role in stabilising the contact points of tumours to the ECM (Kong & Korthuis, 1997). It has been shown that increased TG2 expression in ovarian cancer promotes adhesion with fibronectin and cell migration (Satpathy et al., 2007). In this mode, TG2 could be implicated in the survival of cancer cells. In contrast, TG2's enzymatic transamidation activity suggests that it has a role in promoting cancer cell death, as it has been shown to establish cell apoptosis in some cancer cell lines (Milakovic et al., 2004). These opposing functions of TG2 in cancer biology suggest that it could have both cell death and cell survival roles.

1.7.3 The cell death and cell survival roles of TG2

In the past decade, a considerable number of studies have established the contradictory role of TG2 in promoting cell survival and apoptosis (Fesus & Szondy, 2005; Mehta et al., 2006; Verma & Mehta, 2007). TG2's multifunctional, conformational change and localisation properties make it complex to identify the possible trigger to initiate this dual role. It has been found that TG2 modulates caspase-dependent cell death and is involved in another mechanism to control cell death that is independent of caspase (Fesus & Szondy, 2005). It has also been found that TG2 transamidation activity can both facilitate and inhibit apoptosis. However, TG2 has been shown to have an anti-apoptotic effect via its crosslinking activity (Fesus & Szondy, 2005; Sarang et al., 2005).

TG2's role in cell death and survival has been widely studied using neuronal models, as TG2 is the most predominant TG isoform expressed in the brain (Kim et al., 1999; Bailey et al., 2004). Moreover, it has been found to be up-regulated in the human brain associated with acute and chronic neurodegenerative diseases, suggesting a possible role in neuronal cell death or survival. It has been found that in a mouse model of Huntington's disease $TG2^{-/-}$ knockout revealed a delay in motor dysfunction onset. Furthermore, prolonged survival of transgenic $TG2^{-/-}$ mice has been reported (Mastroberardino et al., 2002; Bailey & Johnson, 2005; Mishra et al., 2007). However, the reason that the TG2 knockout caused protection in the Huntington disease mouse model has not yet been established. In contrast, in the SH-SY5Y human neuroblastoma hypoxia model, TG2 binding to hypoxia inducible factor 1β (HIF1β) protected neuronal cells from hypoxia induced-cell death (Filiano et al., 2008).

Several studies have reported that overexpression of TG2 under apoptotic conditions leads to more neuronal phenotypes in human neuroblastoma SH-SY5Y cells (Zhang et al., 1998). These data provide evidence that TG2 up-regulation is not necessarily associated with apoptosis; instead, it could lead to differentiation and axon outgrowth. Furthermore, the up-regulation of TG2 was found to suppress the apoptosis and cell death induced by Ca^{2+} overload via Bax suppression, decreased activation of caspase-3 and 9, decreased release of cytochrome C and inhibition of mitochondrial permeability transition pore (Cho et al., 2010). This revealed the protective and anti-apoptotic role of TG2 in diseases involving Ca^{2+} overload. Although TG2 has long been known to be involved in the apoptosis process, a definitive answer to whether it is pro-apoptotic or anti-apoptotic has not yet been determined. Altogether, these studies suggest a role for TG2 in mediating the cellular response in pathological conditions, such as ischaemia and stroke. Thus, it is likely to be a target for pharmacological manipulation to alleviate

associated neuropathology. Several extensive reviews discuss the potential complicated role of TG2 in cell survival and cell death (Fesus & Szondy, 2005; Chhabra et al. 2009; Iismaa et al., 2009; Caccamo et al., 2012).

1.7.4 TG2's neuroprotective role

Although TG2 plays a role in various cellular processes, its neuroprotective function by regulating cell survival and death has been an area of especial interest. In the past decade, increasing evidence has suggested the potential role of TG2 in protecting and stabilising cells and tissue, especially in neuronal cells (Eckert et al., 2014).

Ischaemia/stroke

Inadequate oxygen and glucose levels in cerebral tissue as a consequence of stroke/ischaemia, induce various processes involving adaptive responses and apoptotic and excitotoxic cell death. They also initiate hypoxic signalling via HIFs (Lee et al. 2000; Thornton et al. 2017). There is a growing awareness that TG2 is up-regulated in response to hypoxic/ischaemic stress (Tolentino et al., 2004). In addition, it has been documented that the TG2 activity and expression are increased in an animal model of cerebral ischaemia and stroke (Ientile et al., 2004; Tolentino et al., 2004). Therefore, it is reasonable to hypothesise a functional role of TG2 in response to ischaemic insult. Studies on cardiomyocytes from $TG2^{-/-}$ mice revealed that TG2 had a protective role against cardiac ischaemia (Szondy et al., 2006). In contrast, astrocytes of $TG2^{-/-}$ mice showed resistance to ischaemia and increased survival compared to wild-type mouse astrocytes (Colak & Johnson, 2012). These conflicting finding suggests that the TG2 cell survival function depends on the cell context.

At the neuronal level, a considerable amount of evidence has been gathered concerning TG2's role in hypoxia/ischaemia, and this has confirmed its neuroprotective functions. Neuronal selective TG2 over-expression in mice resulted in smaller infarct volumes compared to wild-type mice after ischaemic stroke (Filiano et al. 2010). The possible cellular protective mechanisms of TG2 were investigated previously by the same group in 2008, and it was shown that TG2 protected against oxygen and glucose deprivation (OGD)-induced cell death in the SH-SY5Y neuroblastoma cell line. This protective role of TG2 is due to its interaction with HIF1β and suppression of the HIF1 hypoxic response pathway (Filiano et al. 2008).

Neuronal differentiation

Considerable progress has been made in understanding the role of TG2 in neuronal differentiation. The first study conducted to identify this role was performed by Maccioni and Seeds (1986), who reported that TG2 activity increased 10-fold in association with neuronal outgrowth during neuroblastoma cell differentiation. In addition, a localisation study of TG2 in neuroblastoma cell lines showed that TG2 was predominantly found in the tips of neurites and the perinuclear area, suggesting a role in neurite outgrowth (Tucholski et al., 2001). These findings indicate that TG2 acts as a positive regulator of neuronal differentiation. Further research has demonstrated that inhibition of TG2 blocks neurite outgrowth and the expression of neuronal markers (Singh et al., 2003). It has also recently been found that the overexpression of active TG2 in neuroblastoma cell lines promotes neurite outgrowth (Tee et al., 2010). The possible underlying molecular mechanism has been studied, and it was found for the first time that the transamidation of RhoA by TG2 is required for activation of ERK1/2 and p38 MAPK pathways, which are involved in neuronal differentiation (Singh et al., 2003). It has been found that TG2 contributes to neuronal differentiation by facilitating AC, thereby activating the cAMP/CREB pathway, which plays a critical role in neuronal differentiation process (Tucholski and Johnson 2003). Various studies have found that TG2 most likely contributes to neuronal differentiation by enhancing AC activity; however, further studies are still required to identify the clear mechanism by which this occurs. Therefore, one of the research aims of the work presented in this thesis was to determine this possible underlying mechanism.

1.8 The use of *In vitro* mammalian cell models for the assessment of neuronal cell survival and neurite outgrowth

Neuronal cell signalling is a complex molecular interaction that stimulates the surrounding cell components, resulting in the modulation and induction of various cellular processes and complicated intermolecular reactions. The capacity of *in vitro* model systems has changed the field of neurobiology and contributed to the understanding of most neuronal cell processes. Furthermore, it has produced a useful platform for characterising protein functionality and molecular processes associated with specific conditions to understand their pathogenesis and implement pharmacological assessments. The ethical issues and economic costs associated with animal experiments for neurological studies have encouraged researchers to rely more and more on *in vitro* cell cultures (Gordon et al., 2013). The disadvantages of *in vitro* cell cultures are that

they could show some physiological differences due to lack cell to cell interaction and partial manipulation of pharmacokinetic factors (Rice & Barone, 2000). However, this cell culture method also has numerous potential advantages, making it suitable for this project. This approach can grow cell cultures relatively easily, give unlimited numbers of homogenous cells and be easily maintained for long periods of time to conduct assessments with minimal time and much lower financial costs (Radio & Mundy, 2008; Flaskos, 2012). Furthermore, it is appropriate for assessing cellular, molecular and morphological alterations.

1.8.1 The mouse N2a neuroblastoma cell line

The mouse N2a neuroblastoma cell line was derived from the mouse C1300 neuroblastoma (Klebe and Ruddle, 1969). Due to its immediate response to stimuli to express signalling molecules and to serum deprivation to induce differentiation within a short time, it is broadly used to study neuronal differentiation, neurite outgrowth and signalling pathways. Serum withdrawal and the addition of retinoic acid (RA) is one method used to differentiate the cells into neurons and have them undergo several morphological changes. Upon differentiation, N2a cells show a neuron-like morphology, expressing various adrenergic and cholinergic neuronal markers (Sajithlal et al. 2002, Klebe and Ruddle, 1969). Furthermore, differentiated N2a cells can develop axon-like processes and dendrites and express important axon outgrowth associated proteins such as neurofilaments (NFs) and microtubules (MTs; Evangelopoulos et al., 2005; Tremblay et al. 2010). All these factors make N2a cells a suitable model for the purpose of this study on the screening of cell signalling and morphology alterations. However, appreciation of the pharmacological and functional differences between neurons and neuron-like cell lines is essential, including an understanding of species–specific differences in some cellular processes when compared to humans. Therefore, a human cell line has been also used in the current study, as discussed in the following section.

1.8.2 Human SH-SY5Y neuroblastoma

Human SH-SY5Y neuroblastoma cells have been cultured and used extensively in neurobiology research. They were derived by sub-cloning from the parental metastatic bone tumour cell line SK-N-SH, which was generated from bone marrow biopsy. Undifferentiated SH-SY5Y cells exhibit a large, flat, epithelial-like phenotype with several short outward extending processes. The differentiated cells are morphologically similar to primary neurons, exhibiting numerous neurite projections that connect to surrounding cells, as well as long branched processes. In

addition, they express various neuronal markers, such as axon growth-associated protein 43 (GAP-43), NFs and MT-associated proteins (MAPs). SH-SY5Y cells are characterised by having a stable karyotype, and they can be differentiated into mature human neurons via different approaches, including the use of RA. The use of RA with serum removal induces SH-SY5Y cells to differentiate into neurons with a dopaminergic phenotype (Presgraves et al., 2004; Korecka et al., 2013). These differentiated SH-SY5Y neurons are similar to mature human neurons found *in vivo* and provide an appropriate model for understanding cellular processes, cell signalling and morphology.

1.9 Framework and aims of this study

As discussed previously, the multifunctional enzyme TG2 has a strong relationship with hypoxic stress, and its protective role against cell death under ischaemia-like conditions and induction of neuronal outgrowth has been reported in the literature (Maccioni and Seeds 1986; Filiano et al. 2008; Filiano et al. 2010). It has also been shown that protein kinases, such as PKA and PKC, regulate the activity of TG2 via GPCRs to modulate cytoprotection (Almami et al., 2014). However, not much is known about the GPCRs and signalling pathways involved. It is well established that neurotrophic factors, such as PACAP and NGF, stimulate via their receptors (PAC_1 and TrKA, respectively) signalling pathways including ERK1/2, PKA, PKC and Akt, thereby inducing neuronal cell growth and survival. As some of these pathways are associated with the modulation of intracellular TG2 activity, it is conceivable that these neurotrophic factors directly regulate TG2 activity and induce neuroprotection. Understanding the pathways involved in hypoxia stress and the implications they may have for TG2 on activation of the PAC_1 receptor by PACAP or the TrKA receptor by NGF, would provide a clear view as to how this enzyme may be involved in neuroprotection. Accordingly, the aims of this study were to investigate the modulation of TG2 by PACAP and NGF via their receptors to induce neuronal cell growth and survival.

In this research, a series of studies is completed with the objective of characterising TG2's ability to modulate neuronal outgrowth and survival via the kinase signalling cascade induced by neurotrophic factors (PACAP and NGF) in differentiating N2a mouse neuroblastoma and SH-SY5Y human neuroblastoma cells. To begin, the ability of these neurotrophic factors to induce TG2 transamidase activity through their receptors is characterised (chapter 4 and 5). Next, the neuroprotective potential of PACAP- and NGF-induced TG2 activity following exposure of N2a and SH-SY5Y cells to hypoxia is assessed (chapter 6). Finally, high-

throughput approaches are applied to evaluate the role of PACAP- and NGF-induced TG2 activity on different neurite outgrowth parameters, such as the average cell number, average neurite number, average and maximum neurite length, mean processes and branches per cell (chapter 6).

1.10 Aims of the thesis

This study had the following experimental aims:

1. To investigate the modulation of TG2 activity by PACAP via the PAC_1 receptor;
2. To investigate the modulation of TG2 activity by NGF via the TrkA receptor;
3. To assess the neuroprotective and cell survival potential of PACAP- and NGF-induced TG2 activity;
4. To apply high-throughput approaches to evaluate the involvement of TG2 in PACAP- and NGF-modulation of neuronal outgrowth.

Chapter 2

2 Materials and Methods

2.1 Materials

All reagents used in the laboratory were of the highest grade and purchased from Sigma-Aldrich Co Ltd (Gillingham, UK) unless otherwise specified.

2.1.1 Cell culture reagents

Dulbecco's modified Eagle's Medium (DMEM), glucose free DMEM, foetal bovine serum (FBS), L- glutamine (200 mM), penicillin (10,000 U/ml)/streptomycin (10,000 µg/ml) and trypsin (10 X) were purchased from BioWhittaker Lonza Group Ltd., UK. Phosphate buffered saline (PBS) was obtained from Life Technologies (Invitrogen, UK). *All-trans* retinoic acid was obtained from Sigma-Aldrich Co. Ltd (Gillingham, UK).

2.1.2 Cell lines

Murine N2a and human SH-SY5Y neuroblastoma cells were obtained from the European Collection of Animal Cell Cultures (Porton Down, Salisbury, UK).

2.1.3 Kinase inhibitors

Akt inhibitor XI (PKB/Akt, 100 nM; Hu et al., 2000), KT 5720 (PKA, 5 µM; Cabell et al., 1993), Rp-cAMPs (PKA, 50 µM; Gjertsen et al., 1995) and Ro 31-8220 (PKC, 10 µM; Han et al., 2000) were obtained from Calbiochem (San Diego, CA). PD 98059 (MEK1/2, 50 µM; Dudley et al., 1995), SB 203580 (p38 MAPK; 20 µM; Davis et al., 2000), and SP 600 125 (JNK1/2; 20 µM; Bennett et al.,2001) were purchased from Tocris Bioscience (Bristol, UK). All protein kinase inhibitors used in this study are listed in Table 2.1.

Table 2.1 Protein kinase inhibitor compounds used in this study

Compound	Concentration	Target	Supplier
Akt inhibitor XI	1 μM	Akt inhibitor	Calbiochem (San Diego, CA)
KT 5720	5 μM	PKA inhibitor	
***Rp*-8-Cl-cAMPS**	50 μM	PKA inhibitor	
Ro-31-8220	10 μM	PKC inhibitor	
PD 98059	50 μM	MEK1/2 inhibitor	Tocris Bioscience (Bristol, UK)
SB 203580	30 μM	p38 MAPK inhibitor	
SP 600 125	20 μM	JNK1/2 inhibitor	

2.1.4 Chemical compounds and reagents

[Ala11,22,28] VIP, Bay 55-9837, PACAP-27, PACAP 6-38 were obtained from Tocris Bioscience (Bristol, UK). Nerve growth factor (NGF) was obtained from Merck Millipore (Watford, UK). Casein, N',N'-dimethylcasein, IBMX (3-isobutyl-1-methylxanthine), IGEPAL, MTT (3-(4-5-dimethylthiazol-2-yl)-2,5-diphenyltetrazolium bromide), paraformaldehyde, TritonTM X-100, Protease Inhibitor Cocktail (AEBSF – [4-(2-aminoethyl) benzenesulfonyl fluoride hydrochloride], aprotinin, bestatin hydrochloride, E-64 – [N-(trans-epoxysuccinyl)-L leucine 4-guanidinobutylamide], leupeptin hemisulfate salt, pepstatin A), Phosphatase Inhibitor Cocktails 2 (sodium orthovanadate, sodium molybdate, sodium tartrate and imidiazole) and 3 (cantharidin, (–)-p-bromolevamisole oxalate, calyculin A), Ammonium persulphate (APS), ExtrAvidin-horseradish Peroxidase (HRP) and ExtrAvidin-FITC were obtained from Sigma-Aldrich Co. Ltd. (Gillingham, UK). The TG2 inhibitors Z-DON (Z-DON-Val-Pro-Leu-OMe) and R283, together with purified guinea-pig liver TG2 were obtained from Zedira GmbH (Darmstadt, Germany). VectaShield® containing 4,6-diamidino- 2-phenylinole (DAPI) was from Vector Laboratories Inc (Peterborough, UK). Fluo-8/AM was purchased from Stratech Scientific Ltd (Newmarket, UK). Biotin-TVQQEL was purchased from Pepceuticals (Enderby, UK). Biotin cadaverine (N-(5 aminopentyl)biotinamide) and biotin-X-cadaverine (5-([(N-(biotinoyl)amino)hexanoyl]amino) pentylamine) were purchased from Invitrogen, UK (Loughborough, UK). N,N,N',N'- tetramethylethylenediamine (TEMED) was from (National Diagnostics, USA.

2.1.5 Antibodies

Table 2.2 Monoclonal and polyclonal primary antibodies

Antibody	Dilution Western blotting	Dilution Immunocyto -chemistry	Molecular wt. kDa	Supplier and catalogue number
Monoclonal phospho-specific ERK1/2 (Thr^{202}/Tyr^{204})	1:1000	-	44-42	Sigma-Aldrich, UK, M8159
Monoclonal anti-total ERK1/2	1:1000	-	44-42	New England Biolab, UK, 9107
Polyclonal phospho-specific PKB (Ser^{473})	1:1000	-	60	New England Biolab, UK, 9271
Polyclonal anti-total PKB	1:1000	-	60	New England Biolab, UK, 9272
Polyclonal anti-total JNK	1:1000	-	54-46	New England Biolab, UK, 9252
Monoclonal phospho-specific JNK (Thr^{183}/Tyr^{185})	1:1000	-	54-46	New England Biolab, UK, 9251
Monoclonal phospho-specific p38 MAPK (Thr^{180}/Tyr^{182})	1:1000	-	43	New England Biolab, UK, 9216
Polyclonal anti-total p38 MAPK	1:1000	-	43	New England Biolab, UK, 9212
Monoclonal cleaved caspase-3	1:500	-	19-17	New England Biolab, UK, 9661
Monoclonal anti-TG2	1:1000	-	78	Thermo Scientific (CUB 7402)
Polyclonal anti-TG1	1:1000	-	90	Zedira GmbH A018
Polyclonal anti-TG3	1:1000	-	78	Zedira GmbH A015
Monoclonal anti-α-tubulin clone B512	1:2000	1:100	50	Sigma-Aldrich, UK, T6074
Monoclonal anti-tyrosine Hydroxylase	1:1000	1:200	60	Sigma-Aldrich, UK, T1299
Polyclonal anti-choline acetyltransferase	1:1000	1:200	82	Santa Cruz Biotechnology, SC20672
Monoclonal anti-GAPDH	1:1000	-	36	Abcam, Uk, ab8245
polyclonal anti-phosphoserine	1:1000 IP	-	-	Abcam (Cambridge, UK) ab9332
polyclonal anti-phosphothreonine	1:1000 IP	-	-	Abcam (Cambridge, UK) ab9337

Table 2.3 Secondary antibodies

Antibody	Dilution Western blotting	Dilution Immunocyto-chemistry	Supplier and catalogue number
Anti-mouse IgG-HRP	1:1000	-	Sigma-Aldrich, UK (A4416)
Anti-rabbit IgG-HRP	1:1000	-	Sigma-Aldrich, UK (A0545)
Anti-mouse-Alexa 568	-	1:500	Molecular Probes (Invitrogen, UK) (A-11031)
Anti-rabbit-Alexa 568	-	1:500	Molecular Probes (Invitrogen, UK) (A10042)
ExtrAvidin®-FITC	-	1:200	Sigma-Aldrich, UK (E2761)

2.2 Methods

2.2.1 Cell culture

Maintenance of cells

Mouse N2a cells and human SH-SY5Y cells were grown and maintained as a monolayer in DMEM, supplemented with 2 mM L-glutamine, 10% (v/v) FBS, penicillin (100 U/ml) and streptomycin (100 µg/ml). Cells were incubated at 37°C in a humidified atmosphere of 95% air /5% CO_2.

Sub-culture of cells

Cells were passaged or sub-cultured when growth reached 70-80% confluence (i.e. every 3-4 days). On reaching 80% confluence, the cell cultures were either used to seed monolayers on cell culture plates for assays, (for example; T75 flasks for Western blot analysis, chamber slides for immunofluorescence staining and high throughput screening of neurite outgrowth) or passaged to maintain the cell line. N2a cells were mechanically removed from the flask surface using a sterile Pasteur pipette to detach the cells by aspirating growth medium and squirting it out on the monolayer surface. In contrast, SH-SY5Y cells were passaged by removing the growth medium and washing cells with sterile phosphate buffered saline (PBS), then detached using trypsin (0.05 % w/v)/EDTA (0.02 % w/v) in PBS. Following trypsinisation, 10 ml of fully supplemented DMEM medium were added to the trypsinized cells. Then both suspended N2a and SH-SY5Y cells were harvested by centrifugation at 300 x g at room temperature for 5 min. The supernatant was discarded, and the cell pellet resuspended in 1 ml of growth medium and further sub-cultured (1:5 split ratio). Experiments were performed on passage numbers 8-20 for N2a and 18-25 for SH-SY5Y because later passages would be more susceptible to the effect of genetic drift.

Counting and plating cells for experimental analysis

Cells were plated out for experimental analysis when they reached 70-80% confluence in the maintenance flasks. Initially, cells were passaged as described in the previous section and, after resuspending in 1 ml of the growth medium, automated cell counting carried on using a TC20 automated cell counter (BioRad, Hemel Hempstead, UK). The device utilised prepared TC20 Trypan blue dye (0.4% Trypan blue (w/v) in 0.81% (w/v) sodium chloride and 0.06% (w/v) potassium phosphate dibasic solution). Trypan blue is a vital stain that differentiates between live and dead cells (Wang, 2006). The principle of this dye is based on the blue acid dye chromophores which react and are taken up by the internal region of dead (non-viable) cells through a damaged membrane, whereas live (viable) cells do not take up this dye. A volume of 10 µl of cell suspension was added to 10 µl of Trypan blue solution and left for 4 min to allow for cells to be exposed to the stain. A volume of 10 µl of this mixture was then loaded into a chamber of the counting slide. The slide was inserted into the slide slot of the TC20 cell counter and cell counting was automatically initiated as soon as the cell counter detected the presence of the slide and Trypan blue dye. Viable cell counts per ml were used to determine the volume necessary to seed the cells at a required cell density in growth medium. Cell density of 50,000 cells/ml was used to plate out mouse N2a cells and 100,000 cells/ml was used for SH-SY5Y cells (Table 2.4). Flasks were then incubated at 37ºC in a humidified atmosphere of 95% air/5% CO_2 for 24 h to allow for cell recovery.

Table 2.4 Cell density for experiments with N2a and SH-SY5Y cells.

Cell culture dish/plate	Loading volume	Total cells number	
		N2a	SH-SY5Y
T175 flask	50 ml/flask	2,5000,000	5,000,000
T75 flask	40 ml/flask	2000,000	4,000,000
T25 flask	10 ml/flask	500,000	1,000,000
8 well slide	300 µl/well	15,000	30,000
24 well plate	500 µl/well	25,000	50,000
96 well plate	200 µl/well	10,000	20,000

Differentiation of cells

Differentiation of N2a cells was induced by culturing cells in serum-free DMEM containing 1 µM *all-trans* retinoic acid for 48 h, unless otherwise specified. Differentiation of SH-SY5Y cells was induced by culturing cells in serum-free DMEM containing 10 µM *all-trans* retinoic acid for 5 days. The addition of retinoic acid induced N2a and SH-SY5Y cells to develop the

characteristic phenotype of differentiated neurons with neurite extensions (Tremblay et al., 2010).

Measurement of cell differentiation

Coomassie Brilliant Blue staining

Differentiation of N2a and SHSY-5Y cells was monitored for morphological change under a light microscope (mitotic cells were used as control) using Coomassie Brilliant Blue staining solution. Cells were cultured and differentiated as mentioned previously. The growth medium was aspirated, and the cells were washed with PBS three times. The cells were then fixed at -20 °C with 90 % (v/v) methanol solution for 15 min. The methanol fixing solution was then removed and Coomassie blue staining solution ((0.1% (w/v) Coomassie brilliant blue G, 50 % (v/v) methanol, 10 % (v/v) acetic acid)) was added the cells for 10 min to stain the cells. Staining solution was aspirated, and stained cells were washed three times with deionised water and left to air dry at room temperature then examined with the aid of a light microscope. Five randomly selected fields were examined in each well. Cells showed neuronal-like phenotype and neurite extension by forming axon like process in N2a cells and showed consistently slender and longer bipolar morphology in SH-SY5Y cells (Biedler et al., 1973).

2.2.2 Experimental treatment procedure

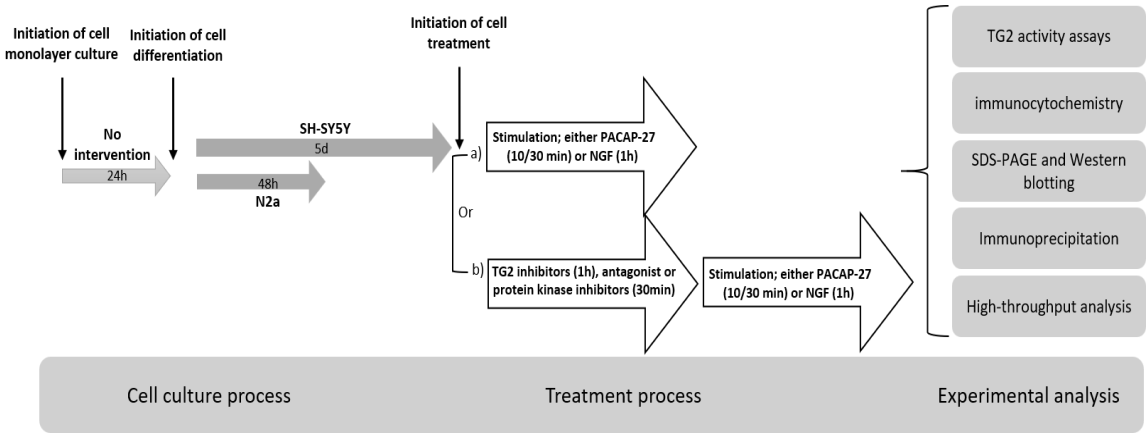

Figure 2.1 Flow diagram representing the cell culture, treatment and experimental process

a) Neurotrophic factor (stimulus) treatment (PACAP-27 or NGF). N2a and SH-SY5Y cells were exposed for 10 or 30 min, respectively, to PACAP-27 or to NGF for 1 h in both cell lines. b) TG2 inhibitors were applied for 1 h, and PAC_1 receptor antagonist and protein kinase inhibitors for 30 min prior to neurotrophic factor (stimulus) treatment.

2.2.3 Protein estimation assay

Protein concentration in cell lysates was measured based on the Bicinchoninic acid (BCA) method of Smith et al. (1985) using a commercially available kit (Sigma-Aldrich Co Ltd, Gillingham, UK). Bovine serum albumin (BSA) was used as the protein standard. In brief, protein standards were prepared using dilutions of 1 mg/ml BSA to produce a linear standard curve. Standards (20 µl) and cell lysate samples (20 µl) were added to a 96-well flat-bottomed plate in triplicate. A volume of 200 µl of working BCA reagent (50 parts of reagent A to 1 part of reagent B) was added to each of the wells and the plate incubated at 37^{o}C for 30 min. Absorbance was read at 570 nm using a standard 96-well plate reader. Protein content of samples was obtained by measuring them against the BSA standard curve.

2.2.4 Tissue transglutaminase activity assays

Cell extraction for measurement of TG2 activity

N2a and SH-SY5Y cells were grown in T75 tissue culture flasks and induced to differentiate as described in section 2.2.1. Following the treatments, cells were washed twice with ice cold PBS and then lysed with 500 µl of ice cold-lysis buffer (50 mM Tris-HCl pH 8.0, containing 0.5% (w/v) sodium deoxycholate, 0.1% (v/v) protease inhibitor cocktail and 1% (v/v) phosphatase inhibitor cocktails 2 and 3). The cells were incubated in the lysis buffer on ice for 30 min, scraped and clarified by centrifugation at 4°C for 10 min at 14000 x g. The supernatant was collected and stored at -80°C until assayed for TG transamidase activity. Protein levels were determined by BCA protein assay (section 2.2.3). Transglutaminase activity was subsequently monitored by two different transamidase assays; amine incorporation and peptide cross-linking.

Biotin-labeled cadaverine incorporation assay

The amine incorporating activity of TG2 was measured via biotin-cadaverine incorporation into N, N'-dimethylcasein. The assay was performed as per the method described by Slaughter et al. (1992) with the modifications of Lilley et al. (1998). Briefly, 96-well microtitre plates were coated overnight at 4°C with 250 µl of N′,N′-dimethylcasein (10 mg ml-1 in 100 mM Tris-HCl, pH 8.0). The plate was washed twice with distilled water and blocked with 250 µl of 3% (w/v) BSA in 100 mM Tris-HCl, pH 8.0 and incubated for 1 h at room temperature with gentle agitation. The plate was washed twice with distilled water before the application of 150 µl of either 6.67 mM calcium chloride (required for enzyme activity) or 13.3 mM EDTA (used to detect background TG activity) assay buffer containing 225 µM biotin cadaverine (a widely used substrate to monitor TG amine incorporating activity) and 2 mM 2-mercaptoethanol. The reaction was started by the addition of 50 µl of samples or positive control (50 ng/well of guinea-pig liver TG2) and negative control (100 mM Tris-HCl, pH 8.0). After incubation for 1 h at 37°C, plates were washed as before. Then, 200 µl of 100 mM Tris-HCl pH 8.0 containing 1% (w/v) BSA and ExtrAvidin®-HRP (1:5000 dilution) were added to each well and the plate incubated at 37°C for 45 min then washed as before. The plate was developed with 200 µl of freshly made developing buffer (7.5 µg ml-1 3,3',5,5'-tetramethylbenzidine (TMB) and 0.0005% (v/v) $H2O_2$ in 100 mM sodium acetate buffer, pH 6.0) and incubated at room temperature for 15 min. The reaction was terminated by adding 50 µl of 5 M sulphuric acid and

the absorbance read at 450 nm. One unit of transglutaminase activity was defined as a change in absorbance at 450nm/1 h.

Biotin-labeled peptide cross-linking assay

The crosslinking activity of TG2 was measured via biotin-TVQQEL peptide incorporation into casein as described by Trigwell et al., (2004) with minor modifications. The 96-well microtitre plates were coated and incubated overnight at 4°C with casein at 1.0 mg ml^{-1} in 100 mM Tris-HCl pH 8.0 (250 µl per well). The wells were washed twice with distilled water, before being blocked with 250 µl of 3% (w/v) BSA in 100 mM Tris-HCl, pH 8.0 and incubated for 1 h at room temperature with gentle agitation. The plate was washed twice with distilled water before the application of 150 µl of either 6.67 mM calcium chloride and or 13.3 mM EDTA assay buffer containing 5 µM biotin-TVQQEL and 2 mM 2-mercaptoethanol. The reaction was started by the addition of 50 µl of samples or positive control (50 ng/well of guinea-pig liver TG2) and negative control (100 mM Tris-HCl, pH 8.0) and allowed to proceed for 1 h at 37°C. Reaction development and termination were performed as described for biotin-cadaverine assays. One unit of TG2 activity was defined as a change in absorbance at 450nm/1 h.

2.2.5 Visualisation of *in situ* TG2 transamidase activity

N2a (15,000 cells/well) and SH-SY5Y (30,000 cells/well) cells were seeded on 8-well chamber slides and induced to differentiate as described in section 2.2.1. The the medium was then removed, and slides incubated for 6 h with 1 mM biotin-X-cadaverine (a cell permeable TG2 substrate; Perry et al., 1995) in serum-free DMEM before experimentation. Then cells were treated as required, washed three times (five min per wash) with PBS, fixed with 3.7 % (w/v) paraformaldehyde and permeabilised with 0.1% (v/v) Triton-X100, both in PBS for 15 min at room temperature. After washing, cells were blocked with 3% (w/v) BSA in PBS for 1 h at room temperature. The transglutaminase mediated biotin-X-cadaverine labeled protein substrates were detected by FITC-conjugated ExtrAvidin® (Sigma-Aldrich) (1:200 v/v) in blocking buffer. The slides were incubated overnight at 4°C. The next day, cells were washed as before and nuclei counter-stained using DAPI in Vectashield mounting medium. The slides were sealed with coverslips and secured with clear nail varnish and stored at 4°C until required. Images were acquired using a Leica TCS SP5 II confocal microscope (Leica Microsystems, GmbH, Manheim, Germany) equipped with a 20x air objective. Optical sections were typically 1–2 µm; the highest fluorescence intensity values were acquired and fluorescence intensity

relative to DAPI stain was quantified for each field of view. Image analysis and quantification were carried out using Leica LAS AF software from five fields of view per culture well.

2.2.6 Visualisation of neuronal markers

N2a (15,000 cells/well) and SH-SY5Y (30,000 cells/well) cells were seeded on 8-well chamber slides and induced to differentiate as described in section 2.2.1. The medium was then removed, and the cells washed three times (five min per wash) with PBS, fixed with 3.7 % (w/v) paraformaldehyde for 15 min at room temperature then washed three times with 300 µl/well of ice cold PBS (2 min/rinse). Then cells were permeabilised with 0.05% (v/v) Triton-X100 in PBS, for 15 min at room temperature. Following three further rinses with PBS, non-specific binding was prevented by blocking the fixed cells with 500 µl of BSA/PBS per well for 1 h at room temperature. Then, cells were incubated overnight at 4ºC with rabbit anti-choline acetyltransferase antibody or mouse anti-tyrosine hydroxylase antibody all diluted 1:200 in 3% (w/v) BSA/PBS. Unbound primary antibody was then removed, and the cells washed three times for 5 min with PBS. Cells were then incubated for 2 h at room temperature with either goat anti-mouse or anti-rabbit FITC-conjugated immunoglobulin G (Abcam, Cambridge, UK) diluted 1:1000 in 3% (w/v) BSA/PBS. The chamber slide was subsequently washed three times for 5 min with PBS, air-dried and mounted with Vectashield® mountant (Vector Laboratories Ltd, Peterborough, UK) containing DAPI counterstain for nuclei visualisation. Finally, slides were sealed using clear, colourless nail varnish and stained cells visualised using a Leica TCS SP5 II confocal microscope (Leica Microsystems, GmbH, Manheim, Germany) equipped with a 20x air objective. Optical sections were typically 1-2 µm; the highest fluorescence intensity values were acquired and fluorescence intensity relative to DAPI stain was quantified for each field of view. Image analysis and quantification were carried out using Leica LAS AF software.

2.2.7 cAMP accumulation assay

N2a (5,000 cells/well) and SH-SY5Y (10,000 cells/well) cells were plated in 96-well microtitre plates, with clear bottomed wells (Corning; Fisher Scientific, Loughborough, UK) and induced to differentiate as described in section 2.2.1. The medium was then removed, and the cell monolayer treated with the neurotrophic (100nM PACAP-27) in serum-free DMEM (50 µl/well) in the presence of 20 mM $MgCl_2$ and 500 µM 3-isobutyl-1-methylxanthine (IBMX). Following stimulation, cAMP levels within cells were determined using the cAMPGlo™ Max Assay kit (Promega; Southampton, UK). Briefly, following cell treatment, 10 µl of cAMP

detection solution were added to all wells and incubated for 20 min at room temperature. After incubation, Kinase- Glo® reagent (50 µl/well) was added and incubated for 10 min at room temperature, following which luminescence levels across the plate were recorded using a plate-reading FLUOstar Optima luminometer (BMG Labtech Ltd, UK,). Treatment with forskolin (10 µM) was used as a positive control and the luminescence values were converted to cAMP levels using a cAMP standard curve (0-100 nM), according to the manufacturer's instructions.

2.2.8 Measurement of intracellular calcium

N2a (25,000 cells/well) and SH-SY5Y (50,000 cells/well) cells were plated in 24-well flat-bottomed plates and induced to differentiate as described in section 2.2.1. Cells were loaded with Fluo-8 AM; a cell-permeable medium affinity green fluorescent calcium binding dye, diluted 1:2000 in imaging buffer (134 mM NaCl, 6 mM KCl, 1.3 mM $CaCl_2$, 1 mM $MgCl_2$, 10 mM HEPES, and 10 mM glucose; pH 7.4) for 30 min before mounting on the stage of a Leica TCS SP5 II confocal microscope (Leica Microsystems, GmbH, Manheim, Germany) equipped with a 20x air objective. Cells were incubated at 37°C using a temperature controller and micro incubator (The Cube, Life Imaging Services, Basel, Switzerland) in the presence of imaging buffer (134 mM NaCl, 6 mM KCl, 1.3 mM $CaCl_2$, 1 mM $MgCl_2$, 10 mM HEPES, and 10 mM glucose; pH 7.4). Using an excitation wavelength of 490 nm, emissions over 514 nm were recorded. Images were collected every 1.7 s for 10 min. Increases in intracellular Ca^{2+} were defined as F/F_0 where F was the fluorescence at any given time, and F_0 was the initial basal level of fluorescence.

2.2.9 One dimensional polyacrylamide gel electrophoresis (SDS- PAGE) and Western blotting

To examine the activation or the expression of the proteins of interest, SDS- PAGE and Western blotting were employed.

Preparation of cell lysates for SDS-PAGE and Western blot analysis

N2a and SH-SY5Y cells were grown in T75 tissue culture flasks and induced to differentiate as described in section 2.2.1. Following the treatments, serum free medium was carefully removed, and cells washed twice with PBS (room temperature). Cell monolayers were then subjected to 500 µl of boiling sodium dodecyl sulphate buffer (0.5% w/v SDS in Tris buffered saline) after

which cells were removed by a scraper from the flask surface and collected in 1.5 ml Eppendorf™ tubes, boiled for 10 min and then allowed to cool to room temperature for 10-15 min. The lysates were stored at -20°C until use. The amount of protein presentin each sample was then estimated by BCA assay (section 2.2.3).

Sodium Dodecyl Sulphate-Polyacrylamide Gel Electrophoresis (SDS-PAGE)

Once the protein concentration of the samples was determined, the desired amount of protein was diluted in a 3:1 ratio with 4x reducing Laemmli buffer (8 % w/v SDS, 40 % (v/v) glycerol, 10 % (v/v) β-mercaptoethanol, 0.01 % (w/v) bromophenol blue, 250 mM Tris- HCl pH 6.8; Laemmli, (1970)) and boiled for 10 min at 95°C to denature the proteins. Based on the molecular weight of the investigated proteins, a 10% (w/v) acrylamide resolving gel was prepared for all experiments. The gels were prepared according to manufacturer's instructions (Geneflow Ltd, Staffordshire, UK). The resolving gel is also called separating gel, which separates the proteins by size. A Bio-Rad mini-PROTEAN III™ electrophoresis chamber was used. Two glass plates with combs and spacers of 1.5 mm thickness were used. The 10% (w/v) acrylamide resolving gel mixture was prepared according to the required number of gels, as indicated in Table 2.5. Acrylamide polymerisation was initiated by the addition of the volumes indicated of 10 % (w/v) APS (Ammonium persulfate in deionised water) and TEMED (N,N,N',N'-tetramethylethylenediamine), after which the mixture was swirled gently. For each gel, about 8 ml of resolving gel mixture was transferred into the glass cast to allow sufficient space for a stacking gel to be added later. Distilled water was carefully overlaid on the top layer of the freshly poured gel mixture to create a smooth interface and prevent any gel shrinkage. The gel mix was allowed to polymerise at room temperature for approximately 30 to 40 min. Once the resolving gel had polymerised, water was removed, the required amount of 4% (w/v) polyacrylamide stacking gel was prepared and polymerised by the adding of 10% APS and TEMED as indicated in Table 2.5. The stacking gel is used because it allows proteins entry and accumulation at its interface with the resolving gel. Immediately after the stacking gel was poured, a plastic comb was placed to form the sample wells. Following polymerisation, the gels were placed in the electrophoretic tank to which electrophoresis buffer (0.01 % (w/v) SDS, 2.5 mM Tris, 19.2 mM glycine, pH 8.3) was added. The protein samples (15-20 µg/well) were loaded along with 5 µl of protein ladder (BioRad, Hemel Hempstead, UK, 1610374). Electrophoresis was conducted at 120 V through the stacking gel and then at 160 V through the resolving gel.

Table 2.5 Preparation of SDS-PAGE gels

Reagent	Volume (for 2 gels)	
	10% (w/v) acrylamide resolving gel	4% (w/v) acrylamide stacking gel
30% (w/v) acrylamide: bisacrylamide (37.5:1)	6.66 ml	1.3 ml
Protogel® Resolving buffer (1.5 M Tris-HCl buffer pH 8.8, 0.4% (w/v) SDS)	5 ml	-
Protogel® stacking buffer (0.5 M Tris-HCl buffer pH 6.8, 0.4% (w/v) SDS)	-	2.5 ml
deionised water	8.12 ml	6.1
10 % (w/v) Ammonium persulfate (APS) solution	200 µl	50 µl
TEMED	20 µl	10 µl

Western blotting

Proteins were transferred to nitrocellulose membranes in a Bio-Rad Trans-Blot system. A set up of a wet transfer was performed, with the blotting cassettes set up as follows; pre-wet sponge - filter paper - gel- nitrocellulose membrane filter - filter paper – pre-wet sponge. The layers were then placed into a Western blotting cassette and closed gently to avoid air bubbles and placed in the transfer tank that contained chilled transfer buffer (25 mM Tris, 192 mM glycine pH 8.3 and 20% (v/v) MeOH). Proteins were transferred at 100 V for 1 h. After electrotransfer of the proteins, the nitrocellulose membrane was stained by Ponceau red stain (Sigma-Aldrich Co Ltd, Gillingham, UK) to confirm protein transfer from the gel. The membranes were washed with Tris-buffered saline (TBS) then blocked for 1 h at room temperature with 3% (w/v) skimmed milk powder in TBS containing 0.1% (v/v) Tween-20 with mild agitation. Blocking is essential to prevent non-specific binding of the antibodies to the membrane in subsequent steps. Blots were then incubated overnight with gentle agitation at 4°C in blocking buffer containing one of the following primary antibodies (1:1000 unless otherwise stated): Phospho-specific ERK1/2, phospho-specific JNK (1:500), phospho-specific p38 MAPK (1:500), phospho-specific PKB (1:500), cleaved active caspase-3 (1:200), Glyceraldehyde 3-phosphate dehydrogenase (GAPDH), TG1, TG2, TG3, anti-phosphoserine or anti-phosphothreonine (Table 2.2). After incubation, the primary antibodies were removed, and blots washed three times for 5 min in TBS/Tween 20. After washing, blots were probed with the appropriate (1:1000) horseradish peroxidase (HRP)-conjugated secondary antibodies (New England Biolabs Ltd; Hitchin, UK) for 2 h at room temperature in blocking buffer (Table 2.3). Following

removal of the secondary antibody, blots were extensively washed as above and developed using the Enhanced Chemiluminescence Detection System (Uptima, Interchim, France). Images of the blots were captured by the LAS 4000 system and the bands were quantified by densitometry using Advanced Image Data Analysis software (AIDA) (Fuji; version 3.52). All band densities were measured and corrected for background, then normalised to band densities for internal control. Data are expressed as a percentage of the average value of the peak area compared to its corresponding control ± SEM. To confirm uniform protein loading in the gel primary antibodies specific to GAPDH were used.

2.2.10 Immunoprecipitation analysis of TG2 phosphorylation

Immunoprecipitation (IP) was used to monitor the phosphorylation status of TG2 under different conditions.

Preparation of cell lysates

Briefly, N2a and SH-SY5Y cells were grown in T175 tissue culture flasks and induced to differentiate as described in section 2.2.1. Following treatments, cells were washed twice with ice cold PBS. The cells were then scraped, collected in 5 ml of PBS and subjected to centrifugation at 300 x g at room temperature for 5 min. Cells were then washed by suspending the cell pellet in PBS followed by centrifugation at 300 x g at room temperature for 5 min to pellet cells. The supernatant was discarded and the cell pellet resuspended in 500 µl of ice cold lysis buffer (2 mM EDTA, 1.5 mM $MgCl_2$, 10% (v/v) glycerol, 0.5% (v/v) IGEPAL, 0.1% (v/v) protease inhibitor cocktail (AEBSF–[4-(2-aminoethyl) benzenesulfonyl fluoride hydrochloride], aprotinin, bestatin hydrochloride, E-64 – [N-(trans-epoxysuccinyl)-L leucine 4-guanidinobutylamide], leupeptin hemisulfate salt, pepstatin A), and 1% (v/v) phosphatase inhibitor cocktail 2 (sodium orthovanadate, sodium molybdate, sodium tartrate and imidiazole) and 3 (cantharidin, (–)-p-bromolevamisole oxalate, calyculin A). The cells were incubated with lysis buffer for 30 min and then clarified by centrifugation at 4°C for 10 min at 14000 x g. The supernatant was collected and transferred to a new Eppendorf tube for protein estimation and further analysis.

Preparation of the Immune complex

A total of 500 µg of protein (cell lysate) was incubated overnight at 4°C with 2 µg of anti-TG2 monoclonal antibody (CUB 7402) or non-specific IgG using an Eppendorf tube revolver.

Precipitation of the Immune complex

Immune complexes were precipitated using a Pierce™ Classic Magnetic IP/Co-IP kit (Thermo Scientific, Loughborough, UK). The eluted proteins were resolved by SDS-PAGE in a 10 % polyacrylamide gel and levels of TG2 bound phosphoserine and phosphothreonine assessed via Western blotting using anti-phosphoserine or anti-phosphothreonine antibodies. The blots were developed using the ECL detection system and quantified by densitometry, as described in section 2.2.6.

2.2.11 Assessing the protection against hypoxia

Stimulation of hypoxia

Differentiating N2a and SH-SY5Y cells in glucose-free and serum-free DMEM (Gibco™, Life Technologies Ltd, Paisley, UK) were exposed to 8 h hypoxia (except for time interval experiments) using a hypoxic incubator (5% CO_2/1% O_2 at 37°C) in which O_2 was replaced by N_2. Normoxic incubation of cells at similar passage numbers were used as controls. Cells were treated as required in serum-free DMEM prior to it being replaced with glucose-free and serum-free DMEM for the hypoxic/normoxic incubation.

Cell viability assessment

1. *MTT reduction assay*

Cell viability was determined by measuring the activity of cellular dehydrogenases via MTT (3-(4,5-dimethylthiazol-2-yl)-2,5 diphenyltetrazolium bromide) reduction assay (Mosmann, 1983). MTT is a tetrazolium dye that is converted to water-insoluble purple formazan on the reductive cleavage of its tetrazolium ring by the respiratory enzyme succinate dehydrogenase in active mitochondria and by other cellular dehydrogenases. The assay was used to assess cell viability after exposure to hypoxia under different pharmacological treatments. N2a (25,000 cells/well) and SH-SY5Y (50,000 cells/well) cells were plated in 24-well flat-bottomed plates and induced to differentiate as described in section 2.2.1 Cells were exposed to hypoxia and required treatment and cell viability subsequently determined by incubating with 0.5 mg/ml MTT at 37 °C for 1 h prior to completion of periods of hypoxia. After completion of this final hour, the medium in each well was carefully aspirated, and replaced with 500 µl of DMSO. The plate was then gently agitated to ensure sufficient dissolution of the water-insoluble purple formazan crystals. After that, 200 µl of the resultant solution was transferred into a 96-well plate

and the absorbance of the solutions was read at 570 nm using a standard 96-well plate reader. The absorbance of the blank (DMSO) was subtracted from each sample absorbance reading and the viability of the cells is directly proportional to the basal MTT reduction, which determined by the absorbance of the solubilized formazan product at 570 nm.

2. *Lactate dehydrogenase (LDH) assay*

Cytotoxicity induced by hypoxia was also assessed by lactate dehydrogenase (LDH) release into the culture medium. The LDH assay was performed according to the manufacturer's instructions using a CytoTox 96® non-radioactive cytotoxic assay kit (Promega, Southampton, UK). The assay is a colorimetric assay based on the measurement of LDH release from damaged tissue that catalyses the conversion of lactate to pyruvate via reduction of NAD^+ to NADH. Then, the dehydrogenase enzyme diaphorase (present in the substrate mix in the kit) coupled with NADH results in the formation of a red formazan product tetrazolium salt (INT). Thus, the amount of LDH released is proportional to the red formazan product. N2a (5,000 cells/well) and SH-SY5Y (10,000 cells/well) cells were plated in 96-well flat-bottomed plates and induced to differentiate as described in section 2.2.1 Following exposure to hypoxia and required treatment, the plate was centrifuged (5 min, 300 x g) to allow cellular debris to be compacted to the bottom of the wells. A volume of 50 µl of the supernatant was then transferred to a new non-sterile 96 well plate and 50 µl of the reconstituted assay buffer (10 ml assay buffer added to one bottle of substrate mix, in kit) added to each sample well. The plate was then covered with foil and incubated at room temperature for 30 min using a mixer shaker. After that, a volume of 50 µl of assay stop solution (1 M acetic acid) was added to stop the reaction. The change in absorbance was monitored at 490 nm using a standard plate reader.

3. *Caspase-3 activation*

N2a and SH-SY5Y cells were grown in T75 tissue culture flasks and induced to differentiate as described in section 2.2.1. Where appropriate, treatments were performed in the respective medium, which was replaced with glucose-free and serum-free DMEM for the 8 h incubation under hypoxic conditions. Following incubations, cells were lysed and subjected to Western blotting to detect cleaved caspase-3 (Section 2.2.9).

2.2.12 High-throughput analysis

The role of TG2 in neurite outgrowth involving PACAP and NGF in N2a and SH-SY5Y cells was further determined using the ImageXpress Micro Widefield High Content Analysis System (Molecular Devices, Wokingham, UK). This technique permits rapid assessment of the effects of a wide range of pharmacological treatments at different concentrations on multiple parameters of neurite outgrowth. The screening system integrates an inverted epifluorescence microscope combined with automated image acquisition and analysis software to quantify different subcellular measurements of neurite outgrowth such as cell count, neurite count, neurite length and cell body area (Smith and Eisenstein, 2005).

Briefly, cells were seeded on 8-well Ibidi µ-slides: 15,000 cells/well for N2a and 30,000 cells/well for SH-SY5Y and cultured for 24 h in fully supplemented DMEM. Where appropriate, cells were treated for 1 h with TG2 inhibitors Z-DON (150 µM) or R283 (200 µM) or for 30 min with the PAC_1 receptor antagonist PACAP 6-38 (100nM). The medium containing the previous treatment was removed and replaced with fresh medium before the addition of either 100 nM PACAP-27 or 100 ng/ml NGF for 48 h. Following stimulation, cells were fixed with 3.7 % (w/v) paraformaldehyde for 15 min at room temperature then washed three times with 300 µl/well of ice cold PBS (2 min/rinse). Then cells were permeabilised with 0.05% (v/v) Triton-X100 in PBS, for 15 min at room temperature. After three further rinses with PBS, cells were blocked with 3% (w/v) BSA in PBS for 1 h at room temperature. Cells were then stained overnight at 4˚C with monoclonal primary antibodies to total α-tubulin (B512) diluted 1:1000 in BSA/PBS after which primary antibody was removed and the monolayers washed 3 times for 2 min with TBS. This was followed by incubation with Alexa Fluor®488 goat anti-mouse IgG labelled secondary antibody diluted 1:500 in BSA/PBS for 2 h at room temperature. The slides were subsequently washed three times for 5 min with PBS and incubated for 1 min with Vectashield® mountant (Vector Laboratories Ltd, Peterborough, UK) containing DAPI counterstain for nuclei visualisation. Slides were preserved in PBS containing 0.01% (w/v) sodium azide as a preservative and stored at 4˚C prior to image acquisition and analysis. Neurite outgrowth was monitored using an ImageXpress® Micro Widefield High Content Screening (HCS) System (Molecular Devices, Wokingham, UK). Fluorescence images were acquired using a 10× objective lens in order to acquire all neurites in one field of view, thus enabling more reliable analysis of neurite outgrowth. The acquired images were then segmented by multi-coloured tracing masks on neurites and cell bodies. Segmentation masks were generated using the MetaXpress imaging and analysis software (version 5.1.0.46; Molecular devices, USA),

where each neurite segment is given the same coloured mask as that of their parent neuronal cell bodies. The segmentation images were then analysed by the neurite outgrowth module integrated within the MetaXpress imaging and analysis software, to measure a number of morphological parameters including average number of cells/field, average cell body area/cell, neurite length/cell, mean processes/cell, mean branches/cell, percentage of cells with significant outgrowth and average intensity of staining within the positive cells. Particles from each image were identified as cells if valid nuclei width between 5 to 10 μm had been detected and cell body width ranged from 15 to 20 μm. Outgrowth was recorded as significant when minimum cell outgrowth was more than 10 μm (approximately half a cell body diameter in length). Analysis was performed on a total of four fields and at least 200 cells per well from four independent experiments.

2.2.13 Statistical analysis

All graphs and statistics (one-way ANOVA followed by Dunnet's multiple comparison test and two-way ANOVA for group comparison) were performed using GraphPad Prism® software (GraphPad Software, Inc., USA). All sets of data were based on a minimum of four separate experiments and expressed as mean ± standard error of the mean (SEM) and p values <0.05 were considered statistically significant.

Chapter 3

3 Characterisation of N2a and SH-SY5Y neuroblastoma cells

3.1 Introduction

The mouse N2a and human SH-SY5Y neuroblastoma cell lines have been widely used as a suitable *in vitro* model to study cell signalling pathways, differentiation, neurite outgrowth and molecular mechanisms associated with neuronal apoptosis (Li et al., 2007; Kim et al., 2011; Sahu et al., 2013; Murillo et al., 2017; Pirou et al. 2017). N2a and SH-SY5Y cells can be induced to differentiate and develop into a more mature neuron-like phenotype following serum withdrawal and retinoic acid (RA) treatment (Pahlman et al., 1984; Mao et al., 2000; Sajithlal et al., 2002; Korecka et al., 2013). Differentiating N2a and SH-SY5Y cells were chosen as model systems in this study for assessing the possible molecular intervention of TG2 in neurotrophic factor-induced neurite outgrowth and cell survival function.

N2a mouse neuroblastoma cells have a rapid and reproducible potential to differentiate within a few hours of serum withdrawal (Evangelopoulos et al., 2005). However, effects may be observed that could be unique to the species due to lack of a human component, genetic drift or clonal/species-related effects. Therefore, it is essential to use a more homogenous, consistent model of human neurological system to avoid these variations. To validate this research observations were also made in a human-species-related cell model, namely human SH-SY5Y neuroblastoma cells. SH-SY5Y cells were derived from a neuroblastoma patient's bone marrow biopsy, and the cell line can be induced to differentiate into neuronal like phenotypes (Biedler et al., 1973). Differentiating SH-SY5Y cells have been widely used as a model for *in vitro* experiments requiring neuron-like cells (Ross et al., 1983).

It is critical to ensure that the *in vitro* neuronal system used properly differentiates into neurons to generate data that represent the best possible approximation of what could happen in neurons *in vivo*. Several mechanisms exist for inducing cultured neuronal cells to differentiate *in vitro*; RA treatment is the most widespread, successful technique (Mao et al., 2000; Shipley et al.,

2016). Inducing cells to differentiate using RA involves several processes, including the formation and extension of axonal processes and expression of neuron-specific enzymes (Adem et al., 1987; Mao et al., 2000; Tremblay et al., 2010). Furthermore, RA can drive N2a and SH-SY5Y cells toward various mature neuronal phenotypes involving cholinergic, adrenergic and dopaminergic neurons (Zimmermann et al., 2004; Cheung et al., 2009; Lopes et al., 2010; Tremblay et al., 2010; Korecka et al., 2013). The specific neuronal phenotype induced in response to RA treatment in N2a and SH-SY5Y cells is still unclear. Thus, it was essential to characterise the molecular phenotype of differentiating N2a and SH-SY5Y cells as an initial step in this research.

The first aim of the work in this chapter was to define the RA-induced differentiation of N2a and SH-SY5Y cells morphologically and biochemically. Prior to investigating the possible modulation of TG2 activity by the neurotrophic factors PACAP and NGF, it was also important to examine whether TG2 and other neuronally expressed TG isoforms (TG1 and TG3) were expressed in RA-induced differentiating N2a and SH-SY5Y cells.

3.2 Results

3.2.1 Morphological characterisation of N2a and SH-SY5Y cells

N2a and SH-SY5Y neuroblastoma cells were induced to differentiate into a more neuron-like phenotype by treatment with 1 µM and 10 µM RA, respectively, as described in section 2.2.1. After the required period of differentiation, the cells were stained with Coomassie Brilliant Blue, and cell morphology was assessed microscopically (section 2.2.1). As shown in Figure 3.1, after 24 h under normal culture conditions, mitotic N2a cells grew as round neuroblasts. N2a cells responded to serum withdrawal and RA treatment (48 h). As shown in Figure 3.1B, the differentiating N2a cells underwent morphological changes by developing axon-like processes and dendrites. Undifferentiated SH-SY5Y cells were characterised by elongated cell bodies and short neurite-like processes, as shown in Figure 3.2. In contrast, differentiating SH-SY5Y cells treated with 10 µM RA displayed extended long, branched processes (Figure 3.2). These changes in the morphological parameters of mouse and human neuroblastoma cells treated with RA combined with serum deprivation all suggest the differentiation into a neuron-like phenotype in both cell lines.

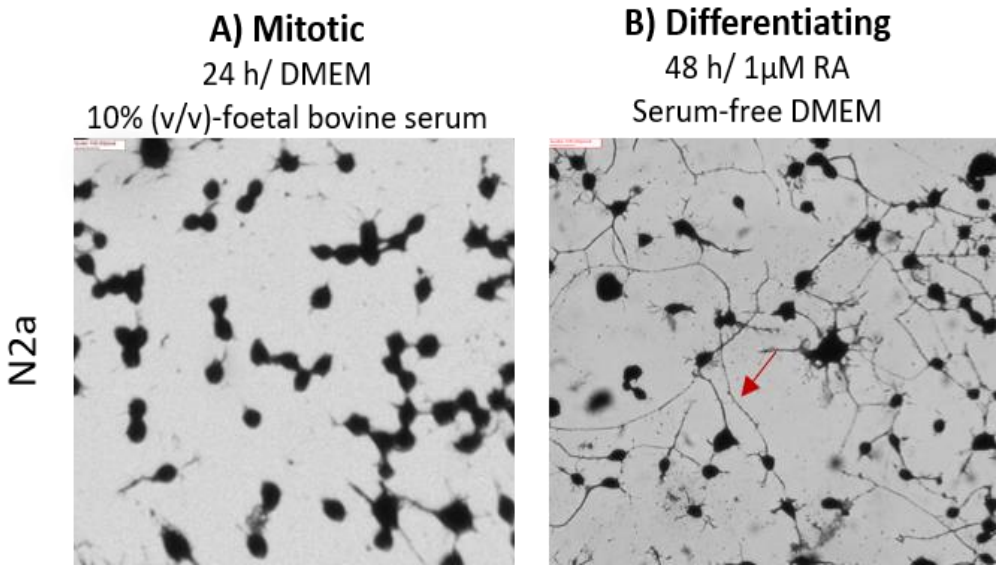

Figure 3.1 Light microscopy examination of morphological differentiation of N2a cells.

Images represent cellular morphologies viewed with the aid of an inverted light microscope. A) Mitotic N2a cells (24 h/DMEM 10% (v/v)-foetal bovine serum) grow as round neuroblasts. B) Differentiating N2a cells (48 h/1 µM RA serum-free DMEM) exhibit neurite extensions (red arrow). Images were visualised using a 20× objective lens. Scale bar = 100 µm.

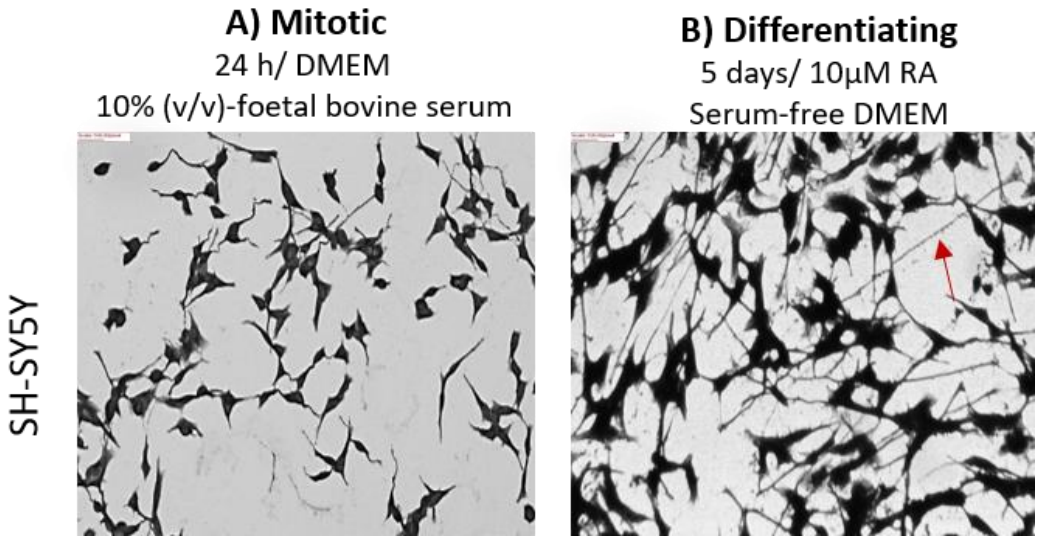

Figure 3.2 Light microscopy examination of morphological differentiation of SH-SY5Y cells.

Images represent cellular morphologies viewed with the aid of an inverted light microscope. A) Mitotic SH-SY5Y cells (24 h/DMEM 10% (v/v) foetal bovine serum) show short branched processes. B) Differentiating SH-SY5Y cells (5 days/10 μM RA serum-free DMEM) display neurite extensions (arrow). Images were visualised using a 20× objective lens. Scale bar = 100 μm

3.2.2 Characterisation of the neuronal phenotypes of N2a and SH-SY5Y cells

A substantial body of evidence indicates that the use of different methods to induce N2a and SH-SY5Y cell differentiation can select for specific neurotransmitter phenotypes, such as dopaminergic and cholinergic neurons (Pahlman et al., 1984; Xie et al., 2010). Thus, the characterisation of the specific neuronal phenotype induced on the induction of differentiation of N2a and SH-SY5Y by using RA should be considered when using these cells for *in vitro* studies. After exhibiting successful differentiation by RA into a more mature neuron-like morphological phenotype in the previous section, the next aim was to investigate RA's effect on the specific neuronal phenotype markers, namely tyrosine hydroxylase (TH) for the dopaminergic and choline acetyl transferase (ChAT) for the cholinergic neuronal marker. Changes in the protein expression levels of these neuronal markers in mitotic and RA-differentiating N2a and SH-SY5Y were assessed by Western-blot analysis. As shown in Figure 3.3, the quantitative values showed a significant increase in the expression of the cholinergic neuronal marker ChAT in RA-differentiating N2a cells and the dopaminergic neuronal marker TH in differentiating SH-SY5Y cells compared with the mitotic cells. The data were confirmed by immunocytochemistry, whereby the changes in the fluorescence intensity of ChAT and TH were compared between mitotic and RA-differentiating N2a and SH-SY5Y cells, as shown in Figure 3.4. The observations illustrated a significant increase in the fluorescence intensity of ChAT in differentiating N2a cells and TH in differentiating SH-SY5Y cells compared with undifferentiated cells (Figure 3.4). These findings agree with the data revealed by Western blot analysis.

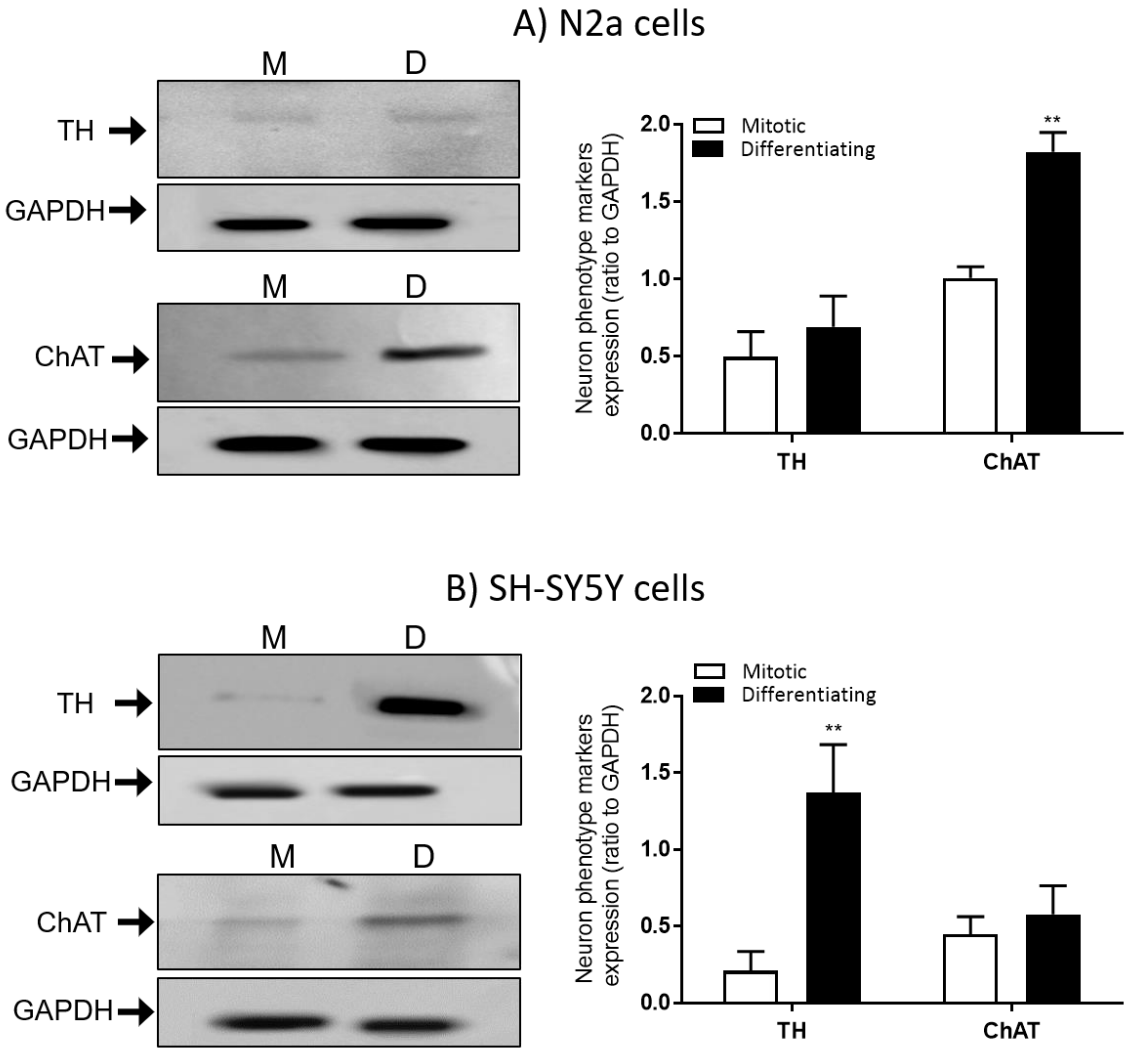

Figure 3.3 Expression of choline acetyltransferase and tyrosine hydroxylase in differentiating neuroblastoma cells.

A) N2a and **B)** SH-SY5Y cells were differentiated with retinoic acid in serum-free medium. Expression levels of cholinergic and dopaminergic neuronal protein biomarkers were assessed by Western blot analysis using anti-choline acetyltransferase (ChAT) antibody (cholinergic neuronal marker) and anti-tyrosine hydroxylase (TH) antibody (dopaminergic and noradrenergic neuronal marker). Cell lysates were also analysed on separate blots for GAPDH expression to confirm equal protein loading. Quantified data are expressed as the ratio of the TG isoform to GAPDH and represent the mean ± SEM from three independent experiments. $^{**}p < 0.01$ versus control (mitotic) cells.

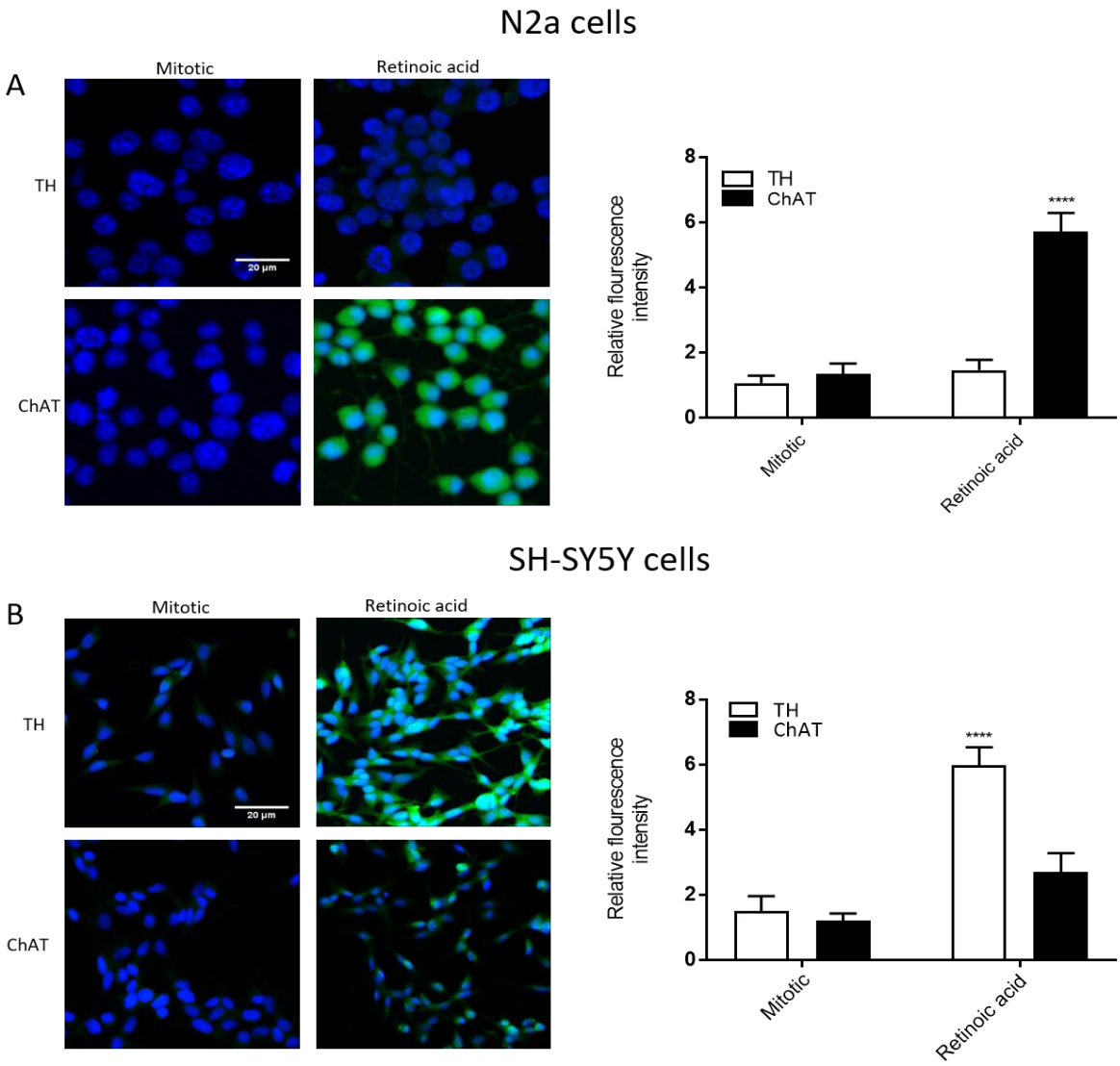

Figure 3.4 Immunocytochemical analysis of neuronal markers in differentiating neuroblastoma cells.

A) N2a and **B)** SH-SY5Y cells were induced to differentiate with retinoic acid in serum-free medium. Immunocytochemistry was performed via fluorescence microscopy using anti-choline acetyltransferase (ChAT) antibody (cholinergic neuronal marker; green) and anti-tyrosine hydroxylase (TH) antibody (dopaminergic and noradrenergic neuronal marker; green) and DAPI counterstain for visualisation of nuclei (blue). Images presented are from one experiment and are representative of three assays. Quantified immunocytochemistry data represent the mean ± SEM. of fluorescence intensity relative to DAPI stain for five fields of view each from three independent experiments. ****$p < 0.0001$ versus mitotic cells.

3.2.3 Characterisation of TG expression patterns in N2a and SH-SY5Y cells

To elucidate the expression patterns of the TG isoforms that are most susceptible to expression in neuronal cells (Kim et al., 1999; Condello et al., 2008), Western blot analysis was performed to compare the expression of TG isoforms in mitotic and RA-differentiating N2a and SH-SY5Y cells. TG1, TG2 and TG3 expression were detected in both mitotic and differentiating N2a cells (Figure 3.5). This suggests that not only TG2, but also TG1 and TG3 isoforms exist in differentiating N2a cells. In addition, the observations showed a significant increase in the expression of the three isoforms in N2a cells after RA-induced differentiation. In SH-SY5Y cells, Western blot analysis revealed that mitotic SH-SY5Y cells expressed comparable levels of TG1, TG2 and TG3, and only TG2 expression significantly increased following RA-induced differentiation (Figure 3.6).

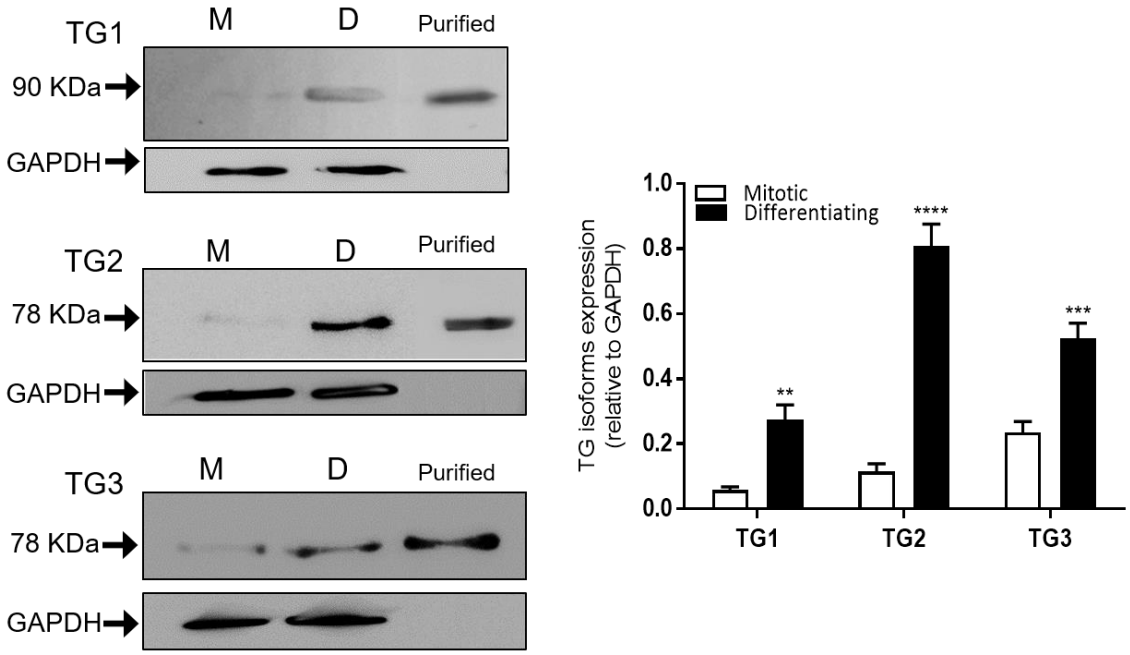

Figure 3.5 TG isoform expression in differentiating N2a neuroblastoma cells.

Protein expression of TG isoforms in mitotic and differentiating N2a cells. Cell lysates from mitotic (M) and differentiating (D) N2a cell lysates were analysed for TG1, TG2 and TG3 expression by Western blotting using TG isoform-specific antibodies. Cell lysates were also analysed on separate blots for GAPDH expression to confirm equal protein loading, and 0.1 ng from purified enzymes was used as positive control. Quantified data are expressed as the ratio of TG isoform to GAPDH and represent the mean ± SEM from three independent experiments. **$p < 0.01$, ***$p < 0.001$ and ****$p < 0.0001$ versus control (mitotic) cells.

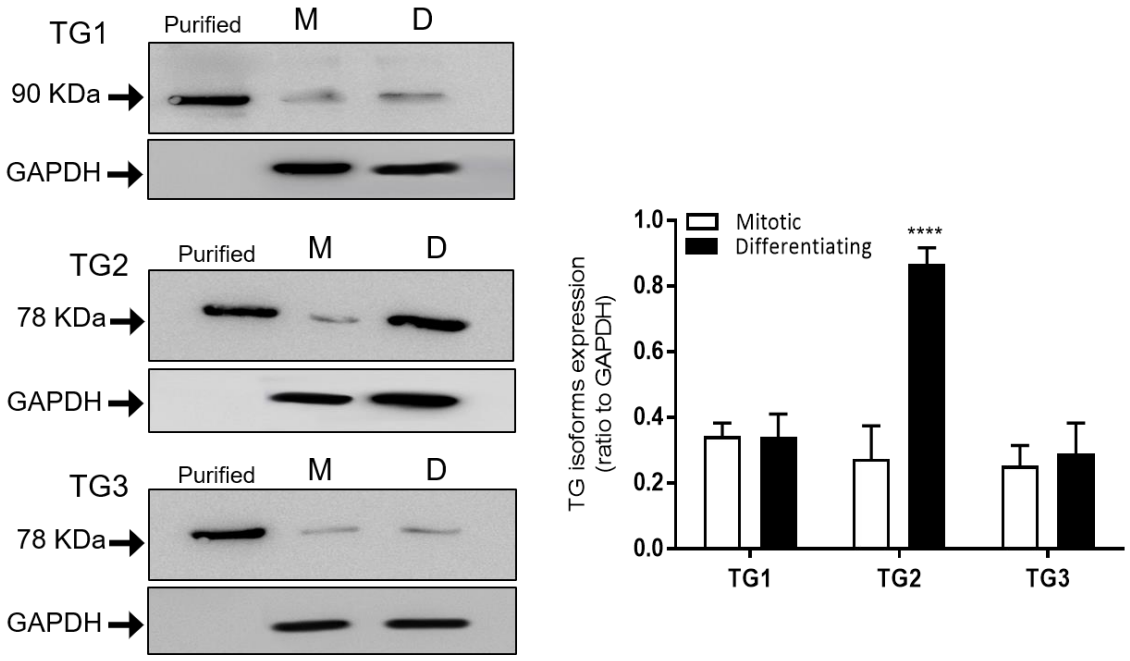

Figure 3.6 TG isoform expression in differentiating SH-SY5Y neuroblastoma cells.

Protein expression of TG isoforms in mitotic and differentiating N2a cell lysates from mitotic (M) and differentiating (D) SH-SY5Y cell lysates were analysed for TG1, TG2 and TG3 expression by Western blotting using TG isoform-specific antibodies. Cell lysates were also analysed on separate blots for GAPDH expression to confirm equal protein loading, and 0.1 ng from purified enzymes was used as positive control. Quantified data are expressed as the ratio of TG isoform to GAPDH and represent the mean ± SEM from three independent experiments. **$p < 0.01$, ***$p < 0.001$ and ****$p < 0.0001$ versus control (mitotic) cells.

3.3 Discussion

3.3.1 Assessment of the differentiating N2a- and SH-SY5Y neuron-like phenotype

N2a and SH-SY5Y neuroblastoma cells have been widely used in neuroscience research, and they are accepted as reliable models for neuronal cells in their differentiating form. In some cases, undifferentiated cells are used; however, the assessment is complicated because of cell replication and division during the experimental processing. Hence, the first part of this study aimed to characterise and validate the effect of the most widely used differentiation agent *all-trans* RA on cell morphology and neuronal markers. The current study showed the detailed characteristics of RA-differentiating N2a and SH-SY5Y cellular morphology, the immunocytochemistry and molecular expression of dopaminergic (e.g. TH) and cholinergic (e.g. ChAT) neuronal markers. The findings confirm that the N2a and SH-SY5Y neuroblastoma cells were induced to differentiate into well-established neuron-like phenotypes.

Mouse N2a and human SH-SY5Y neuroblastoma cells can be induced to differentiate by different methods, such as using dibutyryl cyclic AMP (Kuramoto et al., 1981; Kume et al., 2008; Tremblay et al., 2010) and *all-trans* RA (Pahlman et al., 1984; Manabe et al., 2005; Cheung et al., 2009). RA is an efficient differentiation factor; it was used in the current study to avoid potential problems with using dibutyryl cAMP when assessing functional responses mediated by the G_s-protein-coupled PAC_1 receptor. Morphologically, N2a cells exhibited considerable long extending axon-like processes induced by RA and fully visible neurite extension was observed in the SH-SY5Y cells. These findings suggest similar processes to those exhibited in earlier work, whereby RA enhanced the differentiation of N2a and SH-SY5Y neuroblastoma cells into well-established neuron-like cells (Encinas et al., 2000; Wu et al., 2009; Tremblay et al., 2010; Korecka et al., 2013).

Previous studies have suggested that differentiation of N2a cells into different neuronal phenotypes depends on the method used (Manabe et al., 2005; Tremblay et al., 2010). For example, serum withdrawal in the presence of RA induces differentiation into cholinergic neurons, whereas dibutyryl cAMP promotes the development of dopaminergic neurons (Manabe et al., 2005; Tremblay et al., 2010). In the current study, the immunocytochemical staining indicated that the expression of the cholinergic neuronal marker, choline acetyl-transferase (ChAT) increased markedly after 48 h, confirming that RA promotes differentiation of N2a cells into a cholinergic neuronal phenotype (Figure 3.4). Moreover, as shown in Figure

3.3, Western blot analysis demonstrated that differentiating N2a cells highly expressed ChAT protein and lacked expression of TH. These findings agree with many previous *in vitro* studies demonstrating that RA treatment enhances cholinergic characteristics in N2a cells (Berrard et al., 1993; Pedersen et al., 1995; Zeller and Strauss 1995; Hill and Robertson 1997; Kornyei et al., 1998; Malik et al., 2000; Personett et al., 2000; Chu et al., 2003).

The effects of the differentiation process induced by RA in SH-SY5Y cells were similarly investigated. Using RA to induce neuron-like differentiation in human neuroblastoma SH-SY5Y cells is a widely applied method (Kaplan et al., 1993; Kito et al., 1997); however, to date, there is no consensus in the profiling of the developed specific neuronal phenotype (Korecka et al., 2013). The observed increases in the immunocytochemical staining intensity and Western blot analysis of TH, together with the lack of a statistically significant effect on ChAT, revealed that RA induces differentiation of SH-SY5Y cells into the dopaminergic neuronal phenotype. These findings agree with a great majority of studies that aimed to characterise the neuronal phenotype of RA-differentiating SH-SY5Y. Tyrosine hydroxylase, the dopaminergic neuronal marker, has been previously demonstrated to be highly expressed in RA-differentiating SH-SY5Y cells, suggesting the development of a dopaminergic neuronal phenotype (Presgraves et al. 2004; Cheung et al. 2009). Although the current study and others confirm that RA induced this cell line to differentiate into a dopaminergic neuron-like phenotype (Lopes et al., 2010), some studies claim that in SH-SY5Y cells RA enhances the cholinergic-specific neuronal phenotype (Adem et al., 1987; Zimmermann et al., 2004).

3.3.2 Characterisation of TG expression patterns in differentiating neuroblastoma cells

The mouse and human differentiating neuroblastoma cell models employed in the current study are suitable for studying the molecular events associated with neuronal survival and neurite outgrowth (Li et al., 2007; Kim et al., 2011; Sahu et al., 2013; Pirou et al. 2017; Murillo et al. 2017). To assess the role of TG2 in the neurotrophic activity of PACAP and NGF, it was necessary as an initial step in this research to investigate which TG isoform(s) are expressed in the differentiating neuroblastoma cells. In the current study, the expression patterns of TG1, TG2 and TG3 – the transglutaminase members predominantly expressed in neuronal tissue (Kim et al. 1999; Condello et al. 2008) – were assessed. The presented findings confirmed the differential nature of TG1, TG2 and TG3 expression in neuroblastoma cells.

Previously, the presence of TG activity in the nervous system was reported (Thomázy & Fésüs, 1989; Reichelt & Poulsen, 1992; Facchiano et al., 1993; Johnson et al., 1997). Most of these activities were attributed to the TG2 isoform, since TG2 is the enzyme member of the transglutaminase family that has been identified as the most abundant isoform expressed in the adult human brain (Thomázy & Fésüs, 1989). Although TG2 is the most abundant isoform that has been identified in neuronal tissue, the differential expression of other transglutaminase isoforms, namely TG1 and TG3, has also been reported (Facchiano et al., 1993; Kim et al., 1999; Lesort et al. 2000; Condello et al., 2008). In the current study, Western blot analysis was performed to compare the expression of TG isoforms in mitotic and differentiating N2a cells. TG1, TG2 and TG3 expression increased significantly in N2a cells following differentiation for 48 h with *all-trans* RA (Figure 3.5). These observations are in agreement with those of previous studies (Condello et al., 2008; Currò et al., 2009). Furthermore, the findings revealed that mitotic SH-SY5Y cells expressed comparable levels of TG1, TG2 and TG3, but only TG2 expression significantly increased following RA-induced differentiation (Figure 3.6). Multiple studies have confirmed the expression of TG2 in SH-SY5Y cells (Tucholski et al., 2001; Singh et al., 2003; Joshi et al., 2006; Filiano et al., 2008); however, there is no evidence on relating TG1 and TG3 to this cell line.

In conclusion, the results presented in this chapter indicate that N2a and SH-SY5Y cells differentiate into cholinergic and dopaminergic neuronal phenotypes, respectively, following treatment with RA. Furthermore, data presented confirms the expression of the TG2 isoform in both cell lines and its increase on cell differentiation.

Chapter 4

4 Modulation of TG2 activity by PACAP in differentiating neuroblastoma cells

4.1 Introduction

Pituitary adenylate cyclase–activating polypeptide (PACAP) is a neurotrophic factor that has neuroprotective activity arising through activation of the pituitary adenylate cyclase type 1 receptor (PAC_1). This receptor belongs to the glucagon/ secretin family of GPCR. Previous studies have shown that the PAC_1 receptor is widely expressed in the brain (Vaudry et al., 2000; Jolivel et al., 2009) and modulates neurite outgrowth activity through signalling cascade initiated by PACAP (Deutsch and Sun, 1992; Kambe and Miyata 2012). In the central nervous system (CNS), activation of the PAC_1 receptor stimulates G_s and G_q proteins, leading to activation of adenylyl cyclase/cAMP/PKA and phospholipase C/DAG/PKC signalling pathways, respectively (Dickson & Finlayson, 2009; Vaudry et al., 2009). Moreover, PACAP has long been known to activate PKA, ERK1/2 and p38 MAPK signalling cascades, which contribute to its neuroprotective effect (Vaudry et al., 2009). However, very little is known about the specific signal transduction pathways that mediate this neuroprotective activity. It has been found previously that the multifunctional enzyme transglutaminase 2 (TG2) protects neuronal cells against cell death under ischaemia-like conditions (Filiano et al., 2008). Also, the activity of TG2 and other TG family members can be regulated by protein kinases. For example, it has been shown that protein kinases, such as PKA and PKC, regulate the activity of TG2 (Almami et al., 2014). Furthermore, phosphorylation of TG2 by protein kinase A (PKA) inhibits its transamidating activity but enhances its kinase activity (Mishra et al., 2007). The transamidating activity of TG1 (keratinocyte transglutaminase) is enhanced by phorbol ester-induced stimulation of PKC and ERK1/2 (Bollag et al., 2005). These findings suggest that the activity of TG can be regulated by signalling pathways associated with GPCRs. Indeed, examples include muscarinic receptor-mediated increases in TG2 activity in SH-SY5Y cells (Zhang et al.,

1998), 5-HT_{2A} receptor-mediated transamidation of Rac1 in the rat A1A1v cortical cell line (Dai et al., 2008) and β_2-adrenoceptor and A_1 adenosine receptor-mediated increases in TG2 transamidase activity in rat H9c2 cardiomyoblasts (Vyas et al., 2016; Vyas et al., 2017). However, the regulation of intracellular TG2 following stimulation of GPCRs is not well understood. Since some of these protein kinase pathways are associated with PACAP-induced signalling cascades (PKA, PKC and ERK1/2) it is conceivable that the PAC_1 receptor regulates TG activity. The majority of studies have focused on the regulation of TG by different protein kinases (Bollag et al., 2005; Mishra et al., 2007; Almami et al., 2014). However, little work has been done regarding molecular mechanisms implicit in this regulation.

Therefore, the aims of the current study were to investigate the modulation of TG2 by PACAP via the PAC_1 receptor and identify the possible signalling pathways involved using differentiated neuroblastoma cells. To achieve this aim, the effect of the highly selective PAC_1 receptor agonist PACAP-27 on modulation of TG2 activity was investigated using TG2 transamidase activity assays and immunofluorescence visualisation. Also, the possible molecular mechanisms underlying this modulation has been investigated by assessing the protein kinases involved.

4.2 Results

4.2.1 Functional expression of PAC_1 receptor in differentiating N2a and SH-SY5Y cells

The expression of PAC_1 receptor in N2a and SH-SY5Y cells has been previously investigated (Lelièvre et al., 1998; Monaghan, MacKenzie, Plevin, & Lutz, 2008). In this study the functional expression of the PAC_1 receptor was initially assessed and confirmed using a cAMP accumulation assay (section 2.2.8) and calcium imaging (section 2.2.9).

PAC_1 receptor mediated cAMP accumulation and calcium signalling

cAMP accumulation assays measuring cellular levels of cAMP are dependent on the activity of adenylyl cyclase, which is regulated by GPCRs coupled to $G\alpha_s$ or $G\alpha_{i/o}$ protein (Milligan & Kostenis, 2006). $G\alpha_s$ positively stimulates the activity of adenylate cyclase, resulting in increased cellular cAMP. As shown in Figure 4.1, PACAP-27 induced a robust increase in cAMP accumulation in N2a cells (EC_{50} = 4.0 ± 1.3 nM; p[EC]50= 8.5 ± 0.2; n=3; Figure 4.1 A) and SH-SY5Y cells (EC_{50} = 0.28 ± 0.25 nM; p[EC]50= 9.4 ± 0.7; n=3; Figure 4.1 B). These findings confirm the activation of G_s protein signalling via the PAC_1 receptor by PACAP-27 and confirm the functional expression of PAC_1 receptor in differentiating N2a and SH-SY5Y cells. Further experiments were performed to assess whether the PAC_1 receptor triggers intracellular Ca^{2+} responses in differentiating N2a and SH-SY5Y cells, which would be indicative of G_q protein coupling. Calcium imaging experiments revealed that PACAP-27 (100 nM) also triggered a robust increase in intracellular Ca^{2+} in differentiating N2a cells (Figure 4.2 A and B) that was abolished in the absence of extracellular Ca^{2+} (Figure 4.2 C), ATP (10 μM) was added where indicated as a positive control. The findings suggesting that these responses were dependent upon extracellular Ca^{2+} influx. Similar responses were made in the differentiating SH-SY5Y cells (Figure 4.3). Overall, these data indicate that the PAC_1 receptor is functionally expressed in differentiating mouse N2a and human SH-SY5Y cells.

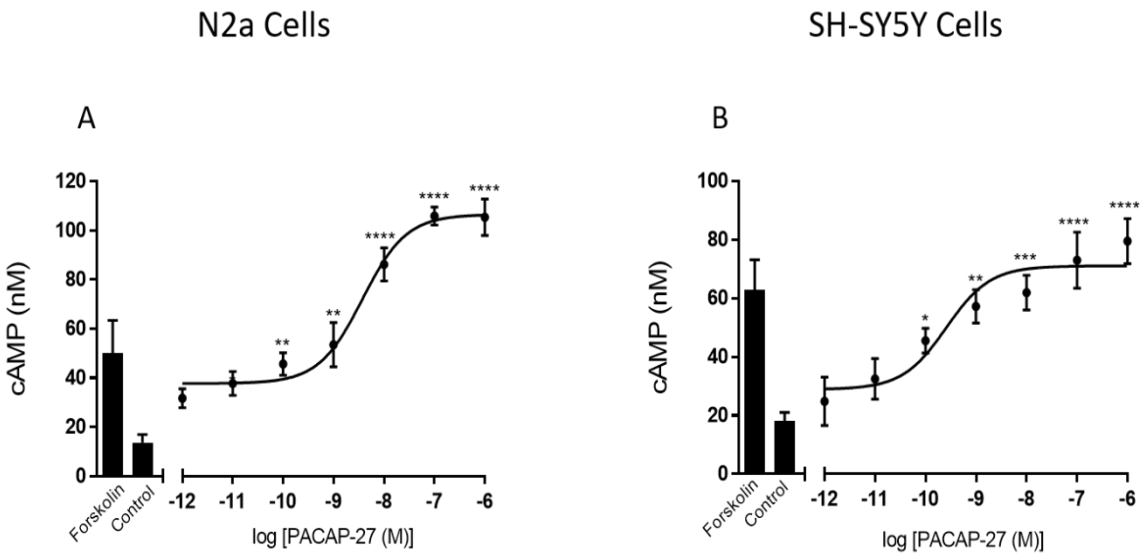

Figure 4.1 PACAP-27-induced cAMP accumulation in differentiating N2a and SH-SY5Y cells.

Differentiating N2a and SH-SY5Y cells were treated with the indicated concentrations of PACAP-27 for 10 min. Levels of cAMP were determined as described in section 2.2.7. The results represent the mean ± S.E.M. of three experiments each performed in triplicate. Forskolin (10 μM) stimulation was used as a positive control. *P<0.05, **P<0.01, ***P<0.001, and ****P<0.0001 versus control (unstimulated cells) response.

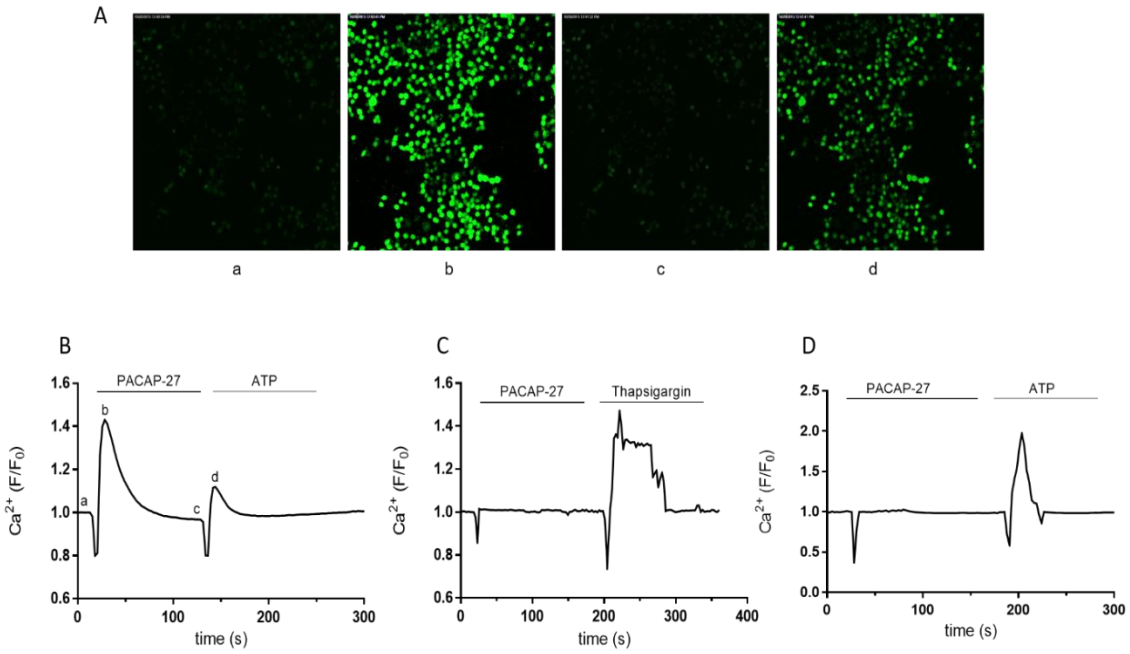

Figure 4.2 Effect of PACAP-27 on $[Ca^{2+}]_i$ in differentiating N2a cells.

(A) Confocal imaging snapshots of PACAP (100 nM) and ATP (10 µM)-induced Ca^{2+} responses in the presence of extracellular Ca^{2+} (1.3 mM). The panel letters (a-d) correspond to the time points shown in (B). (C) Ca^{2+} responses to PACAP were absent in experiments performed in nominally Ca^{2+}-free buffer and 0.1 mM EGTA. In these experiments depletion of intracellular Ca^{2+} stores with thapsigargin (5 µM) was still evident. In (D) responses to PACAP-27 (100 nM) in the presence of extracellular Ca^{2+} and pre-treated with PAC_1 receptor antagonist PACAP 6-38 (100 nM). ATP (10 µM) was added where indicated as a positive control. Similar results were obtained in three other experiments.

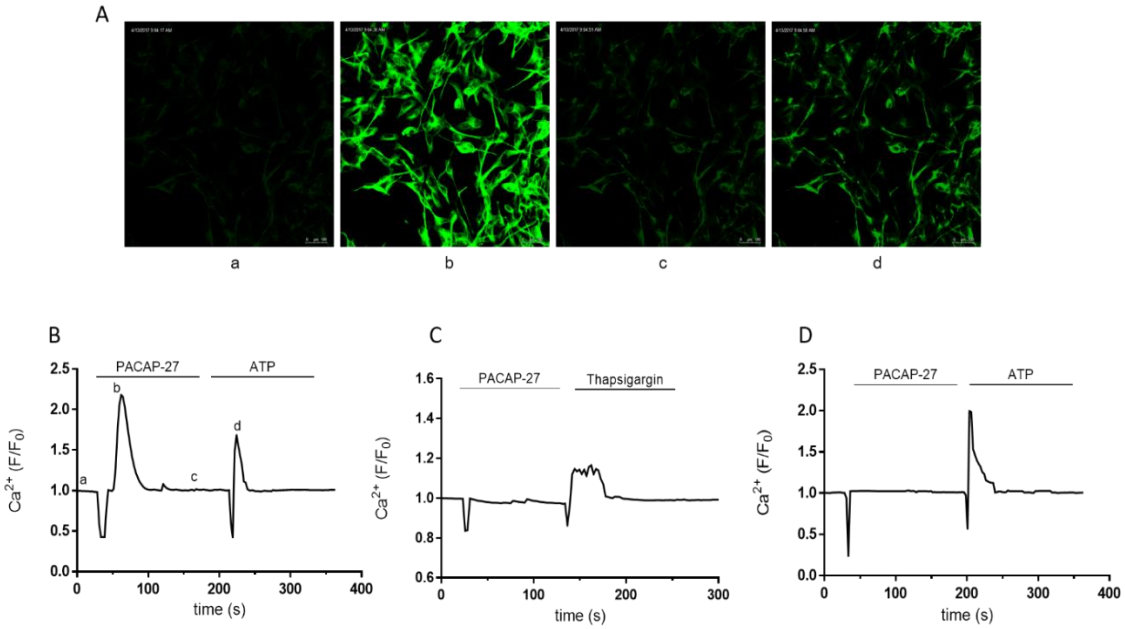

Figure 4.3 Effect of PACAP-27 on $[Ca^{2+}]_i$ in differentiating SH-SY5Y cells.

(A) Confocal imaging snapshots of PACAP (100 nM) and ATP (10 µM)-induced Ca^{2+} responses in the presence of extracellular Ca^{2+} (1.3 mM). The panel letters (a-d) correspond to the time points shown in **(**B). (C) Ca^{2+} responses to PACAP were absent in experiments performed in nominally Ca^{2+}-free buffer and 0.1 mM EGTA. In these experiments depletion of intracellular Ca^{2+} stores with thapsigargin (5 µM) was still evident. In (D) responses to PACAP-27 (100 nM) in the presence of extracellular Ca^{2+} and pre-treated with PAC_1 receptor antagonist PACAP 6-38 (100 nM). ATP (10 µM) was added where indicated as a positive control. Similar results were obtained in three other experiments.

4.2.2 Effect of PACAP-27 on TG2-mediated biotin cadaverine incorporation and protein cross-linking activity

Initial experiments in this study investigated whether the PAC_1 receptor agonist PACAP-27 induced modulation of TG2-mediated amine incorporation and peptide cross-linking activity in differentiating N2a and SH-SY5Y neuroblastoma cells. Cells were treated with PACAP-27 (100 nM) for varying periods of time and cell lysates subjected to the biotin cadaverine incorporation assay and biotin-labelled peptide (Biotin-TVQQEL) cross-linking assay (section 2.2.4). PACAP-27 treatment produced transient increases in TG2 catalysed biotin-cadaverine incorporation and protein cross-linking activity, peaking at 10 min in N2a cells (Figure 4.4 A and B) and 30 min in SH-SY5Y cells (Figure 4.5 A and B). Furthermore, various concentrations of PACAP-27 were tested for their ability to modulate TG2 activity. As shown in Figure 4.4 C and D, PACAP-27 stimulated concentration-dependent increases in biotin-cadaverine incorporation activity (EC50 = 0.08 ± 0.01 nM; p[EC50] = 10.1 ± 0.1; n=5) and protein cross-linking activity (EC50 = 0.4 ± 0.2 nM; p[EC50] = 9.7 ± 0.2; n=6) in N2a cells. In SH-SY5Y cells (Figure 4.5 C and D) PACAP-27 also triggered concentration-dependent increases in both biotin-cadaverine incorporation activity (EC50 = 2.2 ± 1.0 nM; p[EC50] = 8.9 ± 0.4; n=3) and protein cross-linking activity (EC50 = 1.3 ± 0.5 nM; p[EC50] = 9.0 ± 0.2; n=3). Overall, these data indicate that PACAP-27 triggers a marked increase in TG2 biotin-cadaverine incorporation and protein cross-linking activity in neuroblastoma cells.

Since PACAP-27 also acts as a $VAPC_1$ and $VAPC_2$ receptor agonist (Vaudry et al. 2009), testing of its selectivity for the PAC_1 receptor in modulating TG2 activity in differentiating N2a and SH-SY5Y cell lines was required. The effects of various concentrations of $[Ala^{1,22,28}]VIP$ (Ala-VIP; a potent and highly selective agonist for $VPAC_1$ receptor) and Bay 55-9837 (a selective $VPAC_2$ receptor agonist) on TG2 activity were assessed (Nicole et al., 2000, Dickson et al., 2006, Vaudry et al. 2009). As shown in Figure 4.6, no noticeable stimulation of TG2 activity was shown with Ala-VIP or Bay 55-9837 in both differentiating neuroblastoma cell lines. Furthermore, those selective $VAPC_1$ and $VAPC_2$ receptor agonists had no significant effect on cAMP accumulation (Figure 4.7). Thus, it appears likely that this TG2 activity is mediated principally through the PAC_1 receptor.

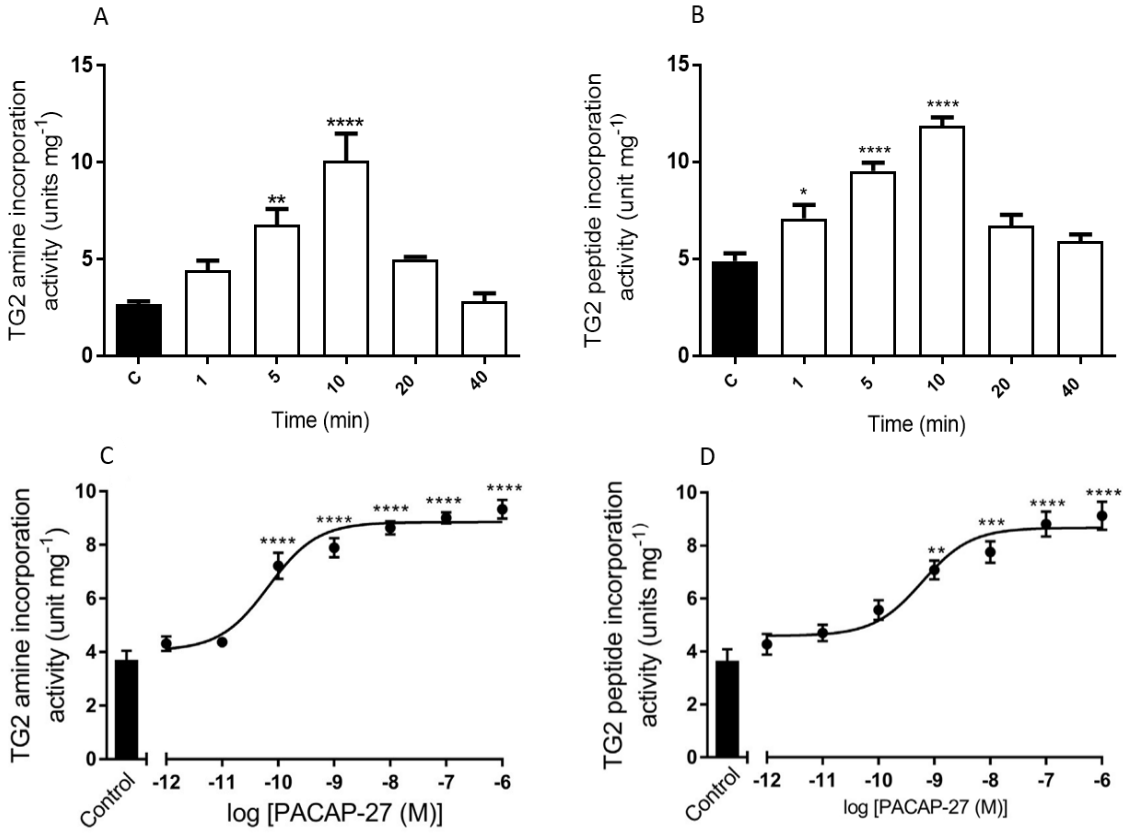

Figure 4.4 Effect of PACAP-27 on TG2 activity in N2a cells.

Differentiating N2a cells were either incubated with 100 nM PACAP-27 for the indicated time periods or for 10 min with the indicated concentrations of PACAP-27. Cell lysates were then subjected to the biotin-cadaverine incorporation (A and C) or peptide cross-linking assay (B and D). Data points represent the mean TG specific activity ± S.E.M. from four (A and C), five (B) or six (D) independent experiments. *P < 0.05, **P <0.01, ***P < 0.001, and ****P < 0.0001 versus control response.

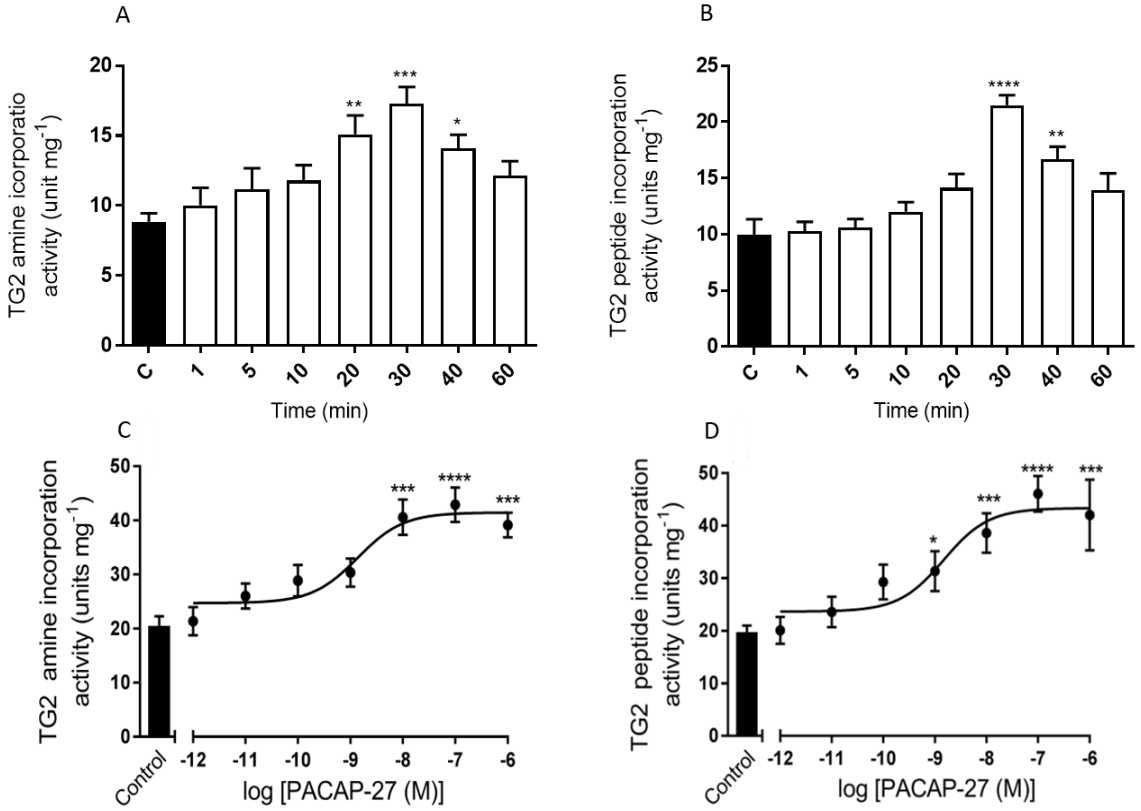

Figure 4.5 Effect of PACAP-27 on TG2 activity in SH-SY5Y cells.

Differentiating SH-SY5Y cells were either incubated with 100 nM PACAP-27 for the indicated time periods or for 30 min with the indicated concentrations of PACAP-27. Cell lysates were then subjected to the biotin-cadaverine incorporation (A and C) or peptide cross-linking assay (B and D). Data points represent the mean TG specific activity ± S.E.M. from four (A and B) or three (C and D) independent experiments. *P<0.05, **P<0.01, ***P<0.001, and ****P<0.0001 versus control response.

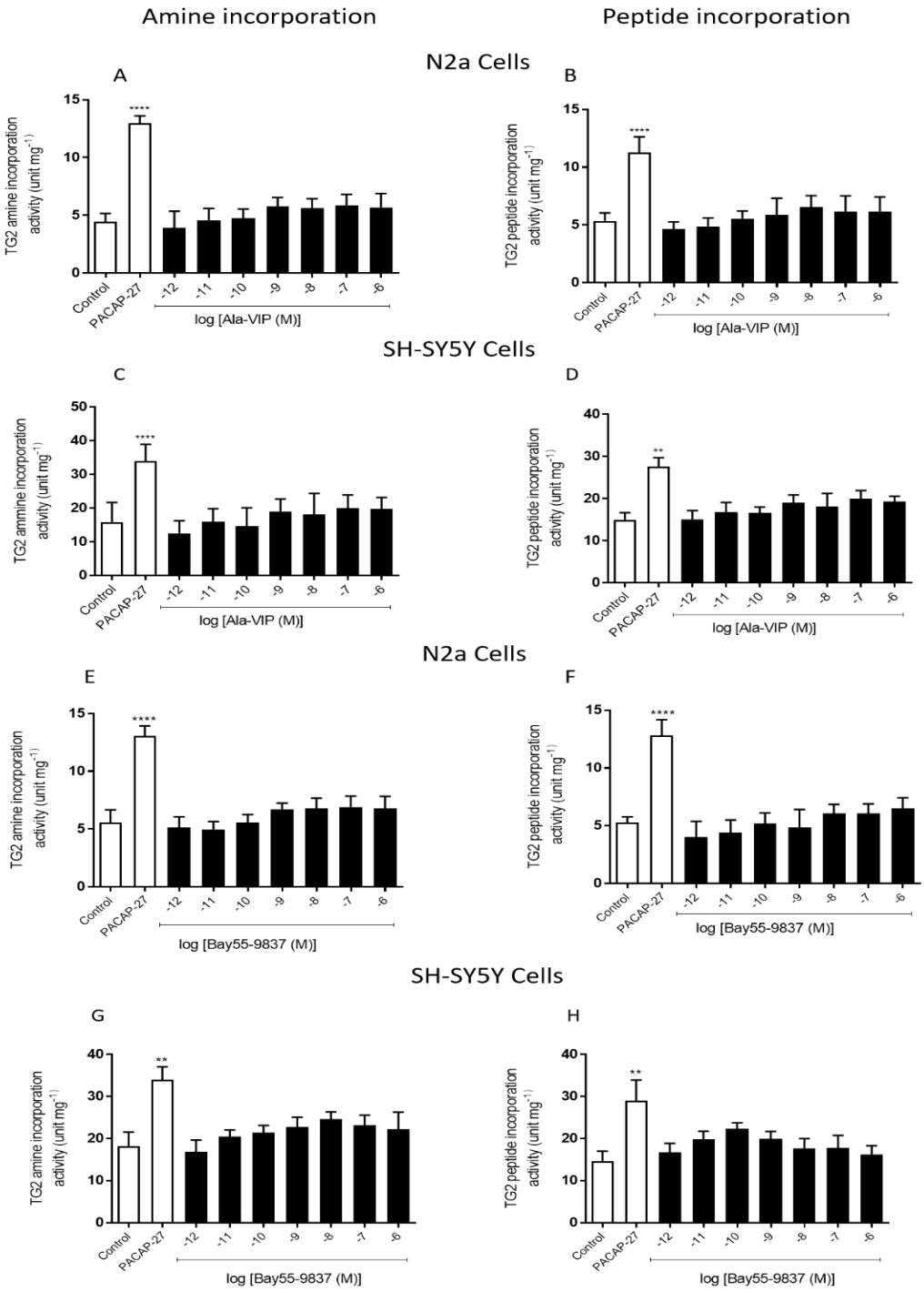

Figure 4.6 Effect of $VAPC_1$ and $VAPC_2$ agonist on TG2 activity in differentiating N2a and SH-SY5Y cells.

Cells were treated with increasing concentrations of Ala-VIP (panels A-D) and Bay55-9837 (panels E-H) for 10 min. Cell lysates were subjected to biotin cadaverine incorporation assay (A, C, E and G) or peptide crosslinking assay (B, D, F and H). PACAP-27 (100 nM, 10 min) stimulation was used as a positive control. Data points represent the mean of TG2-specific activity ±SEM from four to six independent experiments. **P<0.01 and ****P<0.0001 versus basal TG2 activity.

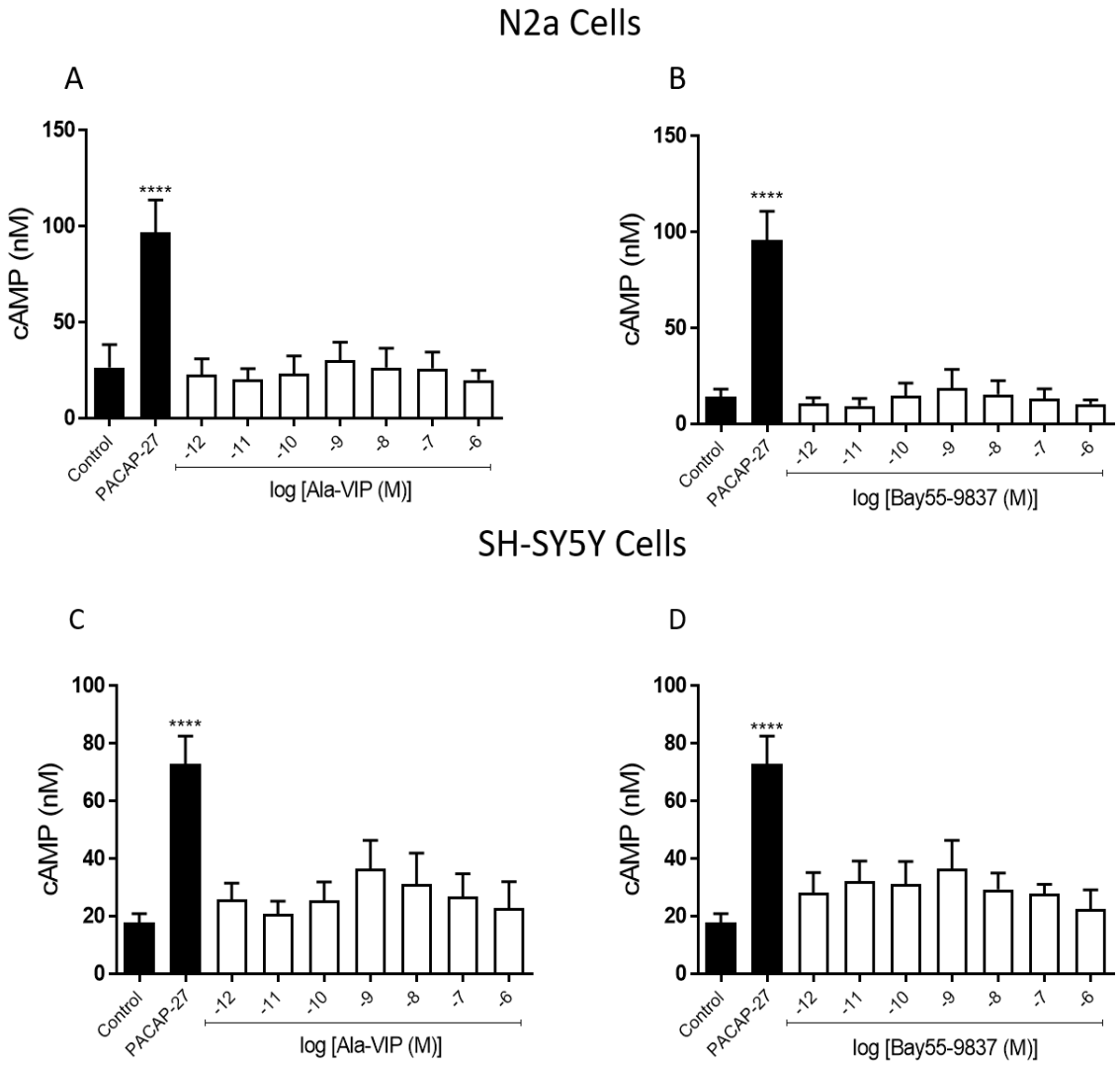

Figure 4.7 Effect of $VAPC_1$ and $VAPC_2$ agonists on cAMP accumulation in differentiating N2a and SH-SY5Y cells.

Cells were treated with increasing concentrations of Ala-VIP (panels A and C) and Bay55-9837 (panels B and D) for 10 min. Levels of cAMP were determined as described in (section 2.2.7). PACAP-27 (100 nM, 10 min) stimulation was used as a positive control. Data points represent the mean of TG2-specific activity ±SEM from four to six independent experiments. ****P<0.0001 versus basal TG2 activity.

4.2.3 Effect of PAC_1 receptor antagonist and TG2 inhibitors on PACAP-27-induced TG2 activity

To determine whether the induced TG2 activity was via the PAC_1 receptor, differentiating N2a and SH-SY5Y cells were treated for 30 min with PAC_1 receptor selective antagonist PACAP 6-38 (100 nM) prior to stimulation with 100 nM PACAP-27. PACAP 6-38 attenuated PACAP-27 induced TG2 biotin-cadaverine incorporation and protein crosslinking activity in differentiating N2a (Figure 4.8 A and B) and SH-SY5Y cells (Figure 4.9 A and B), confirming the involvement of the PAC_1 receptor.

To confirm that TG2 was responsible for PAC_1 receptor-mediated transglutaminase activity in differentiating N2a and SH-SY5Y cells, two structurally different cell permeable TG2 specific inhibitors were tested; R283 (a small molecule; Freund et al., 1994) and Z-DON (peptide-based; Schaertl et al., 2010). Cells were pre-treated for 1 h with Z-DON (150 µM) or R283 (200 µM) prior to stimulation with PACAP-27 (100 nM) for 10 min (N2a) and 30 min (SH-SY5Y). Both inhibitors completely blocked PACAP-27-induced TG-mediated amine incorporation and peptide cross-linking activity in both cell lines (Fig. 4.8 C and D and Fig. 4.9 C and D). It is important to note that, despite these TG2 inhibitors being cell-permeable, inhibition of cellular TG2 is only achieved at concentrations significantly above their IC_{50} value (Z-DON 150 nM and R283 1 µM) versus purified enzyme (Freund et al., 1994; Schaertl et al., 2010). Overall, these data indicate that TG2 is the TG isoform activated by the PAC_1 receptor.

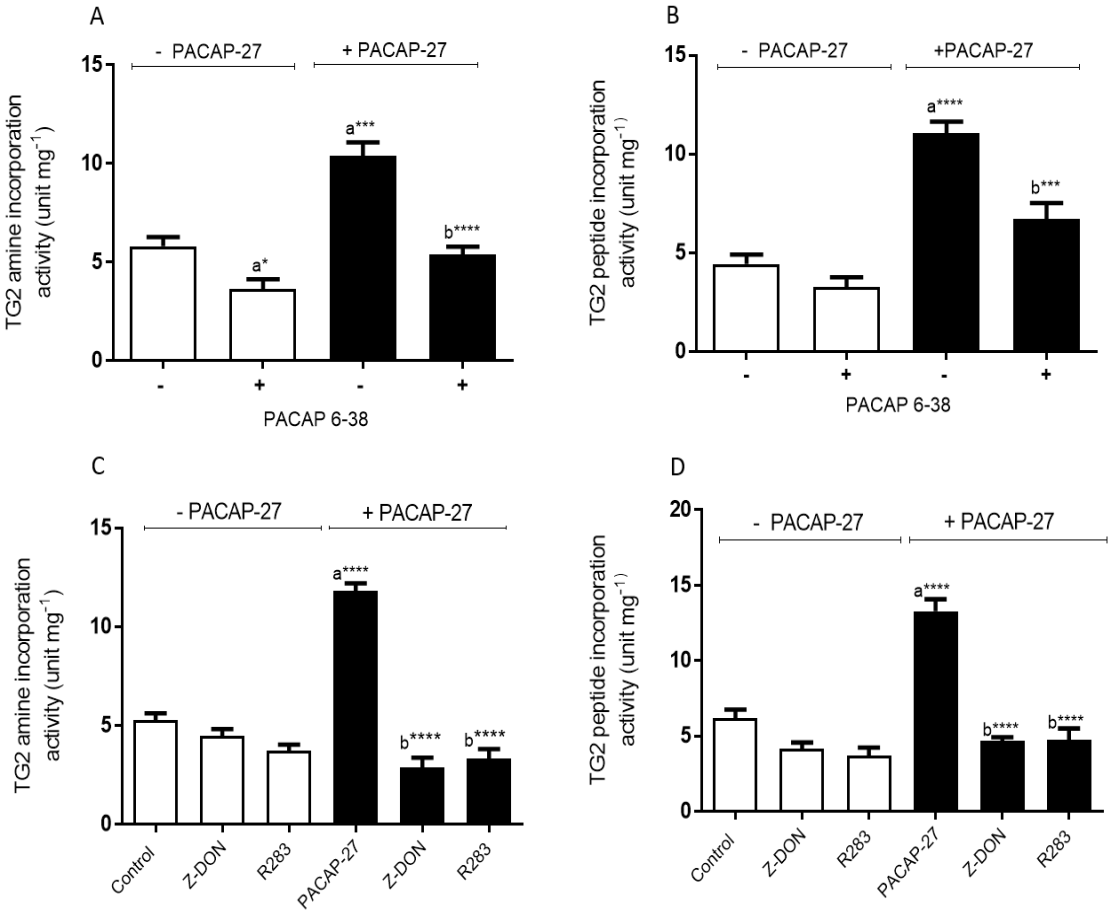

Figure 4.8 Effect of the selective PAC_1 receptor antagonist PACAP 6-38 and inhibitors of TG2 on PACAP-27 induced TG2 activity in differentiating N2a cells.

Differentiated N2a cells were pre-treated for 1 h with the TG2 inhibitors Z-DON (150 µM) and R283 (200 µM) or for 30 min with the selective PAC_1 receptor antagonist PACAP 6-38 (100 nM) prior to 10 min stimulation with PACAP-27 (100 nM). Cell lysates were then subjected to the biotin-cadaverine incorporation (panels A and C) or protein cross-linking assay (panels B and D). Data points represent the mean TG specific activity ± S.E.M. from four independent experiments. *P<0.05, ***P<0.001, and ****P<0.0001, (a) versus control and (b) versus 100 nM PACAP-27 alone.

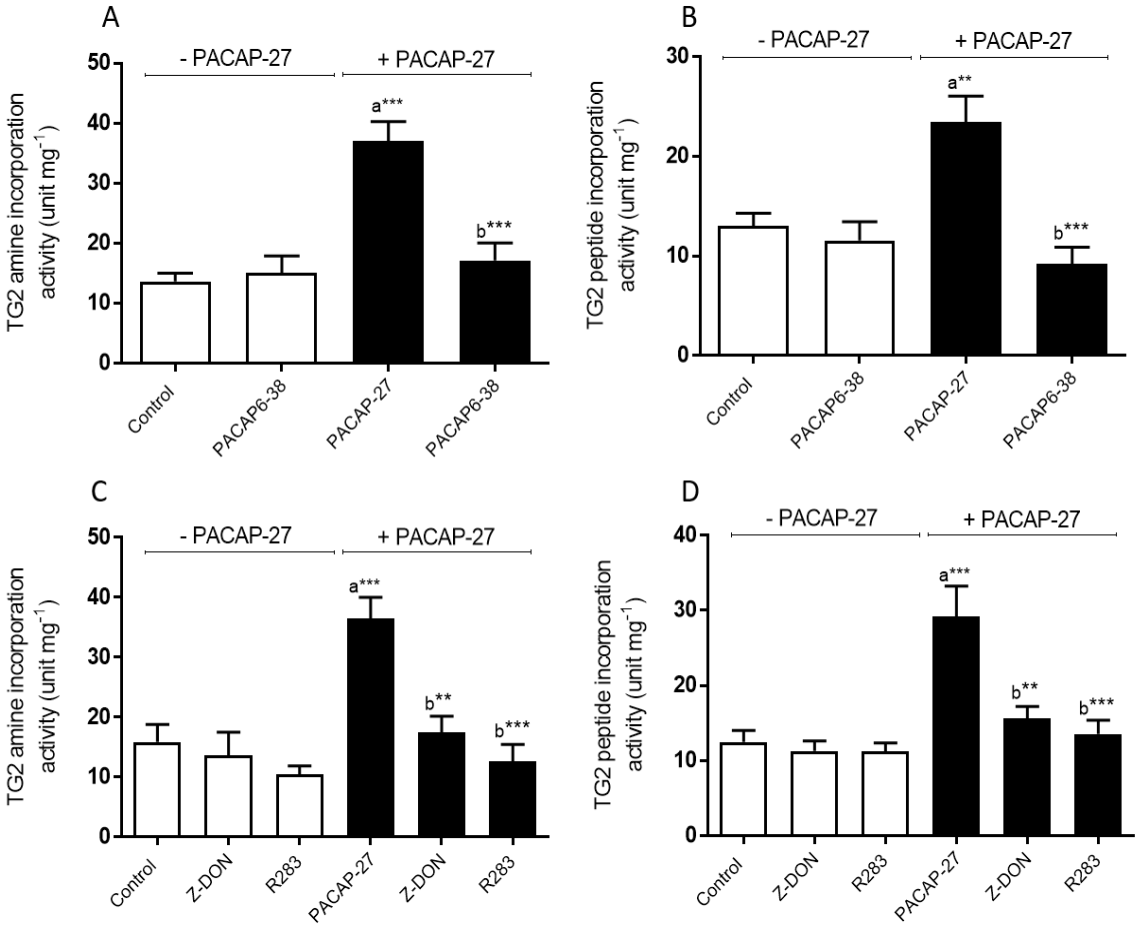

Figure 4.9 Effect of the selective PAC_1 receptor antagonist PACAP 6-38 and inhibitors of TG2 on PACAP-27 induced TG2 activity in differentiating SH-SY5Y cells.

Differentiating SH-SY5Y cells were pre-treated for 1 h with the TG2 inhibitors Z-DON (150 µM) and R283 (200 µM) or for 30 min with the selective PAC_1 receptor antagonist PACAP 6-38 (100 nM) prior to 30 min stimulation with PACAP-27 (100 nM). Cell lysates were then subjected to the biotin-cadaverine incorporation (panels A and C) or peptide cross-linking assay (panels B and D). Data points represent the mean TG specific activity ± S.E.M. from four independent experiments. **P<0.01 and ***P<0.001, (a) versus control and (b) versus 100 nM PACAP-27 alone.

4.2.4 The effect of protein kinase inhibitors on PACAP-27 induced TG2 activity

PACAP-27-induced TG2 activity in differentiating N2a and SH-SY5Y cells may involve the modulation of pro-survival and/or other signalling pathways. Hence, in this section the role of protein kinases in PAC_1 receptor-induced TG2 activity was determined.

Effect of PACAP-27 on protein kinase activation

Modulation of protein kinase activity following PAC_1 receptor activation by PACAP-27 was assessed by Western blot analysis using phospho-specific antibodies that recognise phosphorylated motifs within activated ERK1/2 ($pT^{202}EpY^{204}$), p38 MAPK ($pT^{180}GpY^{182}$), JNK ($pT^{183}pPy^{185}$) and PKB (S^{473}). PACAP-27 (100 nM) stimulated significant increases in ERK1/2 and PKB phosphorylation in differentiating N2a (Figure 4.10 A and B) and SH-SY5Y cells (Figure 4.10 C and D). As expected PACAP-27-mediated increases in ERK1/2 and PKB phosphorylation were inhibited by PD 98059 (50 µM; MEK1/2 inhibitor) and Akt inhibitor XI (0.1, 1 µM and 10 µM; PKB inhibitor), respectively in both cell lines (Figure 4.10). Furthermore, PACAP-27 significantly increased JNK1/2 phosphorylation in differentiating N2a cells but no significant increase was observed in SH-SY5Y cells (Figure 4.11 A and C). Finally, p38 MAPK was significantly activated by PACAP-27 in differentiating SH-SY5Y cells but not in N2a cells (Figure 4.11 B and D). As depicted PACAP-27-mediated increases in JNK1/2 phosphorylation were inhibited by SP 600125 (20 µM; JNK1/2 inhibitor; Figure 4.11 B) in N2a cells only while SB 203580 (20 µM; p38 MAPK inhibitor; Figure 4.11 D) reversed the activation of p38 MAPK induced by PACAP-27 in SH-SY5Y cells only.

Role of PKA, PKC and Ca^{2+} in PACAP-27 induced ERK1/2 activation

Since activation of ERK1/2 by phosphorylation is a major and central regulatory event in neurite outgrowth and cell survival in PC12 (Ravni et al., 2006), N2a (Biernat et al., 2002) and SHSY-5Y cells (Monaghan et al., 2008) therefore it was of interest to examine the effect of other protein kinase inhibitors on PACAP-27 induced ERK1/2 phosphorylation. As it has been previously reported that PKA can activate ERK1/2 (Emery & Eiden, 2012; Clason et al., 2017), the effect of the PKA inhibitor KT 5720 (5 µM) on PACAP-27 induced ERK1/2 phosphorylation was assessed. As shown in Figure 4.12 A and 4.13 A, PACAP-27–induced increases in ERK1/2 were attenuated by KT 5720 in both cell lines, suggesting an up-stream role of PKA in PACAP-27 induced ERK1/2 activation. PAC_1 receptor-induced ERK1/2 is

dependent on Ca^{2+} influx and PLC/DAG/PKC (Vaudry et al., 2009) and hence the role of PKC and Ca^{2+} was determined. PACAP-27–induced increases in ERK1/2 were partially attenuated by Ro 31-8220 (10 μM; PKC inhibitor; Figure 4.12 B) in N2a and showed no significant effect in SH-SY5Y cells (Figure 4.13 B). Finally, removal of extracellular Ca^{2+} in both cell lines did not block PACAP-27 induced ERK1/2 activation (Figure 4.12 C and 4.13 C).

In summary, these data have shown that PAC_1 receptor activation by PACAP-27 in differentiating N2a and SH-SY5Y cells triggers robust increases in phosphorylation of ERK1/2, PKB, JNK1/2 (N2a cells only) and p38 MAPK (SH-SY5Y cells only) and that ERK1/2 activation is PKA-dependent in both cell lines.

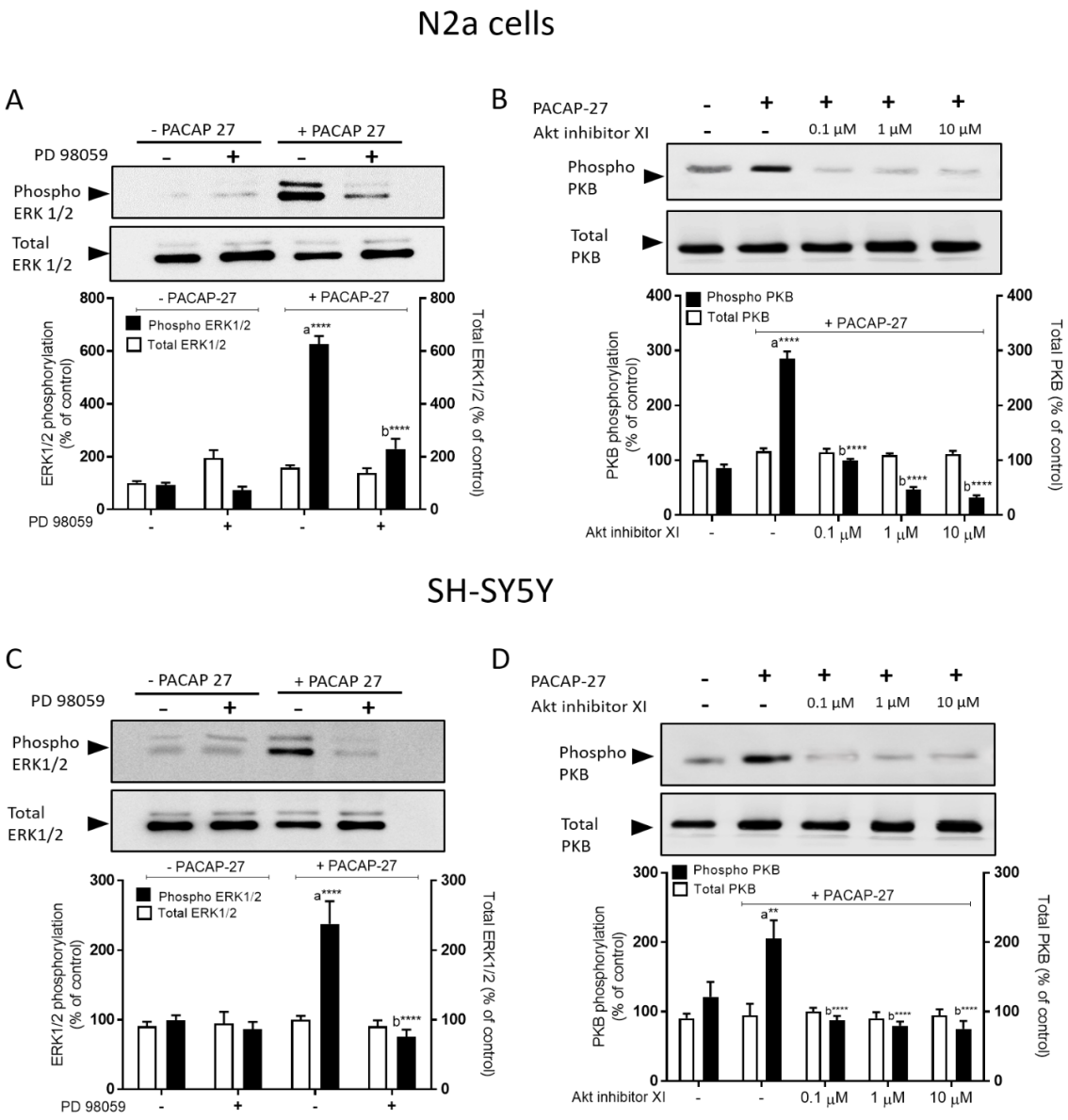

Figure 4.10 Effect of PACAP-27 on ERK1/2 and PKB phosphorylation in differentiating N2a and SH-SY5Y cells.

Where indicated N2a and SH-SY5Y cells were pre-treated for 30 min with PD 98059 (50 μM) or Akt inhibitor X1 (0.1 μM, 1 μM or 10 μM) prior to stimulation with PACAP-27 (100 nM) for 10 min (N2a) and 30 min (SH-SY5Y). Cell lysates were analysed by Western blotting for activation of ERK1/2 (panels A and C) and PKB (panels B and D) using phospho-specific antibodies. Samples were subsequently analysed on separate blots using antibodies that recognize total ERK1/2 and PKB. Quantified data are expressed as the percentage of the value for control cells (=100%) in the absence of protein kinase inhibitor and represent the mean ± S.E.M. of four independent experiments. **P<0.01, ***P<0.001 and ****P<0.0001, (a) versus control and (b) versus 100 nM PACAP-27.

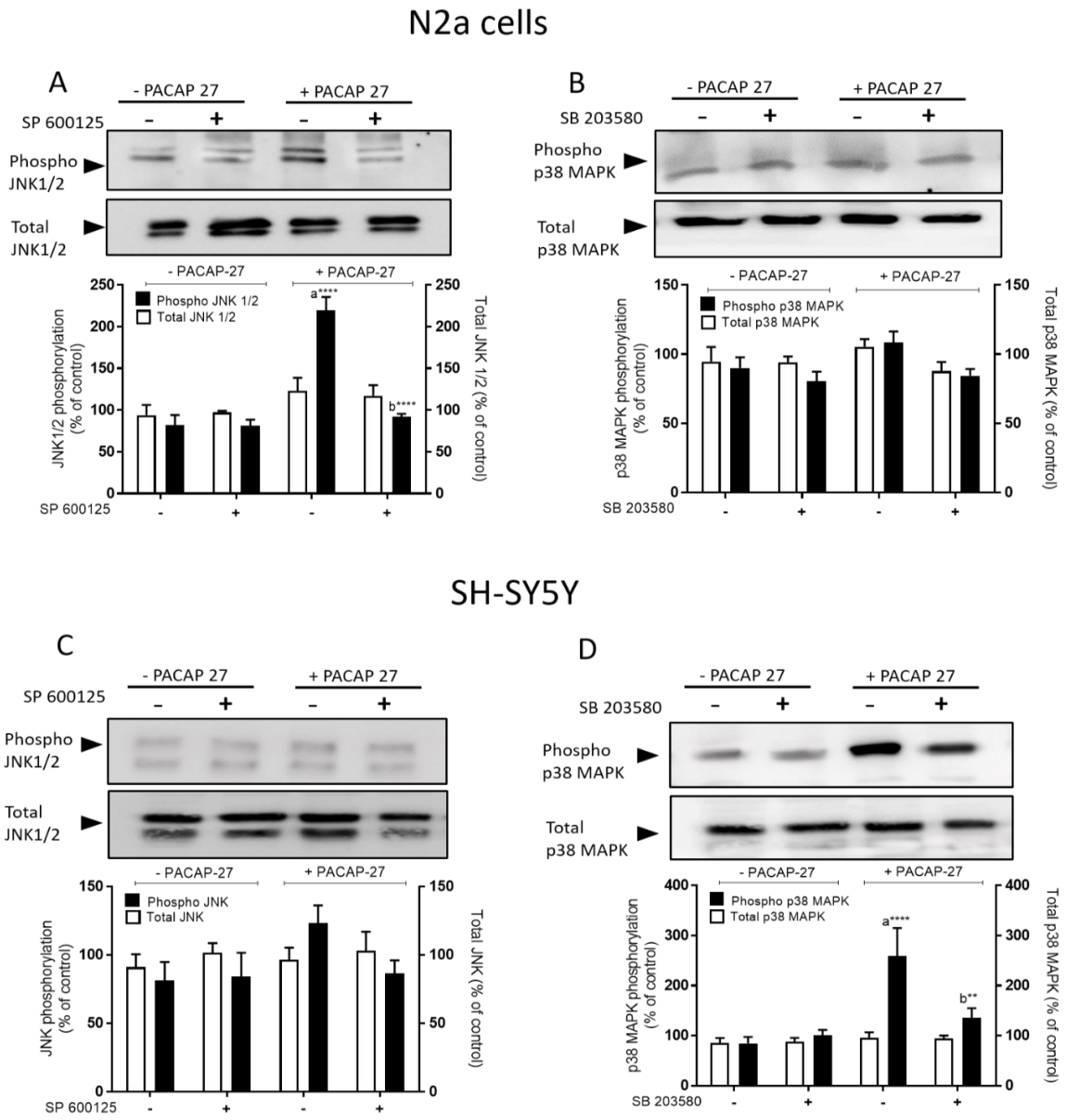

Figure 4.11 Effect of PACAP-27 on JNK 1/2 and p38 MAPK phosphorylation in differentiating N2a and SH-SY5Y cells.

Where indicated N2a and SH-SY5Y cells were pre-treated for 30 min with SP 600 125 (20 µM) or SB 203580 (20 µM) prior to stimulation with PACAP-27 (100 nM) for 10 min (N2a) and 30 min (SH-SY5Y). Cell lysates were analysed by Western blotting for activation of JNK1/2 (panels A and C) and p38 MAPK (panels B and D) using phospho-specific antibodies. Samples were subsequently analysed on separate blots using antibodies that recognize total JNK1/2 and p38 MAPK. Quantified data are expressed as the percentage of the value for control cells (=100%) in the absence of protein kinase inhibitor and represent the mean ± S.E.M. of four independent experiments. **P<0.01 and ****P<0.0001, (a) versus control and (b) versus 100 nM PACAP-27.

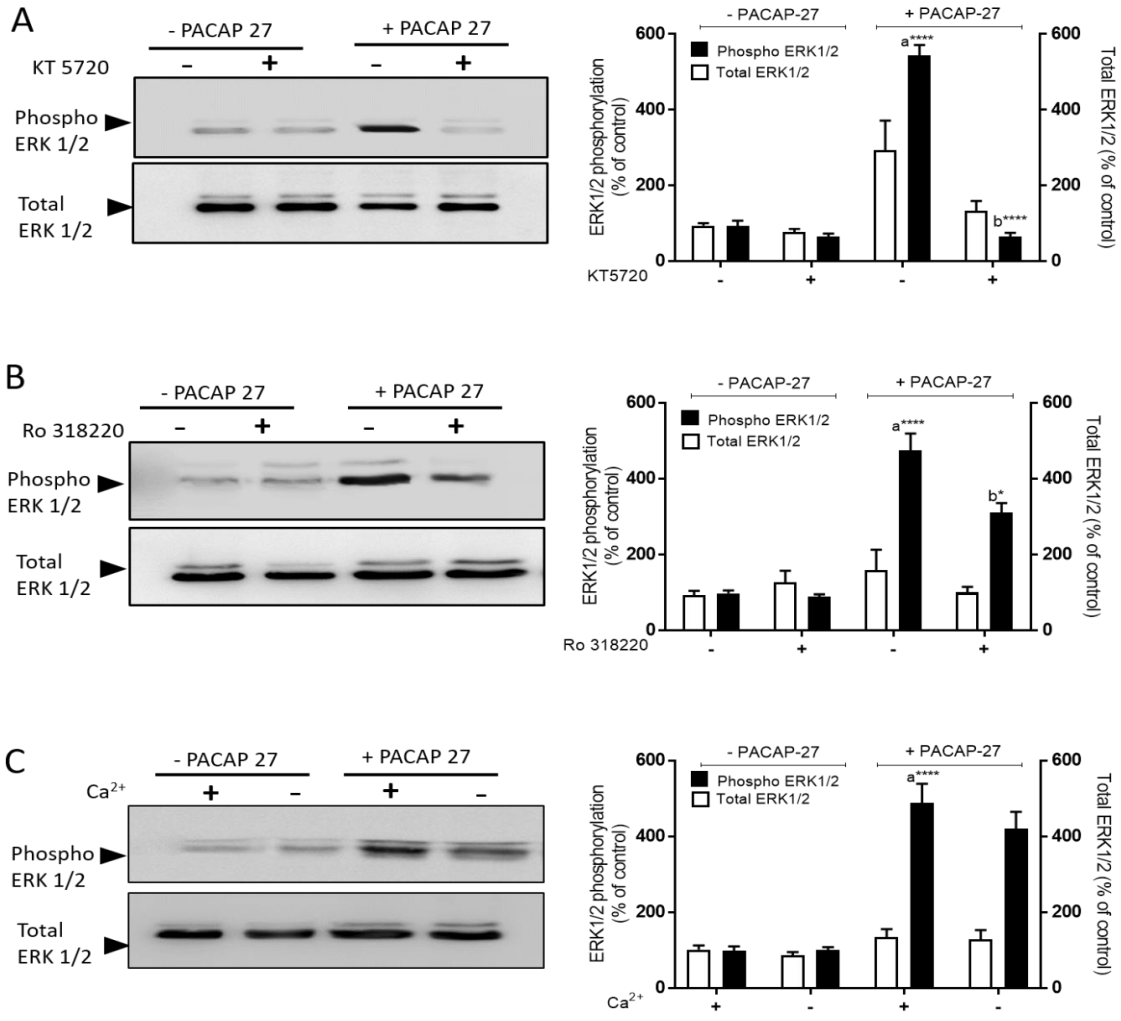

Figure 4.12 Effect of protein kinase inhibitors (PKA and PKC) and role of extracellular Ca^{2+} on PACAP-27 induced ERK1/2 activation in differentiating N2a cells.

Where indicated differentiating N2a cells were pre-treated for 30 min with (A) KT 5720 (5 µM) or (B) Ro 318220 (10 µM) prior to stimulation with PACAP-27 (100 nM) for 10 min. (C) cells were stimulated for 10 min with PACAP-27 (100 nM) either in the presence (1.8 mM $CaCl_2$) or absence of extracellular Ca^{2+} (nominally Ca^{2+}-free Hanks/HEPES buffer containing 0.1 mM EGTA). Cell lysates were analysed by Western blotting for activation of ERK1/2 using a phospho-specific antibody. Samples were subsequently analysed on separate blots using an antibody that recognizes total ERK1/2. Quantified data are expressed as the percentage of the value for control cells (=100%) in the absence of protein kinase inhibitor or presence of extracellular Ca^{2+} and represent the mean ± S.E.M. of four independent experiments. *P<0.05 and ****P<0.0001, (a) versus control and (b) versus 100 nM PACAP-27.

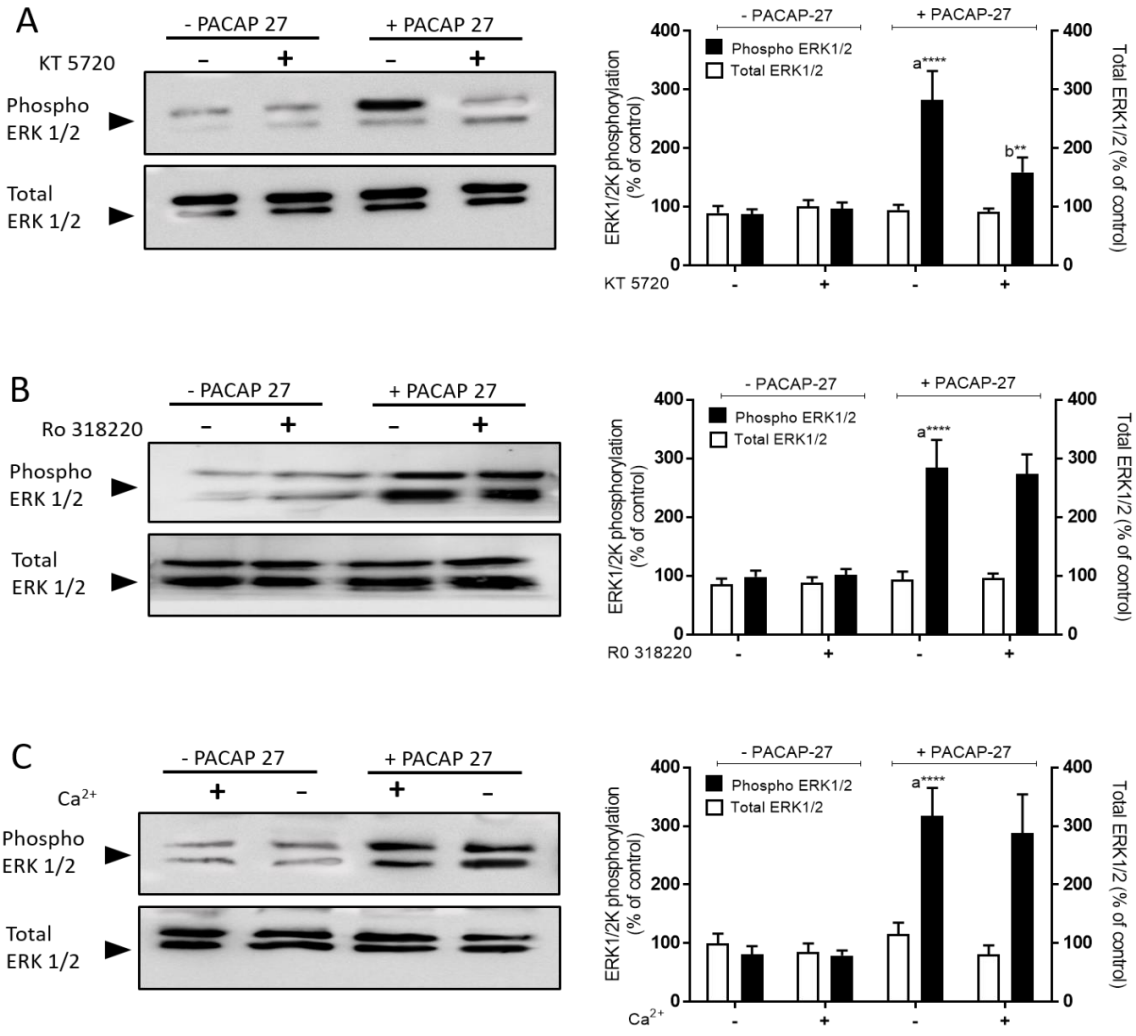

Figure 4.13 Effect of protein kinase inhibitors (PKA and PKC) and role of extracellular Ca^{2+} on PACAP-27 induced ERK1/2 activation in differentiating SH-SY5Y cells.

Where indicated differentiating SH-SY5Y cells were pre-treated for 30 min with (A) KT 5720 (5 µM) or (B) Ro 318220 (10 µM) prior to stimulation with PACAP-27 (100 nM) for 30 min. (C) cells were stimulated for 30 min with PACAP-27 (100 nM) either in the presence (1.8 mM $CaCl_2$) or absence of extracellular Ca^{2+} (nominally Ca^{2+} -free Hanks/HEPES buffer containing 0.1 mM EGTA). Cell lysates were analysed by Western blotting for activation of ERK1/2 using a phospho-specific antibody. Samples were subsequently analysed on separate blots using an antibody that recognizes total ERK1/2. Quantified data are expressed as the percentage of the value for control cells (=100%) in the absence of protein kinase inhibitor or presence of extracellular Ca^{2+} and represent the mean ± S.E.M. of four independent experiments. **P<0.01and ****P<0.0001, (a) versus control and (b) versus 100 nM PACAP-27.

Effect of protein kinase inhibitors on PACAP-27-induced TG2 activity

The role ERK1/2, PKA, PKB, PKC, p38 MAPK and JNK1/2 in PACAP-27-induced TG2 activation was determined using pharmacological inhibitors of these protein kinases. Pre-treatment with PD 98950, Akt inhibitor XI and PKA inhibitors (KT 5720; 5 µM or *Rp*-cAMPs; 50 µM), completely abolished PACAP-27-induced amine incorporation and peptide cross-linking activity, confirming the involvement of ERK1/2, PKB and PKA respectively, in PACAP-27-mediated TG2 responses in differentiating N2a and SH-SY5Y cells (Figure 4.14 and 4.15). In N2a cells the JNK1/2 inhibitor SP 6000125 attenuated PACAP-27-induced peptide cross-linking activity (Figure 4.16 B) but was without effect on TG2-mediated amine incorporation (Figure 4.16 A). In SH-SY5Y cells SP 600125 had no significant effect either of the TG2 activities (Figure 4.16 C and D). The PKC inhibitor Ro 318220 blocked PACAP-27-induced TG2 activities in N2a cells but not in SH-SY5Y cells (Figure 4.16). Finally, the p38 MAPK inhibitor SB 203580 showed no effect on PACAP-27-induced TG2 activation in either cell line (Figure 4.16).

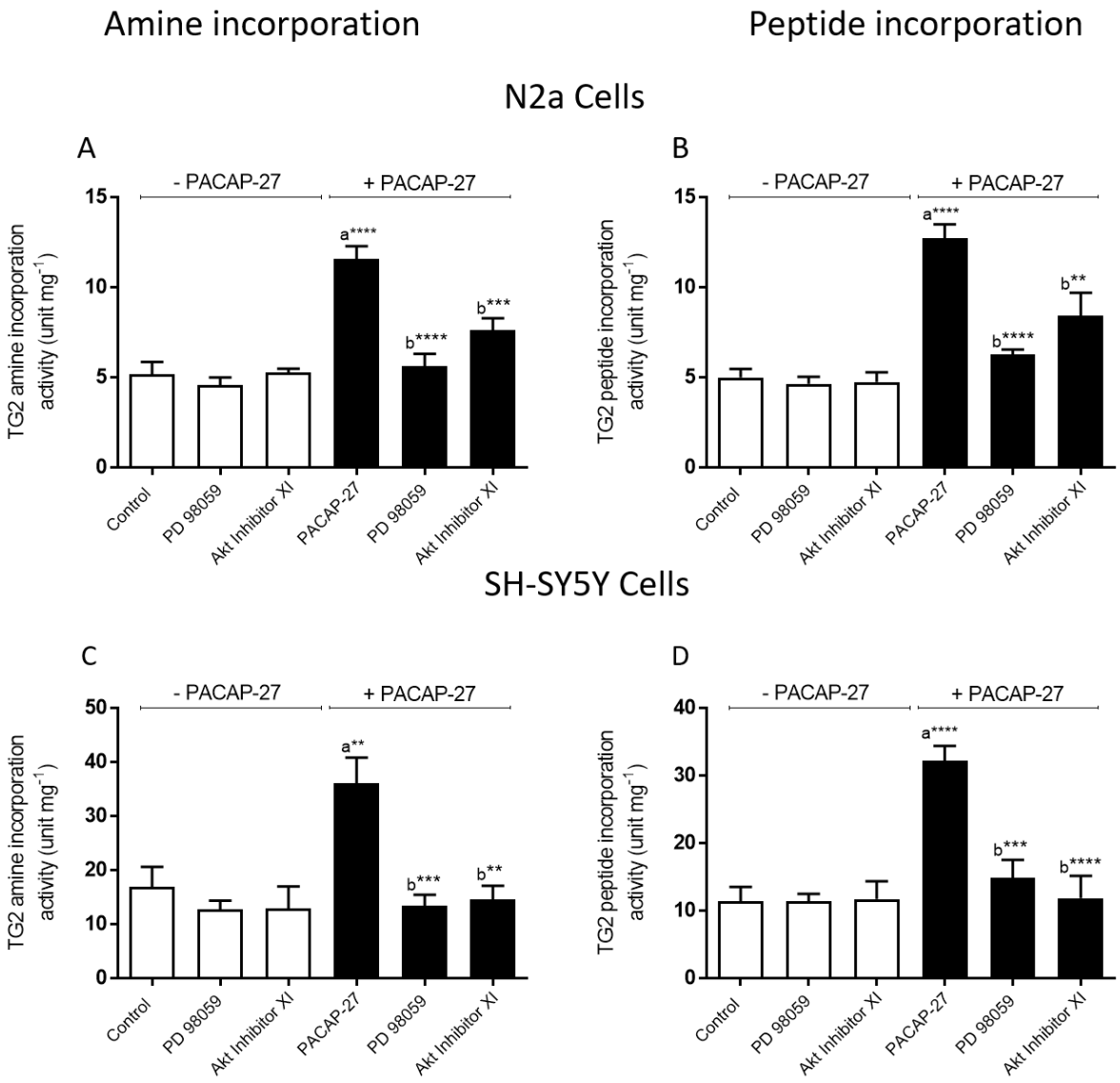

Figure 4.14 Effect of protein kinase inhibitors (ERK1/2 and PKB) on PACAP-27-induced TG2 activity in differentiating N2a and SH-SY5Y cells.

Differentiating N2a and SH-SY5Y cells were pre-treated for 30 min with PD 98059 (50 µM) or Akt inhibitor XI (100 nM) prior to stimulation with PACAP-27 (100 nM) for 10 min (N2a) and 30 min (SH-SY5Y). Cell lysates subjected to biotin-cadaverine incorporation (panels A and C) or peptide cross-linking assay (panels B and D). Data points represent the mean ± S.E.M. TG specific activity from four independent experiments. ** P<0.01, ***P<0.001 and **** P<0.0001, (a) versus control and (b) versus 100 nM PACAP-27 alone.

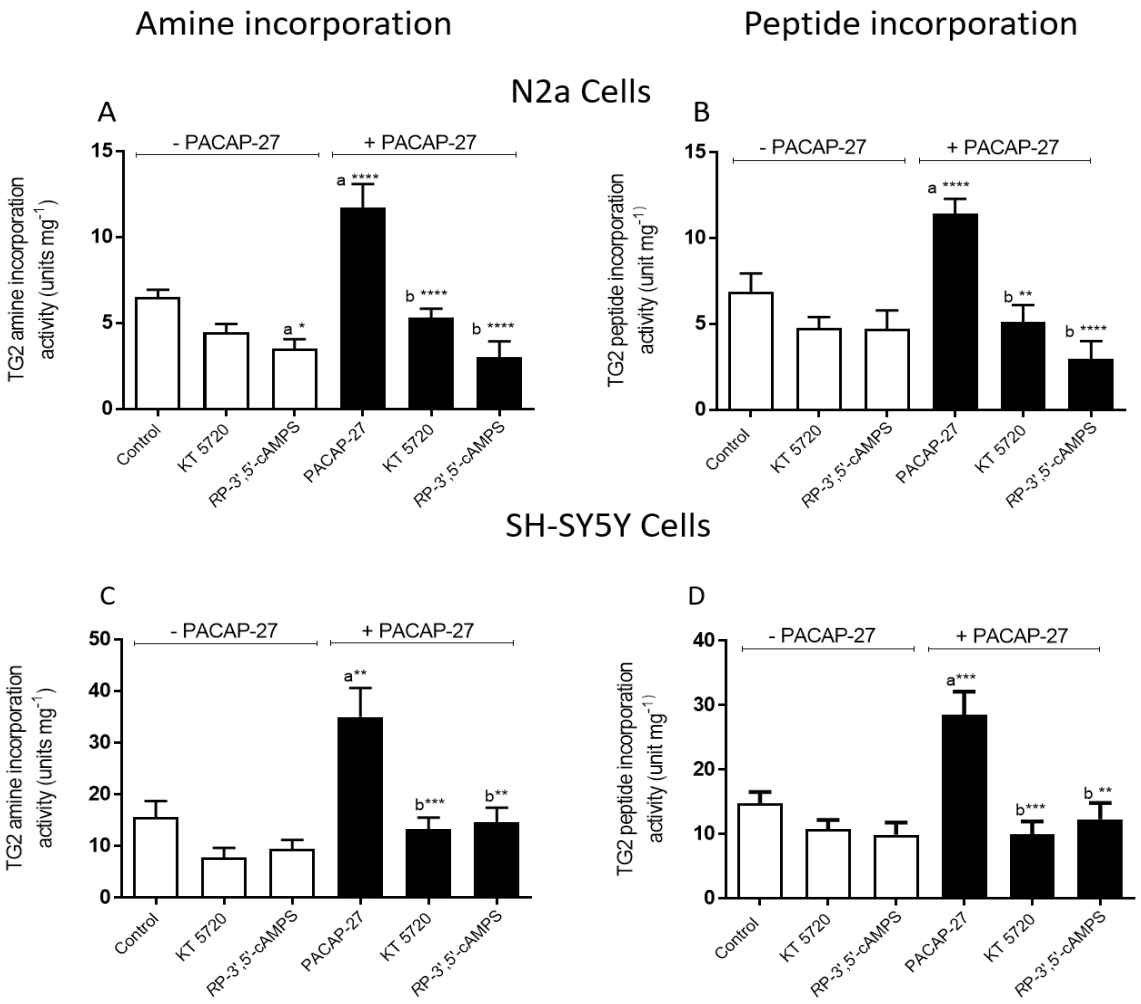

Figure 4.15 Effect of PKA inhibitors on PACAP-27-induced TG2 activity in differentiating N2a and SH-SY5Y cells.

Differentiating N2a and SH-SY5Y cells were pre-treated for 30 min with KT 5720 (5 µM) or Rp-3',5'-cAMPs (50 µM) prior to stimulation with PACAP-27 (100 nM) for 10 min (N2a) and 30 min (SH-SY5Y). Cell lysates subjected to biotin-cadaverine incorporation (panels A and C) or peptide cross-linking assay (panels B and D). Data points represent the mean ± S.E.M. TG specific activity from four independent experiments. *P<0.05, ** P<0.01, *** P<0.001 and **** P<0.0001, (a) versus control and (b) versus 100 nM PACAP-27 alone.

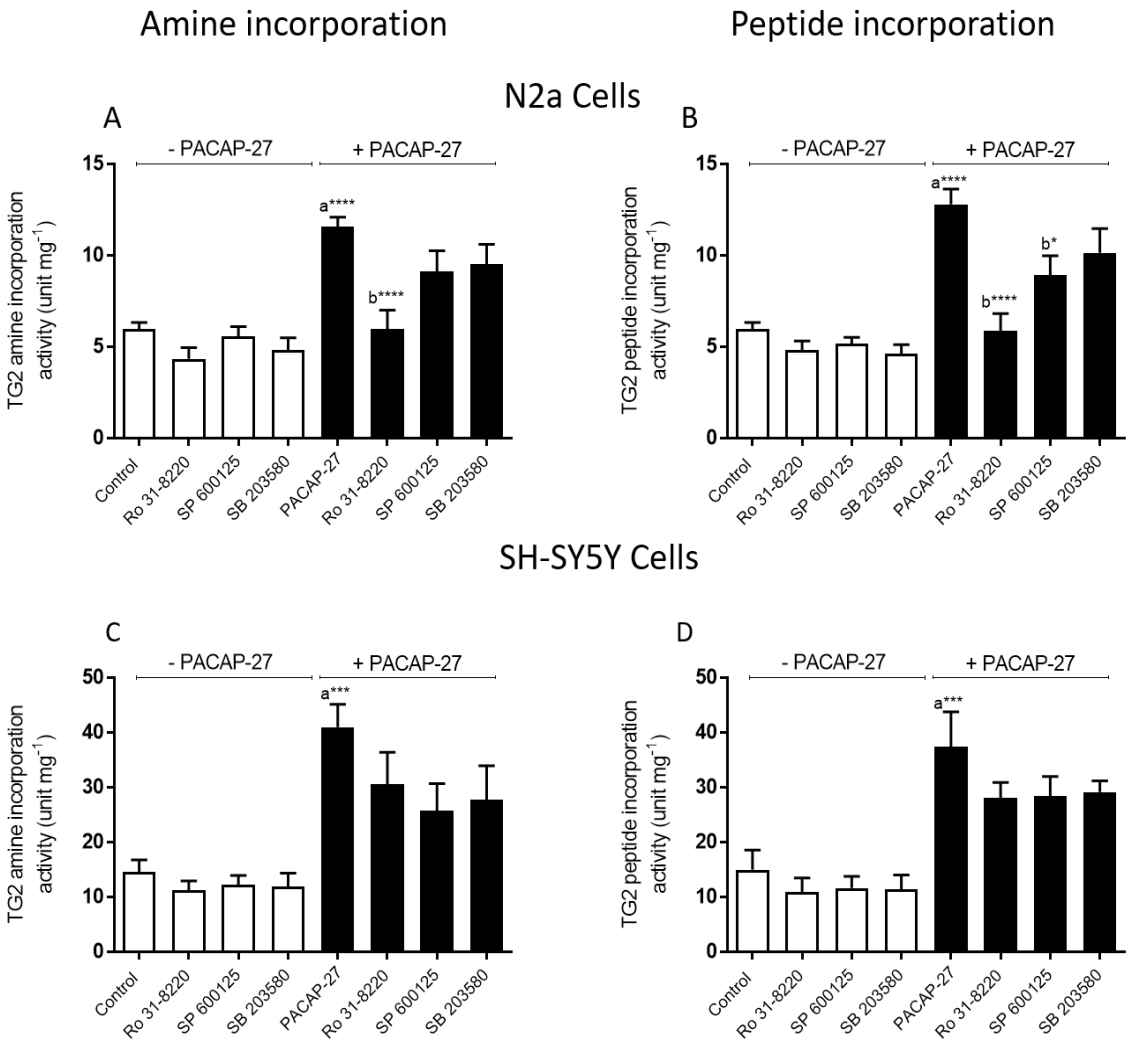

Figure 4.16 Effect of protein kinase inhibitors (PKC, JNK 1/2 and p38 MAPK) on PACAP-27-induced TG2 activity in differentiating N2a and SH-SY5Y cells.

Differentiating N2a and SH-SY5Y cells were pre-treated for 30 min with Ro 31-8220 (10 µM), SP 600 125 (20 µM) or SB 203580 (20 µM) prior to stimulation with PACAP-27 (100 nM) for 10 min (N2a) and 30 min (SH-SY5Y). Cell lysates subjected to biotin-cadaverine incorporation (panels A and C) or peptide cross-linking assay (panels B and D). Data points represent the mean ± S.E.M. TG specific activity from four independent experiments. *P<0.05, ** P<0.01, *** P<0.001 and **** P<0.0001, (a) versus control and (b) versus 100 nM PACAP-27 alone.

It was important to assess the effect of the compounds used in this study; PACAP-27, PACAP 6-38, Ala-VIP, Bay55-9837 and protein kinase inhibitors on purified guinea pig liver TG2 activity. TG2 amine incorporating and peptide crosslinking assays were carried out using purified guinea pig liver TG2 (50 ng/ well) after incubated with the indicated concentrations of the compounds for 30 min then, subjected to the biotin-cadaverine incorporation or peptide cross-linking assays. As shown in Figure 4.17 the compounds used in this study had no significant effect on purified guinea pig liver TG2 activity. Overall, these data suggest that the activating of PAC_1 receptor with PACAP-27 stimulates TG2 activity in differentiating N2a and SH-SY5Y cells via a multi protein kinase-dependent pathway.

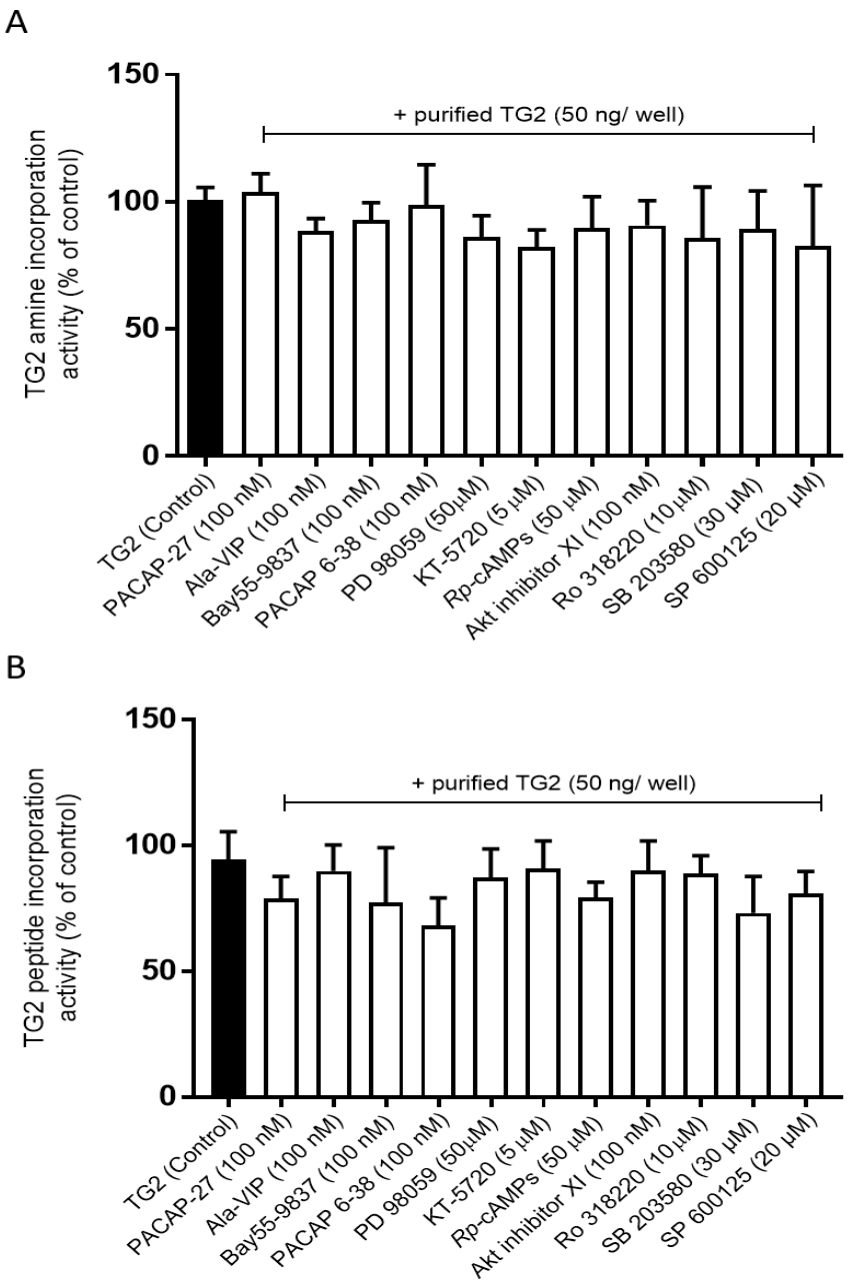

Figure 4.17 Effect of compounds used in this study on purified guinea pig liver TG2 activity.

TG2 amine incorporating (A) and peptide crosslinking (B) assays were carried out using purified guinea pig liver TG2 (50 ng/ well). Briefly, 50 ng of purified guinea pig liver TG2 was incubated with concentrations of the compounds as indicated for 30 min prior to 1 h incubation in presence of either 6.67 mM calcium chloride or 13.3 mM EDTA containing 225 μM biotin-cadaverine and 2mM 2-mercaptoethanol. Following incubation, the plates were processed as described in section 2.2.4 of chapter 2. Data points represent the mean ± S.E.M. TG2 specific activity from 4 independent experiments at basal level of purified guinea pig liver TG2 (control 100%).

4.2.5 The role of Ca^{2+} in PACAP-27 induced TG2 activity

Since TG2 is a Ca^{2+}-dependent enzyme, it was of interest to investigate the role of extracellular Ca^{2+} in TG2 activation. This was achieved by monitoring PACAP-27 induced TG2 activity in the absence of extracellular Ca^{2+} using nominally Ca^{2+}-free Hanks/HEPES buffer containing 0.1 mM EGTA. Removal of extracellular Ca^{2+} abolished PACAP-27-induced TG2 activation in differentiating N2a (Figure 4.18 A and B) and SH-SY5Y cells (Figure 4.18 C and D). In order to assess the role of intracellular Ca^{2+} in TG2 activities, differentiated cells were pre-treated with the Ca^{2+} chelator (BAPTA-AM, 50 µM) for 30 min in the absence of the extracellular Ca^{2+} prior to stimulation with PACAP-27 and measurement of TG2 activities. PACAP-27-induced TG2 activities were not further affected by Ca^{2+} chelating in the absence of extracellular Ca^{2+} (Figure 4.18). These observations suggest that PAC_1 receptor-induced TG2 activation is dependent upon extracellular Ca^{2+}.

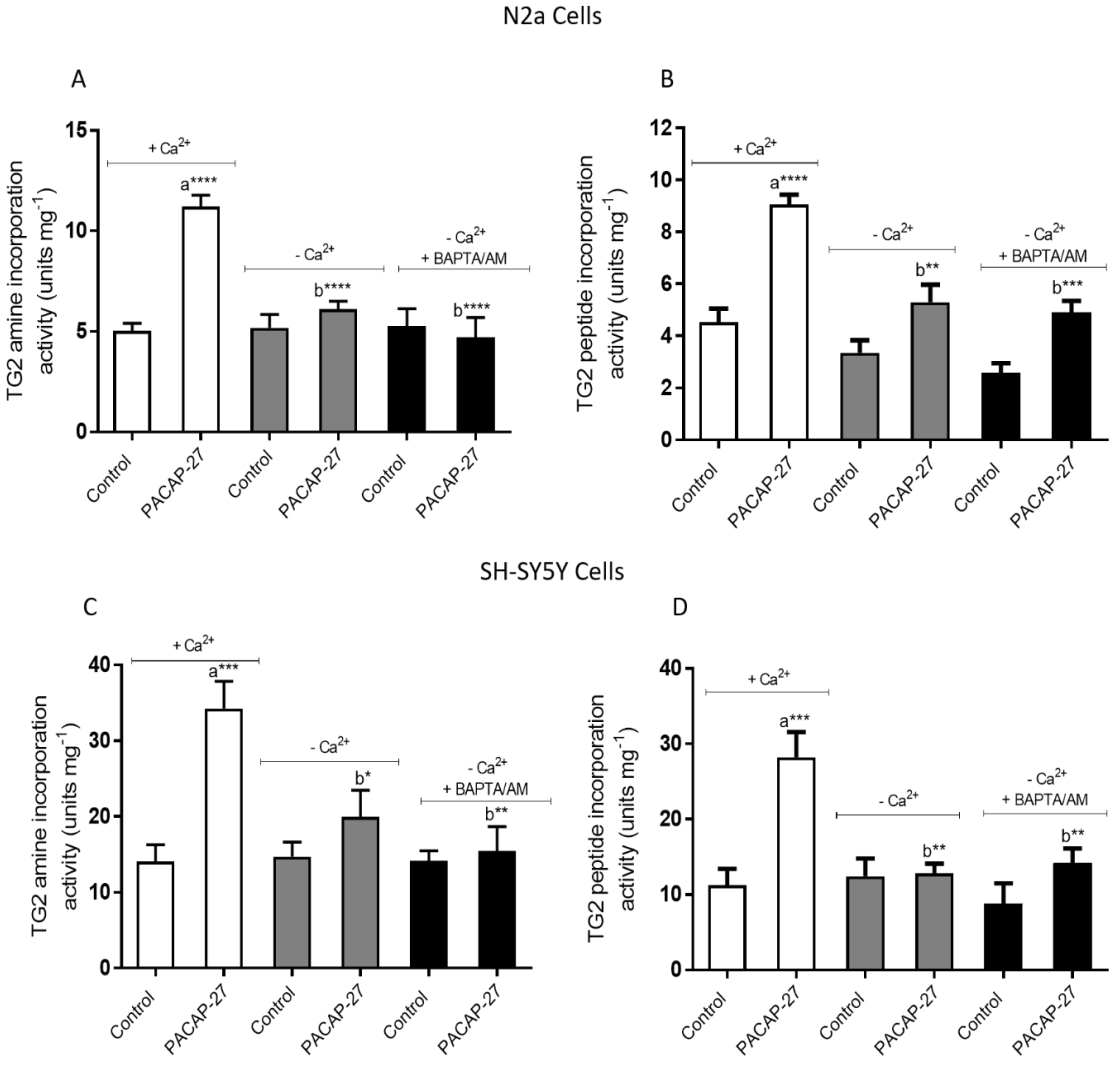

Figure 4.18 The role of intracellular and extracellular Ca^{2+} in PACAP-27-induced TG2 activity in differentiating N2a and SH-SY5Y cells.

Differentiating cells were treated with PACAP-27 for 10 min (N2a cells) and 30 min (SH-SY5Y cells) either in the presence (1.8 mM $CaCl_2$) or absence of extracellular Ca^{2+} (nominally Ca^{2+}-free Hanks/HEPES buffer containing 0.1 mM EGTA). Experiments were also performed using cells pre-incubated for 30 min with 50 µM BAPTA/AM and in the absence of extracellular Ca^{2+} (nominally Ca^{2+} -free Hanks/HEPES buffer containing 0.1 mM EGTA) to chelate intracellular Ca^{2+}. Cell lysates were subjected to biotin-cadaverine incorporation assay (A and C) or peptide cross-linking assay (B and D). Data points represent the mean TG specific activity ± S.E.M. from four independent experiments. *P<0.05, ** P<0.01, *** P<0.001 and **** P<0.0001, (a) versus control in presence of extracellular Ca^{2+}, (b) versus 100 nM PACAP-27 in presence of extracellular Ca^{2+}.

4.2.6 Visualisation of *in situ* TG2 activity

Since PACAP-27 was able to induce *in vitro* TG2 amine incorporation activity via a multi protein kinase dependent pathway, it was of interest to assess the capability of PACAP-27 to induce *in situ* TG2 activity using biotin-X-cadaverine, a cell penetrating primary amine, which enables the *in situ* visualisation of endogenous protein substrates of TG2, when combined with FITC-ExtrAvidin® (Lee et al., 1993). Differentiating cells were pre-incubated for 6 h with biotin-X-cadaverine prior to treatment with PACAP-27 (100 nM) for varying periods of time or various concentrations. After fixation and permeabilization, intracellular proteins with covalently attached biotin-X-cadaverine were visualised using FITC-ExtrAvidin® (section 2.2.5). The data from these experiments revealed that PACAP-27 induced a time-dependent increases in *in situ* TG2 activity peaking at 10 min in N2a (Figure 4.19 A and C) and 30 min in SH-SY5Y cells (Figure 4.20 A and C). These observations are similar to the pattern of *in vitro* TG2 activity (section 4.2.3). Similarly, PACAP-27 induced a concentration-dependent increase in TG2 *in situ* incorporation of biotin-X-cadaverine into endogenous protein substrates in differentiating N2a (EC_{50}= 6.7 ± 3 nM; pEC_{50} = 8.3 ± 0.2; n=3; Figure 4.19 B and D) and SH-SY5Y (EC_{50}= 0.82 ± 0.5 nM; pEC_{50} = 9.4 ± 0.4; n=3; Figure 4.20 B and D.) Finally, *in situ* responses to PACAP-27 were attenuated by the PAC_1 receptor selective antagonist (PACAP 6-38; 100 nM) and the TG2 inhibitors Z-DON (150 µM) and R283 (200 µM) in both cell lines (Figure 4.21 A and Figure 4.22 A) confirming that the induced activity was mediated by the PAC_1 receptor and TG2 is the responsible TG isoform of the observed activity. Overall, these data indicate that PACAP-27 induces a marked increase in TG2 *in situ* activity that is comparable to the pattern of TG2 activation observed *in vitro.*

The *in situ* responses to PACAP-27 were also significantly reversed by inhibitors of MEK1/2 (PD 98059, 50 µM), PKB (Akt Inhibitor XI, 100 nM), PKA (KT 5720, 5 µM), PKC (Ro 31-8220, 10 µM) and following removal of extracellular Ca^{2+} in N2a cells (Figure 4.21 B and C). Similarly, in SH-SY5Y cells, PACAP-27-mediated biotin-X-cadaverine incorporation into protein substrates was attenuated by PD 98059, Akt Inhibitor XI, KT 5720 but showed no significant inhibition with Ro 31-8220 or Ca^{2+} removal (Figure 4.22 B and C).

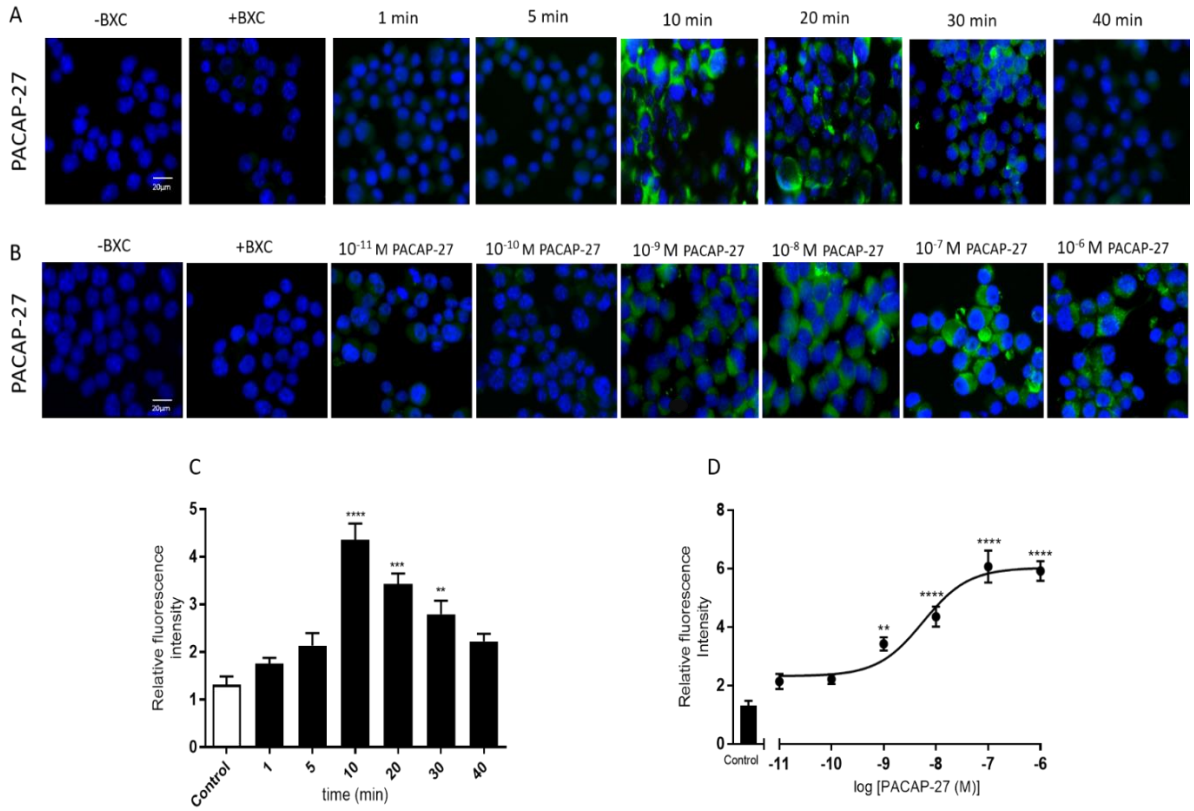

Figure 4.19 Effect of PACAP-27 on *in situ* TG2 activity in differentiating N2a cells.

Cells were incubated with 1 mM biotin-X-cadaverine (BXC) for 6 h, after which they were incubated with (A, C) 100 nM PACAP-27 for 1, 5, 10, 20, 30 or 40 min or (B, D) the indicated concentrations of PACAP-27 for 10 min. TG2-mediated biotin-X-cadaverine incorporation into intracellular proteins was visualized using FITC-conjugated ExtrAvidin® (green). Nuclei were stained with DAPI (blue) and viewed using a Leica TCS SP5 II confocal microscope (20x objective magnification). Images presented are from one experiment and representative of three. Quantified data represent the mean ± S.E.M. of fluorescence intensity relative to DAPI stain for five fields of view each from at least three independent experiments. **P<0.01, *** P<0.001 and ****P<0.0001 versus control response.

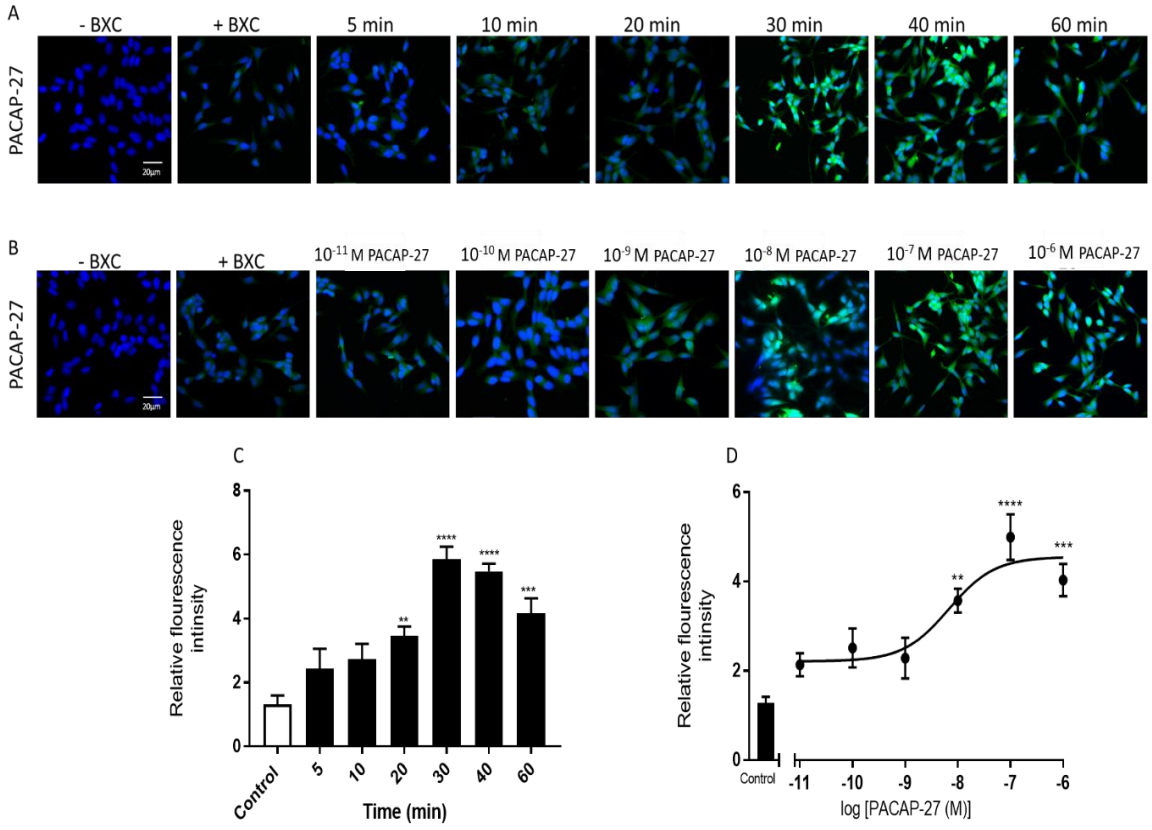

Figure 4.20 Effect of PACAP-27 on *in situ* TG2 activity in differentiating SH-SY5Y cells.

Cells were incubated with 1 mM biotin-X-cadaverine (BXC) for 6 h, after which they were incubated with (A) 100 nM PACAP-27 for 5, 10, 20, 30, 40 or 60 min or (B) the indicated concentrations of PACAP-27 for 30 min. TG2-mediated biotin-X-cadaverine incorporation into intracellular proteins was visualized using FITC-conjugated ExtrAvidin® (green). Nuclei were stained with DAPI (blue) and viewed using a Leica TCS SP5 II confocal microscope (20x objective magnification). Images presented are from one experiment and representative of three. Quantified data represent the mean ± S.E.M. of fluorescence intensity relative to DAPI stain for five fields of view each from at least three independent experiments. **P<0.01, *** P<0.001 and ****P<0.0001 versus control response.

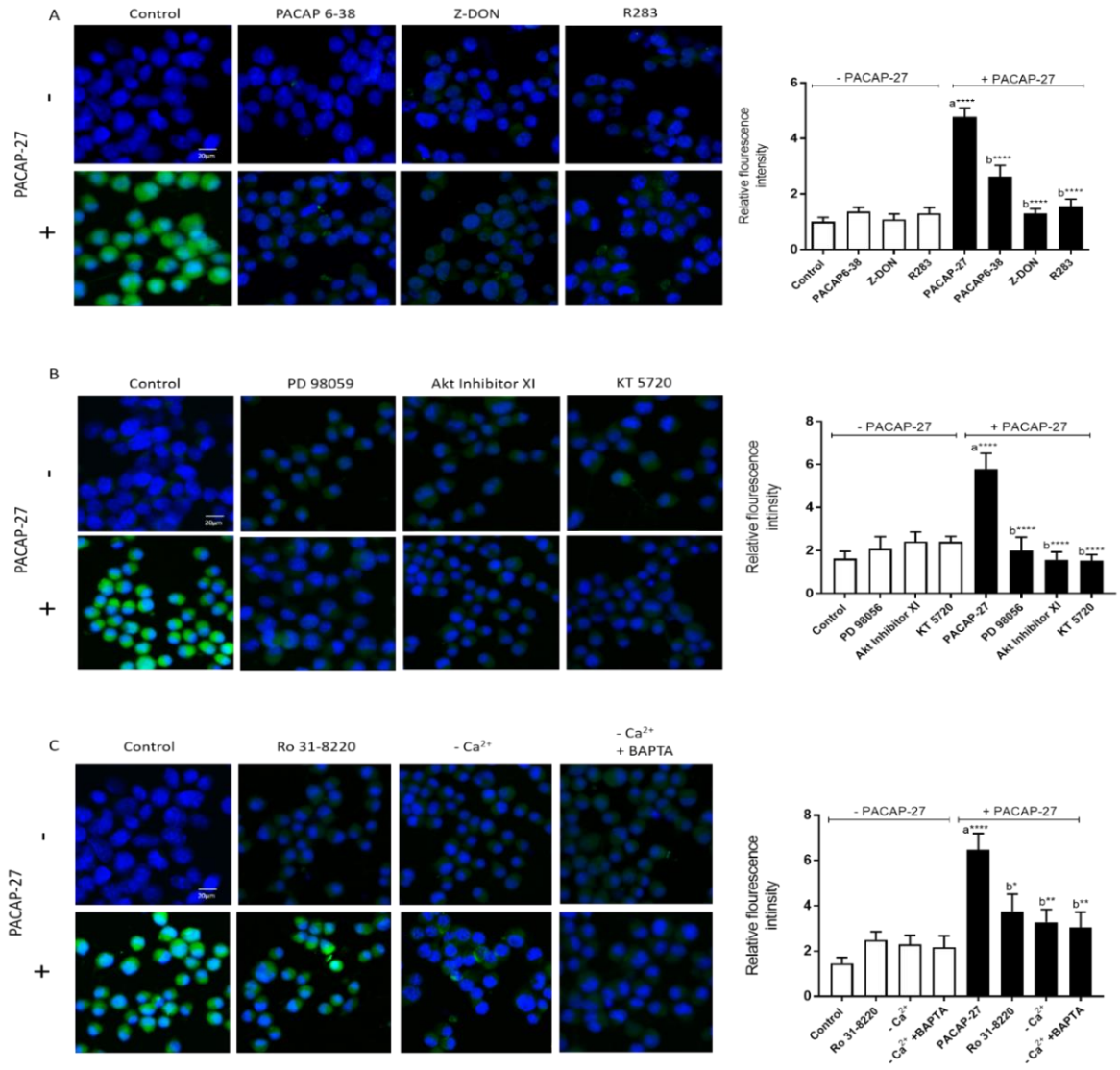

Figure 4.21 Effect of PAC_1 receptor antagonist, TG2 inhibitors, protein kinase inhibitors and removal of extracellular Ca^{2+} on PACAP-27-induced *in situ* TG2 activity in differentiating N2a cells.

Cells were incubated with 1 mM biotin-X-cadaverine (BXC) for 6 h, after which they were incubated with (A) the PAC_1 receptor antagonist PACAP6-38 (100 nM) for 30 min or for 1 h with TG2 inhibitors Z-DON (150 µM) and R283 (200 µM),(B) PD 98059 (50 µM), Akt Inhibitor XI (100 nM) and KT 5720 (5 µM) for 30 min, or (C) Ro 31-8220 (10 µM) for 30 min or in the absence of extracellular Ca^{2+} (nominally Ca^{2+}-free Hanks/HEPES buffer containing 0.1 mM EGTA) or pre-incubated for 30 min with 50µM BAPTA/AM and in the absence of extracellular Ca^{2+} (nominally Ca^{2+}-free Hanks/HEPES buffer containing 0.1 mM EGTA) prior to stimulation with PACAP-27 (100 nM) for 10 min. TG2-mediated biotin-X-cadaverine incorporation into intracellular proteins was visualized using FITC-conjugated ExtrAvidin® (green). Nuclei were stained with DAPI (blue) and viewed using a Leica TCS SP5 II confocal microscope (20x objective magnification). Scale bar = 20 µm. Images presented are from one experiment and representative of three. Quantified data represent the mean ± S.E.M. of fluorescence intensity relative to DAPI stain for five fields of view each from at least three independent experiments. *P<0.05, **P<0.01 and ****P<0.0001 versus control response.

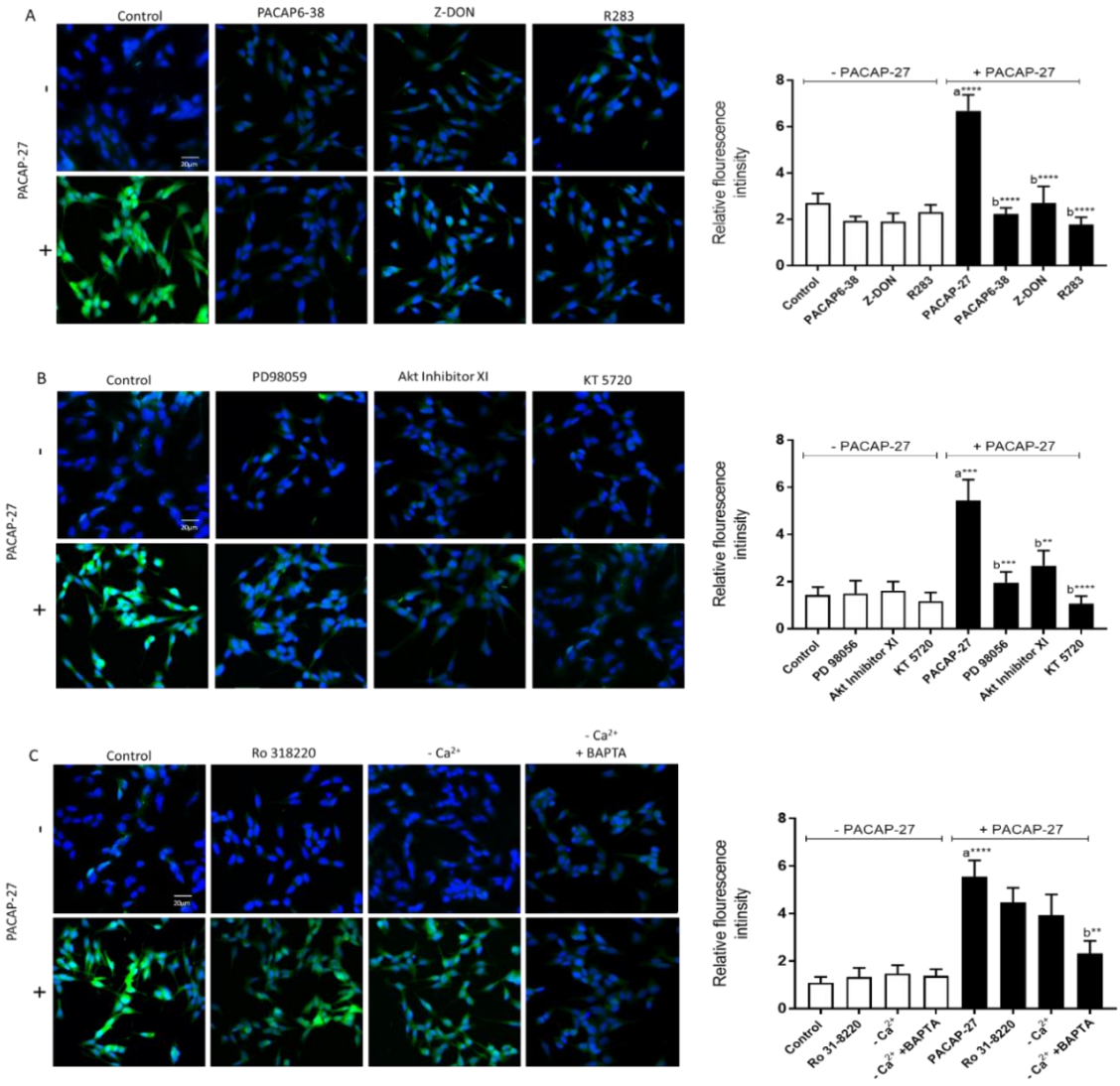

Figure 4.22 Effect of PAC_1 receptor antagonist, TG2 inhibitors, protein kinase inhibitors and Ca^{2+} on PACAP-27-induced *in situ* TG2 activity in differentiating SH-SY5Y cells.

Cells were incubated with 1 mM biotin-X-cadaverine (BXC) for 6 h, after which they were incubated with (A) the PAC_1 receptor antagonist PACAP6-38 (100 nM) for 30 min or for 1 h with TG2 inhibitors Z-DON (150 µM) and R283 (200 µM), (B) PD 98059 (50 µM) and Akt Inhibitor XI (100 nM) for 30 min, or (C) Ro 31-8220 (10 µM) for 30 min or in the absence of extracellular Ca^{2+} (nominally Ca^{2+}-free Hanks/HEPES buffer containing 0.1 mM EGTA) or pre-incubated for 30 min with 50µM BAPTA/AM and in the absence of extracellular Ca^{2+} (nominally Ca^{2+}-free Hanks/HEPES buffer containing 0.1 mM EGTA) prior to stimulation with PACAP-27 (100 nM) for 30 min. TG2-mediated biotin-X-cadaverine incorporation into intracellular proteins was visualized using FITC-conjugated ExtrAvidin® (green). Nuclei were stained with DAPI (blue) and viewed using a Leica TCS SP5 II confocal microscope (20x objective magnification). Scale bar = 20 µm. Images presented are from one experiment and representative of three. Quantified data represent the mean ± S.E.M. of fluorescence intensity relative to DAPI stain for five fields of view each from at least three independent experiments. **P*<0.05, ***P*<0.01, *** *P*<0.001 and *****P*<0.0001 versus control response.

4.2.7 Phosphorylation of TG2 following PAC_1 receptor activation with PACAP-27

The effect of PAC_1 receptor activation on the phosphorylation status of TG2 was monitored via immunoprecipitation of TG2 followed by SDS-PAGE and Western blot analysis using anti-phosphoserine and anti-phosphothreonine antibodies. PACAP-27 (100 nM) triggered a robust increase in the levels of TG2-bound phosphoserine and phosphothreonine in N2a (Figure 4.23 and 4.25) and SH-SY5Y cells (Figure 4.24 and 4.26). Pre-treatment with PD 98059 (50 µM) and KT 5720 (5 µM) attenuated PACAP-27-mediated increases in TG2 phosphorylation in differentiating N2a (Figure 4.23) and SH-SY5Y cells (Figure 4.24). In contrast, Ro 318220 (10 µM) had no significant effect in either cell line (Figure 4.25 and Figure 4.26). Finally, removal of extracellular Ca^{2+} partially attenuated PACAP-27-induced TG2 phosphorylation in N2a but had no significant effect in SH-SY5Y cells (Figure 4.25 and Figure 4.26). These data indicate that activation of the PAC_1 receptor promotes robust increases in TG2 phosphorylation and this process is mainly ERK1/2 and PKA dependent.

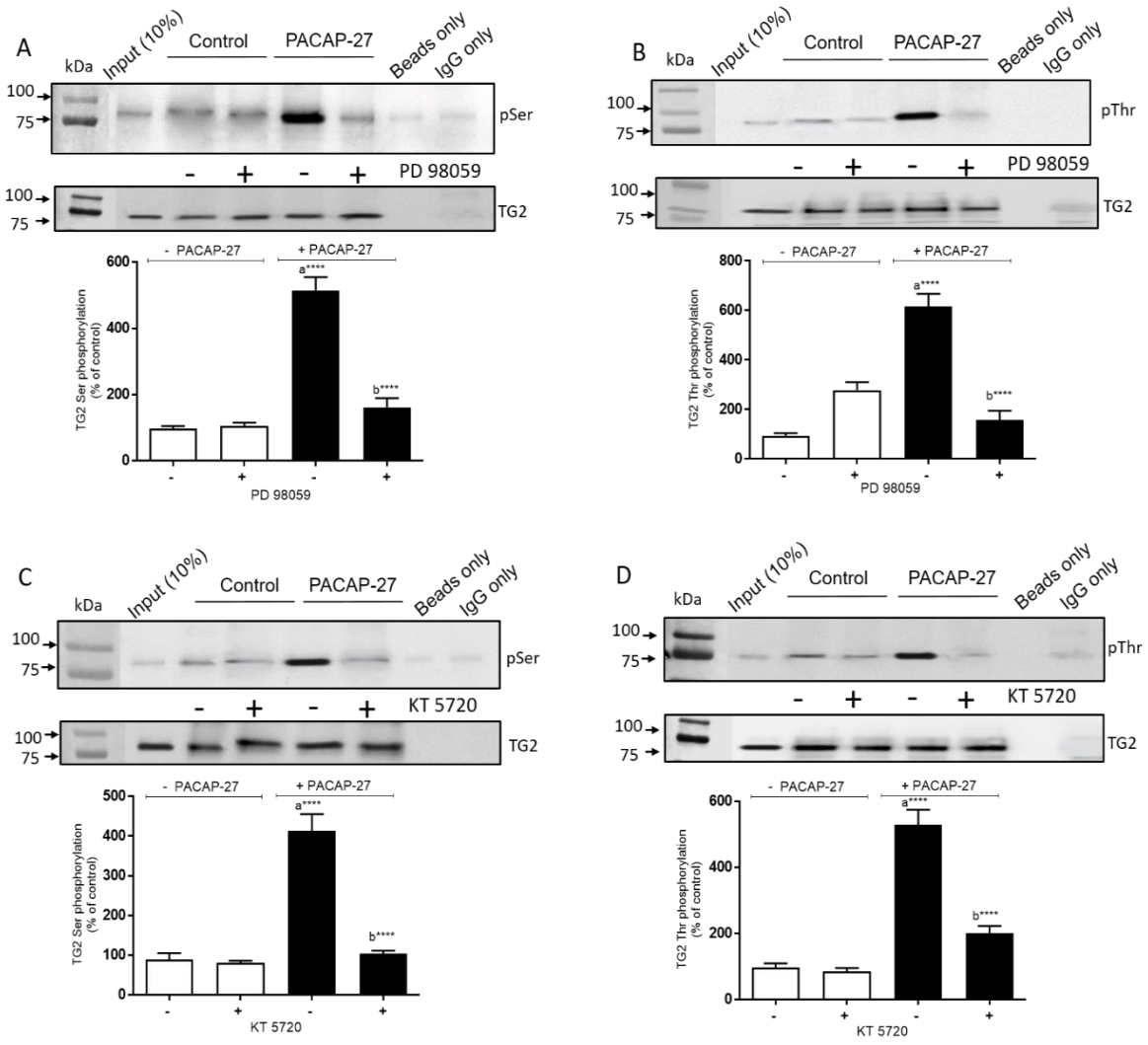

Figure 4.23 Effect of the ERK1/2 inhibitor (PD 98059) and PKA inhibitor (KT 5720) on PACAP-27-induced phosphorylation of TG2 in differentiating N2a cells.

Where indicated, differentiating N2a cells were pre-treated for 30 min with PD 98059 (50 µM) or KT 5720 (5 µM) prior to stimulation with PACAP-27 (100 nM) for 10 min. Following stimulation with PACAP-27, cell lysates were subjected to immunoprecipitation using anti-TG2 monoclonal antibody as described in section 2.2.10. The resultant immunoprecipitated protein(s) were subjected to SDS-PAGE and Western blot analysis using anti-phosphoserine (panels A and C) and anti-phosphothreonine (panels B and D) antibodies. One tenth of the total input was applied to the first lane to show the presence of phosphorylated proteins prior to immunoprecipitation and negative controls with the immunoprecipitation performed with immunobeads only were included to demonstrate the specificity of the band shown. Quantified data for PACAP-induced increases in TG2-bound serine and threonine phosphorylation are expressed as a percentage of the TG2 phosphorylation observed in control cells (=100%). Levels of TG2 are shown for comparison as internal loading control. Data points represent the mean ± S.E.M. from three independent experiments. ****P<0.0001 (a) versus control and (b) versus 100 nM PACAP-27 alone.

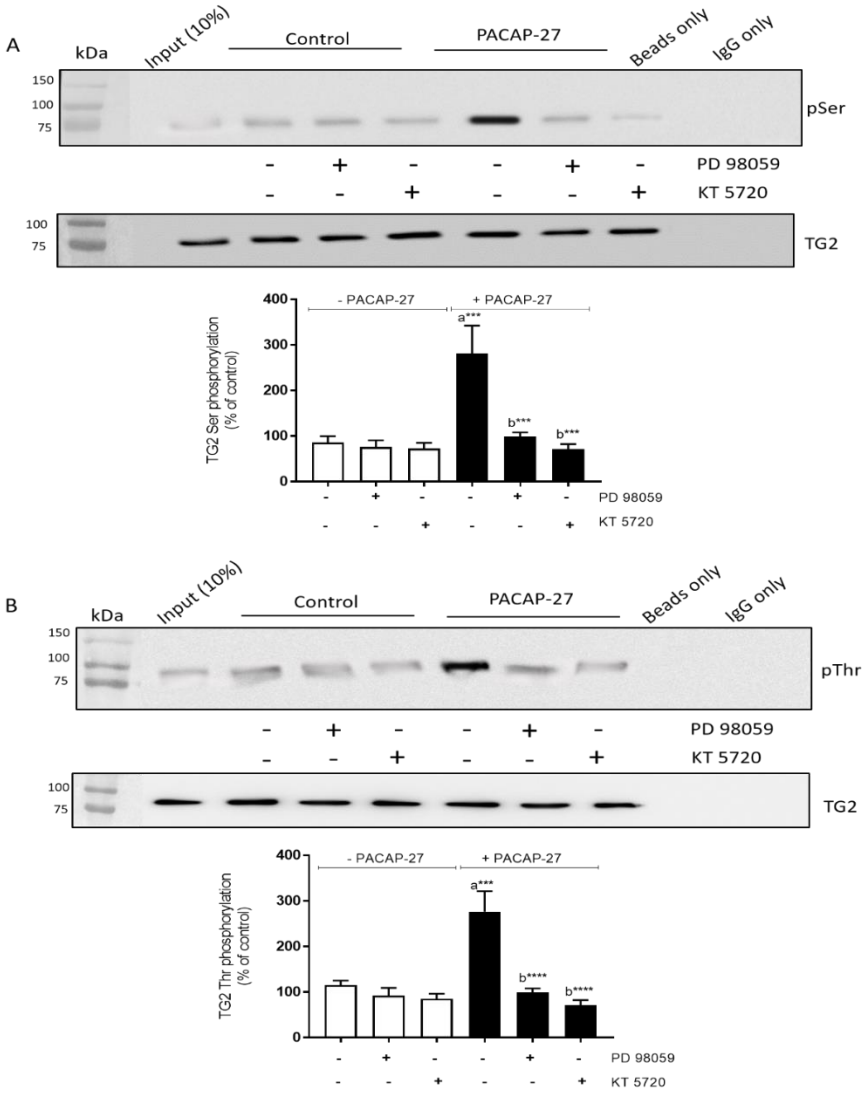

Figure 4.24 Effect of the ERK1/2 inhibitor (PD 98059) and PKA inhibitor (KT 5720) on PACAP-27-induced phosphorylation of TG2 in differentiating SH-SY5Y cells.

Where indicated, differentiating SH-SY5Y cells were pre-treated for 30 min with PD 98059 (50 µM) or KT 5720 (5 µM) prior to stimulation with PACAP-27 (100 nM) for 30 min. Following stimulation with PACAP-27, cell lysates were subjected to immunoprecipitation using anti-TG2 monoclonal antibody as described in section 2.2.10. The resultant immunoprecipitated protein(s) were subjected to SDS-PAGE and Western blot analysis using (A) anti-phosphoserine and (B) and anti-phosphothreonine antibodies. One tenth of the total input was applied to the first lane to show the presence of phosphorylated proteins prior to immunoprecipitation and negative controls with the immunoprecipitation performed with immunobeads only were included to demonstrate the specificity of the band shown. Quantified data for PACAP-induced increases in TG2-bound serine and threonine phosphorylation are expressed as a percentage of the TG2 phosphorylation observed in control cells (=100%). Levels of TG2 are shown for comparison as internal loading control. Data points represent the mean ± S.E.M. from three independent experiments. ***P<0.001 and ****P<0.0001 (a) versus control and (b) versus 100 nM PACAP-27 alone.

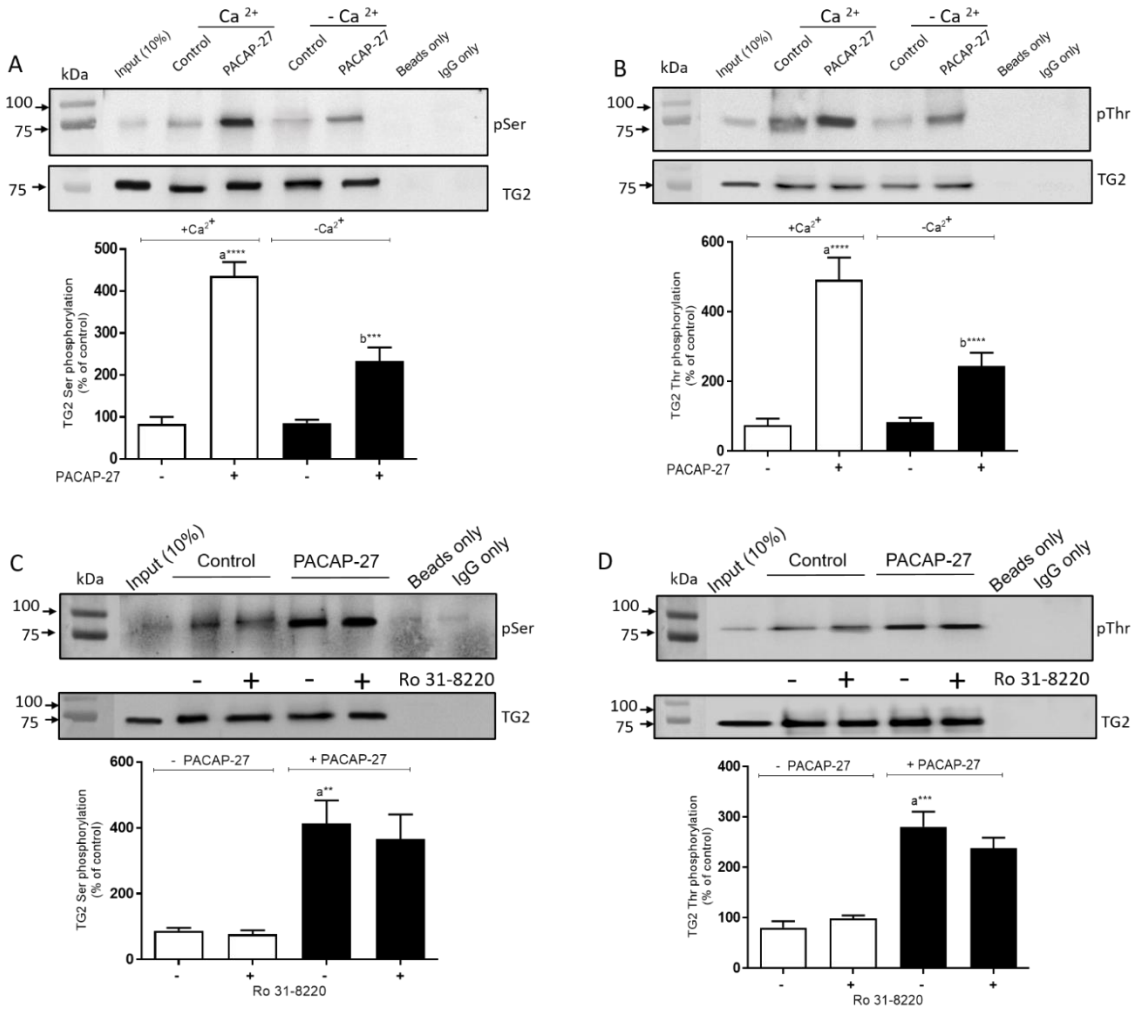

Figure 4.25 Effect of the Ca^{2+} and PKC inhibitor (Ro 31-8220) on PACAP-27-induced phosphorylation of TG2 in differentiating N2a cells.

Where indicated, differentiating N2a cells were subjected to the absence of extracellular Ca^{2+} (nominally Ca^{2+}-free Hanks/HEPES buffer containing 0.1 mM EGTA) or pre-treated for 30 min with Ro 31-8220 (10 µM) prior to stimulation with PACAP-27 (100 nM) for 10 min. Following stimulation with PACAP-27, cell lysates were subjected to immunoprecipitation using anti-TG2 monoclonal antibody as described in section 2.2.10. The resultant immunoprecipitated protein(s) were subjected to SDS-PAGE and Western blot analysis using anti-phosphoserine (panels A and C) and anti-phosphothreonine (panels B and D) antibodies. One tenth of the total input was applied to the first lane to show the presence of phosphorylated proteins prior to immunoprecipitation and negative controls with the immunoprecipitation performed with immunobeads only were included to demonstrate the specificity of the band shown. Quantified data for PACAP-induced increases in TG2-bound serine and threonine phosphorylation are expressed as a percentage of the TG2 phosphorylation observed in control cells (=100%). Levels of TG2 are shown for comparison as internal loading control. Data points represent the mean ± S.E.M. from three independent experiments. ****P<0.0001 (a) versus control and (b) versus 100 nM PACAP-27 alone.

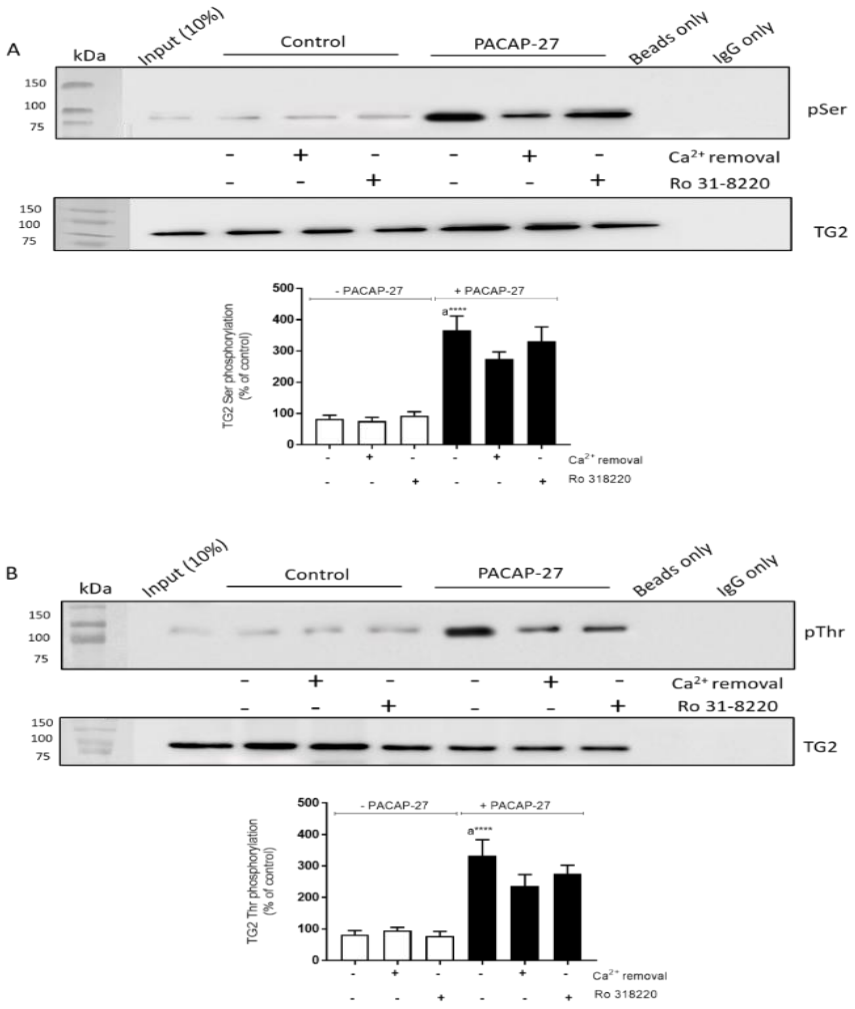

Figure 4.26 Effect of the Ca^{2+} and PKC inhibitor (Ro 31-8220) on PACAP-27-induced phosphorylation of TG2 in differentiating SH-SY5Y cells.

Where indicated, differentiating SH-SY5Y cells were subjected to the absence of extracellular Ca^{2+} (nominally Ca^{2+}-free Hanks/HEPES buffer containing 0.1 mM EGTA) or pre-treated for 30 min with Ro 31-8220 (10 µM) prior to stimulation with PACAP-27 (100 nM) for 30 min. Following stimulation with PACAP-27, cell lysates were subjected to immunoprecipitation using anti-TG2 monoclonal antibody as described in section 2.2.10. The resultant immunoprecipitated protein(s) were subjected to SDS-PAGE and Western blot analysis using anti-phosphoserine (A) and anti-phosphothreonine (B) antibodies. One tenth of the total input was applied to the first lane to show the presence of phosphorylated proteins prior to immunoprecipitation and negative controls with the immunoprecipitation performed with immunobeads only were included to demonstrate the specificity of the band shown. Quantified data for PACAP-induced increases in TG2-bound serine and threonine phosphorylation are expressed as a percentage of the TG2 phosphorylation observed in control cells (=100%). Levels of TG2 are shown for comparison as internal loading control. Data points represent the mean ± S.E.M. from three independent experiments. **P<0.01, ***P<0.001 and ****P<0.0001 (a) versus control and (b) versus 100 nM PACAP-27 alone.

4.3 Discussion

In this study, the modulation of TG2 activity by the neurotrophic factor PACAP-27 through PAC_1 receptor was investigated in differentiating mouse (N2a) and human (SH-SY5Y) neuroblastoma cells and the molecular mechanisms underlying this modulation were determined. PAC_1 receptor agonist; PACAP-27, TG2 inhibitors, PAC_1 receptor antagonist and different protein kinase inhibitors were used to assess the *in vitro* and *in situ* TG2 activity and to investigate the pathways involved. The results provide evidence that PACAP-27 modulates TG2 activity in differentiating N2a and SHSY5Y cells occurs via a multi protein kinase dependent pathways.

4.3.1 Modulation of TG2 transamidation activity by PACAP-27

Functional expression of PAC_1 receptors on differentiating N2a and SH-SY5Y

Previous studies have been reported that the PAC_1 receptor is expressed in mitotic N2a, and both mitotic and differentiating SH-SY5Y cells (Lelièvre et al., 1998; Lutz et al., 2006; Miura et al., 2013). Initially in the current study, functional expression of the PAC_1 receptor was investigated in differentiating N2a and SH-SY5Y cells, first via measuring cAMP accumulation and mediating of Ca^{2+} signalling. Hence, this study has demonstrated functional expression of the PAC_1 receptor in N2a and SH-SY5Y cells induced to differentiate with retinoic acid. The results revealed the potential ability of PACAP-27 to mediate robust activation of cAMP production (up to 60-fold of basal activity) with potencies of approximately 4 nM and 2.8 nM in differentiating N2a and SH-SY5Y cells respectively. Live calcium imaging enabled further characterisation of the functional expression of the PAC_1 receptor in differentiating N2a and SH-SY5Y cells. Previous studies have shown that the PAC_1 receptor promotes Ca^{2+} mobilization from intracellular stores and Ca^{2+} influx via N-type calcium channels in rat cerebellar granule cells (Basille-Dugay et al., 2013). The data presented in the current work support these findings by showing that PACAP-27-triggered Ca^{2+} responses were abolished in the absence of extracellular Ca^{2+}, which is indicative of extracellular Ca^{2+} influx as the intracellular stores were still intact. In order to confirm the involvement of PAC_1 receptor in mediating these Ca^{2+} responses, the PAC_1 receptor selective antagonist (PACAP 6-38) was used. As expected, PACAP-27 induced Ca^{2+} responses were attenuated by the PAC_1 receptor antagonist in both cell lines, confirming the involvement of PAC_1 receptor. Overall, these data

demonstrated the functional expression of the PAC_1 receptor in differentiating N2a and SH-SY5Y neuroblastoma cells. These findings are broadly comparable to those shown in another neuroblastoma cells model N1E 115, where PACAP-27 stimulates cAMP accumulation and increases $[Ca^{2+}]_i$ through the PAC_1 receptor (Chik et al., 1996).

Modulation of TG2 transamidation activity by PACAP-27

The neurotrophic factor PACAP mediates neurite outgrowth and neuroprotection; however, it is not known if these events involve PAC_1 receptor-induced TG2 activation (Monaghan et al., 2008; Manecka et al., 2013; Jóźwiak-Bębenista et al., 2015). It has been shown that TG2 is regulated by signaling pathways associated with GPCRs such as PKC and PKA in rat H9c2 cardiomyoblasts (Almami et al., 2014) and further investigation has shown A_1 adenosine receptor-mediated increases in TG2 transamidase activity in the same cell line (Vyas et al., 2016). Hence, it was of interest to investigate whether PACAP could modulate TG2 transamidase activity via the PAC_1 receptor in neuroblastoma cell lines prior to assessing the possible neuroprotection role.

TG2 can catalyse two types of transamidation, namely (i) intra-, and/or inter-molecular covalent cross-links between protein-bound glutamine and protein-bound lysine residues, and (ii) cross-links between primary amines and protein-bound glutamine (Nurminskaya and Belkin, 2013). In the current study the PAC_1 receptor agonist PACAP-27 triggered time- and concentration-dependent increases in TG2-mediated biotin-cadaverine incorporation and peptide cross-linking activity in differentiating N2a and SH-SY5Y cells. The EC_{50} values for PACAP-27-mediated transglutaminase-catalysed amine incorporation (0.08 nM in N2a and 2.2 nM in SH-SY5Y) and protein cross-linking activity (0.4 nM in N2a and 1.3 nM in SH-SY5Y) are in-line with the affinity of PACAP-27 for the PAC_1 receptor (Dickson et al., 2006; Dickson and Finlayson, 2009; Harmar et al., 2012). Interestingly, the response was peaking at 10 min in N2a and 30 min in SH-SY5Y cells, also the potency of PACAP-27 in N2a cells was significantly higher than in human SH-SY5Y neuroblastoma cells, suggesting that the N2a cells are more sensitive than SHSY5Y cells to this neuropeptide. These findings are similar to those reported in previous work on N2a and SH-SY5Y cells, indicated that mouse N2a cells are more sensitive than human SH-SY5Y neuroblastoma in cytotoxic assessment study (Li et al., 2007; Sahu et al., 2013). This could be attributed to species dependent differences in the sensitivity of the signalling cascades activated via the PAC_1 receptor.

The findings in this section were confirmed by using an immunocytochemistry-based assay that enabled fluorescence microscopy visualisation of *in situ* TG2 activity. Increases in *in situ* TG2

activity following PAC_1 receptor stimulation with the PACAP-27 occurred in a time- and concentration- dependent manner. However, given the covalent nature of biotin-X-cadaverine incorporation into protein substrates, it was surprising to observe that *in situ* TG2 activity returned to basal levels after 40 min. Possible explanations for this include reversal of amine incorporation by TG itself (Stamnaes et al. 2008), targeting of modified proteins for degradation or their rapid removal from the cell. Previous studies have reported the rapid expulsion of biotinylated proteins from H9c2 cells following treatment with PMA or forskolin (Almami et al. 2014). It could be that the rapid expulsion of biotinylated proteins from neuroblastoma cells occurs via exosomes (Kalani et al. 2014). Since neuroblastoma cells secrete exosomes it will be interest to determine whether amine-labelled proteins can be detected in exosomes purified from cell culture supernatants obtained from these cells following PACAP-27 treatment (Chivet et al. 2014).

Selectivity of PACAP-27 to PAC_1 receptor in modulation of TG2 activity

It is known that PACAP and its structurally related neuropeptide VIP act through the three GPCRs, namely PAC_1, $VAPC_1$ and $VAPC_2$ receptors, with varying potencies (Monaghan et al., 2008; Harmar et al., 2012). The naturally occur peptide PACAP has 100-fold greater potency than VIP for the PAC_1 receptor (Lutz et al., 2006; Dickson and Finlayson 2009). The only available selective agonist for PAC_1 receptor is maxadilan (Uchida et al., 1998), which was isolated from salivary gland of sand flies and is structurally unrelated to PACAP/VIP (Lerner et al., 1991). It is a 61-amino acid peptide with three disulfide-bonds but is rarely used as it is difficult to synthesize (Harmar et al., 2012). A previous study aimed to develop PAC_1 receptor selective agonists by designing PACAP analogues that were conformationally restricted for their receptor-selectivity position (Ramos-A`lvarez et al., 2015). However, the variety of PAC_1 receptor splice-variants and their differences in affinities/potencies for PACAP-27/PACAP-38, as well as the high sequence identity (68%) between VIP and PACAP27, made the process particularly difficult (Ramos-A‘lvarez et al., 2015). Hence, in the current study it was necessary to examine the PAC_1 receptor specificity for induction of TG2 activity. Experiments were performed with the $VAPC_1$ and $VAPC_2$ receptor-specific agonists Ala-VIP and Bay 55-9837, respectively. The data presented indicated that Ala-VIP and Bay 55-9837 had no significant effect on cAMP accumulation or TG2 transamidase activity. The findings confirm that the TG2 responses obtained occur via the PAC_1 receptor in differentiating N2a and SH-SY5Y. Further investigation used the PAC_1 receptor antagonist PACAP 6-38 (Robberecht et al., 1992) which blocked PACAP-27-induced TG2 activity, confirming that the induced activity was via the

PAC_1 receptor. It is important to note that PACAP 6-38 also displays high affinity for the $VPAC_2$ receptor (Dickinson et al.,1997); however, since the $VPAC_2$ agonist Bay 55-9837 did not trigger increased TG2 activity, it is likely that the effects of PACAP 6-38 are mediated entirely via the PAC_1 receptor. Finally, PAC_1 receptor-induced increases in TG2 activity were inhibited by R283 and Z-DON, structurally different TG2 inhibitors, confirming that the observed increases in TG activity were via TG2. It is important to note that the inhibition effect of these TG2 inhibitors on cellular TG2 is only achieved at a concentration significantly higher than their IC50 value versus purified enzyme (Freund et al., 1994; Schaertl et al., 2010). The observed increases in *in situ* TG2 responses induced by PACAP-27 were also reversed by the PAC_1 receptor antagonist PACAP 6-38, confirming the role of the PAC_1 receptor in the reported TG2 activity. Furthermore, the TG2 *in situ* PACAP-27-induced polyamine incorporation was sensitive to TG2 inhibitors Z-DON and R283, further confirming that TG2 is the TG isoform responsible for the observed activity. Since differentiating N2a and SH-SY5Y cells also express TG1 and TG3 isoforms (Chapter 3), it would be of interest to investigate if PACAP-27 also regulates the activity of these enzymes. It is difficult to establish an assay for discriminating between the different TG isoform activities; however Hitomi et al. (2009) have established a highly sensitive colorimetric assay using selective substrate peptides to some of the TG isoforms (Hitomi et al., 2009). It would be interesting in future work to use such substrates to determine whether the other TGs isoform are also regulated by PACAP-27 in neuroblastoma cells; such types of future testing paradigms could help to assess the possible differences in responses and sensitivity of TG1 and TG3 to PACAP-27 and the related alterations in cell signalling. However, in the current study, the improved understanding of function and role of TG2 in PACAP-27-induced neurite outgrowth and cell survival suggests that TG2 represents a potential target.

4.3.2 Role of protein kinases

There is increasing evidence showing that TG2 activity can be modulated by different kinases such as ERK1/2 and PKC in different models (Bollag et al., 2005; Mishra et al., 2007; Almami et al., 2014). However, there is very little known about the role of protein kinases in modulating TG2 activity in differentiating mouse N2a and human SH-SY-5Y neuroblastoma cells. To determine whether various protein kinase signaling pathways were involved in PACAP-27-induced TG2 activity, the current study investigated the effect different protein kinase inhibitors on PACAP-27 induced modulation of protein kinase phosphorylation and PACAP-27-induced TG2 activity. It was presumed that activation of the PAC_1 receptor would induce activation of

ERK1/2, p38 MAPK (Monaghan et al., 2008), PKA (Dickson & Finlayson, 2009; Vaudry et al., 2009), PKC (May et al., 2014), and PKB (May et al., 2010; Castorina et al., 2014) signalling pathways. In the current study it appears that PACAP-27-induced the activation of ERK1/2 and PKB in both neuroblastoma cell lines. However, the activation of p38 MAPK by PACAP-27 was shown only in human neuroblastoma SH-SY5Y cells and the activation of JNK1/2 was shown in N2a cells only. These findings could be attributed to species dependent differences in the signalling cascades activated via the PAC_1 receptor. These findings were also consistent with the observed reduction of PACAP-27-induced TG2-medaited amine incorporation and peptide crosslinking activity by pharmacological inhibition of the protein kinases. The MEK1/2 (upstream activator of ERK1/2) inhibitor PD 98059 and Akt inhibitor XI significantly blocked PACAP-27-induced TG2 activity, suggesting a prominent role for ERK1/2 and PKB. While, SP 600125 (JNK1/2 inhibitor; Figure 4.16) and SB 203580 (p38 MAPK inhibitor; Figure 5B) had no significant effect on TG2 activity in either cell line.

The phosphorylation of TG2 by PKA inhibits its transamidating activity but augments its kinase activity (Mishra et al. 2007). These contrasting effects on TG2 activity were obtained using histidine-tagged TG2 immobilized on nickel-agarose and incubated with the catalytic subunit of PKA. In the current study, the PKA inhibitors KT 5720 and Rp-cAMPs completely blocked PACAP-27-induced TG2 transamidating activity, which reflects PAC_1 receptor signaling via cAMP/PKA. The PAC_1 receptor also activates PLC/DAG/PKC (via Gq-protein coupling) signalling and hence the role of PKC was investigated. The broad-spectrum PKC inhibitor Ro 318220 inhibited PACAP-27-induced TG2 activity, indicating that Gq-protein coupling is involved in PAC_1 receptor-mediated TG2 activation in N2a cells. The observed response is in good agreement with that noted in H9c2 cells, where the A_1 adenosine receptor-mediated activation of TG2, was also sensitive to ERK1/2 and PKC inhibition (Vyas et al., 2016). In transfected HEK293 cells, PAC_1 receptor-induced ERK1/2 is dependent upon calcium influx and PLC/DAG/PKC (May et al., 2014) and hence the inhibition of PACAP-27-induced TG2 activity by removal of extracellular Ca^{2+} and inhibition of PKC may reflect their up-stream role(s) in ERK1/2 activation. However, in the current study, PAC_1 receptor-induced ERK1/2 activation was found to be independent of Ca^{2+} influx in both cell lines and partially sensitive to PKC inhibition in N2a cells and PKC-independent in SH-SY5Y cells. Similarly, PKA can activate ERK1/2 (Stork and Schmitt, 2002) and therefore the effect of PKA inhibitors on PAC_1 receptor TG2 activation may also reflect the up-stream role of PKA in ERK1/2 activation. In guinea-pig cardiac neurons PAC_1 receptor-induced ERK1/2 activation is PKA-independent (Clason et al., 2016). In the current study, PAC_1 receptor-induced ERK1/2 signalling was shown

to be PKA-dependent in both neuroblastoma cell lines. Hence, PKA-mediated inhibition of TG2 activation may indeed reflect the up-stream role of PKA in ERK1/2 activation.

Role of protein kinases in PACAP-27-mediated in situ TG2 activation

PACAP-27 induced *in situ* TG2 responses were also blocked by pharmacological inhibition of MEK1/2 (PD 98059), PKB (Akt inhibitor XI) and PKA (KT 5720) (figures 4.21 and 4.22), further confirming the role of these signalling pathways. The finding also demonstrates that the observed response was attenuated by PKC (Ro 31-8220) and removal of Ca^{2+} in N2a cells but not in SH-SY5Y cells. Overall these observations are comparable to PACAP-27-induced TG2 activation observed *in vitro*. As previously discussed, the conflicting data as to whether PKC plays a role in PACAP-27-induced TG2 activity in differentiating N2a cells, suggests that PKC may regulate targets involved in TG2 activation other than the targets assessed in this study. Furthermore, the effective role of Ca^{2+} removal was observed only in mouse N2a cells. These finding suggest that, in differentiating N2a cells, PACAP-27 stimulates the PAC_1 receptor to modulate TG2 activity either via G_s protein leading to activation of adenylyl cyclase/cAMP/PKA or through phospholipase C/DAG/PKC via G_q protein coupling-dependent signalling pathways. In contrast, TG2 responses in human neuroblastoma SH-SY5Y cells are insensitive to either PKC inhibition or removal of Ca^{2+} and display higher sensitivity to PKA inhibition, suggesting that the ability of PAC_1 receptor to induced TG2 activity is mainly via G_s protein dependent adenylyl cyclase/cAMP/PKA-signalling in human neuroblastoma cells. The effect of protein kinase inhibitors on PACAP-27-induced TG2 activation in summarized in Figure 4.27 and Table 4.1.

Role of protein kinases in PACAP-27-mediated TG2 phosphorylation

Since Vyas et al., (2016) showed that TG2 was phosphorylated following activation of the A_1 adenosine receptor in H9c2 cells (Vyas et al., 2016), it was of interest to examine the phosphorylation status of TG2 following activation of the PAC_1 receptor with PACAP-27. The data presented in the current study demonstrate that TG2 is phosphorylated following PAC_1 receptor activation. Furthermore, PAC_1 receptor-induced TG2 phosphorylation was attenuated by pharmacological inhibition of MEK1/2 and PKA in both neuroblastoma cell lines and by removal of extracellular Ca^{2+} in N2a cells only. It is not clear how the absence of extracellular Ca^{2+} blocks TG2 phosphorylation since the PAC_1 receptor-induced ERK1/2 activation is independent of Ca^{2+} influx in N2a cells. One possible explanation is that changes in $[Ca^{2+}]_i$ promote conformational changes in TG2 that facilitate its phosphorylation by protein kinase(s).

Alternatively, Ca^{2+} influx may play a role in augmenting PAC_1 receptor-induced PLC/PKC signalling. However, the fact that the PKC inhibitor Ro 31-8220 did not block TG2 phosphorylation, suggests that PKC may regulate other targets involved in TG2 activation. The next logical step would be to identify the specific site(s) of TG2-associated serine and threonine phosphorylation. In human cells, various TG2 phosphorylation sites have been identified namely Ser^{56}, Ser^{60}, Tyr^{219}, Thr^{368}, Tyr^{369}, Ser^{419}, Ser^{427}, Ser^{538}, Ser^{541} and Ser^{608} (Rikova et al., 2007; Imami et al., 2008; Kettenbach et al., 2011; Bian et al., 2014). Previous studies have shown that TG2 is phosphorylated by PKA at Ser^{215} and Ser^{216} (Mishra and Murphy, 2006) and at an unknown site(s) by PTEN-induced putative kinase 1 (PINK1; Min et al., 2015). At present the precise role of PAC_1 receptor-induced TG2 phosphorylation is not known. However, PKA-mediated phosphorylation of TG2 enhances its interaction with the scaffolding protein 14-3-3 and increases TG2 kinase activity, whereas PINK1-mediated phosphorylation of TG2 blocks its proteasomal degradation (Mishra and Murphy, 2006; Mishra et al., 2007; Min et al., 2015). It is also conceivable that TG2 phosphorylation sensitizes TG2 to low levels of intracellular $[Ca^{2+}]_i$ or alters its subcellular location. Further work to determine the functional consequences of PAC_1 receptor-induced TG2 phosphorylation would be of value.

Role of Ca^{2+} in PACAP-27-mediated TG2 activation

Previous studies have shown that PACAP-induced increases in $[Ca^{2+}]_i$ are blocked by the PAC_1 receptor antagonist PACAP 6–38 in human fetal chromaffin cells (Payet et al., 2003). In the current study, PACAP-27-triggered Ca^{2+} responses in neuroblastoma cell lines loaded with Fluo-8 AM were abolished in the absence of extracellular Ca^{2+}, which is indicative of Ca^{2+} influx. The transamidating activity of TG2 is dependent upon Ca^{2+}, which promotes the "open" form of TG2 and negates the inhibitory actions of the nucleotides GTP, GDP and ATP (Király et al., 2011). Previous studies have shown that release of Ca^{2+} from intracellular Ca^{2+} stores or influx of extracellular Ca^{2+} is linked to TG activation in response to GPCR stimulation (Zhang et al., 1998; Walther et al., 2003; Vyas et al., 2016). The data presented in the current work indicate that PAC_1 receptor-induced TG2 transamidase activity is dependent upon extracellular Ca^{2+}. Clearly, further studies are required to determine the mechanism(s) of PAC_1 receptor-induced Ca^{2+} influx in differentiating N2a and SH-SY5Y cells and its role in TG2 activation. It is interesting to note that changes in intracellular $[Ca^{2+}]$ required for TG2 transamidating activity are typically in the order 3-100 µM (Király et al., 2011). However, there is growing evidence that intracellular $[Ca^{2+}]$ can reach levels sufficient to activate TG2, for example in calcium microdomains that occur near the cell membrane following the opening of voltage gated Ca^{2+}

channels or near internal stores (Berridge, 2006; Király et al., 2011). Alternatively, the role of Ca^{2+} in PAC_1 receptor-induced TG2 activation may require the sensitization of TG2 to low levels of intracellular [Ca^{2+}]. For example, interaction of TG2 with protein binding partners and/or membrane lipids have been proposed to induce a conformational change that promotes activation at low levels of intracellular [Ca^{2+}] (Király et al., 2011).

4.4 Conclusion

From the results presented in this chapter, it can be concluded that exposure of differentiating mouse N2a and human SH-SY5Y neuroblastoma cells to the neurotrophic factor PACAP-27 mediated activation of TG2 activity through the PAC_1 receptor. The findings also demonstrate that this activity is sensitive to the inhibition of various protein kinases, suggesting that the stimulation of TG2 activity via the PAC_1 receptor is associated with a multi-protein kinase dependent pathway. Overall the data describe a strong correlation between the signalling pathway trigger by neurotrophic factor PACAP-27 and TG2 activity that could be part of the neuronal survival and neurite outgrowth process. This principle could also be applicable to another neurotrophic factor e.g. nerve growth factor, which is investigated in the next chapter.

Table 4.1 The overall ability of different treatments to inhibit PACAP-27-induced TG2 activity assessed by different approaches

Treatment	Assessment following PACAP-27 treatment									
	Amine incorporation		Peptide crosslinking		In-situ		IP		WB	
	N2a	SH-SY5Y	N2a	SH-SY5Y	N2a	SH-SY5Y	N2a	SH-SY5Y	N2a	SH-SY5Y
PACAP 6-38 (100 nM; PAC_1 receptor antagonist)	****	***	***	***	****	****	nd	nd	nd	nd
Z-DON (150 µM; TG2 inhibitors)	****	**	****	**	****	****	nd	nd	nd	nd
R283 (200 µM; TG2 inhibitors)	****	***	****	***	****	****	nd	nd	nd	nd
PD 98059 (50 µM; MEK1/2 inhibitor)	****	***	****	***	****	***	****	***	****	****
Akt inhibitor XI (0.1 µM; PKB inhibitor)	***	**	***	****	****	**	nd	nd	****	****
KT 5720 (5 µM; PKA inhibitors)	****	***	****	***	****	****	****	***	**** vs ERK1/2	** vs ERK1/2
Rp-3',5'-cAMPS (50 µM; PKA inhibitors)	****	**	****	**	nd	nd	nd	nd	nd	nd
Ro 31-8220 (10 µM; PKC inhibitor)	****	ns	****	ns	*	ns	ns	ns	* vs ERK1/2	ns vs ERK1/2
Nominally Ca^{2+}-free Hanks/HEPES buffer containing 0.1 mM EGTA	****	*	**	**	**	ns	***	ns	ns vs ERK1/2	ns vs ERK1/2
50 µM BAPTA-AM in nominally Ca^{2+}-free Hanks/HEPES buffer containing 0.1 mM EGTA	****	**	***	**	**	**	nd	nd	nd	nd
SP 600125 (20 µM; JNK1/2 inhibitor)	ns	ns	*	ns	nd	nd	nd	nd	****	ns
SB 203580 (20 µM; p38 MAPK inhibitor)	ns	ns	ns	ns	nd	nd	nd	nd	ns	**

The results of range of treatments used in this study to investigate the role of PACAP-27 in modulating of TG2 activity. Differentiating neuroblastoma N2a or SH-SY5Y cells were treated with the compounds in the table, then cells were stimulated with PACAP-27 and the TG2 activity assessed by different approaches; *in vitro* amine incorporation and peptide crosslinking assays, visualisation of *in situ* amine incorporation activity, protein kinase activation by Western blotting (WB) and TG2 phosphorylation via immunoprecipitation (IP). ns= no significant change, nd= not determined, *P<0.05, **P<0.01, ***P<0.001, and ****P<0.0001.

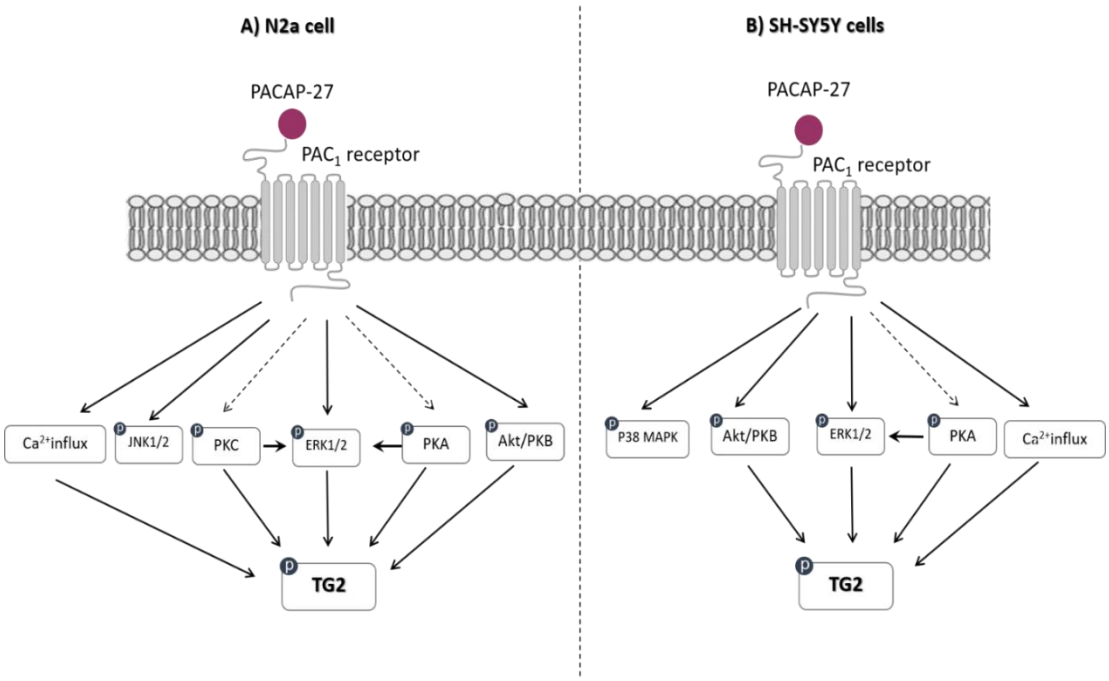

Figure 4.27 Schematic summary of PAC_1 receptor-induced TG2 activation.

Activation of PAC_1 receptor by PACAP-27 trigger activation of various targets. (A) In differentiating mouse N2a cells, PACAP-27 induced TG2 activity and TG2 phosphorylation by triggering the activation of protein kinases (ERK1/2, PKA, Akt/PKB, PKC and JNK1/2) and Ca^{2+} influx. (B) In differentiating human SH-SY5Y cells, TG2 activity and TG2 phosphorylation induced by PACAP-27 occurs as a result of activation of protein kinases (ERK1/2, PKA, Akt/PKB and p38 MAPK) and Ca^{2+} influx. Solid black arrows represent findings of the current study, dashed arrows represent findings from other studies.

Chapter 5

5 Modulation of TG2 activity by nerve growth factor NGF in differentiating neuroblastoma cells

5.1 Introduction

Nerve growth factor (NGF) was the first neurotrophin to be characterised (Levi-Montalcini & Hamburger, 1951). NGF modulates a wide range of biological functions and signalling in the nervous system; it regulates cell proliferation, differentiation and survival (Kawamoto and Matsuda 2004; Chao et al., 2006). It triggers its functions via the high affinity tyrosine kinase receptor A (TrkA; Wang et al., 2014). A substantial body of evidence indicates that NGF-induced activation of TrkA evokes neurite outgrowth and survival in neuronal cells (Lavenius et al., 1995; Eggert et al., 2000; Schramm et al., 2005). Receptor tyrosine kinases represent a large family of receptors; this family's prominent members include receptors for epidermal growth factor (EGF), platelet-derived growth factor (PDGF) and vascular endothelial growth factor (VEGF). Transglutaminase 2, the most widely expressed form of TG in the nervous system, as well as the most ubiquitous and studied transglutaminase isoform, has been found to mediate transamidase activity and participate in EGF receptor signalling, whereas the interaction of extracellular TG2 with PDGF and VEGF receptors promotes their activation (Dardik & Inbal, 2006; Zemskov et al., 2009; Li et al., 2010). These observations suggest a major role for TG2 in the modulation of receptor tyrosine kinases. However, at present, it is not known whether receptor tyrosine kinase activation by NGF promotes intracellular TG2 activation. NGF's activation of TrkA leads to a multitude of signalling pathways, including the ERK1/2, PI-3K/PKB and PLC-γ/PKC cascades (Wang et al., 2014). As some of these pathways are associated with the modulation of intracellular TG2 activity (PKC, ERK1/2 and Ca^{2+}), it is conceivable that NGF directly regulates TG2 activity.

Considering that mouse N2a and human SH-SY5Y neuroblastoma cells are responsive to NGF (Eggert et al., 2000; Price et al., 2003; Dwan et al., 2013), as well as the already established

interplay between NGF and TG2 in neuroblastoma cells (Condello et al., 2008), the current study sought to determine whether short-term treatment with NGF (<4 h) could modulate TG2-mediated transamidase activity in these cells and identify the possible signalling pathways involved. To achieve this aim, NGF's effect on the modulation of TG2 activity was investigated using TG2 transamidase activity assays and immunofluorescence visualisation. In addition, the possible molecular mechanisms underlying this modulation were investigated by assessing the protein kinases involved.

5.2 Results

5.2.1 The effect of NGF on TG2 activity

Although it has been determined that long-term exposure to NGF has neurotrophic effects, its possible potential actions as a fast-acting neurotrophin have not been investigated as thoroughly. The initial experiments in this study assessed the effects of short-term exposure of differentiating neuroblastoma cells to NGF. Following NGF exposure, cell lysates were initially subjected to biotin cadaverine amine–incorporated and biotin-labelled peptide (biotin-TVQQEL) crosslinking assay. From the results, NGF (100 ng/ml) was shown to rapidly (1 h) and robustly enhance biotin–cadaverine incorporation and protein crosslinking activity at a significant level in differentiating N2a (Figure 5.1 A and B) and SH-SY5Y (Figure 5.2 A and B) cells. Furthermore, NGF also stimulated concentration-dependent increases in biotin–amine incorporation activity and peptide crosslinking activity in N2a (Figure 5.1 C and D) and SH-SY5Y (Figure 5.2 C and D) cells.

To confirm that the observed increase in NGF-induced TG2 activation was not simply a consequence of increased levels of TG2 protein expression, the level of TG2 protein expression was monitored by Western blotting. The data obtained indicated no significant change in the level of TG2 protein expression during the time course (up to 4 h) of NGF treatment in differentiated N2a and SH-SY5Y cells (Figure 5.3), confirming that NGF increased TG2 activity but not TG2 protein expression during the indicated times.

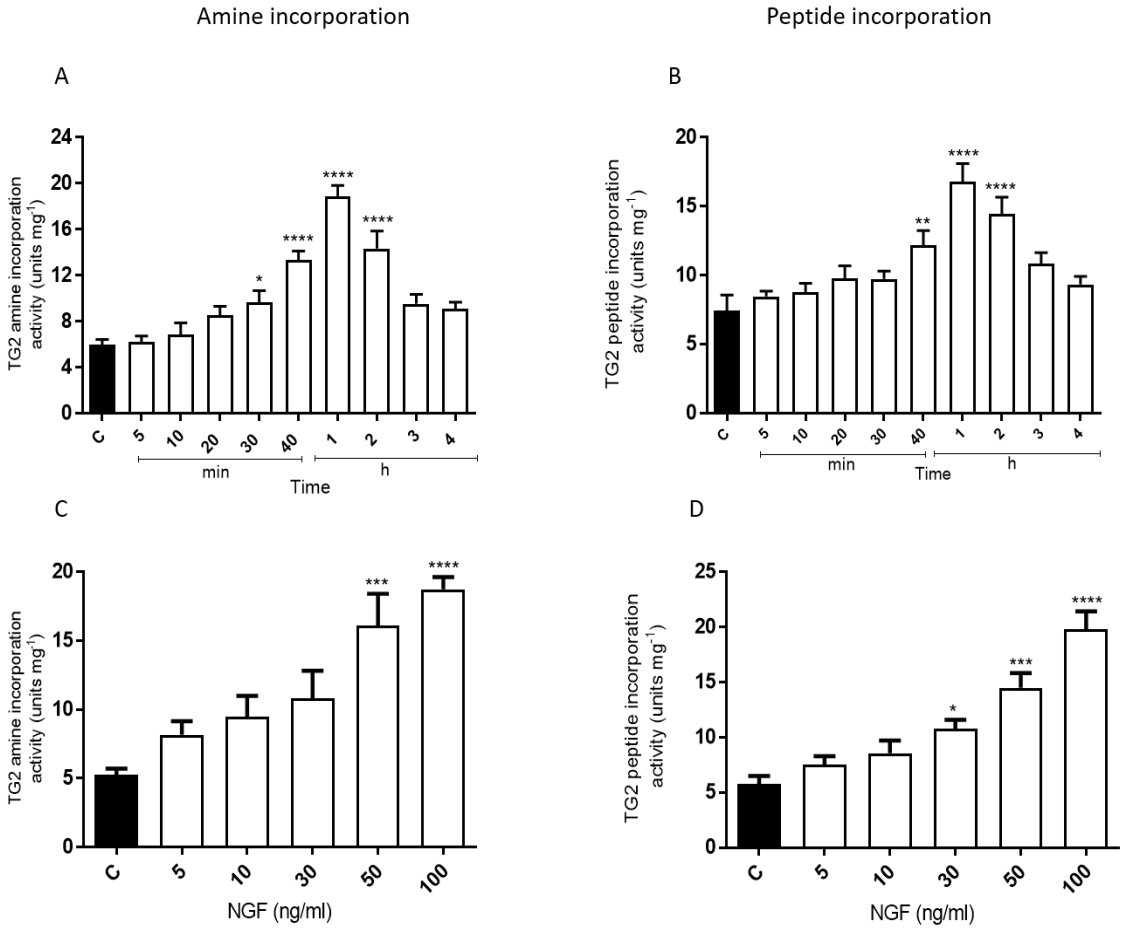

Figure 5.1 Effects of NGF on TG2 activity in differentiating mouse N2a cells.

Differentiating N2a cells were either incubated with 100 ng/ml NGF for the indicated times or for 1 h with the indicated concentrations of NGF. The cell lysates were then subjected to the biotin–cadaverine incorporation (A and C) or peptide crosslinking assay (B and D). The data points represent the mean TG2-specific activity ± S.E.M. from four independent experiments. *P < 0.05, **P <0.01, ***P < 0.001 and ****P < 0.0001 versus the control response.

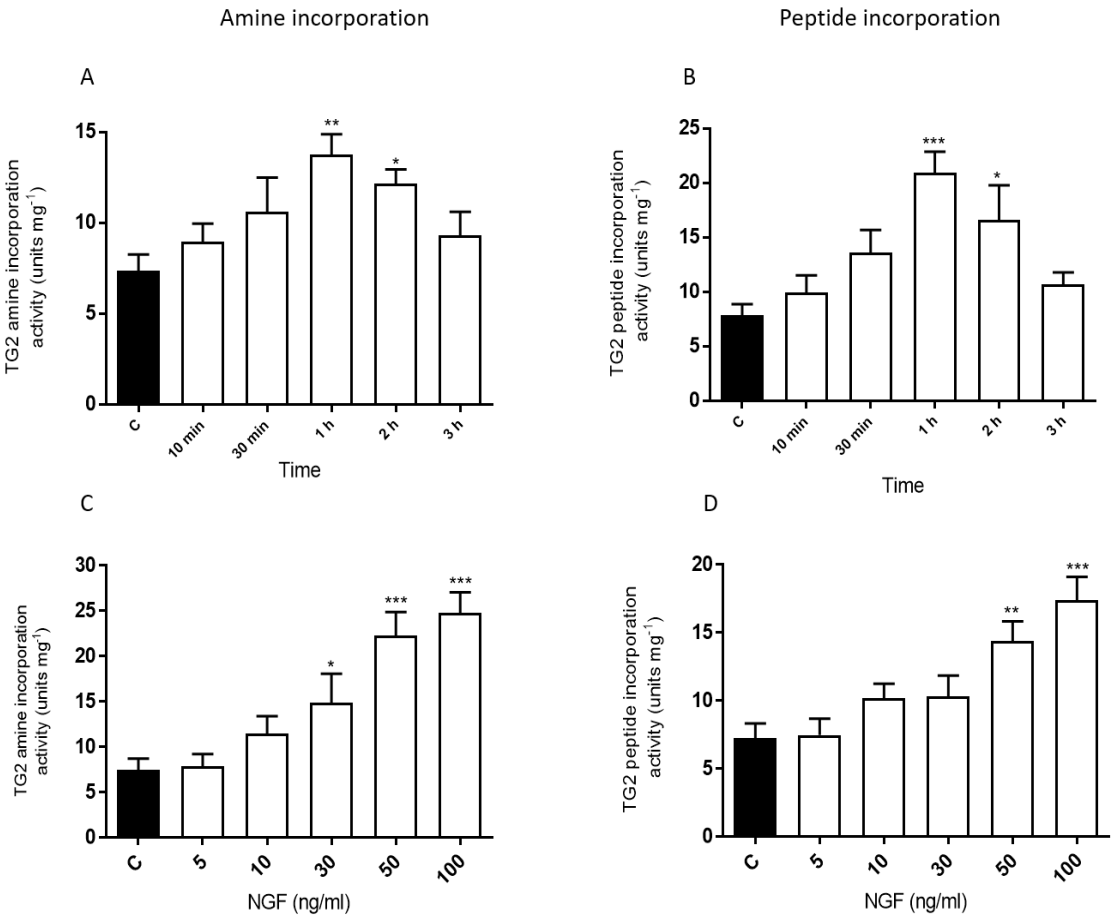

Figure 5.2 Effects of NGF on TG2 activity in differentiating human SH-SY5Y cells.

Differentiating SH-SY5Y cells were either incubated with 100 ng/ml NGF for the indicated times or for 1 h with the indicated concentrations of NGF. The cell lysates were then subjected to the biotin–cadaverine incorporation (A and C) or peptide crosslinking assay (B and D). Data points represent the mean TG2 specific activity ± S.E.M. from four independent experiments. *p < 0.05, **P <0.01 and, ***P < 0.001 versus control response.

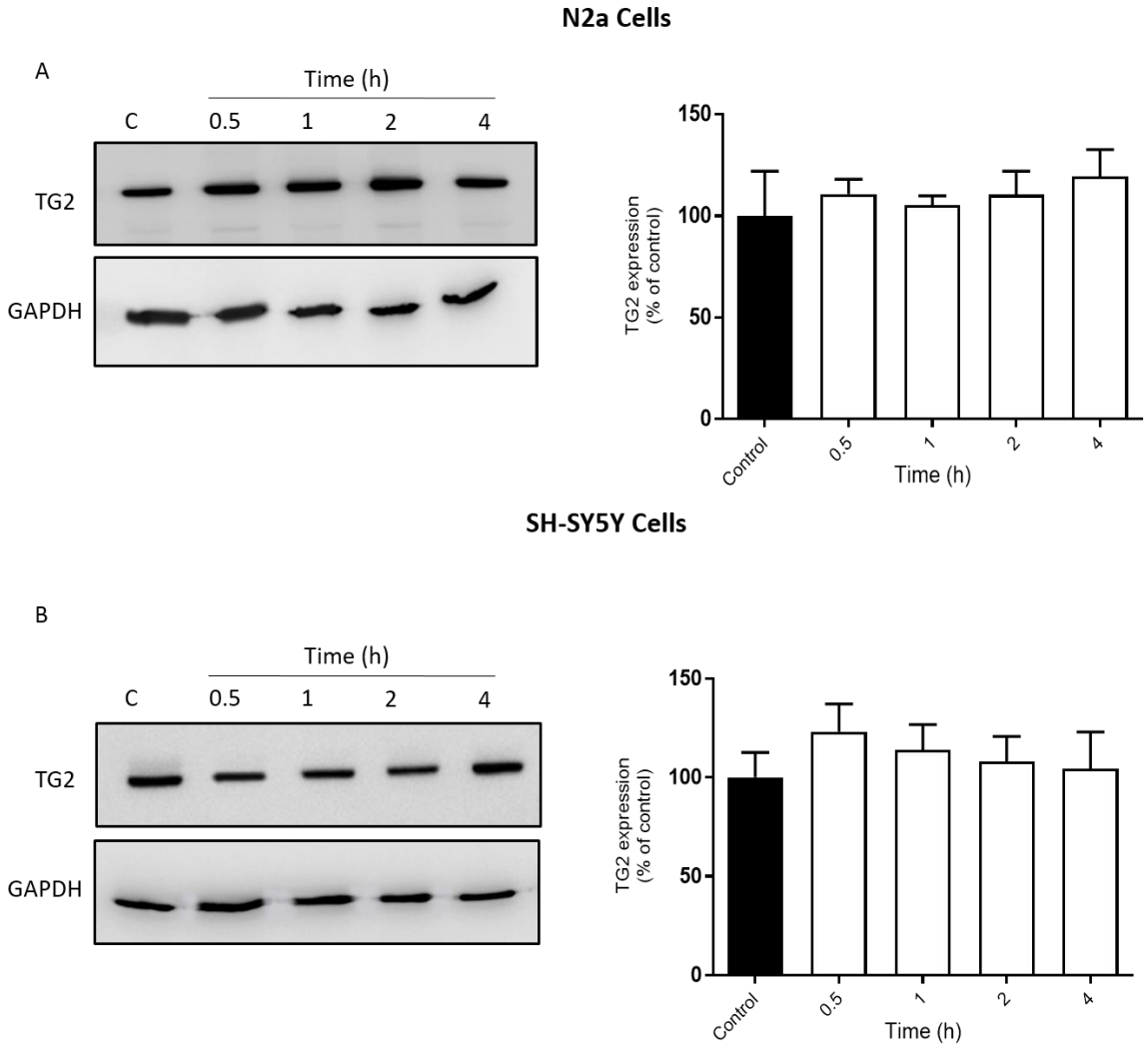

Figure 5.3 Effect of acute NGF-treatment on TG2 protein expression in differentiating N2a and SH-SY5Y cells.

Differentiating N2a (A) and SH-SY5Y (B) cells were incubated with 100 ng/ml NGF for the indicated times. Cell lysates (20 µg protein) were analysed for TG2 expression by Western blotting with anti-TG2 antibody. Levels of GAPDH are included for comparison. Quantified data are expressed as the percentage of TG2 expression in control cells (100%) and represent the mean ± S.E.M. of four independent experiments.

To confirm that TG2 was responsible for NGF-mediated transglutaminase activity, TG2-specific inhibitors were tested, namely R283 and Z-DON. Cells were pre-treated for 1 h with Z-DON (150 µM) or R283 (200 µM) prior to stimulation with NGF (100 ng/ml) for 1 h. Both inhibitors completely blocked NGF-induced TG-mediated amine incorporation (Figure 5.4A and C) and peptide crosslinking activity (Figure 5.4B and D) in N2a and SH-SY5Y cells. The data from these experiments revealed that TG2 was the transglutaminase form involved in these responses. It is important to note that, although the TG2 inhibitors are cell permeable, the inhibition of cellular TG2 is only achieved at concentrations significantly above their IC50 values versus purified enzymes (Freund et al., 1994; Schaertl et al., 2010). Overall, these data indicate that NGF stimulates robust TG2-mediated transamidase activity in differentiating N2a and SH-SY5Y cells.

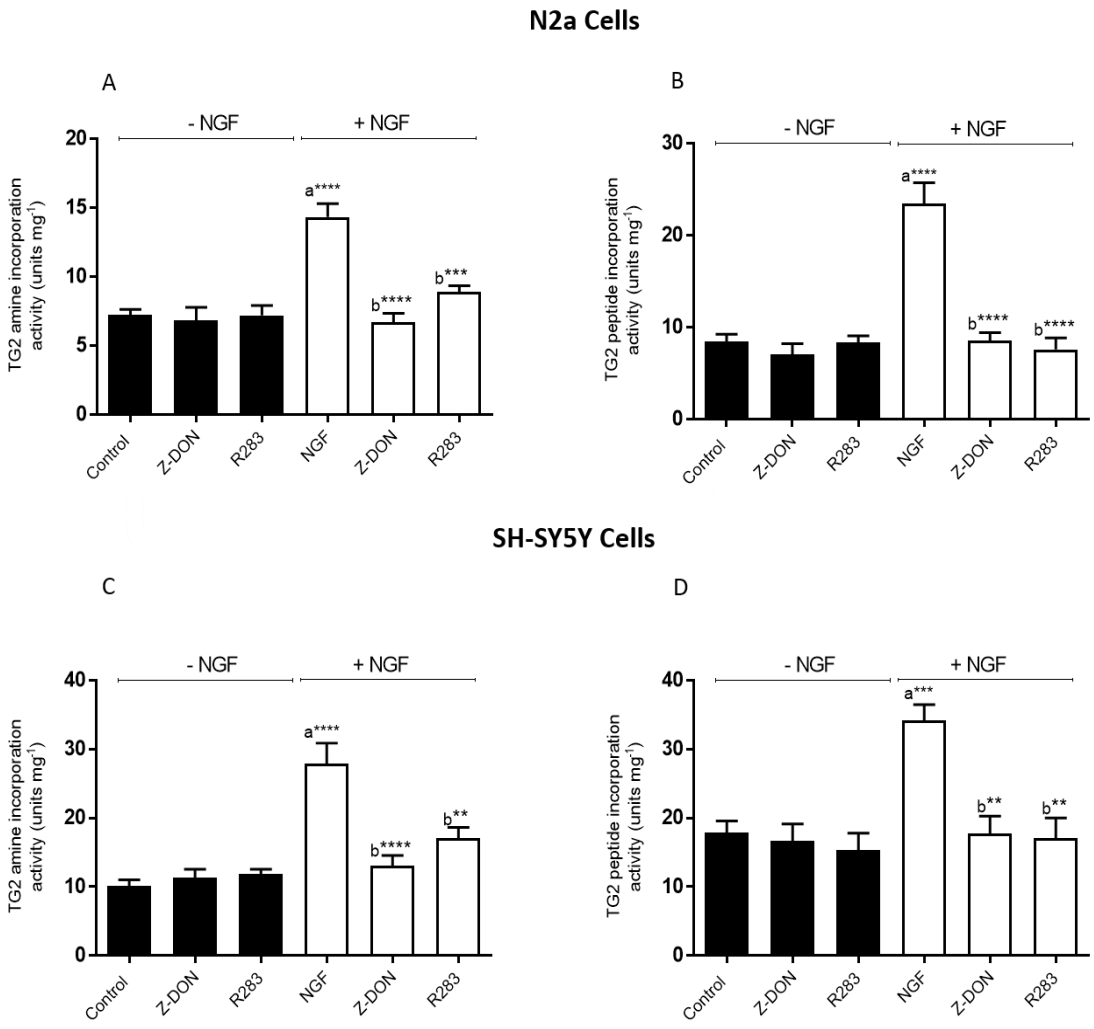

Figure 5.4 Effects of TG2 inhibitors on NGF-induced TG activity.

Differentiating N2a (A and B) and SH-SY5Y (C and D) cells were pre-treated for 1 h with the TG2 inhibitors Z-DON (150 µM) and R283 (200 µM) prior to 1 h of stimulation with NGF (100 ng/ml). The cell lysates were then subjected to the biotin-cadaverine incorporation (A and C) or peptide crosslinking assay (B and D). The data points represent the mean TG-specific activity ± S.E.M. from four independent experiments. **P <0.01, ***P<0.001, and ****P<0.0001, (a) versus control and (b) versus NGF alone.

5.2.2 The effects of ERK1/2, PI-3K/PKB and PKC inhibitors on NGF-induced TG2 activity

The roles of ERK1/2 and PI-3K/PKB

Several signalling proteins are known to act downstream of NGF, including ERK1/2, PI-3K/PKB and PKC (Wang et al., 2014). In the current study, initial experiments assessed NGF induced ERK1/2 and PKB activation via Western blotting using phospho-specific antibodies that recognise phosphorylated motifs in activated ERK1/2 ($pT^{202}EpY^{204}$**)** and PKB (S^{473}). As expected, NGF (100 ng/ml) stimulated robust increases in ERK1/2 and PKB phosphorylation in differentiating N2a (Figure 5.5 A and B) and SH-SY5Y cells (Figure 5.5 C and D). NGF-mediated increases in ERK1/2 and PKB were inhibited by PD 98059 (50 µM; MEK1/2 inhibitor) and Akt Inhibitor XI (100 nM; PKB inhibitor), respectively (Figure 5.5). Furthermore, inhibiting of PKB using Akt Inhibitor XI did not influence the NGF-induced increase in ERK1/2 phosphorylation, and inhibition of MEK1/2 using PD 98059 had no effect on the PKB phosphorylation induced by NGF in N2a or SH-SY5Y cells (Fig. 5.6). The data from these experiments suggest inhibitor selectivity and a lack of 'crosstalk' between the two kinase pathways.

Turning to the next experimental evidence on whether ERK1/2 and PKB were involved in NGF-induced TG2 activation, the pharmacological inhibitors of these protein kinases were used prior to stimulating the cells with NGF and subjected to biotin-cadaverine incorporation and biotin-labelled peptide (biotin-TVQQEL) crosslinking assay**.** As depicted in Figure 5.7, NGF-induced TG-mediated amine incorporation activity and peptide crosslinking activity were significantly inhibited by PD 98950 (MEK1/2 inhibitor (50 µM) and Akt inhibitor XI (100 nM), suggesting the involvement of ERK1/2 and PKB, respectively.

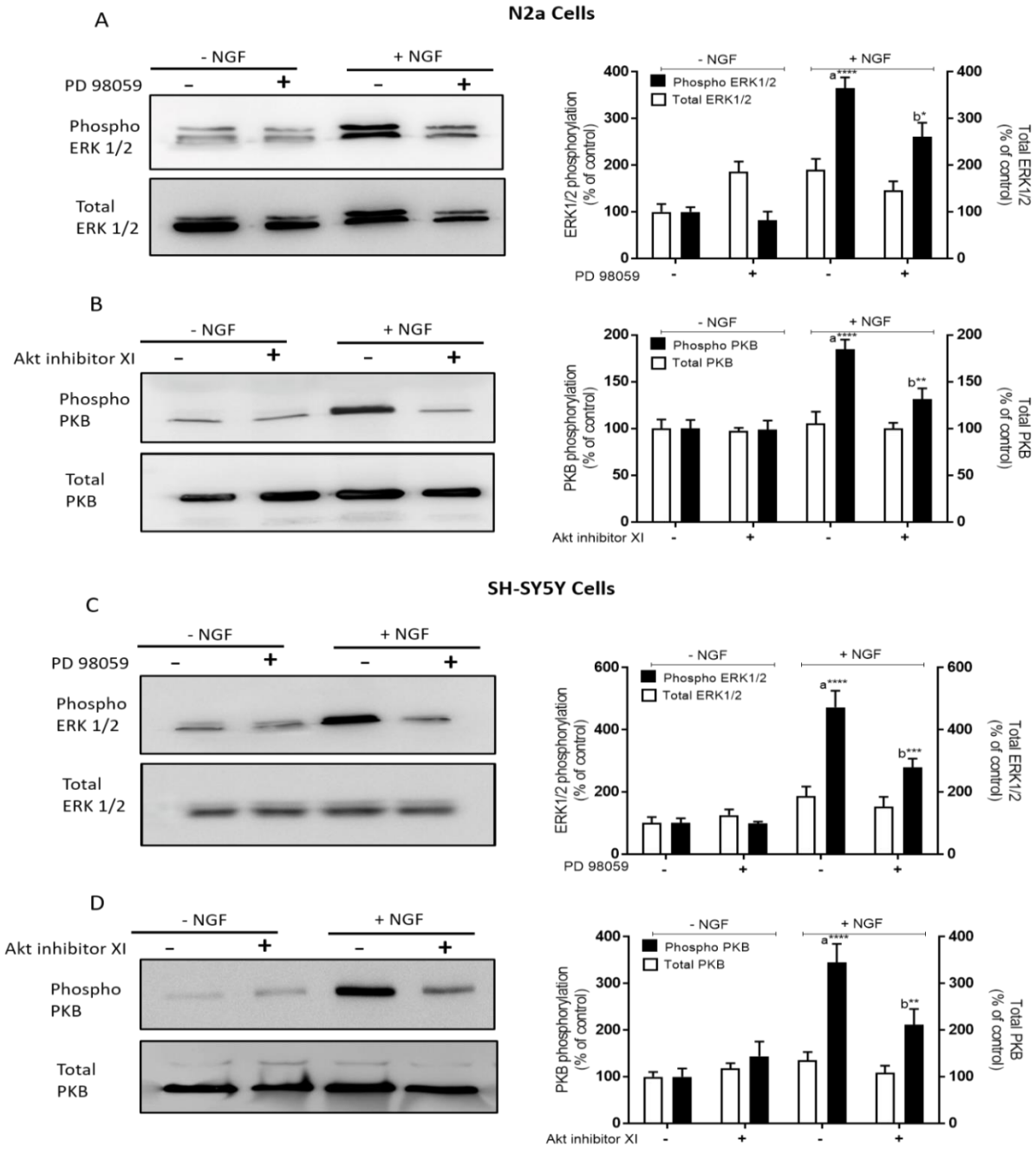

Figure 5.5 Effects of PD 98959 and Akt inhibitor XI on NGF-induced ERK1/2 and PKB activation in differentiating N2a and SH-SY5Y cells.

Where indicated, differentiating cells were pre-treated for 30 min with (A and C) PD 98059 (50 μM) or (B and D) Akt Inhibitor XI (100 nM) prior to stimulation with NGF (100 ng/ml) for 1 h. The cell lysates were analysed by Western blotting for activation of ERK1/2 and PKB using phospho-specific antibodies. The samples were subsequently analysed on separate blots using an antibody that recognises total ERK1/2 and PKB. Quantified data are expressed as the percentage of the value for control cells (= 100%) in the absence of protein kinase inhibitor and represent the mean ± S.E.M. of four independent experiments. *P<0.05, **P<0.01, *** P<0.001 and ****P<0.0001, (a) versus control and (b) versus NGF.

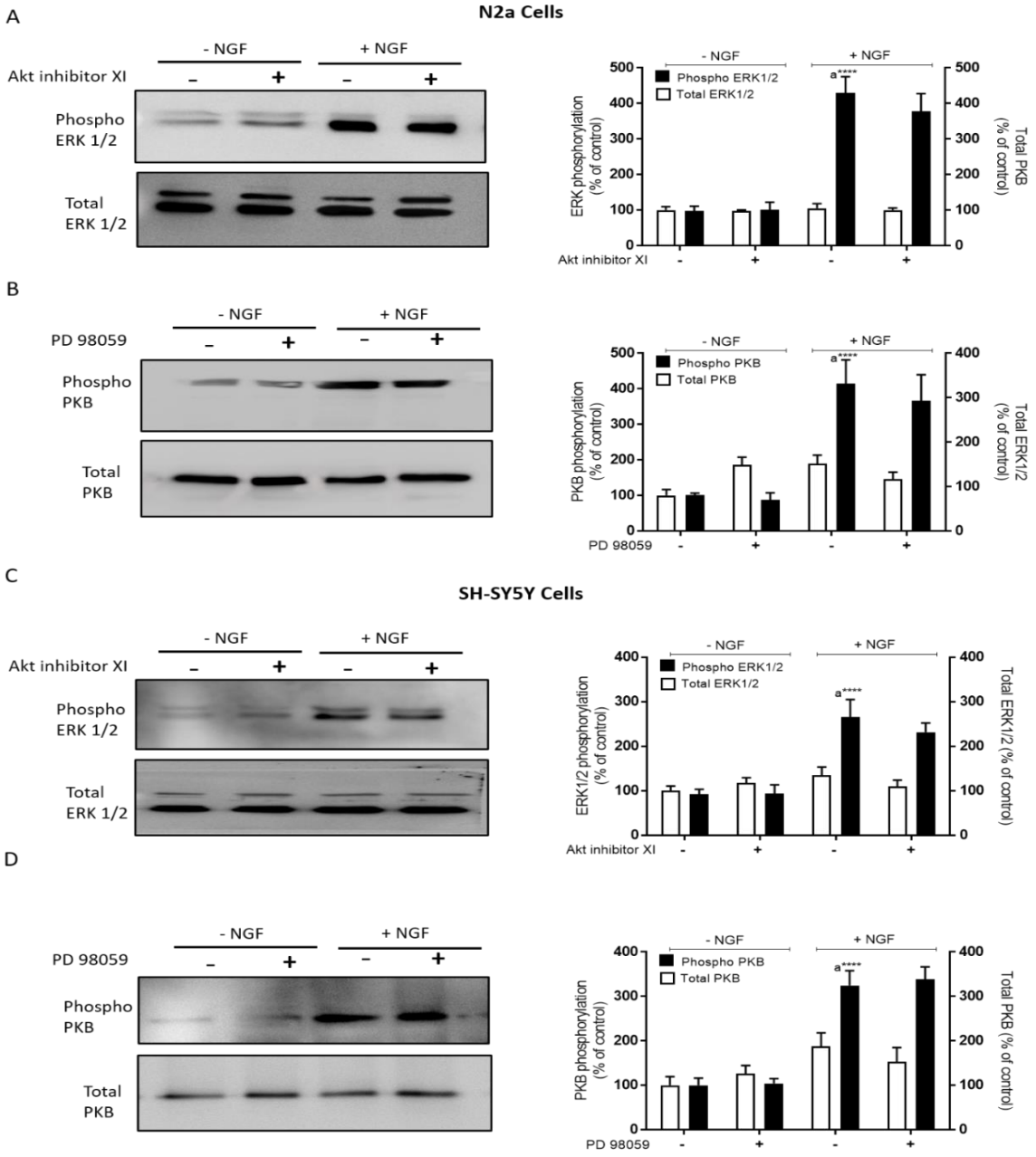

Figure 5.6 Effects of Akt inhibitor XI and PD 98959 on NGF-induced ERK1/2 and PKB activation in differentiating N2a and SH-SY5Y cells.

Where indicated, differentiating cells were pre-treated for 30 min with (A and C) Akt Inhibitor XI (100 nM) or (B and D) PD 98059 (50 μM) prior to stimulation with NGF (100 ng/ml) for 1 h. The cell lysates were analysed by Western blotting for ERK1/2 and PKB activation using phospho-specific antibodies. The samples were subsequently analysed on separate blots using antibodies that recognise total ERK1/2 and PKB. The quantified data are expressed as the percentage of the value for control cells (= 100%) in the absence of protein kinase inhibitor and represent the mean ± S.E.M. of four independent experiments. *** P<0.001 and ****P<0.0001, (a) versus control.

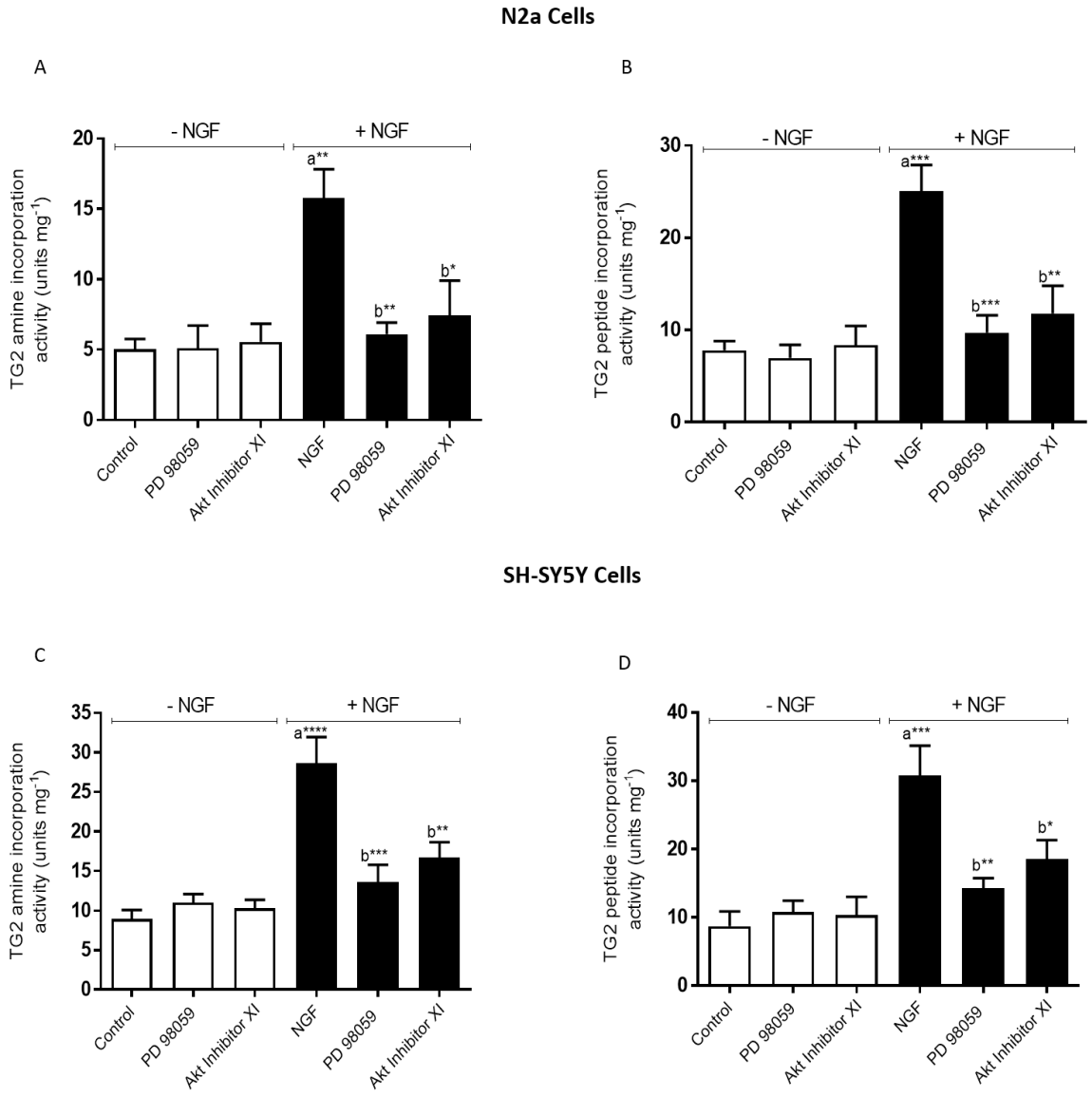

Figure 5.7 Effects of ERK1/2 and PKB inhibition on NGF induced TG2 activity.

Differentiating N2a and SHSY5Y cells were pre-treated for 30 min with PD 98059 (50 μM) or Akt inhibitor XI (100 nM) prior to 1 h stimulation with NGF (100 ng/ml). The cell lysates were subjected to biotin–cadaverine incorporation (A and C) or biotin-peptide crosslinking assay (B and D). The data points represent the mean TG-specific activity ± S.E.M. from four independent experiments. *P<0.05, ** P<0.01, *** P<0.001 and **** P<0.0001, (a) versus control and (b) versus NGF alone.

The role of PKC

Previous studies have reported an upstream role of PKC in NGF-induced ERK1/2 activation (Lloyd & Wooten, 1992; Wooten et al., 2000). Hence, in the present study, the effects of the pharmacological inhibition of PKC with Ro 31-8220 in modulating NGF-induced ERK1/2 and PKB activation in N2a and SH-SY5Y cells were determined. Treatment with Ro 31-8220 (10 µM) attenuated NGF-induced ERK1/2 activation in both cell lines (Figure 5.8A and C). Conversely, Ro 31-8220 did not block NGF-induced PKB activation in N2a or SH-SY5Y cells (Figure 5.8 B and D). These findings suggest an upstream role of PKC in NGF induced ERK1/2 activation. Subsequent experiments assessed the effects of the pharmacological inhibition of PKC on TG2 activity. Differentiated neuroblastoma cells were treated with the PKC inhibitor Ro 31-8220 (10 µM) for 30 min prior to stimulation with NGF (100 ng/ml) for 1 h. Cell lysates were then subjected to biotin-cadaverine incorporation and biotin-labelled peptide (biotin-TVQQEL) crosslinking assay. Interestingly, in this case, the inhibition of PKC abolished NGF-induced TG2-mediated amine incorporation and peptide crosslinking activity in both N2a and SH-SY5Y cells (Figure 5.9), suggesting that PKC may play a mediator role in NGF-induced TG2 activity. Taken together, the data presented in this section suggest that NGF stimulates TG2 activity in differentiating N2a and SHSY5Y cells via a multi–protein kinase–dependent pathway involving ERK1/2, PKB and the upstream role of PKC.

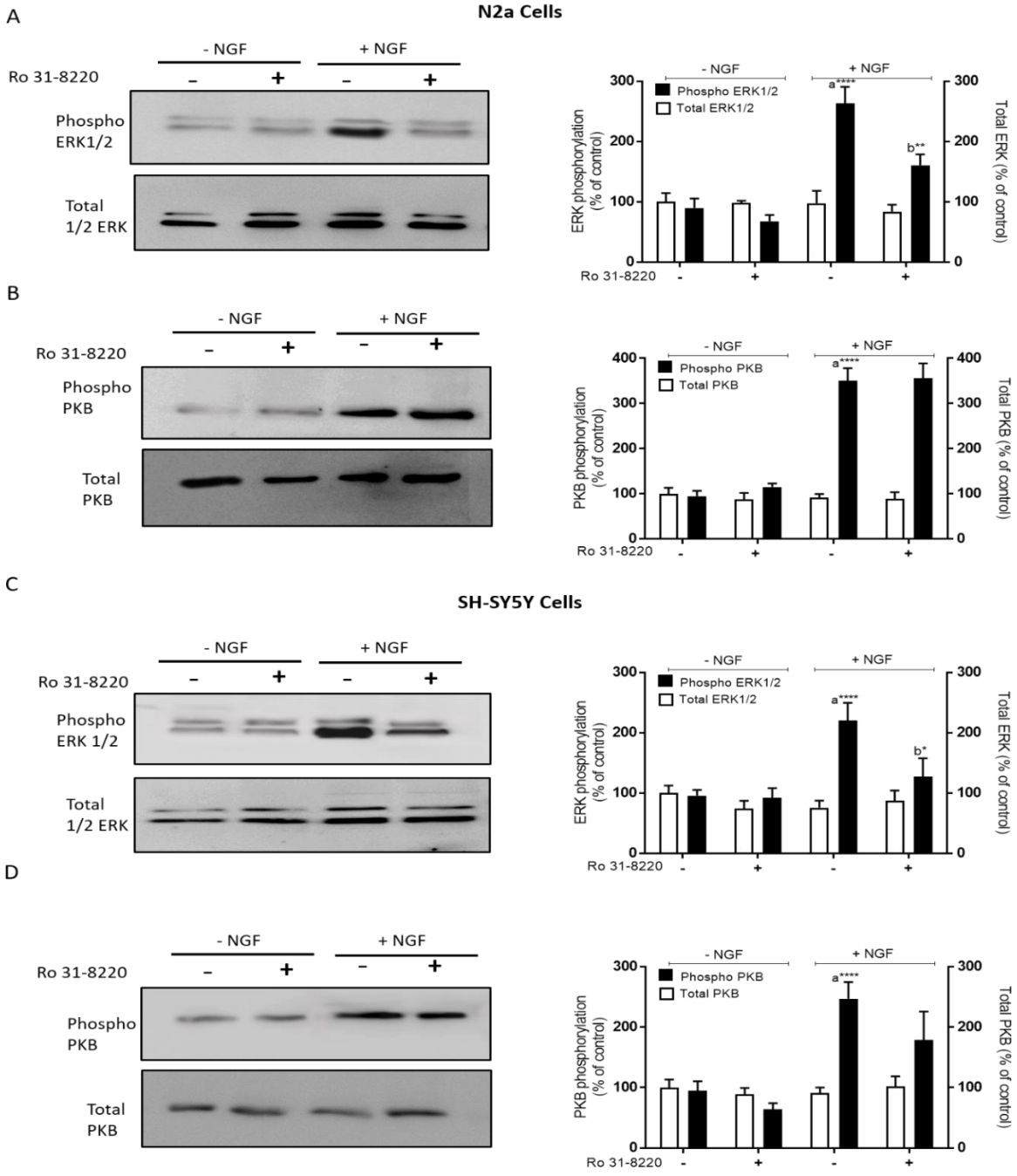

Figure 5.8 Effects of the protein kinase C inhibitor Ro 318220 on NGF-induced ERK1/2 and PKB activation in differentiating N2a and SH-SY5Y cells.

Where indicated, differentiating cells were pre-treated for 30 min with Ro 318220 (10 µM) prior to stimulation with NGF (100 ng/ml) for 1 h. The cell lysates were analysed by Western blotting for activation of ERK1/2 (A and C) and PKB (B and D) using phospho-specific antibodies. The samples were subsequently analysed on separate blots using antibodies recognising total ERK1/2 and PKB. The quantified data are expressed as the percentage of the value for control cells (= 100%) in the absence of protein kinase inhibitor and represent the mean ± S.E.M. of four independent experiments. *P<0.05, **P<0.01, *** P<0.001 and ****P<0.0001, (a) versus control and (b) versus NGF.

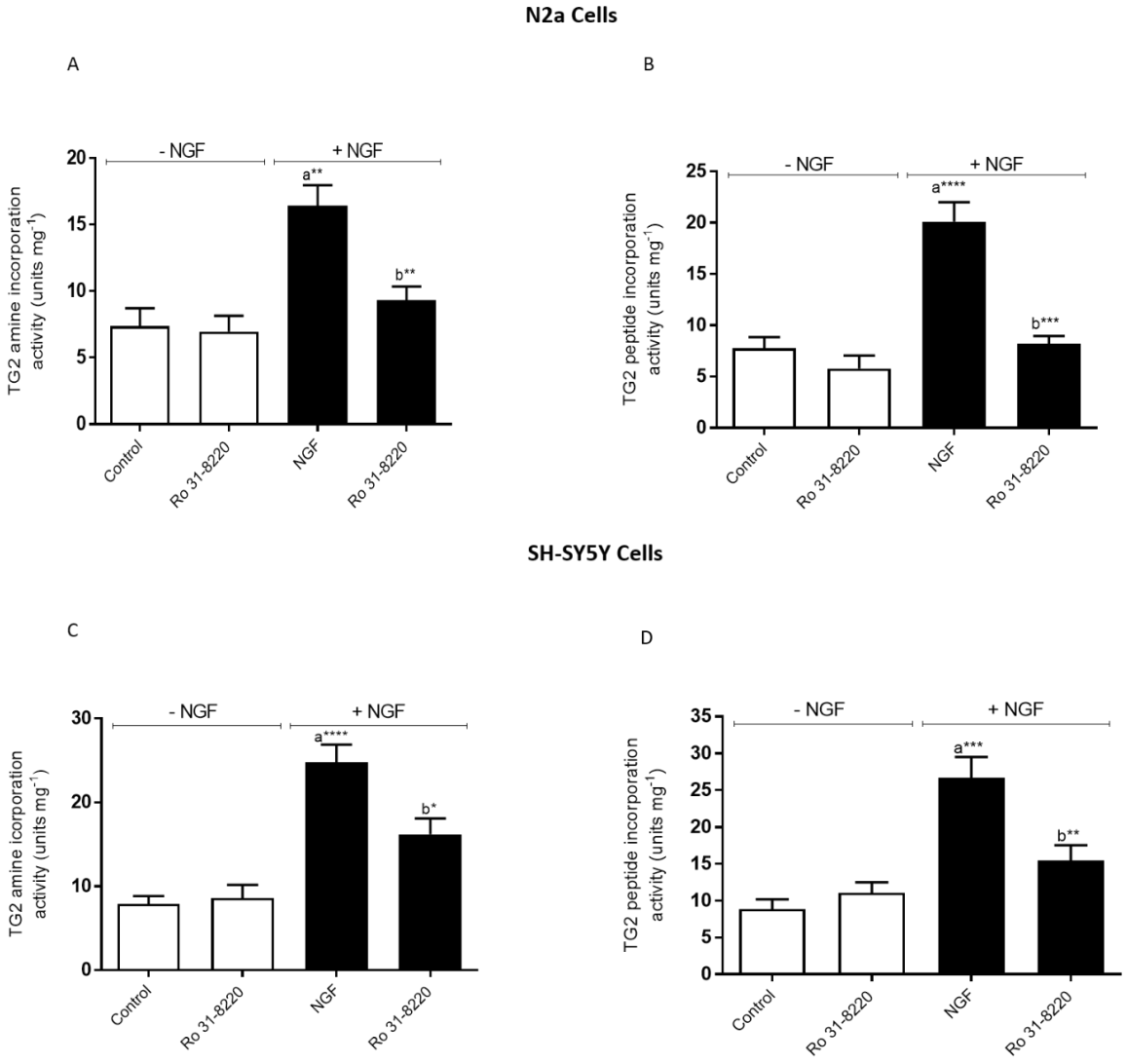

Figure 5.9 Effects of PKC inhibition on NGF-induced TG2 activity.

Differentiating N2a and SHSY5Y cells were pre-treated for 30 min with Ro 318220 (10 µM) prior to 1 h of stimulation with NGF (100 ng/ml). The cell lysates were subjected to biotin-cadaverine incorporation (A and C) or biotin-peptide crosslinking assay (B and D). The data points represent the mean TG-specific activity ± S.E.M. from four independent experiments. *P<0.05, **P<0.01, ***P<0.001 and ****P<0.0001, (a) versus control, (b) versus NGF alone.

It was important to assess the effect of the compounds used in this study; NGF and protein kinase inhibitors on purified guinea pig liver TG2 activity. TG2 amine incorporating and peptide crosslinking assays were carried out using purified guinea pig liver TG2 (50 ng/ well) after incubated with the indicated concentrations of the compounds for 30 min then, subjected to the biotin-cadaverine incorporation or peptide cross-linking assays. As shown in Figure 5.10 NGF and Figure 4.17 (in Chapter 4), protein kinase inhibitors used in this study had no significant effect on purified guinea pig liver TG2 activity. Overall, these data suggest that NGF stimulates TG2 activity in differentiating N2a and SH-SY5Y cells via a multi protein kinase-dependent pathway.

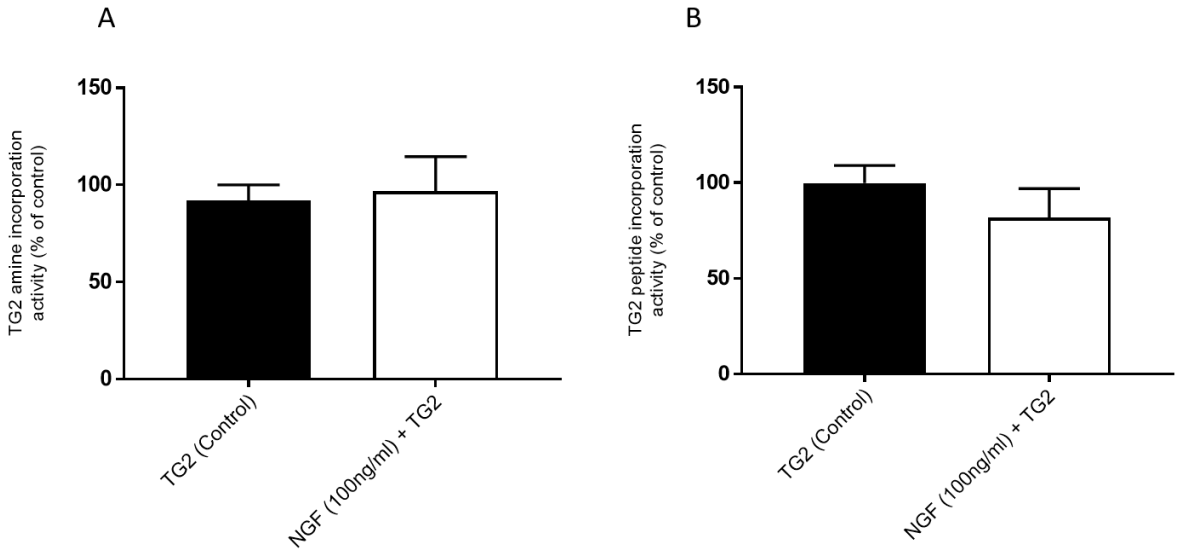

Figure 5.10 Effect of compounds used in this study on purified guinea pig liver TG2 activity.

TG2 amine incorporating (A) and peptide crosslinking (B) assays were carried out using purified guinea pig liver TG2 (50 ng/ well). Briefly, 50 ng of purified guinea pig liver TG2 was incubated with NGF (100 ng/ml) for 1 h prior to incubation in presence of either 6.67 mM calcium chloride or 13.3 mM EDTA containing 225 μM biotin-cadaverine and 2mM 2-mercaptoethanol for 1 h. Following incubation, the plates were processed as described in section 2.2.4 of chapter 2. Data points represent the mean ± S.E.M. TG2 specific activity from 4 independent experiments at basal level of purified guinea pig liver TG2 (control 100%).

5.2.3 The role of Ca^{2+} in NGF-induced TG2 activation

The transamidating activity of TG2 is Ca^{2+} dependent (Nurminskaya & Belkin, 2013; Eckert et al., 2014); hence, it was important to determine the possible involvement of extracellular Ca^{2+} in the NGF-induced increases in TG2 activity. The involvement of extracellular Ca^{2+} was determined by measuring TG2 stimulation in the absence of extracellular Ca^{2+} using Ca^{2+}-free Hanks/HEPES buffer containing 0.1 mM EGTA. Removal of extracellular Ca^{2+} moderately inhibited NGF-induced TG2 transamidation activity in N2a and SH-SY5Y cells (Figure 5.11). To ascertain the role of intracellular Ca^{2+}, measurements of TG2 activation were also implemented using cells loaded with the intracellular Ca^{2+} chelator BAPTA-AM (50 µM for 30 min) in the absence of extracellular Ca^{2+}. Loading cells with BAPTA, in the continued absence of extracellular Ca^{2+}, did not lead to further attenuation of NGF-induced TG2 activation (Figure 5.11). These data indicate that NGF-induced TG2 activation partially depends on the influx of extracellular Ca^{2+}.

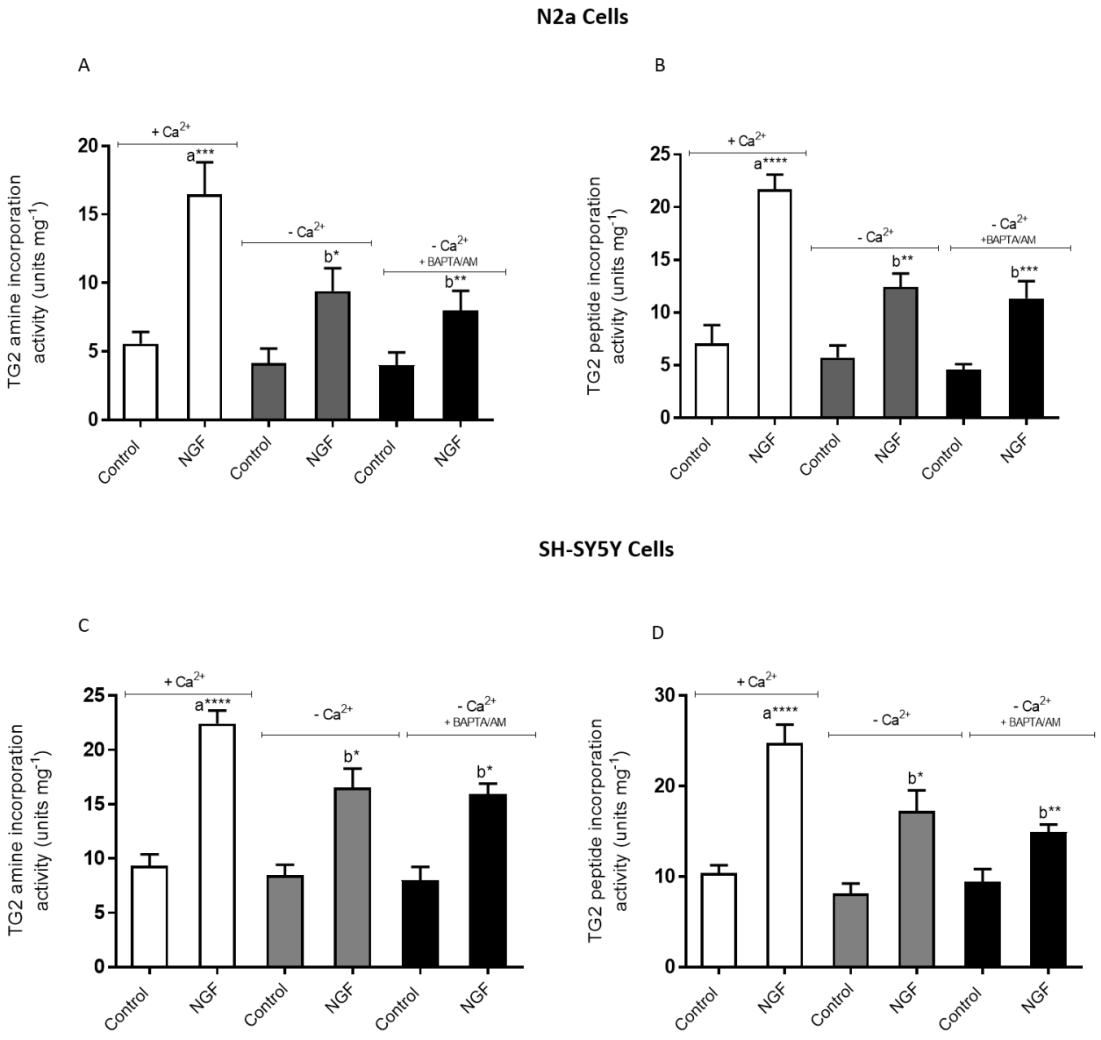

Figure 5.11 The role of Ca^{2+} in NGF-induced TG2 activity.

Differentiating N2a and SH-SY5Y cells were stimulated with NGF (100 ng/ml) for 1 h, either in the presence (1.8 mM $CaCl_2$) or absence of extracellular Ca^{2+} (nominally Ca^{2+}-free Hanks/HEPES buffer containing 0.1 mM EGTA). Experiments were also performed using cells pre-incubated for 30 min with 50 µM BAPTA/AM and in the absence of extracellular Ca^{2+} (nominally Ca^{2+}-free Hanks/HEPES buffer containing 0.1 mM EGTA) to chelate intracellular Ca^{2+}.Cell lysates were subjected to biotin-cadaverine incorporation assay (A and C) or protein crosslinking assay (B and D). Data points represent the mean TG specific activity ± S.E.M. from four independent experiments. *P<0.05, **P<0.01, ***P<0.001 and ****P<0.0001, (a) versus control, (b) versus NGF in the presence of extracellular Ca^{2+}.

5.2.4 Visualisation of *in situ* TG2 activity following NGF treatment

Since NGF-induced TG2 activity was evident at 1 h with 100 ng/ml exposure and involved various protein kinases, the present study determined the effect of time- and concentration-dependent NGF-induced TG2 activity at these earlier time points via immunocytochemistry, as described in Chapter 2 (section 2.2.5). Cells cultured in chamber slides were incubated with 1 mM biotin-X-cadaverine (BXC) for 4 h; following this, they were incubated with either NGF (100 ng/ml) for the indicated time or the indicated concentrations of NGF for 1 h. TG2-mediated BXC incorporation into intracellular proteins was visualised with Extravidin®-FITC (green). As shown in Figures 5.12 and 5.13, in N2a and SH-SY5Y cells, NGF stimulated the incorporation of BXC into endogenous protein substrates of TG2 in a time- and concentration-dependent manner. Furthermore, the *in situ* responses to NGF in both cell lines were attenuated by the TG2 inhibitors Z-DON and R283, as well as the protein kinase inhibitors PD 98059, Akt Inhibitor XI and Ro 31-8220 and following removal of extracellular Ca^{2+} (Figures 5.14 and 5.15). Overall, these data indicate a similar pattern of TG2 activation observed *in vitro*.

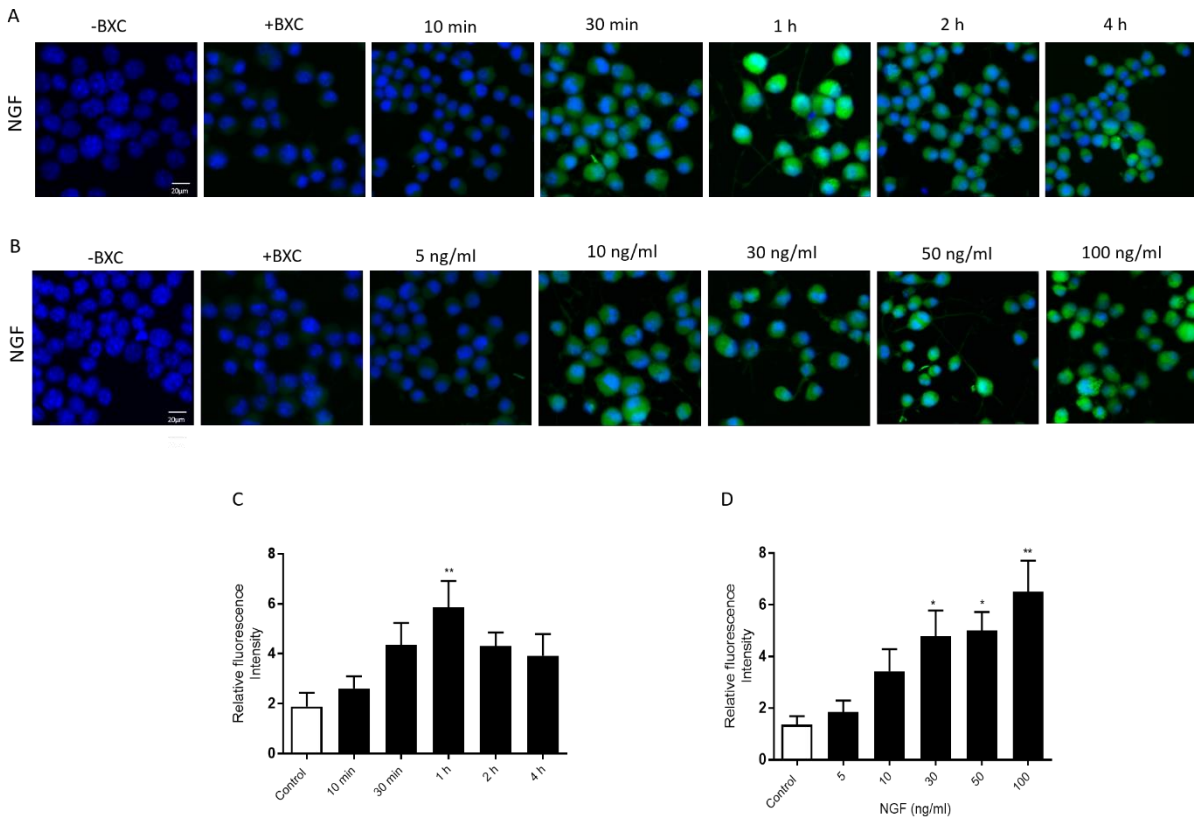

Figure 5.12 Effect of NGF on *in situ* TG2 activity in differentiating N2a cells.

The cells were incubated with 1 mM biotin-X-cadaverine (BXC) for 6 h, after which, they were incubated with (A) NGF (100 ng/ml) for the indicated time or (B) the indicated concentration of NGF for 1 h. TG2-mediated BXC incorporation into intracellular proteins was visualised using FITC-conjugated ExtrAvidin® (green). Nuclei were stained with DAPI (blue) and viewed using a Leica TCS SP5 II confocal microscope (20x objective magnification). The images presented are from one experiment and representative of three assays. Quantified data points for (C) time course and (D) concentration response represent the mean ± S.E.M. of fluorescence intensity relative to DAPI stain for five fields of view each from at least three independent experiments. *P<0.05 and **P<0.01 versus the control response.

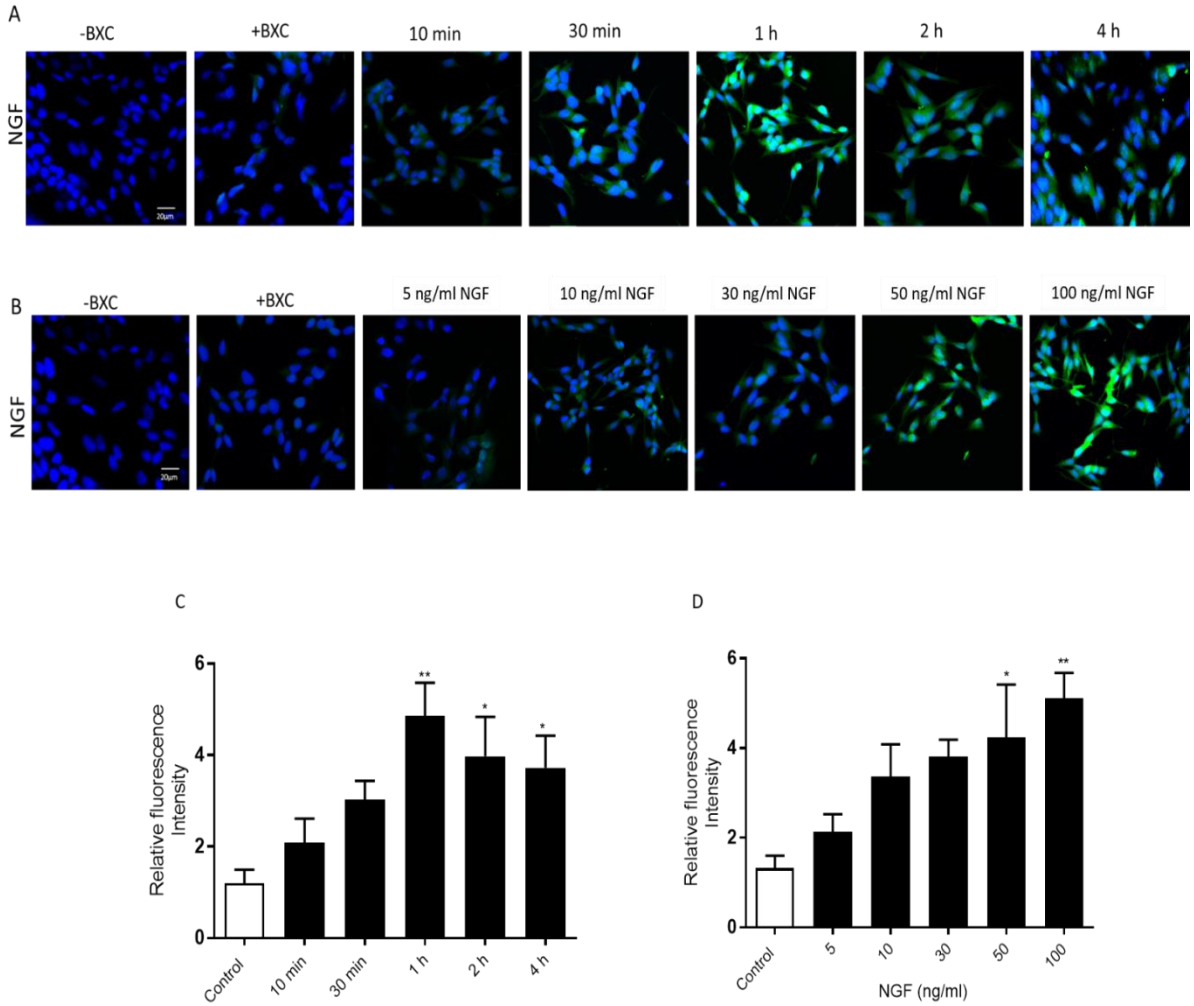

Figure 5.13 Effects of NGF on *in situ* TG2 activity in differentiating SH-SY5Y cells.

The cells were incubated with 1 mM biotin-X-cadaverine (BXC) for 6 h, after which, they were incubated with (A) NGF (100 ng/ml) for indicated time or (B) the indicated concentration of NGF for 1 h. The TG2-mediated BXC incorporation into intracellular proteins was visualised using FITC-conjugated ExtrAvidin® (green). Nuclei were stained with DAPI (blue) and viewed using a Leica TCS SP5 II confocal microscope (20x objective magnification). The images presented are from one experiment and representative of three assays. Quantified data points for (C) time course and (D) concentration response represent the mean ± S.E.M. of fluorescence intensity relative to DAPI staining for five fields of view each from at least three independent experiments. *P<0.05 and **P<0.01 versus the control response.

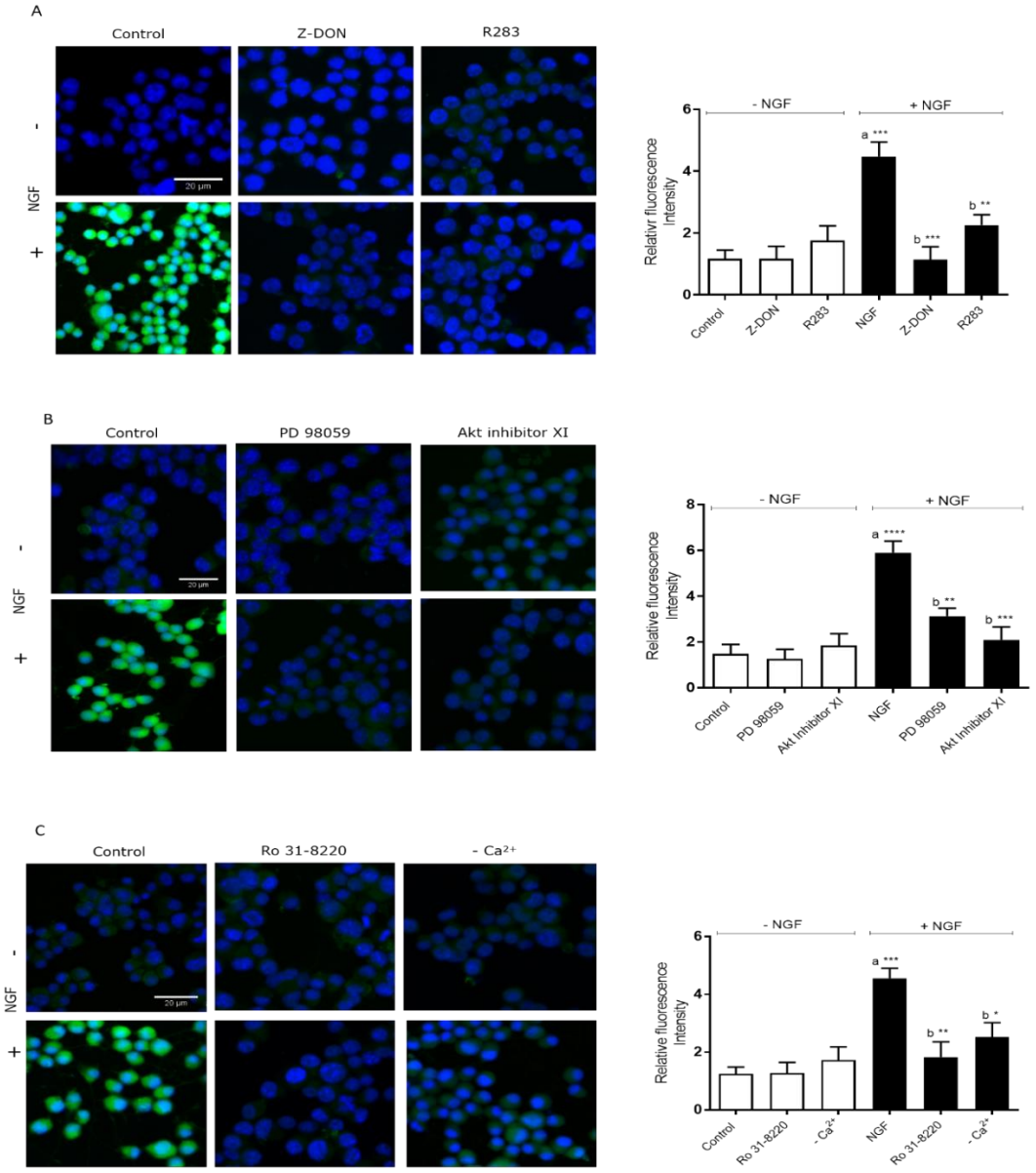

Figure 5.14 NGF-induced *in situ* TG activity in differentiating N2a cells.

The cells were incubated with 1 mM biotin-X-cadaverine (BXC) for 6 h, after which, they were incubated with (A) TG2 inhibitors Z-DON (150 µM) and R283 (200 µM) for 1 h, (B) PD 98059 (50 µM) and Akt Inhibitor XI (100 nM) for 30 min, or (C) Ro 31-8220 (10 µM) for 30 min or the absence of extracellular Ca^{2+} (nominally Ca^{2+}-free Hanks/HEPES buffer containing 0.1 mM EGTA) prior to stimulation with NGF (100 ng/ml) for 1 h. TG2-mediated BXC incorporation into intracellular proteins was visualised using FITC-conjugated ExtrAvidin® (green). Nuclei were stained with DAPI (blue) and viewed using a Leica TCS SP5 II confocal microscope (20× objective magnification). Scale bar = 20 µm. The images presented are from one experiment and representative of three assays. Quantified data represent the mean ± S.E.M. of fluorescence intensity relative to DAPI staining for five fields of view each from at least three independent experiments. *P<0.05, ** P<0.01, *** P<0.001 and ****P<0.0001 versus the control response.

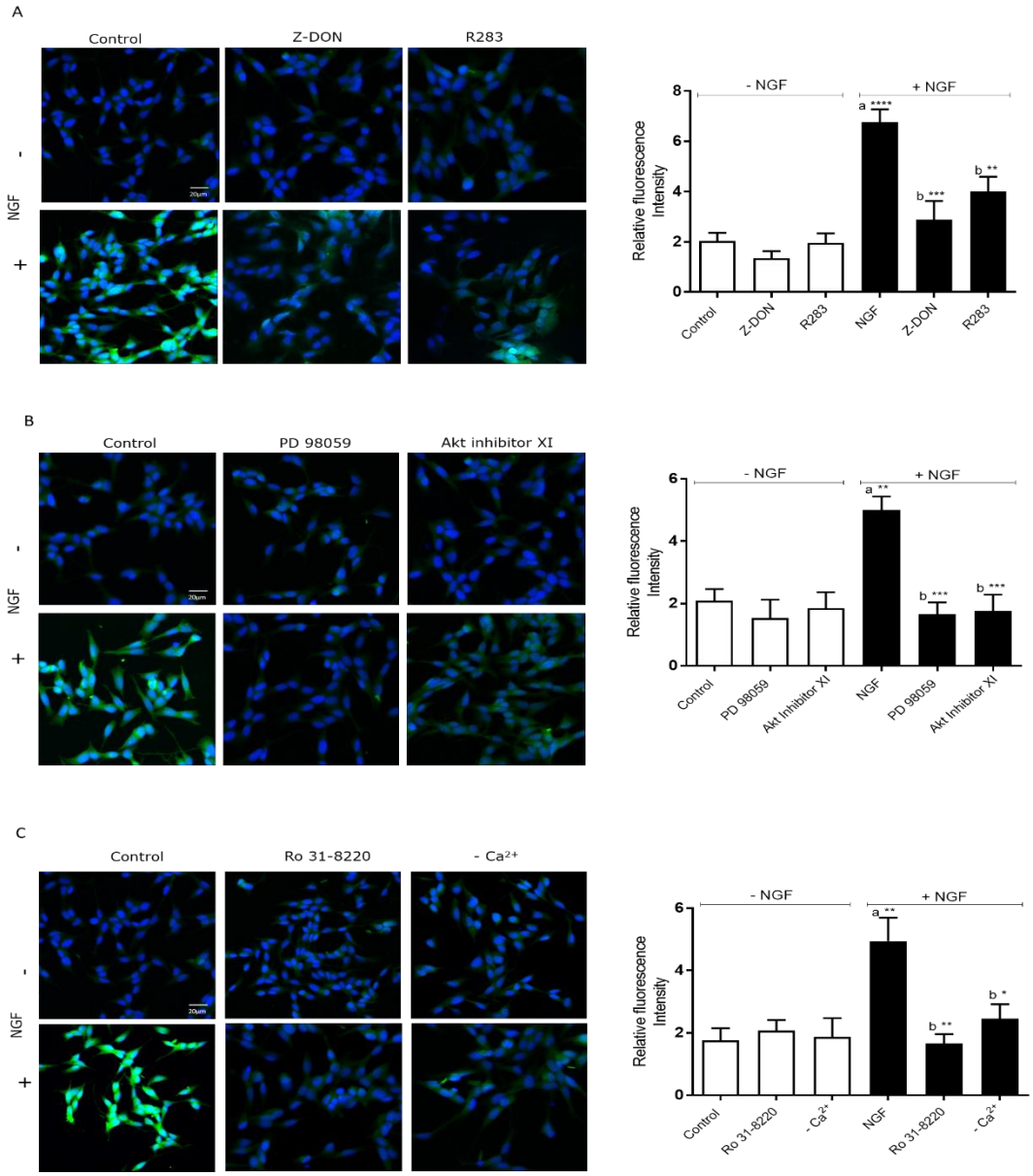

Figure 5.15 NGF-induced *in situ* TG activity in differentiating SH-SY5Y cells.

The cells were incubated with 1 mM biotin-X-cadaverine (BXC) for 6 h, after which, they were incubated with (A) TG2 inhibitors Z-DON (150 µM) and R283 (200 µM) for 1 h, (B) PD 98059 (50 µM) and Akt Inhibitor XI (100 nM) for 30 min, or (C) Ro 31-8220 (10 µM) for 30 min or the absence of extracellular Ca^{2+} (nominally Ca^{2+}-free Hanks/HEPES buffer containing 0.1 mM EGTA) prior to stimulation with NGF (100 ng/ml) for 1 h. TG2-mediated BXC incorporation into intracellular proteins was visualised using FITC-conjugated ExtrAvidin® (green). Nuclei were stained with DAPI (blue) and viewed using a Leica TCS SP5 II confocal microscope (20× objective magnification). Scale bar = 20 µm. The images presented are from one experiment and representative of three assays. Quantified data represent the mean ± S.E.M. of fluorescence intensity relative to DAPI stain for five fields of view each from at least three independent experiments. *P<0.05, ** P<0.01, *** P<0.001 and ****P<0.0001 versus the control response.

5.2.5. Phosphorylation of TG2 in response to NGF

Based on previous observations, NGF-induced TG2 activity involved various signalling proteins; it can be speculated that NGF could phosphorylate TG2 via those protein kinases. Therefore, the effect of NGF on the phosphorylation status of TG2 was next examined via the immunoprecipitation of TG2, followed by SDS-PAGE and Western blot analysis, using anti-phosphoserine and anti-phosphothreonine antibodies, as described in Chapter 2 (section 2.2.10). The observation from these experiments clearly revealed that NGF (100 ng/ml) enhanced TG2-bound phosphoserine and phosphothreonine in differentiating N2a (Figures 5.16 and 5.18) and SH-SY5Y cells (Figures 5.17 and 5.19). In addition, pre-treatment with PD 98059 (50 µM), Akt Inhibitor XI (100 nM) and Ro 31-8220 (10 µM) significantly inhibited NGF-mediated TG2 phosphorylation in differentiating N2a (Figures 5.16 and 5.18) and SH-SY5Y cells (Figures 5.17 and 5.19). In marked contrast, removal of extracellular Ca^{2+} had no significant influence on NGF-induced TG2 phosphorylation, and this result was similar in both cell lines (Figures 5.18 and 5.19). These data indicate that NGF promotes robust increases in TG2 phosphorylation, and this process is mainly ERK1/2, PKB and PKC dependent.

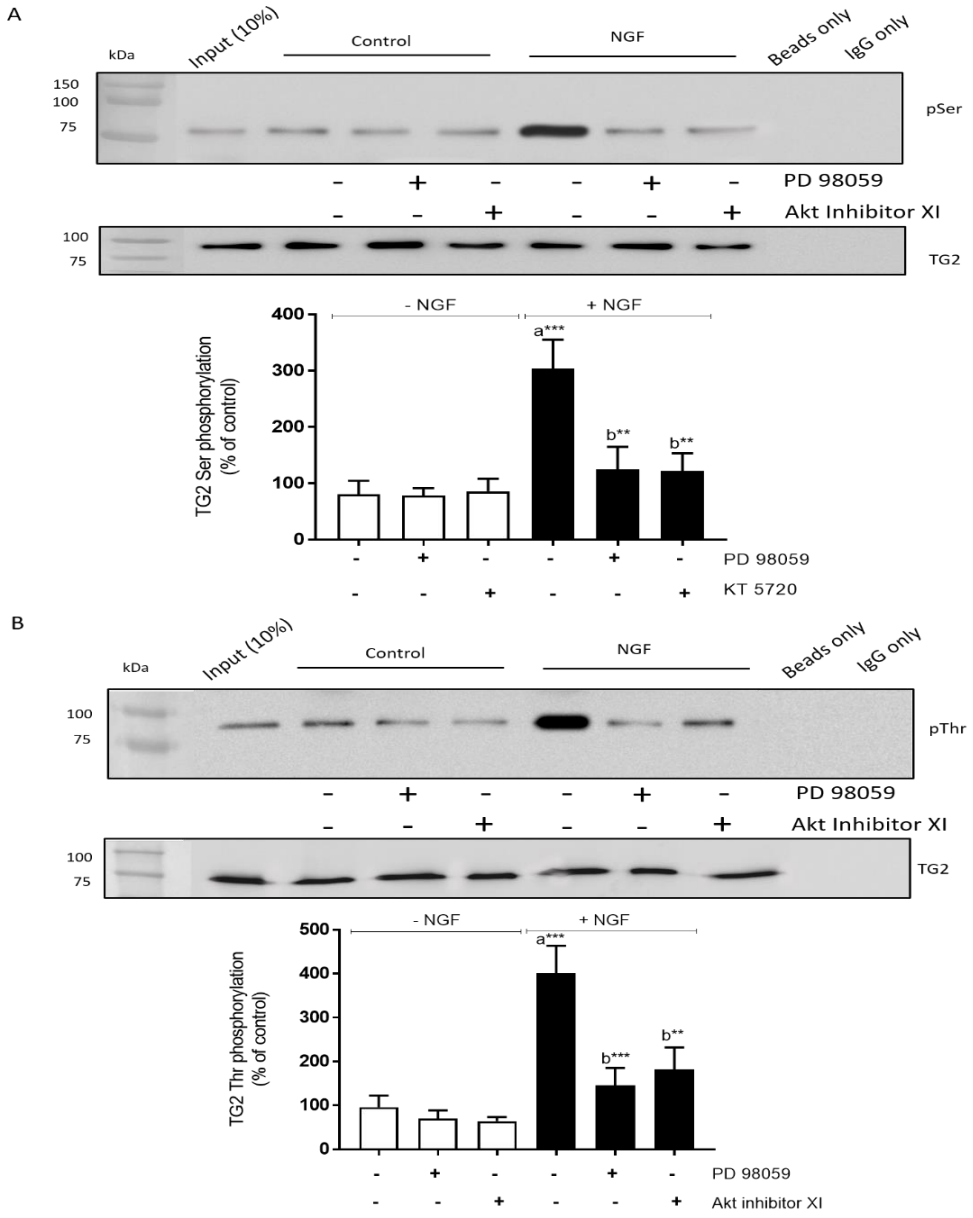

Figure 5.16 Effects of the ERK1/2 inhibitor PD 98059 and Akt inhibitor XI on NGF-induced phosphorylation of TG2 in differentiating N2a cells.

Where indicated, differentiating N2a cells were pre-treated for 30 min with PD 98059 (50 µM) or Akt Inhibitor XI (100 nM) prior to stimulation with NGF (100 ng/ml) for 1 h. Following stimulation with NGF, the cell lysates were subjected to immunoprecipitation using anti-TG2 monoclonal antibody as described in section 2.2.10. The resultant immunoprecipitated protein(s) were subjected to SDS-PAGE and Western blot analysis using (A) anti-phosphoserine and (B) anti-phosphothreonine antibodies. One-tenth of the total input was applied to the first lane to show the presence of phosphorylated proteins prior to immunoprecipitation, and negative controls with the immunoprecipitation performed with immunobeads only were included to demonstrate the specificity of the band shown. Quantified data for NGF-induced increases in TG2-bound serine and threonine phosphorylation are expressed as a percentage of the TG2 phosphorylation observed in control cells (= 100%). Data points represent the mean ± S.E.M. from three independent experiments. ** $P<0.01$ and *** $P<0.001$ (a) versus control and (b) versus NGF alone.

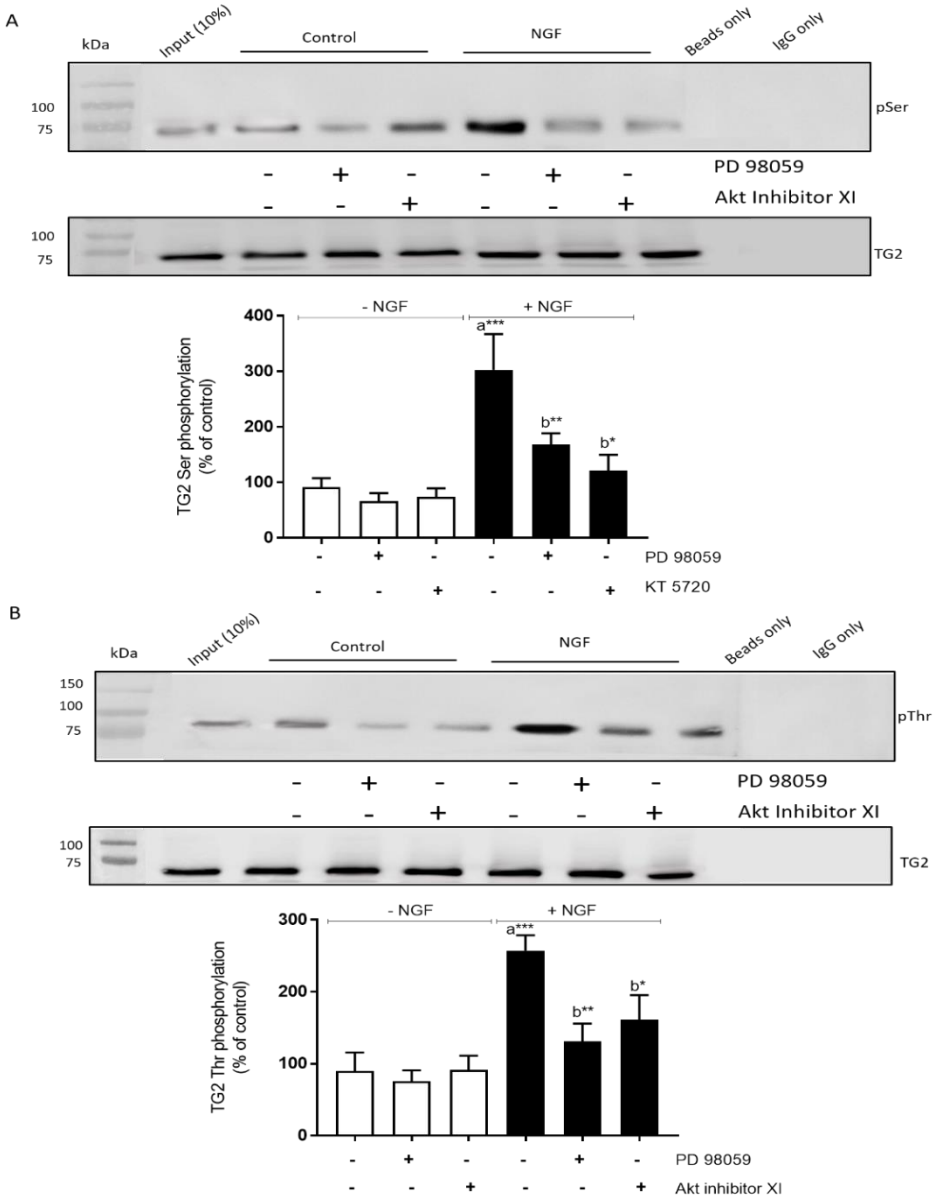

Figure 5.17 Effects of the ERK1/2 inhibitor PD 98059 and Akt inhibitor XI on NGF-induced phosphorylation of TG2 in differentiating SH-SY5Y cells.

Where indicated, differentiating SH-SY5Y cells were pre-treated for 30 min with PD 98059 (50 µM) or Akt Inhibitor XI (100 nM) prior to stimulation with NGF (100 ng/ml) for 1 h. Following stimulation with NGF, cell lysates were subjected to immunoprecipitation using anti-TG2 monoclonal antibody, as described in section 2.2.10. The resultant immunoprecipitated protein(s) were subjected to SDS-PAGE and Western blot analysis using (A) anti-phosphoserine and (B) anti-phosphothreonine antibodies. One-tenth of the total input was applied to the first lane to show the presence of phosphorylated proteins prior to immunoprecipitation and negative controls with the immunoprecipitation performed with immunobeads only were included to demonstrate the specificity of the band shown. Quantified data for NGF-induced increases in TG2-bound serine and threonine phosphorylation are expressed as a percentage of the TG2 phosphorylation observed in control cells (= 100%). Data points represent the mean ± S.E.M. from three independent experiments. *P<0.05, ** P<0.01 and *** P<0.001 (a) versus control and (b) versus NGF alone.

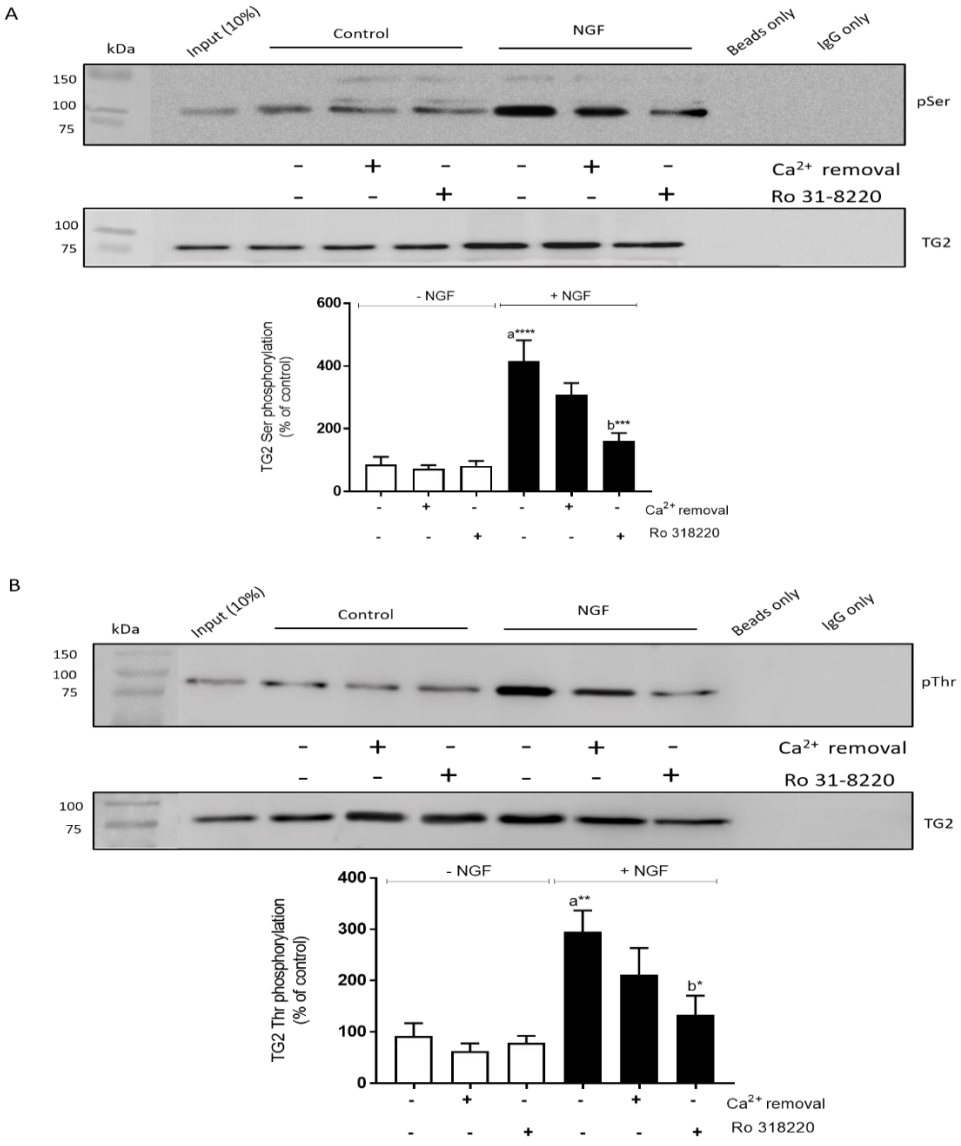

Figure 5.18 Effect of the Ca^{2+} and PKC inhibitor Ro 31-8220 on NGF-induced phosphorylation of TG2 in differentiating N2a cells.

Where indicated, differentiating N2a cells were subjected to the absence of extracellular Ca^{2+} (nominally Ca^{2+}-free Hanks/HEPES buffer containing 0.1 mM EGTA) or pre-treated for 30 min with Ro 31-8220 (10 µM) prior to stimulation with NGF (100 ng/ml) for 1 h. Following stimulation with NGF, the cell lysates were subjected to immunoprecipitation using anti-TG2 monoclonal antibody, as described in section 2.2.10. The resultant immunoprecipitated protein(s) were subjected to SDS-PAGE and Western blot analysis using (A) anti-phosphoserine and (B) and anti-phosphothreonine antibodies. One-tenth of the total input was applied to the first lane to show the presence of phosphorylated proteins prior to immunoprecipitation, and negative controls with the immunoprecipitation performed with immunobeads only were included to demonstrate the specificity of the band shown. Quantified data for NGF-induced increases in TG2-bound serine and threonine phosphorylation are expressed as a percentage of the TG2 phosphorylation observed in control cells (= 100%). Data points represent the mean ± S.E.M. from three independent experiments. *P<0.05, ** P<0.01 and *** P<0.001 (a) versus control and (b) versus NGF alone.

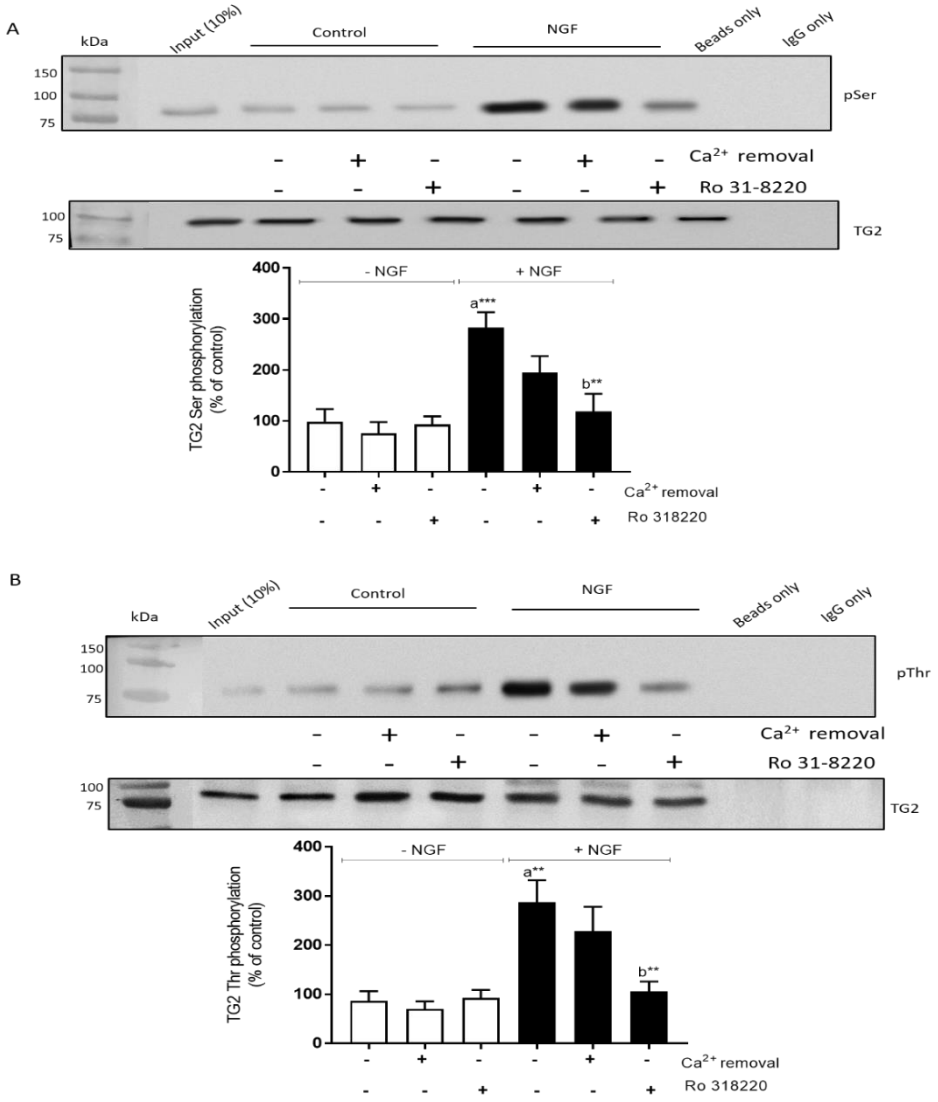

Figure 5.19 Effect of the Ca^{2+} and PKC inhibitor Ro 31-8220 on NGF-induced phosphorylation of TG2 in differentiating SH-SY5Y cells.

Where indicated, differentiating SH-SY5Y cells were subjected to the absence of extracellular Ca^{2+} (nominally Ca^{2+}-free Hanks/HEPES buffer containing 0.1 mM EGTA) or pre-treated for 30 min with Ro 31-8220 (10 µM) prior to stimulation with NGF (100 ng/ml) for 1 h. Following stimulation with NGF, cell lysates were subjected to immunoprecipitation using anti-TG2 monoclonal antibody, as described in section 2.2.10. The resultant immunoprecipitated protein(s) were subjected to SDS-PAGE and Western blot analysis using (A) anti-phosphoserine and (B) and anti-phosphothreonine antibodies. One-tenth of the total input was applied to the first lane to show the presence of phosphorylated proteins prior to immunoprecipitation, and negative controls with the immunoprecipitation performed with immunobeads only were included to demonstrate the specificity of the band shown. Quantified data for NGF-induced increases in TG2-bound serine and threonine phosphorylation are expressed as a percentage of the TG2 phosphorylation observed in the control cells (= 100%). Data points represent the mean ± S.E.M. from three independent experiments. ** $P<0.01$ and *** $P<0.001$ (a) versus control and (b) versus NGF alone.

5.3 Discussion

As the neurotrophic factor PACAP-27 induces TG2 activity via multiple protein kinase pathways (Chapter 4), determining the role of NGF – another member of the neurotrophin family – will provide insight into the molecular mechanisms underlying the correlation of these neurotrophic factors and the multifunctional enzyme TG2. This will also aid in studying the possible neuroprotective effect associated with this activation. The present study focussed on identifying whether TG2 is modulated by NGF in mouse and human neuroblastoma cells and determining the molecular mechanisms underlying such modulation. The data in this study provide sufficient evidence to support the notion that TG2 activity is modulated by NGF in differentiated neuroblastoma cells via ERK1/2, PKB and PKC-dependent pathways.

5.3.1 Modulation of TG2 transamidation activity by NGF

Over the years, NGF has been demonstrated to mediate neurite outgrowth and neuroprotection (Howe, & Mobley, 2001; Huang & Reichardt, 2001; Oe et al., 2005; Tang et al., 2005). TG2 has been shown to be necessary for enhancing neurite outgrowth (Tucholski et al., 2001). However, it is not known whether TG2 has a role in the growth-promoting action of NGF. In a previous study, the interplay between NGF and TG2 in neuroblastoma cells was established; it was found that exposure of RA-differentiated N2a cells to NGF (4 days) caused a higher level of TG2 activity compared with that shown in cells treated with NGF alone (Condello et al., 2008). This suggests that NGF and RA act synergistically to promote TG2 activation (Condello et al., 2008). However, to date, there is no evidence concerning crosstalk between short-term treatment with NGF, which is not carried out for differentiation purposes, and TG2 activity in neuroblastoma cells. In the current study, it appears that short-term treatment with NGF (<4 h) triggered time- and concentration-dependent increases in *in vitro* TG2-mediated biotin-cadaverine incorporation and protein crosslinking activity in differentiating N2a (Figure 5.1) and SH-SY5Y (Figure 5.2) cells. This peaked at 1 h and a concentration of 100 ng/ml. The findings were further confirmed by quantitative analysis of fluorescence microscopy of the *in situ* intracellular TG2 activity following NGF stimulation, which indicated a time- and concentration-dependent NGF induction of *in situ* TG2-mediated polyamine incorporation into the protein substrate activity in both differentiating neuroblastoma cell lines (Figures 5.12 and 5.13). The results were comparable to those concerning the NGF-induced amine incorporation activity observed *in vitro*. Overall, these initial observations suggest that NGF has a direct

stimulation effect on inducing TG2 activity. Since the main aim of this study was to investigate NGF-induced TG2 activity and its possible involvement in neuroprotection and cell survival effects, in this context, the data obtained here are in line with previous observations suggesting that NGF exerts rapid neuroprotective effects (30 min treatment) and maximum protection within 1 h; this research also showed that 100 ng/ml of NGF is efficient in inducing sufficient neuroprotective action (Nguyen et al., 2010). This protective effect has been sustained up to 24 h through the downstream signalling cascade (Nguyen et al., 2010).

A previous study revealed that exposure of N2a cells to NGF (50 ng/ml) for 4 days mediated the induction of TG2 expression (Condello et al., 2008). However, from the findings of the current study, it is important to note that the levels of TG2 protein expression did not change during a short time period (<4 h), emphasising that the enhancement of TG2 activity induced by NGF is not a consequence of increased levels of TG2 expression. The possible explanation for this variation is that, in neuroblastoma cells, the optimum incubation time for NGF to enhance TG2 protein expression is up to 4 days, while a shorter time would be sufficient to induce TG2 enzymatic activity. Although differentiating N2a and SH-SY5Y cells also express TG1 and TG3 isoforms, NGF-induced increases in TG activity were inhibited by R283 and Z-DON, confirming that the observed increases in TG activity occurred selectively via TG2 (Figure 5.4). This observation was also confirmed by assessing TG2's *in situ* activity, and the findings revealed an equivalent pattern to reverse the NGF-induced *in situ* TG2 activity by the TG2 inhibitors R283 and Z-DON in both neuroblastoma cell lines (Figures 5.14 A and 5.15 A).

5.3.2 The role of protein kinases

It has recently been shown that the stimulation of intracellular TG2-mediated transamidase activity by the A_1 adenosine receptor depends on ERK1/2, PKC, and TG2 phosphorylation (Vyas et al., 2016). There is increasing evidence for NGF-induced activation of the MAPK/ERK, phospholipase C (PLC)-γ1 and (PI3K/Akt) signalling cascades via the TrkA receptor, which are required for neuronal survival (Patapoutian and Reichardt 2001; Lemmon et al., 2010). These NGF signalling networks, which are initiated and controlled by Ras, represent a precise cascade of events that directly regulate protein–protein interactions. Since the crosslinking activity of TG1 is regulated via ERK1/2 and PKC, it is conceivable that NGF may modulate the activity of multiple TG isoforms through the induced kinases (Bollag et al., 2005). Moreover, as the data in the previous section 5.3.1 showed that NGF significantly enhanced TG2 activity, it is presumed that NGF-induced activation of MAPKs (especially

ERK1/2, PKC and PKB/Akt) would be involved in enhancing of TG2 activity. The roles of protein kinases in NGF-induced TG2 activity and TG2 phosphorylation are discussed in the following sections.

The role of protein kinases in NGF-mediated TG2 activation

Since NGF via the TrkA receptor stimulates protein kinase cascades involving ERK1/2, PKB and PKC (Wang et al., 2014), the current study explored the roles of these kinases in NGF-induced TG2 activation. Initially, the protein kinases activated by NGF in differentiating N2a and SH-SY5Y were characterised, and the effects of the appropriate protein kinase pharmacological inhibitors were assessed. The findings confirmed that NGF stimulates the phosphorylation of ERK1/2 and PKB; these findings are broadly comparable to those of previous studies, which have reported the activation pattern of ERK1/2 and PKB by NGF (Wang et al., 2014). As depicted in Figure 5.5, the induced activation of ERK1/2 and PKB was attenuated by the MEK1/2 inhibitor PD 98059 and Akt Inhibitor XI, respectively, in both neuroblastoma cell lines. ERK1/2 and Akt/PKB are independent signalling programs that generate compensatory mechanisms, which are especially important and sufficient for controlling cell survival and the differentiation process. Moreover, they have been found to be essential for NGF to induce the cell survival of different neuronal cell types (Yao & Cooper, 1995; Philpott et al., 1997; Nguyen et al., 2010). In addition, there is extensive crosstalk between those pathways for regulating each other (Yu et al., 200; Moelling et al., 2002; Lemmon et al., 2010; Mendoza et al.,2011). For example, in various cancer models, the inhibition of both pathways conjointly has been found to effectively minimise tumour growth (Engelman et al., 2008; Kinkade et al., 2008). Thus, in this project, it was of interest to determine whether they could have a negative cross-inhibition effect on each other. As shown in Figure 5.6**,** inhibiting of PKB using Akt Inhibitor XI did not influence the NGF-induced increase in ERK1/2 phosphorylation; in addition, inhibition of MEK1/2 using PD 98059 had no effect on the PKB phosphorylation induced by NGF in N2a and SH-SY5Y cells. The data from these experiments suggest inhibitor selectivity and a lack of 'crosstalk' between the two kinase pathways in differentiating N2a and SH-SY5Y cells.

Increasing evidence suggests that TG2 is regulated by phosphorylation. As in the previously mentioned example, phosphorylation of TG2 by PKA inhibits its transamidating activity, but augments its kinase activity (Mishra et al., 2007), whereas PTEN-induced putative kinase 1 (PINK1) mediated phosphorylation of TG2 inhibits its proteasomal degradation (Min et al.,

2015). As mentioned previously, TG2 activity could be modulated by ERK1/2, PKB and PKC induced by GPCRs, such as the A_1 adenosine receptor (Vyas et al., 2016) or receptor tyrosine kinases (Sivaramakrishan et al., 2013). Thus, it was necessary to assess their role in NGF-induced TG2 activity. The observation that pharmacological inhibition of ERK1/2, PKB and PKC attenuated NGF-induced TG2 transamidase activity in N2a and SH-SY5Y cells suggests prominent roles for these protein kinases in NGF-modulating TG2 activity (Figures 5.7 and 5.9). These observations agree with previous research, which has revealed roles for ERK1/2, PKB and PKC in TG2 activation triggered by members of the GPCR family (Vyas et al., 2016, 2017). Furthermore, NGF-induced *in situ* TG2 responses were also sensitive to the pharmacological inhibition of ERK1/2, PKB and PKC, confirming the role of these kinase pathways. Finally, it is important to note that the attenuation of NGF-induced TG2 activation by the inhibition of PKC reflected the reported upstream role of PKC isozymes in NGF-induced ERK1/2 activation (Lloyd & Wooten, 1992; Wooten et al., 2000). Clearly, further assessment is required to establish whether NGF activation promotes TG2 phosphorylation and, if so, identify the protein kinases involved. These targets are discussed in the next section. Such assessment would provide a better understanding of how the NGF-modulated TG2 activity may induce neuronal survival and neurite outgrowth.

The role of protein kinases in NGF-mediated TG2 phosphorylation

Considering the evident roles of ERK1/2, PKB and PKC in modulating TG2 activity (described in the previous section), it was of interest to investigate the role of these kinases in the phosphorylation status of TG2 following NGF stimulation. TG2 phosphorylation was monitored by immunoprecipitation, and the data demonstrated that TG2 was phosphorylated in response to NGF (Figures 5.16, 5.17, 5.18 and 5.19) in both neuroblastoma cell lines. Therefore, it is conceivable that the modulation of TG2 phosphorylation represents a downstream target of NGF-induced signalling. In this context, several studies have previously outlined the role of protein kinases in the regulation of TG2 activity. For example, a previous study reported that TG2 is phosphorylated by PKA at Ser^{215} and Ser^{216} which promotes its interaction with the scaffolding protein 14-3-3, leading to the attenuation of TG2 kinase activity (Mishra & Murphy, 2006). Furthermore, TG2 is phosphorylated at an unknown site(s) by PINK1 (Min et al., 2015). It is also known that phosphorylation of TG2 by PKA at Ser^{216} inhibits its transamidase activity and enhances its kinase activity (Mishra et al., 2007; Wang et al., 2012). In the current study, it was also reasonable to investigate the influence of the inhibition of the involved protein kinases

on NGF-induced TG2 phosphorylation. From the findings in this chapter, it is quite clear that pharmacological inhibition of ERK 1/2 (PD 98059), PKB (Akt inhibitor XI) or PKC (Ro 31-8220) significantly attenuated the NGF-induced promotion of TG2 serine and threonine phosphorylation. This suggests similar roles to those reported in earlier work, which showed that inhibition of ERK 1/2 and PKC reversed the TG2 phosphorylation induced by the activation of the A_1 receptor in a cardiomyocyte model (Vyas et al., 2016). However, it is not known whether ERK1/2, PKB and PKC directly phosphorylate TG2, leading to direct enhancement of enzymic activity, or whether these kinases may phosphorylate downstream targets that subsequently interact with TG2, resulting in enhanced activity. Furthermore, as TG2 possesses kinase activity, the process possibly involves auto-phosphorylation; thus, further work to determine the possible auto-phosphorylation site, if it exists, in response to NGF would be worthwhile for improving the understanding of the signalling mechanism of the induced response.

The role of Ca^{2+} in NGF-induced TG2 activation

Previous studies have shown that NGF triggers intracellular Ca^{2+} release in C6-2B glioma cells (De Bernardi et al., 1996) and extracellular Ca^{2+} influx in PC12 and bovine chromaffin cells (Pandiella Alonso et al., 1986). Moreover, since TG2 transamidase activity is Ca^{2+} dependent, it was of interest to investigate the potential involvement of extracellular and intracellular Ca^{2+} in NGF-induced TG2 activation. The data presented indicate that NGF-induced TG2-mediated *in vitro* (Figure 5.11) and *in situ* (Figures 5.14 C and 5.15 C) transamidase activity partially depends on extracellular Ca^{2+}, suggesting that NGF triggers Ca^{2+} influx in N2a and SH-SY5Y cells. However, no measurable increases in intracellular Ca^{2+} were observed following stimulation of these cells with NGF. The reason(s) for this are not currently known, but may reflect localised NGF-induced increases in $[Ca^{2+}]_i$ that were not detectable using the technique employed. While the levels of Ca^{2+} required for TG2 activation are typically in the order of 3–100 μM, there is evidence that $[Ca^{2+}]_i$ can reach levels sufficient to activate intracellular TG2 (Király et al., 2011). Alternatively, the participation of Ca^{2+} in NGF-induced TG2 activation may necessitate the sensitisation of TG2 to low levels of $[Ca^{2+}]_i$. It has been suggested that the interaction of TG2 with protein binding partners and/or membrane lipids promotes a conformational change that enables activation at low levels of intracellular $[Ca^{2+}]$ (Király et al., 2011). It is also important to note that removal of extracellular Ca^{2+} has no effect on NGF-induced TG2 phosphorylation (Figures 5.18 and 5.19). It has been reported that conformational changes in TG2 triggered by Ca^{2+} facilitate its subsequent phosphorylation by PKA and/or

ERK1/2. However, in the current study, the removal of extracellular Ca^{2+} showed no effect on TG2 phosphorylation induced by NGF. It could be that TG2 phosphorylation induced by NGF sensitises TG2 to activate, and this reaction exists even in the presence of low Ca^{2+} levels. It would be of interest to study the effects of Ca^{2+} removal and either of the protein kinases simultaneously on TG2 phosphorylation to further understand the selective role of Ca^{2+} on this process. Clearly, further studies are required to determine how NGF-induced TG2 activation occurs in the absence of detectable increases in $[Ca^{2+}]_i$, but the kinase-dependent pathways outlined in the present study could be central to these novel aspects of TG2 regulation.

5.4 Conclusion

The data presented in this chapter indicate that the neurotrophic factor NGF (100 ng/ml, 1 h) induces TG2 transamidase activity and TG2 phosphorylation in differentiating N2a and SH-SY5Y neuroblastoma cells. Furthermore, the findings demonstrate that this modulation is carried out at the molecular level via ERK1/2-, PKB/Akt- and PKC-dependent pathways; summarised in Figure 5.20. The results in this chapter highlight the existence of crosstalk between neurotrophic NGF and TG2 activity in neuroblastoma cells, and this discussion may provide the basic components of the novel modulation of neuronal cell function (Table 5.1)

Table 5.1 The overall ability of different treatments to inhibit NGF-induced TG2 activity assessed by different approaches

Treatment	Assessment following NGF treatment									
	Amine incorporation		Peptide crosslinking		In-situ		IP		WB	
	N2a	SH-SY5Y	N2a	SH-SY5Y	N2a	SH-SY5Y	N2a	SH-SY5Y	N2a	SH-SY5Y
Z-DON (150 µM; TG2 inhibitors)	****	****	****	**	***	***	nd	nd	nd	nd
R283 (200 µM; TG2 inhibitors)	***	**	****	**	**	**	nd	nd	nd	nd
PD 98059 (50 µM; MEK1/2 inhibitor)	**	***	***	**	**	***	**	**	* vs ERK1/2 ns vs PKB	*** vs ERK1/2 ns vs PKB
Akt inhibitor XI (0.1 µM; PKB inhibitor)	*	**	**	*	***	***	**	*	ns vs ERK1/2 ** vs PKB	ns vs ERK1/2 ** vs PKB
Ro 31-8220 (10 µM; PKC inhibitor)	**	*	***	**	**	**			** vs ERK1/2 ns vs PKB	* vs ERK1/2 ns vs PKB
Nominally Ca^{2+}-free Hanks/HEPES buffer containing 0.1 mM EGTA	*	*	**	*	**	*	ns	ns	nd	nd
50 µM BAPTA-AM in nominally Ca^{2+}-free Hanks/HEPES buffer containing 0.1 mM EGTA	**	*	***	**	**	nd	nd	nd	nd	nd

Results of the range of treatments used in this study to investigate the role of NGF in modulating of TG2 activity. Differentiated N2a or SH-SY5Y neuroblastoma cells were treated with the compounds in the table; then, the cells were stimulated with NGF, and the TG2 activity was assessed by different approaches, as follows: *in vitro* amine incorporation and peptide crosslinking assays, visualisation of *in situ* amine incorporation activity, protein expression by Western blotting (WB) and immunoprecipitation (IP). ns= no significant decrease, nd= not determined, *P<0.05, **P<0.01, ***P<0.001, and ****P<0.0001, compared to the control

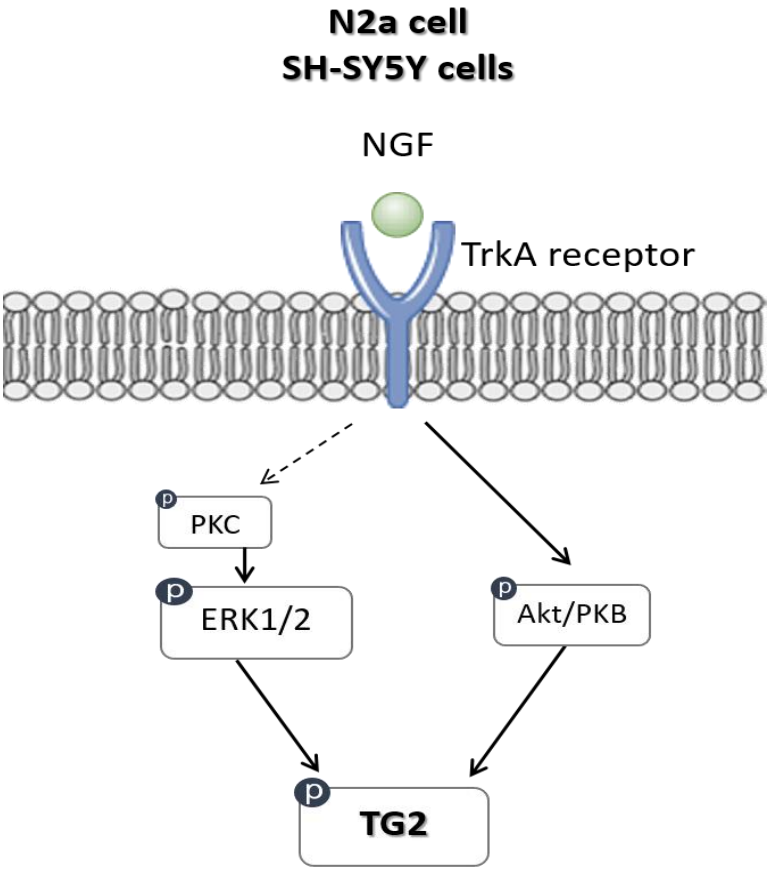

Figure 5.20 Schematic summary of the NGF-induced TG2 activation.

NGF triggers activation of various downstream targets in differentiated mouse N2a and SH-SY5Y cells. NGF induces TG2 activity and phosphorylation by triggering the activation of protein kinases (ERK1/2, Akt/PKB and PKC). Solid black arrows represent the findings of the current study; dashed arrows represent findings from other research (Sivaramakrishan et al., 2013).

Chapter 6

6 The role of TG2 in PACAP-27- and NGF-induced neuroblastoma cell survival and neurite outgrowth

6.1 Introduction

A substantial body of evidence indicates that one of the key roles of neurotrophic factors is protecting neuronal cells from cell death after cerebral ischaemia and inducing neurite outgrowth (Kromer, 1987; Wang et al., 1993; Gonzalez et al., 1997; Erhardt & Sherwood, 2004; Oliveira et al., 2013). Both NGF and PACAP have neurotrophic effects, which have been studied extensively; they promote differentiation, maturation, neurite outgrowth and survival of neurons *in vivo* and *in vitro* (Williams et al., 1986; Hatanaka et al., 1988; akei et al., 2000; Yuhara et al., 2001). In addition, the intracellular transduction pathways involved in their neurotrophic effects are now well established (Kaplan & Miller, 2000; Ravni et al., 2006). For example, in the PC12 cell line, PACAP prevents cell apoptosis by activating the PKA signalling cascade (Reglodi et al., 2004), whereas NGF inhibits apoptosis and induces neuroprotection through the PI-3K/PKB pathway (Shimoke & Chiba, 2001; Salinas et al. 2003; Wu & Wong, 2005). In agreement with the previous studies outlined above, the two trophic factors exerted similar effects in the present study, especially neurite outgrowth and neuronal survival; thus, it can be speculated that they may be protecting neuronal cell death via a similar modulator. It was recently suggested that TG2 has a neuronal cell protection and differentiation role (Tatsukawa et al., 2016). In addition, it has been reported that TG2 is activated via protein kinases, such as ERK1/2, PKB and PKC (Vyas et al., 2016, 2017). It is conceivable that these trophic factors could modulate TG2 activity to play a role in neuronal cell survival and neurite outgrowth. Hence, the aims of the work presented in this chapter were to assess the possible role of the multifunctional enzyme TG2 in the following: i) PACAP- and NGF-induced neuroprotection, which were determined after hypoxia exposure by assessing the cell viability and activation of caspase-3, and ii) their neurite outgrowth, as examined by high-throughput

screening for quantitatively analysing multiple parameters of neurite outgrowth in neuroblastoma cells. It was of interest to investigate whether the neurotrophic factor-induced TG2 activity has a protective role against hypoxia-induced neuronal cell injury, as well as whether it is involved in the neurite outgrowth process; such findings could reveal a new therapeutic target for neurodegenerative and hypoxia-associated neuronal injury.

6.2 Results

6.2.1 The role of TG2 in cell survival

Determination of the time course for hypoxia-induced cell death

Initially, the time course of simulated hypoxia (5% CO_2/1% O_2 in glucose- and serum-free medium at 37°C)-induced cell death was examined. Differentiating N2a and SH-SY5Y cells were exposed to hypoxia for different durations (0, 1, 2, 4, 6, 8 and 24 h). Then, cell viability was monitored by MTT reduction assay, cytotoxicity was measured by LDH activity assay (section 2.2.11), and the activation of caspase-3; an enzyme involved in programmed cell death (apoptosis), which was monitored via Western blotting (section 2.2.9). In both N2a and SH-SY5Y cells, exposure to simulated hypoxia (1% O_2) resulted in a time-dependent decrease in MTT reduction, increase in LDH release and gradual increase in caspase-3 activation. As shown in Figures 6.1 A and 6.2 A, cell viability was significantly decreased at 8 h of exposure to hypoxia in both cell lines, with a decrease in MTT reduction to about 60% of the control value. Notably, the release of LDH release was highly statistically significant ($p < 0.001$) at 8 h of hypoxia exposure compared with the control (at 0 h of hypoxia) in both cell lines (Figures 6.1B and 6.2B). Exposing neuroblastoma cells to 8 h of hypoxia triggered a significant increase ($p < 0.001$) in caspase-3 activation (Figures 6.1 C-D and 6.2 C-D). Furthermore, to determine the timescale of the morphological changes induced by hypoxia in differentiated N2a and SH-SY5Y cells, the cells were stained with Coomassie Blue, and changes in cell morphology were assessed microscopically. As shown in Figure 6.3, about 25% of the neurites retracted in the first 2 h after hypoxia exposure. At 8 h of hypoxia, both N2a and SH-SY5Y cell images showed cell body shape and size alterations; these observations provided evidence of neuroblastoma cell deterioration occurring after 8 h of exposure to hypoxia. The previous cell viability and morphology findings were clearly comparable in both the mouse and human neuroblastoma cell lines, and they showed that exposing the cells to 8 h of hypoxia is sufficient to induce cell death; hence, an 8-h duration was chosen for the subsequent experiments.

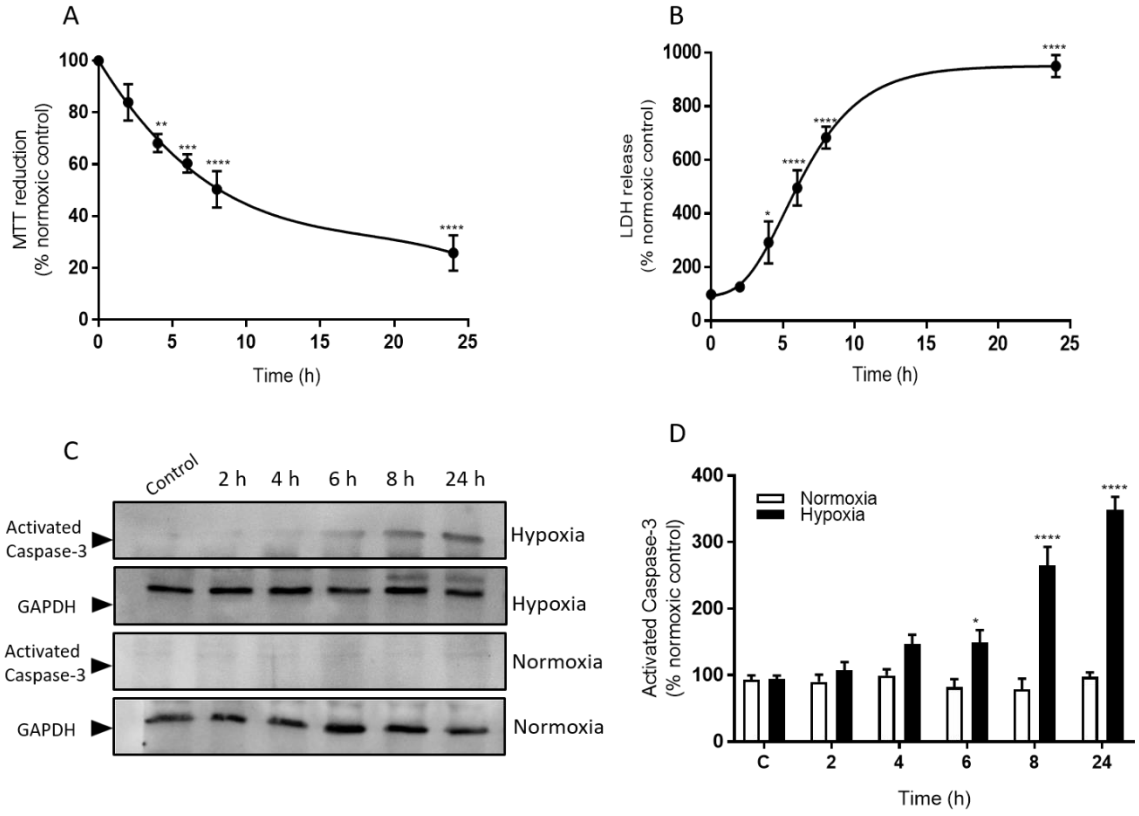

Figure 6.1 Effect of simulated hypoxia on cell viability in terms of MTT reduction, LDH release and caspase-3 activity in differentiating N2a cells.

Cells in glucose- and serum-free DMEM were exposed to hypoxia (1% O_2) for the indicated times. Cell viability was assessed by measuring (A) the metabolic reduction of MTT by cellular dehydrogenases, (B) release of LDH into the culture medium and (C) caspase-3 activity via Western blot analysis using the anti-active caspase-3 antibody. Levels of GAPDH are shown for comparison. (D) Quantified caspase-3 activity data. Data are expressed as the percentage of the normoxic control (=100%) and represent the mean ± SEM of four independent experiments. *$p < 0.05$, **$p < 0.01$, ***$p < 0.001$ and ****$p < 0.0001$ versus normoxic control.

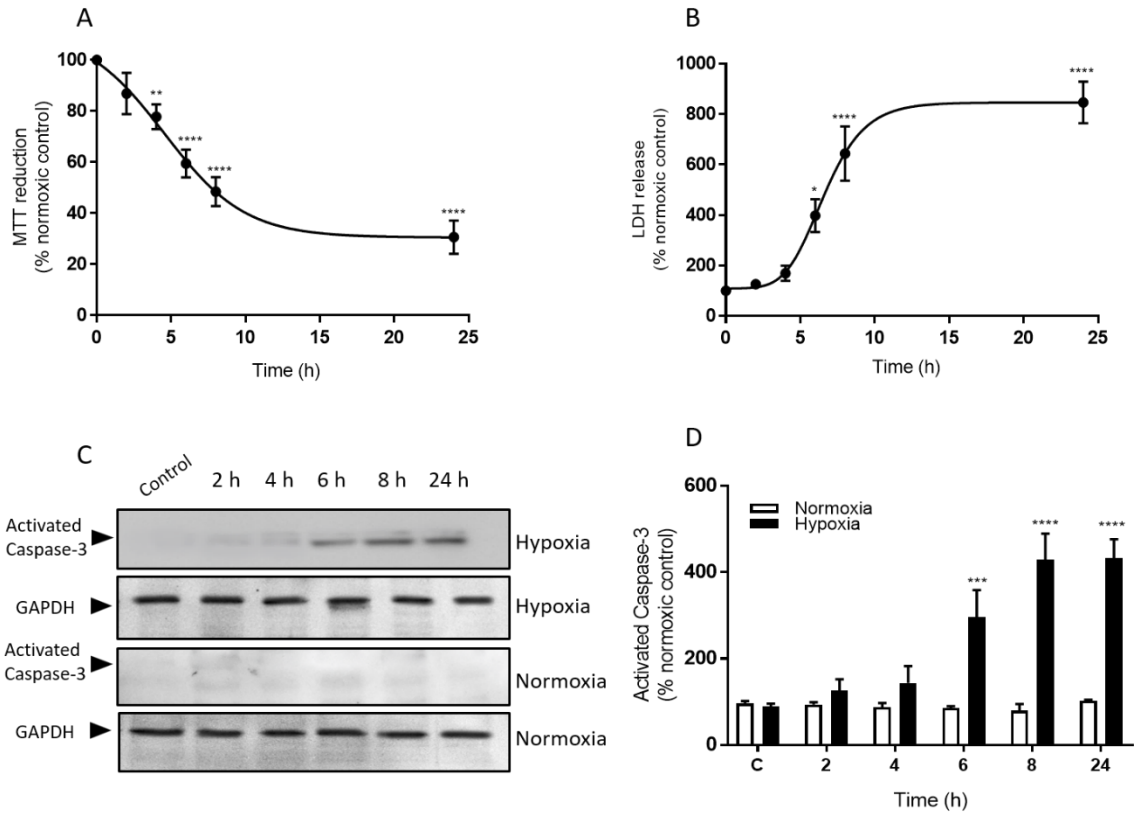

Figure 6.2 Effect of simulated hypoxia on cell viability MTT reduction, LDH release and caspase-3 activity in differentiating SH-SY5Y cells.

Cells in glucose- and serum-free DMEM were exposed to hypoxia (1% O_2) for the indicated times. Cell viability was assessed by measuring (A) the metabolic reduction of MTT by cellular dehydrogenases, (B) release of LDH into the culture medium and (C) caspase-3 activity via Western blot analysis using the anti-active caspase-3 antibody. Levels of GAPDH are shown for comparison. (D) Quantified caspase-3 activity data. Data are expressed as the percentage of the normoxic control (=100%) and represent the mean ± SEM from four independent experiments. *$p < 0.05$, **$p < 0.01$, ***$p < 0.001$ and ****$p < 0.0001$.

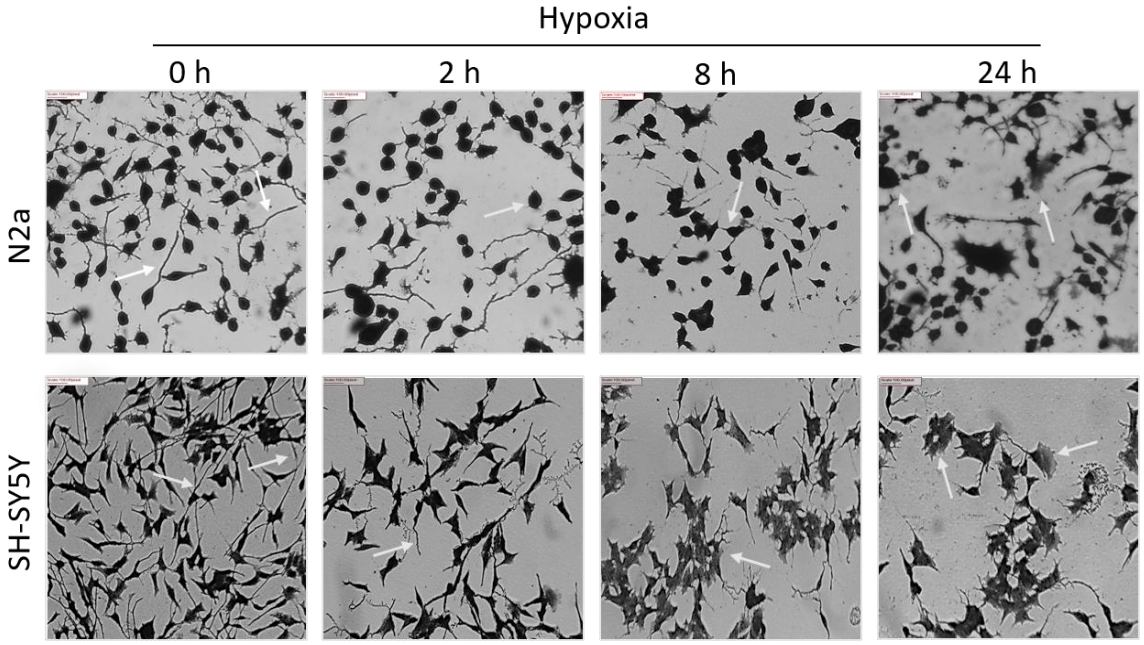

Figure 6.3 Effect of simulated hypoxia on differentiating N2a and SH-SY5Y cell morphology.

Morphological evidence of injury and death in neurons exposed to hypoxia for 0, 2, 8 and 24 h in differentiating N2a and SH-SY5Y cells. Cells were exposed to hypoxia (1% O_2) for the indicated times. Cells were fixed with 90% (v/v) methanol and stained with Coomassie Brilliant Blue; the changes in neuronal cell morphology following hypoxia exposure were then visualised using light microscopy (20× objective lens). Arrows indicate the changes in neurite length and cell disintegration. The images presented are from one experiment and representative of three independent experiments. Scale bar = 100 μm.

Role of TG2 in PACAP-27-induced cell survival against hypoxia-induced cell death

Initially, the identification of PACAP-27's cytoprotective role against hypoxia injury was assessed. Differentiating N2a and SH-SY5Y cells were pre-treated with PACAP-27 (100 nM) for 10 min and 30 min, respectively, prior to 8 h of hypoxia exposure. Following hypoxia incubation, cell viability was assessed. As shown in Figures 6.4, 6.5, 6.6 and 6.7, the findings revealed that pre-treatment with PACAP-27 significantly attenuated the hypoxia-induced decrease in MTT reduction, release of LDH and activation of caspase-3, thereby indicating the protective role of PACAP-27. This protection was abolished when cells were pre-treated with the PAC_1 receptor antagonist PACAP 6-38 (100 nM; 30 min), confirming that the induced cytoprotection was modulated via the PAC_1 receptor (Figure 6.4 and Figure 6.5). Finally, to determine if TG2 was involved in the PACAP-27-induced cell survival in neuroblastoma cells, the TG2 inhibitors R283 and Z-DON were used. Differentiating neuroblastoma cells were pre-treated for 1 h with Z-DON (150 μM) or R283 (200 μM) prior to stimulation with PACAP-27 (100 nM) and exposed to hypoxia. Both TG2 inhibitors attenuated PACAP-27-induced cell survival (Figures 6.6 and 6.7). Overall, these results demonstrate a role of TG2 in PACAP-27-induced cell survival and protection against hypoxia via the PAC_1 receptor in both mouse N2a and human SH-SY5Y cells.

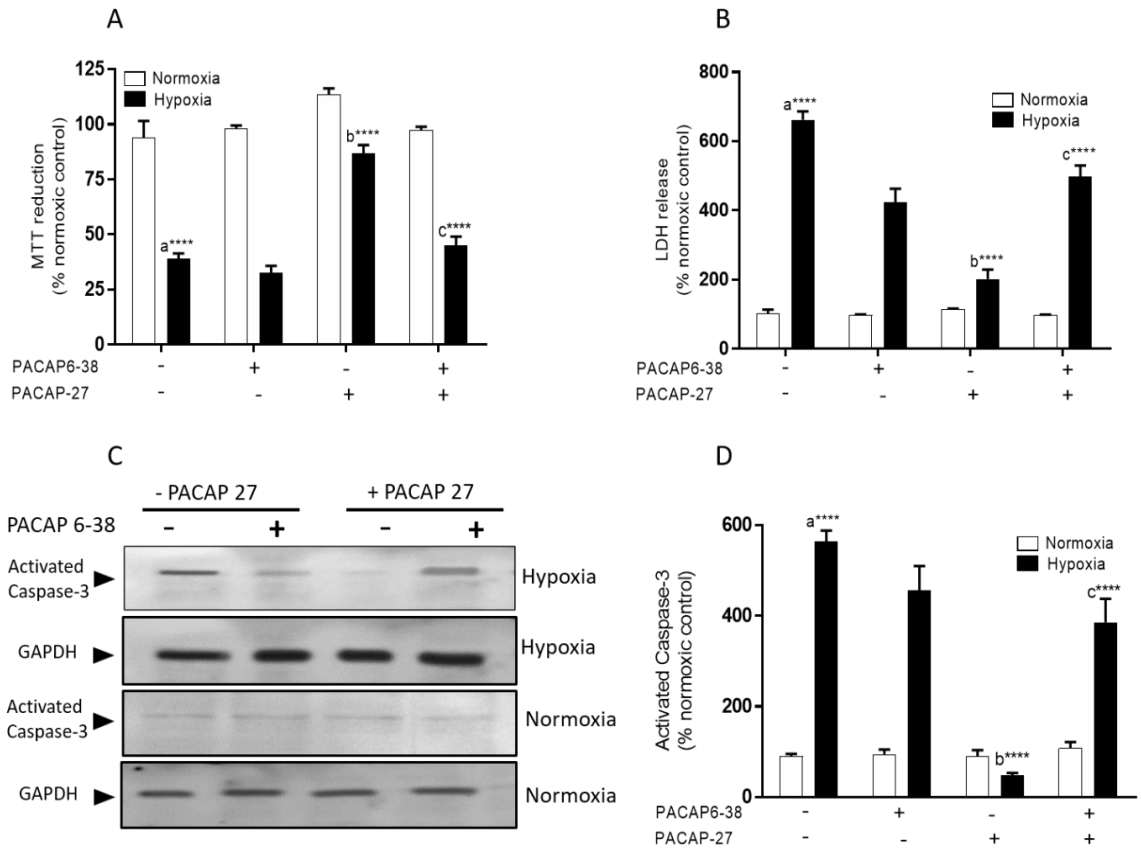

Figure 6.4 Effect of PACAP-27 on hypoxia-induced cell death in N2a cells.

Differentiating N2a cells were pre-treated with the PAC_1 receptor antagonist PACAP 6-38 (100 nM) for 30 min before the addition of PACAP-27 (100 nM) for 10 min prior to 8 h of hypoxia (1% O_2) or normoxia. Cell viability was assessed by measuring (A) the metabolic reduction of MTT by cellular dehydrogenases, (B) release of LDH into the culture medium and (C) caspase-3 activity via Western blot analysis using the anti-active caspase 3 antibody. (D) Quantified caspase-3 activity data. Data are expressed as a percentage of normoxia control cell values (=100%) and represent the mean ± SEM from four independent experiments. ****$p < 0.0001$ versus (a) normoxic control, (b) hypoxic control, (c) 100 nM PACAP-27 in the presence of hypoxia.

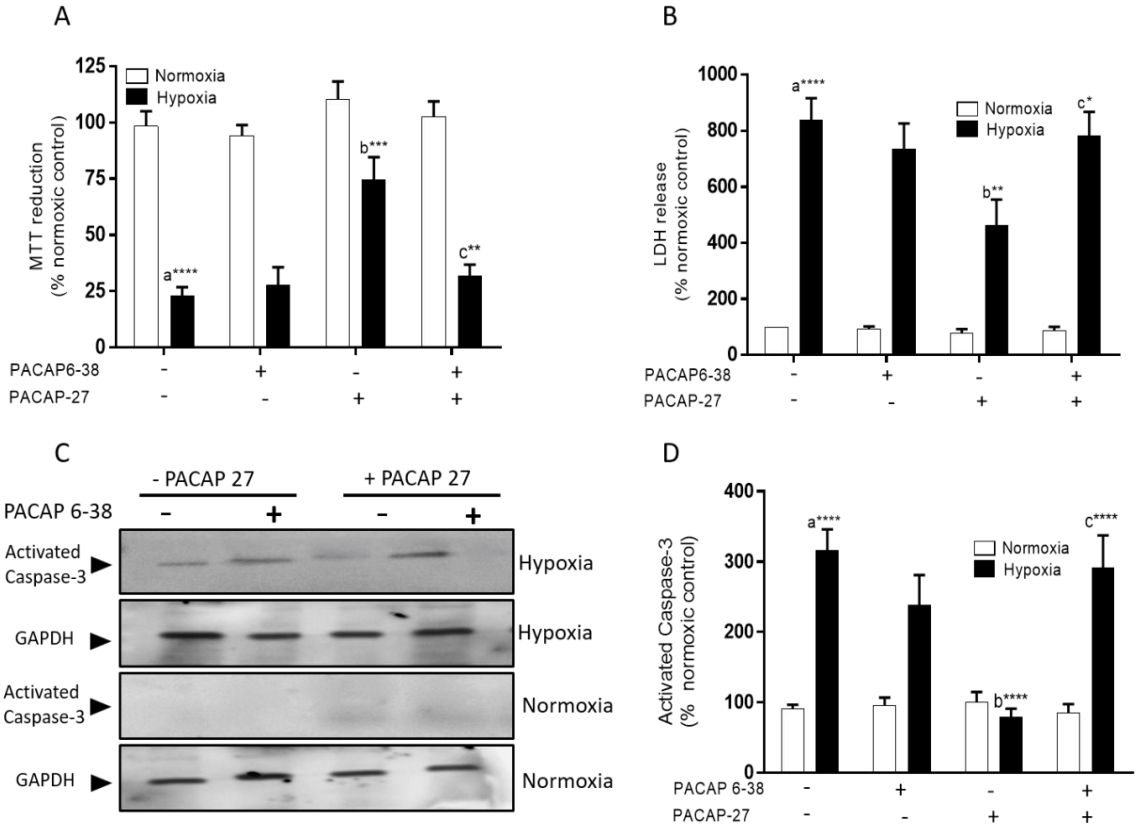

Figure 6.5 Effect of PACAP-27 on hypoxia-induced cell death in SH-SY5Y cells.

Differentiating SH-SY5Y cells were pre-treated with the PAC_1 receptor antagonist PACAP 6-38 (100 nM) for 30 min before the addition of PACAP-27 (100 nM) for 30 min prior to 8 h of hypoxia (1% O_2) or normoxia. Cell viability was assessed by measuring (A) the metabolic reduction of MTT by cellular dehydrogenases, (B) release of LDH into the culture medium and (C) caspase-3 activity via Western blot analysis using anti-active caspase-3 antibody. (D) Quantified caspase-3 activity data. Data are expressed as a percentage of normoxia control cell values (=100%) and represent the mean ± SEM from four independent experiments. ****$p < 0.0001$ versus (a) normoxic control, (b) hypoxic control, (c) 100 nM PACAP-27 in the presence of hypoxia.

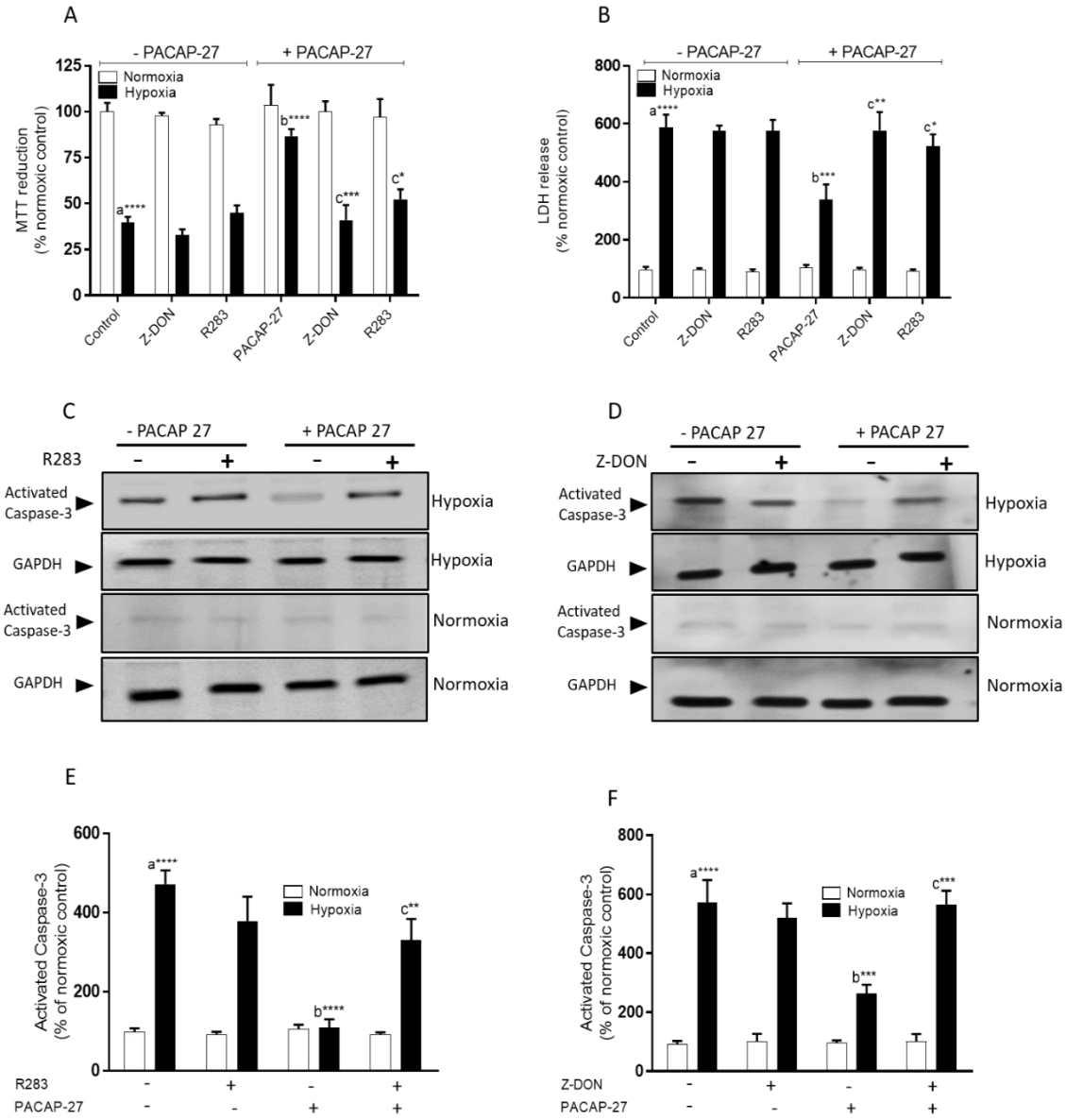

Figure 6.6 Effects of the TG2 inhibitors Z-DON and R283 on PACAP-27 induced cell survival in N2a cells.

Differentiating N2a cells were pre-treated for 1 h with the TG2 inhibitor Z-DON (150 µM) or R283 (200 µM) before the addition of PACAP-27 (100 nM) for 10 min prior to 8 h of hypoxia (1% O_2) or normoxia. Cell viability was assessed by measuring (A) the metabolic reduction of MTT by cellular dehydrogenases, (B) release of LDH into the culture medium and (C) caspase-3 activity via Western blot analysis using the anti-active caspase-3 antibody. (D) Quantified caspase-3 activity data. Data are expressed as a percentage of normoxia control cell values (=100%) and represent the mean ± SEM from four independent experiments. *$p < 0.05$, **$p < 0.01$, ***$p < 0.001$ and ****$p < 0.0001$ versus (a) normoxic control, (b) hypoxic control, (c) 100 nM PACAP-27 in the presence of hypoxia.

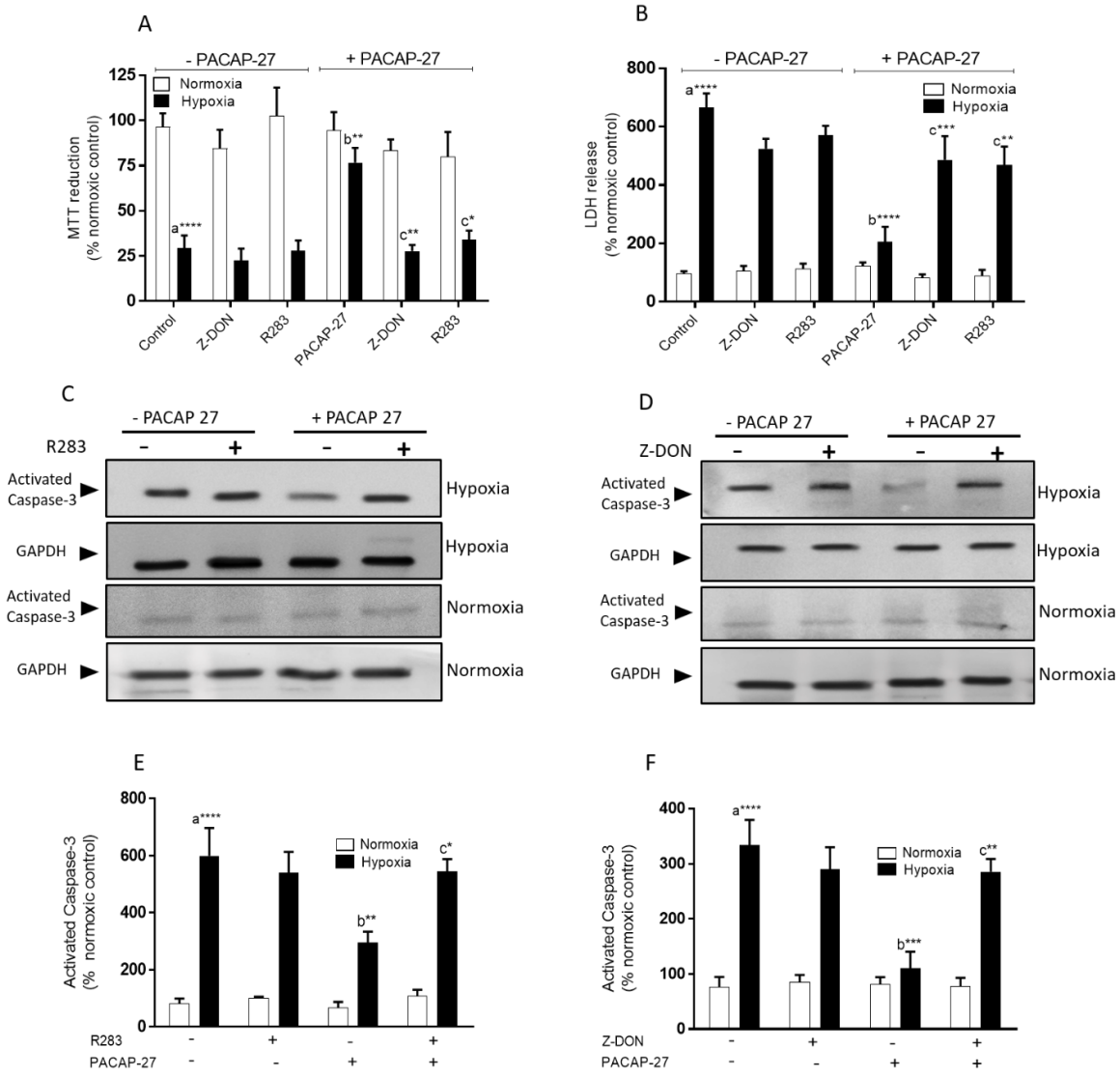

Figure 6.7 The effects of the TG2 inhibitors Z-DON and R283 on PACAP-27-induced cell survival in SH-SY5Y cells.

Differentiating SH-SY5Y cells were pre-treated for 1 h with the TG2 inhibitors Z-DON (150 µM) or R283 (200 µM) before the addition of PACAP-27 (100 nM) for 30 min prior to 8 h of hypoxia (1% O_2) or normoxia. Cell viability was assessed by measuring (A) the metabolic reduction of MTT by cellular dehydrogenases, (B) release of LDH into the culture medium and (C) caspase-3 activity via Western blot analysis using the anti-active caspase 3 antibody. (D) Quantified caspase-3 activity data. Data are expressed as a percentage of normoxia control cell values (=100%) and represent the mean ± SEM from four independent experiments. *$p < 0.05$, **$p < 0.01$, ***$p < 0.001$ and ****$p < 0.0001$ versus (a) normoxic control, (b) hypoxic control, (c) 100 nM PACAP-27 in the presence of hypoxia.

Role of TG2 in NGF-induced cell survival against hypoxia-induced cell death

To determine the role of TG2 in NGF-induced cell survival, differentiating neuroblastoma cells were treated with NGF (100 ng/ml; 1 h) prior to exposure to 8 h of hypoxia. After this, cell viability was assessed by measuring the metabolic reduction of MTT, release of LDH and activation of caspase-3. As expected, NGF significantly attenuated hypoxia-induced reduction in MTT, release of LDH and activation of caspase-3 in both N2a and SH-SY5Y neuroblastoma cells (Figures 6.8 and 6.9). Then, to determine the role of TG2 in this protection activity, the TG2-specific inhibitors Z-DON and R283 were implemented. Both differentiating neuroblastoma cells were pre-treated with Z-DON (150 μM) or R283 (200 μM) prior to stimulation with NGF 100 ng/ml and exposure to hypoxia. The TG2 inhibitors Z-DON and R283 attenuated NGF-induced neuronal cell protection in both cell lines (Figures 6.8 and 6.9).

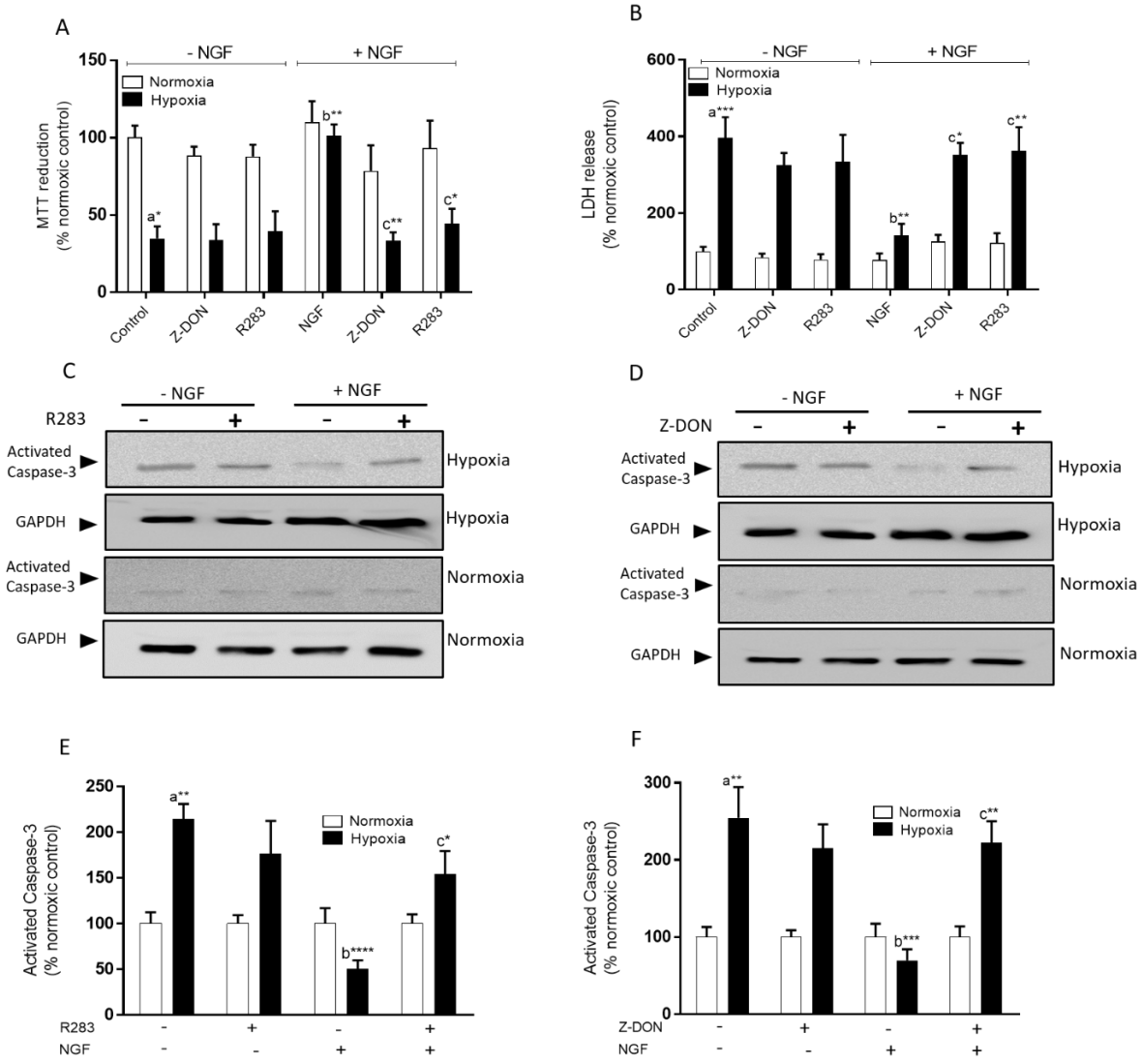

Figure 6.8 Effects of the TG2 inhibitors Z-DON and R283 on NGF-induced cell survival in N2a cells.

Differentiating N2a cells were pre-treated for 1 h with the TG2 inhibitors Z-DON (150 µM) or R283 (200 µM) before the addition of NGF (100 ng/ml) for 1 h prior to 8 h of hypoxia (1% O_2) or normoxia. Cell viability was assessed by measuring (A) the metabolic reduction of MTT by cellular dehydrogenases, (B) release of LDH into the culture medium and (C) caspase-3 activity via Western blot analysis using anti-active caspase 3 antibody. (D) Quantified caspase-3 activity data. Data are expressed as a percentage of normoxia control cell values (=100%) and represent the mean ± SEM from four independent experiments. *$p < 0.05$, **$p < 0.01$, ***$p < 0.001$ and ****$p < 0.0001$ versus (a) normoxic control, (b) hypoxic control, (c) NGF in the presence of hypoxia.

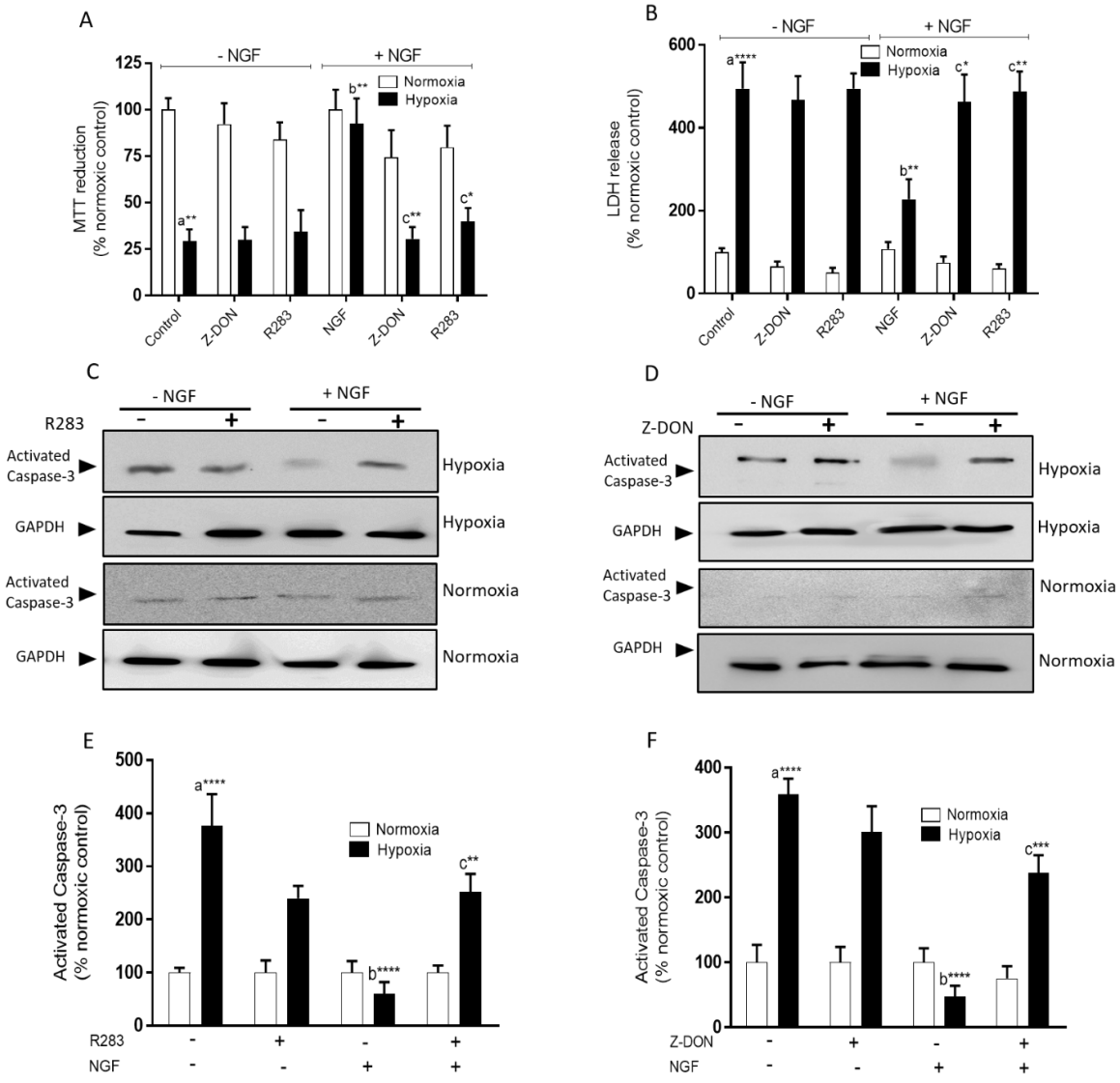

Figure 6.9 Effects of the TG2 inhibitors Z-DON and R283 on NGF induced cell survival in SH-SY5Y cells.

Differentiating SH-SY5Y cells were pre-treated for 1 h with the TG2 inhibitors Z-DON (150 µM) or R283 (200 µM) before the addition of NGF (100 ng/ml) for 1 h prior to 8 h of hypoxia (1% O_2) or normoxia. Cell viability was assessed by measuring (A) the metabolic reduction of MTT by cellular dehydrogenases, (B) release of LDH into the culture medium and (C) caspase-3 activity via Western blot analysis using anti-active caspase 3 antibody. (D) Quantified caspase-3 activity data. Data are expressed as a percentage of normoxic control cell values (=100%) and represent the mean ± SEM from four independent experiments. *$p < 0.05$, **$p < 0.01$, ***$p < 0.001$ and ****$p < 0.0001$ versus (a) normoxic control, (b) hypoxic control, (c) NGF in the presence of hypoxia.

6.2.2 The role of TG2 in neurite outgrowth

Neurite outgrowth is the extension of axonal processes (axons and dendrites) from the cell body; it is the main morphological characteristic of neuronal development (reviewed by Craig and Banker, 1994; Szu-Yu Ho and Rasband, 2011). Variation in neurite outgrowth processing is implicated in neuronal disorders or injury, such as ischaemic stroke/hypoxia (Qian et al., 2001). The role of TG2 in the neuroprotective effects of neurotrophic factors, PACAP-27 and NGF, on multiple-parameters of neurite outgrowth in differentiated N2a and SH-SY5Y were assessed in this section using high-throughput analysis.

Development of high-throughput analysis of neurite outgrowth

The main aim of this study was to develop an accurate high-throughput approach to investigate the role TG2 in neurotrophic factor–induced neurite outgrowth. To accomplish this, initially, multiple parameters of neurite outgrowth were quantitatively analysed in differentiating N2a and SH-SY5Y cells following PACAP-27 and NGF treatment for 48 h in serum-free medium to induce neurite outgrowth. Cells were then fixed and stained using indirect immunofluorescence with a monoclonal antibody against α-tubulin (clone B512), which enabled staining of the microtubules in axons, dendrites and cell bodies. B512 was used because tubulin is an abundant cytoskeletal protein that is found in both cell bodies and neurites, permitting examination of the PACAP-27 and NGF-induced effects on different parameters of neurite outgrowth in differentiating neuroblastoma cells. The stained cell monolayers were examined using a fluorescence microscope with the ImageXpress Micro Widefield High Content Screening System. The images were analysed with high-content image processing software MetaXpress for neurite outgrowth parameters, and the obtained outputs were given in a mathematical algorithm, as explained in section 2.2.12.

Image segmentation of the acquired images was carried out using ImageXpress. Examples of image segmentation from PACAP-27- and NGF-treated N2a and SH-SY5Y neuroblastoma cells probed with B512 are depicted in Figure 6.10. Two wavelengths were used, namely FITC green to detect the cell body and neurites and DAPI blue for nuclei. Multicoloured mask images show segmentation tracing neurites and cell bodies, which were identified by setting up the MetaXpress imaging and analysis software segmentation parameters. The analysis settings were optimised and configured to identify the maximum relevant neuronal outgrowth processing details and minimum background noise until the most accurate image segmentation was obtained, as shown in Figure 6.10. Since this study was conducted to assess the neurite

outgrowth under different treatment conditions, the cell-by-cell neurite outgrowth parameters were selected accordingly, as follows:

- Average number of cells per field (total number of neural cell bodies averaged by the number of fields);
- Average cell body area per cell (total area of cell bodies in square micron averaged by the number of cell);
- Average number of neurites (total number of neurites produced from the cell bodies averaged by the number of fields);
- Significant outgrowth (neurites longer than 10 μm in length);
- Maximum neurite length per cell (length in microns of the longest neurite from the neuronal cell body to an extreme segment per cell);
- Average neurite length per cell (total length in microns of all significant outgrowths averaged by the number of cells);
- Mean processes per cell (average number of neurites longer than 10 μm in length); and
- Mean branches per cell (average number of branches originating from neurites produced by each cell).

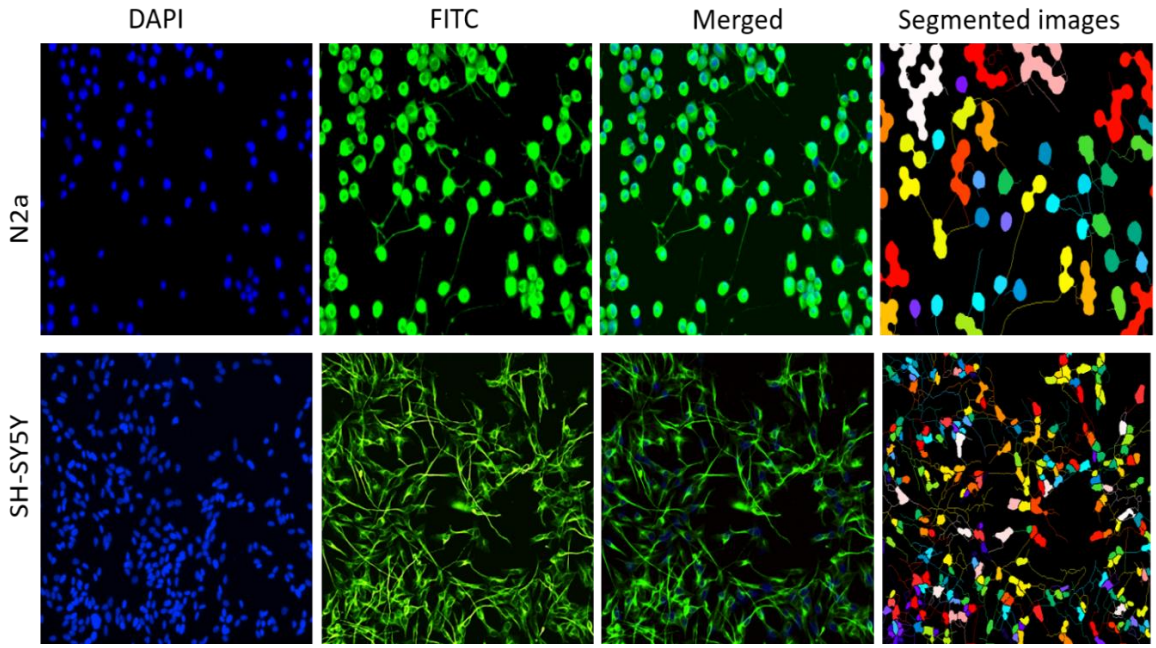

Figure 6.10 Image segmentation of stained N2a and SH-SY5Y cells using the high-throughput screening system.

Segmentation of stained N2a and SH-SY5Y cells using high-throughput screening assays. Cells were fixed and stained with an antibody recognising α-tubulin (B512), followed by Alexa Fluor® –conjugated anti-IgG secondary antibody. All images shown are from PACAP-27- and NGF-treated controls from a single field of view. Acquired images were obtained using the ImageXpress Micro system (10× objective) with two wavelengths, namely FITC for cell body and neurite detection and DAPI for nucleus counting. Segmented images with multicoloured tracing masks on neurites and cell bodies were generated using the Neurite Outgrowth Module in the MetaXpress imaging and analysis software for monitoring different parameters of neurite outgrowth.

Role of TG2 in PACAP-27-induced neurite outgrowth

The neurotrophic effects of PACAP-27 (100 nM, 48 h) on inducing neurite outgrowth in N2a and SH-SY5Y cells were monitored using high-throughput assay. Figure 6.11 shows the initial, automated images for the effect of TG2 inhibitors on PACAP-27-induced neurite outgrowth in differentiating N2a and SH-SY5Y cells. In the absence of TG2 inhibitors, the cells had the typical neuronal cell morphology – round cell bodies with long extending axons for N2a and flat, extensive with elongated neuritic projections for SH-SY5Y cells**.** After pre-treatment with TG2 inhibitors prior to stimulation with PACAP-27, smaller neurite projections were apparent in comparison with the cells treated with PACAP-27 alone.

The high-throughput quantitative data analysis obtained show that PACAP-27 had no effects on the average neuronal cell number per field or on the measurement of cell body area of N2a and SH-SY5Y by analysis of B512 staining (Figure 6.12***)***. Treatment with the TG2 inhibitor Z-DON (150 μM) or R283 (200 μM) prior to stimulation with PACAP-27 (100 nM) caused no significant changes in neuronal cell number or cell body area measurements (Figure 6.12). The quantitative analysis of B512 staining for the average number of neurites per field and the percentage of cells with a neurite of length above 10 μm (i.e. significant outgrowth) were also assessed, as shown in Figure 6.13. The presented data show that PACAP-27 caused a significant increase in the average number of neurites and number of cells with neurites compared with control untreated cells (Figure 6.13). In addition, exposing the cells to the TG2 inhibitors prior to stimulation with PACAP-27 significantly inhibited the average neurite number per field and the percentage of cells with significant outgrowth that stimulated with PACAP-27 in N2a and SH-SY5Y cells (Figure 6.13).

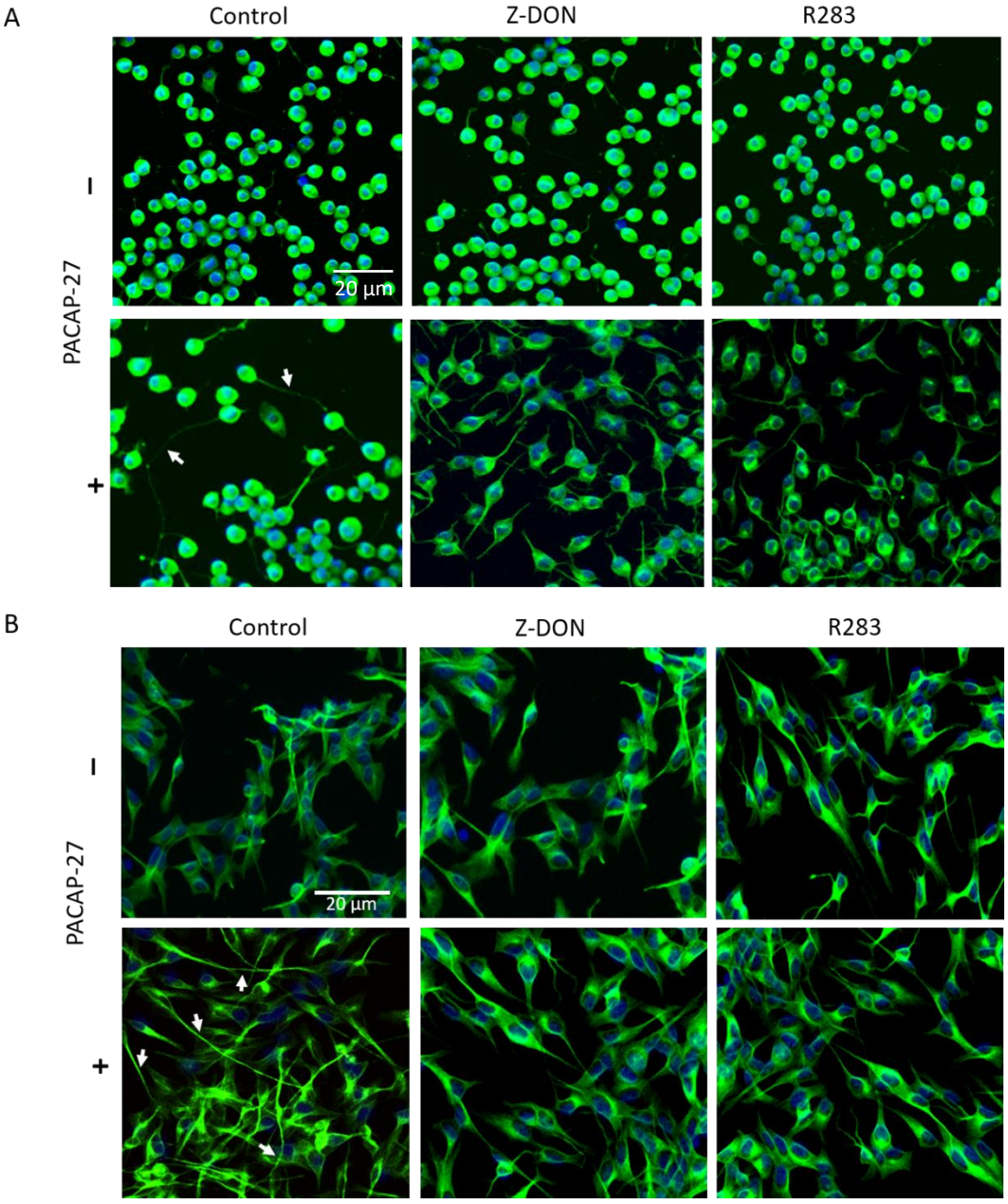

Figure 6.11 Representative, automated images for the effect of TG2 inhibitors on PACAP-27-induced neurite outgrowth in differentiating N2a and SH-SY5Y cells.

(A) N2a and (B) SH-SY5Y cells were incubated for 1 h with the TG2 inhibitor Z-DON (150 µM) or R283 (200 µM) before treatment with PACAP-27 (100 nM) in serum-free DMEM for 48 h. Following stimulation, high-throughput immunocytochemistry was performed using the anti-tubulin antibody and visualised using Alexa Fluor® 488–labelled goat anti-mouse IgG secondary antibody (green). Nuclei were visualised using DAPI counterstain (blue). Images are from one experiment and representative of four. White arrows indicate typical neurite outgrowths.

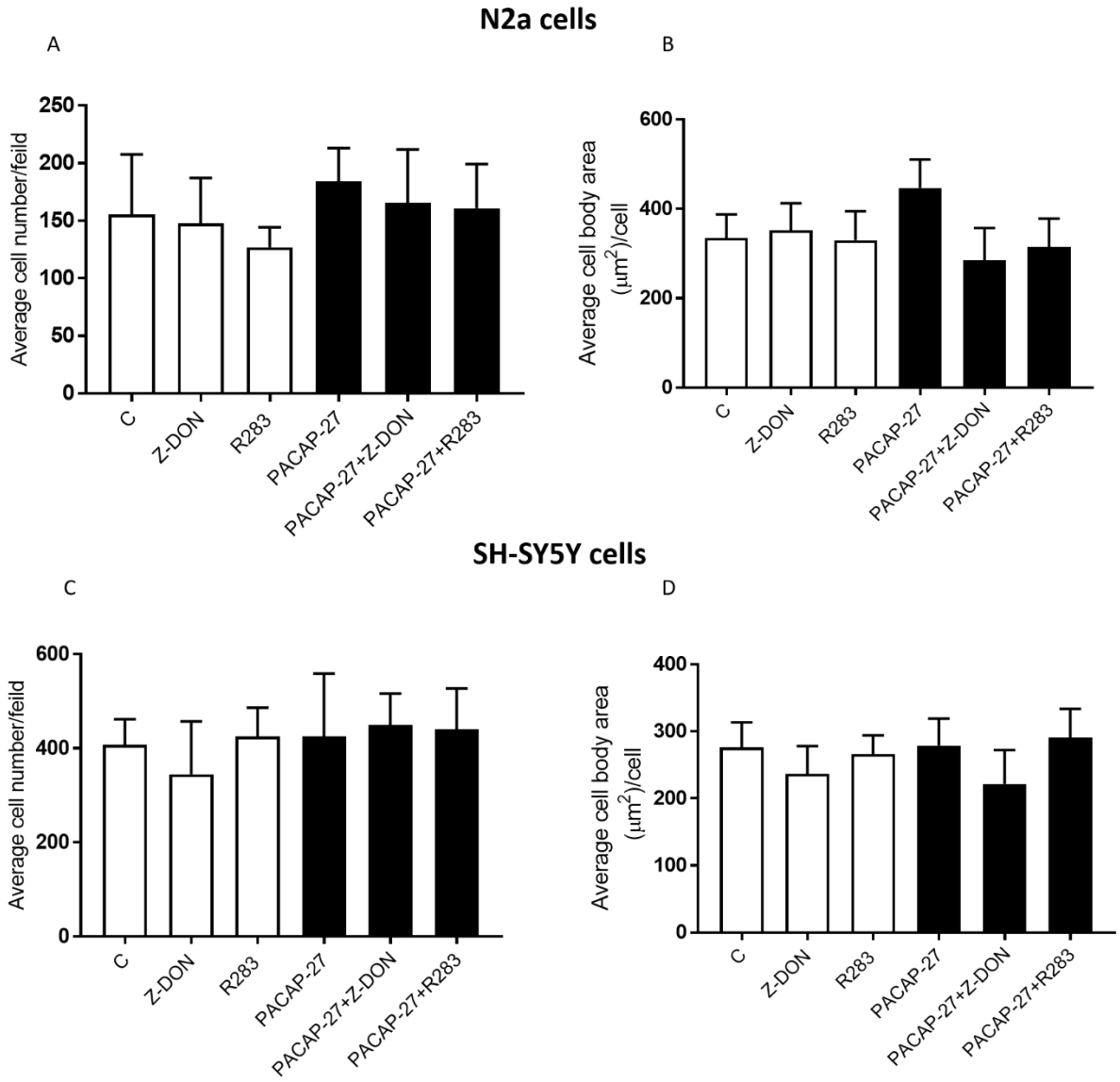

Figure 6.12 Effects of TG2 inhibitors on PACAP-27-induced neurite outgrowth (average cell number and cell body area) in differentiating N2a and SH-SY5Y cells.

N2a (panels A and B) and SH-SY5Y (panels C and D) cells were incubated for 1 h with the TG2 inhibitors Z-DON (150 µM) or R283 (200 µM) before treatment with PACAP-27 (100 nM) in serum-free DMEM for 48 h. Following stimulation, high-throughput immunocytochemistry was performed using the anti-tubulin antibody (B512). Data were acquired using the ImageXpress Micro system, and the cell number (A and C) and cell body area (B and D) were measured using MetaXpress imaging and analysis software. High-throughput data are expressed as a mean value ± SEM from four independent experiments.

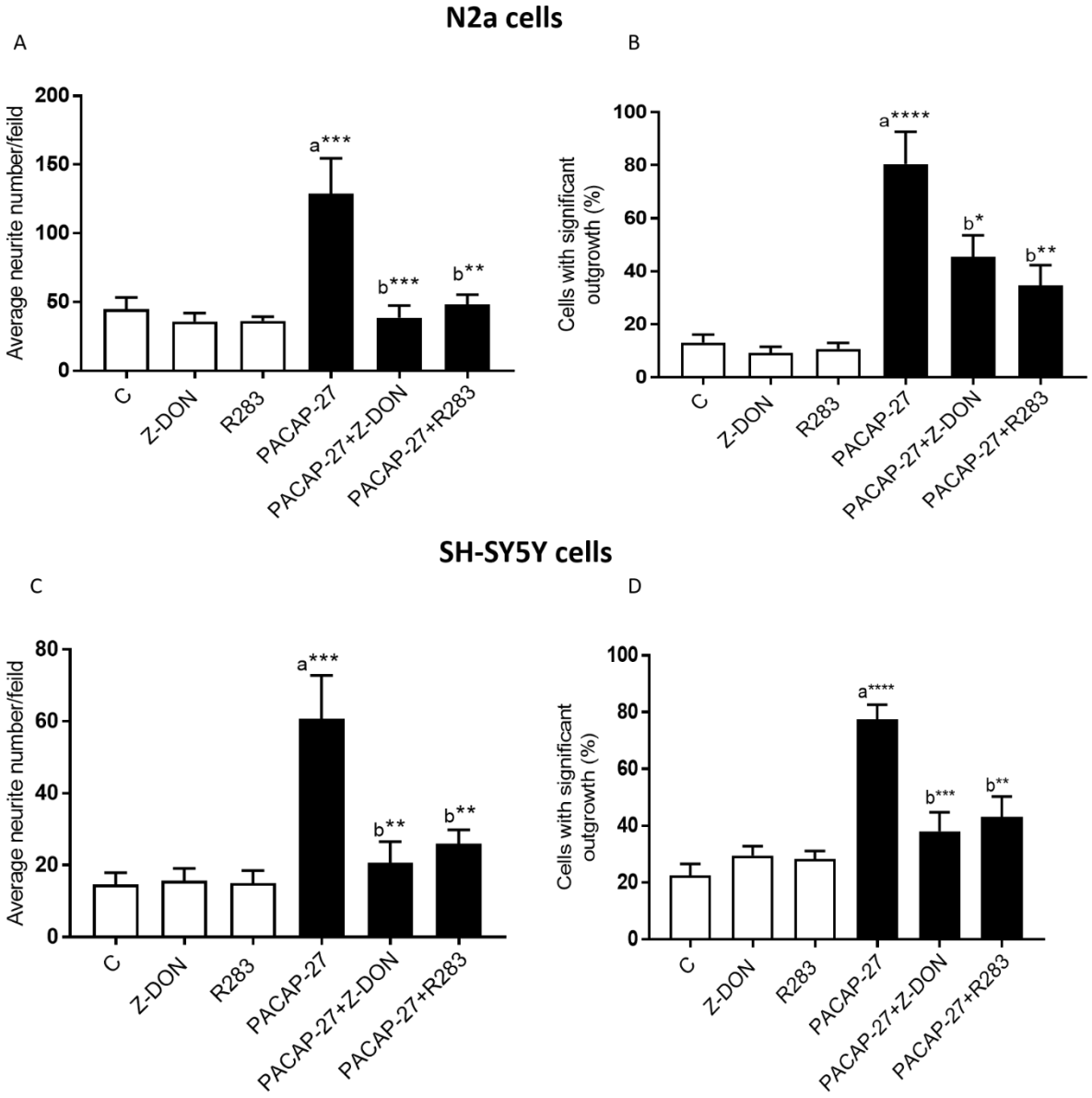

Figure 6.13 Effects of TG2 inhibitors on PACAP-27 induced neurite outgrowth (average number of neurites and significant outgrowth) in differentiating N2a and SH-SY5Y cells.

N2a (panels A and B) and SH-SY5Y (panels C and D) cells were incubated for 1 h with the TG2 inhibitors Z-DON (150 µM) or R283 (200 µM) before treatment with PACAP-27 (100 nM) in serum-free DMEM for 48 h. Following stimulation, high-throughput immunocytochemistry was performed using the anti-tubulin antibody (B512). Data were acquired using the ImageXpress Micro system, and the average number of neurites (A and C) and significant outgrowth (B and D) were measured using MetaXpress imaging and analysis software. High-throughput data are expressed as a mean value ± SEM from four independent experiments *$p < 0.05$, **$p < 0.01$, ***$p < 0.001$ and ****$p < 0.0001$ versus (a) control, (b) PACAP-27 alone.

The maximum and average neurite length per neuronal cell were also assessed (Figure 6.14). Quantitation of B512 staining showed significant increases in the maximum and the average neurite length per cell in response to PACAP-27. It revealed that the maximum neurite lengths per cell in PACAP-27-treated cells were 60 μm for N2a and 45 μm for SH-SY5Y cells. Exposure to the TG2 inhibitors significantly decreased the maximum length of B512-positive neurite per cell by about 60% ($p < 0.0001$).

B512 is expected to detect the neurite outgrowth–related processes and branches; thus, the measurement of the mean number of cell processes and branches per neuronal cell were considered. As shown in Figure 6.15, B512 staining detected that PACAP-27 significantly increased the average number of neuronal cell processes and branches in both N2a and SH-SY5Y cells. A significant attenuation in the cell processes and branches per neuronal cell ($p < 0.01$) was observed when the cells were pre-treated with the TG2 inhibitors prior to stimulation with PACAP-27 (Figure 6.15).

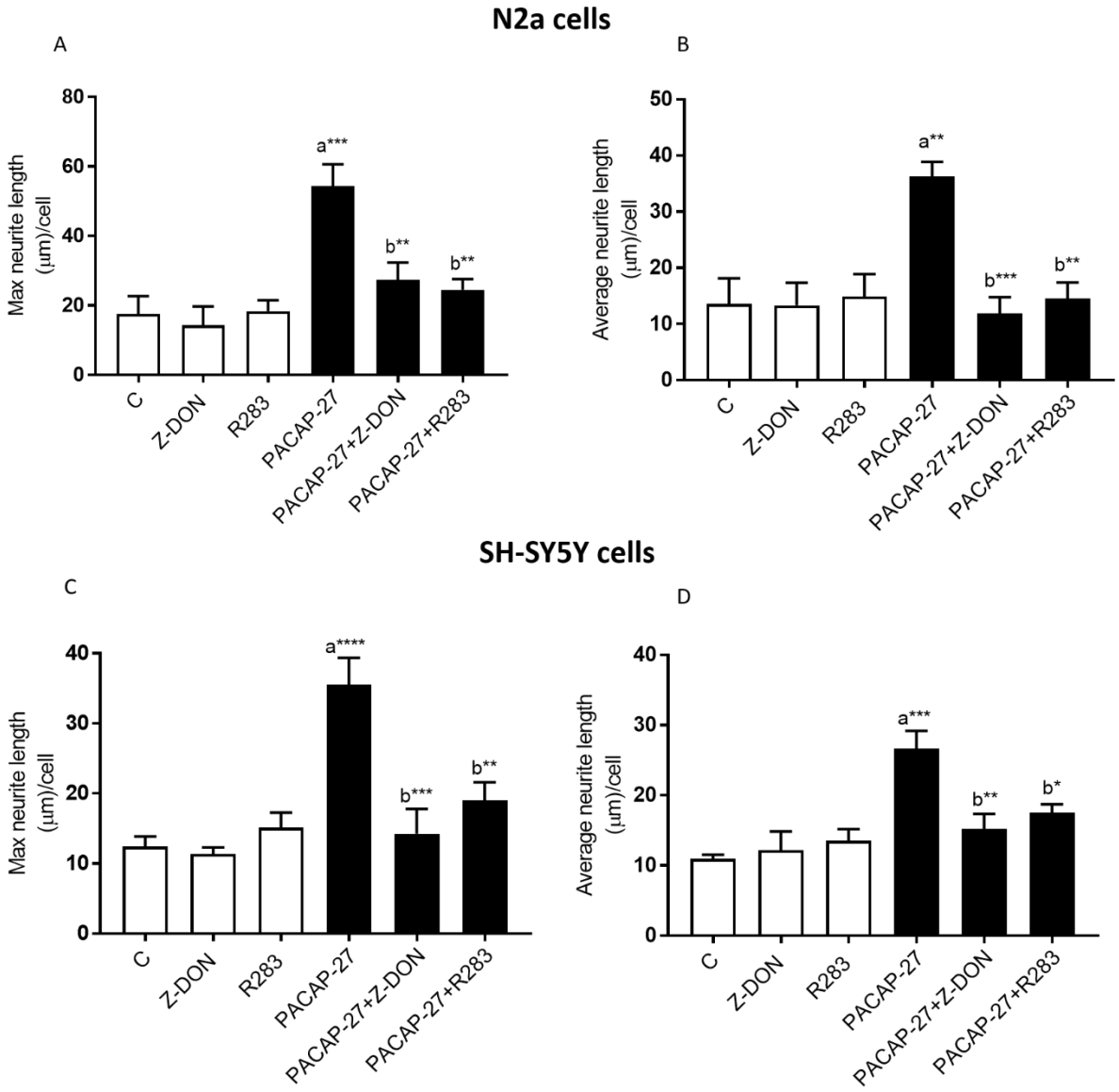

Figure 6.14 Effects of TG2 inhibitors on PACAP-27-induced neurite outgrowth (maximum neurite length and average neurite length) in differentiating N2a and SH-SY5Y cells.

N2a (panels A and B) and SH-SY5Y (panels C and D) cells were pre-treated for 1 h with the TG2 inhibitors Z-DON (150 µM) or R283 (200 µM) before treatment with PACAP-27 (100 nM) in serum-free DMEM for 48 h. Following stimulation, high-throughput immunocytochemistry was performed using the anti-tubulin antibody (B512). Data were acquired using the ImageXpress Micro system, and maximum neurite length (A and C) and average neurite length (B and D) were measured using MetaXpress imaging and analysis software. High-throughput data are expressed as mean values ± SEM from four independent experiments *$p < 0.05$, **$p < 0.01$, ***$p < 0.001$ and ****$p < 0.0001$ versus (a) control, (b) PACAP-27 alone.

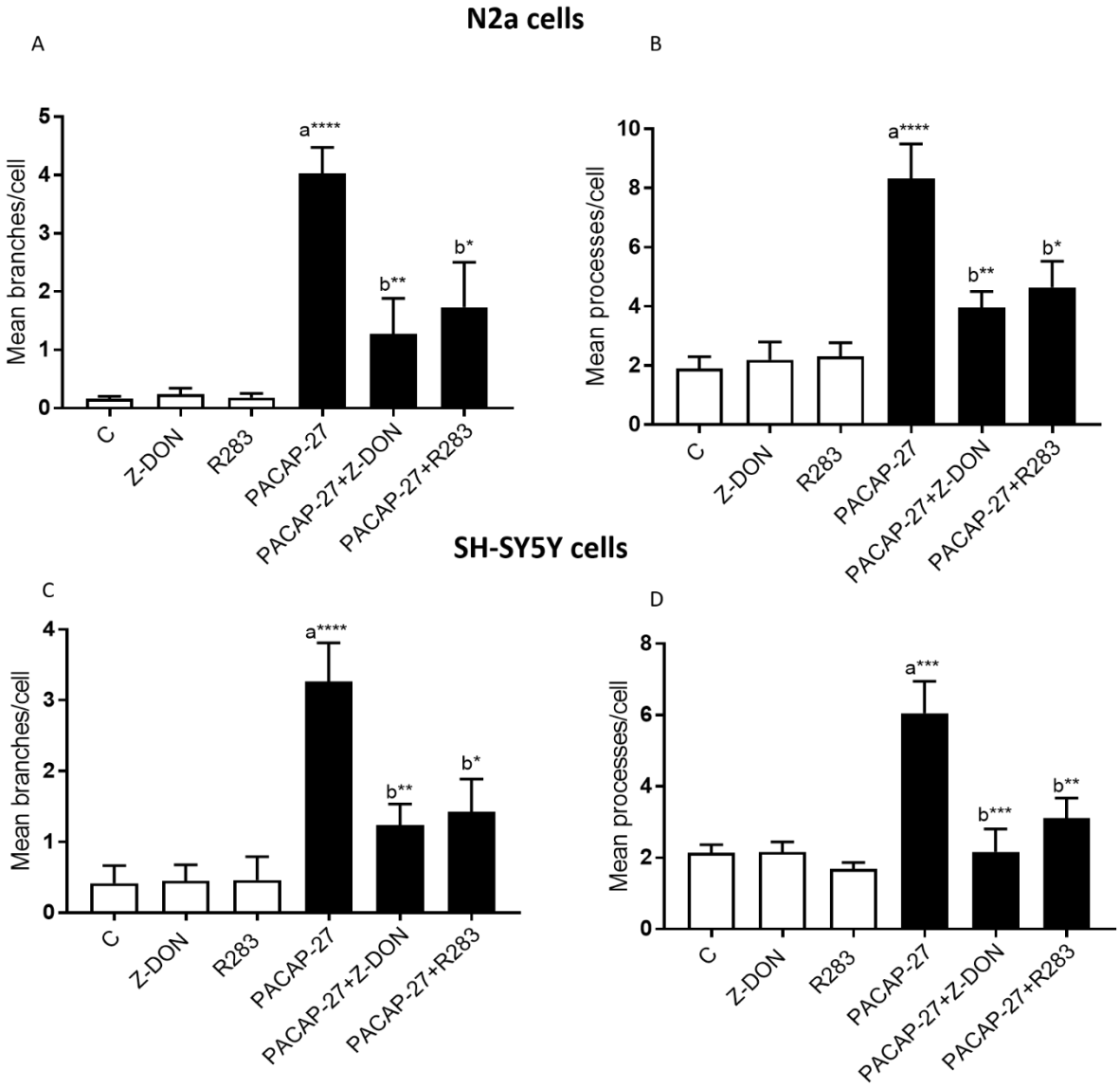

Figure 6.15 Effects of TG2 inhibitors on PACAP-27-induced neurite outgrowth (mean processes and mean branches in differentiating N2a and SH-SY5Y cells.

N2a (panels A and B) and SH-SY5Y (panels C and D) cells were pre-treated for 1 h with the TG2 inhibitors Z-DON (150 µM) or R283 (200 µM) before treatment with PACAP-27 (100 nM) in serum-free DMEM for 48 h. Following stimulation, high-throughput immunocytochemistry was performed using anti-tubulin antibody (B512). Data were acquired using the ImageXpress Micro system, and mean processes (A and C) and mean branches (B and D) were measured using MetaXpress imaging and analysis software. High-throughput data are expressed as mean values ± SEM from four independent experiments. *$p < 0.05$, **$p < 0.01$, ***$p < 0.001$ and ****$p < 0.0001$ versus (a) control, (b) PACAP-27 alone.

Role of TG2 in NGF-induced neurite outgrowth

The role of TG2 in NGF-induced neurite outgrowth was assessed by high-throughput monitoring of different neurite outgrowth related parameters following 48 h treatment with NGF (100 ng/ml) in N2a and SH-SY5Y cells. The effect of TG2 inhibitors on the neuronal cell morphology were assessed. As shown in Figure 6.16, the presented automated images illustrate that treatment with TG2 inhibitors resulted in retraction of the neurites and axons extending in both neuroblastoma cell lines.

Like PACAP-27, NGF showed no significant changes in the average neuronal cell number per field of N2a and SH-SY5Y cells (Figure 6.17). In addition, no changes were observed in the measurement of cell body area per field in N2a cells; however, a slight increase in the SH-SY5Y cell body area per field in response to NGF was observed. Treatment with TG2 inhibitors Z-DON (150 µM) and R283 (200 µM) caused no changes in the observed responses of the average neuronal cell number and body area (Figure 6.17). Furthermore, the quantification of the average number of neurites per field and number of cells with a neurite length above 10 µm (i.e. significant outgrowth) in N2a and SH-SY5Y cells treated with NGF in the presence or absence of the TG2 inhibitors was performed. The findings indicated that NGF induced a significant enhancement effect on the neurite number per field and significant outgrowth, and these responses were reversed by TG2 inhibitors (Figure 6.18).

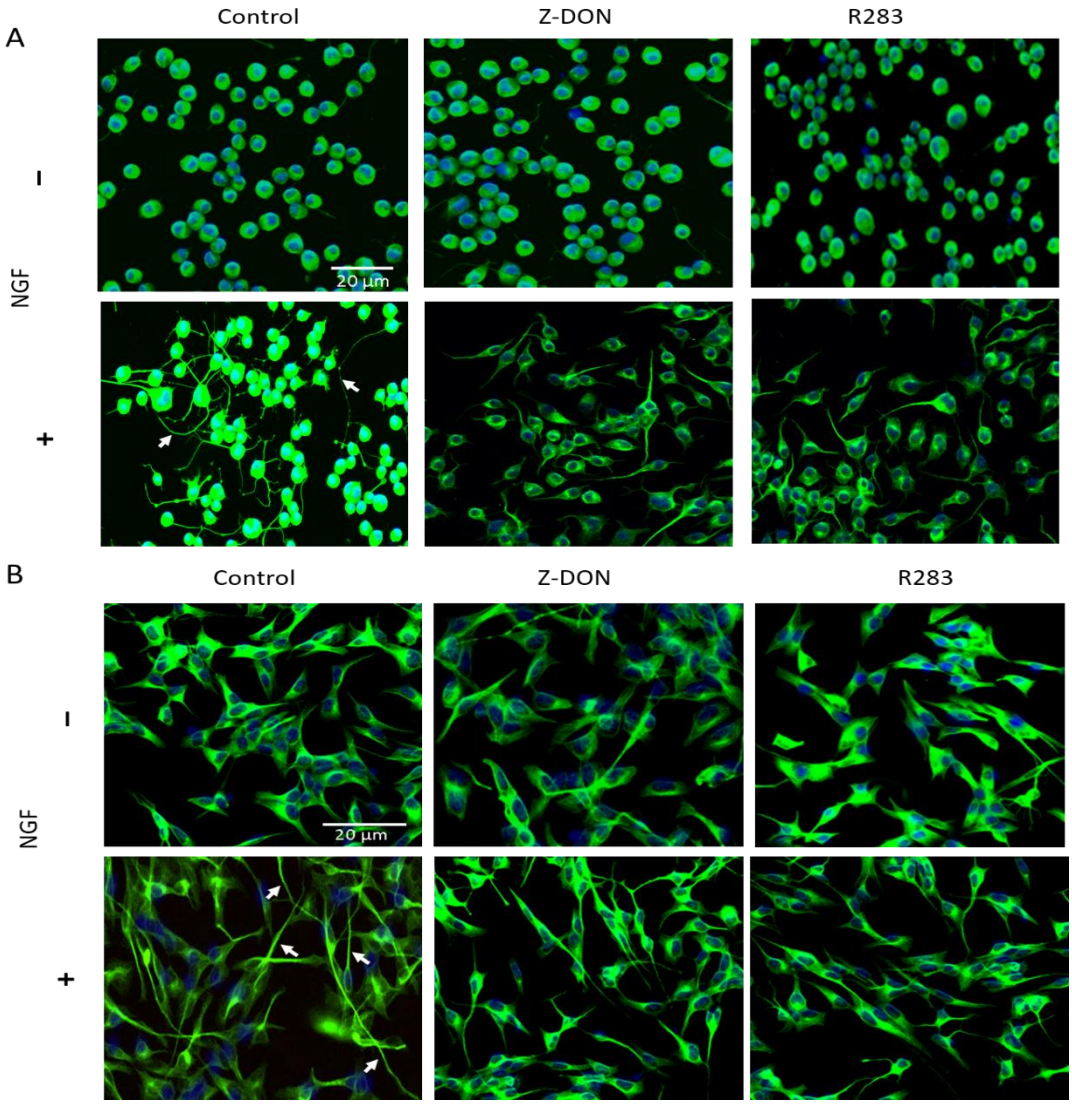

Figure 6.16 Representative automated images for the effect of TG2 inhibitors on NGF induced neurite outgrowth in differentiating N2a and SH-SY5Y cells.

(A) N2a and (B) SH-SY5Y cells were incubated for 1 h with the TG2 inhibitors Z-DON (150 µM) or R283 (200 µM) before treatment with NGF (100 ng/ml) in serum-free DMEM for 48 h. Following stimulation, high-throughput immunocytochemistry was performed using the anti-tubulin antibody and visualised using Alexa Fluor® 488–labelled goat anti-mouse IgG secondary antibody (green). Nuclei were visualised using DAPI counterstain (blue). Images are from one experiment and representative of four. White arrows indicate typical neurite outgrowths.

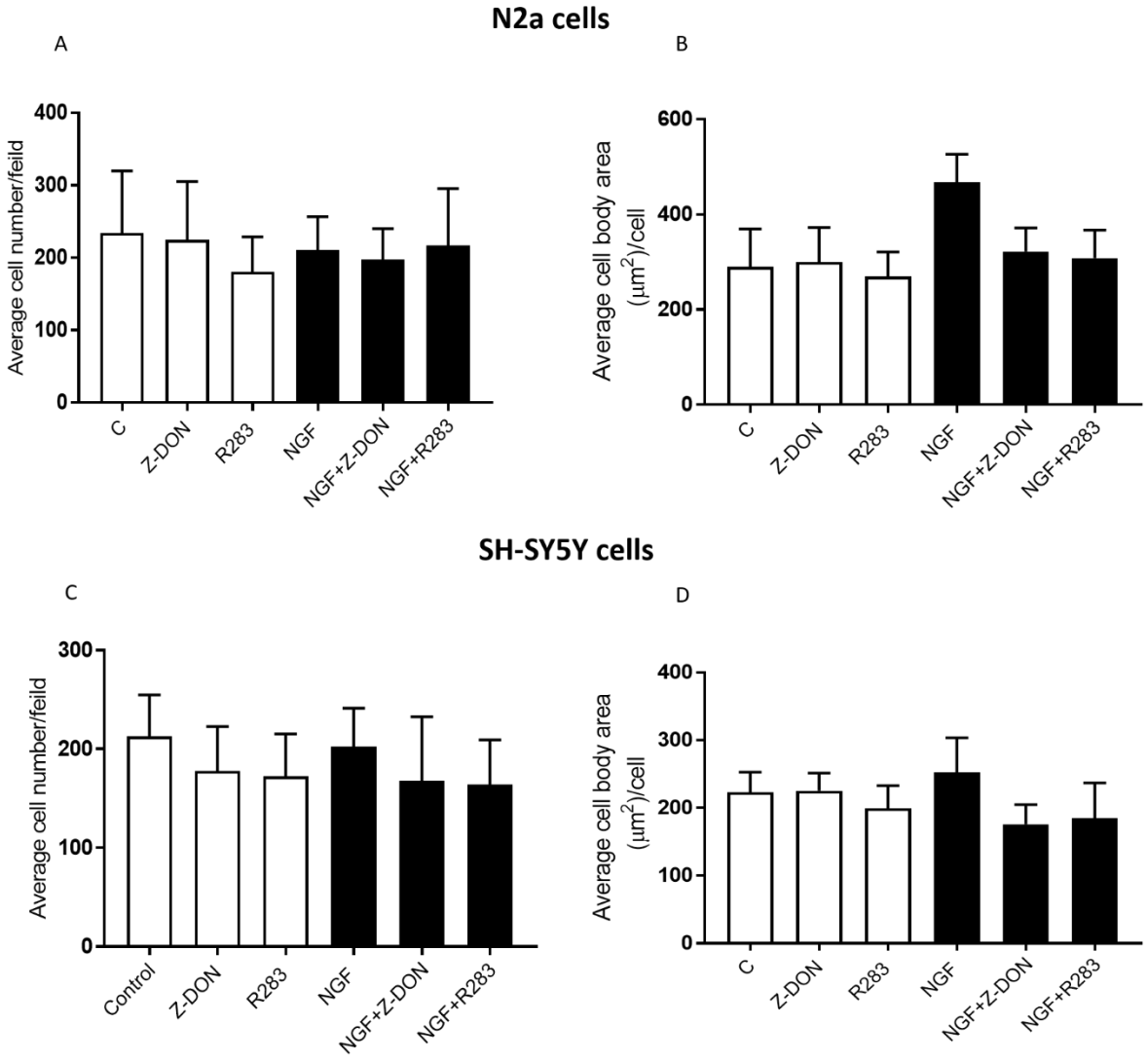

Figure 6.17 Effects of TG2 inhibitors on NGF-induced neurite outgrowth (average cell number and cell body area) in differentiating N2a and SH-SY5Y cells.

N2a (panels A and B) and SH-SY5Y (panels C and D) cells were incubated for 1 h with the TG2 inhibitors Z-DON (150 µM) or R283 (200 µM) before treatment with NGF (100 ng/ml) in serum-free DMEM for 48 h. Following stimulation, high-throughput immunocytochemistry was performed using the anti-tubulin antibody (B512). Data were acquired using the ImageXpress Micro system, and the cell number (A and C) and cell body area (B and D) were measured using MetaXpress imaging and analysis software. High-throughput data are expressed as mean values ± SEM from four independent experiments.

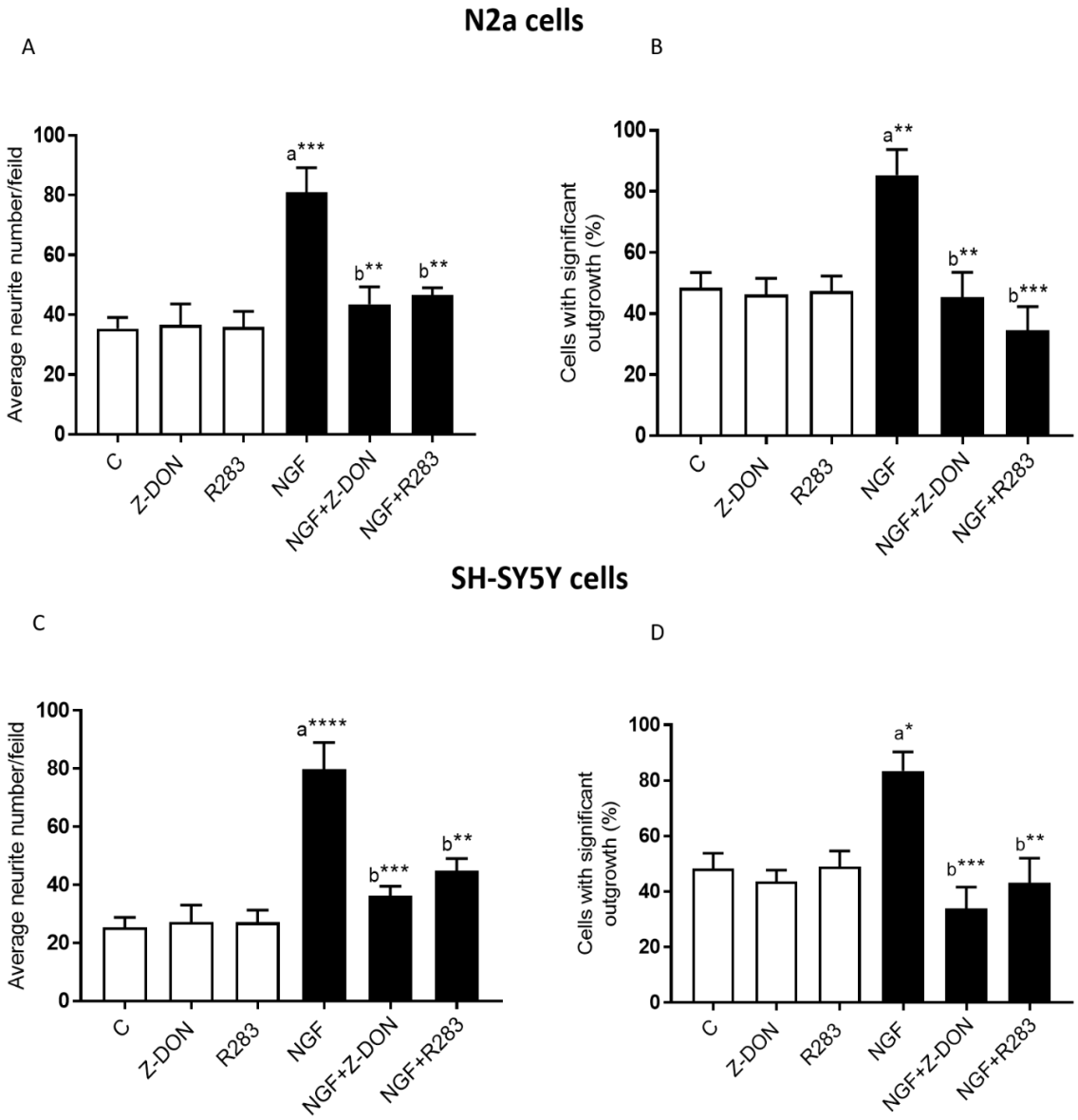

Figure 6.18 Effects of TG2 inhibitors on NGF-induced neurite outgrowth (average number of neurites and significant outgrowth) in differentiating N2a and SH-SY5Y cells.

N2a (panels A and B) and SH-SY5Y (panels C and D) cells were pre-treated for 1 h with the TG2 inhibitors Z-DON (150 µM) or R283 (200 µM) before treatment with NGF (100 ng/ml) in serum-free DMEM for 48 h. Following stimulation, high-throughput immunocytochemistry was performed using the anti-tubulin antibody (B512). Data were acquired using the ImageXpress Micro system, and the average number of neurites (A and C) and significant outgrowth (B and D) were measured using MetaXpress imaging and analysis software. High-throughput data are expressed as mean values ± SEM from four independent experiments *$p < 0.05$, **$p < 0.01$, ***$p < 0.001$ and ****$p < 0.0001$ versus (a) control, (b) NGF alone.

Exposure to NGF was also shown to have a significant enhancement effect on the average number of neurites per field and number of cells with a neurite length above 10 μm in length (i.e. significant outgrowth) in both neuroblastoma cell lines (Figure 6.19). To assess the role of TG2, cells were pre-treated with the TG2 inhibitors prior to exposure to NGF; both inhibitors significantly impaired NGF's ability to stimulate the neurite number per field and percentage of cells with significant outgrowth. Finally, measurements with B512 staining showed that there was a significant increase in the mean number of processes and branches in N2a and SH-SY5Y cells in response to NGF (Figure 6.20). In addition, a significant reversal of these responses was observed with the TG2 inhibitors, suggesting a prominent role of TG2 in NGF-induced neurite outgrowth. Table 6.1 summarises the findings of this section. Overall, the high-throughput data presented in this section indicated a prominent role for TG2 in PACAP-27- and NGF-mediated neurite outgrowth.

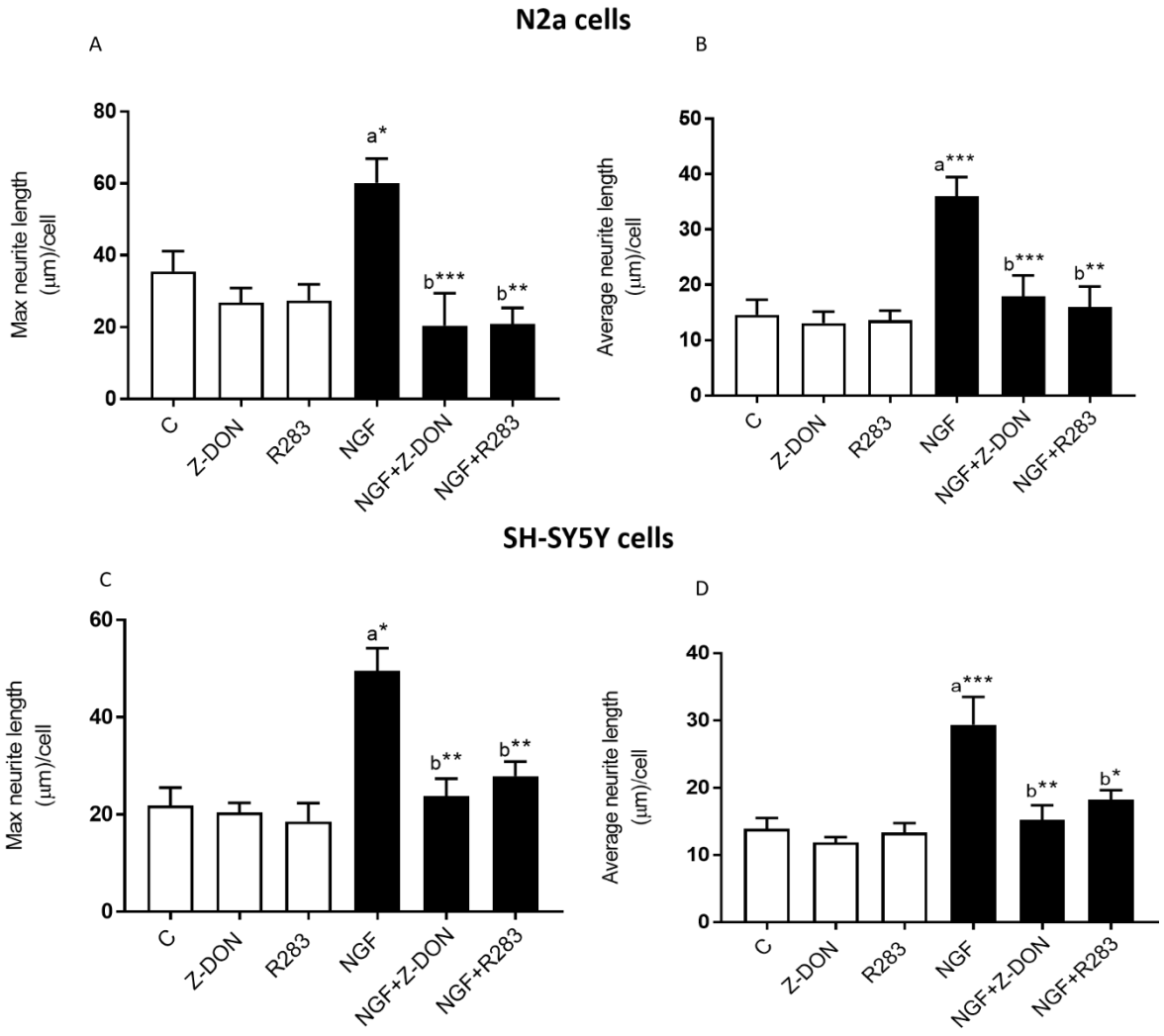

Figure 6.19 Effects of TG2 inhibitors on NGF-induced neurite outgrowth (maximum and average neurite lengths) in differentiating N2a and SH-SY5Y cells.

N2a (panels A and B) and SH-SY5Y (panels C and D) cells were pre-treated for 1 h with the TG2 inhibitors Z-DON (150 µM) or R283 (200 µM) before treatment with NGF (100 ng/ml) in serum-free DMEM for 48 h. Following stimulation, high-throughput immunocytochemistry was performed using the anti-tubulin antibody (B512). Data were acquired using the ImageXpress Micro system, and the maximum neurite length (A and C) and average neurite length (B and D) were measured using MetaXpress imaging and analysis software. High-throughput data are expressed as mean values ± SEM from four independent experiments. *$p < 0.05$, **$p < 0.01$, ***$p < 0.001$ and ****$p < 0.0001$ versus (a) control, (b) NGF alone.

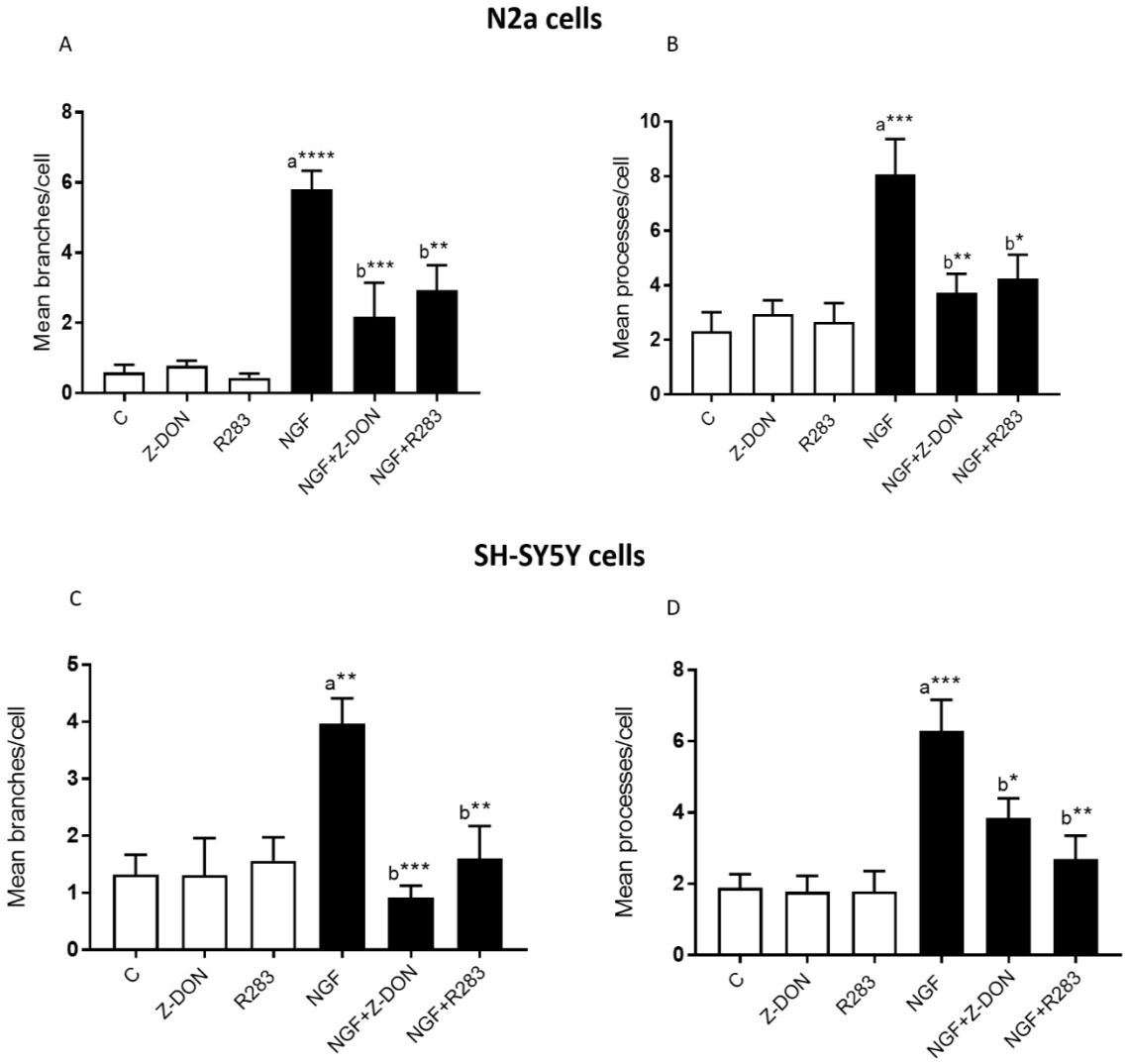

Figure 6.20 Effects of TG2 inhibitors on NGF-induced neurite outgrowth (mean processes and mean branches) in differentiating N2a and SH-SY5Y cells.

N2a (panels A and B) and SH-SY5Y (panels C and D) cells were pre-treated for 1 h with the TG2 inhibitors Z-DON (150 µM) or R283 (200 µM) before treatment with NGF (100 ng/ml) in serum-free DMEM for 48 h. Following stimulation, high-throughput immunocytochemistry was performed using the anti-tubulin antibody (B512). Data were acquired using the ImageXpress Micro system, and mean branches (A and C) and mean processes (B and D) were measured using MetaXpress imaging and analysis software. High-throughput data are expressed as mean values ± SEM from four independent experiments. *$p < 0.05$, **$p < 0.01$, ***$p < 0.001$ and ****$p < 0.0001$ versus (a) control, (b) NGF alone.

Table 6.1 Overall effect of TG2 inhibitors on PACAP-27 and NGF induced neurite outgrowth assessed by high throughput assay

Parameter	N2a			SH-SY5Y		
	PACAP-27	PACAP-27 + Z-DON	PACAP-27 + R283	PACAP-27	PACAP-27 + Z-DON	PACAP-27 + R283
	Average ± SEM					
Average neurite number/field	129±10	39±15	48±14	60±12	21±5	26±4
Cell with significant outgrowth %	80±12	45±10	34±7	77±5	38±7	42±8
Maximum neurite length (µm)/cell	45±6	27±5	25±3	36±4	14±3	19±3
Average neurite length(µm)/cell	36±5	12±3	15±2	27±3	15±2	18±4
Mean branches/cell	6±0.2	2±0.6	3±0.7	4±0.5	2±0.3	2±0.5

Parameter	N2a			SH-SY5Y		
	NGF	NGF + Z-DON	NGF + R283	NGF	NGF + Z-DON	NGF + R283
	Average ± SEM					
Average neurite number/field	81±8	35±6	42±3	72±9	36±3	45±4
Cell with significant outgrowth %	85±8	43±6	32±8	80±7	34±10	42±6
Maximum neurite length (µm)/cell	60±11	20±9	18±4	50±5	24±7	28±2
Average neurite length(µm)/cell	40±15	18±7	16±4	29±7	132±2	17±6
Mean branches/cell	8±0.5	2±0.9	2±0.9	3±0.2	0.9±0.2	2±0.3

Shown is a summary of the results of the range of treatments used in this study to investigate the role of TG2 in PACAP-27 and NGF in modulating of neurite outgrowth. Differentiating neuroblastoma N2a or SH-SY5Y cells were treated with the compounds indicated in the table, then the cells were stimulated with PACAP-27 or NGF with or without TG2 inhibitors. Results (average ± SEM) were calculated from the data generated from MetaXpress imaging and analysis software.

6.3 Discussion

Several studies have investigated the neuronal protection and neurite outgrowth role of TG2 (Tucholski et al., 2001; Singh et al., 2003; Filiano et al., 2008, 2010; Tatsukawa et al., 2016). However, little was known about the exact underlying cellular mechanism(s) involved. The main aim of the work presented in this chapter was to evaluate TG2's role in the neuroprotective and neurite outgrowth potential of PACAP and NGF. In the present study, the pharmacological inhibition of TG2 resulted in attenuation of the neuronal protection and neurite outgrowth induced by the neurotrophic factors PACAP-27 and NGF in differentiating N2a and SH-SY5Y cells. These observations are in good agreement with previous findings on TG2's neuronal survival (Tucholski et al., 2001; Filiano et al., 2008, 2010; Tatsukawa et al., 2016) and neurite outgrowth roles (Tucholski et al., 2001; Singh et al., 2003). For the first time, the current study has revealed the potential role of TG2 in neurotrophic factor–induced cell survival and neurite outgrowth.

6.3.1 Role of TG2 in neurotrophic factor–induced cytoprotection

There are currently conflicting data as to whether TG2 plays an anti-apoptotic or pro-apoptotic role in neuronal cell death (Tatsukawa et al., 2016). These opposing roles appear to depend on the cell type, trigger mechanism of cell death, intracellular location of TG2 and specific TG2 enzymatic activity (Tatsukawa et al., 2016). One study, using a hippocampal ischaemic model, revealed that either TG2 knockout mice or mice treated with the TG2 inhibitor cystamine showed a smaller infarction size compared with control mice, suggesting that TG2 has a role in ischaemic cell death (Saiki et al., 2011). In contrast, increasing evidence indicates the neuronal protection role of TG2. For example, it has been found that TG2-mediated neuronal cell survival includes protection against heat shock-induced cell death in SH-SY5Y cells (Tucholski et al., 2001), protection of rat primary cortical neurons against hypoxia and oxygen/glucose deprivation-induced cell death (Filiano et al., 2008) and *in vivo* protection against ischaemic stroke (Filiano et al., 2010). TG2 is considered to mediate protection of neuronal cells against hypoxia by attenuating the hypoxia inducible factor (HIF)-induced activation of pro-apoptotic genes (Filiano et al., 2008, 2010). Furthermore, the transamidating activity of TG2 appears to play a role in protection against oxygen/glucose deprivation-induced cell death (Filiano et al., 2008). However, the precise cellular mechanism underlying the TG2 anti-apoptotic effect remains poorly understood.

The neurotrophic effects of PACAP-27 and NGF are widely recognised as activators of neuroprotective/cell survival mechanisms via reducing apoptosis, and they are considered potential therapeutic agents for the treatment of neuronal cell death associated with neurodegenerative disorders (Batistatou & Greene 1993; Tanaka et al., 1997; Allen et al., 2013). The complex cellular mechanisms and signal transduction pathways involved in this activity of either PACAP or NGF are well documented. The PACAP-induced neuronal survival and anti-apoptotic effects have been reported to involve mainly PKA (Reglodi et al., 2004), as well as other signalling pathways, such as PKB, ERK1/2, NF-κB and Ca^{2+} mobilisation (May et al., 2010; Manecka et al., 2013). The neuroprotection and cell survival mechanisms associated with NGF are thought to involve the activation of PI-3K/ Akt cascade (Shimoke & Chiba, 2001; Koh et al., 2003; Salinas et al., 2003; Wu & Wong, 2005). Recent studies have shown that TG2 can be modulated by multi protein kinase dependent pathways, and it plays a role in cytoprotection in cardiomyoblasts (Almami et al., 2014; Vyas et al., 2016, 2017). Thus, it would be reasonable to assess the possible involvement of TG2 in neuronal cell survival induced by PACAP and NGF.

In the current study, cell survival was assessed following exposure to hypoxia to investigate the neuronal protection effect of both neurotrophic factors and the possible involvement of TG2. Initially, hypoxia conditions were induced by incubating the differentiated N2a and SH-SY5Y cells in 5% CO_2/1% O_2 at 37°C in serum/glucose-free medium; then, different hypoxia exposure times were investigated for cell viability tests to determine which time exposures were sufficient for inducing cell death in differentiating N2a and SH-SY5Y cells. Cell viability was assessed by measuring the levels of MTT reduction and LDH release. As shown in Figure 6.1, Figure 6.2 and Figure 6.3, an 8-h period was optimum for inducing significant MTT reduction and LDH release, and it was shown to induce morphological changes in differentiating N2a and SH-SY5Y cells, with the degree of deterioration ranging from mild to severe. The question was asked whether the observed hypoxia-induced cell death was associated with apoptosis or necrosis; thus, activation of caspase-3 was assessed in differentiating N2a and SH-SY5Y cells exposed to hypoxia for various durations. The present findings showed that caspase-3 was gradually activated, suggesting that the cells were undergoing apoptosis, inducing cell death. Caspase-3 sensitivity in the early response to hypoxia exposure is comparable to that observed in a previous study, which identified a significant increase in caspase-3 expression 8h after exposure to hypoxia (Qian et al., 2001).

The experiments performed in this part of the study were designed to relate the PACAP-27 and NGF modulation of TG2 activity observed in chapters 4 and 5, respectively, to the neuronal

protection/cell survival and associated regulatory proteins in differentiating N2a and SH-SY5Y cells. The present study identified that PACAP-27 and NGF significantly attenuated the hypoxia-induced decreases in MTT reduction and release of LDH. An apoptosis-induced cell death marker caspase-3 was also assessed, and the present findings showed that caspase-3 activation induced by hypoxia was significantly decreased by PACAP-27 or NGF. These findings are in agreement with other studies that have reported the neuronal protection and anti-apoptotic power of PACAP-27 and NGF against hypoxia (Masmoudi-Kouki et al., 2011; Mnich et al., 2014). It has been found that PACAP induces a transient intrinsic inhibition of caspase-3 gene expression, providing additional evidence of PACAP's anti-apoptotic properties (Douiri et al., 2016). Similarly, NGF has been reported to exert its neuronal protection function through mechanisms that also involve caspase-3. A recent study demonstrated that NGF-induced neuroprotection is through mechanisms that require lysosomes for the direct removal of active caspase-3 (Mnich et al., 2014). Furthermore, it has been reported that, in the PC12 model, NGF protects the neurons from apoptosis-induced death by down-regulation the expression of the pro-apoptotic factor Bcl-2 homology 3 [BH3] domain-only protein (BIM) via a MEK/ERK-dependent pathway (Biswas & Greene, 2002). All of these previous literature findings provide evidence that the neuronal cell survival effects of PACAP and NGF are mostly carried out through anti-apoptotic activity. Based on the previous observations and the current data showing that PACAP and NGF potentially modulate TG2 activity in differentiating neuroblastoma cell lines, it can be speculated that TG2 has a role in the neuroprotection and in the anti-apoptotic effect of PACAP and NGF. Therefore, investigations into the intracellular protein targets involved in the cellular death process, such as the apoptosis biochemical markers caspase-3, and the mechanistic contribution of TG2 with the survival effect of PACAP and NGF, would be of interest. The noticeable differences in the activity of activated caspase-3 presented in this study suggested that the apoptotic cell death pathway was a major target to evaluate the role of TG2 in the cell survival induced by PACAP and NGF.

To assess the role of TG2, differentiating neuroblastoma cells were pre-treated with the TG2 inhibitors Z-DON (150 μM) or R283 (200 μM) prior to stimulation with PACAP-27 (100 nM) or NGF (100 ng/ml) and exposed to hypoxic conditions. The obtained data revealed that inhibition of TG2 could significantly reverse the protection offered by PACAP-27 or NGF, providing the first suggestion for a key role of TG2 in PACAP-27- and NGF-induced cytoprotection in differentiating mouse N2a and human SH-SY5Y neuroblastoma cells. The signalling system involved in this process would be a fundamental area of research to consider for the development of new therapeutic approaches to cure various pathologies involving

hypoxic/ischaemic neurodegeneration. However, while it is not clear how PACAP/PAC_1 receptor-induced TG2 activation mediates cell survival, TG2 is known to regulate pathways associated with PACAP neuroprotection. For example, TG2 activates adenylyl cyclase and enhances cAMP/PKA-dependent CRE-reporter gene activity in SH-SY5Y neuroblastoma cells (Tucholski & Johnson, 2003) and promotes NF-κB signalling via crosslinking of $I_{\kappa}B\alpha$ (Eckert et al., 2014). It is also unclear how NGF-induced TG2 activation mediates cell survival, although TG2 is known to regulate pathways associated with NGF neuroprotection. For example, TG2 mediates 5-HT-induced serotonylation of PKB in vascular smooth muscle cells (Penumatsa et al., 2014). While the data presented suggest that PKB is upstream of TG2 (i.e. NGF-induced TG2 activation is blocked by PKB inhibition) it is conceivable that NGF-induced TG2 activation functions to augment and sustain PKB activity. From the results obtained in chapters 4 and 5, PACAP-27 clearly induces TG2 enzymatic activity and phosphorylation in the PKA-dependent pathway, while NGF does so in the Akt/PKB dependent pathway. Accordingly, PACAP-27-induced PKA-dependent and NGF-induced Akt/PKB-dependent modulation of TG2 activity could be the possible cell survival and protection pathways under this study's experimental conditions.

In the current study, inhibition of TG2 blocked PACAP-27- and NGF-mediated attenuation of hypoxia-induced activation of caspase-3, which is indicative of an anti-apoptotic role of TG2. One potential anti-apoptotic mechanism is TG2's inhibition of apoptosis via the downregulation of Bax expression and inhibition of caspase-3 and 9 (Cho et al., 2010). Furthermore, the reported effect of TG2 to act as a new type of apoptosis inhibitor by crosslinking caspase-3 and inactivating its enzymatic activity, resulting in the suppression of apoptosis (Yamaguchi & Wang, 2006), could be another possible mechanism. The findings indicate that TG2's anti-apoptotic role is involved in PACAP and NGF-induced neuronal cell protection; and this may provide a target for future attempts at modulating its anti-apoptotic potential for therapeutic benefit. Further work is required to determine the role and mechanisms of TG2 in PACAP- and NGF-induced cell survival. Taken together, these and the previous findings indicate that the PACAP- and NGF-induced TG2 activity have neuroprotective/anti-apoptotic potential against hypoxia-induced cell death in differentiating mouse and human neuroblastoma cells. Overall these data highlight the need to carefully consider the identification of the TG2 substrate(s) possibly involved in TG2-mediated neuroprotective activity.

6.3.2 The role of TG2 in neurotrophic factor-induced neurite outgrowth

The data presented in this part of the study demonstrate for the first time that TG2 inhibition reverses the PACAP- and NGF-induced neurite outgrowth process, indicating the involvement of TG2 in the neurite outgrowth activity induced by PACAP and NGF. This conclusion is supported by three major pieces of evidence, as follows: i) PACAP-27 and NGF modulate TG2 activity in neuroblastoma cell lines, ii) PACAP-27 and NGF induce neurite outgrowth in different neuronal cell models and iii) TG2 has been shown to be essential for the neurite outgrowth of neuronal cells. TG2 is a normal constituent found in the brain, spinal cord and neurons, and its expression and activation levels in different physiological and pathological conditions have been investigated. Previously, it was shown that TG activity was significantly elevated during the foetal stages when the axonal outgrowth process is occurring in rats and during the regeneration of the sciatic nerve following injury (Chakraborty et al., 1987). In addition, previous studies have shown that, in human neuroblastoma SH-SY5Y cells, TG2-mediated neurite outgrowth depends on the transamidating activity (Tucholski et al., 2001; Singh et al., 2003). These studies provide confirmatory evidence that TG2 is essential for differentiation/neurite outgrowth in neuronal cells. Furthermore, modulation of TG2 transamidation activity in neuroblastoma cells by the neurotrophic factors PACAP and NGF was confirmed in chapters 4 and 5. Although there is overwhelming evidence supporting the notion that PACAP and NGF have a potential role in inducing neurite outgrowth in neuronal cells (Grimes et al., 1996; Zhang et al. 2000; Monaghan et al., 2008; Kambe & Miyata, 2012), the TG2 functional implementation in this interaction has not been demonstrated. Accordingly, in this study, the role of TG2 in the PACAP-27 and NGF-induced neurite outgrowth of N2a and SH-SY5Y cells was investigated. The auto-quantified assay high-throughput ImageXpress screening and analysis system was developed and applied for this purpose.

The *in vitro* high-throughput analysis system permitted precise quantification of the changes in the different neurite parameters under different treatment conditions. This approach is a powerful, accurate, fast, reproducible tool that can provide homogenous detection and recognition of even fine neuronal cell processes and branches. In this part of the study, the primary aim was evaluating TG2's role in the neurite outgrowth via multiparametric measurements of morphological changes induced by PACAP-27 and NGF in differentiating N2a and SH-SY5Y cells. Initially, the high-throughput quantification indicated that the inhibition of TG2 had no significant effect on the average number of cells per field or average

cell body area per field in mouse N2a or human SH-SY5Y neuroblastoma. Furthermore, the analysis provided valuable neurite outgrowth parameters data to interpret, namely the average number of neurites, significant outgrowth, maximum neurite length per cell, average neurite length per cell, mean processes per cell and mean number of processes and branches per cell. All these parameters were significantly enhanced in response to PACAP-27 and NGF in both cell lines, and this activity was attenuated by TG2 inhibition; these findings indicate a potential role of TG2 in the PACAP-27 and NGF modulation of neurite outgrowth. It is important to note that the lack of effect of the TG2 inhibitors Z-DON (150 µM) and R283 (200 µM) on the average cell number per field confirmed that the observed reductions in the neurite outgrowth parameters were mainly due to their inhibitory effect, and they were not because of any reduction in the average counting of the cell number.

Several previous studies have found that PACAP has a triggering effect on different neurite outgrowth morphological characteristics, such as the neurite length or number (Shi et al., 2008; Kambe & Miyata, 2012; Ogata et al., 2015). For example, a morphological study on PC12 cells confirmed that PACAP enhances the neurite number per cell (Shi et al., 2008), and in cultured hippocampal neurons, PACAP increases neurite length in the first 2 days (Kambe & Miyata, 2012). In SH-SY5Y human neuroblastoma cells, PACAP has been shown to induce neurite outgrowth and increase the expression of cytoskeletal proteins (Héraud et al., 2004). Reports from some researchers have addressed the underlying mechanism for this; one study showed that PACAP increases the total neurite length in human SH-SY5Y cells via a cAMP-dependent pathway requiring the activation of ERK1/2 and p38 MAPK (Monaghan et al., 2008). However, the mechanism by which TG2 involved in PACAP promotes neurite outgrowth in neuroblastoma cells has not yet been investigated. The PACAP/PAC_1 receptors cause activation of adenylyl cyclase (May et al., 2014), and the available evidence seems to suggest that PACAP-modulated neurite outgrowth is cAMP dependent and PKA-independent (Monaghan et al., 2008). The present work also sheds light on the signalling cascade involved in the PACAP modulation of TG2 enzymatic activity and phosphorylation status, confirming that it is ERK1/2-dependent modulation (chapter 4). Based on the currently available evidence, it seems reasonable to suggest that PACAP-mediated TG2 activation could promote neurite outgrowth via cAMP and ERK1/2 signalling.

It is also prominent in the literature that the intracellular stream of the NGF-TrkA (a high-affinity NGF receptor) complex is essential for an effective NGF signal transduction process to induce neurite outgrowth (Grimes et al., 1996; Zhang et al., 2000). Further research in this area indicated that PKC provides a positive signal for the neurite outgrowth response induced by

NGF via activation of ERK1/2 signalling (Brodie et al., 1999). It has also been established that crosstalk between NGF and TG2 induces neurite outgrowth in neuroblastoma cells (Oe et al., 2005; Condello et al., 2008). It is conceivable that this may involve modulation of the PKC signalling pathway, as earlier in the current study, the obtained findings confirmed that NGF modulation of TG2 activity was PKC dependent (chapter 5). It could also be one or more of the pathways described above, such as TG2-induced modulation of adenylyl cyclase/CREB signalling. Indeed, studies have shown that NGF can modulate cAMP levels in neuronal cells (Nikodijevic et al., 1975; Berg et al., 1995).

Functional considerations

TG2's involvement in the stimulatory effect of PACAP and NGF on cell survival and neurite outgrowth strongly suggests a role for TG2 in their neurotrophic activity in mouse and human neuroblastoma cell lines. This conclusion leads to the suggestion that the observed response may share a common mechanism. Neurite branching has a fundamental role in connecting neuronal cells, and it is one of the sensitive parameters of neurite outgrowth. It has been reported that changes in axonal branching are associated with neurodegenerative disorders (Yu et al., 1996). The current findings showed that neurite branching and processing were significantly increased in response to PACAP-27 and NGF, and this activity was reduced by the inhibition of TG2, suggesting that it has a key role in PACAP- and NGF-induced neurite branching. The observed reduction in the mean branches and mean processes per cell may indicate a disruption in the cytoskeletal proteins required for the development of neurite branching and enhanced microtubule stability, which is required for neurite stability. Accordingly, microtubule stability would be essential for preventing neurite deterioration associated with neurodegenerative disorders or neuronal hypoxia. Hence, TG2 could be neuroprotective due to its role in microtubule and neurite stability enhancement.

6.4 Conclusion

In conclusion, the results of this study indicate a role for TG2 as a useful neuroprotective/anti-apoptotic agent involved in the modulation of neurite outgrowth and neuronal cell stability induced by PACAP and NGF. Thus, further studies are required to elucidate the downstream substrates of TG2 and signalling pathways associated with the role of TG2 in neuroprotection and neurite outgrowth induced by the neurotrophic factors PACAP and NGF.

Chapter 7

7 Conclusion and future works

7.1 Summary of findings

This study aimed to determine whether the neurotrophic factors, PACAP and NGF, could modulate tissue transglutaminase (TG2) transamidase activity in morphologically and biochemically characterised differentiating mouse N2a and human SH-SY5Y neuroblastoma cell lines. In addition, it was intended to assess the role of TG2 in PACAP- and NGF-induced neuroprotection and neurite outgrowth in mouse N2a and human SH-SY5Y neuroblastoma cells.

7.1.1 Characterisation of differentiating neuroblastoma cell lines

The differentiating mouse N2a and human SH-SY5Y neuroblastoma cell lines have been reported to be suitable for use in the study of cell signalling pathways, differentiation, neurite outgrowth and neuronal survival (Li et al., 2007; Kim et al., 2011; Sahu et al., 2013; Murillo et al., 2017; Pirou et al., 2017). The SH-SY5Y cell line was used to validate the results observed in mouse N2a cells in a related human cell line. The findings were mostly comparable in both cell lines, except for minor variations that could be attributed to genetic drift and/or species- or cell line-related responses. Initially, both cell lines' ability to differentiate into a neuron-like phenotype by *all-trans* retinoic acid RA was evaluated. The generation of neuron-like phenotype cells was confirmed by monitoring the morphological alterations following RA treatment and the expression of neuronal phenotype-specific markers, such as the cholinergic neuronal marker choline acetyltransferase (ChAT) and the dopaminergic neuronal marker tyrosine hydroxylase (TH). N2a cells became more cholinergic neuron–like, with developing axon-like processes and dendrites, whereas SH-SY5Y cells became more adrenergic neuron–like with extended, long, and branched processes. Furthermore, Western blot analysis showed that differentiating N2a and SH-SY5Y cells expressed higher levels of TG2 compared with undifferentiated cells. In addition, the other transglutaminase members that are predominantly

expressed in neuronal tissue, TG1 and TG3, increased significantly in differentiating N2a cells and were present at comparable levels in differentiated and undifferentiated SH-SY5Y cells. Thus, the characterisation of differentiated N2a and SH-SY5Y cells could provide a potential aid for understanding the molecular mechanisms that contribute to the obtained responses.

7.1.2 Modulation of TG2 activity by PACAP and NGF

The neurotrophic effects of PACAP and NGF have been extensively studied; they both promote neurite outgrowth and neuronal survival (Williams et al., 1986; Hatanaka et al., 1988; Takei et al., 2000; Yuhara et al. 2001). However, it was essential to assess the possible modulation of TG2 activity by these neurotrophic factors prior to assessing its role in neuronal survival and neurite outgrowth. The first part of this thesis aimed to investigate the possible modulation of TG2 activity by the neurotrophic factors PACAP and NGF.

The neurotrophic effect of PACAP and NGF mediates neurite outgrowth and neuroprotection (Allen and Dawbarn 2006; Monaghan et al., 2008; Lomb et al., 2009; Jóźwiak-Be¸benista et al., 2015); however, it is not known whether these events involve modulation of TG2 activity. Therefore, initial experiments assessed the modulation of TG2 activity in response to PACAP and NGF. Modulation of TG2 was assessed by monitoring two types of transamidation activity, namely amine incorporation and crosslinking activity. The amine incorporating activity of TG2 was measured via biotin-cadaverine incorporation into N, N'-dimethylcasein, as described by Slaughter et al. (1992), and the crosslinking activity of TG2 was measured via biotin-TVQQEL peptide incorporation into casein, as described by Trigwell et al. (2004). The results showed that the neuropeptide PACAP-27 (PAC_1 receptor agonist) and NGF triggered transient time- and concentration-dependent increases in TG2-mediated biotin-cadaverine incorporation and peptide crosslinking activity in differentiating N2a and SH-SY5Y cells with no accompanying changes in TG2 expression level. In addition, the PAC_1 receptor-induced increases in TG activity were attenuated by the PAC_1 receptor antagonist PACAP 6-38, confirming that the activity is mediated through the PAC_1 receptor. Furthermore, the TG2 inhibitors R283 and Z-DON resulted in significant inhibition of the PACAP- and NGF-induced transamidation activity; on this basis, it can be confirmed that the observed increases in TG activity modulated by PACAP and NGF occurred via TG2. This was verified using *in situ* FITC-cadaverine incorporation and immunocytochemistry.

TG2 enzymatic activity is tightly regulated by the allosteric regulators Ca^{2+} and guanine nucleotides (Király et al., 2009). The presence of Ca^{2+} is essential for TG2 catalytic activity,

which induces TG2 to develop an open and active conformational structure and exposes the active site to the substrates and produces its enzymatic activity (Pinkas et al., 2007). Previous studies have shown that the release of Ca^{2+} from intracellular stores or influx of extracellular Ca^{2+} is linked to TG activation in response to GPCR stimulation, such as muscarinic receptor, 5-HT_{2A}, A_1 adenosine receptor and the β_2-adrenoceptor (Zhang et al., 1998; Walther et al., 2003; Vyas et al., 2016). Cells were stimulated with PACAP-27/NGF in either the presence (1.8 mM $CaCl_2$) or absence of extracellular Ca^{2+} (nominally Ca^{2+}-free Hanks/HEPES buffer containing 0.1 mM EGTA) and cell lysates were subjected to biotin-cadaverine incorporation or peptide crosslinking assays. The data presented in the current work indicate that PAC_1 receptor-induced transamidase activity was dependent on extracellular Ca^{2+}. In contrast, the NGF modulation of TG2 activity was partially dependent on the extracellular $Ca^{2+.}$

Although TG2 activity is regulated by intracellular [Ca^{2+}] changes, there is a growing and compelling body of evidence suggesting that TG activity can also be modulated by protein kinases and phosphorylation (Bollag et al, 2005; Mishra et al, 2007). For example, it has been shown that protein kinases, such as PKA and PKC, regulate the activity of TG2 (Almami et al. 2014) and that phosphorylation of TG2 by protein kinase A (PKA), inhibits its transamidating activity but enhances its kinase activity (Mishra et al., 2007). Moreover, PACAP has long been known to activate PKA, ERK1/2 and p38 MAPK signalling cascades, which contribute to its neuroprotective effect (Vaudry et al., 2009, 2000b), while NGF's activation of TrkA leads to the up-regulation of a multitude of signalling pathways, including the ERK1/2, PI-3K/PKB and PLC-γ/PKC cascades (Wang et al., 2014). However, very little is known about the specific signal transduction pathways that mediate this neuroprotective activity. As some of these pathways are associated with the modulation of intracellular TG2 activity, it is conceivable that PACAP or NGF directly regulates TG2 activity. Thus, the role of different protein kinases, which have been found to be more involved in the modulation of TG2 activity in the literature, was evaluated in this study. Accordingly, different protein kinase inhibitors were used to determine whether these signalling pathways are involved in PACAP-27- and NGF-induced TG2 activity. In brief, the observed inhibition in PACAP-27-induced TG2 activity in response to MEK1/2, PKB and PKA inhibition suggests that PACAP-27 modulates TG2 activity via these signalling proteins in both differentiating neuroblastoma cell lines. However, inhibition of PKC attenuated PACAP-27-induced TG2 activity in N2a, but not in SH-SY5Y, differentiating cells. As PACAP-27 has a significant activation effect on the central regulatory protein ERK1/2, it is conceivable that this phosphorylation of ERK1/2 would depend upon an up-stream role of other protein kinases and/or Ca^{2+} signalling. Therefore, the effect of protein kinase inhibitors and

removal of extracellular Ca^{2+} on PACAP-27-induced ERK1/2 phosphorylation were considered. The findings indicatethat PACAP-27 stimulation of the PAC_1 receptor to induce ERK1/2 activation is independent on Ca^{2+} influx in both cell lines, partially sensitive to PKC inhibition in N2a cells but PKC independent in SH-SY5Y cells. Furthermore, as a previous study showed that PKA can activate ERK1/2 (Stork and Schmitt, 2002), in the current work, the inhibition effect of PKA inhibitor on PACAP-27 induced ERK1/2 activation indicated the upstream role of PKA in ERK1/2 activation. Hence, PKA-mediated inhibition of TG2 activation may indeed reflect the upstream role of PKA in ERK1/2 activation. In addition, NGF is known to activate different downstream signalling proteins, including ERK1/2, PI-3K/PKB and PKC (Wang et al., 2014); therefore, assessment of these kinases to understand the modulation of TG2 activity by NGF was considered. The data elucidated that the NGF-induced TG2 activity was significantly attenuated by inhibiting ERK1/2, PKB and PKC, indicating their involvement in this modulation process and the lack of any 'crosstalk' between the ERK1/2 and PKB; however, PKC's upstream role in ERK1/2 activation was identified. Figure 7.1 summarises the common identified kinase pathways in both N2a and SH-SY5Y cells. In regard to the protein kinases' roles, the obtained data provide sufficient evidence to highlight the signalling pathways involved in the modulation of TG2 activity in neuron by neurotrophins which would be an initial platform to consider in future research in the field.

The findings obtained from this study may also reflect the potential effect of both neurotrophic factors (PACAP and NGF) on TG2 phosphorylation. The robust increase in the levels of TG2 phosphorylation after exposure to the PACAP or NGF was blocked by the inhibition of different protein kinases or removal of Ca^{2+}; these findings suggested their involvement in the neurotrophic modulation of TG2 phosphorylation activity. The findings indicated a prominent role of PKA and ERK1/2 in PACAP-27-induced TG2 phosphorylation, and more interestingly, the removal of Ca^{2+} only blocked the PACAP-induced phosphorylation of TG2 in mouse N2a cells and showed no effect in human SH-SY5Y cells. In contrast, the TG2 phosphorylation modulated by NGF was mainly regulated by ERK1/2, PKB and PKC.

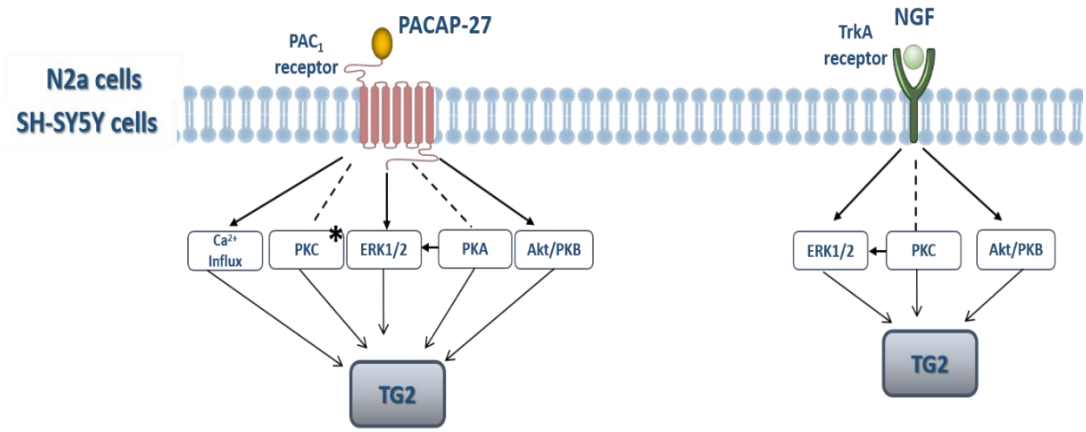

Figure 7.1 Schematic representation summarise the possible protein kinase pathways involved in PACAP- and NGF-induced TG2 activation in N2a and SH-SY5Y cells.

PACAP-27 promotes TG2 transamidase activity via a signalling pathway dependent upon PKC, ERK1/2, PKA and PKB along with influx of extracellular Ca^{2+} leading to increases in TG2 activity. The finding reflects the up- stream involvement of PKA in PACAP-induced ERK1/2 activation. NGF promotes TG2 transamidase activity in mouse N2a and human SH-SY5Y neuroblastoma cells via a signalling pathway dependent upon PKC, ERK1/2 and PKB. The role of PKC reflects the up- stream involvement of PKC in NGF-induced ERK1/2 activation. * represent signalling in N2a cells only, black lines represent this study's findings and dashed lines represent effects that are not from the present study.

7.1.3 The role of TG2 in neurotrophic factor–induced cytoprotection

The second part of this research evaluated the possible role of TG2 in the neuroprotection activity induced by PACAP or NGF in differentiating neuroblastoma cells after exposure to hypoxia conditions. Using the MTT and LDH assays and measuring the activity of caspase-3, decreased cell viability was observed within 8 h of hypoxia exposure in both N2a and SH-SY5Y cells. Treatment with PACAP and NGF prior to hypoxia exposure significantly attenuated the hypoxia-induced decrease in cell viability assessed by MTT reduction, LDH release and caspase-3 activation. The inhibition of TG2 attenuated the protective effect of PACAP and NGF under hypoxia condition and reversed their blocking effect on hypoxia-induced caspase-3 activation. These findings suggested that TG2 has a prominent role in the neuroprotective and anti-apoptotic effect of PACAP and NGF under hypoxic conditions.

7.1.4 The role of TG2 in neurotrophic factor-induced neurite outgrowth

The last part of the current study involved the development of an automated, quantitative, high-throughput imaging system for multiple-parameter measurement to evaluate the role of TG2 in the neurite outgrowth induced by PACAP and NGF in differentiating N2a and SH-SY5Y cells. Establishment of such automated measurement permitted quantitative evaluation of the morphological features of neurite outgrowth staining with the cytoskeleton-specific antibody B512 (which stained microtubules in the cell body, axons and dendrites). In brief, PACAP and NGF significantly enhanced the neurite number/field, cells with significant outgrowth, neurite length and branching, but with no effect on the cell number or cell body area. Inhibition of TG2 significantly reversed the PACAP and NGF enhancement of the neurite outgrowth parameters, which suggests a role for TG2 in the neurite outgrowth induced by neurotrophic factors. Taken together, the findings indicate that TG2 is essential for neurite outgrowth process modulated by PACAP and NGF.

Taking all of the results together, considering the role of TG2 in the stimulatory effect of PACAP and NGF for inducing neuronal cell survival/anti-apoptotic and neurite outgrowth, it may can be suggested that the observed response could share one mechanism. Based on the role of TG2 in PACAP- and NGF-enhanced neurite branching, which is required for neuronal stability and for preventing neuronal retrogradation associated with hypoxia, it can be hypothesised that TG2 could be neuroprotective due to its role in microtubule and neurite stability enhancement. The key findings of the current study are summarised in Figure 7.2.

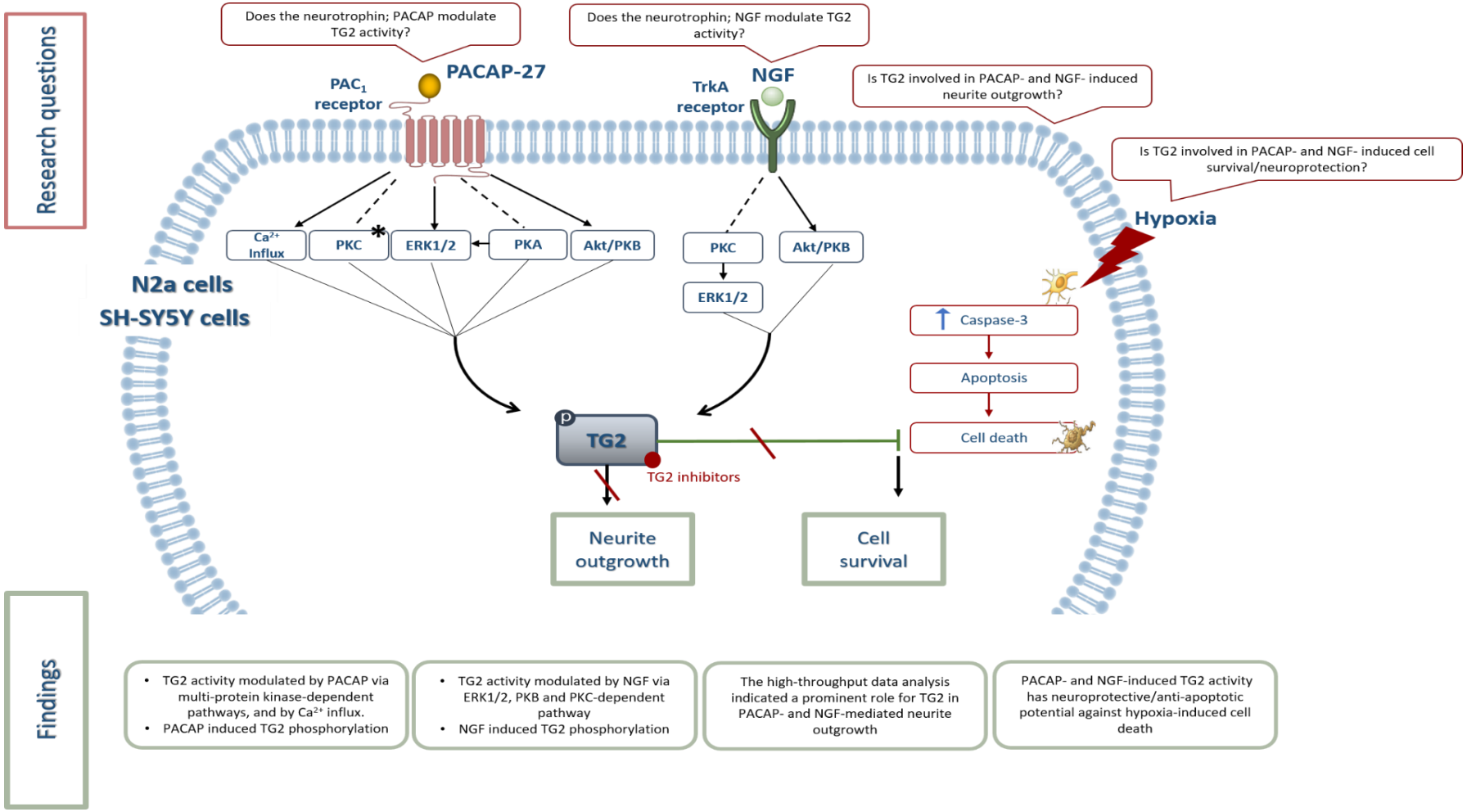

Figure 7.2 Schematic diagram of the findings in this study

7.2 Future work

Based on the findings of the present study, recommendations can be made for future work. This study evaluated the modulation of TG2 activity by PACAP and NGF and the possible involvement of such phenomena in cell survival and neurite outgrowth. Assessment of TG2 transamidase enzymatic activities were used in this study to evaluate this modulation response. Other TG2 biochemical activities, such as GTPase, kinase and/or isopeptidase are assigned for various TG2 cellular functions; therefore, it would be of interest in future work to investigate the potential of PACAP and NGF in modulation of these other TG2 activities. Due to the existence of other TG isoforms, for example TG1 and TG3 in the models used in this study, it would be of value to evaluate the possible modulation of these enzymes by the neurotrophic factors PACAP and NGF.

The data presented in this thesis suggest that pharmacological inhibition of TG2 attenuates the neuroprotective and the neurite outgrowth function of PACAP and NGF. TG2 structure homogeneity with other transglutaminase family members could interfere with the selectivity profile of the applied TG2 inhibitors. Thus, it would be worthwhile to apply a method of eliminating the TG2 activity other than with pharmacological inhibition, such as siRNA, which allows selective reduction of the TG2 without using chemicals, to confirm the findings of this study. In addition, it would be of further interest to assess this modulation and the responses in TG2 null neuronal cell lines.

The current study suggests the role of TG2 in PACAP- and NGF-induced cell survival and neurite outgrowth; extending this study to identify the downstream substrates of TG2 would be of value. One available approach could be using CaptAvidin™-agarose affinity chromatography to isolate TG2 substrates, followed by mass spectrometry and bioinformatics approaches to identify the labelled TG2 substrate and interacting proteins and relating them to the identified pathways. This would allow a better understanding of the signalling pathway(s) associated with the role of TG2 in PACAP and NGF neuroprotection.

The findings revealed that TG2 was phosphorylated in response to the neurotrophic factors used, where TG2 and the protein kinases possibly involved in this process were identified. However, the precise TG2 phosphorylation site(s) under this experimental condition were not investigated. To extend this work, it would be beneficial to apply phosphoproteomic analysis to identify the site(s) on TG2 that are being phosphorylated in response to PACAP or NGF. Such a finding could conceivably provide sufficient knowledge to determine whether regulation of

the TG2 phosphorylation site(s) has a neuroprotective, anti-apoptotic or neurite stabilisation effect that would be a therapeutic target in hypoxia or neurodegeneration-associated neuronal damage.

Having confirmed the neuroprotective role of PACAP and NGF in differentiating N2a and SH-SY5Y cells exposed to hypoxia and having shown the effect of TG2 inhibition on interfering with cell survival promoted by PACAP and NGF, the functional role of TG2 in the context of cell survival was addressed. The findings indicated the inhibition of TG2 blocked PACAP- and NGF-mediated reduction in hypoxia-induced activation of caspase-3, which is indicative of an anti-apoptotic role. Since it is known that TG2 inhibits apoptosis via the down-regulation of Bax expression and inhibition of caspases 3 and 9 (Cho et al., 2010), this regulation could account for the anti-apoptotic activity of TG2 under the current study conditions. In addition, TG2 cell survival studies highlighted the association of TG2 anti-apoptotic and growth-stimulating functions with its GTPase activity, and this biochemical activity depends on its subcellular localisation (Antonyak et al., 2001). Thus, the detrimental effect on this signalling pathway could be further expanded by assessing the proteins associated with the apoptosis pathway and GTPase biochemical activity of TG2. Additional work could also examine TG2's interaction with hypoxia inducible factor (HIF) signalling in differentiating mouse and human neuroblastoma cells, as it has been proven that, in neurons, TG2 binds to HIF, attenuating its activity under ischaemic conditions (Filiano et al., 2008). Also, it would be of interest assess the role of TG2 during the hypoxia and in hypoxia/reoxygenation condition. Thus, it is desirable to further characterise the mechanism by which this activity developed; thus, considering this in the future work would be of value. Taken together, such extensions in future works would further help in elucidating the exact mechanism of TG2's role in neuroprotection and neurite outgrowth, modulated by PACAP and NGF, in differentiating N2a and SH-SY5Y cells.

7.3 Concluding remarks

The mechanism by which TG2 promotes anti-apoptotic and neurite outgrowth of neuronal cells remains a matter of speculation. The present study addressed the question of whether TG2 could be modulated by two neurotrophins, PACAP and NGF, and assessed the role of TG2 in neuronal survival under hypoxic conditions and neurite outgrowth in differentiating N2a and SH-SY5Y cells. Indeed, the findings demonstrate for the first time that the neurotrophins PACAP and NGF induce TG2 activity via multiple protein kinase-dependent pathways. Furthermore, PACAP and NGF-induced neuronal cell survival and neurite outgrowth depend on TG2 transamidation activity. These results highlight the importance of TG2 in the cellular functions of neurotrophins in neuronal cells. Continued research on these signalling mechanisms would be highly recommended to understand the precise role of TG2 in neuronal development and cell protection. This knowledge would provide valuable insight into how neurons behave under various conditions and development of therapeutic targets for pharmacological intervention to alleviate the neuronal damage associated with neurodegenerative disease, ischaemic stroke or apoptosis.

8 References

Achyuthan, K. E., & Greenberg, C. S. (1987). Identification of a guanosine triphosphate-binding site on guinea pig liver transglutaminase. Role of GTP and calcium ions in modulating activity. *Journal of Biological Chemistry*, *262*(4), 1901–06.

Adem, A., Mattsson, M. E., Nordberg, a, & Påhlman, S. (1987). Muscarinic receptors in human SH-SY5Y neuroblastoma cell line: regulation by phorbol ester and retinoic acid-induced differentiation. *Brain Research*, *430*, 235–42.

Aeschlimann, D., & Paulsson, M. (1991). Cross-linking of laminin-nidogen complexes by tissue transglutaminase: A novel mechanism for basement membrane stabilization. *Journal of Biological Chemistry*, *266*(23), 15308–17.

Aeschlimann, D., & Thomazy, V. (2000). Protein crosslinking in assembly and remodelling of extracellular matrices: the role of transglutaminases. *Connective Tissue Research*, *41*(1), 1–27.

Agerman, K., Baudet, C., Fundin, B., Willson, C., & Ernfors, P. (2000). Attenuation of a caspase-3 dependent cell death in NT4- and p75-deficient embryonic sensory neurons. *Molecular and Cellular Neurosciences*, *16*(3), 258–68.

Ahn, J. S., Kim, M. kyung, Hahn, J. hee, Park, J. H., Park, K. H., Cho, B. R. & Kim, D. joong. (2008). Tissue transglutaminase-induced down-regulation of matrix metalloproteinase-9. *Biochemical and Biophysical Research Communications*, *376*(4), 743–47.

Akimov, S. S., & Belkin, A. M. (2001). Cell surface tissue transglutaminase is involved in adhesion and migration of monocytic cells on fibronectin. *Blood*, *98*(5), 1567–76.

Akimov, S. S., Krylov, D., Fleischmana, L. F., & Belkin, A. M. (2000). Tissue transglutaminase is an integrin-binding adhesion coreceptor for fibronectin. *Journal of Cell Biology*, *148*(4), 825–38.

Akpan, N., & Troy, C. M. (2013). Caspase inhibitors: prospective therapies for stroke. *The Neuroscientist : A Review Journal Bringing Neurobiology, Neurology and Psychiatry*, *19*(2), 129–36.

Alessandrini, A., Namura, S., Moskowitz, M. A., & Bonventre, J. V. (1999). MEK1 protein kinase inhibition protects against damage resulting from focal cerebral ischemia. *Proceedings of the National Academy of Sciences of the United States of America*, *96*(22), 12866–09.

Allen, S. J., & Dawbarn, D. (2006). Clinical relevance of the neurotrophins and their receptors. *Clinical Science*, *110*(2), 175–91.

Allen, S. J.,Watson J. J., Shoemark D. K., Barua N. U., Patel N. K. (2013). GDNF, NGF and BDNF as therapeutic options for neurodegeneration. *Pharmacology & Therapeutics,138*(2), 155–75.

Almami, I., Dickenson, J. M., Hargreaves, A. J., & Bonner, P. L. R. (2014). Modulation of transglutaminase 2 activity in H9c2 cells by PKC and PKA signalling: A role for transglutaminase 2 in cytoprotection. *British Journal of Pharmacology 171*(16), 3946–60.

Aloe, L., Rocco, M. L., Bianchi, P., & Manni, L. (2012). Nerve growth factor: from the early discoveries to the potential clinical use. *Journal of Translational Medicine*, *10*(1), 239.

Andringa, G., Lam, K. Y., Chegary, M., Wang, X., Chase, T. N., & Bennett, M. C. (2004). Tissue transglutaminase catalyzes the formation of alpha-synuclein crosslinks in Parkinson's disease. *The FASEB Journal : Official Publication of the Federation of American Societies for Experimental Biology*, *18*(7), 932–34.

Antonyak, M. A., Singh, U. S., Lee, D. A., Boehm, J. E., Combs, C., Zgola, M. M. & Cerione, R. A. (2001). Effects of Tissue Transglutaminase on Retinoic Acid-induced Cellular Differentiation and Protection against Apoptosis. *Journal of Biological Chemistry*, *276*(36), 33582–87.

Atwal, J. K., Massie, B., Miller, F. D., & Kaplan, D. R. (2000). The TrkB-Shc site signals neuronal survival and local axon growth via MEK and PI3-Kinase. *Neuron*, *27*(2), 265–77.

Aubert, N., Falluel-Morel, A., Vaudry, D., Xifro, X., Rodriguez-Alvarez, J., Fisch, C. & Gonzalez, B. J. (2006). PACAP and C2-ceramide generate different AP-1 complexes through a MAP-kinase-dependent pathway: Involvement of c-Fos in PACAP-induced Bcl-2 expression. *Journal of Neurochemistry*, *99*(4), 1237–50.

Bai, Y., Dergham, P., Nedev, H., Xu, J., Galan, A., Rivera, J. C., & Saragovi, H. U. (2010). Chronic and acute models of retinal neurodegeneration TrkA activity are neuroprotective whereas p75NTR activity is neurotoxic through a paracrine mechanism. *Journal of Biological Chemistry*, *285*(50), 39392–39400.

Bailey, C. D., Graham, R. M., Nanda, N., Davies, P. J., & Johnson, G. V. (2004). Validity of mouse models for the study of tissue transglutaminase in neurodegenerative diseases. *Mol Cell Neurosci*, *25*(3), 493–503.

Bailey, C. D., & Johnson, G. (2005). Tissue transglutaminase contributes to disease progression in the R6/2 Huntington's disease mouse model via aggregate-independent mechanisms. *Journal of Neurochemistry*, *92*(1), 83–92.

Bamji, S. X., Majdan, M., Pozniak, C. D., Belliveau, D. J., Aloyz, R., Kohn, J., & Miller, F. D. (1998). The p75 neurotrophin receptor mediates neuronal apoptosis and is essential for naturally occurring sympathetic neuron death. *The Journal of Cell Biology*, *140*(4), 911–23.

Barres, B. A., & Barde, Y. (2000). Neuronal and glial cell biology. *Current Opinion in Neurobiology*, *10*(5), 642–48.

Basille-Dugay, M., Vaudry H., Fournier A., Gonzalez B., & Vaudry D. (2013). Activation of PAC_1 receptors in rat cerebellar granule cells stimulates both calcium mobilization from intracellular stores and calcium influx through N-type calcium channels. *Front Endocrinol (Lausanne) 10*(4): 56.

Batistatou, A., & Greene L. A., (1993). Internucleosomal DNA cleavage and neuronal cell survival/death *The Journal of Cell Biology*, *122* (3), 523–32.

Baxter, P. S., Martel, M. A., McMahon, A., Kind, P. C., & Hardingham, G. E. (2011). Pituitary adenylate cyclase-activating peptide induces long-lasting neuroprotection through the induction of activity-dependent signaling via the cyclic AMP response element-binding protein-regulated transcription co-activator 1. *Journal of Neurochemistry*, *118*(3), 365–78.

Bayascas, J. R., & Alessi, D. R. (2005). Regulation of Akt/PKB Ser473 phosphorylation. *Molecular Cell*, *18*(2), 143–45.

Belkin, A. M. (2011). Extracellular TG2: Emerging functions and regulation. *FEBS Journal*., *278*(24), 4704–16.

Bennett, B. L., Sasaki, D. T., Murray, B. W., O'Leary, E. C., Sakata, S. T., Xu, W., Leisten, J. C., Motiwala, A., Pierce, S., Satoh, Y., Bhagwat, S. S., Manning, A. M., & Anderson, D. W. (2001) *Proc. Natl. Acad. Sci. U. S. A.*, *98*(24), 13681–86.

Berg, K.A., Maayani, S., McKay, R., & Clarke, W.P. (1995). Nerve Growth Factor Amplifies Cyclic AMP Production in the HT4 Neuronal Cell Line. *Journal of Neurochemistry, 64* (1), 220–28.

Bergamini, C. M., & Signorini, M. (1993). Studies on tissue transglutaminases: interaction of erythrocyte type-2 transglutaminase with GTP. *The Biochemical Journal*, *291 (Pt 1)*, 37–9.

Berridge, M. J. (2006) Calcium microdomains: organization and function. *Cell Calcium 40*(5-6), 405-412.

Bezzi, P., & Volterra, A. (2001). A neuron-glia signalling network in the active brain. *Current Opinion in Neurobiology*, *11*(1), 387–94.

Bian, Y., Song C., Cheng K., Dong M., Wang F., Huang J., Sun D., Wang L., Ye M., & Zou H. (2014). An enzyme assisted RP-RPLC approach for in-depth analysis of human liver phosphoproteome. *J Proteomics. 96*:253-62.

Bibel, M., & Barde, Y. (2000). vertebrate nervous system Neurotrophins : key regulators of cell fate and cell shape in the vertebrate nervous system. *Genes & Development*, (Bargmann 1998), 2919–2937.

Biedler, J. L., Helson, L., & Spengler, B. A. (1973). Morphology and Growth, Tumorigenicity, and Cytogenetics of Human Neuroblastoma Cells in Continuous Culture. *Cancer Research*, *33*(11), 2643–52.

Biernat, J., Wu, Y.-Z., Timm, T., Zheng-, Q. F., Mandelkow, E., Meijer, L., & Mandelkow. (2002). Protein Kinase MARK/PAR-1 Is Required for Neurite Outgrowth and Establishment of Neuronal Polarity. *Molecular Biology of the Cell*, *13*, 4013–28.

Bijur, G. N., & Jope, R. S. (2003). Rapid accumulation of Akt in mitochondria following phosphatidylinositol 3-kinase activation. *Journal of Neurochemistry*, *87*(6), 1427–35.

Björkblom, B., Vainio, J. C., Hongisto, V., Herdegen, T., Courtney, M. J., & Coffey, E. T. (2008). All JNKs can kill, but nuclear localization is critical for neuronal death. *Journal of Biological Chemistry*, *283*(28), 19704–13.

Biswas, S.C. & Greene, L.A. NGF down-regulates the BH3-only protein Bim and suppresses its pro-apoptotic activity by phosphorylation. (2002). *J. Biol. Chem. 277*(51),49511–16.

Blaskó, B., Mádi, A., & Fésüs, L. (2003). Thioredoxin motif of Caenorhabditis elegans PDI-3 provides Cys and His catalytic residues for transglutaminase activity. *Biochemical and Biophysical Research Communications*, *303*(4), 1142–1147.

Blechman, J., & Levkowitz, G. (2013). Alternative splicing of the pituitary adenylate cyclase-activating polypeptide receptor PAC1: Mechanisms of fine tuning of brain activity. *Frontiers in Endocrinology*, *4*(MAY), 1–19.

Bollag, W. B., Zhong, X., Dodd, M. E., Hardy, D. M., Zheng, X., & Allred, W. T. (2005). Phospholipase d signaling and extracellular signal-regulated kinase-1 and -2 phosphorylation (activation) are required for maximal phorbol ester-induced transglutaminase activity, a marker of keratinocyte differentiation. *J.Pharmacol.Exp.Ther.*, *312*(3), 1223–31.

Botia, B., Basille, M., Allais, A., Raoult, E., Falluel-Morel, A., Galas, L., & Vaudry, D. (2007). Neurotrophic effects of PACAP in the cerebellar cortex. *Peptides*, *28*(9), 1746–52.

Bozyczko-Coyne, D., O'Kane, T. M., Wu, Z. L., Dobrzanski, P., Murthy, S., Vaught, J. L., & Scott, R. W. (2001). CEP-1347/KT-7515, an inhibitor of SAPK/JNK pathway activation, promotes survival and blocks multiple events associated with A??-induced cortical neuron apoptosis. *Journal of Neurochemistry*, *77*(3), 849–63.

Braithwaite, S. P., Schmid, R. S., He, D. N., Sung, M. L. A., Cho, S., Resnick, L., & Lo, D. C. (2010). Inhibition of c-Jun kinase provides neuroprotection in a model of Alzheimer's disease. *Neurobiology of Disease*, *39*(3), 311–17.

Brazil, D. P., & Hemmings, B. A. (2001). Ten years of protein kinase B signalling: A hard Akt to follow. *Trends in Biochemical Sciences*, *26*(11), 657–64.

Briani, C., Samaroo, D., & Alaedini, A. (2008). Celiac disease: From gluten to autoimmunity. *Autoimmunity Reviews*, *7*(8), 644–50.

Brodie, C., Bogi, K., Acs, P., Lazarovici, P., Petrovics, G., Anderson, W. B., & Blumberg, P. M. (1999). Protein kinase C-epsilon plays a role in neurite outgrowth in response to epidermal growth factor and nerve growth factor in PC12 cells. *Cell Growth & Differentiation*, *10*(3), 183–91.

Bruce, S. E., Bjarnason, I., & Peters, T. J. (1985). Human jejunal transglutaminase: demonstration of activity, enzyme kinetics and substrate specificity with special relation to gliadin and coeliac disease. *Clinical Science (London, England : 1979)*, *68*(5), 573–79.

Brunet, A., Bonni, A., Zigmond, M. J., Lin, M. Z., Juo, P., Hu, L. S., & Greenberg, M. E. (1999). Akt promotes cell survival by phosphorylating and inhibiting a forkhead transcription factor. *Cell*, *96*(6), 857–68.

Cabell, L., & Audesirk, G., (1993). Effects of selective inhibition of protein kinase C, cyclic AMP-dependent protein kinase, and Ca^{2+}-calmodulin-dependent protein kinase on neurite development in cultured rat hippocampal neurons. *Int. J. Dev. Neurosci.*, *11*(1993),357–368.

Cabeza, C., Figueroa, A., Lazo, O. M., Galleguillos, C., Pissani, C., Klein, A., & Bronfman, F. C. (2012). Cholinergic abnormalities, endosomal alterations and up-regulation of nerve growth factor signaling in Niemann-Pick type C disease. *Molecular Neurodegeneration*, *7*(1), 11.

Caccamo, D., Curro, M., Ferlazzo, N., Condello, S., & Ientile, R. (2012). Monitoring of transglutaminase 2 under different oxidative stress conditions. *Amino Acids*, *42*(2–3), 1037–43.

Cai, J., Hua, F., Yuan, L., Tang, W., Lu, J., Yu, S., & Hu, Y. (2014). Potential therapeutic effects of neurotrophins for acute and chronic neurological diseases. *BioMed Research International*.

Carlsson, Y., Schwendimann, L., Vontell, R., Rousset, C. I., Wang, X., Lebon, S., & Jacotot, E. (2011). Genetic inhibition of caspase-2 reduces hypoxic-ischemic and excitotoxic neonatal brain injury. *Annals of Neurology*, *70*(5), 781–789.

Carracedo, A., & Pandolfi, P. P. (2008). The PTEN-PI3K pathway: Of feedbacks and cross-talks. *Oncogene*, *27*(41), 5527–41.

Carriere, A., Romeo, Y., Acosta-Jaquez, H. A., Moreau, J., Bonneil, E., Thibault, P., & Roux, P. P. (2011). ERK1/2 phosphorylate raptor to promote ras-dependent activation of mTOR complex 1 (mTORC1). *Journal of Biological Chemistry*, *286*(1), 567–77.

Casaccia-Bonnefil, P., Carter, B. D., Dobrowsky, R. T., & Chao, M. V. (1996). Death of oligodendrocytes mediated by the interaction of nerve growth factor with its receptor p75. *Nature*, *383*(6602), 716–719.

Castorina, A., Scuderi, S., D'Amico, A. G., Drago, F., & D'Agata, V. (2014). PACAP and VIP increase the expression of myelin-related proteins in rat schwannoma cells: Involvement of PAC1/VPAC2 receptor-mediated activation of PI3K/Akt signaling pathways. *Experimental Cell Research*, *322*(1), 108–121.

Chakraborty, G., Leach, T., Zanakis, M. F., Sturman, J. A., & Ingoglia, N. A. (1987). Posttranslational Protein Modification by Polyamines in Intact and Regenerating Nerves. *Journal of Neurochemistry*, *48*(3), 669–675.

Chao, M. V., Rajagopal, R., & Lee, F. S. (2006). Neurotrophin signalling in health and disease: Figure 1. *Clinical Science*, *110*(2), 167–173.

Chao, M. V, Bothwell, M. A., Ross, A. H., Koprowski, H., Lanahan, A. A., Buck, C. R., & Sehgal, A. (1986). Gene transfer and molecular cloning of the human NGF receptor. *Science*, *232*(4749), 518–521.

Chauvier, D., Renolleau, S., Holifanjaniaina, S., Ankri, S., Bezault, M., Schwendimann, L., & Jacotot, E. (2011). Targeting neonatal ischemic brain injury with a pentapeptide-based irreversible caspase inhibitor. *Cell Death and Disease*, *2*(9), e203.

Cheung, Y. T., Lau, W. K. W., Yu, M. S., Lai, C. S. W., Yeung, S. C., So, K. F., & Chang, R. C. C. (2009). Effects of all-trans-retinoic acid on human SH-SY5Y neuroblastoma as in vitro model in neurotoxicity research. *NeuroToxicology*, *30*(1), 127–135.

Chhabra, A., Verma, A., & Mehta, K. (2009). Tissue transglutaminase promotes or suppresses tumors depending on cell context. *Anticancer Research*, *29*(6), 1909–19.

Chik, C. L.,Inukai T., Ogiwara T., Boyd H., Li B., Karpinski E. & Ho. A.K. (1996). Characterization of pituitary adenylate cyclase-activating polypeptide 38 (PACAP38)- PACAP27-, and vasoactive intestinal peptide-stimulated responses in N1E-115 neuroblastoma cells. *J. Neurochem. 67*: 1005–1013.

Chivet M., Javalet C., Laulagnier K., Blot B., Hemming F. J., & Sadoul R. (2014). Exosomes secreted by cortical neurons upon glutamatergic synapse activation specifically interact with neurons. *J. Extracell. Vesicles 3*, 24722.

Cho, S.-Y., Lee, J.-H., Bae, H.-D., Jeong, E. M., Jang, G.-Y., Kim, C.-W., & Kim, I.-G. (2010). Transglutaminase 2 inhibits apoptosis induced by calcium- overload through down-regulation of Bax. *Experimental & Molecular Medicine*, *42*(9), 639–650.

Ciccocioppo, R., Finamore, A., Mengheri, E., Millimaggi, D., Esslinger, B., Dieterich, W., & Corazza, G. R. (2010). Isolation and characterization of circulating tissue transglutaminase-specific T cells in coeliac disease. *Int J Immunopathol Pharmacol*, *23*(1), 179–191.

Citron, B. A., SantaCruz, K. S., Davies, P. J. A., & Festoff, B. W. (2001). Intron-Exon Swapping of Transglutaminase mRNA and Neuronal Tau Aggregation in Alzheimer's Disease. *Journal of Biological Chemistry*, *276*(5), 3295–3301.

Clarke, D. D., Mycek, M. J., Neidle, a., & Waelsch, H. (1959). The incorporation of amines into protein. *Archives of Biochemistry and Biophysics*, *79*(1959), 338–354.

Clason, T. A., Girard B. M., May V., & Parsons R. L. (2016). Activation of MEK/ERK signaling by PACAP in guinea pig cardiac neurons. *J. Mol. Neurosci. 59*(2): 309-316.

Colak, G., & Johnson, G. V. W. (2012). Complete transglutaminase 2 ablation results in reduced stroke volumes and astrocytes that exhibit increased survival in response to ischemia. *Neurobiology of Disease*, *45*(3), 1042–1050.

Collins, L. M., Downer, E. J., Toulouse, A., & Nolan, Y. M. (2015). Mitogen-Activated Protein Kinase Phosphatase (MKP)-1 in Nervous System Development and Disease. *Molecular Neurobiology*, *51*(3), 1158–1167.

Compston, A, Zajicek, J., Sussman, J., Webb, a, Hall, G., Muir, D., & Scolding, N. (1997). Glial lineages and myelination in the central nervous system. *Journal of Anatomy*, *190 (Pt 2)*, 161–200.

Condello, S., Caccamo, D., Currò, M., Ferlazzo, N., Parisi, G., & Ientile, R. (2008). Transglutaminase 2 and NF-κB interplay during NGF-induced differentiation of neuroblastoma cells. *Brain Research*, *1207*(2008), 1–8.

Corrêa, S. A. L., & Eales, K. L. (2012). The Role of p38 MAPK and Its Substrates in Neuronal Plasticity and Neurodegenerative Disease. *Journal of Signal Transduction*, *2012*, 1–12.

Courtney, K. D., Corcoran, R. B., & Engelman, J. A. (2010). The PI3K pathway as drug target in human cancer. *Journal of Clinical Oncology : Official Journal of the American Society of Clinical Oncology*, *28*(6), 1075–83.

Couvineau, A., Amiranoff, B., & Laburthe, M. (1986). Solubilization of the Liver Vasoactive Intestinal

Peptide Receptor and evidence for an association with with a functional GTP regulatory protein.*The Journal of Biological Chemistry*, *261*(31), 14482–89.

Craig, A. M., & Banker, G. (1994). Neuronal Polarity. *Annual Review of Neuroscience*, *17*(1), 267–310.

Creedon, D. J., Johnson, E. M., & Lawrence, J. C. (1996). Mitogen-activated protein kinase-independent pathways mediate the effects of nerve growth factor and cAMP on neuronal survival. *J Biol Chem*, *271*(34), 20713–20718.

Crowder, R. J., & Freeman, R. S. (1998). Phosphatidylinositol 3-kinase and Akt protein kinase are necessary and sufficient for the survival of nerve growth factor-dependent sympathetic neurons. *J Neurosci*, *18*(8), 2933–2943.

Crowley, C., Spencer, S. D., Nishimura, M. C., Chen, K. S., Pitts-Meek, S., Armaninl, M. P., & Phillips, H. S. (1994). Mice lacking nerve growth factor display perinatal loss of sensory and sympathetic neurons yet develop basal forebrain cholinergic neurons. *Cell*, *76*(6), 1001–1011.

Cuenda, A., & Rousseau, S. (2007). p38 MAP-Kinases pathway regulation, function and role in human diseases. *Biochimica et Biophysica Acta (BBA) - Molecular Cell Research*, *1773*(8), 1358–1375.

Currò, M., Condello, S., Caccamo, D., Ferlazzo, N., Parisi, G., & Ientile, R. (2009). Homocysteine-induced toxicity increases TG2 expression in Neuro2a cells. *Amino Acids*, *36*(4), 725–730.

Dai, Y, Dudek N.L. , Patel T.B. , & Muma N. A. (2008). Transglutaminase-catalyzedtransamidation:a novel mechanism for Rac1 activation by 5-hydroxytryptamine 2 A receptor stimulation. J *Pharmacol Exp Ther 326*(1): 153–162.

Dardik, R., & Inbal, A. (2006). Complex formation between tissue transglutaminase II (tTG) and vascular endothelial growth factor receptor 2 (VEGFR-2): Proposed mechanism for modulation of endothelial cell response to VEGF. *Experimental Cell Research*, *312*(16), 2973–2982.

Das, T., Baek, K. J., Gray, C., & Im, M. J. (1993). Evidence that the Gh protein is a signal mediator from α1-adrenoceptor to a phospholipase C: II. Purification and characterization of a Gh-coupled 69-kDa phospholipase C and reconstitution of α1-adrenoceptor, Gh family, and phospholipase C. *Journal of Biological Chemistry*, *268*(36), 27398–27405.

Davies, S. P., Reddy, H., Caivano, M. & Cohen, P. (2000). Specificity and mechanism of action of some commonly used protein kinase inhibitors. *Biochem. J. 351*(pt 1), 95–105.

De Bernardi M. A., Rabin S. J., Colangelo A. M., Brooker G., & Mocchetti I. (1996). TrkA mediates the nerve growth factor-induced intracellular calcium accumulation. *J Biol Chem 271*(11), 6092–98.

Dejda, A., Sokołowska, P., & Nowak, J. Z. (2005). Neuroprotective potential of three neuropeptides PACAP, VIP and PHI. *Pharmacological Reports*, *57*(3), 307–320.

Deppmann, C. D., Mihalas, S., Sharma, N., Lonze, B. E., Niebur, E., & Ginty, D. D. (2008). A Model for Neuronal Competition During Development. *Science*, *320*(5874), 369–373.

Derijard, B., Hibi, M., Wu, I. H., Barrett, T., Su, B., Deng, T. L., & Davis, R. J. (1994). JNK1 - A protein-kinase stimulated by uv-light and ha-ras that binds and phosphorylates the c-jun activation domain. *Cell*, *76*(6), 1025–1037.

Descloux, C., Ginet, V., Clarke, P. G. H., Puyal, J., & Truttmann, A. C. (2015). Neuronal death after perinatal cerebral hypoxia-ischemia: Focus on autophagy-mediated cell death. *International Journal of Developmental Neuroscience*, *45*(2015), 75–85.

Deutsch, PJ & Su NY. (1992). The 38-amino acid form of pituitary adenylate cyclase-activating polypeptide stimulates dual signaling cascades in PC12 cells and promotes neurite outgrowth. *J Biol Chem 267*(8): 5108–13.

Dhanasekaran, D. N., & Reddy, E. P. (2008). JNK signaling in apoptosis. *Oncogene*, *27*(48), 6245–6251.

Di Sabatino A., & Corazza G. R. (2009). Coeliac disease. *Lancet*,*373*(9673):1480–1493.

Dickinson, T., Fleetwood-Walker, S. M., Mitchell, R., & Lutz, E. M. (1997). Evidence for roles of vasoactive intestinal polypeptide (VIP) and pituitary adenylate cyclase activating polypeptide (PACAP) receptors in modulating the responses of rat dorsal horn neurons to sensory inputs. *Neuropeptides*, *31*(2), 175–185.

Dickson, L., & Finlayson, K. (2009). VPAC and PAC receptors: From ligands to function. *Pharmacology and Therapeutics*, *121*(3), 294–316.

Dillon, R. L., White, D. E., & Muller, W. J. (2007). The phosphatidyl inositol 3-kinase signaling network: Implications for human breast cancer. *Oncogene*, *26*(9), 1338–45.

Douiri, S., Bahdoudi, S., Hamdi, Y., Cubì, R., Basille, M., Fournier, A., & Masmoudi-Kouki, O. (2016). Involvement of endogenous antioxidant systems in the protective activity of pituitary adenylate cyclase-activating polypeptide against hydrogen peroxide-induced oxidative damages in cultured rat astrocytes. *Journal of Neurochemistry*, *137*(6), 913–930.

Dudley DT, Pang L, Decker SJ, Bridges AJ, & Saltiel AR (1995) A syntheticinhibitorofthemitogen-activatedproteinkinasecascade. *Proc Natl Acad Sci USA, 92*(17):7686–7689

Durukan, A., & Tatlisumak, T. (2007). Acute ischemic stroke: Overview of major experimental rodent models, pathophysiology, and therapy of focal cerebral ischemia. *Pharmacology Biochemistry and Behavior*, *87*(1), 179–197.

Dwane, S., Durack, E., & Kiely, P. A. (2013). Optimising parameters for the differentiation of SH-SY5Y cells to study cell adhesion and cell migration. *BMC Research Notes*, *6*(1), 366.

Eckert, R. L., Kaartinen, M. T., Nurminskaya, M., Belkin, A. M., Colak, G., Johnson, G. V. W., & Mehta, K. (2014). Transglutaminase regulation of cell function. *Physiological Reviews*, *94*(2), 383–417.

Eggert, A., Ikegaki, N., Liu, X., Chou, T. T., Lee, V. M., Trojanowski, J. Q., & Brodeur, G. M. (2000). Molecular dissection of TrkA signal transduction pathways mediating differentiation in human neuroblastoma cells. *Oncogene*, *19*(16), 2043–51.

Elli, L., Bergamini, C. M., Bardella, M. T., & Schuppan, D. (2009). Transglutaminases in inflammation and fibrosis of the gastrointestinal tract and the liver. *Digestive and Liver Disease*. *41*(8), 541–50.

Elmore, S. (2007). Apoptosis: A Review of Programmed Cell Death. *Toxicologic Pathology*, *35*(4), 495–516.

Emery, A. C., & Eiden, L. E. (2012). Signaling through the neuropeptide GPCR PAC1 induces neuritogenesis via a single linear cAMP- and ERK-dependent pathway using a novel cAMP sensor. *The FASEB Journal*, *26*(8), 3199–3211.

Encinas, M., Iglesias, M., Liu, Y., Wang, H., Muhaisen, A., Ceña, V., & Comella, J. X. (2000). Sequential treatment of SH-SY5Y cells with retinoic acid and brain-derived neurotrophic factor gives rise to fully differentiated, neurotrophic factor-dependent, human neuron-like cells. *Journal of Neurochemistry*, *75*(3), 991–1003.

Engelman, J. A., Chen, L., Tan, X., Crosby, K., Guimaraes, A. R., Upadhyay, R., & Wong, K. K. (2008). Effective use of PI3K and MEK inhibitors to treat mutant Kras G12D and PIK3CA H1047R murine lung cancers. *Nature Medicine*, *14*(12), 1351–56.

Erhardt, N. M., & Sherwood, N. M. (2004). PACAP maintains cell cycling and inhibits apoptosis in chick neuroblasts. *Molecular and Cellular Endocrinology*, *221*(1–2), 121–134.

Esposito, C. L., D'Alessio, A., de Franciscis, V., & Cerchia, L. (2008). A cross-talk between TrkB and ret tyrosine kinase receptors mediates neuroblastoma cells differentiation. *PLoS ONE*, *3*(2), 1643

Evangelopoulos, M. E., Weis, J., & Krüttgen, A. (2005). Signalling pathways leading to neuroblastoma differentiation after serum withdrawal: HDL blocks neuroblastoma differentiation by inhibition of EGFR. *Oncogene*, *24*(20), 3309–3318.

Facchiano, F., Benfenati, F., Valtorta, F., & Luini, A. (1993). Covalent modification of synapsin I by a tetanus toxin-activated transglutaminase. *Journal of Biological Chemistry*, *268*(7), 4588–4591.

Falluel-Morel, A., Aubert, N., Vaudry, D., Basille, M., Fontaine, M., Fournier, A., & Gonzalez, B. J. (2004). Opposite regulation of the mitochondrial apoptotic pathway by C2-ceramide and PACAP through a MAP-kinase-dependent mechanism in cerebellar granule cells. *Journal of Neurochemistry*, *91*(5), 1231–1243.

Fantacci, C., Capozzi, D., Ferrara, P., & Chiaretti, A. (2013). Neuroprotective Role of Nerve Growth Factor in Hypoxic-Ischemic Brain Injury. *Brain Sci. Brain Sci*, *3*(3), 1013–1022.

Feng, Y., Fratkin, J. D., & LeBlanc, M. H. (2003). Inhibiting caspase-8 after injury reduces hypoxic-ischemic brain injury in the newborn rat. *European Journal of Pharmacology*, *481*(2–3), 169–173.

Feriche, B., Delgado, M., Calderón, C., Lisbona, O., Chirosa, I. J., Miranda, M. T., & Alvarez, J. (2007). The effect of acute moderate hypoxia on accumulated oxygen deficit during intermittent exercise in nonacclimatized men. *Journal of Strength and Conditioning Research*, *21*(2), 413–8.

Fesus, L., & Piacentini, M. (2002). Transglutaminase 2: An enigmatic enzyme with diverse functions. *Trends in Biochemical Sciences*, *27*(10), 534–9.

Fesus, L., & Szondy, Z. (2005). Transglutaminase 2 in the balance of cell death and survival. *FEBS Letters*, *579*(15), 3297–3302.

Filiano, A. J., Bailey, C. D. C., Tucholski, J., Gundemir, S., & Johnson, G. V. W. (2008). Transglutaminase 2 protects against ischemic insult, interacts with HIF1 , and attenuates HIF1 signaling. *The FASEB Journal*, *22*(8), 2662–2675.

Filiano, A. J., Bailey, C. D. C., Tucholski, J., Gundemir, S., & Johnson, G. V. W. (2008). Transglutaminase 2 protects against ischemic insult, interacts with HIF1beta, and attenuates HIF1 signaling. *The FASEB Journal : Official Publication of the Federation of American Societies for Experimental Biology*, *22*(8), 2662–2675.

Filiano, A. J., Tucholski, J., Dolan, P. J., Colak, G., & Johnson, G. V. W. (2010). Transglutaminase 2 protects against ischemic stroke. *Neurobiology of Disease*, *39*(3), 334–343.

Fink, K., Zhu, J., Namura, S., Shimizu-Sasamata, M., Endres, M., Ma, J., & Moskowitz, M. A. (1998). Prolonged therapeutic window for ischemic brain damage caused by delayed caspase activation. *Journal of Cerebral Blood Flow and Metabolism*, *18*(10), 1071–1076.

Flaskos, J. (2012). The developmental neurotoxicity of organophosphorus insecticides: A direct role for the oxon metabolites. *Toxicology Letters*, *209*(1), 86–93.

Folk, J. E. (1983). Mechanism and basis for specificity of transglutaminase-catalyzed ε-(γ-glutamyl) lysine bond formation. *Advances in Enzymology and Related Areas of Molecular Biology*, *54*(83), 1–56.

Freund, K. F., Doshi, K. P., Gaul, S. L., Claremon, D. a, Remy, D. C., Baldwin, J. J.,& Stern, a M. (1994). Transglutaminase inhibition by 2-[(2-oxopropyl)thio]imidazolium derivatives: mechanism of factor XIIIa inactivation. *Biochemistry*, *33*(33), 10109–19.

Friedlander, R. M. (2003). Apoptosis and Caspases in Neurodegenerative Diseases. *New England Journal of Medicine*, *348*(14), 1365–1375.

Galluzzi, L., & Kroemer, G. (2008). Necroptosis: A Specialized Pathway of Programmed Necrosis. *Cell*. *135*(7):1161-3.

Gaudry, C. A., Verderio, E., Aeschlimann, D., Cox, A., Smith, C., & Griffin, M. (1999). Cell surface localization of tissue transglutaminase is dependent on a fibronectin-binding site in its N-terminal β-sandwich domain. *Journal of Biological Chemistry*, *274*(43), 30707–30714.

Gentile, V., Porta, R., Chiosi, E., Spina, A., Valente, F., Pezone, R., Davies, P.J.A., Alaadik, A., & Illiano, G. (1997). TGase/Gah protein expres- sion inhibits adenylate cyclase activity in Balb-C 3T3 fibroblasts mem- branes. *Biochim. Biophys. Acta*, *1357*(1), 115–122.

Ghatei, M. a, Takahashi, K., Suzuki, Y., Gardiner, J., Jones, P. M., & Bloom, S. R. (1993). Distribution, molecular characterization of pituitary adenylate cyclase-activating polypeptide and its precursor encoding messenger RNA in human and rat tissues. *The Journal of Endocrinology*, *136*(1), 159–166.

Gjertsen, B. T., Mellgren, G., Otten, A., Maronde, E., Genieser, H. G., Jastorff, B., Vintermyr, O. K., McKnight, G. S., & Døskeland, S. O. (1995). Novel (Rp)-cAMPS Analogs as Tools for Inhibition of cAMP-kinase in Cell Culture basal cAMP-Kinase activity modulates interleukin-1β action *J. Biol. Chem*. *270*(35), 20599–20607

Gonzalez, B. J., Basille, M., Vaudry, D., Fournier, A., & Vaudry, H. (1997). Pituitary adenylate cyclase-activating polypeptide promotes cell survival and neurite outgrowth in rat cerebellar neuroblasts. *Neuroscience*, *78*(2), 419–430.

Gordon, J., Amini, S., & White, M. K. (2013). General Overview of Neuronal Cell Culture. In *Neuronal Cell Culture: Methods and Protocols 1078*(2013), 1–8.

Gorman, A. M. (2008). Neuronal cell death in neurodegenerative diseases: Recurring themes around protein handling: Apoptosis Review Series. *Journal of Cellular and Molecular Medicine*, *12*(6A), 2263–2280.

Greenberg, C. S., Birckbichler, P. J., & Rice, R. H. (1991). Transglutaminases: multifunctional cross-linking enzymes that stabilize tissues. *FASEB Journal : Official Publication of the Federation of American Societies for Experimental Biology*, *5*(15), 3071–7.

Grenard, P., Bates, M. K., & Aeschlimann, D. (2001). Evolution of transglutaminase genes: Identification of a transglutaminase gene cluster on human chromosome 15q15: Structure of the gene encoding transglutaminase X and a novel gene family member, transglutaminase Z. *Journal of Biological Chemistry*, *276*(35), 33066–33078.

Griffin, M., Casadio, R., & Bergamini, C. M. (2002). Transglutaminases : Nature's biological glues. *Biochem. J*, *368*, 377–396.

Grimes, M. L., Zhou, J., Beattie, E. C., Yuen, E. C., Hall, D. E., Valletta, J. S.,& Mobley, W. C. (1996). Endocytosis of activated TrkA: evidence that nerve growth factor induces formation of signaling endosomes. *The Journal of Neuroscience : The Official Journal of the Society for Neuroscience*, *16*(24), 7950–7964.

Hamanoue, M., Middleton, G., Wyatt, S., Jaffray, E., Hay, R. T., & Davies, A. M. (1999). p75-mediated NF-κB activation enhances the survival response of developing sensory neurons to nerve growth factor. *Mol Cell Neurosci*, *14*, 28–40.

Hammack, S. E., Roman, C. W., Lezak, K. R., Kocho-Shellenberg, M., Grimmig, B., Falls, W. A., & May, V. (2010). Roles for pituitary adenylate cyclase-activating peptide (PACAP) expression and signaling in the bed nucleus of the stria terminalis (BNST) in mediating the behavioral consequences of chronic stress. *Journal of Molecular Neuroscience*, *42*(3), 327–40.

Han, Z., Pantazis P., Lange T. S., Wyche J. H., & Hendrickson E. A. (2000). The staurosporine analog, Ro-31-8220, induces apoptosis independently of its ability to inhibit protein kinase C. *Cell Death Differ*. *7*(6):521–530.

Hang, J., Zemskov, E. A., Lorand, L., & Belkin, A. M. (2005). Identification of a novel recognition sequence for fibronectin within the NH2-terminal β-sandwich domain of tissue transglutaminase. *Journal of Biological Chemistry*, *280*(25), 23675–23683.

Hara, M. R., & Snyder, S. H. (2007). Cell signaling and neuronal death. *Annual Review of Pharmacology and Toxicology*, *47*(July 2006), 117–141.

Harding, T. C., Xue, L., Bienemann, A., Haywood, D., Dickens, M., Tolkovsky, A. M., & Uney, J. B. (2001). Inhibition of JNK by Overexpression of the JNK Binding Domain of JIP-1 Prevents Apoptosis in Sympathetic Neurons. *Journal of Biological Chemistry*, *276*(7), 4531–4534.

Harmar, A. J., Fahrenkrug, J., Gozes, I., Laburthe, M., May, V., Pisegna, J. R., & Said, S. I. (2012). Pharmacology and functions of receptors for vasoactive intestinal peptide and pituitary adenylate cyclase-activating polypeptide: IUPHAR Review 1. *British Journal of Pharmacology*, *166*(1), 4–17.

Haroon, Z. a, Hettasch, J. M., Lai, T. S., Dewhirst, M. W., & Greenberg, C. S. (1999). Tissue transglutaminase is expressed, active, and directly involved in rat dermal wound healing and angiogenesis. *The FASEB Journal : Official Publication of the Federation of American Societies for Experimental Biology*, *13*(13), 1787–1795.

Hasegawa, G., Suwa, M., Ichikawa, Y., Ohtsuka, T., Kumagai, S., Kikuchi, M., & Saito, Y. (2003). A novel function of tissue-type transglutaminase: protein disulphide isomerase. *Biochem. J*, *373*, 793–803.

Hashimoto, H., Shintani, N., & Baba, A. (2006). New insights into the central PACAPergic system from the phenotypes in PACAP- and PACAP receptor-knockout mice. In *Annals of the New York Academy of Sciences 1070*(2006), 75–89.

Hatanaka, H., Nihonmatsu, I., & Tsukui, H. (1988). Nerve growth factor promotes survival of cultured magnocellular cholinergic neurons from nucleus basalis of Meynert in postnatal rats. *Neuroscience Letters*, *90*(1–2), 63–68.

Hausott, B., Kurnaz, I., Gajovic, S., & Klimaschewski, L. (2009). Signaling by neuronal tyrosine kinase receptors: Relevance for development and regeneration. *Anatomical Record*, *292*(12), 1976–1985.

Hefti, F. F., Rosenthal, A., Walicke, P. A., Wyatt, S., Vergara, G., Shelton, D. L., & Davies, A. M. (2006). Novel class of pain drugs based on antagonism of NGF. *Trends in Pharmacological Sciences*, *27*(2), 85–91.

Héraud, C. , Hilairet, S. , Muller, J. , Leterrier, J. & Chadéneau, C. (2004), Neuritogenesis induced by vasoactive intestinal peptide, pituitary adenylate cyclase-activating polypeptide, and peptide histidine methionine in SH-SY5Y cells is associated with regulated expression of cytoskeleton mRNAs and proteins. *J. Neurosci. Res.*, *75*(3): 320–29.

Hetman, M., Kanning, K., Cavanaugh, J. E., & Xia, Z. (1999). Neuroprotection by brain-derived neurotrophic factor is mediated by extracellular signal-regulated kinase and phosphatidylinositol 3-kinase. *J Biol Chem*, *274*(32), 22569–22580.

Hitomi, K., Kitamura, M., Alea, M. P., Ceylan, I., Thomas, V., & El Alaoui, S. (2009). A specific colorimetric assay for measuring transglutaminase 1 and factor XIII activities. *Analytical Biochemistry*, *394*(2), 281–283.

Holtzman, D. M., Sheldon, R. A., Jaffe, W., Cheng, Y., & Ferriero, D. M. (1996). Nerve growth factor protects the neonatal brain against hypoxic-ischemic injury. *Annals of Neurology*, *39*(1), 114–122.

Horton, A., Laramee, G., Wyatt, S., Shih, A., Winslow, J., & Davies, A. M. (1997). NGF Binding to p75 Enhances the Sensitivity of Sensory and Sympathetic Neurons to NGF at Different Stages of Development. *Molecular and Cellular Neuroscience*, *10*(3–4), 162–172.

Hu, Y., Qiao, L., Wang, S., Rong, S., Meuillet, E.J., Berggren, M., Gallegos, A., Powis, G., & Kozikowski, A.P. (2000). 3-(Hydroxymethyl)bearing phosphatidylinositol ether lipid analogues and carbonate surrogates block PI3-K, akt, and cancer cell growth. *J. Med. Chem. 43*(16), 3045–51.

Huang, E. J., & Reichardt, L. F. (2001). Neurotrophins: Roles in Neuronal Development and Function. *Annual Review of Neuroscience*, *24*(1), 677–736.

Ientile, R., Caccamo, D., Marciano, M. C., Currò, M., Mannucci, C., Campisi, A., & Calapai, G. (2004). Transglutaminase activity and transglutaminase mRNA transcripts in gerbil brain ischemia. *Neuroscience Letters*, *363*(2), 173–177.

Iismaa, S. E., Mearns, B. M., Lorand, L., & Graham, R. M. (2009). Transglutaminases and disease: lessons from genetically engineered mouse models and inherited disorders. *Physiological Reviews*, *89*(3), 991–1023.

Im, M. J., Russell, M. a, & Feng, J. F. (1997). Transglutaminase II: a new class of GTP-binding protein with new biological functions. *Cellular Signalling*, *9*(7), 477–82.

Imami K., Sugiyama N., Kyono Y., Tomita M.,& Ishihama Y. (2008) Automated phosphoproteome analysis for cultured cancer cells by two-dimensional nanoLC-MS using a calcined titania/C18 biphasic column. *Anal Sci. 24*(1):161-6.

Ishii, I., & Ui, M. (1994). Retinoic acid-induced gene expression of tissue transglutaminase via protein kinase C-dependent pathway in mouse peritoneal macrophages. *Journal of Biochemistry*, *115*(6), 1197–202.

Jang, G.-Y., Jeon, J.-H., Cho, S.-Y., Shin, D.-M., Kim, C.-W., Jeong, E. M., & Kim, I.-G. (2010). Transglutaminase 2 suppresses apoptosis by modulating caspase 3 and NF-κB activity in hypoxic tumor cells. *Oncogene*, *29*(3), 356–367.

Jaworski, D. M. (2000). Expression of pituitary adenylate cyclase-activating polypeptide (PACAP) and the PACAP-selective receptor in cultured rat astrocytes, human brain tumors, and in response to acute intracranial injury. *Cell and Tissue Research*, *300*(2), 219–30.

Jin, Z., & El-Deiry, W. S. (2005). Overview of cell death signaling pathways. *Cancer Biology and Therapy*, *4*(2), 147–71.

Johnson, K., Hashimoto, S., Lotz, M., Pritzker, K., & Terkeltaub, R. (2001). Interleukin-1 induces pro-mineralizing activity of cartilage tissue transglutaminase and factor XIIIa. *The American Journal of Pathology*, *159*(1), 149–63.

Johnson, G. V, Cox, T. M., Lockhart, J. P., Zinnerman, M. D., Miller, M. L., & Powers, R. E. (1997). Transglutaminase activity is increased in Alzheimer's disease brain. *Brain Research*, *751*(2), 323–329.

Jolivel, V., Basille, M., Aubert, N., de Jouffrey, S., Ancian, P., Le Bigot, J. F., & Vaudry, D. (2009). Distribution and functional characterization of pituitary adenylate cyclase-activating polypeptide receptors in the brain of non-human primates. *Neuroscience*, *160*(2), 434–451.

Joshi, S., Guleria, R., Pan, J., DiPette, D., & Singh, U. S. (2006). Retinoic acid receptors and tissue-transglutaminase mediate short-term effect of retinoic acid on migration and invasion of neuroblastoma SH-SY5Y cells. *Oncogene*, *25*(2), 240–247.

Jóźwiak-Bębenista M, Kowalczyt E, & Nowak JZ (2015). The cyclic AMP effects and neuroprotective activities of PACAP and VIP in cultured astrocytes and neurons exposed to oxygen-glucose deprivation. *Pharmacol. Reports*, *67*(2), 332-338.

Kalani A., Tyagi A., & Tyagi N. (2014) Exosomes: mediators of neurodegeneration, neuroprotection and therapeutics. *Mol. Neurobiol. 49*(1), 590-600.

Kambe, Y., & Miyata, A. (2012). Role of mitochondrial activation in PACAP dependent neurite outgrowth. *Journal of Molecular Neuroscience*, *48*(3), 550–557.

Kang, S.-K., Lee, J.-Y., Chung, T.-W., & Kim, C.-H. (2004). Overexpression of transglutaminase 2 accelerates the erythroid differentiation of human chronic myelogenous leukemia K562 cell line through PI3K/Akt signaling pathway. *FEBS Letters*, *577*(3), 361–366.

Kaplan, D. R., Matsumoto, K., Lucarelli, E., & Thielet, C. J. (1993). Induction of TrkB by retinoic acid mediates biologic responsiveness to BDNF and differentiation of human neuroblastoma cells. *Neuron*, *11*(2), 321–331.

Kaplan, D. R., & Miller, F. D. (2000). Neurotrophin signal transduction in the nervous system. *Current Opinion in Neurobiology*, *10*(3), 381–91.

Katso, R., Okkenhaug, K., Ahmadi, K., White, S., Timms, J., & Waterfield, M. D. (2001). Cellular Function of Phosphoinositide 3-Kinases: Implications for Development, Immunity, Homeostasis, and Cancer. *Annual Review of Cell and Developmental Biology*, *17*(1), 615–75.

Kawamoto, K., & Matsuda, H. (2004). Nerve growth factor and wound healing. In *Progress in Brain Research*, *146*(2004), 369–84.

Kenchappa, R. S., Zampieri, N., Chao, M. V., Barker, P. A., Teng, H. K., Hempstead, B. L., & Carter, B. D. (2006). Ligand-Dependent Cleavage of the P75 Neurotrophin Receptor Is Necessary for NRIF Nuclear Translocation and Apoptosis in Sympathetic Neurons. *Neuron*, *50*(2), 219–32.

Kettenbach A. N., Schweppe D. K., Faherty B. K., Pechenick D., Pletnev A. A., & Gerber S. A. (2011) Quantitative phosphoproteomics identifies substrates and functional modules of Aurora and Polo-like kinase activities in mitotic cells. *Sci Signal. 4*(179):rs5.

Kim, J. K., Choi, J. W., Lim, S., Kwon, O., Seo, J. K., Ryu, S. H., & Suh, P.-G. (2011). Phospholipase C-η1 is activated by intracellular Ca^{2+} mobilization and enhances GPCRs/PLC/Ca^{2+} signaling. *Cellular Signalling*, *23*(26), 1022–29.

Kim, S.-Y., Grant, P., Lee, J.-H., Pant, H. C., & Steinert, P. M. (1999). Differential Expression of Multiple Transglutaminases in Human Brain. *Journal of Biological Chemistry*, *274*(43), 30715–30721.

Kim, S. Y., Grant, P., Lee, J. H., Pant, H. C., & Steinert, P. M. (1999). Differential expression of multiple transglutaminases in human brain. Increased expression and cross-linking by transglutaminases 1 and 2 in Alzheimer's disease. *Journal of Biological Chemistry*, *274*(43), 30715–30721.

Kimura, S., Uchiyama, S., Takahashi, H. E., & Shibuki, K. (1998). cAMP-dependent long-term potentiation of nitric oxide release from cerebellar parallel fibers in rats. *The Journal of Neuroscience : The Official Journal of the Society for Neuroscience*, *18*(21), 8551–8.

Kinkade, C. W., Castillo-Martin, M., Puzio-Kuter, A., Yan, J., Foster, T. H., Gao, H., & Abate-Shen, C. (2008). Targeting AKT/mTOR and ERK MAPK signaling inhibits hormone-refractory prostate cancer in a preclinical mouse model. *Journal of Clinical Investigation*, *118*(9), 3051–64.

Király, R., Cssz, É., Kurtán, T., Antus, S., Szigeti, K., Simon-Vecsei, Z., & Fésüs, L. (2009). Functional significance of five noncanonical Ca^{2+}-binding sites of human transglutaminase 2 characterized by site-directed mutagenesis. *FEBS Journal*, *276*(23), 7083–7096.

Király, R, Demény MA, & Fésös L (2011) Protein transamidation by transglutaminase 2 in cells: a disputed Ca^{2+}-dependent action of a multifunctional protein. *FEBS J. 278*(24), 4717-4739.

Kito, K., Ito, T., & Sakaki, Y. (1997). Fluorescent differential display analysis of gene expression in differentiating neuroblastoma cells. *Gene*, *184*(1), 73–81.

Klebe, R. J. & Ruddle, F. H. (1969). Neuroblastoma: cell culture analysis of a differentiating stem cell system. *Journal of Cell Biology*, *43*(69).

Klöock, C., & Khosla, C. (2012). Regulation of the activities of the mammalian transglutaminase family of enzymes. *Protein Science*, *21*(12), 1781–91.

Knight, R. A., & Verkhratsky, A. (2010). Neurodegenerative diseases: failures in brain connectivity. *Cell Death and Differentiation*, *17*(7), 1069–1070.

Koh, S., Kim S. H., Kwon H., Park Y., Kim K. S., Song C. W., Kim J., Kim M., Yu H., Henkel J. S., & Jung H. K. (2003). Epigallocatechin gallate protects nerve growth factor differentiated PC12 cells from oxidative-radical-stress-induced apoptosis through its effect on phosphoinositide 3-kinase/Akt and glycogen synthase kinase-3. *Molecular Brain Research*, *118*(1–2)72–81.

Kong, L., & Korthuis, R. J. (1997). Melanoma cell adhesion to injured arterioles: Mechanisms of stabilized tethering. *Clinical and Experimental Metastasis*, *15*(4), 426–431.

Koning, F., Schuppan, D., Cerf-Bensussan, N., & Sollid, L. M. (2005). Pathomechanisms in celiac disease. *Best Practice and Research: Clinical Gastroenterology*, *19*(3 SPEC. ISS.), 373–387.

Korecka, J. A., van Kesteren, R. E., Blaas, E., Spitzer, S. O., Kamstra, J. H., Smit, A. B., & Bossers, K. (2013). Phenotypic Characterization of Retinoic Acid Differentiated SH-SY5Y Cells by Transcriptional Profiling. *PLoS ONE*, *8*(5), 63862-79.

Korsching, S., & Thoenen, H. (1983). Quantitative demonstration of the retrograde axonal transport of endogenous nerve growth factor. *Neuroscience Letters*, *39*(1), 1–4.

Kotsakis, P., & Griffin, M. (2007). Tissue transglutaminase in tumour progression: Friend or foe? *Amino Acids*, *33*(2), 373–84.

Krasnikov, B. F., Kim, S. Y., McConoughey, S. J., Ryu, H., Xu, H., Stavrovskaya, I., & Cooper, A. J. L. (2005). Transglutaminase activity Is present in highly purified nonsynaptosomal mouse brain and liver mitochondria. *Biochemistry*, *44*(21), 7830–7843.

Kromer, L. F. (1987). Nerve growth factor treatment after brain injury prevents neuronal death. *Science*, *235*(4785), 214–216.

Kumar, V., & Mahal, B. A. (2012). NGF - The TrkA to successful pain treatment. *Journal of Pain Research*, *5*(2012), 279–87.

Kume, T., Kawato, Y., Osakada, F., Izumi, Y., Katsuki, H., Nakagawa, T., & Akaike, A. (2008). Dibutyryl cyclic AMP induces differentiation of human neuroblastoma SH-SY5Y cells into a noradrenergic phenotype. *Neuroscience Letters*, *443*(3), 199–203.

Kummer, J. L., Rao, P. K., & Heidenreich, K. A. (1997). Apoptosis induced by withdrawal of trophic factors is mediated by p38 mitogen-activated protein kinase. *J Biol Chem*, *272*(33), 20490–20494.

Kuramoto, T., Werrbach-Perez, K., Perez-Polo, J. R., & Haber, B. (1981). Membrane properties of a human neuroblastoma II: Effects of differentiation. *Journal of Neuroscience Research*, *6*(4), 441–449.

Laburthe, M., Couvineau, A., & Tan, V. (2007). Class II G protein-coupled receptors for VIP and PACAP: Structure, models of activation and pharmacology. *Peptides*, *144*(1-3), 91–100.

Laemmli, U. K., Mölbert E., Showe M., & Kellenberger E. (1970). Form-determining function of the genes required for the assembly of the head of bacteriophage T4. *J Mol Biol. 49*(1):99-113.

Lallemend, F., Hadjab, S., Hans, G., Moonen, G., Lefebvre, P. P., & Malgrange, B. (2005). Activation of protein kinase CbetaI constitutes a new neurotrophic pathway for deafferented spiral ganglion neurons. *Journal of Cell Science*, *118*(19), 4511–25.

Lane, N. E., Schnitzer, T. J., Birbara, C. a, Mokhtarani, M., Shelton, D. L., Smith, M. D., & Brown, M.

T. (2010). Tanezumab for the treatment of pain from osteoarthritis of the knee. *The New England Journal of Medicine*, *363*(16), 1521–1531.

Lavenius, E., Gestblom, C., Johansson, I., Nånberg, E., & Påhlman, S. (1995). Transfection of TRK-A into human neuroblastoma cells restores their ability to differentiate in response to nerve growth factor. *Cell Growth & Differentiation : The Molecular Biology Journal of the American Association for Cancer Research*, *6*(6), 727–736.

Le-Niculescu, H., Bonfoco, E., Kasuya, Y., Claret, F. X., Green, D. R., & Karin, M. (1999). Withdrawal of survival factors results in activation of the JNK pathway in neuronal cells leading to Fas ligand induction and cell death. *Molecular and Cellular Biology*, *19*(1), 751–63.

Lee, E. H., & Seo, S. R. (2014). Neuroprotective roles of pituitary adenylate cyclase-activating polypeptide in neurodegenerative diseases. *BMB Reports*, *47*(7), 369–375.

Lee, J., Kim, Y.-S., Choi, D.-H., Bang, M. S., Han, T. R., Joh, T. H., & Kim, S.-Y. (2004). Transglutaminase 2 induces nuclear factor-kappaB activation via a novel pathway in BV-2 microglia. *The Journal of Biological Chemistry*, *279*(51), 53725–35.

Lee, J. M., Grabb, M. C., Zipfel, G. J., & Choi, D. W. (2000). Brain tissue responses to ischemia. *The Journal of Clinical Investigation*, *106*(6), 723–31.

Lee K. N., Arnold S. A., Birckbichler P. J., Patterson M. K Jr, Fraij B. M., Takeuchi Y., & Carter H. A. (1993) Site-directed mutagenesis of human tissue transglutaminase: Cys-277 is essential for transglutaminase activity but not for GTPase activity. *Biochim Biophys Acta. 1202*(1):1-6.

Lee, K. H., Lee, N., Lim, S., Jung, H., Ko, Y. G., Park, H. Y., & Hwang, K. C. (2003). Calreticulin inhibits the MEK1,2-ERK1,2 pathway in α1-adrenergic receptor/Gh-stimulated hypertrophy of neonatal rat cardiomyocytes. *Journal of Steroid Biochemistry and Molecular Biology*, *84*(1), 101–107.

Lee, K. N., Birckbichler, P. J., & Patterson, M. K. (1989). GTP hydrolysis by guinea pig liver transglutaminase. *Biochemical and Biophysical Research Communications*, *162*(3), 1370–1375.

Lelièvre, V., Pineau, N., Du, J., Wen, C. H., Nguyen, T., Janet, T., & Waschek, J. A. (1998). Differential effects of peptide histidine isoleucine (PHI) and related peptides on stimulation and suppression of neuroblastoma cell proliferation. A novel VIP-independent action of PHI via MAP kinase. *Journal of Biological Chemistry*, *273*(31), 19685–90.

Lemmon, M. A., & Schlessinger J. (2010). Cell signaling by receptor tyrosine kinases. *Cell*, *141*(7), 1117–34.

Lerner, E. A., Ribeiro, J. M. C., Nelson, R. J., & Lerner, M. R. (1991). Isolation of maxadilan, a potent vasodilatory peptide from the salivary glands of the sand fly Lutzomyia longipalpis. *Journal of Biological Chemistry*, *266*(17), 11234–11236.

Lesort, M., Tucholski, J., Ml, M., & Gvw, J. (2000). Tissue transglutaminase: a possible role in neurodegenerative diseases. *Progress in Neurobiology*, *61*(5), 439–463.

Levi-Montalcini, R., & Hamburger, V. (1951). Selective growth stimulating effects of mouse sarcoma on the sensory and sympathetic nervous system of the chick embryo. *Journal of Experimental Zoology*, *116*(2), 321–361.

Li, B., Antonyak, M. A., Druso, J. E., Cheng, L., Nikitin, A. Y., & Cerione, R. A. (2010). EGF potentiated oncogenesis requires a tissue transglutaminase-dependent signaling pathway leading to Src activation. *Proceedings of the National Academy of Sciences*, *107*(4), 1408–1413.

Li, M. (2000). Functional Role of Caspase-1 and Caspase-3 in an ALS Transgenic Mouse Model. *Science*, *288*(5464), 335–339.

Li, X. H., Long, D. X., Li, W., & Wu, Y. J. (2007). Different mechanisms of lysophosphatidylcholine-induced Ca^{2+}mobilization in N2a mouse and SH-SY5Y human neuroblastoma cells. *Neuroscience Letters*, *424*(1), 22–26.

Li, Y., Liu, L., Barger, S. W., & Griffin, W. S. (2003). Interleukin-1 mediates pathological effects of microglia on tau phosphorylation and on synaptophysin synthesis in cortical neurons through a p38-MAPK pathway. *J Neurosci*, *23*(5), 1605–1611.

Lilley, G. R., Skill, J., Griffin, M., Bonner, P. L.. (1998) Detection of Ca^{2+}-dependent transglutaminase activity in root and leaf tissue of monocotyledonous and dicotyledonous plants. *Plant Physiol. 117*(3):1115–23.

Lloyd, E. D. & Wooten, M. W. (1992), $pp^{42/44}$MAP Kinase Is a Component of the Neurogenic Pathway Utilized by Nerve Growth Factor in PC12 Cells. *Journal of Neurochemistry, 59* 1099–109.

Lizcano, J. M., Morrice, N., & Cohen, P. (2000). Regulation of BAD by cAMP-dependent protein kinase is mediated via phosphorylation of a novel site, Ser155. *The Biochemical Journal*, *349*(2), 547–57.

Lomb, D. J., Desouza, L. A., Franklin, J. L., & Freeman, R. S. (2009). Prolyl Hydroxylase Inhibitors Depend on Extracellular Glucose and Hypoxia-Inducible Factor (HIF)-2 to Inhibit Cell Death Caused by Nerve Growth Factor (NGF) Deprivation: Evidence that HIF-2 Has a Role in NGF-Promoted Survival of Sympathetic Neurons. *Molecular Pharmacology*, *75*(5), 1198–1209.

Lopes, F. M., Schröder, R., Júnior, M. L. C. da F., Zanotto-Filho, A., Müller, C. B., Pires, A. S., & Klamt, F. (2010). Comparison between proliferative and neuron-like SH-SY5Y cells as an in vitro model for Parkinson disease studies. *Brain Research, 1337*(6), 85–94.

Lorand, L., & Graham, R. M. (2003). Transglutaminases: crosslinking enzymes with pleiotropic functions. *Nature Reviews Molecular Cell Biology*, *4*(2), 140–156.

Lutz, E. M., Ronaldson, E., Shaw, P., Johnson, M. S., Holland, P. J., & Mitchell, R. (2006). Characterization of novel splice variants of the PAC1 receptor in human neuroblastoma cells: Consequences for signaling by VIP and PACAP. *Molecular and Cellular Neuroscience*, *31*(2), 193–209.

Lutz-Bucher B., Monnier D., & Koch B. (1996). Evidence for the presence of receptors for pituitary adenylate cyclase-activating polypeptide in the neurohypophysis that are positively coupled to cyclic AMP formation and neurohypophyseal hormone secretion. *Neuroendocrinology 64*(2):153–161.

Maccioni, R. B., & Seeds, N. W. (1986). Transglutaminase and neuronal differentiation. *Molecular and Cellular Biochemistry*, *69*(2), 161–68.

Mahura, I. S. (2003). Cerebral ischemia-hypoxia and biophysical mechanisms of neurodegeneration and neuroprotection effects. *Fiziol Zh*, *49*(2), 7–12.

Malorni, W., Farrace, M. G., Matarrese, P., Tinari, A., Ciarlo, L., Mousavi-Shafaei, P., & Piacentini, M. (2009). The adenine nucleotide translocator 1 acts as a type 2 transglutaminase substrate: implications for mitochondrial-dependent apoptosis. *Cell Death and Differentiation*, *16*(11), 1480–1492.

Manabe, T., Tatsumi, K., Inoue, M., Matsuyoshi, H., Makinodan, M., Yokoyama, S., & Wanaka, A. (2005). L3/Lhx8 is involved in the determination of cholinergic or GABAergic cell fate. *Journal of Neurochemistry*, *94*(3), 723–730.

Manecka, D. L., Mahmood, S. F., Grumolato, L., Lihrmann, I., & Anouar, Y. (2013). Pituitary Adenylate Cyclase-activating Polypeptide (PACAP) Promotes Both Survival and Neuritogenesis in PC12 Cells through Activation of Nuclear Factor-kB (NF-kB) Pathway. *The Journal of Biological Chemistry*, *288*(21), 14936–48.

Mann, A. P., Verma, A., Sethi, G., Manavathi, B., Wang, H., Fok, J. Y., & Mehta, K. (2006). Overexpression of tissue transglutaminase leads to constitutive activation of nuclear factor-kappaB in cancer cells: delineation of a novel pathway. *Cancer Res*, *66*(17), 8788–8795.

Mao, A. J., Bechberger, J., Lidington, D., Galipeau, J., Laird, D. W., & Naus, C. C. (2000). Neuronal differentiation and growth control of neuro-2a cells after retroviral gene delivery of connexin43. *The Journal of Biological Chemistry*, *275*(44), 34407–34414.

María Frade, J., Rodríguez-Tébar, A., & Barde, Y.-A. (1996). Induction of cell death by endogenous nerve growth factor through its p75 receptor. *Nature*, *383*(6596), 166–168.

Martinez, J., Chalupowicz, D. G., Roush, R. K., Sheth, A., & Barsigian, C. (1994). Transglutaminase-Mediated Processing of Fibronectin by Endothelial Cell Monolayers. *Biochemistry*, *33*(9), 2538–2545.

Masmoudi-Kouki, O., Douiri, S., Hamdi, Y., Kaddour, H., Bahdoudi, S., Vaudry, D., & Amri, M. (2011). Pituitary adenylate cyclase-activating polypeptide protects astroglial cells against oxidative stress-induced apoptosis. *Journal of Neurochemistry*, *117*(3), 403–411.

Mastroberardino, P. G., Iannicola, C., Nardacci, R., Bernassola, F., De Laurenzi, V., Melino, G., & Piacentini, M. (2002). "Tissue" transglutaminase ablation reduces neuronal death and prolongs survival in a mouse model of Huntington's disease. *Cell Death and Differentiation*, *9*(9), 873–80.

Matysiak-Budnik, T., Moura, I. C., Arcos-Fajardo, M., Lebreton, C., Ménard, S., Candalh, C., & Heyman, M. (2008). Secretory IgA mediates retrotranscytosis of intact gliadin peptides via the transferrin receptor in celiac disease. *The Journal of Experimental Medicine*, *205*(1), 143–154.

May, V., Buttolph, T. R., Girard, B. M., Clason, T. A., & Parsons, R. L. (2014). PACAP-induced ERK activation in HEK cells expressing PAC1 receptors involves both receptor internalization and PKC signaling. *AJP: Cell Physiology*, *306*(11), 1068–1079.

May, V., Lutz, E., MacKenzie, C., Schutz, K. C., Dozark, K., & Braas, K. M. (2010). Pituitary Adenylate Cyclase-activating Polypeptide (PACAP)/PAC1HOP1 Receptor Activation Coordinates Multiple Neurotrophic Signaling Pathways: Akt activation through phosphatidylinositol 3-kinase and vesicle endocytosis for neuronal survival. *Journal of Biological Chemistry*, *285*(13), 9749–9761.

McConoughey, S. J., Basso, M., Niatsetskaya, Z. V., Sleiman, S. F., Smirnova, N. A., Langley, B. C., & Ratan, R. R. (2010). Inhibition of transglutaminase 2 mitigates transcriptional dysregulation in models of Huntington's disease. *EMBO Molecular Medicine*, *2*(9), 349–370.

McCulloch, D. a, Lutz, E. M., Johnson, M. S., Robertson, D. N., MacKenzie, C. J., Holland, P. J., & Mitchell, R. (2001). ADP-ribosylation factor-dependent phospholipase D activation by VPAC receptors and a PAC(1) receptor splice variant. *Molecular Pharmacology*, *59*(6), 1523–32.

Mehta, K., Fok, J. Y., & Mangala, L. S. (2006). Tissue transglutaminase: from biological glue to cell survival cues. *Frontiers in Bioscience : A Journal and Virtual Library*, *11*(3), 173–185.

Mehta, K., & Han, A. (2011). Tissue Transglutaminase (TG2)-induced inflammation in initiation, progression, and pathogenesis of pancreatic cancer. *Cancers*, *3*(1), 897–912.

Meloni, B. P. (2017). Pathophysiology and Neuroprotective Strategies in Hypoxic-Ischemic Brain Injury and Stroke. *Brain Sciences*, *7*(8), 11–14.

Mendoza, M. C., Er, E. E., & Blenis, J. (2011). The Ras-ERK and PI3K-mTOR pathways: Cross-talk and compensation. *Trends in Biochemical Sciences*, *36*(6), 320–8.

Mhaouty-Kodja, S. (2004). Ghα/tissue transglutaminase 2: An emerging G protein in signal transduction. *Biology of the Cell*, *96*(5), 363–367.

Mian, S., El Alaoui, S., Lawry, J., Gentile, V., Davies, P. J. A., & Griffin, M. (1995). The importance of the GTP-binding protein tissue transglutaminase in the regulation of cell cycle progression. *FEBS Letters*, *370*(1–2), 27–31.

Milakovic, T., Tucholski, J., McCoy, E., & Johnson, G. V. W. (2004). Intracellular Localization and Activity State of Tissue Transglutaminase Differentially Impacts Cell Death. *Journal of Biological Chemistry*, *279*(10), 8715–8722.

Milligan, G., & Kostenis, E. (2006). Heterotrimeric G-proteins: A short history. *British Journal of Pharmacology*, *147*(1), 64–55.

Min B., Kwon Y. C., Choe K. M., & Chung K. C. (2015) PINK1 phosphorylates transglutaminase 2 and blocks its proteasomal degradation. *J Neurosci Res. 93*(5):722-35.

Mishra, S., Melino, G., & Murphy, L. J. (2007). Transglutaminase 2 kinase activity facilitates protein kinase A-induced phosphorylation of retinoblastoma protein. *Journal of Biological Chemistry*, *282*(25), 18108–18115.

Mishra, S., & Murphy, L. J. (2004). Tissue transglutaminase has intrinsic kinase activity. Identification of transglutaminase 2 as an insulin-like growth factor-binding protein-3 kinase. *Journal of Biological Chemistry*, *279*(23), 23863–23868.

Mishra, S., & Murphy, L. J. (2006). Phosphorylation of transglutaminase 2 by PKA at Ser216 creates 14-3-3 binding sites. *Biochemical and Biophysical Research Communications*, *347*(4), 1166–1170.

Miura, A., Kambe, Y., Inoue, K., Tatsukawa, H., Kurihara, T., Griffin, M., & Miyata, A. (2013). Pituitary adenylate cyclase-activating polypeptide type 1 receptor (PAC1) gene is suppressed by transglutaminase 2 activation. *The Journal of Biological Chemistry*, *288*(45), 32720–30.

Miyata, A., Arimura, A., Dahl, R. R., Minamino, N., Uehara, A., Jiang, L., & Coy, D. H. (1989). Isolation of a novel 38 residue-hypothalamic polypeptide which stimulates adenylate cyclase in pituitary cells. *Biochemical and Biophysical Research Communications*, *164*(1), 567–574.

Mnich, K., Carleton, L. A., Kavanagh, E. T., Doyle, K. M., Samali, A., & Gorman, A. M. (2014). Nerve growth factor-mediated inhibition of apoptosis post-caspase activation is due to removal of active caspase-3 in a lysosome-dependent manner. *Cell Death and Disease*, *5*(5),1202–15.

Moelling, K., Schad, K., Bosse, M., Zimmermann, S., & Schweneker, M. (2002). Regulation of Raf-Akt cross-talk. *Journal of Biological Chemistry*, *277*(34),31099–106.

Monaghan, T. K., MacKenzie, C. J., Plevin, R., & Lutz, E. M. (2008). PACAP-38 induces neuronal differentiation of human SH-SY5Y neuroblastoma cells via cAMP-mediated activation of ERK and p38 MAP kinases. *Journal of Neurochemistry*, *104*(1), 74–88.

Mookherjee, P., Quintanilla, R., Roh, M. S., Zmijewska, A. A., Jope, R. S., & Johnson, G. V. W. (2007). Mitochondrial-targeted active Akt protects SH-SY5Y neuroblastoma cells from staurosporine-induced apoptotic cell death. *Journal of Cellular Biochemistry*, *102*(1), 196–210.

Morooka, T., & Nishida, E. (1998). Requirement of p38 mitogen-activated protein kinase for neuronal differentiation in PC12 cells. *The Journal of Biological Chemistry*, *273*(38), 24285–24288.

Mosmann, T. (1983). Rapid colorimetric assay for cellular growth and survival: application to proliferation and cytotoxicity assays. *J Immunol Methods*, *65*(1-2), 55-63.

Murad, F. (2011). Nitric oxide: the coming of the second messenger. *Rambam Maimonides Medical Journal*, *2*(2), 38–44.

Murillo, J. R., Goto-Silva, L., Sánchez, A., Nogueira, F. C. S., Domont, G. B., & Junqueira, M. (2017). Quantitative proteomic analysis identifies proteins and pathways related to neuronal development in differentiated SH-SY5Y neuroblastoma cells. *EuPA Open Proteomics*, *16*(2017), 1–11.

Nakaoka, H., Perez, D. M., Baek, K. J., Das, T., Husain, A., Misono, K., & Graham, R. M. (1994). Gh: a GTP-binding protein with transglutaminase activity and receptor signaling function. *Science (New York, N.Y.)*, *264*(5165), 1593–1596.

Nanda, N., Iismaa, S. E., Owens, W. A., Husain, A., Mackay, F., & Graham, R. M. (2001). Targeted Inactivation of Gh/Tissue Transglutaminase II. *Journal of Biological Chemistry*, *276*(23), 20673–78.

Napoli, I., Noon, L. A., Ribeiro, S., Kerai, A. P., Parrinello, S., Rosenberg, L. H., & Lloyd, A. C. (2012). A Central Role for the ERK-Signaling Pathway in Controlling Schwann Cell Plasticity and Peripheral Nerve Regeneration In Vivo. *Neuron*, *73*(4), 729–42.

Neary, J. T. (2005). Protein kinase signaling cascades in CNS trauma. *IUBMB Life*, *57*(11), 711–8.

Nguyen, T. L., Kim, C. K., Cho, J.-H., Lee, K.-H., & Ahn, J.-Y. (2010). Neuroprotection signaling pathway of nerve growth factor and brain-derived neurotrophic factor against staurosporine induced apoptosis in hippocampal H19-7 cells. *Experimental and molecular medicine*, *42*(8), 583–595.

Nikodijevic B., Nikodijevic O.,Yu M. Y., Pollard H., & Guroff G. (1975). The effect of nerve growth factor on cycle AMP levels in superior cerival ganglia of the rat. *Proceedings of the National Academy of Sciences*, *72* (12) 4769–71.

Nicole, P., Lins, L., Rouyer-Fessard, C., Drouot, C., Fulcrand, P., Thomas, A., & Laburthe, M. (2000). Identification of key residues for interaction of vasoactive intestinal peptide with human VPAC1 and VPAC2 receptors and development of a highly selective VPAC1 receptor agonist: Alanine scanning and molecular modeling of the peptide. *Journal of Biological Chemistry*, *275*(31), 24003–24012.

Nikoletopoulou, V., Markaki, M., Palikaras, K., & Tavernarakis, N. (2013). Crosstalk between apoptosis, necrosis and autophagy. *Biochimica et Biophysica Acta - Molecular Cell Research*, *1833*(12), 3448–59.

Northington, F. J., Chavez-Valdez, R., & Martin, L. J. (2011). Neuronal cell death in neonatal hypoxia-ischemia. *Annals of Neurology*, *69*(5), 743–758.

Nozaki, K., Nishimura, M., & Hashimoto, N. (2001). Mitogen-activated protein kinases and cerebral ischemia. *Molecular Neurobiology*, *23*(1), 1–19.

Nurminskaya, M. V., & Belkin, A. M. (2013). Cellular functions of tissue transglutaminase. *International Review of Cell and Molecular Biology*, *294*(2012), 1–9.

Odii, B. O., & Coussons, P. (2014). Biological functionalities of transglutaminase 2 and the possibility of its compensation by other members of the transglutaminase family. *The Scientific World Journal*, *2014*(3), 1–13.

Oe, T., Sasayama, T., Nagashima, T., Muramoto, M., Yamazaki, T., Morikawa, N., & Kita, Y. (2005). Differences in gene expression profile among SH-SY5Y neuroblastoma subclones with different neurite outgrowth responses to nerve growth factor. *Journal of Neurochemistry*, *94*(5), 1264–1276.

Ogata, K., Shintani, N., Hayata-Takano, A., Kamo, T., Higashi, S., Seiriki, K., & Hashimoto, H. (2015). PACAP enhances axon outgrowth in cultured hippocampal neurons to a comparable extent as BDNF. *PLoS ONE*, *10*(3), 1–13.

Oh, J. E., Bae, G. U., Yang, Y. J., Yi, M. J., Lee, H. J., Kim, B. G., & Kang, J. S. (2009). Cdo promotes neuronal differentiation via activation of the p38 mitogen-activated protein kinase pathway. *FASEB Journal*, *23*(7), 2088–2099.

Ohnou, T., Yokai, M., Kurihara, T., Hasegawa-Moriyama, M., Shimizu, T., Inoue, K., & Miyata, A. (2016). Pituitary adenylate cyclase-activating polypeptide type 1 receptor signaling evokes long-lasting nociceptive behaviors through the activation of spinal astrocytes in mice. *Journal of*

Pharmacological Sciences, *130*(4), 194–203.

Oliveira, S. L. B., Pillat, M. M., Cheffer, A., Lameu, C., Schwindt, T. T., & Ulrich, H. (2013). Functions of neurotrophins and growth factors in neurogenesis and brain repair. *Cytometry Part A*, *83*(1), 76–89.

Orrenius, S., Zhivotovsky, B., & Nicotera, P. (2003). Regulation of cell death: The calcium-apoptosis link. *Nature Reviews Molecular Cell Biology*, *4*(7), 552–65.

Otten, U., Ehrhard, P., & Peck, R. (1989). Nerve growth factor induces growth and differentiation of human B lymphocytes. *Proceedings of the National Academy of Sciences*, *86*(24), 10059–10063.

Pahlman, S., Ruusala, A. I., Abrahamsson, L., Mattsson, M. E., & Esscher, T. (1984). Retinoic acid-induced differentiation of cultured human neuroblastoma cells: a comparison with phorbolester-induced differentiation. *Cell Differ*, *14*(2), 135–144.

Pandiella-Alonso A.,Malgaroli A.,Vicentini L. M. & Meldolesi J. (1986). Early rise of cytosolic Ca^{2+} induced by NGF in PC12 and chromaffin cells, *FEBS Letters*, *208*(1),48–51.

Patapoutian, A., & Reichardt, L. F. (2001). Trk receptors: Mediators of neurotrophin action. *Current Opinion in Neurobiology*, *11*(3), 272–80.

Paulmann, N., Grohmann, M., Voigt, J. P., Bert, B., Vowinckel, J., Bader, M., & Walther, D. J. (2009). Intracellular serotonin modulates insulin secretion from pancreatic β-cells by protein serotonylation. *PLoS Biology*, *7*(10), 1–10.

Payet, M. D., Bilodeau, L., Breault, L., Fournier, A., Yon, L., Vaudry, H., & Gallo-Payet, N. (2003). PAC1 receptor activation by PACAP-38 mediates Ca^{2+} release from a cAMP-dependent pool in human fetal adrenal gland chromaffin cells. *The Journal of Biological Chemistry*, *278*(3), 1663–70.

Penumatsa K., Abualkhair S., Wei L., Warburton R., Preston I., Hill N., Watts S., Fanburg B., & Toksoz D. (2014). Tissue transglutaminase promotes serotonin-induced AKT signaling and mitogenesis in pulmonary vascular smooth muscle cells. *Cellular Signalling*, *26*(12) 2818–25.

Perron, J. C. & Bixby, J. L. (1999). Distinct neurite outgrowth signaling pathways converge on ERK activation. *Mol Cell Neurosci, 13*(5), 362-78.

Perry MJ, Mahoney SA, & Haynes LW. (1995). Transglutaminase C in cerebellar granule neurons: regulation and localization of substrate cross-linking. *Neuroscience*. *65*(4):1063-76.

Philpott, K. L., McCarthy, M. J., Klippel, A., & Rubin, L. L. (1997). Activated phosphatidylinositol 3-kinase and Akt kinase promote survival of superior cervical neurons. *J Cell Biol*, *139*(3), 809–815.

Picarelli, A., Di Tola, M., Sabbatella, L., Vetrano, S., Anania, M. C., Spadaro, A., & Taccari, E. (2003). Anti-Tissue Transglutaminase Antibodies in Arthritic Patients: A Disease-specific Finding. *Clinical Chemistry*, *49*(12), 2091–2094.

Pierchala, B. A., Ahrens, R. C., Paden, A. J., & Johnson, E. M. (2004). Nerve growth factor promotes the survival of sympathetic neurons through the cooperative function of the protein kinase C and phosphatidylinositol 3-kinase pathways. *Journal of Biological Chemistry*, *279*(27), 27986–27993.

Pinkas DM, Strop P, Brunger AT, & Khosla C (2007). Transglutaminase 2 Undergoes a Large Conformational Change upon Activation . *PLOS Biology 5*(12): e327.

Pirou, C., Montazer-Torbati, F., Jah, N., Delmas, E., Lasbleiz, C., Mignotte, B., & Renaud, F. (2017). FGF1 protects neuroblastoma SH-SY5Y cells from p53-dependent apoptosis through an intracrine pathway regulated by FGF1 phosphorylation. *Cell Death and Disease*, *8*(8), 1–10.

Pisano, J. J., Finlayson, J. S., & Peyton, M. P. (1969). Chemical and Enzymic Detection of Protein Cross-Links. Measurement of ϵ-(γ-Glutamyl)Lysine in Fibrin Polymerized by Factor Iii. *Biochemistry*, *8*(3), 871–876.

Pisegna, J., & Wanks, S. (1996). Cloning and Characterization of the Signal Transduction of Four Splice Variants of the Human Pituitary Adenylate Cyclase Activating Polypeptide Receptor. *The Journal of Biological Chemistry*, *271*(29), 17267–17274.

Pozuelo-Rubio, M., Leslie, N. R., Murphy, J., & MacKintosh, C. (2010). Mechanism of Activation of PKB/Akt by the Protein Phosphatase Inhibitor Calyculin A. *Cell Biochemistry and Biophysics*, *58*(3), 147–156.

Presgraves, S. P., Ahmed, T., Borwege, S., & Joyce, J. N. (2004). Terminally differentiated SH-SY5Y cells provide a model system for studying neuroprotective effects of dopamine agonists. *Neurotoxicity Research*, *5*(8), 579–598.

Price, R. D., Yamaji, T., & Matsuoka, N. (2003). FK506 potentiates NGF-induced neurite outgrowth via the Ras/Raf/MAP kinase pathway. *British Journal of Pharmacology*, *140*(5), 825–9.

Pun, P. B. L., Lu, J., & Moochhala, S. (2009). Involvement of ROS in BBB dysfunction. *Free Radical Research*, *43*(4), 348–364.

Putney, J. W., & Tomita, T. (2011). Phospholipase C Signaling and Calcium Influx. *Advances in Biological Regulation*, *52*(1), 152–164.

Qian, J., Ramroop, K., McLeod, A., Bandari, P., Livingston, D. H., Harrison, J. S., & Rameshwar, P. (2001). Induction of hypoxia-inducible factor-1alpha and activation of caspase-3 in hypoxia-reoxygenated bone marrow stroma is negatively regulated by the delayed production of substance P. *Journal of Immunology (Baltimore, Md : 1950)*, *167*(8), 4600–4608.

Qiao, J., Paul, P., Lee, S., Qiao, L., Josifi, E., Tiao, J. R., & Chung, D. H. (2012). PI3K/AKT and ERK regulate retinoic acid-induced neuroblastoma cellular differentiation. *Biochemical and Biophysical Research Communications*, *424*(3), 421–6.

Quan, G., Choi, J. Y., Lee, D. S., & Lee, S. C. (2005). TGF-b1 up-regulates transglutaminase two and fibronectin in dermal fibroblasts: A possible mechanism for the stabilization of tissue inflammation. *Archives of Dermatological Research*, *297*(2), 84–90.

Radio, N. M., & Mundy, W. R. (2008). Developmental neurotoxicity testing in vitro: Models for assessing chemical effects on neurite outgrowth. *NeuroToxicology*, *297*(3),361–76.

Ramos-A`lvarez, I., Mantey, S. A., Nakamura, T., Nuche-Berenguer, B., Moreno, P., Moody, T. W., & Jensen, R. T. (2015). A structure-function study of PACAP using conformationally restricted analogs: Identification of PAC1 receptor-selective PACAP agonists. *Peptides*, *66*(4), 26–42.

Ravni, A., Bourgault, S., Lebon, A., Chan, P., Galas, L., Fournier, A., & Vaudry, D. (2006). The neurotrophic effects of PACAP in PC12 cells: Control by multiple transduction pathways. *Journal of Neurochemistry*, *98*(2), 321–9.

Reglodi, D., Fábián, Z., Tamás, A., Lubics, A., Szeberényi, J., Alexy, T., & Lengvári, I. (2004). Effects of PACAP on in vitro and in vivo neuronal cell death, platelet aggregation, and production of reactive oxygen radicals. *Regulatory Peptides*, *123*(1–3), 51–59.

Reglodi, D., Somogyvari-vigh, A., Vigh, S., Maderdrut, J. L., & Arimura, A. (2000). Neuroprotective Effects of PACAP38 in a Rat Model of Transient Focal Ischemia under Various Experimental Conditions. *Biomedical Research*, *31*(2000), 1411–17.

Reglodi, D., Tamás, A., Somogyvári-Vigh, A., Szántó, Z., Kertes, E., Lénárd, L., & Lengvári, I. (2002). Effects of pretreatment with PACAP on the infarct size and functional outcome in rat permanent focal cerebral ischemia. *Peptides*, *23*(12), 2227–34.

Reichardt, L. F. (2006). Neurotrophin-regulated signalling pathways. *Philosophical Transactions of the Royal Society B: Biological Sciences*, *361*(1473), 1545–1564.

Reichelt, K. L., & Poulsen, E. (1992). gamma-Glutamylaminotransferase and transglutaminase in subcellular fractions of rat cortex and in cultured astrocytes. *J.Neurochem.*, *59*(2), 500–4.

Rice, D., & Barone, S. (2000). Critical periods of vulnerability for the developing nervous system: Evidence from humans and animal models. *Environmental Health Perspectives*, *108*(3), 511–33.

Riedl, S. J., & Shi, Y. (2004). Molecular mechanisms of caspase regulation during apoptosis. *Nature Reviews Molecular Cell Biology*, *5*(11), 897–907.

Rikova, K., Guo, A., Zeng, Q., Possemato, A., Yu, J., Haack, H., & Comb, M. J. (2007). Global Survey of Phosphotyrosine Signaling Identifies Oncogenic Kinases in Lung Cancer. *Cell*, *131*(6), 1190–1203.

Robberecht P., Gourlet P., De Neef P., Woussen-Colle M. C., Vandermeers-Piret M. C., Vandermeers A., & Christophe J. (1992). Structural requirements for the occupancy of pituitary adenylate cyclase activating polypeptide (PACAP) receptors and adenylate cyclase activation in human neuroblastoma NB-OK-1 cell membranes. Discovery of PACAP(6-38) as a potent antagonist. *Eur. J. Biochem. 207*(1), 239-246.

Roskoski, R. (2012). ERK1/2 MAP kinases: Structure, function, and regulation. *Pharmacological Research*, *66*(2), 105–143.

Ross, R. A., Spengler, B. A., & Biedler, J. L. (1983). Coordinate Morphological and Biochemical Interconversion of Human Neuroblastoma Cells. *Journal of the National Cancer Institute*, *71*(4), 741–747.

Ruan, Q., Tucholski, J., Gundemir, S., & Johnson Voll, G. V. W. (2008). The Differential Effects of R580A Mutation on Transamidation and GTP Binding Activity of Rat and Human Type 2 Transglutaminase. *International Journal of Clinical and Experimental Medicine*, *1*(3), 248–59.

Ruberti, F., Capsoni, S., Comparini, A, Di Daniel, E., Franzot, J., Gonfloni, S., & Cattaneo, A. (2000). Phenotypic knockout of nerve growth factor in adult transgenic mice reveals severe deficits in basal forebrain cholinergic neurons, cell death in the spleen, and skeletal muscle dystrophy. *The Journal of Neuroscience : Journal of the Society for Neuroscience*, *20*(7), 2589–601.

Sahu, U., Sidhar, H., Ghate, P. S., Advirao, G. M., Raghavan, S. C., & Giri, R. K. (2013). A Novel Anticancer Agent, 8-Methoxypyrimido[4′,5′:4,5]thieno(2,3-b) Quinoline-4(3H)-One Induces Neuro 2a Neuroblastoma Cell Death through p53-Dependent, Caspase-Dependent and -Independent Apoptotic Pathways. *PLoS ONE*, *8*(6), 1–18.

Saiki, R., Park, H., Ishii, I., Yoshida, M., Nishimura, K., & Toida, T. (2011). Brain infarction correlates more closely with acrolein than with reactive oxygen species. *Biochem Biophys Res Commun 2011; 404*(4),1044–49.

Saito, A., Hayashi, T., Okuno, S., Ferrand-Drake, M., & Chan, P. H. (2003). Overexpression of copper/zinc superoxide dismutase in transgenic mice protects against neuronal cell death after transient focal ischemia by blocking activation of the Bad cell death signaling pathway. *J Neurosci*, *23*(5), 1710–1718.

Sajithlal, G., Huttunen, H., Rauvala, H., & Münch, G. (2002). Receptor for advanced glycation end products plays a more important role in cellular survival than in neurite outgrowth during retinoic acid-induced differentiation of neuroblastoma cells. *Journal of Biological Chemistry*, *277*(9), 6888–6897.

Salinas, M., Diaz, R., Abraham, N. G., De Galarreta, C. M. R., & Cuadrado, A. (2003). Nerve growth factor protects against 6-hydroxydopamine-induced oxidative stress by increasing expression of heme oxygenase-1 in a phosphatidylinositol 3-kinase-dependent manner. *Journal of Biological*

Chemistry, *278*(16), 13898–13904.

Sarang, Z., Molnár, P., Németh, T., Gomba, S., Kardon, T., Melino, G., & Szondy, Z. (2005). Tissue transglutaminase (TG2) acting as G protein protects hepatocytes against Fas-mediated cell death in mice. *Hepatology*, *42*(3), 578–587.

Sarkar, N. K., Clarke, D. D., & Waelsch, H. (1957). An enzymically catalyzed incorporation of amines into proteins. *Biochimica et Biophysica Acta*, *25*(2), 451–52.

Satpathy, M., Cao, L., Pincheira, R., Emerson, R., Bigsby, R., Nakshatri, H., & Matei, D. (2007). Enhanced peritoneal ovarian tumor dissemination by tissue transglutaminase. *Cancer Research*, *67*(15), 7194–7202.

Schaertl, S., Prime, M., Wityak, J., Dominguez, C., Munoz-Sanjuan, I., Pacifici, R. E., & Macdonald, D. (2010). A profiling platform for the characterization of transglutaminase 2 (TG2) inhibitors. *Journal of Biomolecular Screening : The Official Journal of the Society for Biomolecular Screening*, *15*(5), 478–487.

Schramm, A., Schulte, J. H., Astrahantseff, K., Apostolov, O., Van Limpt, V., Sieverts, H., & Eggert, A. (2005). Biological effects of TrkA and TrkB receptor signaling in neuroblastoma. *Cancer Letters*, *228*(1-2), 143–53.

Seaborn, T., Ravni, A., Au, R., Chow, B. K. C., Fournier, A., Wurtz, O., & Vaudry, D. (2014). Induction of serpinb1a by PACAP or NGF is required for PC12 cells survival after serum withdrawal. *Journal of Neurochemistry*, *131*(1), 21–32.

Semenza, G. L. (2011). Oxygen Sensing, Homeostasis, and Disease. *New England Journal of Medicine*, *365*(6), 537–547.

Shao, N., Wang, H., Zhou, T., & Liu, C. (1993). 7S nerve growth factor has different biological activity from 2.5S nerve growth factor in vitro. *Brain Res*, *609*(1–2), 338–340.

Sharp, F. R., & Bernaudin, M. (2004). HIF1 and oxygen sensing in the brain. *Nature Reviews Neuroscience*, *5*(6), 437–448.

Shaw, R. J., & Cantley, L. C. (2006). Ras, PI(3)K and mTOR signalling controls tumour cell growth. *Nature*, *441*(7092), 424–30.

Shi, G.-X., Jin, L., & Andres, D. A. (2008). Pituitary Adenylate Cyclase-Activating Polypeptide 38-Mediated Rin Activation Requires Src and Contributes to the Regulation of Hsp27 Signaling during Neuronal Differentiation. *Molecular and Cellular Biology*, *28*(16), 4940–4951.

Shimoke, K., & Chiba, H. (2001). Nerve growth factor prevents 1-methyl-4-phenyl-1,2,3,6-tetrahydropyridine-induced cell death via the Akt pathway by suppressing caspase-3-like activity using PC12 cells: Relevance to therapeutical application for Parkinson's disease. *Journal of Neuroscience Research*, *63*(5), 402–409.

Shioda, S., & Arimura, A. (1995). Pituitary adenylate cyclase activating polypeptide (PACAP) and its receptors: neuroendocrine and endocrine interaction. *Front Neuroendocrinol*, *16*(1), 53–88.

Shipley, M. M., Mangold, C. A., & Szpara, M. L. (2016). Differentiation of the SH-SY5Y Human Neuroblastoma Cell Line. *Journal of Visualized Experiments : JoVE*, *2016*(108), 1–11.

Siegel, M., & Khosla, C. (2007). Transglutaminase 2 inhibitors and their therapeutic role in disease states. *Pharmacology & Therapeutics*, *115*(2), 232–45.

Singh, U. S., Pan, J., Kao, Y. L., Joshi, S., Young, K. L., & Baker, K. M. (2003). Tissue transglutaminase mediates activation of RhoA and MAP kinase pathways during retinoic acid-induced neuronal differentiation of SH-SY5Y cells. *Journal of Biological Chemistry*, *278*(1), 391–399.

Sivaramakrishnan, M., Croll T. I., Gupta R., Stupar D., Van Lonkhuyzen D. R., Upton Z., & Shooter G. (2013). Lysine residues of IGF-I are substrates for transglutaminases and modulate downstream IGF-I signalling. *Biochimica et Biophysica Acta (BBA) - Molecular Cell Research. 1833*(12) 12, 3176–85.

Slaughter, T. F., Achyuthan, K. E., Lai, T. S., & Greenberg, C..S. (1992). A microtiter plate transglutaminase assay utilizing 5-(biotinamido)pentylamine as substrate. *Anal Biochem. 205*(1):166–71.

Smith, C. & Eisenstein, M. (2005). Automated imaging: data as far as the eye can see. *Nature methods, 2*, 547–55.

Smith, P. K., Krohn, R. I., Hermanson, G. T., Mallia, A. K., Gartner, F. H., Provenzano, M. D., Fujimoto, E. K., Goeke, N. M., Olson, B. J., Klenk, D. C. (1985). Measurement of protein using bicinchoninic acid. *Anal Biochem. 150*(1):76–85.

Sofroniew, M. V, Howe, C. L., & Mobley, W. C. (2001). Nerve growth factor signaling, neuroprotection, and neural repair. *Annual Review of Neuroscience*, *24*, 1217–81.

Stamnaes J., Fleckenstein B., Sollid L.M. (2008) The propensity for deamidation and transamidation of peptides by transglutaminase 2 is dependent on substrate affinity and reaction conditions. *Biochim Biophys Acta. 1784*(11):1804-11.

Stork, P. J. & Schmitt, J. M. Crosstalk between cAMP and MAP kinase signaling in the regulation of cell proliferation. (2002).*Trends Cell Biol. 12*(6), 258–266.

Suda, K., Smith, D. M., Ghatei, M. A., & Bloom, S. R. (1992) Investigation of the interaction of VIP binding sites with VIP and PACAP in human brain. *Neurosci Lett 137*(1):19– 23.

Suda, K., Smith, D. M., Ghatei, M. A., & Bloom, S. R. (1991) Investigation and characterization of receptors for pituitary adenylate cyclase-activating polypeptide in human brain by radioligand bind- ing and chemical cross-linking. *J Clin Endocrinol Metab, 72*(5), 958–964.

Sugawara, T., Fujimura, M., Noshita, N., Kim, G. W., Saito, A., Hayashi, T., & Chan, P. H. (2004). Neuronal Death/Survival Signaling Pathways in Cerebral Ischemia. *NeuroRx*, *1*(1), 17–25.

Suto, N., Ikura, K., & Sasaki, R. (1993). Expression induced by interleukin-6 of tissue-type transglutaminase in human hepatoblastoma HepG2 cells. *Journal of Biological Chemistry*, *268*(10), 7469–7473.

Suzuki, R., Arata, S., Nakajo, S., Ikenaka, K., Kikuyama, S., & Shioda, S. (2003). Expression of the receptor for pituitary adenylate cyclase-activating polypeptide (PAC1-R) in reactive astrocytes. *Brain Research. Molecular Brain Research*, *115*(1), 10–20.

Szondy, Z., Mastroberardino, P. G., Váradi, J., Farrace, M. G., Nagy, N., Bak, I., & Piacentini, M. (2006). Tissue transglutaminase (TG2) protects cardiomyocytes against ischemia/reperfusion injury by regulating ATP synthesis. *Cell Death and Differentiation*, *13*(10), 1827–1829.

Szu-Yu Ho, T., & Rasband, M. N. (2011). Maintenance of neuronal polarity. *Developmental Neurobiology*, *71*(6), 474–482.

Tabakman, R., Jiang, H., Schaefer, E., Levine, R. A., & Lazarovici, P. (2004). Nerve growth factor pretreatment attenuates oxygen and glucose deprivation-induced c-Jun amino-terminal kinase 1 and stress-activated kinases p38alpha and p38beta activation and confers neuroprotection in the pheochromocytoma PC12 Model. *J Mol Neurosci*, *22*(3), 237–250.

Tabakman, R., Jiang, H., Shahar, I., Arien-Zakay, H., Levine, R. A., & Lazarovici, P. (2005). Neuroprotection by NGF in the PC12 in vitro OGD model: Involvement of mitogen-activated protein kinases and gene expression. In *Annals of the New York Academy of Sciences*, *1053*(8), 84–96.

Takeda, K., & Ichiijo, H. (2002). Neuronal p38 MAPK signalling: An emerging regulator of cell fate and function in the nervous system. *Genes to Cells*, *7*(11), 1099–1111.

Takei, N., Torres, E., Yuhara, A., Jongsma, H., Otto, C., Korhonen, L., & Lindholm, D. (2000). Pituitary adenylate cyclase-activating polypeptide promotes the survival of basal forebrain cholinergic neurons in vitro and in vivo: comparison with effects of nerve growth factor. *European Journal of Neurosci*, *12*(7), 2273–2280.

Tanaka, K., & Tsukahara, T., Hashimoto, N., Ogata, N., Yonekawa, Y., Kimura, T., & Taniguchi, T. (1994). Effect of nerve growth factor on delayed neuronal death after cerebral ischaemia. *Acta Neurochir (Wien)*, *129*(1–2), 64–71.

Tanaka T., Knapp D., Nasmyth K.(1997). Loading of an Mcm protein onto DNA replication origins is regulated by Cdc6p and CDKs. Cell, 90(4): 649–60.

Tang, L. L., Wang, R., & Tang, X. C. (2005). Huperzine A protects SHSY5Y neuroblastoma cells against oxidative stress damage via nerve growth factor production. *European Journal of Pharmacology*, *519*(1–2), 9–15.

Tatsukawa, H., Fukaya, Y., Frampton, G., Martinez-Fuentes, A., Suzuki, K., Kuo, T. F., & Kojima, S. (2009). Role of Transglutaminase 2 in Liver Injury via Cross-linking and Silencing of Transcription Factor Sp1. *Gastroenterology*, *136*(5), 1783–95.

Tatsukawa, H., Furutani, Y., Hitomi, K., & Kojima, S. (2016). Transglutaminase 2 has opposing roles in the regulation of cellular functions as well as cell growth and death. *Cell Death and Disease*.

Tee, A. E. L., Marshall, G. M., Liu, P. Y., Xu, N., Haber, M., Norris, M. D., & Liu, T. (2010). Opposing effects of two tissue transglutaminase protein isoforms in neuroblastoma cell differentiation. *The Journal of Biological Chemistry*, *285*(6), 3561–3567.

Ter Horst, G. J. & Korf, H. J. (1997). Clinical Pharmacology of Cerebral Ischemia. *Journal of Neurochemistry*, *69*(6), 2624.

Thomázy, V., & Fésüs, L. (1989). Differential expression of tissue transglutaminase in human cells. An immunohistochemical study. *Cell and Tissue Research*, *255*(1), 215–24.

Thornton, C., Leaw, B., Mallard, C., Nair, S., Jinnai, M., & Hagberg, H. (2017). Cell Death in the Developing Brain after Hypoxia-Ischemia. *Frontiers in Cellular Neuroscience*, *11*(8), 1–19.

Thorpe, L. W., & Perez-Polo, J. R. (1987). The influence of nerve growth factor on the in vitro proliferative response of rat spleen lymphocytes. *J Neurosci Res*, *18*(1), 134–139.

Tolentino, P. J., Waghray, A., Wang, K. K. W., & Hayes, R. L. (2004). Increased expression of tissue-type transglutaminase following middle cerebral artery occlusion in rats. *Journal of Neurochemistry*, *89*(5), 1301–1307.

Tomaselli, B., Podhraski, V., Heftberger, V., Böck, G., & Baier-Bitterlich, G. (2005). Purine nucleoside-mediated protection of chemical hypoxia-induced neuronal injuries involves p42/44 MAPK activation. *Neurochemistry International*, *46*(7), 513–521.

Tremblay, R. G., Sikorska, M., Sandhu, J. K., Lanthier, P., Ribecco-Lutkiewicz, M., & Bani-Yaghoub, M. (2010). Differentiation of mouse Neuro 2A cells into dopamine neurons. *Journal of Neuroscience Methods*, *186*, 60–67.

Trigwell SM, Lynch PT, Griffin M, Hargreaves AJ, Bonner PL. (2004). An improved colorimetric assay for the measurement of transglutaminase (type II)-(gammaglutamyl) lysine cross-linking activity. *Anal Biochem. 330*(1):164-6.

Tucholski, J., & Johnson, G. V. W. (2002). Tissue transglutaminase differentially modulates apoptosis in a stimuli-dependent manner. *Journal of Neurochemistry*, *81*(4), 780–791.

Tucholski, J., & Johnson, G. V. W. (2003). Tissue transglutaminase directly regulates adenylyl cyclase resulting in enhanced cAMP-response element-binding protein (CREB) activation. *Journal of Biological Chemistry*, *278*(29), 26838–26843.

Tucholski, J., Lesort, M., & Johnson, G. V. (2001). Tissue transglutaminase is essential for neurite outgrowth in human neuroblastoma SH-SY5Y cells. *Neuroscience*, *102*(2), 481–491.

Tuszynski, M. H., Yang, J. H., Barba, D., U, H. S., Bakay, R., Pay, M. M. & Nagahara, A. H. (2015). Nerve Growth Factor Gene Therapy Activates Neuronal Responses in Alzheimer's Disease. *JAMA Neurology*, *72*(10), 1139–1147.

Uchida, D., Tatsuno, I., Tanaka, T., Hirai, A., Saito, Y., Moro, O., & Tajima, M. (1998). Maxadilan is a specific agonist and its deleted peptide (M65) is a specific antagonist for PACAP type 1 receptor. In *Annals of the New York Academy of Sciences 865*(1), (253–258).

Uings, I. J., & Farrow, S. N. (2000). Cell receptors and cell signalling. *Molecular Pathology : MP*, *53*(6), 295–9.

Van der Zee, C. E. E. M., Ross, G. M., Riopelle, R. J., & Hagg, T. (1996). Survival of Cholinergic Forebrain Neurons in Developing p75NGFR-Deficient Mice. *Science*, *274*(5293), 1729–1732.

Vanhaesebroeck, B., & Alessi, D. R. (2000). The PI3K–PDK1 connection : more than just a road to PKB. *Biochem. J*, *346*(3), 561–76.

Vanhaesebroeck, B., Stephens, L., & Hawkins, P. (2012). PI3K signalling: the path to discovery and understanding. *Nature Reviews Molecular Cell Biology*, *13*(3), 195–203.

Vaudry, D., Gonzalez, B. J., Basille, M., Yon, L., Fournier, A., & Vaudry, H. (2000a). Pituitary adenylate cyclase-activating polypeptide and its receptors: From structure to functions. *Pharmacological Reviews*, *52*(2), 269–324.

Vaudry, D., Falluel-morel, A., Bourgault, S., Basille, M., Burel, D., Wurtz, O., & Sante, D. (2009). Pituitary Adenylate Cyclase-Activating Polypeptide and Its Receptors : 20 Years after the Discovery. *Peptide Research*, *61*(3), 283–357.

Vaudry, D., Gonzalez, B. J., Basille, M., Pamantung, T. F., Fontaine, M., Fournier, A, & Vaudry, H. (2000b). The neuroprotective effect of pituitary adenylate cyclase-activating polypeptide on cerebellar granule cells is mediated through inhibition of the CED3-related cysteine protease caspase-3/CPP32. *Proceedings of the National Academy of Sciences of the United States of America*, *97*(24), 13390–5.

Verbeke, S., Meignan, S., Lagadec, C., Germain, E., Hondermarck, H., Adriaenssens, E., & Le Bourhis, X. (2010). Overexpression of p75NTR increases survival of breast cancer cells through p21waf1. *Cellular Signalling*, *22*(12), 1864–1873.

Verma, A., & Mehta, K. (2007). Tissue transglutaminase-mediated chemoresistance in cancer cells. *Drug Resistance Updates*, *10*(4–5), 144–151.

Villalba, M., Bockaert, J., & Journot, L. (1997). Pituitary adenylate cyclase-activating polypeptide (PACAP-38) protects cerebellar granule neurons from apoptosis by activating the mitogen-activated protein kinase (MAP kinase) pathway. *The Journal of Neuroscience : The Official Journal of the Society for Neuroscience*, *17*(1), 83–90.

Vyas, F. S. , Hargreaves, A. J. , Bonner, P. L., Boocock, D. J., Coveney, C., & Dickenson, J. M. (2016) A1 adenosine receptor-induced phosphorylation and modulation of transglutaminase 2 activity in H9c2 cells: A role in cell survival. *Biochem Pharmacol 107*:41-58.

Vyas, F. S., Nelson, C. P., Freeman, F., Boocock, D. J., Hargreaves, A. J., & Dickenson, J. M. (2017) β2adrenoceptor-induced modulation of transglutaminase 2 transamidase activity in cardiomyoblasts. *Eur J Pharmacol 813*:105-121.

Walther D. J., Peter J-U., Winter S., Höltje M., Paulmann N., & Grohmann M. (2003) Serotonylation of small GTPases is a signal transduction pathway that triggers platelet α-granule release. *Cell 115*(7), 851-862.

Wang, F. (2006). Culture of animal cells: a manual of basic technique, fifth edition. *In Vitro Cellular & Developmental Biology - Animal*, *42*(5), 169–86.

Wang H., Wang R., Thrimawithana T., Little P. J., Xu J., Feng Z. P., & Zheng W. (2014) The nerve growth factor signaling and its potential as therapeutic target for glaucoma. *Biomed Res Int, 759473*,1–10.

Wang, Y., Ande, S. R., & Mishra, S. (2012). Phosphorylation of transglutaminase 2 (TG2) at serine-216 has a role in TG2 mediated activation of nuclear factor-kappa B and in the downregulation of PTEN. *BMC Cancer*, *12*(277), 1–12.

Wang, Z., & Griffin, M. (2011). TG2, a novel extracellular protein with multiple functions. *Amino Acids*. *42*(2-3),939-49

Waschek, J. A. (2002). Multiple actions of pituitary adenylyl cyclase activating peptide in nervous system development and regeneration. *Developmental Neuroscience*, *24*(1), 14–23.

Williams, L. R., Varon, S., Peterson, G. M., Wictorin, K., Fischer, W., Bjorklund, A., & Gage, F. H. (1986). Continuous infusion of nerve growth factor prevents basal forebrain neuronal death after fimbria fornix transection. *Proceedings of the National Academy of Sciences of the United States of America*, *83*(23), 9231–5.

Wooten, M. W., Seibenhener, M. L., Neidigh, K. B. W., & Vandenplas, M. L. (2000). Mapping of atypical protein kinase C within the nerve growth factor signaling cascade: Relationship to differentiation and survival of PC12 cells. *Molecular and Cellular Biology*, *20*(13), 4494–4504.

Wortzel, I., & Seger, R. (2011). The ERK Cascade: Distinct Functions within Various Subcellular Organelles. *Genes & Cancer*, *2*(3), 195–209.

Wu, E. H. T., & Wong, Y. H. (2005). Pertussis toxin-sensitive Gi/o proteins are involved in nerve growth factor-induced pro-survival Akt signaling cascade in PC12 cells. *Cellular Signalling*, *17*(7), 881–890.

Wu, P.Y., Lin, Y.C., Chang, C.L., Lu, H.T., Chin, C.H., Hsu, T.T., & Sun, S. H. (2009). Functional decreases in P2X 7 receptors are associated with retinoic acid-induced neuronal differentiation of Neuro-2a neuroblastoma cells. *Cellular Signalling*, *21*(6), 881–91.

Wyatt, S., & Davies, A. M. (1993). Regulation of expression of mRNAs encoding the nerve growth factor receptors p75 and trkA in developing sensory neurons. *Development*, *119*(3), 635–648.

Wyatt, S., & Davies, A. M. (1995). Regulation of nerve growth factor receptor gene expression in sympathetic neurons during development. *J Cell Biol*, *130*(6), 1435–1446.

Xie, H., Hu, L., & Li, G. (2010). SH-SY5Y human neuroblastoma cell line: in vitro cell model of dopaminergic neurons in Parkinson's disease. *Chinese Medical Journal*, *123*(8), 1086–1092.

Yamaguchi, H., & Wang, H.-G. (2006). Tissue Transglutaminase Serves as an Inhibitor of Apoptosis by Cross-Linking Caspase 3 in Thapsigargin-Treated Cells. *Molecular and Cellular Biology*, *26*(2), 569–579.

Yamaguchi, H., & Wang, H. G. (2001). The protein kinase PKB/Akt regulates cell survival and apoptosis by inhibiting Bax conformational change. *Oncogene*, *20*(53), 7779–86.

Yao, R., & Cooper, G. M. (1995). Requirement for phosphatidylinositol-3 kinase in the prevention of apoptosis by nerve growth factor. *Science*, *267*(5206), 2003–6.

Yeo, T. T., Chua-Couzens, J., Butcher, L. L., Bredesen, D. E., Cooper, J. D., Valletta, J. S., & Longo, F.

M. (1997). Absence of p75NTR causes increased basal forebrain cholinergic neuron size, choline acetyltransferase activity, and target innervation. *The Journal of Neuroscience : The Official Journal of the Society for Neuroscience*, *17*(20), 7594–605.

Yu, S. P., Canzoniero, L. M. T., & Choi, D. W. (2001). Ion homeostasis and apoptosis. *Current Opinion in Cell Biology*, *13*(4), 405–411.

Yu, W., Schwei, M. J., & Baas, P. W. (1996). Microtubule transport and assembly during axon growth. *Journal of Cell Biology*, *133*(1), 151–157.

Yuan, J., Lipinski, M., & Degterev, A. (2003). Diversity in the mechanisms of neuronal cell death. *Neuron*, *40*(2), 401–13.

Yuhara, A., Ishii, K., Nishio, C., Abiru, Y., Yamada, M., Nawa, H., & Takei, N. (2003). PACAP and NGF cooperatively enhance choline acetyltransferase activity in postnatal basal forebrain neurons by complementary induction of its different mRNA species. *Biochemical and Biophysical Research Communications*, *301*(2), 344–349.

Yuhara, A., Nishio, C., Abiru, Y., Hatanaka, H., & Takei, N. (2001). PACAP has a neurotrophic effect on cultured basal forebrain cholinergic neurons from adult rats. *Developmental Brain Research*, *131*(1–2), 41–45.

Zarubin, T., & Han, J. (2005). Activation and signaling of the p38 MAP kinase pathway. *Cell Research*, *15*(1), 11–18.

Zemskov, E. A., Loukinova, E., Mikhailenko, I., Coleman, R. a, Strickland, D. K., & Belkin, A. M. (2009). Regulation of platelet-derived growth factor receptor function by integrin-associated cell surface transglutaminase. *The Journal of Biological Chemistry*, *284*(24), 16693–703.

Zhang, J., Lesort, M., Guttmann, R. P., & Johnson, G. V. W. (1998). Modulation of the in situ activity of tissue transglutaminase by calcium and GTP. *Journal of Biological Chemistry*, *273*(4), 2288–2295.

Zhang, J., Qian, H., Zhao, P., Hong, S. S., & Xia, Y. (2006). Rapid hypoxia preconditioning protects cortical neurons from glutamate toxicity through $^{\delta}$-opioid receptor. *Stroke*, *37*(4), 1094–1099.

Zhang, W., Liu, H. T., & Tu LIU, H. (2002). MAPK signal pathways in the regulation of cell proliferation in mammalian cells. *Cell Research*, *12*(1), 9–18.

Zhang, Y.-Z., Moheban, D. B., Conway, B. R., Bhattacharyya, A., & Segal, R. A. (2000). Cell surface Trk receptors mediate NGF-induced survival while internalized receptors regulate NGF-induced differentiation. *The Journal of Neuroscience*, *20*(15), 5671–5678.

Zhou, C. J., Yada, T., Kohno, D., Kikuyama, S., Suzuki, R., Mizushima, H., & Shioda, S. (2001). PACAP activates PKA, PKC and Ca^{2+} signaling cascades in rat neuroepithelial cells. *Peptides*, *22*(7), 1111–1117.

Zhu, Y., Yang, G. Y., Ahlemeyer, B., Pang, L., Che, X. M., Culmsee, C., & Krieglstein, J. (2002). Transforming growth factor-beta 1 increases bad phosphorylation and protects neurons against damage. *The Journal of Neuroscience : The Official Journal of the Society for Neuroscience*, *22*(10), 3898–3909.

Zimmermann, M., Gardoni, F., Marcello, E., Colciaghi, F., Borroni, B., Padovani, A., & Di Luca, M. (2004). Acetylcholinesterase inhibitors increase ADAM10 activity by promoting its trafficking in neuroblastoma cell lines. *Journal of Neurochemistry*, *90*(6), 1489–1499.

European Journal of Pharmacology 820 (2018) 113–129

Contents lists available at ScienceDirect

European Journal of Pharmacology

journal homepage: www.elsevier.com/locate/ejphar

Neuropharmacology and analgesia

Activation of transglutaminase 2 by nerve growth factor in differentiating neuroblastoma cells: A role in cell survival and neurite outgrowth

Alanood S. Algarni, Alan J. Hargreaves, John M. Dickenson*

School of Science and Technology, Nottingham Trent University, Clifton Lane, Nottingham NG11 8NS, United Kingdom

ARTICLE INFO

Keywords:
Cell survival
Hypoxia
Neuroblastoma cells
Neurite outgrowth
NGF
Transglutaminase 2

ABSTRACT

NGF (nerve growth factor) and tissue transglutaminase (TG2) play important roles in neurite outgrowth and modulation of neuronal cell survival. In this study, we investigated the regulation of TG2 transamidase activity by NGF in retinoic acid-induced differentiating mouse N2a and human SH-SY5Y neuroblastoma cells. TG2 transamidase activity was determined using an amine incorporation and a peptide cross linking assay. In situ TG2 activity was assessed by visualising the incorporation of biotin-X-cadaverine using confocal microscopy. The role of TG2 in NGF-induced cytoprotection and neurite outgrowth was investigated by monitoring hypoxia-induced cell death and appearance of axonal-like processes, respectively. The amine incorporation and protein crosslinking activity of TG2 increased in a time and concentration-dependent manner following stimulation with NGF in N2a and SH-SY5Y cells. NGF mediated increases in TG2 activity were abolished by the TG2 inhibitors Z-DON (Z-ZON-Val-Pro-Leu-OMe; Benzyloxycarbonyl-(6-Diazo-5-oxonorleucinyl)-L-valinyl-L-prolinyl-L-leucinmethylester) and R283 (1,3,dimethyl-2[2-oxo-propyl]thio)imidazole chloride) and by pharmacological inhibition of extracellular signal-regulated kinases 1 and 2 (ERK1/2), protein kinase B (PKB) and protein kinase C (PKC), and removal of extracellular Ca^{2+}. Fluorescence microscopy demonstrated NGF induced in situ TG2 activity. TG2 inhibition blocked NGF-induced attenuation of hypoxia-induced cell death and neurite outgrowth in both cell lines. Together, these results demonstrate that NGF stimulates TG2 transamidase activity via a ERK1/2, PKB and PKC-dependent pathway in differentiating mouse N2a and human SH-SY5Y neuroblastoma cells. Furthermore, NGF-induced cytoprotection and neurite outgrowth are dependent upon TG2. These results suggest a novel and important role of TG2 in the cellular functions of NGF.

1. Introduction

Transglutaminases (TGs) are a family of Ca^{2+}-dependent enzymes that catalyse the post-translational modification of proteins (Nurminskaya and Belkin, 2012; Eckert et al., 2014). There are eight distinct catalytically active members of the TG family which exhibit differential expression (Factor XIIIa and TGs 1–7).

The ubiquitously expressed TG2, which is the most widely studied member of the TG family, is involved in the regulation of numerous cellular processes, including cell adhesion, migration, growth, survival, apoptosis, differentiation, and extracellular matrix organization (Nurminskaya and Belkin, 2012; Eckert et al., 2014). In neuronal cells, TG2 is involved in neurite outgrowth during differentiation and in neuroprotection following cerebral ischaemia (Tucholski et al., 2001; Filiano et al., 2010; Vanella et al., 2015).

Transglutaminase 2 possesses multiple enzymic functions that include transamidation, protein disulphide isomerase and protein kinase activity (Gundemir et al., 2012). Furthermore, TG2 also has non-enzymatic functions which can modulate signal transduction pathways (Nurminskaya and Belkin, 2012).

Receptor tyrosine kinases represent a large family of receptors whose prominent members include receptors for epidermal growth factor (EGF), platelet-derived growth factor (PDGF) and vascular endothelial growth factor (VEGF). It is notable that cytoplasmic TG2-mediated transamidase activity participates in EGF receptor signalling, whereas the interaction of extracellular TG2 with PDGF and VEGF receptors promotes their activation (Dardik and Inbal, 2006; Zemskov et al., 2009; Li et al., 2010). These observations suggest a major role for TG2 in the modulation of receptor tyrosine kinases. However, at present, it is not known if receptor tyrosine kinase activation promotes intracellular TG2 activation. A study has shown that prolonged exposure (3–6 days) of mouse N2a neuroblastoma cells to nerve growth factor (NGF) promoted increased TG2 protein expression and TG2-mediated transamidase activity (Condello et al., 2008). However, it is conceivable that the increased levels of transamidase activity may reflect increased levels of TG2 expression rather than direct activation of

* Corresponding author.
E-mail address: john.dickenson@ntu.ac.uk (J.M. Dickenson).

https://doi.org/10.1016/j.ejphar.2017.12.023
Received 20 September 2017; Received in revised form 5 December 2017; Accepted 8 December 2017
Available online 11 December 2017
0014-2999/

the enzyme itself by NGF-induced signalling. NGF triggers its biological effects via the tyrosine kinase receptor TrkA (Wang et al., 2014), which when activated stimulates a multitude of signalling pathways including ERK1/2 (extracellular signal-regulated kinases 1 and 2), PI-3K (phosphatidylinositol 3-kinase)/PKB (protein kinase B) and PLC-γ (phospholipase C-γ)/PKC (protein kinase C) cascades (Wang et al., 2014). As some of these pathways are associated with modulation of intracellular TG2 activity (PKC, ERK1/2 and Ca^{2+}) it is conceivable that NGF directly regulates TG2 activity. Since mouse N2a and human SH-SY5Y neuroblastoma cells are responsive to NGF (Price et al., 2003; Condello et al., 2008; Dwane et al., 2013), the primary aims of this study were (i) to determine whether short term treatment with NGF (< 4 h) could modulate TG2-mediated transamidase activity in these cells and (ii) to assess the role of TG2 in NGF-induced neuroprotection and neurite outgrowth. The results obtained indicate that NGF triggers robust TG2-mediated amine incorporation and protein cross-linking activity in mouse N2a and human SH-SY5Y cells. Furthermore, inhibition of TG2 attenuated NGF-induced cytoprotection and neurite outgrowth. Overall, these results suggest a novel and prominent role for TG2 in NGF function and signalling.

2. Materials and methods

2.1. Materials

Nerve growth factor (NGF) was obtained from Merck Millipore (Watford, UK). Akt inhibitor XI was purchased from Calbiochem (San Diego, CA). BAPTA/AM (1,2-Bis(2-aminophenoxy)ethane-*N*,*N*,*N*′,*N*′-tetraacetic acid tetrakis acetoxymethyl ester), PD 98059 (2′-amino-3′-methoxyflavone) and Ro 31-8220 (3-[3-[2,5-Dihydro-4-(1-methyl-1*H*-indol-3-yl)-2,5-dioxo-1*H*-pyrrol-3-yl]-1*H*-indol-1-yl]propyl carbamimidothioic acid ester mesylate) were obtained from Tocris Bioscience (Bristol, UK). *All-trans* retinoic acid, casein, Protease Inhibitor Cocktail (for use with mammalian cell and tissue extracts), Phosphatase Inhibitor Cocktail 2 and 3, hordereadish peroxidase conjugated-ExtrAvidin® (ExtrAvidin®-HRP) and fluorescein isothiocyanate conjugated ExtrAvidin® (ExtrAvidin®-FITC) were obtained from Sigma-Aldrich Co. Ltd. (Gillingham, UK). The TG2 inhibitors Z-DON (Z-ZON-Val-Pro-Leu-OMe; Benzyloxycarbonyl-(6-Diazo-5-oxonorleucinyl)-L-valinyl-L-prolinyl-L-leucinmethylester) and R283 (1,3,dimethyl-2[2-oxopropyl]thio)imidazole chloride), together with purified guinea-pig liver TG2 were obtained from Zedira GmbH (Darmstadt, Germany). DAPI (4′,6-diamidino-2-phenylindole) was from Vector Laboratories Inc (Peterborough, UK). Biotin-TVQQEL was purchased from Pepceuticals (Enderby, UK). Biotin cadaverine (N-(5-aminopentyl)biotinamide) and biotin-X-cadaverine (5-([[N-(biotinoyl)amino)hexanoyl]amino)pentylamine) were purchased from Invitrogen (Loughborough, UK). Dulbecco's modified Eagle's medium (DMEM), foetal bovine serum, trypsin (10×), L-glutamine (200 mM), penicillin (10,000 U/ml)/streptomycin (10,000 μg/ml) were purchased from Scientific Laboratory Supplies (Nottingham, UK. All other reagents were purchased from Sigma-Aldrich Co. Ltd. (Gillingham, UK) and were of analytical grade.

Antibodies were obtained from the following suppliers: monoclonal anti-phospho ERK1/2 (Thr^{202}/Tyr^{204}) from Sigma-Aldrich Co. Ltd. (Gillingham, UK); polyclonal anti-phospho PKB (Ser^{473}), polyclonal anti-total PKB, monoclonal anti-total ERK1/2, and polyclonal anti-cleaved caspase 3 from New England Biolabs Ltd. (Hitchin, UK); monoclonal anti-TG2 (CUB 7402) from Thermo Scientific (Loughborough, UK); polyclonal anti-human keratinocyte TG1 and polyclonal anti-human epidermal TG3 from Zedira GmbH (Darmstadt, Germany); monoclonal anti-GAPDH from Santa Cruz Biotechnology Inc (Heidelberg, Germany); Alexa Fluor® 488 goat anti-mouse IgG labelled secondary antibody from Thermo Scientific (Loughborough, UK).

2.2. Cell culture

Murine N2a and human SH-SY5Y neuroblastoma cells were obtained from the European Collection of Animal Cell Cultures (Porton Down, Salisbury, UK). Cells were cultured in DMEM supplemented with 2 mM L-glutamine, 10% (v/v) foetal bovine serum, penicillin (100 U/ml) and streptomycin (100 μg/ml). Cells were maintained in a humidified incubator (95% air/5% CO_2 at 37 °C) until 70–80% confluent and sub-cultured (1:5 split ratio) every 3–4 days. SH-SY5Y cells were sub-cultured using trypsin (0.05% w/v)/EDTA (0.02% w/v). Differentiation of N2a cells was induced by culturing cells in serum-free DMEM containing 1 μM *all-trans* retinoic acid for 48 h, unless otherwise specified. Differentiation of SH-SY5Y cells was induced by culturing cells in serum-free DMEM containing 10 μM *all-trans* retinoic acid for 5 days. Experiments were performed on passage numbers 8–20 for N2a and 18–25 for SH-SY5Y.

2.3. Cell extraction for measurement of TG2 activity

Following prior differentiation with retinoic acid as described above time course profiles and concentration-response curves were obtained for NGF. Where appropriate, cells were also pre-incubated for 30 min in medium with or without the protein kinase inhibitors Akt inhibitor XI (PKB/Akt, 100 nM; Barve et al., 2006), PD 98059 (MEK1/2, 50 μM; Dudley et al., 1995), and Ro 31-8220 (PKC, 10 μM; Davis et al., 1989) prior to treatment with 100 ng/ml NGF. The concentrations of protein kinase inhibitors employed in this study were in the range of values in the literature that are used to inhibit the cellular activity of these kinases: PD 98059 (10–50 μM; Sutter et al., 2004; Kim et al., 2008), Akt inhibitor XI (1 μM; Frampton et al., 2012; Rybchyn et al., 2011) and Ro 31-8220 (1–10 μM; Lee et al., 2013; Montejo-López et al., 2016). In the case of less well known Akt inhibitor XI, effects on PKB inhibition were verified by Western blot analysis.

Following stimulation with NGF, N2a and SH-SY5Y cells were rinsed twice with 2.0 ml of chilled PBS, lysed with 500 μl of ice-cold lysis buffer ((50 mM Tris-HCl pH 8.0, 0.5% (w/v) sodium deoxycholate, 0.1% (v/v) Protease Inhibitor Cocktail, and 1% (v/v) Phosphatase Inhibitor Cocktail 2)). Cell lysates were clarified by centrifugation at 4 °C for 10 min at 14,000 × *g* prior to being assayed for TG transamidase activity. Supernatants were collected and stored at − 80 °C.

Protein levels were determined by the bicinchoninic acid (BCA) protein assay, based on the method of Smith et al. (1985), which was performed using a commercially available kit (Sigma-Aldrich Co. Ltd, UK) using bovine serum albumin (BSA) as the standard. Transglutaminase activity was subsequently monitored by two different transamidase assays; amine incorporation and protein cross-linking.

2.4. Biotin-labelled cadaverine incorporation assay

The assay was performed as per the method described by Slaughter et al. (1992) with the modifications of Lilley et al. (1998). Briefly, 96-well microtitre plates were coated overnight at 4 °C with 250 μl of N′,N′-dimethylcasein (10 mg/ml in 100 mM Tris-HCl, pH 8.0). The plate was washed twice with distilled water and blocked with 250 μl of 3% (w/v) BSA in 100 mM Tris-HCl, pH 8.0 and incubated for 1 h at room temperature. The plate was washed twice before the application of 150 μl of either 6.67 mM calcium chloride and or 13.3 mM EDTA (used to deplete calcium and suppress TG activity) assay buffer containing 225 μM biotin cadaverine (a widely used substrate to monitor TG amine incorporating activity) and 2 mM 2-mercaptoethanol. The reaction was started by the addition of 50 μl of samples or positive

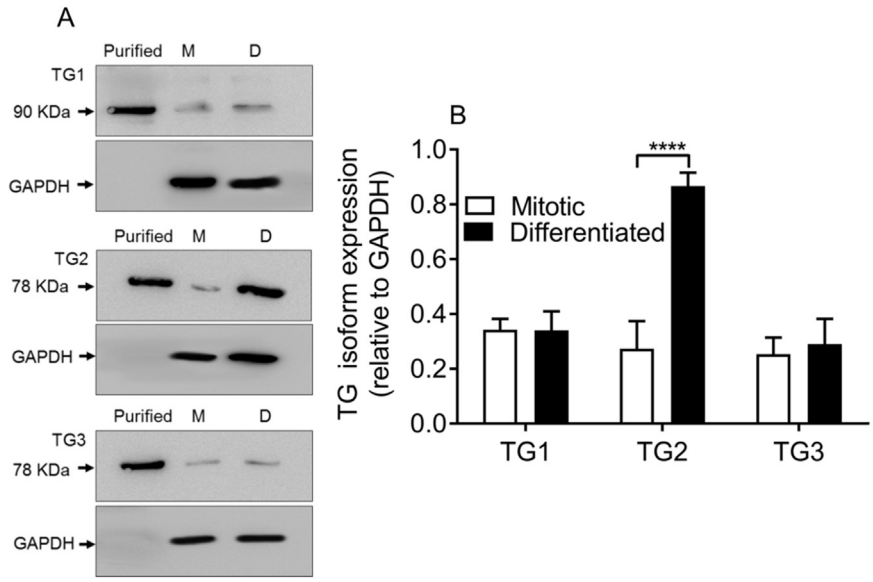

Fig. 1. Protein expression of TG isoforms in mitotic and differentiating SH-SY5Y cells. (A) Cell lysates (20 μg protein) from mitotic (M) and differentiating (D) SH-SY5Y cells (10 μM retinoic acid; for 5 days) were analysed for TG1, TG2 and TG3 expression by Western blotting using TG isoform specific antibodies. Purified TG1, TG2 and TG3 were used as positive controls. Levels of GAPDH are included for comparison. (B) Quantified data are expressed as the ratio of TG isoform to GAPDH and represent the mean ± S.E.M. from four independent experiments. $^{****}P < 0.0001$ versus mitotic cells.

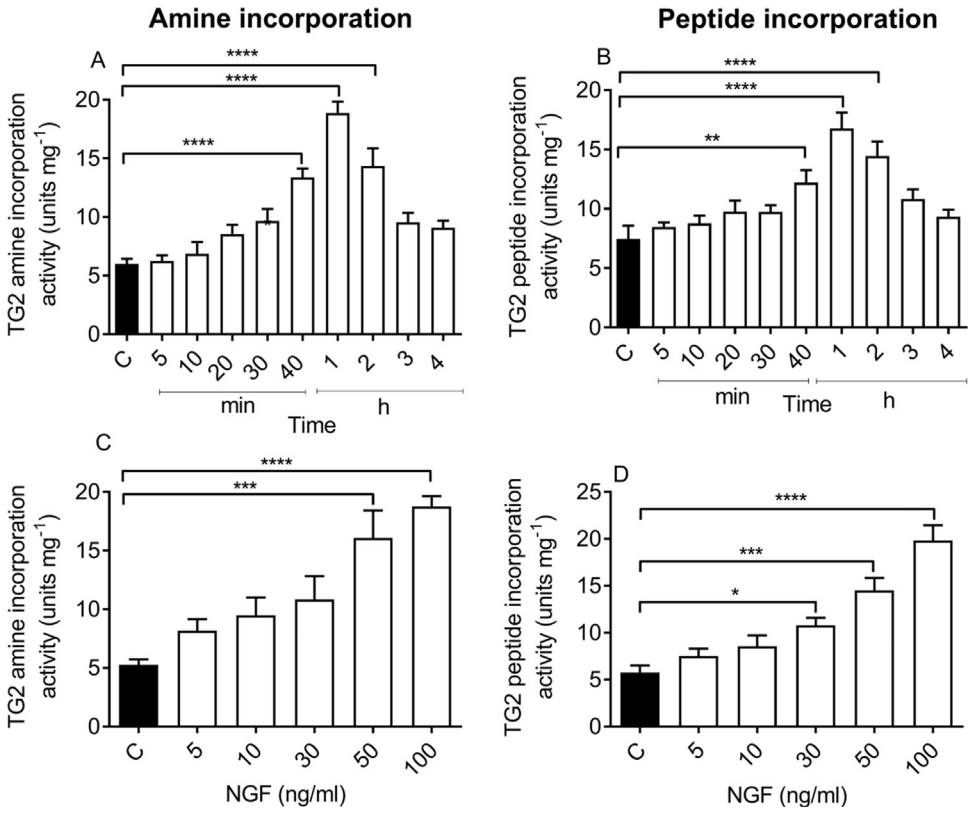

Fig. 2. Effect of NGF on transglutaminase activity in differentiating mouse N2a cells. Cells were either incubated with 100 ng/ml NGF for the indicated time periods or for 1 h with the indicated concentrations of NGF. Cell lysates were then subjected to the biotin-cadaverine incorporation (A and C) or protein cross-linking assay (B and D). Data points represent the mean TG specific activity ± S.E.M. from four independent experiments. $^{*}P < 0.05$, $^{**}P < 0.01$, $^{***}P < 0.001$, and $^{****}P < 0.0001$ versus control response.

control (50 ng/well of guinea-pig liver TG2) and negative control (100 mM Tris-HCl, pH 8.0). After incubation for 1 h at 37 °C plates were washed as before. Then, 200 μl of 100 mM Tris-HCl pH 8.0 containing 1% (w/v) BSA and ExtrAvidin®-HRP (1:5000 dilution) were added to each well and the plate incubated at 37 °C for 45 min then washed as before. The plate was developed with 200 μl of freshly made developing buffer (7.5 μg/ml 3,3′,5,5′-tetramethylbenzidine (TMB) and 0.0005% (v/v) H_2O_2 in 100 mM sodium acetate, pH 6.0) and incubated at room temperature for 15 min. The reaction was terminated by adding 50 μl of 5 M sulphuric acid and the absorbance read at 450 nm. One unit of transglutaminase activity was defined as a change in A_{450} of 1.0 per h. Each experiment was performed in triplicate.

2.5. Biotin-labelled peptide cross-linking assay

The assay was performed according to the method of Trigwell et al. (2004) with minor modifications. Microtitre plates (96-well) were coated and incubated overnight at 4 °C with casein at 1.0 mg/ml in 100 mM Tris-HCl pH 8.0 (250 μl per well). The wells were washed twice with distilled water, before incubation at room temperature for 1 h with 250 μl of blocking solution (100 mM Tris-HCl pH 8.0 containing 3% (w/v) BSA). The plate was washed twice before the application of 150 μl of either 6.67 mM calcium chloride and or 13.3 mM EDTA assay buffer containing 5 μM biotin-TVQQEL and 2 mM 2-mercaptoethanol. The reaction was started by the addition of 50 μl of

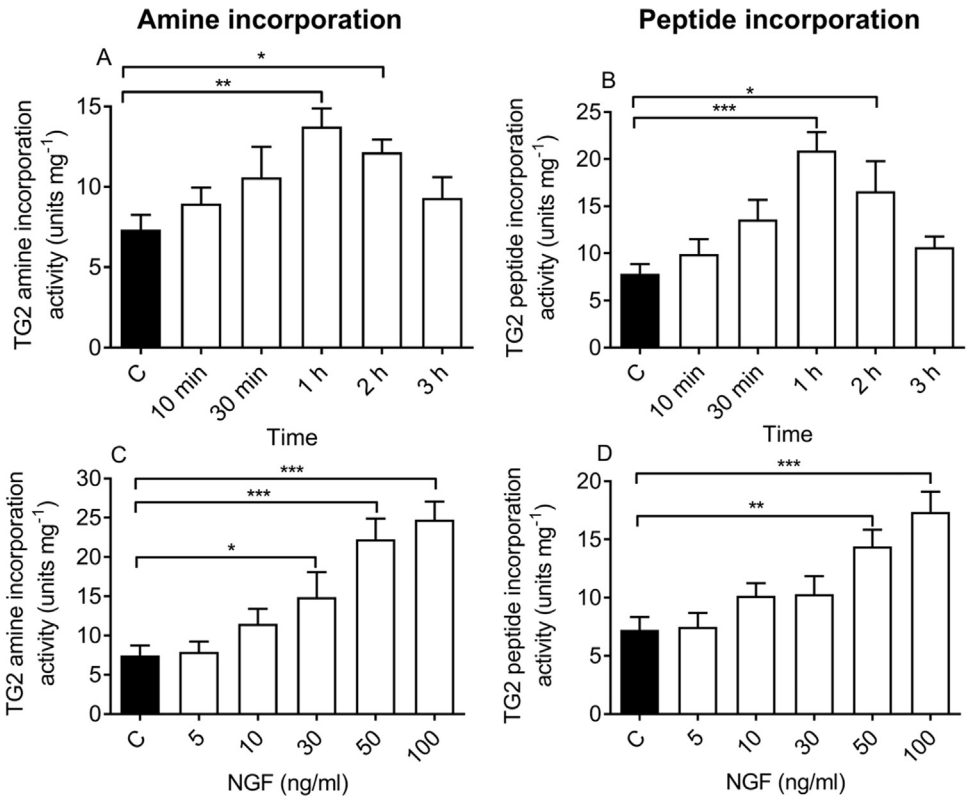

Fig. 3. Effect of NGF on transglutaminase activity in differentiating human SH-SY5Y cells. Cells were either incubated with 100 ng/ml NGF for the indicated time periods or for 1 h with the indicated concentrations of NGF. Cell lysates were then subjected to the biotin-cadaverine incorporation (A and C) or protein cross-linking assay (B and D). Data points represent the mean TG specific activity ± S.E.M. from four independent experiments. $^{*}P < 0.05$, $^{**}P < 0.01$, and $^{***}P < 0.001$ versus control response.

samples or positive control (50 ng/well of guinea-pig liver TG2) and negative control (100 mM Tris-HCl, pH 8.0) and allowed to proceed for 1 h at 37 ˚C. Reaction development and termination were performed as described for biotin-cadaverine assays. One unit of transglutaminase activity was defined as a change in A_{450} of 1.0 per h. Each experiment was performed in triplicate.

2.6. Hypoxia-induced cell death

Differentiating N2a and SH-SY5Y cells in glucose-free and serum-free DMEM (Gibco™, Life Technologies Ltd, Paisley, UK) were exposed to 8 h hypoxia using a hypoxic incubator (5% CO_2/1% O_2 at 37 ˚C) in which O_2 was replaced by N_2.

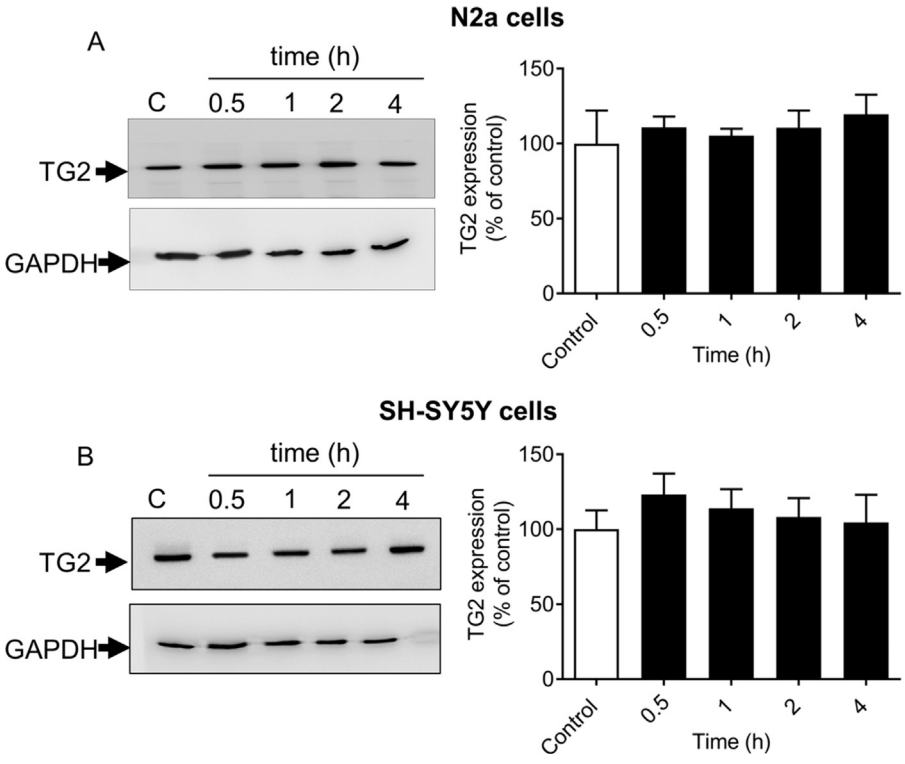

Fig. 4. Effect of acute NGF-treatment on TG2 protein expression in differentiating N2a and SH-SY5Y cells. (A) N2a and (B) SH-SY5Y cells were incubated with 100 ng/ml NGF for the indicated time periods. Cell lysates (20 µg protein) were analysed for TG2 expression by Western blotting using anti TG2 antibody. Levels of GAPDH are included for comparison. Quantified data are expressed as the percentage of TG2 expression in control cells (100%) and represent the mean ± S.E.M. of four independent experiments.

2.7. Cell viability assays

N2a (25,000 cells/well) and SH-SY5Y (50,000 cells/well) cells were plated in 24-well flat bottomed plates and differentiated for 48 h using retinoic acid, as described above, before cell viability was determined by measuring the reduction of MTT (Mosmann, 1983). The amount of DMSO-solubilised reduced formazan product was determined by measurement of absorbance at a wavelength 570 nm. Alternatively, N2a (5,000 cells/well) and SH-SY5Y (10,000 cells/well) cells were plated in 96-well flat bottomed plates and differentiated for 48 h. Following normoxia/hypoxia exposure, the activity of lactate dehydrogenase (LDH) released into the culture medium was detected using the CytoTox 96® non-radioactive cytotoxicity assay (Promega, Southampton, UK) with measurement of absorbance at 490 nm.

2.8. High-throughput analysis of NGF-induced neurite outgrowth

Cells were seeded on 8-well Ibidi μ-slides: 15,000 cells/well for N2a and 30,000 cells/well for SH-SY5Y and cultured for 24 h in fully supplemented DMEM. Where appropriate, cells were treated for 1 h with TG2 inhibitors Z-DON (150 μM) or R283 (200 μM). The medium containing the TG2 inhibitors was removed and replaced with fresh medium before the addition of 100 ng/ml NGF for 48 h. Following stimulation, cells were fixed with 3.7% (w/v) paraformaldehyde and permeabilised with 0.1% (v/v) Triton-X100 (both in PBS) for 15 min at room temperature. After washing, cells were blocked with 3% (w/v) BSA in PBS for 1 h at room temperature. They were then stained overnight at 4 °C with monoclonal antibodies to total α-tubulin (B512), followed by Alexa Fluor® 488 goat anti-mouse IgG labelled secondary antibody for 2 h at room temperature. The slides were subsequently washed three times for 5 min with PBS and incubated for 1 min with Vectashield® medium (Vector Laboratories Ltd, Peterborough, UK) containing DAPI counterstain for nuclei visualisation. Slides were preserved in PBS containing 0.01% (w/v) sodium azide as a preservative and stored at 4 °C prior to image acquisition and analysis. Neurite outgrowth was monitored using an ImageXpress® Micro Widefield High Content Screening (HCS) System (Molecular Devices, Wokingham, UK). Fluorescence images were acquired using a 10× objective lens and analysed by MetaXpress software, using Neurite Outgrowth analysis settings to measure a number of morphological parameters including average neurite length per cell and maximum neurite length per cell. Analysis was performed on a total of four fields and at least 200 cells per well from four independent experiments.

2.9. Western blot analysis

Protein extracts (15–20 μg per lane) were separated by SDS-PAGE (10% w/v polyacrylamide gel) using a Bio-Rad Mini-Protean III system. Proteins were transferred to nitrocellulose membranes in a Bio-Rad Trans-Blot system using transfer buffer comprising 25 mM Tris, 192 mM glycine pH 8.3 and 20% (v/v) MeOH). Following transfer, the membranes were washed with Tris-buffered saline (TBS) and blocked for 1 h at room temperature with 3% (w/v) skimmed milk powder in TBS containing 0.1% (v/v) Tween-20. Blots were then incubated overnight at 4 °C in blocking buffer with primary antibodies to the following targets (1:1000 dilutions unless otherwise indicated): phospho-specific ERK1/2, phospho-specific PKB (1:500), cleaved active caspase-3 (1:500), GAPDH, TG1, TG2 or TG3. The primary antibodies were removed and blots washed three times for 5 min in TBS/Tween 20. Blots were then incubated for 2 h at room temperature with the appropriate secondary antibody (1:1000) coupled to horseradish peroxidase (New England Biolabs Ltd; UK) in blocking buffer. Following removal of the secondary antibody, blots were extensively washed as above and developed using the Enhanced Chemiluminescence Detection System (Uptima, Interchim, France) and quantified by densitometry using Advanced Image Data Analysis Software (Fuji; version 3.52). The uniform transfer of proteins to the nitrocellulose

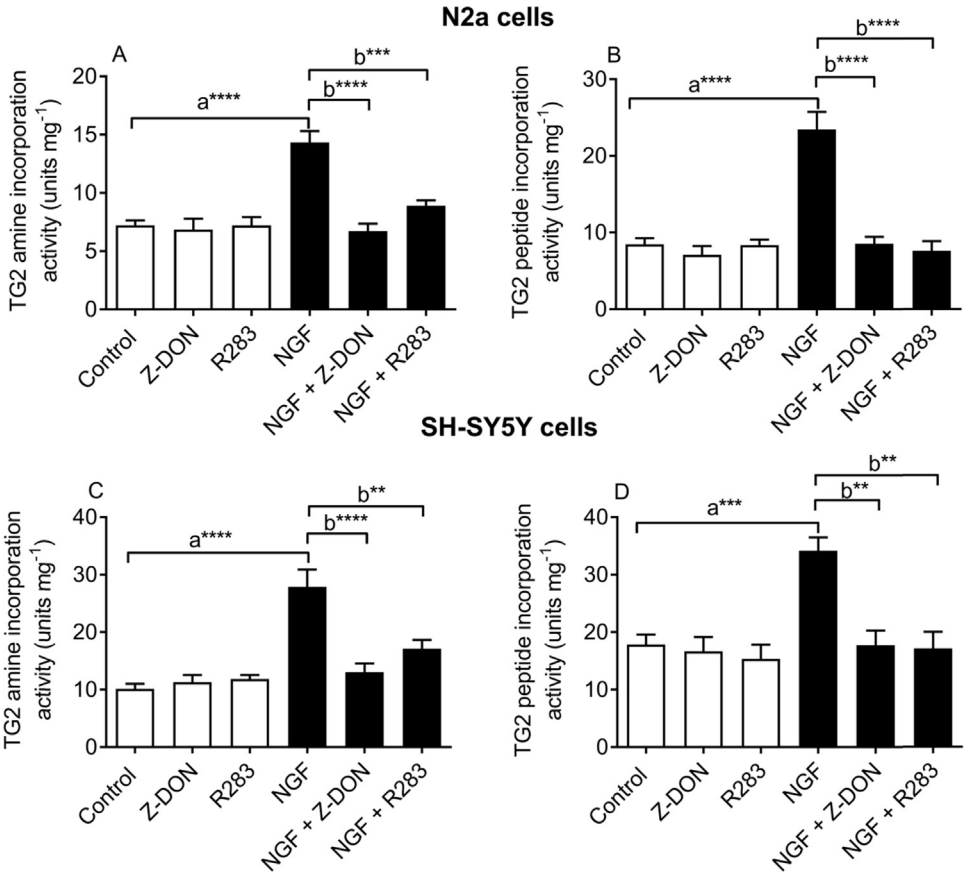

Fig. 5. Effect of TG2 inhibitors on NGF-induced TG2 activity. N2a (A and B) and SH-SY5Y (C and D) cells were pretreated for 1 h with the TG2 inhibitors Z-DON (150 μM) and R283 (200 μM) prior to 1 h stimulation with NGF (100 ng/ml). Cell lysates were then subjected to the biotin-cadaverine incorporation (A and C) or protein cross-linking assay (B and D). Data points represent the mean TG specific activity ± S.E.M. from four independent experiments. $^{**}P < 0.01$, $^{***}P < 0.001$, and $^{****}P < 0.0001$, (a) versus control and (b) versus NGF alone.

membrane was routinely monitored by transiently staining the membranes with Ponceau S stain prior to application of the primary antibody. When assessing protein kinase phosphorylation samples from each experiment were also analysed on separate blots using primary antibodies that recognize total ERK1/2 and PKB, (both at 1:1000 dilution) in order to confirm the uniformity of protein loading.

2.10. Visualisation of in situ TG2 activity

N2a (15,000 cells/well) and SH-SY5Y (30,000 cells/well) cells were seeded on 8-well chamber slides and differentiated using retinoic acid as described above. For the visualisation of in situ TG2 activity, the medium was then removed, monolayer gently washed with PBS and slides incubated for 6 h with 1 mM biotin-X-cadaverine (a cell permeable TG2 substrate; Perry et al., 1995) in serum-free DMEM before experimentation. Where appropriate, cells were treated for 1 h with TG2 inhibitors Z-DON (150 μM) or R283 (200 μM) before the addition of NGF (100 ng/ml). Following stimulation with NGF, cells were fixed with 3.7% (w/v) paraformaldehyde and permeabilised with 0.1% (v/v) Triton-X100 both in PBS for 15 min at room temperature. After washing, cells were blocked with 3% (w/v) BSA for 1 h at room temperature and the transglutaminase mediated biotin-X-cadaverine labelled protein substrates detected by (1:200 v/v) FITC-conjugated ExtrAvidin® (Sigma-Aldrich Co. Ltd., UK). The chamber slide was subsequently washed three times for 5 min with PBS, air-dried and mounted with Vectashield® medium (Vector Laboratories Ltd, Peterborough, UK) containing DAPI counterstain for nuclei visualisation. Finally slides were sealed using clear, colourless nail varnish and stained cells visualised using a Leica TCS SP5 II confocal microscope (Leica Microsystems, GmbH, Manheim, Germany) equipped with a 20× air objective. Optical sections were typically 1–2 μm and the highest fluorescence intensity values were acquired and fluorescence intensity relative to DAPI stain quantified for each field of view. Saturation was

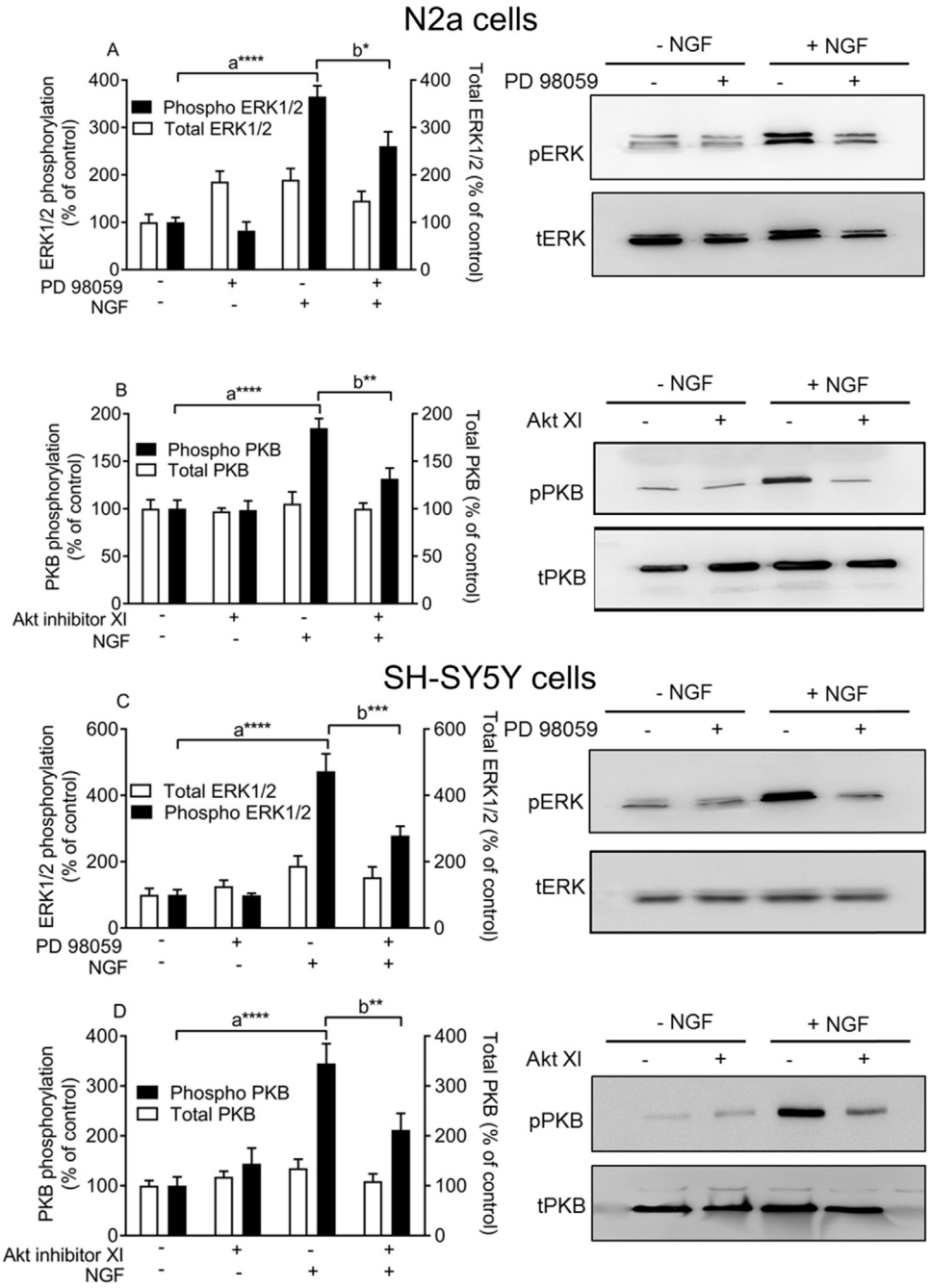

Fig. 6. Effect of PD 98959 and Akt inhibitor XI on NGF-induced ERK1/2 and PKB activation in differentiating N2a and SH-SY5Y cells. Where indicated, cells were pre-treated for 30 min with (A, C) PD 98059 (50 μM) or (B, D) Akt Inhibitor XI (100 nM) prior to stimulation with NGF (100 ng/ml) for 1 h. Cell lysates were analysed by Western blotting for activation of ERK1/2 and PKB using phospho-specific antibodies. Samples were subsequently analysed on separate blots using an antibodies that recognize total ERK1/2 and PKB. Quantified data are expressed as the percentage of the value for control cells (= 100%) in the absence of protein kinase inhibitor and represent the mean ± S.E.M. of four independent experiments. $^{*}P < 0.05$, $^{**}P < 0.01$, $^{***}P < 0.001$ and $^{****}P < 0.0001$, (a) versus control and (b) versus NGF.

avoided using the look-up Table overlay provided by the software. Image analysis and quantification were carried out using Leica LAS AF software.

2.11. Statistical analysis

All graphs and statistics (one-way ANOVA followed by Dunnet's multiple comparison test and two-way ANOVA for group comparison) were performed using GraphPad Prism® software (GraphPad Software, Inc., USA). Results represent mean ± S.E.M. and P values < 0.05 were considered statistically significant.

3. Results

3.1. Effect of NGF on TG2 activity

We have recently reported that TG1, TG2 and TG3 protein expression increased significantly in N2a cells induced to differentiate with retinoic acid (Algarni et al., 2017). In this study, Western blot analysis revealed that mitotic SH-SY5Y cells expressed comparable levels of TG1, TG2 and TG3, and only TG2 expression significantly increased following retinoic acid induced differentiation (Fig. 1).

TG2 catalyses two types of transamidation, namely (i) intra-, and/or inter-molecular covalent cross-links between protein-bound glutamine and protein-bound lysine residues, and (ii) cross-links between primary amines and protein-bound glutamine (Nurminskaya and Belkin, 2012). NGF treatment of differentiating N2a cells produced transient increases in TG2-catalysed biotin-cadaverine incorporation and protein cross-linking activity, peaking at 1 h (Fig. 2A and B). Furthermore, NGF also stimulated concentration-dependent increases in biotin-amine incorporation activity (Fig. 2C) and protein cross-linking activity (Fig. 2D). It is important to demonstrate in vitro changes in more than one cell model, because in cell culture studies there is always a risk that recorded effects may be unique to a specific cell line or due to genetic drift or clonal/species related effects. In order to confirm these observations in another cell model, the ability of NGF to stimulate TG2 activation in differentiating human SH-SY5Y neuroblastoma cells was

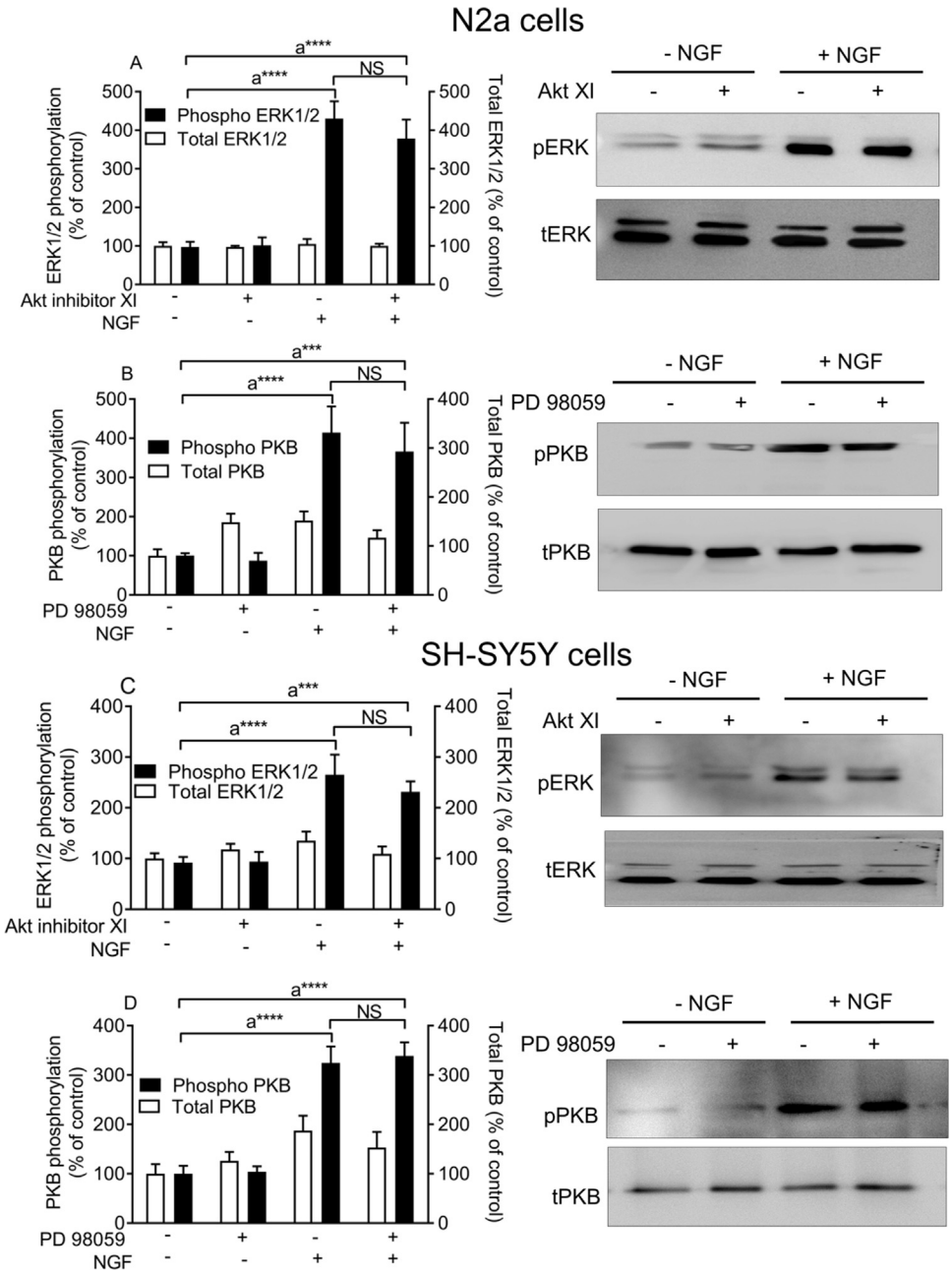

Fig. 7. Effect of Akt inhibitor XI and PD 98959 on NGF-induced ERK1/2 and PKB activation in differentiating N2a and SH-SY5Y cells. Where indicated, cells were pre-treated for 30 min with (A, C) Akt Inhibitor XI (100 nM) or (B, D) PD 98059 (50 μM) prior to stimulation with NGF (100 ng/ml) for 1 h. Cell lysates were analysed by Western blotting for activation of ERK1/2 and PKB using phospho-specific antibodies. Samples were subsequently analysed on separate blots using an antibodies that recognize total ERK1/2 and PKB. Quantified data are expressed as the percentage of the value for control cells (= 100%) in the absence of protein kinase inhibitor and represent the mean ± S.E.M. of four independent experiments. *** $P < 0.001$ and **** $P < 0.0001$, (a) versus control. NS = not significant.

also investigated. NGF treatment of SH-SY5Y cells produced transient increases in TG2 catalysed biotin-cadaverine incorporation and protein cross-linking activity, peaking at 1 h (Fig. 3A and B). Furthermore, NGF also stimulated concentration-dependent increases in biotin-amine incorporation activity (Fig. 3C) and protein cross-linking activity (Fig. 3D) in SH-SY5Y cells. To confirm that the observed increase in NGF-induced TG2 activation is not simply a consequence of increased levels of TG2 protein expression, the level of TG2 protein was monitored by Western blotting. The data obtained indicate no significant change in the level of TG2 protein expression during the time course (up to 4 h) of NGF treatment in N2a and SH-SY5Y cells (Fig. 4). Overall, these data indicate that NGF stimulates robust TG2-mediated transamidase activity in differentiating N2a and SH-SY5Y cells.

3.2. Effect of TG2 inhibitors on NGF induced TG2 activity

To confirm that TG2 was responsible for NGF-mediated transglutaminase activity, two structurally different cell permeable TG2 specific inhibitors were tested; R283 (a small molecule; Freund et al., 1994) and Z-DON (peptide-based; Schaertl et al., 2010). Cells were pre-treated for 1 h with Z-DON (150 μM) or R283 (200 μM) prior to stimulation with NGF (100 ng/ml) for 1 h. Both inhibitors completely blocked NGF-induced TG-mediated amine incorporation (Fig. 5A and C) and protein cross-linking activity (Fig. 5B and D). It is important to note that despite these TG2 inhibitors being cell-permeable, inhibition of cellular TG2 is only achieved at concentrations significantly above their IC_{50} value versus purified enzyme (Schaertl et al., 2010; Freund et al., 1994).

3.3. The effect of ERK1/2, PKB and PKC inhibitors on NGF-induced TG2 activity

NGF triggers the activation of multiple signalling pathways including PI-3K/PKB, ERK1/2, and PKC (Wang et al., 2014). In this study, NGF-induced ERK1/2 and PKB activation was assessed by Western blotting using phospho-specific antibodies that recognize phosphorylated motifs within activated ERK1/2 (pTEpY) and PKB (S^{473}). As

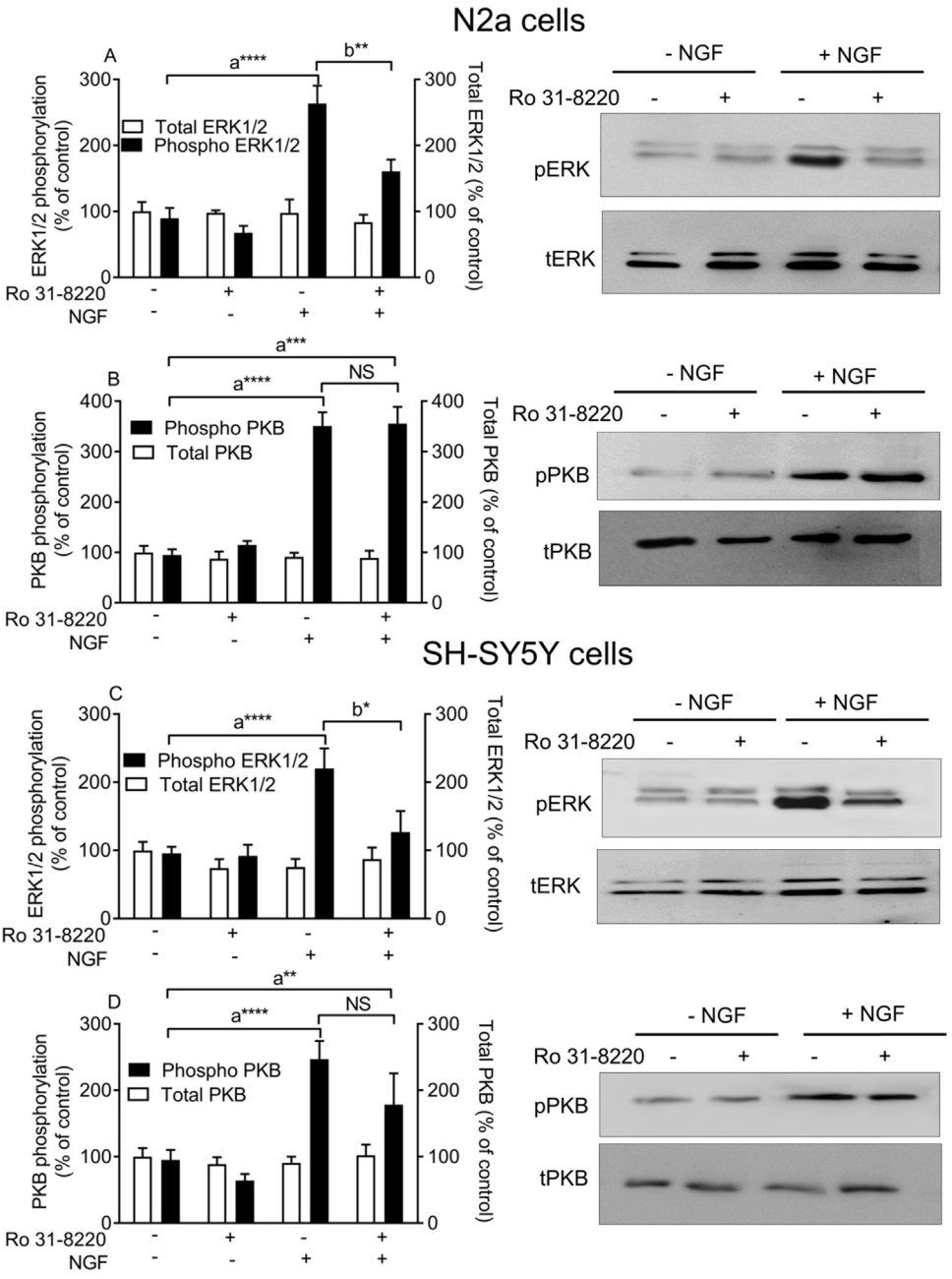

Fig. 8. Effect of the protein kinase C inhibitor Ro 31-8220 on NGF-induced ERK1/2 and PKB activation in differentiating N2a and SH-SY5Y cells. Where indicated, cells were pre-treated for 30 min Ro 31-8220 (10 μM) prior to stimulation with NGF (100 ng/ml) for 1 h. Cell lysates were analysed by Western blotting for activation of ERK1/2 (panels A and C) and PKB (panels B and D) using phospho-specific antibodies. Samples were subsequently analysed on separate blots using an antibodies that recognize total ERK1/2 and PKB. Quantified data are expressed as the percentage of the value for control cells (= 100%) in the absence of protein kinase inhibitor and represent the mean ± S.E.M. of four independent experiments. $^{*}P < 0.05$, $^{**}P < 0.01$, $^{***}P < 0.001$ and $^{****}P < 0.0001$, (a) versus control and (b) versus NGF. NS = not significant.

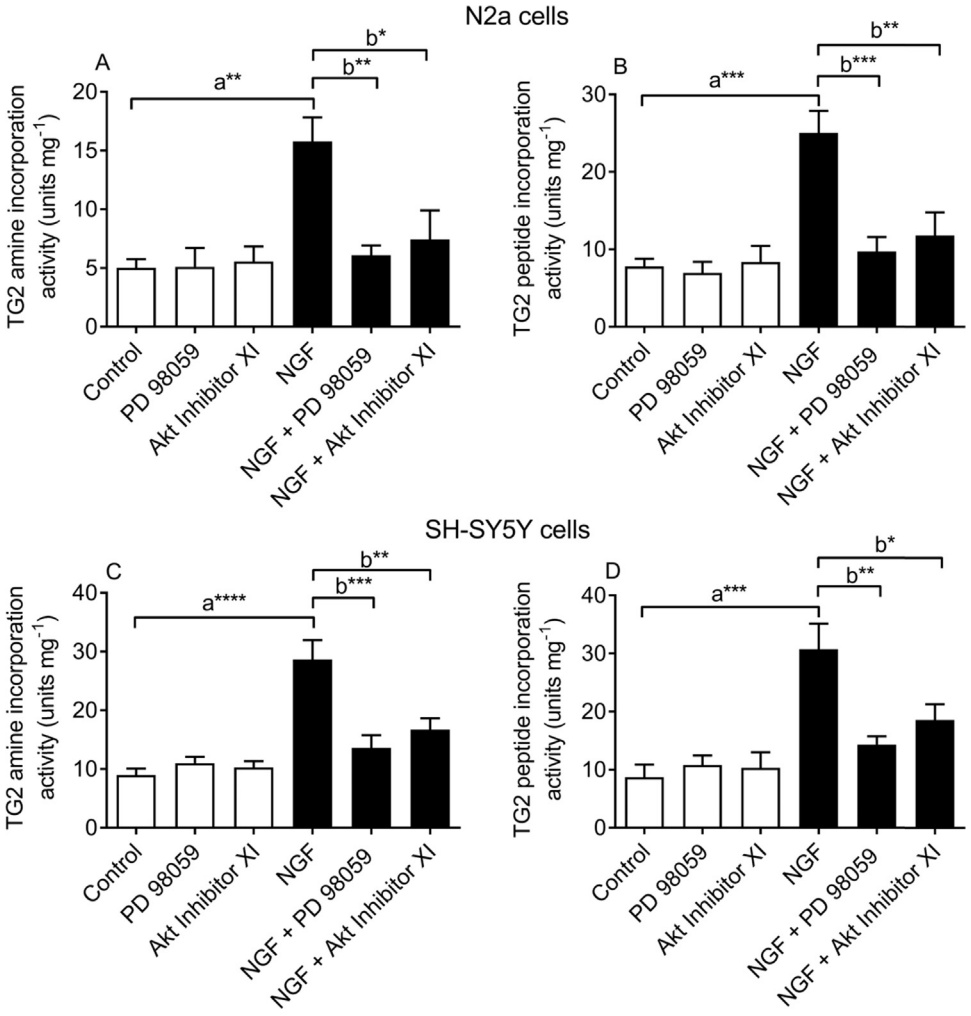

Fig. 9. Effect of ERK1/2 and PKB inhibition on NGF-induced TG activity. Differentiating N2a and SH-SY5Y cells were pretreated for 30 min with PD 98059 (50 μM) or Akt inhibitor XI (100 nM) prior to 1 h stimulation with NGF (100 ng/ml). Cell lysates subjected to biotin-cadaverine incorporation (A, C, E) or protein cross-linking assay (B, D, F). Data points represent the mean TG specific activity ± S.E.M. from four independent experiments. *$P < 0.05$, ** $P < 0.01$, *** $P < 0.001$ and **** $P < 0.0001$, (a) versus control and (b) versus NGF alone.

expected, NGF (100 ng/ml) stimulated robust increases in ERK1/2 and PKB phosphorylation in differentiating N2a (Fig. 6A and B) and SH-SY5Y cells (Fig. 6C and D). NGF-mediated increases in ERK1/2 and PKB were inhibited by PD 98059 (50 μM; MEK1/2 inhibitor) and Akt Inhibitor XI (100 nM; PKB inhibitor) respectively (Fig. 6). Furthermore, NGF-induced increases in ERK1/2 and PKB were insensitive to Akt Inhibitor XI (Fig. 7A and C) and PD 98059 (Fig. 7B and D), respectively suggesting inhibitor selectivity and lack of "cross-talk" between the two kinase pathways. Previous studies have reported an up-stream role of PKC isozymes in NGF-induced ERK1/2 activation (Lloyd and Wooten, 1992; Wooten et al., 2000). Hence in this study we determined if pharmacological inhibition of PKC with Ro 31-8220 modulates NGF-induced ERK1/2 activation in N2a and SH-SY5Y cells. Treatment with Ro 31-8220 (10 μM) attenuated NGF-induced ERK1/2 activation in both cell lines (Fig. 8A and C) suggesting that NGF activates PKC in N2a and SH-SY5Y cells. Finally, Ro 31-8220 did not block NGF-induced PKB activation (Fig. 8B and D).

The role of ERK1/2, PKB and PKC in NGF-induced TG2 activation was determined using pharmacological inhibitors of these protein kinases. NGF-induced transglutaminase-mediated amine incorporation activity and protein cross-linking activity were inhibited by PD 98950 (MEK1 inhibitor; 50 μM; Fig. 9), Akt inhibitor XI (100 nM; Fig. 9), and PKC inhibitor Ro 31-8220 (10 μM; Fig. 10A–D) suggesting the involvement of ERK1/2, PKB and PKC, respectively. Overall, these data suggest that NGF stimulates TG2 activity in differentiating N2a and SH-SY5Y cells via a multi protein kinase-dependent pathway.

3.4. The role of Ca^{2+} in NGF-induced TG2 activation

The transamidating activity of TG2 is a Ca^{2+}-dependent (Nurminskaya and Belkin, 2012; Eckert et al., 2014). Hence we examined the role of Ca^{2+} in NGF-induced TG2 activation. The involvement of extracellular Ca^{2+} was determined by measuring TG2 stimulation in the absence of extracellular Ca^{2+} using Ca^{2+}-free Hanks/HEPES buffer containing 0.1 mM EGTA. Removal of extracellular Ca^{2+} moderately inhibited NGF-induced TG2 transamidation activity in N2a and SH-SY5Y cells (Fig. 10E–H). To ascertain the role of intracellular Ca^{2+}, measurements of TG2 activation were also implemented using cells loaded with the Ca^{2+} chelator BAPTA-AM (50 μM for 30 min) in the absence of extracellular Ca^{2+}. Loading cells with BAPTA, in the continued absence of extracellular Ca^{2+}, did not lead to further attenuation of NGF-induced TG2 activation (Fig. 10E–H). These data indicate that NGF-induced TG2 activation is partially dependent upon extracellular Ca^{2+}. Finally, we assessed whether NGF triggers changes in intracellular Ca^{2+} using the fluorescent Ca^{2+} indicator Fluo-8. NGF did not trigger measurable increases in intracellular Ca^{2+} in N2a and SH-SY5Y cells loaded with Fluo-8AM (data not shown).

3.5. Visualisation of in situ TG2 activity following NGF treatment

Biotin-X-cadaverine, is a cell penetrating primary amine, which enables the in situ visualisation of endogenous protein substrates of TG2, when combined with FITC-ExtrAvidin® (Lee et al., 1993). In N2a and SH-SY5Y cells, NGF (100 ng/ml) stimulated the incorporation of

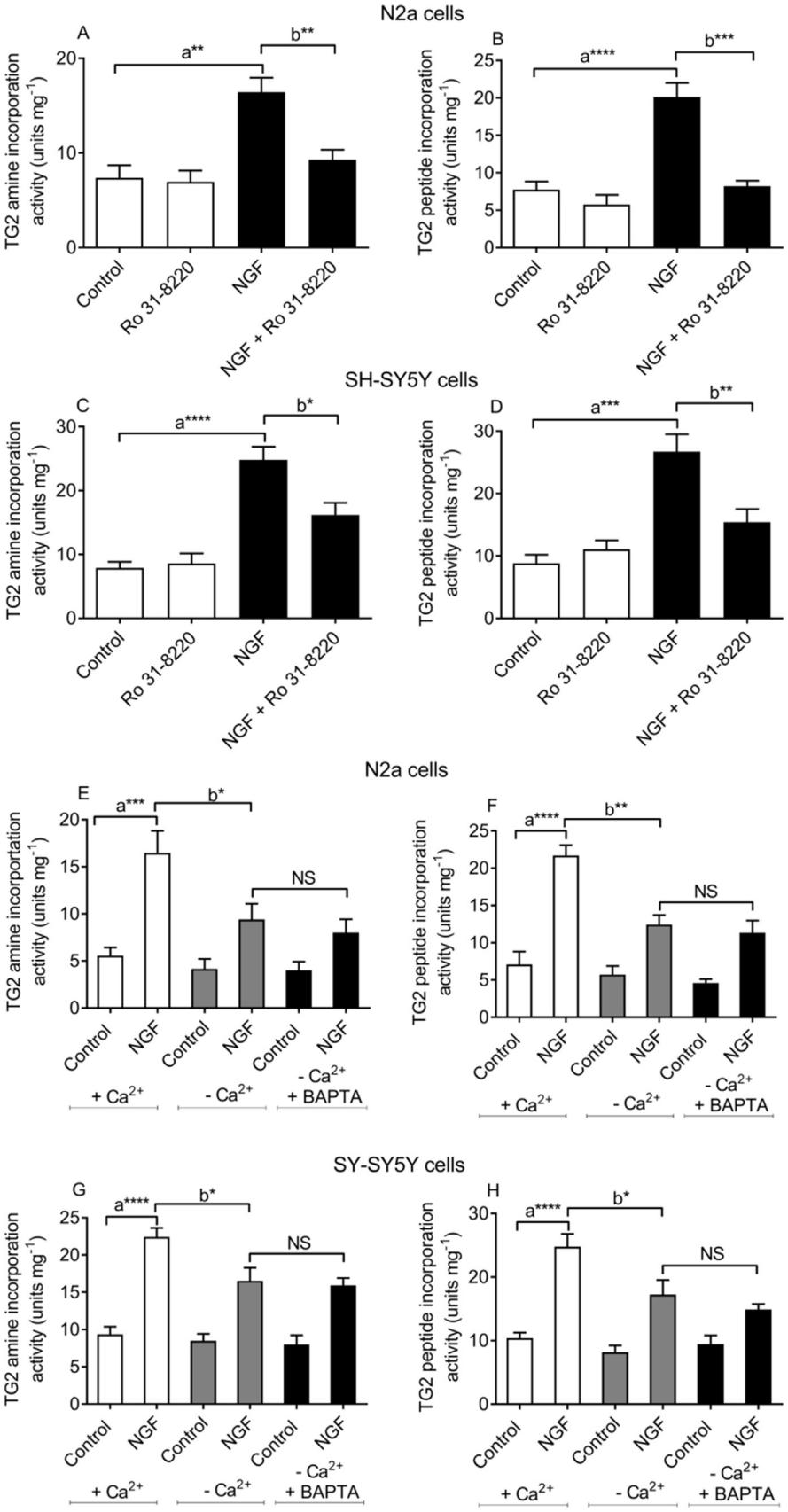

Fig. 10. Effect of PKC inhibition and role of Ca^{2+} in NGF-induced TG2 activation in differentiating N2a and SH-SY5Y cells. In panels (A)–(D) cells were pretreated for 30 min with Ro 31-8220 (10 μM) prior to 1 h stimulation with NGF (100 ng/ml). In panels (E)–(H) cells were stimulated for 1 h with NGF (100 ng/nml) either in the presence (1.8 mM $CaCl_2$) or absence of extracellular Ca^{2+} (nominally Ca^{2+}-free Hanks/HEPES buffer containing 0.1 mM EGTA). Experiments were also performed using cells pre-incubated for 30 min with 50 μM BAPTA/AM and in the absence of extracellular Ca^{2+} (nominally Ca^{2+}-free Hanks/HEPES buffer containing 0.1 mM EGTA) to chelate intracellular Ca^{2+}. Cell lysates were subjected to biotin-cadaverine incorporation assay (A, C, E, G) or protein cross-linking assay (B, D, F, H). Data points represent the mean TG specific activity ± S.E.M. from four independent experiments. *$P < 0.05$, ** $P < 0.01$, *** $P < 0.001$ and **** $P < 0.0001$, (a) versus control, (b) versus NGF alone and in the presence of extracellular Ca^{2+}. Not significant (NS) versus NGF in the absence of extracellular Ca^{2+}.

biotin-X-cadaverine into endogenous protein substrates of TG2 (Figs. 11 and 12). Furthermore, the in situ responses to NGF in both cell lines were attenuated by the TG2 inhibitors Z-DON and R283, the protein kinase inhibitors PD 98059, Akt Inhibitor XI and Ro 31-8220 and following removal of extracellular Ca^{2+} (Figs. 11 and 12). Overall, these data indicate a similar pattern of TG2 activation in live cells.

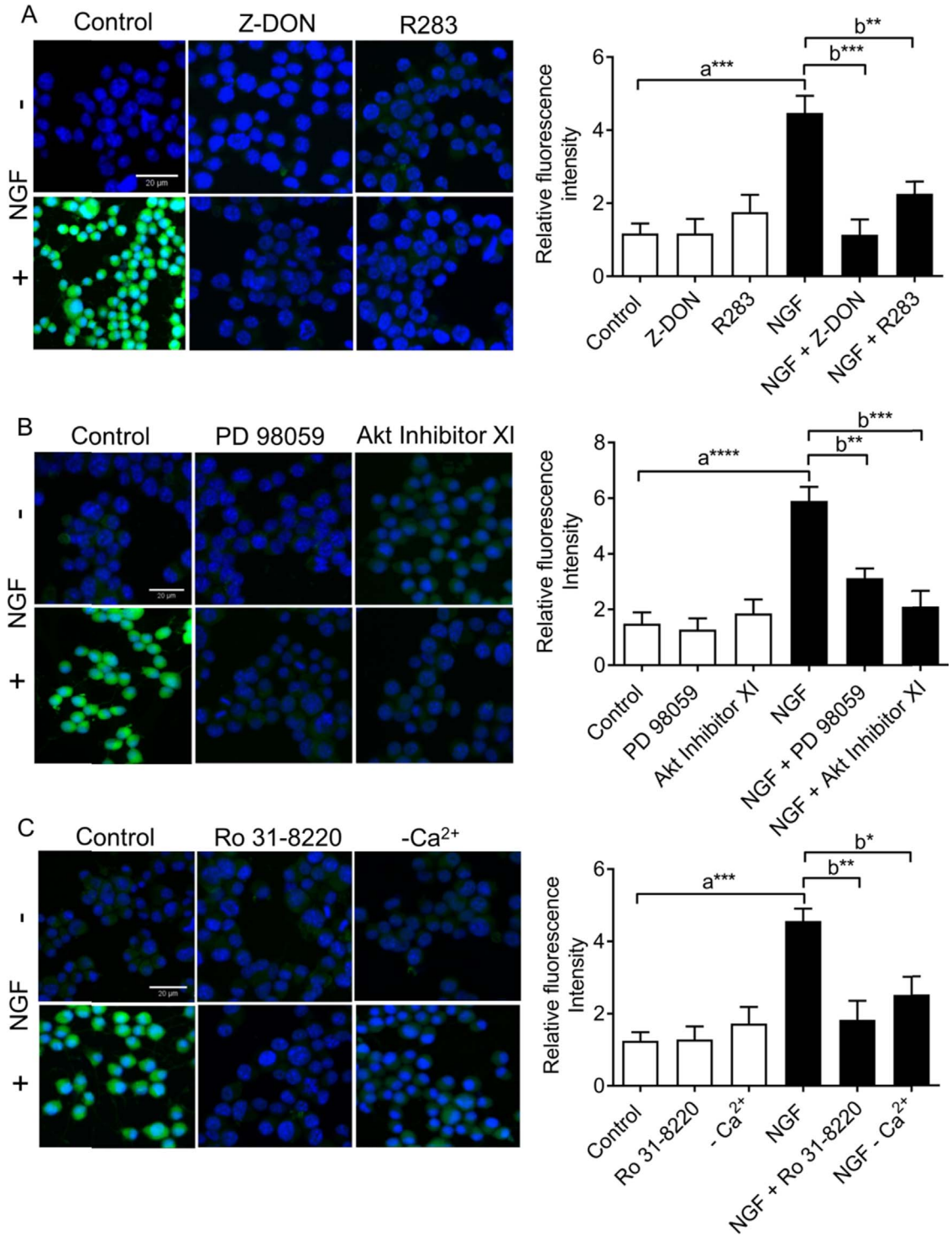

Fig. 11. NGF-induced in situ TG activity in differentiating N2a cells. Cells were incubated with 1 mM biotin-X-cadaverine (BTC) for 6 h, after which they were incubated with (A) TG2 inhibitors Z-DON (150 µM) and R283 (200 µM) for 1 h, (B) PD 98059 (50 µM) and Akt Inhibitor XI (100 nM) for 30 min, or (C) Ro 31-8220 (10 µM) for 30 min or the absence of extracellular Ca^{2+} (nominally Ca^{2+}-free Hanks/HEPES buffer containing 0.1 mM EGTA) prior to stimulation with NGF (100 ng/ml) for 1 h. TG2-mediated biotin-X-cadaverine incorporation into intracellular proteins was visualised using FITC-conjugated ExtrAvidin® (green). Nuclei were stained with DAPI (blue) and viewed using a Leica TCS SP5 II confocal microscope (20× objective magnification). Scale bar = 20 µm. Images presented are from one experiment and representative of three. Quantified data represent the mean ± S.E.M. of fluorescence intensity relative to DAPI stain for five fields of view each from at least three independent experiments. *$P < 0.05$, ** $P < 0.01$, *** $P < 0.001$ and ****$P < 0.0001$ versus control response.

3.6. Role of TG2 in NGF-induced cell survival and neurite outgrowth

The role of TG2 in NGF-induced cell survival was determined in retinoic acid induced differentiating N2a cells and SH-SY5Y cells following exposure of cells to 8 h simulated hypoxia (1% O_2 in glucose-free and serum-free medium; Algarni et al., 2017). Pre-treatment with NGF (100 ng/ml; 1 h) significantly attenuated hypoxia-induced decrease in MTT reduction, release of LDH and activation of caspase-3 in N2a (Fig. 13) and SH-SY5Y (Fig. 14) cells. Furthermore, the TG2 inhibitors R283 and Z-DON attenuated NGF induced cell survival in both

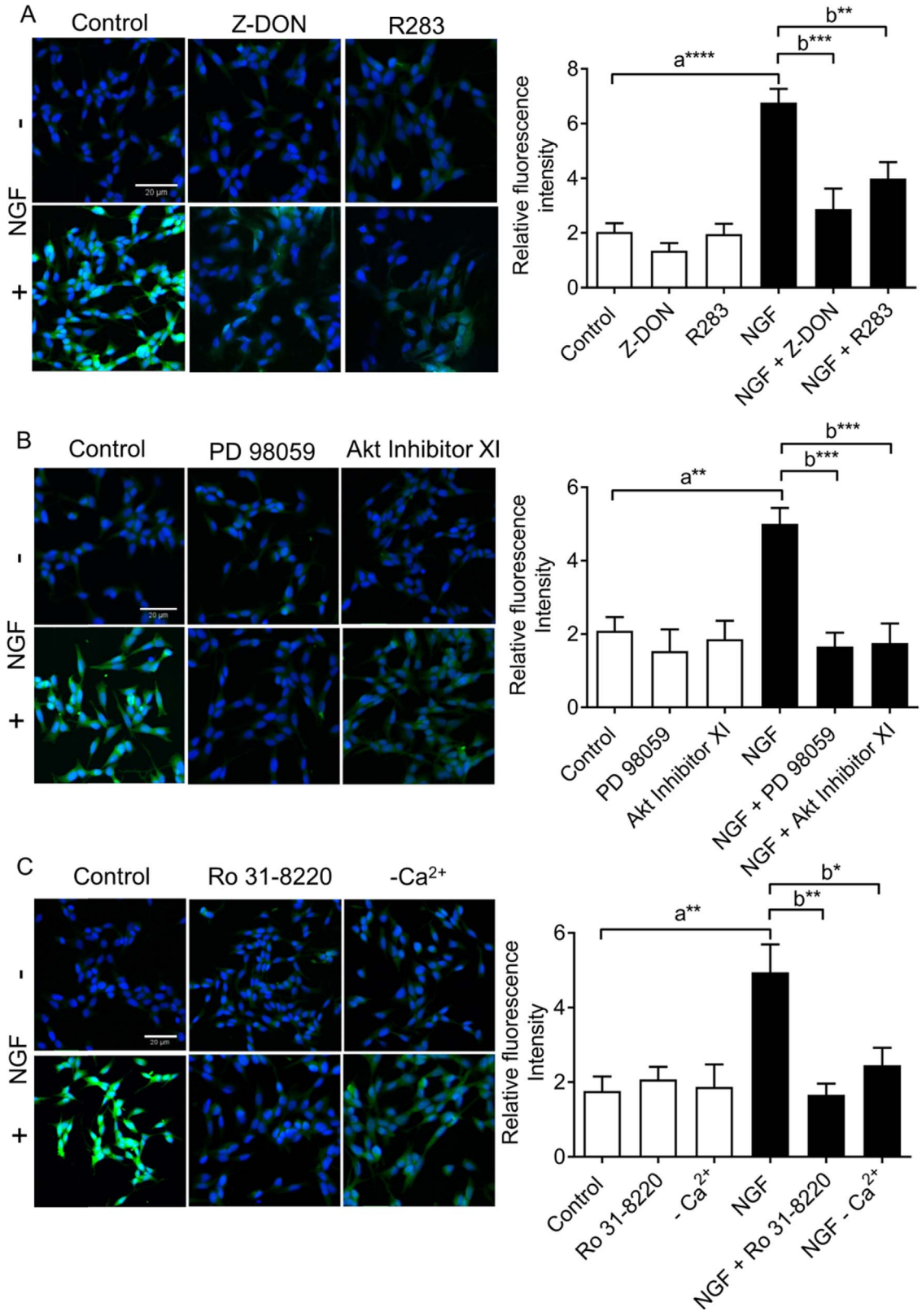

Fig. 12. NGF-induced in situ TG activity in differentiating SH-SY5Y cells. Cells were incubated with 1 mM biotin-X-cadaverine (BTC) for 6 h, after which they were incubated with (A) TG2 inhibitors Z-DON (150 µM) and R283 (200 µM) for 1 h, (B) PD 98059 (50 µM) and Akt Inhibitor XI (100 nM) for 30 min, or (C) Ro 31-8220 (10 µM) for 30 min or the absence of extracellular Ca^{2+} (nominally Ca^{2+}-free Hanks/HEPES buffer containing 0.1 mM EGTA) prior to stimulation with NGF (100 ng/ml) for 1 h. TG2-mediated biotin-X-cadaverine incorporation into intracellular proteins was visualised using FITC-conjugated ExtrAvidin® (green). Nuclei were stained with DAPI (blue) and viewed using a Leica TCS SP5 II confocal microscope (20× objective magnification). Scale bar = 20 µm. Images presented are from one experiment and representative of three. Quantified data represent the mean ± S.E.M. of fluorescence intensity relative to DAPI stain for five fields of view each from at least three independent experiments. *$P < 0.05$, ** $P < 0.01$, *** $P < 0.001$ and ****$P < 0.0001$ versus control response.

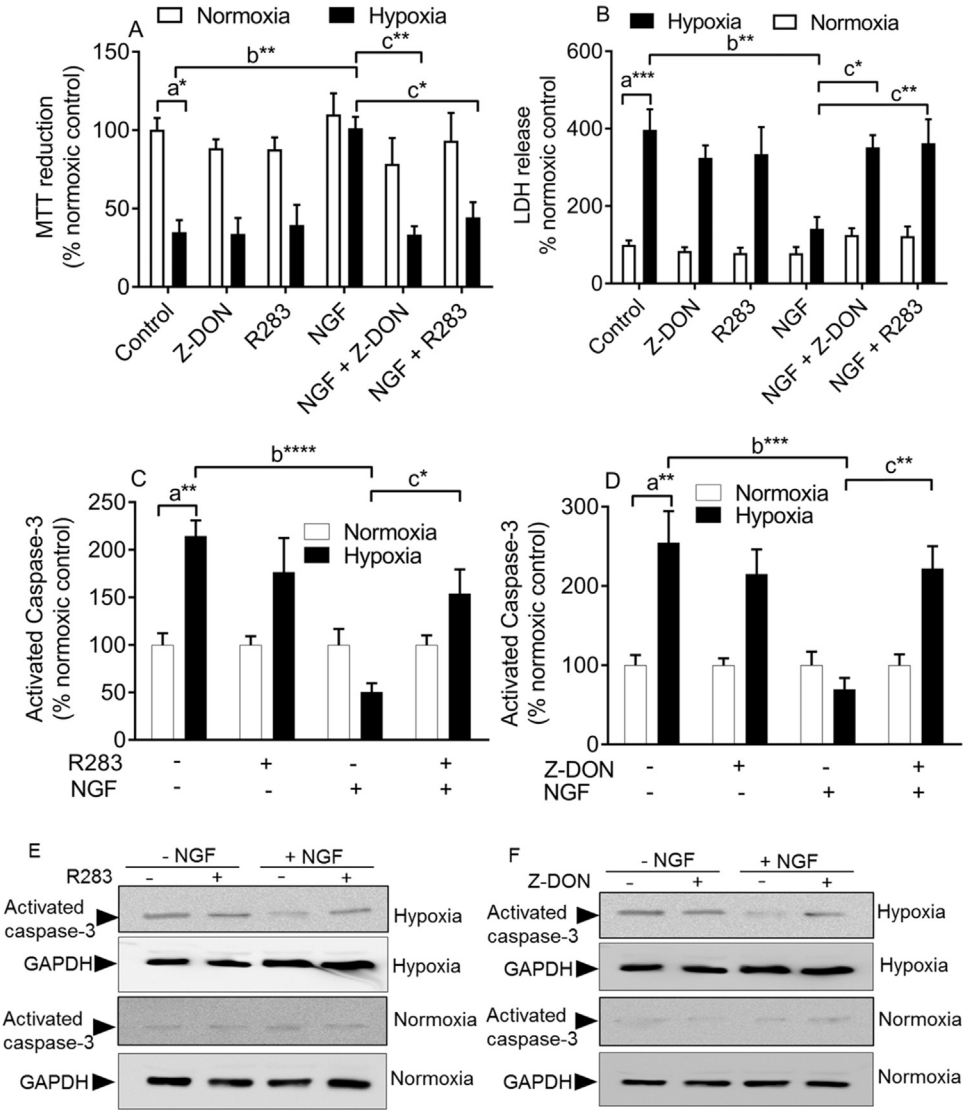

Fig. 13. The effects of the TG2 inhibitors Z-DON and R283 on NGF-induced cell survival against hypoxia-induced cell death in N2a cells. Differentiating N2a cells were pre-treated with NGF (100 ng/ml) for 1 h prior to 8 h hypoxia (1% O_2) or 8 h normoxia. Where indicated cells were pretreated for 1 h with the TG2 inhibitors Z-DON (150 μM) and R283 (200 μM) prior to stimulation with NGF. Cell viability was assessed by measuring (A) the metabolic reduction of MTT by cellular dehydrogenases, (B) release of LDH into the culture medium and (C and D) caspase-3 activity via Western blot analysis using anti-active caspase 3 antibody. Representative Western blots for caspase activation are shown in panels (E) and (F). Levels of GAPDH are shown for comparison. Data are expressed as a percentage of normoxia control cell values (= 100%) and represent the mean ± S.E.M. from four independent experiments, each performed in (a) quadruplicate or (b) sextuplicate. *$P < 0.05$, ** $P < 0.01$, *** $P < 0.001$ and ****$P < 0.0001$, (a) versus normoxia control, (b) versus hypoxia control (c) versus NGF in the presence of hypoxia.

cell lines (Figs. 13 and 14).

The role of TG2 in NGF-induced neurite outgrowth was assessed by high-throughput monitoring of neurite outgrowth following 48 h treatment with NGF (100 ng/ml) in N2a and SH-SY5Y cells. The TG2 inhibitors Z-DON (150 μM) and R283 (200 μM) attenuated maximum neurite outgrowth per cell and average neurite length per cell following treatment with NGF, confirming the involvement of TG2 in N2a (Fig. 15) and SH-SY5Y (Fig. 16) cells. Overall, these data indicate a prominent role for TG2 in NGF-mediated neurite outgrowth.

4. Discussion

The data in this report reveal for the first time that NGF-mediated cell survival and neurite outgrowth are dependent on TG2-mediated transamidase activity.

4.1. In vitro and in situ modulation of TG2 transamidation activity by NGF

NGF mediates neurite outgrowth and neuroprotection; however, it is not known if these events involve NGF-induced TG2 activation (Sofroniew et al., 2001; Huang and Reichardt, 2001; Oe et al., 2005; Condello et al., 2008; Tang et al., 2005). In this study we have shown that short term treatment with NGF (< 4 h) triggered time- and concentration-dependent increases in TG2-mediated biotin-cadaverine incorporation and protein cross-linking activity in differentiating N2a and SH-SY5Y cells. These observations suggest a direct stimulation of TG2 following activation of the TrkA receptor with NGF. It is important to note that levels of TG2 protein expression did not change during this time period (< 4 h). Furthermore, although differentiating N2a and SH-SY5Y cells also express TG1 and TG3 isoforms, NGF-induced increases in TG activity were inhibited by R283 and Z-DON, confirming that the observed increases in TG activity were via TG2. Finally, fluorescence microscopy revealed in situ intracellular TG2 activity following NGF stimulation. The results were comparable to NGF-induced amine incorporation activity observed in vitro. Since the cross-linking activity TG1 is regulated via ERK1/2 and PKC it is conceivable that NGF may modulate the activity of multiple TG isoforms (Bollag et al., 2005).

As detailed in the Introduction, very little is known regarding the regulation of TG2 enzymic activity following receptor tyrosine kinase activation. However, since TG2 transamidase activity modulates protein function by cross-linking and incorporation of small molecule mono- and polyamines into protein substrates, it is likely that activation of TG2 by tyrosine kinase receptors (and in particular other members of the neurotrophin family) plays a major role in the regulation of neuronal cell function (Nurminskaya and Belkin, 2012; Eckert et al., 2014).

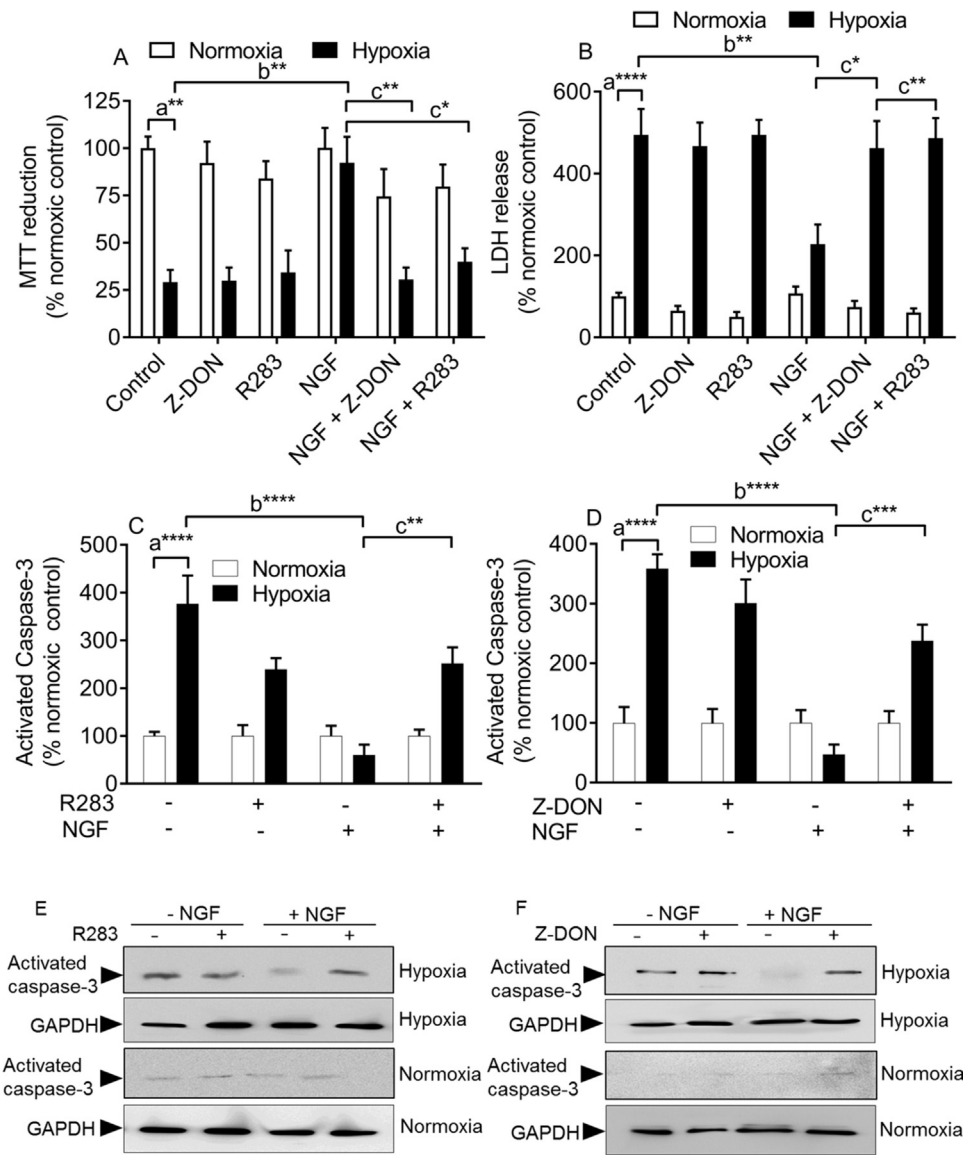

Fig. 14. The effects of the TG2 inhibitors Z-DON and R283 on NGF-induced cell survival against hypoxia-induced cell death in SH-SY5Y cells. Differentiating SH-SY5Y cells were pre-treated with NGF (100 ng/ml) for 1 h prior to 8 h hypoxia (1% O_2) or 8 h normoxia. Where indicated cells were pretreated for 1 h with the TG2 inhibitors Z-DON (150 μM) and R283 (200 μM) prior to stimulation with NGF. Cell viability was assessed by measuring (A) the metabolic reduction of MTT by cellular dehydrogenases, (B) release of LDH into the culture medium and (C and D) caspase-3 activity via Western blot analysis using anti-active caspase 3 antibody. Representative Western blots for caspase activation are shown in panels (E) and (F). Levels of GAPDH are shown for comparison. Data are expressed as a percentage of normoxia control cell values (= 100%) and represent the mean ± S.E.M. from four independent experiments, each performed in (a) quadruplicate or (b) sextuplicate. *$P < 0.05$, ** $P < 0.01$, *** $P < 0.001$ and ****$P < 0.0001$, (a) versus normoxia control, (b) versus hypoxia control (c) versus NGF in the presence of hypoxia.

4.2. Role of protein kinases in NGF-mediated TG2 activation

Increasing evidence suggests that TG2 is regulated by phosphorylation. For example, phosphorylation of TG2 by PKA inhibits its transamidating activity but augments its kinase activity (Mishra et al., 2007), whereas PTEN-induced putative kinase 1 (PINK1) phosphorylation of TG2 inhibits its proteasomal degradation (Min et al., 2015). Furthermore, we have recently shown that stimulation of intracellular TG2 transamidase activity by the A_1 adenosine receptor and PAC_1 receptor is dependent upon ERK1/2, PKC and TG2 phosphorylation (Vyas et al., 2016; Algarni et al., 2017). Since the TrkA receptor stimulates protein kinase cascades involving ERK1/2, PKB and PKC (Wang et al., 2014) we explored the roles of these kinases in NGF-induced TG2 activation. The observation that pharmacological inhibition of ERK1/2, PKB and PKC attenuated NGF-induced TG2 transamidase activity in N2a and SH-SY5Y cells, suggests prominent roles for these protein kinases. These observations are in agreement with our previous studies which have revealed roles for ERK1/2, PKB and PKC in TG2 activation triggered by members of the GPCR family (Vyas et al., 2016, 2017; Algarni et al., 2017). At present it is not known if ERK1/2, PKB and PKC directly phosphorylate TG2, leading to direct enhancement of enzymic activity or whether TG2 phoshorylation promotes its association with interacting proteins. For example, TG2 phosphorylation by PKA promotes its interaction with the scaffolding protein 14-3-3 which leads to the attenuation of TG2 kinase activity (Mishra and Murphy, 2006). Alternatively, these kinases may phosphorylate downstream targets that subsequently interact with TG2, resulting in enhanced activity. Finally, it is important to note that the attenuation of NGF-induced TG2 activation by inhibition of PKC reflects the reported up-stream role of PKC isozymes in NGF-induced ERK1/2 activation (Lloyd and Wooten, 1992; Wooten et al., 2000). Clearly, further studies are required, to establish if NGF activation promotes TG2 phosphorylation and, if so, to subsequently identify the specific site(s).

4.3. Role of Ca^{2+} in NGF-induced TG2 activation

Previous studies have shown that NGF triggers intracellular Ca^{2+} release in C6-2B glioma cells (De Bernardi et al., 1996) and extracellular Ca^{2+} influx in PC12 and bovine chromaffin cells (Pandiella-Alonso et al., 1986). Since TG2 transamidase activity is Ca^{2+} dependent, we investigated the potential involvement of extracellular and intracellular Ca^{2+} in NGF-induced TG2 activation. The data presented indicate that NGF-induced TG2-mediated transamidase activity is partially dependent upon extracellular Ca^{2+}, suggesting that NGF triggers Ca^{2+} influx in N2a and SH-SY5Y cells. However, no measureable increases in intracellular Ca^{2+} were observed following stimulation of

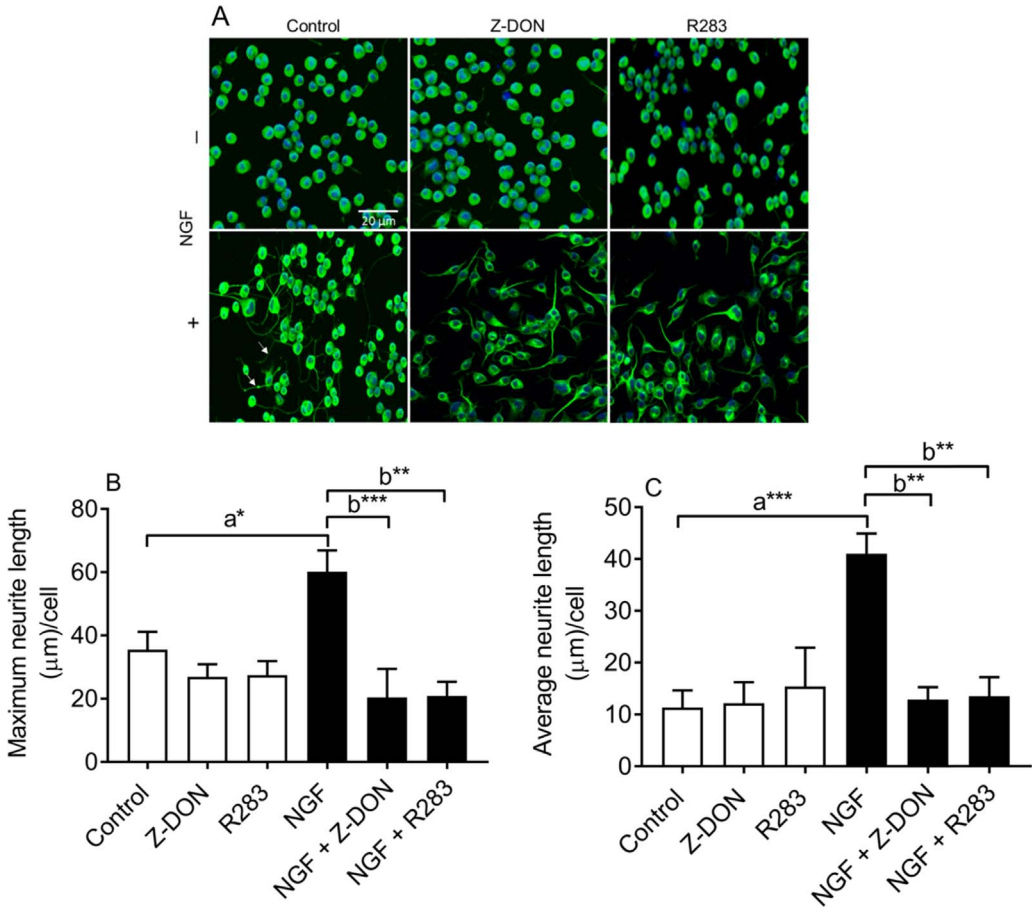

Fig. 15. The effect of TG2 inhibitors on NGF-induced neurite outgrowth in differentiating N2a cells. Cells were incubated for 1 h with the TG2 inhibitors Z-DON (150 µM) or R283 (200 µM) before treatment with NGF (100 ng/ml) in serum-free DMEM for 48 h. (A) Following stimulation high-throughput immunocytochemistry was performed using anti-tubulin antibody and visualised using Alexa Fluor® 488 labelled goat anti-mouse IgG secondary antibody (green). Nuclei were visualised using DAPI counterstain (blue). Images presented are from one experiment and representative of four. High-throughout quantification of (B) the maximum neurite length per cell and (C) the average neurite length per cell as described in Section 2. White arrows indicate typical neurite outgrowths. Data points represent the mean ± S.E.M. from four independent experiments. $^{*}P < 0.05$, $^{**}P < 0.01$ and *** $P < 0.001$ (a) versus mitotic control and (b) versus NGF alone.

these cells with NGF. The reason(s) for this are not currently known but it may reflect localized NGF-induced increases in $[Ca^{2+}]_i$ that were not detectable using the technique employed. Whilst levels of Ca^{2+} required for TG2 activation are typically in the order 3–100 µM, there is evidence that $[Ca^{2+}]_i$ can reach levels sufficient to activate intracellular TG2 (Király et al., 2011). Alternatively, the participation of Ca^{2+} in NGF-induced TG2 activation may necessitate the sensitization of TG2 to low levels of $[Ca^{2+}]_i$. It has been suggested that the interaction of TG2 with protein binding partners and/or membrane lipids promotes a conformational change that enables activation at low levels of intracellular $[Ca^{2+}]$ (Király et al., 2011). Clearly, further studies are required to determine how NGF-induced TG2 activation occurs in the absence of detectable increases in $[Ca^{2+}]_i$, but the kinase-dependent pathways outlined in the present study could be central to these novel aspects of TG2 regulation.

4.4. Role of TG2 in NGF-induced cytoprotection

The role of TG2 in neuronal cell death is controversial with both anti-apoptotic and pro-apoptoric roles reported (Tatsukawa et al., 2016). These opposing roles appear to be dependent upon cell type, trigger mechanism of cell death, intracellular location of TG2 and specific TG2 enzymic activity (Tatsukawa et al., 2016). Examples of TG2-mediated neuronal cell survival include; protection against heat shock–induced cell death in SH-SY5Y cells (Tucholski et al., 2001), protection of rat primary cortical neurons against hypoxia and oxygen/glucose deprivation–induced cell death (Filiano et al., 2008) and in vivo protection against ischaemic stroke (Filiano et al., 2010). TG2 is believed to mediate protection against hypoxia by attenuating HIF-induced activation of pro-apoptotic genes (Filiano et al., 2008, 2010). Furthermore, transamidating activity of TG2 does appear to play a role in protection against oxygen/glucose deprivation–induced cell death (Filiano et al., 2008). Likewise, NGF is widely recognized as a neuroprotective agent and potential therapeutic agent for the treatment of neurodegenerative disorders (Allen et al., 2013). The mechanisms of NGF-induced neuroprotection are complex and involve activation of PI-3K/PKB mediated cell survival signalling (Nguyen et al., 2010). In this study we have shown for the first time a role for TG2 in NGF-induced cytoprotection in differentiating mouse N2a and human SH-SY5Y neuroblastoma cells. However, whilst it is not clear how NGF-induced TG2 activation mediates cell survival, TG2 is known to regulate pathways associated with NGF neuroprotection. For example, TG2 mediates 5-HT induced (serotonylation) of PKB in vascular smooth muscle cells (Penumatsa et al., 2014). However, although the data presented suggest that PKB is up-stream of TG2 (i.e. NGF-induced TG2 activation is blocked by PKB inhibition) it is conceivable that NGF-induced TG2 activation functions to augment and sustain PKB activity. Finally, TG2 inhibition blocked NGF-mediated reduction in hypoxia-induced activation of caspase-3, which is indicative of an anti-apoptotic role. Recent studies have shown that under conditions of Ca^{2+} overload, TG2 inhibits apoptosis via the down-regulation of Bax expression and inhibition of caspase 3 and 9 (Cho et al., 2010). Further work is required to determine the role and mechanisms of TG2 in NGF-induced cell survival.

4.5. Role of TG2 in NGF-induced neurite outgrowth

Previous studies have shown that TG2 is essential for differentiation/neurite outgrowth in human neuroblastoma SH-SY5Y cells (Tucholski et al., 2001; Singh et al., 2003). Furthermore, TG2-mediated neurite outgrowth is dependent upon the transamidating role of TG2 (Tucholski et al., 2001). Postulated mechanisms include the following;

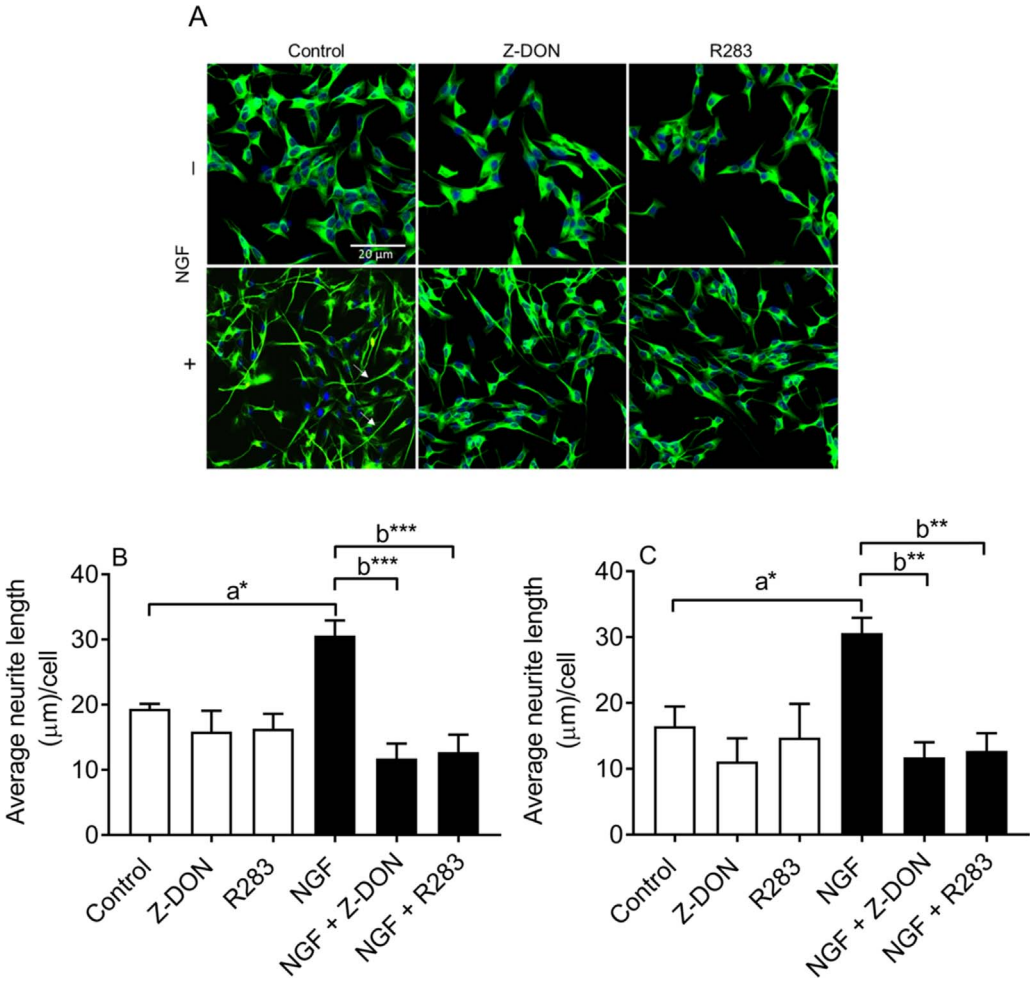

Fig. 16. The effect of TG2 inhibitors on NGF-induced neurite outgrowth in differentiating SH-SY5Y cells. Cells were incubated for 1 h with the TG2 inhibitors Z-DON (150 μM) or R283 (200 μM) before treatment with NGF (100 ng/ml) in serum-free DMEM for 48 h. (A) Following stimulation high-throughput immunocytochemistry was performed using anti-tubulin antibody and visualised using Alexa Fluor® 488 labelled goat anti-mouse IgG secondary antibody (green). Nuclei were visualised using DAPI counterstain (blue). Images presented are from one experiment and representative of four. High-throughout quantification of (B) the maximum neurite length per cell and (C) the average neurite length per cell as described in Section 2. White arrows indicate typical neurite outgrowths. Data points represent the mean ± S.E.M. from four independent experiments. $^{*}P < 0.05$, $^{**}P < 0.01$, and $^{***}P < 0.001$ (a) versus mitotic control and (b) versus NGF alone.

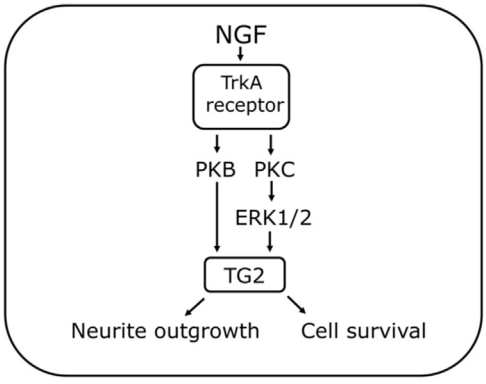

Fig. 17. Schematic representation of the signalling pathways involved in NGF-induced TG2 activation in N2a and SH-SY5Y cells. NGF via the TrkA receptor promotes TG2 transamidase activity in mouse N2a and human SH-SY5Y neuroblastoma cells via a signalling pathway dependent upon PKC, ERK1/2 and PKB. The role of PKC reflects the upstream involvement of PKC in NGF-induced ERK1/2 activation. TG2 is involved in NGF-induced cell survival and neuronal differentiation (neurite outgrowth).

transamidation of RhoA and subsequent activation of ERK1/2, p38 MAPK and JNK (Singh et al., 2003), activation of adenylyl cyclase activity and enhanced phosphorylation of cyclic AMP-response element (CRE) binding protein (CREB; Tucholski and Johnson, 2003), and polyamination of tubulin (Song et al., 2013). Although it is well established that NGF triggers neurite outgrowth in N2a and SH-SY5Y cells, it is not known whether TG2 plays a role in NGF-induced neuronal differentiation (Condello et al., 2008; Oe et al., 2005). In the current study we have shown that pharmacological inhibition of TG2 attenuates NGF-induced neurite outgrowth, suggesting the participation of TG2 in NGF-induced neurite outgrowth. At present it is not known how NGF-mediated TG2 activation promotes neurite outgrowth, but it is conceivable that it may involve modulation of one or more of the pathways described above e.g. TG2-induced modulation of adenylyl cyclase/CREB signalling. Indeed, studies have shown that NGF can modulate cAMP levels in neuronal cells (Nikodijevic et al., 1975; Berg et al., 1995). However, further studies are required to identify the downstream substrates of TG2 and signalling pathways associated with the role of TG2 in NGF-induced neuronal differentiation.

In conclusion, our data show for the first time that TG2 transamidase activity is regulated by NGF in differentiating N2a and SH-SY5Y cells via a ERK1/2, PKB and PKC-dependent pathway (summarised in Fig. 17). Work is currently underway to understand more fully the role of TG2 in NGF signalling and modulation of neuronal cell function.

Acknowledgements and conflicts of interest

This work was supported by a Ph.D. studentship from the Saudi Arabian Government (UMU473). The authors state no conflict of interest.

References

Allen, S.J., Watson, J.J., Shoemark, D.K., Barua, N.U., Patel, N.K., 2013. GDNF, NGF and BDNF as therapeutic options for neurodegeneration. Pharmacol. Ther. 138, 155–175.

Algarni, A.S., Hargreaves, A.J., Dickenson, J.M., 2017. Role of transglutaminase 2 in PAC_1 receptor-mediated protection against hypoxia-induced cell death and neurite outgrowth in differentiating N2a neuroblastoma cells. Biochem. Pharmacol. 128, 55–73.

Barve, V., Ahmed, F., Adsule, S., Banerjee, S., Kulkarni, S., Katiyar, P., Anson, C.E., Powell, A.K., Padhye, S., Sarkar, F.H., 2006. Synthesis, molecular characterization, and biological activity of novel synthetic derivatives of chromen-4-one in human cancer cells. J. Med. Chem. 49, 3800–3808.

Berg, K.A., Maayani, S., McKay, R., Clarke, W.P., 1995. Nerve growth factor amplifies cyclic AMP production in the HT4 neuronal cell line. J. Neurochem. 64, 220–228.

Bollag, W.B., Zhong, X., Dodd, E.M., Hardy, D.M., Zheng, X., Allred, W.T., 2005. Phospholipase D signaling and extracellular signal-regulated kinase-1 and −2 phosphorylation (activation) are required for maximal phorbol-ester-induced transglutaminase activity, a marker of keratinocyte differentiation. J. Pharmacol. Exp. Ther. 312, 1223–1231.

Cho, S.Y., Lee, J.H., Bae, H.D., Jeong, E.M., Jang, G.Y., Kim, C.W., Shin, D.M., Jeon, J.H., Kim, I.G., 2010. Transglutaminase 2 inhibits apoptosis induced by calcium-overload through down-regulation of Bax. Exp. Mol. Med. 42, 639–650.

Condello, S., Caccamo, D., Currò, M., Ferlazzo, N., Parisi, G., Ientile, R., 2008. Transglutaminase 2 and NF-κB interplay during NGF-induced differentiation of neuroblastoma cells. Brain Res. 1207, 1–8.

Dardik, R., Inbal, A., 2006. Complex formation between tissue transglutaminase II (tTG) and vascular endothelial growth factor receptor 2 (VEGFR-2): proposed mechanism for modulation of endothelial cell response to VEGF. Exp. Cell Res. 312, 2973–2982.

Davis, P.D., Hill, C.H., Keech, E., Lawton, G., Nixon, J.S., Sedgewick, A.D., Wadsworth, J., Westmacott, D., Wilkinson, S.E., 1989. Potent selective inhibitors of protein kinase C. FEBS Lett. 259, 61–63.

De Bernardi, M.A., Rabin, S.J., Colangelo, A.M., Brooker, G., Mocchetti, I., 1996. A mediates the nerve growth factor-induced intracellular calcium accumulation. J. Biol. Chem. 271, 6092–6098.

Dudley, D.T., Pang, L., Decker, S.J., Bridges, A.J., Saltiel, A.R., 1995. A synthetic inhibitor of the mitogen-activated protein kinase cascade. Proc. Natl. Acad. Sci. USA 92, 7686–7689.

Dwane, S., Durack, E., Kiely, P.A., 2013. Optimising parameters for the differentiation of SH-SY5Y cells to study cell adhesion and cell migration. BMC Res. Notes 6, 366.

Eckert, R.L., Kaartinen, M.T., Nurminskaya, M., Belkin, A.M., Colak, G., Johnson, G.V.W., Mehta, K., 2014. Transglutaminase regulation of cell function. Physiol. Rev. 94, 383–417.

Filiano, A.J., Bailey, C.D.C., Tucholski, J., Gundemir, S., Johnson, G.V.W., 2008. Transglutaminase 2 protects against ischemic insult, interacts with HIF1β, and attenuates HIF1 signaling. FASEB J. 22, 2662–2675.

Filiano, A.J., Tucholski, J., Dolan, P.J., Colak, G., Johnson, G.V.W., 2010. Transglutaminase 2 protects against ischemic stroke. Neurobiol. Dis. 39, 334–343.

Frampton, G., Invernizzi, P., Bernuzzi, F., Pae, H.Y., Quinn, M., Horvat, D., Galindo, C., Huang, L., McMillin, M., Cooper, B., Rimassa, L., DeMorrow, S., 2012. Interleukin-6-driven progranulin expression increases cholangiocarcinoma growth by an Akt-dependent mechanism. Gut 61, 268–277.

Freund, K.F., Doshi, K.P., Gaul, S.L., Claremon, D.A., Remy, D.C., Baldwin, J.J., Pitzenberger, S.M., Stern, A.M., 1994. Transglutaminase inhibition by 2-[(2-oxopropyl)thio]imidazolium derivatives: mechanism of factor XIIIa inactivation. Biochemistry 33, 10109–10119.

Gundemir, S., Colak, G., Tucholski, J., Johnson, G.V.W., 2012. Transglutaminase 2: a molecular Swiss army knife. Biochim. Biophys. Acta 1823, 406–419.

Huang, E.J., Reichardt, L.F., 2001. Neurotrophins: roles in neuronal development and function. Annu. Rev. Neurosci. 24, 677–736.

Kim, Y.H., Lee, D.H., Jeong, J.H., Guo, Z.S., Lee, Y.J., 2008. Quercetin augments TRAIL-induced apoptotic death: involvement of the ERK signal transduction pathway. Biochem. Pharmacol. 75, 1946–1958.

Király, R., Demény, M.A., Fésüs, L., 2011. Protein transamidation by transglutaminase 2 in cells: a disputed Ca^{2+}-dependent action of a multifunctional protein. FEBS J. 278, 4717–4739.

Lee, I.T., Lin, C.C., Wang, C.H., Cherng, W.J., Wang, J.S., Yang, C.M., 2013. ATP stimulates PGE_2/cyclin D1-dependent VSMCs proliferation via STAT3 activation: role of PKCs-dependent NADPH oxidase/ROS generation. Biochem. Pharmacol. 85, 954–964.

Lee, K.N., Arnold, S.A., Birkbichler, P.J., Patterson Jr, M.K., Fraij, B.M., Takeuchi, Y., Carter, H.A., 1993. Site-directed mutagenesis of human tissue transglutaminase: cys-277 is essential for transglutaminase activity but not for GTPase activity. Biochim. Biophys. Acta 1202, 1–6.

Li, B., Antonyak, M.A., Druso, J.E., Cheng, L., Nikitin, A.Y., Cerione, R.A., 2010. EGF potentiated oncogenesis requires a tissue transglutaminase-dependent signaling pathway leading to Src activation. Proc. Natl. Acad. Sci. USA 107, 1408–1413.

Lilley, G.R., Skill, J., Griffin, M., Bonner, P.L.R., 1998. Detection of Ca^{2+}-dependent transglutaminase activity in root and leaf tissue of monocotyledonous and dicotyledonous plants. Plant Physiol. 117, 1115–1123.

Lloyd, E.D., Wooten, M.W., 1992. pp42/44MAP kinase is a component of the neurogenic pathway utilized by nerve growth factor in PC12 cells. J. Neurochem. 59, 1099–1109.

Min, B., Kwon, Y.C., Choe, K.M., Chung, K.C., 2015. PINK1 phosphorylates transglutaminase 2 and blocks its proteasomal degradation. J. Neurosci. Res. 93, 722–735.

Mishra, S., Murphy, L.J., 2006. Phosphorylation of transglutaminase 2 by PKA at Ser216 creates 14.3.3 binding sites. Biochem. Biophys. Res. Commun. 347, 1166–1170.

Mishra, S., Melino, G., Murphy, L.J., 2007. Transglutaminase 2 kinase activity facilitates protein kinase A-induced phosphorylation of retinoblastoma protein. J. Biol. Chem. 282, 18108–18115.

Montejo-López, W., Rivera-Ramírez, N., Escamilla-Sánchez, J., García-Hernández, U., Arias-Montaño, J.A., 2016. Heterologous, PKC-mediated desensitization of human histamine H_3 receptors expressed in CHO-K1 cells. Neurochem. Res. 41, 2415–2424.

Mosmann, T., 1983. Rapid colorimetric assay for cellular growth and survival – application to proliferation and cyto-toxicity assays. J. Immunol. Methods 65, 55–63.

Nguyen, T.L.X., Kim, C.K., Cho, J.H., Lee, K.H., Ahn, J.Y., 2010. Neuroprotection signaling pathway of nerve growth factor and brain-derived neurotrophic factor against staurosporine induced apoptosis in hippocampal H19-7 cells. Exp. Mol. Med. 42, 583–595.

Nikodijevic, B., Nikodijevic, O., Yu, M.Y.W., Pollard, H., Guroff, G., 1975. The effect of nerve growth factor on cyclic AMP levels in superior cervical ganglia of the rat. Proc. Natl. Acad. Sci. USA 72, 4769–4771.

Nurminskaya, M.V., Belkin, A.M., 2012. Cellular functions of tissue transglutaminase. Int. Rev. Cell Mol. Biol. 294, 1–97.

Oe, T., Sasayama, T., Nagashima, T., Muramoto, M., Yamazaki, T., Morikawa, N., Okitsu, O., Nishimura, S., Aoki, T., Katayama, Y., Kita, Y., 2005. Differences in gene expression profile among SH-SY5Y neuroblastoma subclones with different neurite outgrowth responses to nerve growth factor. J. Neurochem. 94, 1264–1276.

Pandiella-Alonso, A., Malgaroli, A., Vicentini, L.M., Meldolesi, J., 1986. Early rise of cytosolic Ca^{2+} induced by NGF in PC12 and chromaffin cells. FEBS Lett. 208, 48–51.

Penumatsa, K., Abualkhair, S., Wei, L., Warburton, R., Preston, I., Hill, N.S., Watts, S.W., Fanburg, B.L., Toksoz, D., 2014. Tissue transglutaminase promotes serotonin-induced AKT signalling and mitogenesis in pulmonary vascular smooth muscle cells. Cell. Signal. 26, 2818–2825.

Perry, M.J., Mahoney, S.A., Haynes, L.W., 1995. Transglutaminase C in cerebellar granule neurons: regulation and localization of substrate cross-linking. Neuroscience 65, 1063–1076.

Price, R.D., Yamaji, T., Matsuoka, N., 2003. FK506 potentiates NGF-induced neurite outgrowth *via* the Ras/Raf/MAP kinase pathway. Br. J. Pharmacol. 140, 825–829.

Rybchyn, M.S., Slater, M., Conlgrave, A.D., Mason, M.S., 2011. An Akt-dependent increase in canonical Wnt signaling and a decrease in sclerostin protein levels are involved in strontium ranelate-induced osteogenic effects in human osteoblasts. J. Biol. Chem. 286, 23771–23779.

Schaertl, S., Prime, M., Wityak, J., Dominguez, C., Munoz-Sanjuan, I., Pacifici, R.E., Courtney, S., Scheel, A., MacDonald, D., 2010. A profiling platform for the characterization of transglutaminase 2 (TG2) inhibitors. J. Biomol. Screen. 15, 478–487.

Singh, U.S., Pan, J., Kao, Y.-L., Joshi, S., Young, K.L., Baker, K.M., 2003. Tissue transglutaminase mediates activation of RhoA and MAP kinase pathways during retinoic acid-induced neuronal differentiation of SH-SY5Y cells. J. Biol. Chem. 278, 391–399.

Slaughter, T.F., Achyuthan, K.E., Lai, T.S., Greenberg, C.S., 1992. A microtiter plate transglutaminase assay utilizing 5-(biotinamido) pentylamine as substrate. Anal. Biochem. 205, 166–171.

Smith, P.K., Krohn, R.I., Hermanson, G.T., Mallia, A.K., Gartner, F.H., Provenzano, M.D., Fujimoto, E.K., Goeke, N.M., Olson, B.J., Klenk, D.C., 1985. Measurement of protein using bicinchoninic acid. Anal. Biochem. 150, 76–85.

Sofroniew, M.V., Howe, C.L., Mobley, W.C., 2001. Nerve growth factor signaling, neuroprotection, and neural repair. Annu. Rev. Neurosci. 24, 1217–1281.

Song, Y., Kirkpatrick, L.L., Schilling, A.B., Helseth, D.L., Chabot, N., Keillor, J.W., Johnson, G.V.W., Brady, S.T., 2013. Transglutaminase and polyamination of tubulin: posttranslational modification for stabilizing axonal microtubules. Neuron 78, 109–123.

Sutter, A.P., Maaser, K., Gerst, B., Krahn, A., Zeitz, M., Scherübl, H., 2004. Enhancement of peripheral benzodiazepine receptor ligand-induced apoptosis and cell cycle arrest of esophageal cancer cells by simultaneous inhibition of MAPK/ERK kinase. Biochem. Pharmacol. 67, 1701–1710.

Tang, L.L., Wang, R., Tang, X.C., 2005. Huperzine A protects SHSY5Y neuroblastoma cells against oxidative stress damage via nerve growth factor production. Eur. J. Pharmacol. 519, 9–15.

Tatsukawa, H., Furutani, Y., Hitomi, K., Kojima, S., 2016. Transglutaminase 2 has opposing roles in the regulation of cellular functions as well as cell growth and death. Cell Death Dis. 7, e2244.

Tucholski, J., Johnson, G.V.W., 2003. Tissue transglutaminase directly regulates adenylyl cyclase resulting in enhanced cAMP-response element-binding protein (CREB) activation. J. Biol. Chem. 278, 26838–26843.

Tucholski, J., Lesort, M., Johnson, G.V.W., 2001. Tissue transglutaminase is essential for neurite outgrowth in human neuroblastoma SH-SY5Ycells. Neuroscience 102, 481–491.

Trigwell, S.M., Lynch, P.T., Griffin, M., Hargreaves, A.J., Bonner, P.L., 2004. An improved colorimetric assay for the measurement of transglutaminase (type II)-(γ-glutamyl) lysine cross-linking activity. Anal. Biochem. 330, 164–166.

Vanella, L., Raciti, G., Barbagallo, I., Bonfanti, R., Abraham, N., Campisi, A., 2015. Tissue transglutaminase expression during neuronal differentiation of human mesenchymal stem cells. CNS Neurol. Disord. Drug Targets 14, 24–32.

Vyas, F.S., Hargreaves, A.J., Bonner, P.L.R., Boocock, D.J., Coveney, C., Dickenson, J.M., 2016. A_1 adenosine receptor-induced phosphorylation and modulation of transglutaminase 2 activity in H9c2 cells: a role in cell survival. Biochem. Pharmacol. 107, 41–58.

Vyas, F.S., Nelson, C.P., Freeman, F., Hargreaves, A.J., Boocock, D.J., Dickenson, J.M., 2017. β_2-Adrenoreceptor-induced modulation of transglutaminase 2 transamidase activity in cardiomyoblasts. Eur. J. Pharmacol. 813, 105–121.

Wang, H., Wang, R., Thrimawithana, T., Little, P.J., Xu, J., Feng, Z.P., Zheng, W., 2014. The nerve growth factor signaling and its potential as therapeutic target for glaucoma. Biomed. Res. Int. 2014, 759473.

Wooten, M.W., Seibenhener, M.L., Neidigh, K.Y.B.W., Vandenplas, M.L., 2000. Mapping of atypical protein kinase C within the nerve growth factor signaling cascade: relationship to differentiation and survival of PC12 cells. Mol. Cell. Biol. 20, 4494–4504.

Zemskov, E.A., Loukinova, E., Mikhailenko, I., Coleman, R.A., Strickland, D.K., Belkin, A.M., 2009. Regulation of platelet-derived growth factor receptor function by integrin-associated cell surface transglutaminase. J. Biol. Chem. 284, 16693–16703.

Biochemical Pharmacology 128 (2017) 55–73

Contents lists available at ScienceDirect

Biochemical Pharmacology

journal homepage: www.elsevier.com/locate/biochempharm

Role of transglutaminase 2 in PAC_1 receptor mediated protection against hypoxia-induced cell death and neurite outgrowth in differentiating N2a neuroblastoma cells

Alanood S. Algarni, Alan J. Hargreaves, John M. Dickenson *

School of Science and Technology, Nottingham Trent University, Clifton Lane, Nottingham NG11 8NS, United Kingdom

ARTICLE INFO

Article history:
Received 30 September 2016
Accepted 3 January 2017
Available online 5 January 2017

Keywords:
PACAP
PAC_1 receptor
Transglutaminase 2
Neuroblastoma cells
Cytoprotection
Neurite outgrowth

ABSTRACT

The PAC_1 receptor and tissue transglutaminase (TG2) play important roles in neurite outgrowth and modulation of neuronal cell survival. In this study, we investigated the regulation of TG2 activity by the PAC_1 receptor in retinoic acid-induced differentiating N2a neuroblastoma cells. TG2 transamidase activity was determined using an amine incorporation and a peptide cross linking assay. *In situ* TG2 activity was assessed by visualising the incorporation of biotin-X-cadaverine using confocal microscopy. TG2 phosphorylation was monitored via immunoprecipitation and Western blotting. The role of TG2 in PAC_1 receptor-induced cytoprotection and neurite outgrowth was investigated by monitoring hypoxia-induced cell death and appearance of axonal-like processes, respectively. The amine incorporation and protein crosslinking activity of TG2 increased in a time and concentration-dependent manner following stimulation with pituitary adenylate cyclase-activating polypeptide-27 (PACAP-27). PACAP-27 mediated increases in TG2 activity were abolished by the TG2 inhibitors Z-DON and R283 and by pharmacological inhibition of protein kinase A (KT 5720 and *Rp*-cAMPs), protein kinase C (Ro 31-8220), MEK1/2 (PD 98059), and removal of extracellular Ca^{2+}. Fluorescence microscopy demonstrated PACAP-27 induced *in situ* TG2 activity. TG2 inhibition blocked PACAP-27 induced attenuation of hypoxia-induced cell death and outgrowth of axon-like processes. TG2 activation and cytoprotection were also observed in human SH-SY5Y cells. Together, these results demonstrate that TG2 activity was stimulated downstream of the PAC_1 receptor via a multi protein kinase dependent pathway. Furthermore, PAC_1 receptor-induced cytoprotection and neurite outgrowth are dependent upon TG2. These results highlight the importance of TG2 in the cellular functions of the PAC_1 receptor.

1. Introduction

Transglutaminases (TGs) are a family of Ca^{2+}-dependent enzymes that catalyse the post-translational modification of proteins (for extensive reviews see [54,20]). There are eight distinct catalytically active members of the TG family which exhibit differential expression (Factor XIIIa and TGs 1–7).

The ubiquitously expressed TG2 is the most widely studied member of the TG family which is involved in the regulation of numerous cellular processes, including cell adhesion, migration, growth, survival, apoptosis, differentiation, and extracellular matrix organization [54]. In neuronal cells, TG2 is involved in neural differentiation, neurite outgrowth and neuroprotection following cerebral ischaemia [69,22,72].

Transglutaminase 2 (TG2) possesses multiple enzymic functions that include transamidation, protein disulphide isomerase and protein kinase activity [25]. The transamidase activity of TG2 is inhibited by GTP/GDP and evidence suggests that TG2 when bound to GTP/GDP functions as a G-protein (known as Gh; [46]), which is independent of its transamidase activity. Indeed, several members of the G-protein coupled receptor (GPCR) family including the α_{1B}-adrenergic receptor, thromboxane A2 receptor and

Abbreviations: BSA, bovine serum albumin; DAG, diacylglycerol; DMEM, Dulbecco's modified Eagle's medium; ERK1/2, extracellular signal-regulated kinases 1 and 2; FITC, fluorescein isothiocyanate; GPCRs, G-protein coupled receptors; HRP, horseradish peroxidase; JNK, c-Jun N-terminal kinase; LDH, lactate dehydrogenase; MAPK, mitogen activated protein kinase; MEK1/2, mitogen-activated protein kinase kinase 1/2; PACAP, pituitary adenylate cyclase-activating polypeptide; PBS, phosphate-buffered saline; PKA, protein kinase A; PKB, protein kinase B; PKC, protein kinase C; SDS-PAGE, sodium dodecyl sulphate polyacrylamide gel electrophoresis.

* Corresponding author.
E-mail address: john.dickenson@ntu.ac.uk (J.M. Dickenson).

http://dx.doi.org/10.1016/j.bcp.2017.01.001
0006-2952/

oxytocin receptor couple to Gh when activated, promoting exchange of GDP for GTP [25]. Activated Gh-GTP stimulates phospholipase C δ1 promoting phosphoinositide hydrolysis and stimulating increases in intracellular Ca^{2+}.

The activity of TG2 and other TG family members can be regulated by protein kinases. For example, phosphorylation of TG2 by protein kinase A (PKA) inhibits its transamidating activity but enhances its kinase activity [49]. The transamidating activity of TG1 (keratinocyte transglutaminase) is enhanced by phorbol ester-induced stimulation of protein kinase C (PKC) and extracellular signal-regulated kinase 1/2 (ERK1/2; [7]. These findings suggest that the activity of TG can be regulated by signalling pathways associated with GPCRs. However, the regulation of intracellular TG2 following stimulation of GPCRs is not well understood. Examples include muscarinic receptor-mediated increases in TG2 activity in SH-SY5Y cells [78], $5\text{-}HT_{2A}$ receptor-mediated transamidation of Rac1 in the rat A1A1v cortical cell line [13] and A_1 adenosine receptor-mediated increases in TG2 transamidase activity in rat H9c2 cardiomyoblasts [74].

Of particular interest to the current study is pituitary adenylate cyclase-activating polypeptide (PACAP), which is widely distributed in the brain and peripheral organs and displays high affinity for the PAC_1 receptor [73]. The PAC_1 receptor is a member of the GPCR superfamily which activates adenylyl cyclase/cAMP/PKA (via G_s-protein coupling) and phospholipase C/DAG/PKC (via G_q-protein coupling) dependent signalling pathways [18,73]. The PAC_1 receptor also triggers the activation of several other protein kinase cascades such as ERK1/2, JNK1/2, p38 MAPK and PKB [51,44,8]. Since some of these protein kinase pathways are associated with modulation of TG activity (PKA, PKC and ERK1/2) it is conceivable that the PAC_1 receptor regulates TG activity. Since mouse N2a neuroblastoma cells express PAC_1 receptors [39,50] the primary aims of this study were (i) to determine whether the PAC_1 receptor modulates TG2 activity in these cells and (ii) to assess the role of TG2 in PAC_1 receptor-induced neuroprotection and neurite outgrowth. The results obtained indicate that PAC_1 receptor stimulation triggers TG2-mediated amine incorporation and protein cross-linking activity in differentiating N2a and SH-SY5Y cells. Furthermore, inhibition of TG2 attenuates PAC_1 receptor-induced cytoprotection and neurite outgrowth.

2. Materials and methods

2.1. Materials

Akt inhibitor XI, KT 5720, Ro-31-8220 and *R*p-8-Cl-cAMPS (adenosine 3′,5′-cyclic monophosphorothioate, 8-chlro-, Rp-isomer) were purchased from Calbiochem (San Diego, CA). [$Ala^{11,22,28}$]-VIP, Bay 55-9837, PACAP-27, PACAP 6-38, PD 98059, SB 203580, and SP 600 125 were obtained from Tocris Bioscience (Bristol, UK). *All-trans* retinoic acid, casein, Protease Inhibitor Cocktail (for use with mammalian cell and tissue extracts), Phosphatase Inhibitor Cocktail 2 and 3, ExtrAvidin®-HRP and ExtrAvidin®-FITC were obtained from Sigma-Aldrich Co. Ltd. (Gillingham, UK). The TG2 inhibitors Z-DON (Z-DON-Val-Pro-Leu-OMe) and R283, together with purified guinea-pig liver TG2 were obtained from Zedira GmbH (Darmstadt, Germany). DAPI was from Vector Laboratories Inc (Peterborough, UK). Fluo-8/AM was purchased from Stratech Scientific Ltd (Newmarket, UK). Biotin-TVQQEL was purchased from Pepceuticals (Enderby, UK). Biotin cadaverine (N-(5-aminopentyl)biotinamide) and biotin-X-cadaverine (5-([(N-(biotinoyl)amino)hexanoyl]amino)pentylamine) were purchased from Invitrogen, UK. Dulbecco's modified Eagle's medium (DMEM), foetal bovine serum, trypsin (10×), L-glutamine (200 mM), penicillin (10,000 U/ml)/streptomycin (10,000 μg/ml) were purchased from BioWhittaker Ltd, UK. All other reagents were purchased from Sigma-Aldrich Co. Ltd. (Gillingham, UK) and were of analytical grade.

Antibodies were obtained from the following suppliers: monoclonal anti-phospho ERK1/2 (Thr^{202}/Tyr^{204}) and polyclonal anti-tyrosine hydroxylase from Sigma-Aldrich; polyclonal anti-phospho PKB (Ser^{473}), polyclonal anti-total PKB, monoclonal anti-total ERK1/2, monoclonal anti-phospho p38 MAPK, polyclonal anti-total p38 MAPK, monoclonal anti-phospho JNK1/2, polyclonal anti-total JNK1/2 and polyclonal anti-cleaved caspase 3 from New England Biolabs Ltd (UK); polyclonal anti-human keratinocyte TG1 and polyclonal anti-human epidermal TG3 from Zedira GmbH (Darmstadt, Germany); monoclonal anti-TG2 (CUB 7402) from Thermo Scientific (Leicestershire, UK); monoclonal anti-GAPDH, polyclonal anti-phosphoserine and polyclonal anti-phosphothreonine from Abcam (Cambridge, UK); polyclonal anti-choline acetyltransferase from Santa Cruz Biotechnology Inc (Heidelberg, Germany).

2.2. Cell culture

Murine N2a and human SH-SY5Y neuroblastoma cells were obtained from the European Collection of Animal Cell Cultures (Porton Down, Salisbury, UK). Cells were cultured in DMEM supplemented with 2 mM L-glutamine, 10% (v/v) foetal bovine serum, penicillin (100 U/ml) and streptomycin (100 μg/ml). Cells were maintained in a humidified incubator (95% air/5% CO_2 at 37 °C) until 70–80% confluent and sub-cultured (1:5 split ratio) every 3–4 days. SH-SY5Y cells were sub-cultured using trypsin (0.05% w/v)/EDTA (0.02% w/v). Differentiation of N2a cells was induced by culturing cells in serum-free DMEM containing 1 μM *all-trans* retinoic acid for 48 h, unless otherwise specified. Differentiation of SH-SY5Y cells was induced by culturing cells in serum-free DMEM containing 10 μM *all-trans* retinoic acid for 5 days. Experiments were performed on passage numbers 8–20 for N2a and 18–25 for SH-SY5Y.

2.3. cAMP accumulation assay

N2a cells (5000 cells $well^{-1}$) were seeded on a white 96 well microtitre plate, with clear bottomed wells (Corning; Fisher Scientific, Loughborough, UK) and induced to differentiate as described above. The medium was then removed and the monolayer treated with a range of concentrations of PACAP-27 for 20 min in serum-free DMEM (40 μl $well^{-1}$) in the presence of 20 mM $MgCl_2$ and 500 μM 3-isobutyl-1-methylxanthine (IBMX). Following stimulation, cAMP levels within cells were determined using the cAMP-Glo™ Max Assay kit (Promega; Southampton, UK). Briefly, 10 μl of cAMP detection solution was added to all wells and incubated for 20 min at room temperature. After incubation, Kinase-Glo® reagent (50 μl $well^{-1}$) was added and incubated for 10 min at room temperature, following which luminescence levels across the plate were recorded using a plate-reading FLUOstar Optima luminometer (BMG Labtech Ltd, UK,). Treatment with forskolin (10 μM) was used as a positive control and the luminescence values were converted to cAMP levels using a cAMP standard curve (0–100 nM), according to the manufacturer's instructions.

2.4. Cell extraction for measurement of TG2 activity

Time course profiles and concentration-response curves were obtained for PACAP-27. Where appropriate, cells were also pre-incubated for 30 min in medium with or without the protein kinase inhibitors *Rp*-cAMPs (PKA, 50 μM; [15]), KT 5720 (PKA, 5 μM; [31]), Akt inhibitor XI (PKB/Akt, 100 nM; [2]), PD 98059 (MEK1/2, 50 μM; [19]), SP 600125 (JNK1/2, 20 μM; [5]), and Ro

31-8220 (PKC, 10 μM; [14]) prior to treatment with 100 nM PACAP-27. The concentrations of protein kinase inhibitors employed in this study were in the range of values in the literature that are used to inhibit the cellular activity of these kinases: KT 5720 (2–10 μM; [77,43]); *Rp*-cAMPs (10–100 μM; [77]); [43,76,56,71]; Ro 31-8220 1–10 μM; [37,52], PD 98059 (10–50 μM; [66,33]), SP 600125 (20 μM; [26,32]) and Akt inhibitor XI (1 μM; [23,59]). In the case of less well known Akt inhibitor XI effects on PKB inhibition were verified by Western blot analysis.

Following stimulation, N2a and SH-SY5Y cells were rinsed twice with 2.0 ml of chilled PBS, lysed with 500 μl of ice-cold lysis buffer (50 mM Tris-HCl pH 8.0, 0.5% (w/v) sodium deoxycholate, 0.1% (v/v) Protease Inhibitor Cocktail, and 1% (v/v) Phosphatase Inhibitor Cocktail 2). Cell lysates were scraped and clarified by centrifugation at 4 °C for 10 min at 14000*g* prior to being assayed for TG activity using the biotin-labeled cadaverine incorporation assay (see below). Supernatants were collected and stored at −80 °C.

Protein levels were determined by the bicinchoninic acid (BCA) protein assay, based on the method of Smith et al. [63], which was performed using a commercially available kit (Sigma-Aldrich, UK) using bovine serum albumin (BSA) as the standard. Transglutaminase activity was monitored by two different transamidase assays; amine incorporation and protein cross-linking.

2.5. Biotin-labeled cadaverine incorporation assay

The assay was performed as per the method described by Slaughter et al. [62] with the modifications of Lilley et al. [40]. Briefly, 96-well microtitre plates were coated overnight at 4 °C with 250 μl of N′,N′-dimethylcasein (10 mg ml^{-1} in 100 mM Tris-HCl, pH 8.0). The plate was washed twice with distilled water and blocked with 250 μl of 3% (w/v) BSA in 100 mM Tris-HCl, pH 8.0 and incubated for 1 h at room temperature. The plate was washed twice before the application of 150 μl of either 6.67 mM calcium chloride and or 13.3 mM EDTA (used to deplete calcium and suppress TG activity) assay buffer containing 225 μM biotin cadaverine (a widely used substrate to monitor TG amine incorporating activity) and 2 mM 2-mercaptoethanol. The reaction was started by the addition of 50 μl of samples or positive control (50 ng/well of guinea-pig liver TG2) and negative control (100 mM Tris-HCl, pH 8.0). After incubation for 1 h at 37 °C plates were washed as before. Then, 200 μl of 100 mM Tris-HCl pH 8.0 containing 1% (w/v) BSA and ExtrAvidin®-HRP (1:5000 dilution) was added to each well and the plate incubated at 37 °C for 45 min then washed as before. The plate was developed with 200 μl of freshly made developing buffer (7.5 μg ml^{-1} 3,3′,5,5′-tetramethylbenzidine (TMB) and 0.0005% (v/v) H_2O_2 in 100 mM sodium acetate, pH 6.0) and incubated at room temperature for 15 min. The reaction was terminated by adding 50 μl of 5 M sulphuric acid and the absorbance read at 450 nm. One unit of TG2 was defined as a change in absorbance of one unit h^{-1}. Each experiment was performed in triplicate.

2.6. Biotin-labeled peptide-cross-linking assay

The assay was performed according to the method of Trigwell et al. [70] with minor modifications. Microtitre plates (96-well) were coated and incubated overnight at 4 °C with casein at 1.0 mg ml^{-1} in 100 mM Tris-HCl pH 8.0 (250 μl per well). The wells were washed twice with distilled water, before incubation at room temperature for 1 h with 250 μl of blocking solution (100 mM Tris-HCl pH 8.0 containing 3% (w/v) BSA). The plate was washed twice before the application of 150 μl of either 6.67 mM calcium chloride and or 13.3 mM EDTA assay buffer containing 5 μM biotin-TVQQEL and 2 mM 2-mercaptoethanol. The reaction was started by the addition of 50 μl of samples or positive control (50 ng/well of guinea-pig liver TG2) and negative control (100 mM Tris-HCl, pH 8.0) and allowed to proceed for 1 h at 37 °C. Reaction development and termination were performed as described for biotin-cadaverine assays. One unit of TG2 was defined as a change in absorbance of one unit h^{-1}. Each experiment was performed in triplicate.

2.7. Hypoxia-induced cell death

Differentiating N2a and SH-SY5Y cells in glucose-free and serum-free DMEM (Gibco™, Life Technologies Ltd, Paisley, UK) were exposed to hypoxia using a hypoxic incubator (5% CO_2/1% O_2 at 37 °C) in which O_2 was replaced by N_2.

2.8. Cell viability assays

N2a and SH-SY5Y cells were plated in 24-well flat bottomed plates (15,000 cells/well) and differentiated for 48 h, before cell viability was determined by measuring the reduction of MTT [53]. The amount of DMSO-solubilised reduced formazan product was determined by measurement of absorbance at a wavelength of 570 nm. Alternatively, cells were plated in 96-well flat bottomed plates (5000 cells per well) and differentiated for 48 h. Following normoxia/hypoxia exposure, the activity of lactate dehydrogenase (LDH) released into the culture medium was detected using the CytoTox 96® non-radioactive cytotoxicity assay (Promega, Southampton, UK) with measurement of absorbance at 490 nm.

2.9. Outgrowth of axon-like processes

The outgrowth of axon-like processes in N2a cells was assessed as described previously [27]. N2a cells were seeded in 24-well plates (25,000 cells/well) and incubated for 24 h in growth medium prior to treatment with PACAP-27 (100 nM) in serum-free DMEM for 24 or 48 h. After stimulation, the cells were washed with ice cold phosphate buffered saline (PBS) then fixed in 90% (v/v) methanol in PBS at −20 °C for 15 min. After washing, the cells were stained for 1 min at room temperature with Coomassie brilliant blue, washed with PBS then with distilled water. The outgrowth of axon-like processes was morphologically assessed using an inverted light microscope. Five randomly selected fields, containing at least 200 cells, were examined in each well. The total number of cells and the number of axon-like processes, defined as extensions greater than two cell body diameters in length with an extension foot [35] were recorded.

2.10. Western blot analysis

Protein extracts (15–20 μg per lane) were separated by SDS-PAGE (10% w/v polyacrylamide gel) using a Bio-Rad Mini-Protean III system. Proteins were transferred to nitrocellulose membranes in a Bio-Rad trans-Blot system using 25 mM Tris, 192 mM glycine pH 8.3 and 20% (v/v) MeOH). Following transfer, the membranes were washed with Tris-buffered saline (TBS) and blocked for 1 h at room temperature with 3% (w/v) skimmed milk powder in TBS containing 0.1% (v/v) Tween-20. Blots were then incubated overnight at 4 °C in blocking buffer with primary antibodies to the following targets (1:1000 dilutions unless otherwise indicated): phospho-specific ERK1/2, phospho-specific PKB (1:500), phospho-specific p38 MAPK, phospho-specific JNK (1:500), cleaved active caspase-3 (1:500), GAPDH, TG1, TG2 or TG3. The primary antibodies were removed and blots washed three times for 5 min in TBS/Tween 20. Blots were then incubated for 2 h at room temperature with the appropriate secondary antibody (1:1000) coupled to horseradish peroxidase (New England Biolabs Ltd; UK) in blocking buffer. Following removal of the secondary antibody, blots were

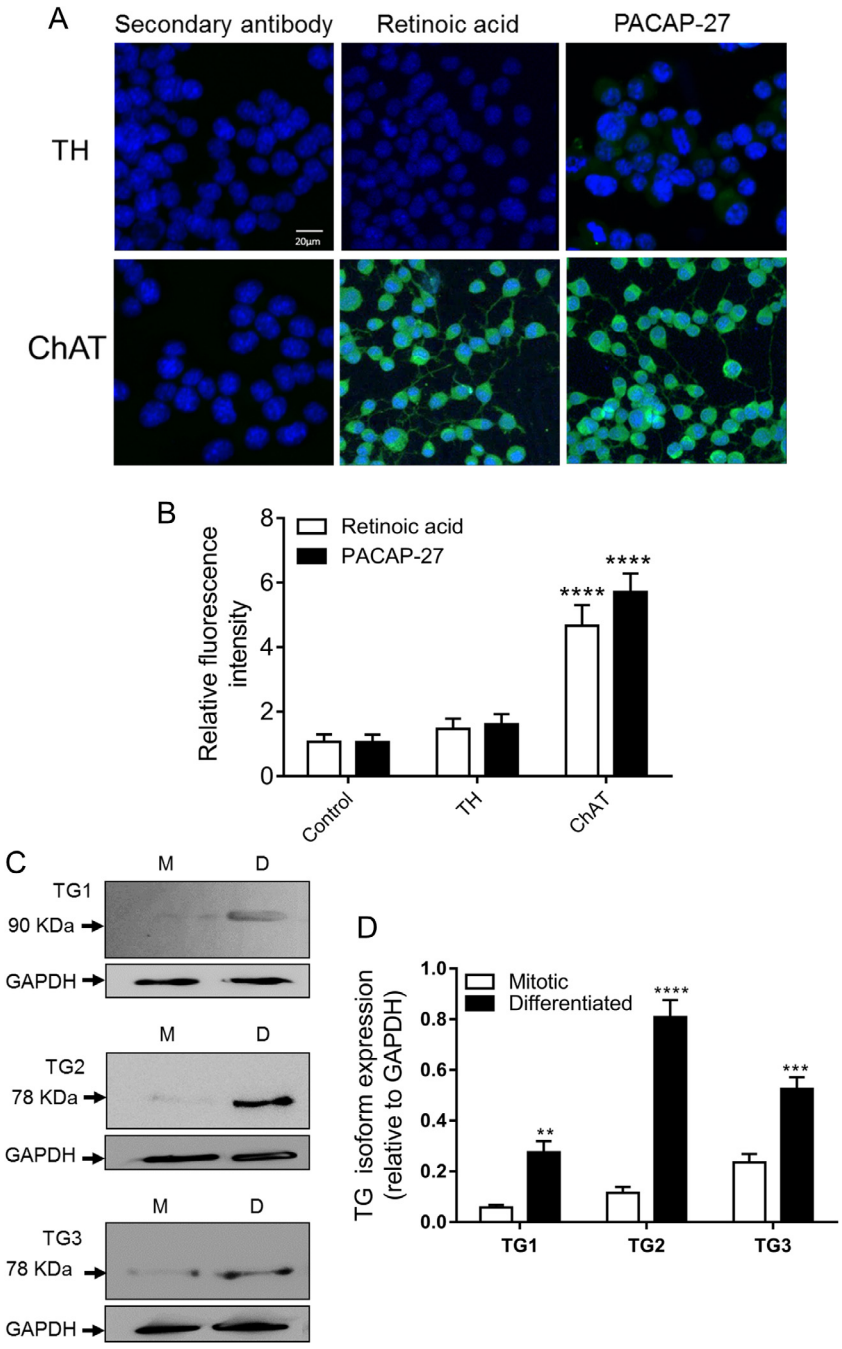

Fig. 1. Protein expression of TG isoforms and neuronal markers in mitotic and differentiated N2a cells. Where indicated cells were differentiated with retinoic acid (1 μM) or PACAP-27 (100 nM) for 48 h in serum-free medium. (A) Immunocytochemistry by fluorescence microscopy was performed using anti-choline acetyltransferase antibody (ChAT; cholinergic neuronal marker; green) and anti-tyrosine hydroxylase antibody (TH; dopaminergic and noradrenergic neuronal marker) and DAPI counterstain for nuclei visualisation (blue). Images presented are from one experiment and representative of three. (B) Quantified immunocytochemistry data represent the mean ± S.E.M. of fluorescence intensity relative to DAPI stain for five fields of view each from three independent experiments. (C) Cell lysates (20 μg protein) from mitotic (M) and differentiating (D) N2a cells were analysed for TG1, TG2 and TG3 expression by Western blotting using TG isoform specific antibodies. Levels of GAPDH are included for comparison. (D) Quantified data are expressed as the ratio of TG isoform to GAPDH and represent the mean ± S.E.M. from four independent experiments. $^{**}P < 0.01$, $^{***}P < 0.001$, and $^{****}P < 0.0001$ versus mitotic cells. (For interpretation of the references to colour in this figure legend, the reader is referred to the web version of this article.)

extensively washed as above and developed using the Enhanced Chemiluminescence Detection System (Uptima, Interchim, France) and quantified by densitometry using Advanced Image Data Analysis Software (Fuji; version 3.52). The uniform transfer of proteins to the nitrocellulose membrane was routinely monitored by transiently staining the membranes with Ponceau S stain prior to application of the primary antibody. When assessing protein kinase phosphorylation samples from each experiment were also analysed on separate blots using primary antibodies that recognise total ERK1/2, PKB, p38 MAPK and JNK1/2 (all 1:1000 dilution) in order to confirm the uniformity of protein loading.

2.11. Visualisation of in situ TG2 activity and neuronal markers

N2a cells were seeded on 8-well chamber slides (15,000 cells well^{-1}) and differentiated for 48 h in serum-free DMEM containing retinoic acid or PACAP-27 (100 nM). The medium was then removed, monolayer gently washed with PBS and

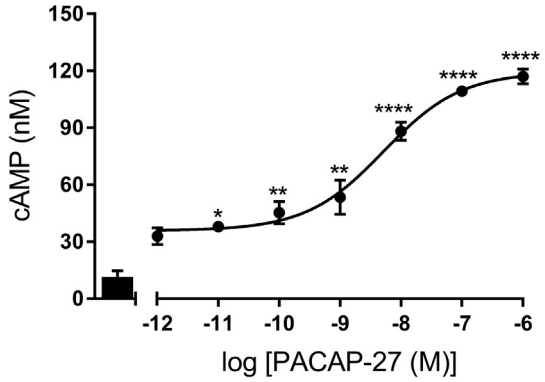

Fig. 2. PACAP-27-induced cAMP accumulation in differentiating N2a cells. Differentiating N2a cells were treated with the indicated concentrations of PACAP-27 for 10 min. The bar represents control. Levels of cAMP were determined as described in Section 2. The results represent the mean ± S.E.M. of three experiments each performed in triplicate. $^{*}P < 0.05$, $^{**}P < 0.01$, and $^{****}P < 0.0001$ versus control response.

slides were incubated for 6 h with 1 mM biotin-X-cadaverine (a cell permeable TG2 substrate; [55]) in serum-free DMEM experimentation. Where appropriate, cells were treated for 1 h with TG2 inhibitors Z-DON (150 μM) or R283 (200 μM) before the addition of 100 nM PACAP-27. Following stimulation, cells were fixed with 3.7 % (w/v) paraformaldehyde and permeabilised with 0.1% (v/v) Triton-X100 both in PBS for 15 min at room temperature. After washing, cells were blocked with 3% (w/v) BSA for 1 h at room temperature and the transglutaminase mediated biotin-X-cadaverine labeled protein substrates detected by (1:200 v/v) FITC-conjugated ExtrAvidin® (Sigma-Aldrich). For the visualisation of neuronal markers fixed cell monolayers were incubated overnight at 4 °C with rabbit anti-choline acetyltransferase antibody (1:200) or mouse anti-tyrosine hydroxylase antibody (1:200) in 3% (w/v) BSA. Unbound primary antibody was then removed, and the cells washed three times for 5 min with PBS. Cells were then incubated for 2 h at 37 °C in a humidified chamber with either goat anti-mouse or anti-rabbit FITC-conjugated immunoglobulin G (Abcam, Cambridge, UK) diluted 1:1000 in 3% (w/v) BSA. The chamber slide was subsequently washed three times for 5 min with PBS, air-dried and mounted with Vectashield® medium (Vector Laboratories Ltd, Peterborough, UK) containing DAPI counterstain for nuclei visualisation. Finally slides were sealed using clear, colourless nail varnish and stained cells visualised using a Leica TCS SP5 II confocal microscope (Leica Microsystems, GmbH, Manheim, Germany) equipped with a 20× air objective. Optical sections were typically 1–2 μm and the highest fluorescence intensity values were acquired and fluorescence intensity relative to DAPI stain quantified for each field of view. Saturation was avoided using the look-up Table overlay provided by the software. Image analysis and quantification were carried out using Leica LAS AF software.

2.12. Measurement of intracellular calcium

N2a cells were plated in 24-well flat-bottomed plates (15,000 cells well^{-1}) and differentiated for 48 h. Cells were loaded with Fluo-8 AM (5 μM, 30–40 min) before mounting on the stage of an Leica TCS SP5 II confocal microscope (Leica Microsystems, GmbH,

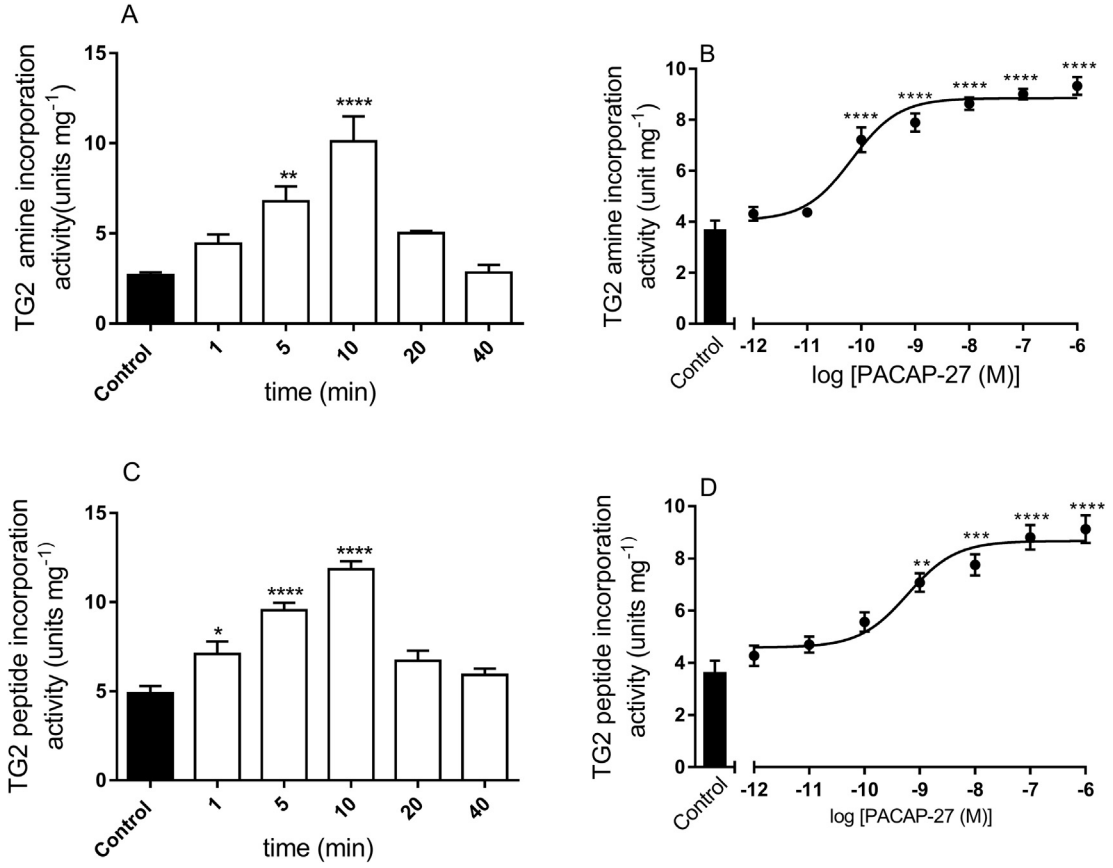

Fig. 3. Effect of PACAP-27 on transglutaminase activity in N2a cells. Differentiating N2a cells were either incubated with 100 nM PACAP-27 for the indicated time periods or for 10 min with the indicated concentrations of PACAP-27. Cell lysates were then subjected to the biotin-cadaverine incorporation (A and B) or peptide cross-linking assay (C and D). Data points represent the mean TG specific activity ± S.E.M. from four (A and C), five (B) or six (D) independent experiments. $^{*}P < 0.05$, $^{**}P < 0.01$, $^{***}P < 0.001$, and $^{****}P < 0.0001$ versus control response.

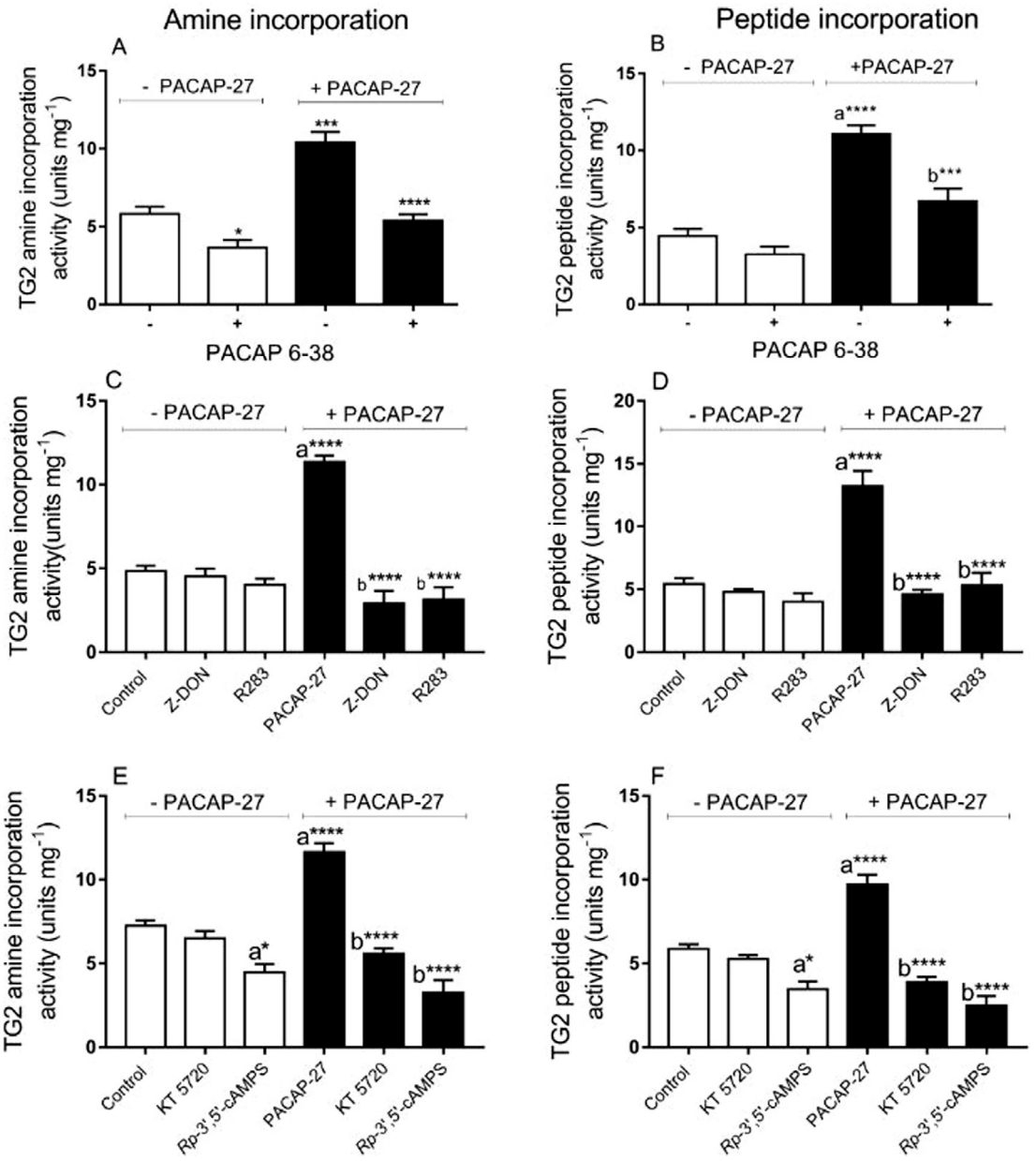

Fig. 4. Effect of the selective PAC_1 receptor antagonist PACAP 6-38 and inhibitors of TG2 and PKA in on PACAP-27 induced TG2 activity in differentiating N2a cells. Cells were pretreated for 1 h with the TG2 inhibitors Z-DON (150 μM) and R283 (200 μM) or for 30 min with the selective PAC_1 receptor antagonist PACAP 6-38 (100 nM) or the PKA inhibitors KT 5720 (5 μM) or Rp-3′,5′-cAMPs (50 μM) prior to 10 min stimulation with PACAP-27 (100 nM). Cell lysates were then subjected to the biotin-cadaverine incorporation (A,C,E) or peptide cross-linking assay (B,D,F). Data points represent the mean TG specific activity ± S.E.M. from four independent experiments. $^{*}P < 0.05$, $^{***}P < 0.001$, and $^{****}P < 0.0001$, (a) versus control and (b) versus 100 nM PACAP-27 alone.

Manheim, Germany) equipped with a 20× air objective. Cells were incubated at 37 °C using a temperature controller and micro incubator (The Cube, Life Imaging Services, Basel, Switzerland) in the presence of imaging buffer (134 mM NaCl, 6 mM KCl, 1.3 mM $CaCl_2$, 1 mM $MgCl_2$, 10 mM HEPES, and 10 mM glucose; pH 7.4). Using an excitation wavelength of 490 nm, emissions over 514 nm were recorded. Images were collected every 1.7 s for 10 min. Relative increases in intracellular Ca^{2+} were defined as F/F_0 where F was the fluorescence at any given time, and F_0 was the initial basal level of Ca^{2+}.

2.13. Determination of TG2 phosphorylation

Following stimulation, differentiated N2a cells were rinsed twice with 2.0 ml of chilled PBS and lysed with 500 μl of ice-cold lysis buffer (2 mM EDTA, 1.5 mM $MgCl_2$, 10% (v/v) glycerol, 0.5% (v/v) IGEPAL, 0.1% (v/v) Protease Inhibitor Cocktail, and 1% (v/v) Phosphatase Inhibitor Cocktail 2 and 3 in PBS). Cell lysates were clarified by centrifugation (4 °C for 10 min at 14000*g*), after which 500 μg of supernatant protein were incubated overnight at 4 °C with 2 μg of anti-TG2 monoclonal antibody or IgG control. Immune complexes were precipitated using Pierce™ Classic Magnetic IP/Co-IP Kit (Loughborough, UK). The precipitates were resolved by SDS-PAGE and Western blotting, then probed using anti-phosphoserine or anti-phosphothreonine antibodies (1:1000). Antibody reactivity was visualised by ECL and quantified densitometrically, as described above.

2.14. Statistical analysis

All graphs and statistics (one-way ANOVA followed by Dunnet's multiple comparison test and two-way ANOVA for group compar-

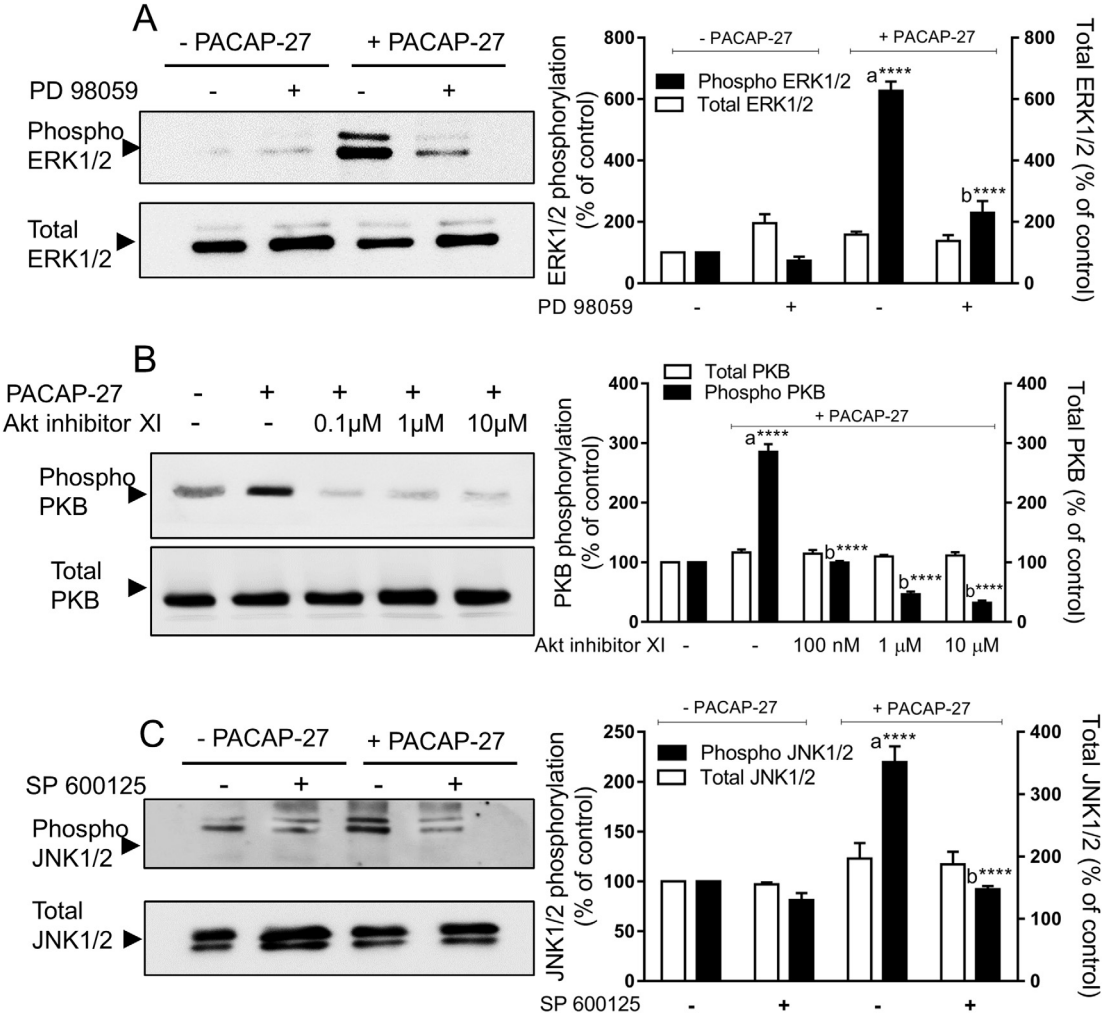

Fig. 5. Effect of PACAP-27 on ERK1/2, PKB and JNK1/2 phosphorylation in differentiating N2a cells. Where indicated, N2a cells were pre-treated for 30 min with PD 98059 (50 μM), SP 600 125 (20 μM) or Akt inhibitor X1 (100 nM, 1 μM or 10 μM) prior to stimulation with PACAP-27 (100 nM) for 10 min. Cell lysates were analysed by Western blotting for activation of (A) ERK1/2, (B) PKB and (C) JNK1/2 using phospho-specific antibodies. Samples were subsequently analysed on separate blots using antibodies that recognise total ERK1/2, PKB and JNK1/2. Quantified data are expressed as the percentage of the value for control cells (=100%) in the absence of protein kinase inhibitor and represent the mean ± S.E.M. of four independent experiments. $^{***}P < 0.001$ and $^{****}P < 0.0001$, (a) versus control and (b) versus 100 nM PACAP-27.

ison) were performed using GraphPad Prism® software (GraphPad Software, Inc., USA). Agonist EC_{50} values (concentration of agonist producing 50% of the maximal stimulation) were obtained by computer-assisted curve fitting using GraphPad Prism® software. Agonist $p[EC_{50}]$ values were subsequently calculated as the negative logarithm to base 10 of the EC_{50}. Results represent mean ± S.E.M. and p values <0.05 were considered statistically significant.

3. Results

3.1. Characterisation of cholinergic neuronal phenotype and TG expression pattern in N2a cells

Mouse N2a neuroblastoma cells can be differentiated into various neuronal types dependent upon the method used [41,67]. For example, serum withdrawal in the presence of retinoic acid induces differentiation into cholinergic neurons, whereas dibutyryl cAMP promotes the development of dopaminergic neurons [41,67]. In this study N2a cells were induced to differentiate using retinoic acid in order to avoid potential problems using dibutyryl cAMP when assessing functional responses mediated by the G_s-protein coupled PAC_1 receptor. Immunocytochemical staining indicated that expression of the cholinergic neuronal marker, choline acetyltransferase increased markedly after 48 h confirming that retinoic acid promotes differentiation of N2a cells into cholinergic neurons (Fig. 1A and B).

Western blot analysis was performed to compare the expression of TG isoforms in mitotic and differentiating N2a cells. TG1, TG2 and TG3 expression increased significantly in N2a cells following differentiation for 48 h with 1 μM *all-trans* retinoic acid (Fig. 1C and D). These observations are in agreement with previous studies [12].

3.2. Effect of PAC_1 receptor activation on TG2 activity

PACAP-27 induced a robust increase in cAMP accumulation (EC_{50} = 4.0 ± 1.3 nM; $p[EC]_{50}$ = 8.5 ± 0.2; n = 3) in retinoic acid-induced differentiating N2a cells (Fig. 2). The selective $VPAC_1$ and $VPAC_2$ agonists, [$Ala^{11,22,28}$]-VIP (1 μM) and Bay 55-9837 (1 μM) respectively, had no significant effect on cAMP accumulation (data not shown). PACAP-27 treatment produced transient increases in TG2 catalysed biotin-cadaverine incorporation and protein cross-linking activity, peaking at 10 min (Fig. 3A and C). Furthermore, as shown in Fig. 3, PACAP-27 stimulated concentration-dependent increases in biotin-amine incorporation activity (EC_{50} = 0.08 ± 0.01 nM; $p[EC_{50}]$ = 10.1 ± 0.1; n = 5) and protein

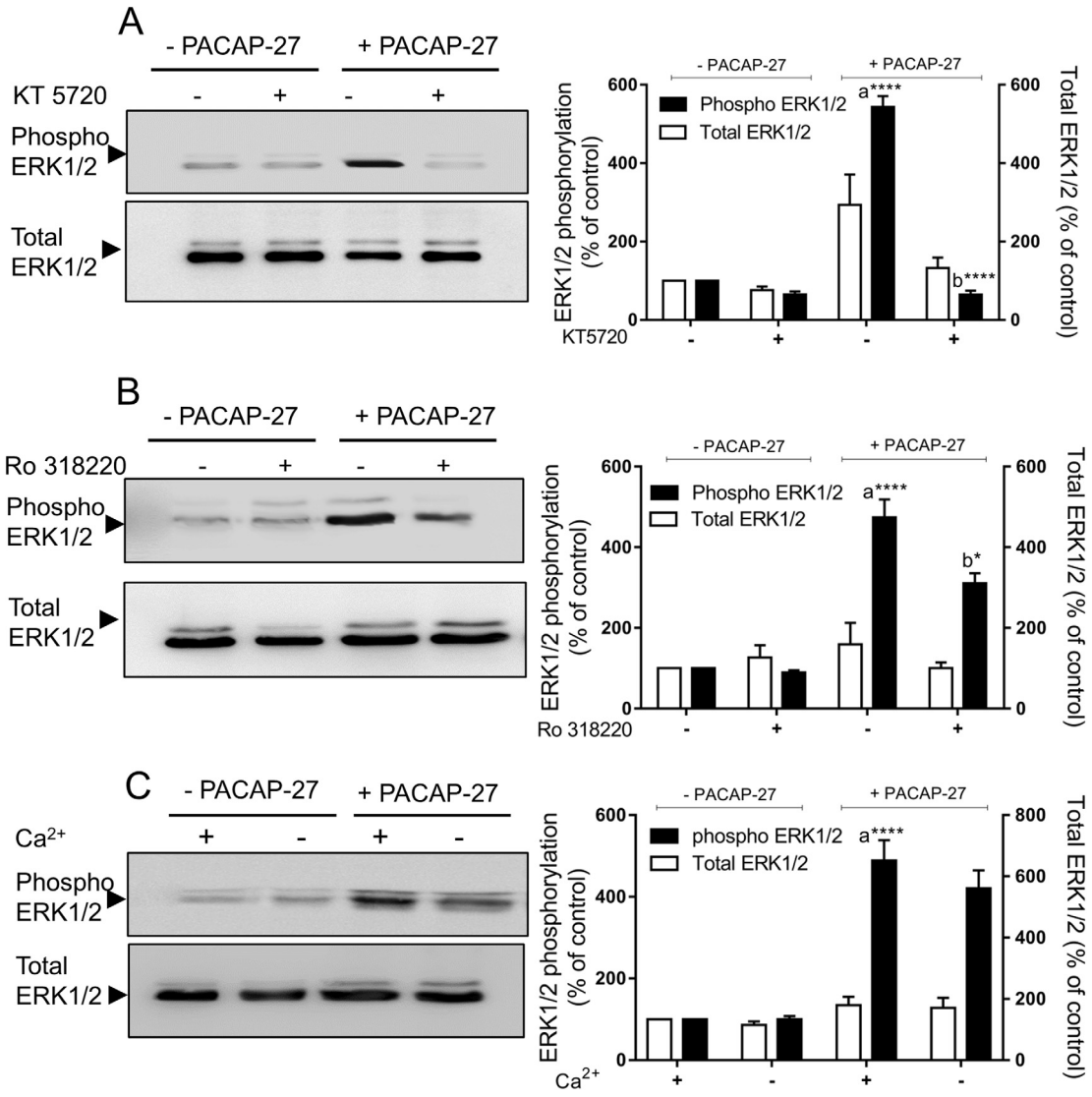

Fig. 6. Effect of protein kinase inhibitors (PKA, PKC) and Ca^{2+} on PACAP-27 induced ERK1/2 activation. Where indicated, differentiating N2a cells were pre-treated for 30 min with (A) KT 5720 (5 μM) or (B) Ro 318220 (10 μM) prior to stimulation with PACAP-27 (100 nM) for 10 min. (C) Cells were stimulated for 10 min with PACAP-27 (100 nM) either in the presence (1.8 mM $CaCl_2$) or absence of extracellular Ca^{2+} (nominally Ca^{2+}-free Hanks/HEPES buffer containing 0.1 mM EGTA). Cell lysates were analysed by Western blotting for activation of ERK1/2 using a phospho-specific antibody. Samples were subsequently analysed on separate blots using an antibody that recognizes total ERK1/2. Quantified data are expressed as the percentage of the value for control cells (=100%) in the absence of protein kinase inhibitor or presence of extracellular Ca^{2+} and represent the mean ± S.E.M. of four independent experiments. $^{***}P < 0.001$ and $^{****}P < 0.0001$, (a) versus control and (b) versus 100 nM PACAP-27.

cross-linking activity (EC_{50} = 0.4 ± 0.2 nM; p[EC_{50}] = 9.7 ± 0.2; n = 6). The selective PAC_1 receptor antagonist PACAP 6-38 attenuated PACAP-27 induced biotin-amine incorporation activity (Fig. 4A) and protein cross-linking activity (Fig. 4B). The selective $VPAC_1$ and $VPAC_2$ agonists, [$Ala^{11,22,28}$]-VIP (1 μM) and Bay 55-9837 (1 μM) respectively, had no significant effect on TG2 activity (data not shown). Overall, these data indicate that the PAC_1 receptor is functionally expressed and stimulates TG2-mediated transamidase activity in differentiated N2a cells.

3.3. Effect of TG2 inhibitors on PAC_1 receptor induced TG2 activity

To confirm that TG2 is responsible for PAC_1 receptor-mediated transglutaminase activity in differentiating N2a cells, two structurally different cell permeable TG2 specific inhibitors were tested; R283 (a small molecule; [24]) and Z-DON (peptide-based; [60]). N2a cells were pre-treated for 1 h with Z-DON (150 μM) or R283 (200 μM) prior to stimulation with PACAP-27 for 10 min. Both inhibitors completely blocked PACAP-27-induced TG-mediated amine incorporation (Fig. 4C) and protein cross-linking activity (Fig. 4D). It is important to note that despite these TG2 inhibitors being cell-permeable, inhibition of cellular TG2 is only achieved at concentrations significantly above their IC_{50} value versus purified enzyme [60,24]. Overall, these data indicate that TG2 is the TG isoform activated by the PAC_1 receptor.

3.4. The effect of protein kinase inhibitors on PAC_1 receptor-induced TG2 activity

Pre-treatment with the PKA inhibitors KT 5720 (5 μM) and *Rp*-cAMPs (50 μM) completely abolished PACAP-27-induced amine incorporation (Fig. 4E) and protein cross-linking activity (Fig. 4F), confirming the involvement of PKA in TG2 activation via the PAC_1 receptor.

Modulation of protein kinase activity following PAC_1 receptor activation was assessed by Western blotting using phospho-

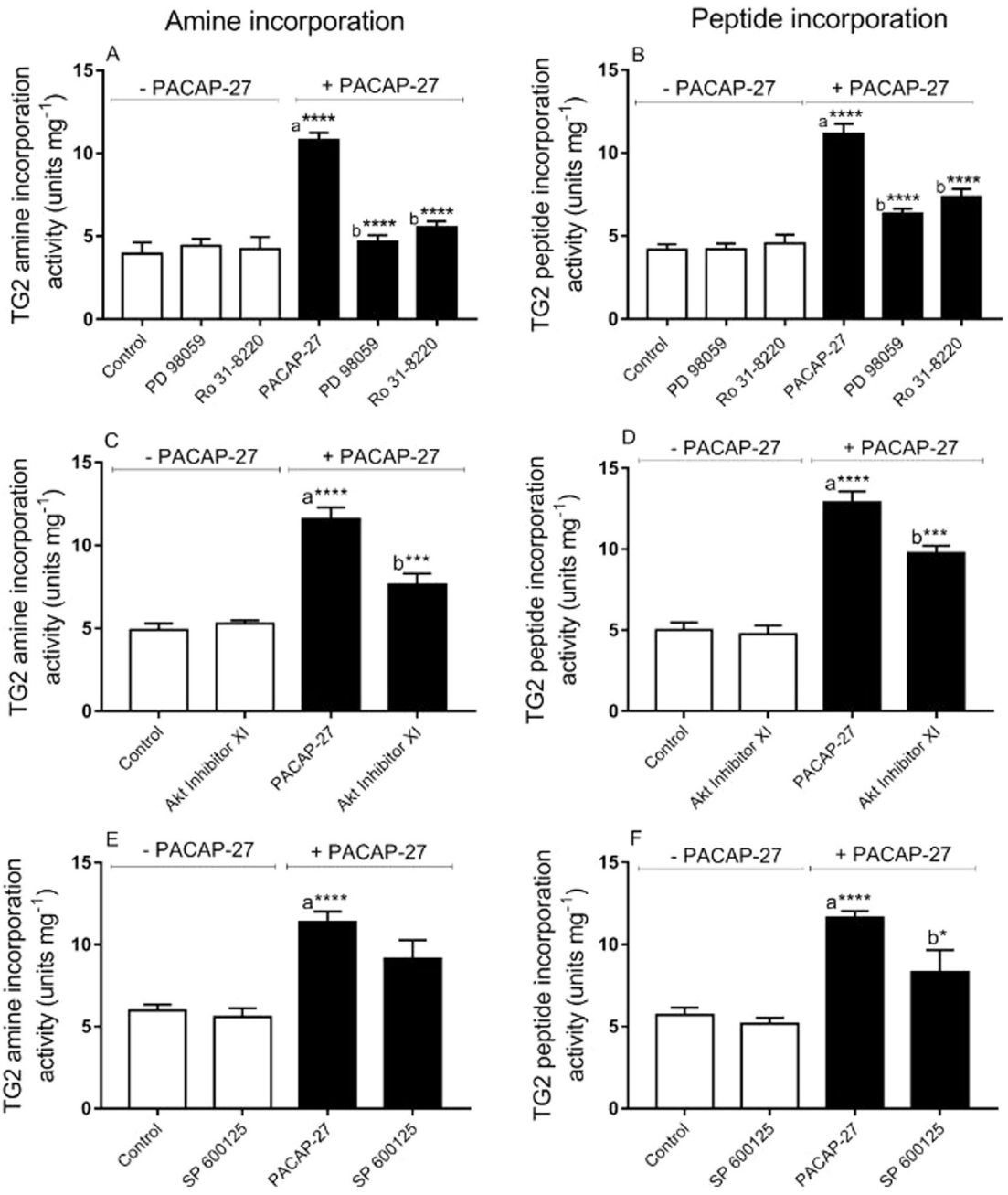

Fig. 7. Effect of protein kinase inhibitors (ERK1/2, PKC, PKB, JNK1/2) on PAC_1 receptor-induced TG activity. Differentiating N2a cells were pretreated for 30 min with PD 98059 (50 μM), Ro 31-8220 (10 μM), Akt inhibitor XI (100 nM) or SP 600125 (20 μM) prior to 10 min stimulation with PACAP-27 (100 nM). Cell lysates subjected to biotin-cadaverine incorporation (A,C,E) or peptide cross-linking assay (B,D,F). Data points represent the mean ± S.E.M. TG specific activity from four independent experiments. $^{*}P < 0.05$, $^{**}P < 0.01$, $^{***}P < 0.001$ and $^{****}P < 0.0001$, (a) versus control and (b) versus 100 nM PACAP-27 alone.

specific antibodies that recognise phosphorylated motifs within activated ERK1/2 (pTEpY), p38 MAPK (pTGpY), JNK (pTPpY) and PKB (S^{473}). PACAP-27 (100 nM) stimulated significant increases in ERK1/2 (Fig. 5A), PKB (Fig. 5B) and JNK1/2 (Fig. 5C) phosphorylation in differentiating N2a cells. As expected PACAP-27-mediated increases in ERK1/2, PKB and JNK1/2 phosphorylation were inhibited by PD 98059 (50 μM; MEK1/2 inhibitor; Fig. 5A), Akt inhibitor XI (0.1, 1 μM and 10 μM; PKB inhibitor; Fig. 5B) and SP 600125 (20 μM; JNK1/2 inhibitor; Fig. 5B), respectively. No significant increases in p38 MAPK phosphorylation were observed following PACAP-27 (100 nM for 10 min) treatment (data not shown). PACAP-27-induced increases in ERK1/2 were also attenuated by KT 5720 (5 μM; PKA inhibitor; Fig. 6A) and Ro 31-8220 (10 μM; PKC inhibitor; Fig. 6B), but not following removal of extracellular Ca^{2+} (Fig. 6C). In summary, these data have shown that PAC_1 receptor activation in differentiating N2a cells triggers robust increases in ERK1/2, PKB and JNK1/2 phosphorylation and that ERK1/2 activation is PKA and PKC dependent.

The role of ERK1/2, PKB, PKC and JNK1/2 in PAC_1 receptor-induced TG2 activation was determined using pharmacological inhibitors of these protein kinases. PACAP-27-induced transglutaminase-mediated amine incorporation activity and protein cross-linking activity were inhibited by PD 98950, Ro 318220, and Akt inhibitor XI, suggesting the involvement of ERK1/2, PKC and PKB, respectively, in PAC_1 receptor-mediated TG2 responses (Fig. 7A–D). In contrast, SP 6000125 attenuated

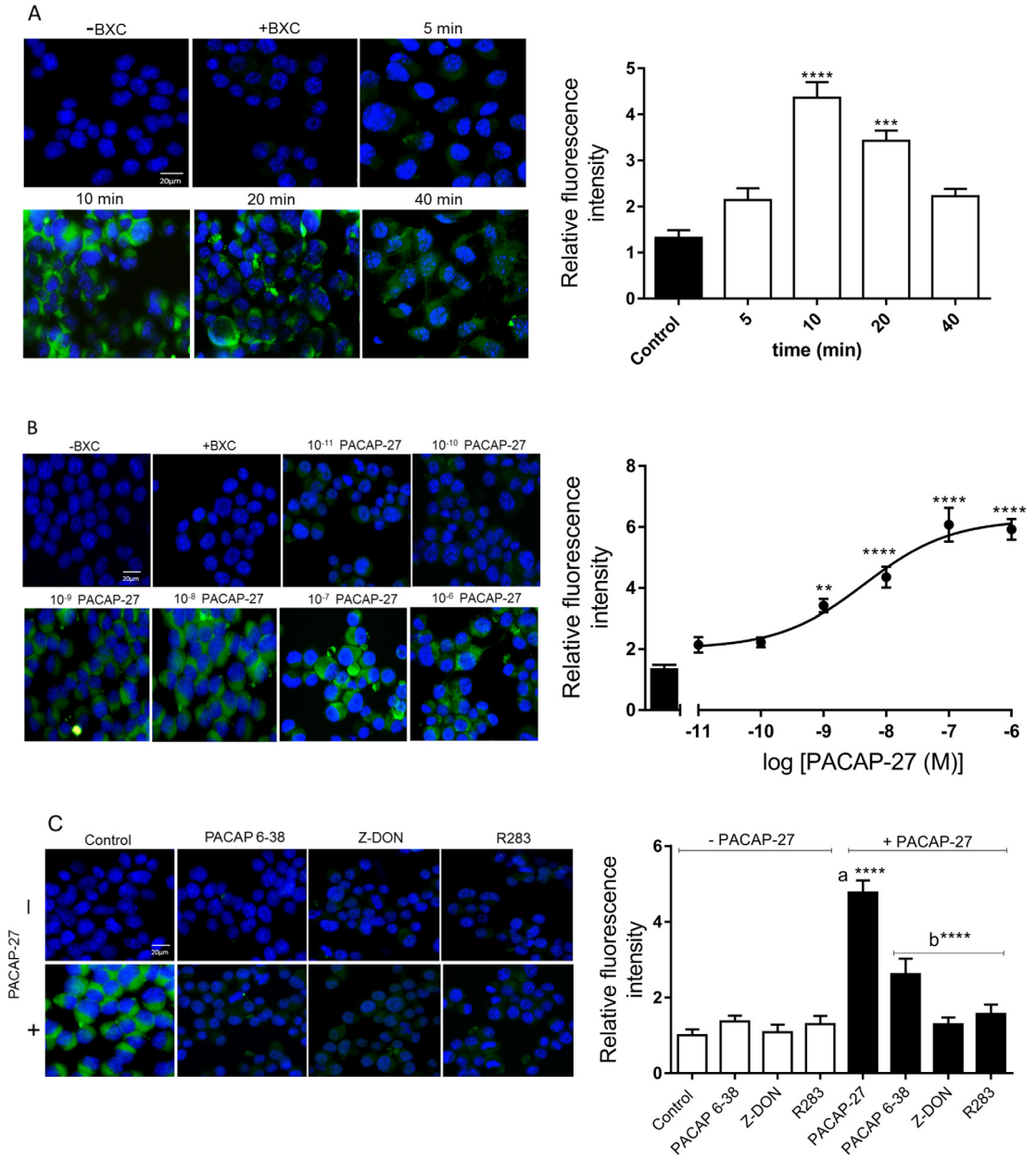

Fig. 8. PACAP-27-induced *in situ* TG activity in differentiating N2a cells. Cells were incubated with 1 mM biotin-X-cadaverine (BTC) for 6 h, after which they were incubated with (A) 100 nM PACAP-27 for 5, 10, 20, or 40 min, (B) the indicated concentrations of PACAP-27 for 10 min, or (C) with the PAC_1 receptor antagonist PACAP 6-38 (100 nM) for 30 min or for 1 h with the TG2 inhibitors Z-DON (150 μM) and R283 (200 μM) prior to 10 min stimulation with PACAP-27 (100 nM). TG2-mediated biotin-X-cadaverine incorporation into intracellular proteins was visualised using FITC-conjugated ExtrAvidin® (green). Nuclei were stained with DAPI (blue) and viewed using a Leica TCS SP5 II confocal microscope (20× objective magnification). Images presented are from one experiment and representative of three. Quantified data represent the mean ± S.E.M. of fluorescence intensity relative to DAPI stain for five fields of view each from at least three independent experiments. $^{*}P < 0.05$, $^{**}P < 0.01$, $^{***}P < 0.001$ and $^{****}P < 0.0001$ versus control response. (For interpretation of the references to colour in this figure legend, the reader is referred to the web version of this article.)

PACAP-27-induced protein cross-linking activity (Fig. 7F) but was without effect on TG2-mediated amine incorporation (Fig. 7E). Finally, PD 98059, Ro 31-8220, Akt inhibitor XI, and SP 600125 had no significant effect on purified guinea pig liver TG2 activity (data not shown). Overall, these data suggest that the PAC_1 receptor stimulates TG2 activity in differentiating N2a cells via a multi protein kinase dependent pathway.

3.5. Visualisation of in situ TG2 activity following PACAP treatment

Biotin-X-cadaverine, is a cell penetrating primary amine, which enables the *in situ* visualisation of endogenous protein substrates of TG2, when combined with FITC-ExtrAvidin® [38]. PACAP-27 (100 nM) induced a time dependent and concentration-dependent (EC_{50} = 6.7 ± 3 nM; pEC_{50} = 8.3 ± 0.2; n = 3) increase in the incorporation of biotin-X-cadaverine into endogenous protein substrates of TG2 (Fig. 8). Finally, the *in situ* responses to PACAP-27 were attenuated by the PAC_1 antagonist PACAP 6-38 and the TG2 inhibitors ZDON and R283 (Fig. 8). Overall, these data indicate a similar pattern of TG2 activation in live cells.

3.6. The role of Ca^{2+} in PAC_1 receptor induced TG2 activity

PACAP-27 (100 nM) triggered a robust increase in intracellular Ca^{2+} that was abolished in the absence of extracellular Ca^{2+} (Fig. 9A and B). The role of extracellular Ca^{2+} in TG2 activation

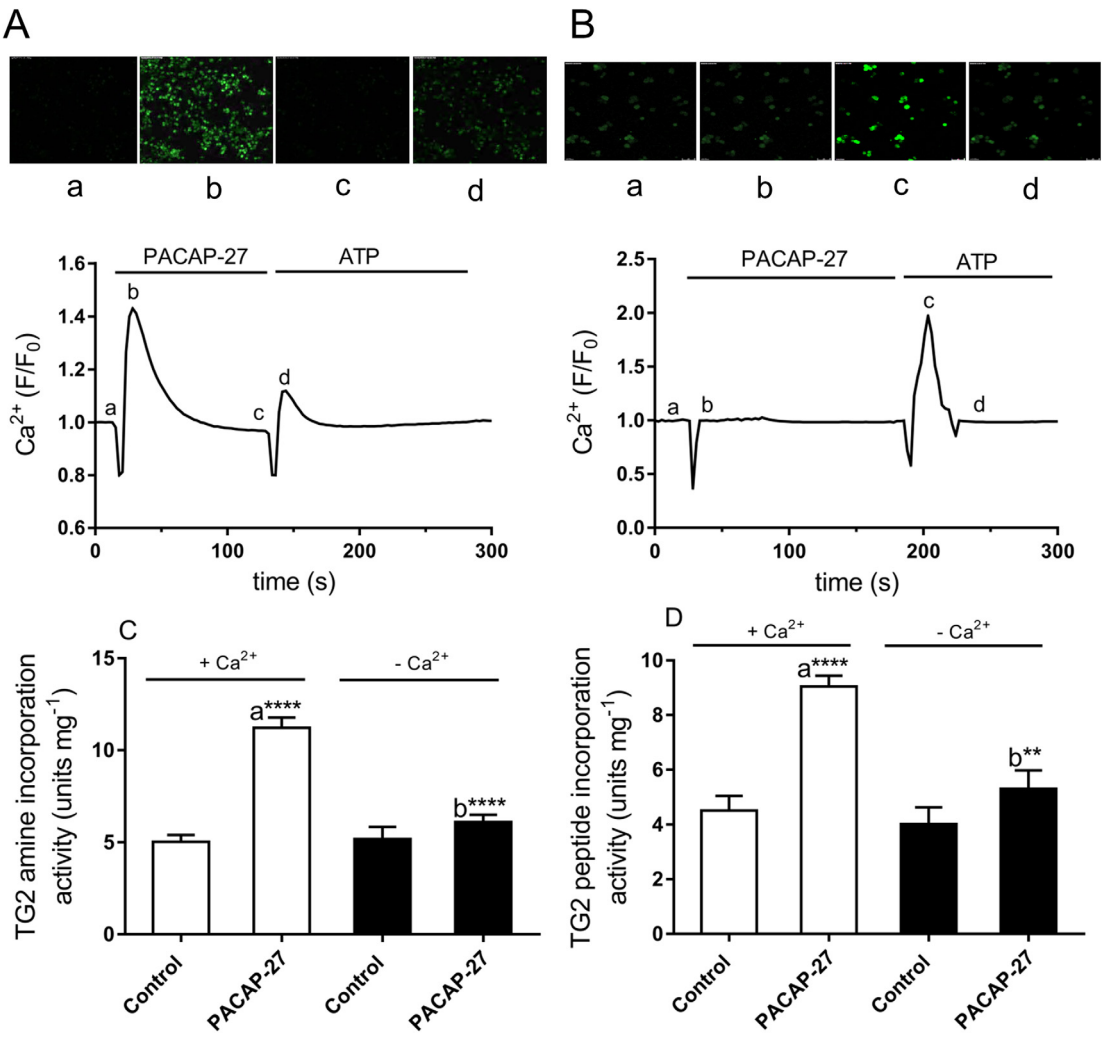

Fig. 9. Effect of PACAP-27 on $[Ca^{2+}]_i$ and role of Ca^{2+} in PACAP-27-induced TG2 activation in differentiating N2a cells. Shown are A) PACAP-27 (100 nM) triggering a rapid and transient rise in intracellular Ca^{2+} in the presence of extracellular Ca^{2+} (1.3 mM). B) The absence of Ca^{2+} responses induced by PACAP-27 during experiments performed in nominally Ca^{2+}-free buffer and 0.1 mM EGTA. In these experiments depletion of intracellular Ca^{2+} stores with thapsigargin (5 μM) was still evident. The panel letters (a–d) correspond to the time points in the traces. Similar results were obtained in three other experiments. For TG2 activity, cells were stimulated for 10 min with PACAP-27 (100 nM) either in the presence (1.8 mM $CaCl_2$) or absence of extracellular Ca^{2+} (nominally Ca^{2+}-free Hanks/HEPES buffer containing 0.1 mM EGTA). Cell lysates were subjected to biotin-cadaverine incorporation assay (C) or protein cross-linking assay (D). Data points represent the mean TG specific activity ± S.E.M. from four independent experiments. $^{**}P < 0.01$, $^{***}P < 0.001$ and $^{****}P < 0.0001$, (a) versus control in presence of extracellular Ca^{2+}, (b) versus 100 nM PACAP-27 in presence of extracellular Ca^{2+}.

was assessed in the absence of extracellular Ca^{2+} using nominally Ca^{2+}-free Hanks/HEPES buffer containing 0.1 mM EGTA. Removal of extracellular Ca^{2+} abolished PACAP-27-induced TG2 activation (Fig. 9C and D). These observations suggest that PAC_1 receptor-induced TG2 activation is dependent upon extracellular Ca^{2+}.

3.7. Phosphorylation of TG2 following PAC_1 receptor activation

The effect of PAC_1 receptor activation on the phosphorylation status of TG2 was monitored via immunoprecipitation of TG2 followed by SDS-PAGE and Western blot analysis using anti-phosphoserine and anti-phosphothreonine antibodies. PACAP-27 (100 nM) triggered a robust increase in the levels of TG2 phosphoserine and phosphothreonine (Fig. 10). Pre-treatment with PD 98059 (50 μM; Fig. 10) and KT 5720 (5 μM; Fig. 11) attenuated PACAP-27 mediated increases in TG2 phosphorylation. In contrast, Ro 318220 (10 μM) had no significant effect (data not shown). Finally, removal of extracellular Ca^{2+} partially attenuated PACAP-27-induced TG2 phosphorylation (data not shown). These data indicate that activation of the PAC_1 receptor promotes robust increases in TG2 phosphorylation.

3.8. Role of TG2 in PAC_1 receptor-induced cell survival and neurite outgrowth

The role of TG2 in PAC_1 receptor-induced cell survival was determined in differentiating N2a cells following exposure of cells to simulated hypoxia (1% O_2 in glucose-free and serum-free medium). Initial experiments determined the time course of simulated hypoxia-induced cell death in differentiated N2a cells. Exposure of cells to simulated hypoxia (1% O_2) resulted in a time dependent decrease in MTT reduction, an increase in LDH release and activation of caspase 3 (Fig. 12). A time period of 8 h hypoxia was used in subsequent experiments. Pre-treatment with PACAP-27 (100 nM; 10 min) significantly attenuated hypoxia-induced decrease in MTT reduction, release of LDH and activation of caspase-3 (Fig. 13). Treatment with PACAP 6-38 (100 nM; 30 min) reversed PACAP-27 induced protection confirming the role of the PAC_1 receptor. Finally, the TG2 inhibitors R283 and Z-DON attenuated

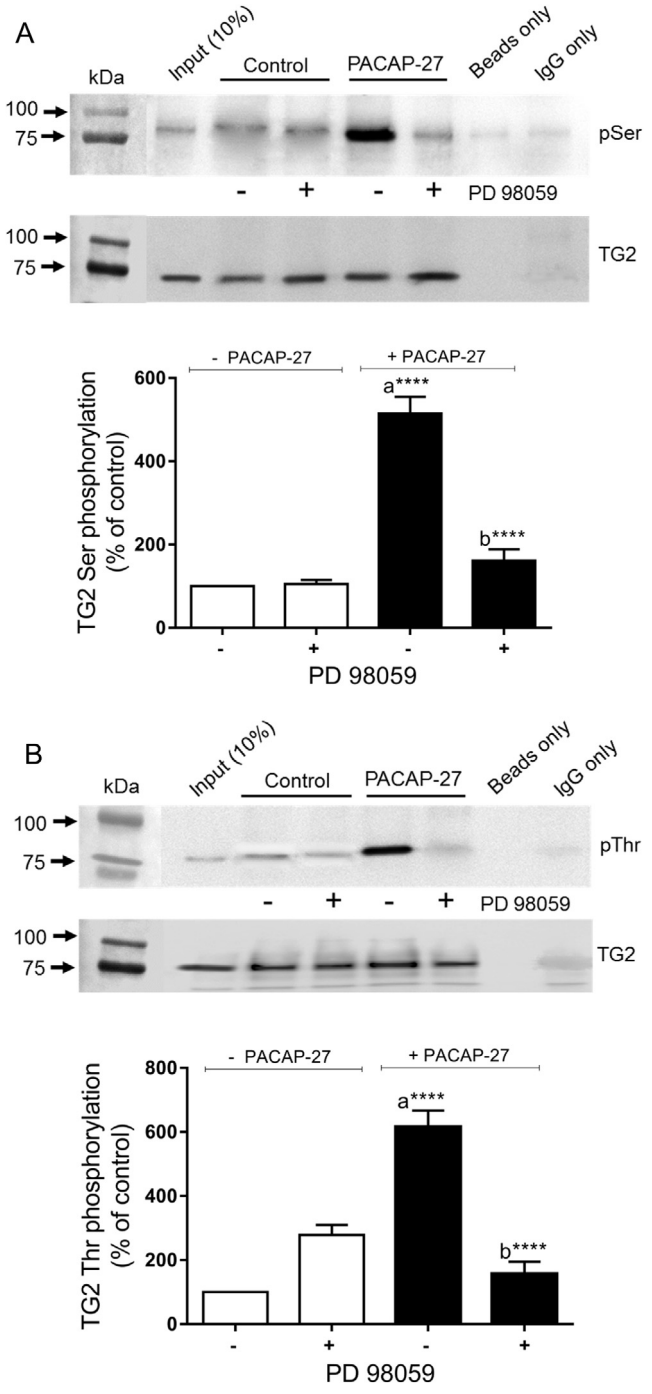

Fig. 10. Effect of the MEK1/2 inhibitor PD 98059 on PACAP-27-induced phosphorylation of TG2. Where indicated, differentiating N2a cells were pre-treated for 30 min with PD 98059 (50 μM) prior to stimulation with PACAP-27 (100 nM) for 10 min. Following stimulation with PACAP-27, cell lysates were subjected to immunoprecipitation using anti-TG2 monoclonal antibody as described under "Section 2". The resultant immunoprecipitated protein(s) were subjected to SDS-PAGE and Western blot analysis using (A) anti-phosphoserine and (B) and anti-phosphothreonine antibodies. One tenth of the total input was applied to the first lane to show the presence of phosphorylated proteins prior to immunoprecipitation and negative controls with the immunoprecipitation performed with immunobeads only were included to demonstrate the specificity of the band shown. Quantified data for PACAP-induced increases in TG2-bound serine and threonine phosphorylation are expressed as a percentage of the TG2 phosphorylation observed in control cells (=100%). Data points represent the mean ± S.E.M. from three independent experiments. $^{*}P < 0.05$, $^{**}P < 0.01$, and $^{***}P < 0.001$, (a) versus control and (b) versus 100 nM PACAP-27 alone.

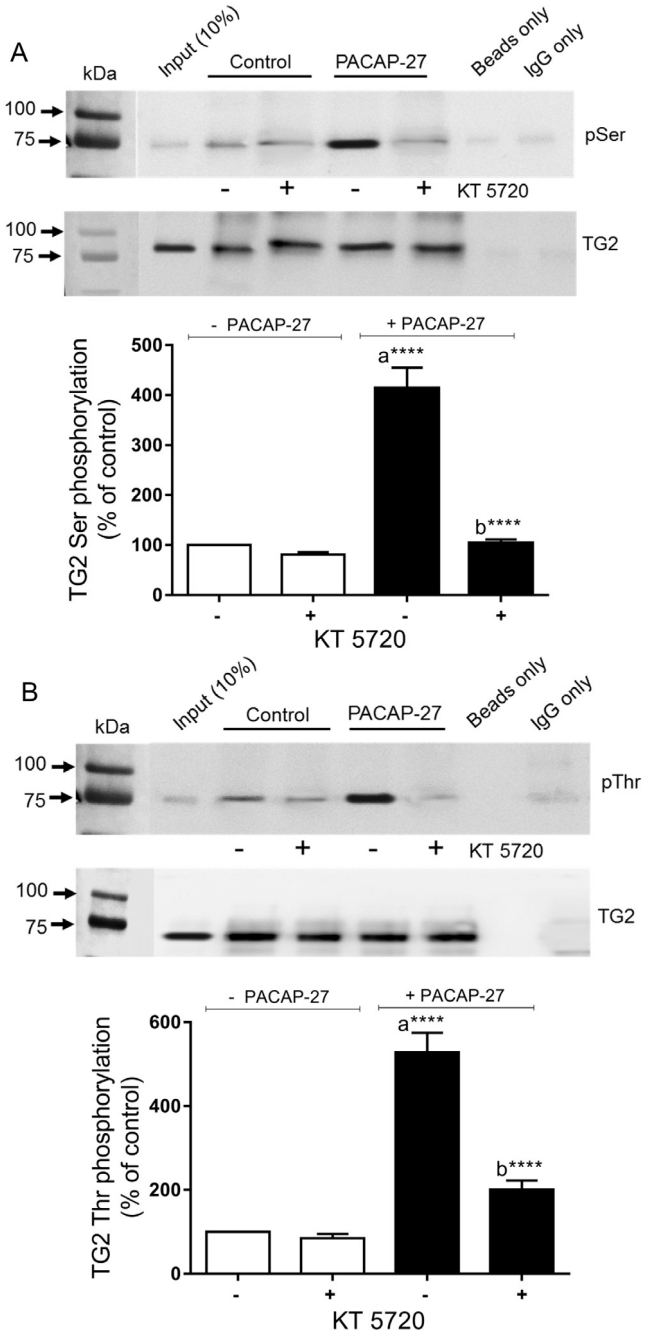

Fig. 11. Effect of the PKA inhibitor KT 5720 on PACAP-27-induced phosphorylation of TG2. Where indicated, differentiating N2a cells were pre-treated for 30 min with KT 5720 (5 μM) prior to stimulation with PACAP-27 (100 nM) for 10 min. Following stimulation with PACAP-27, cell lysates were subjected to immunoprecipitation using anti-TG2 monoclonal antibody as described under "Materials and Methods". The resultant immunoprecipitated protein(s) were subjected to SDS-PAGE and Western blot analysis using (A) anti-phosphoserine and (B) and anti-phosphothreonine antibodies. One tenth of the total input was applied to the first lane to show the presence of phosphorylated proteins prior to immunoprecipitation and negative controls with the immunoprecipitation performed with immunobeads only were included to demonstrate the specificity of the band shown. Quantified data for PACAP-induced increases in TG2-bound serine and threonine phosphorylation are expressed as a percentage of the TG2 phosphorylation observed in control cells (=100%). Data points represent the mean ± S.E.M. from three independent experiments. $^{*}P < 0.05$, $^{**}P < 0.01$, and $^{***}P < 0.001$, (a) versus control and (b) versus 100 nM PACAP-27 alone.

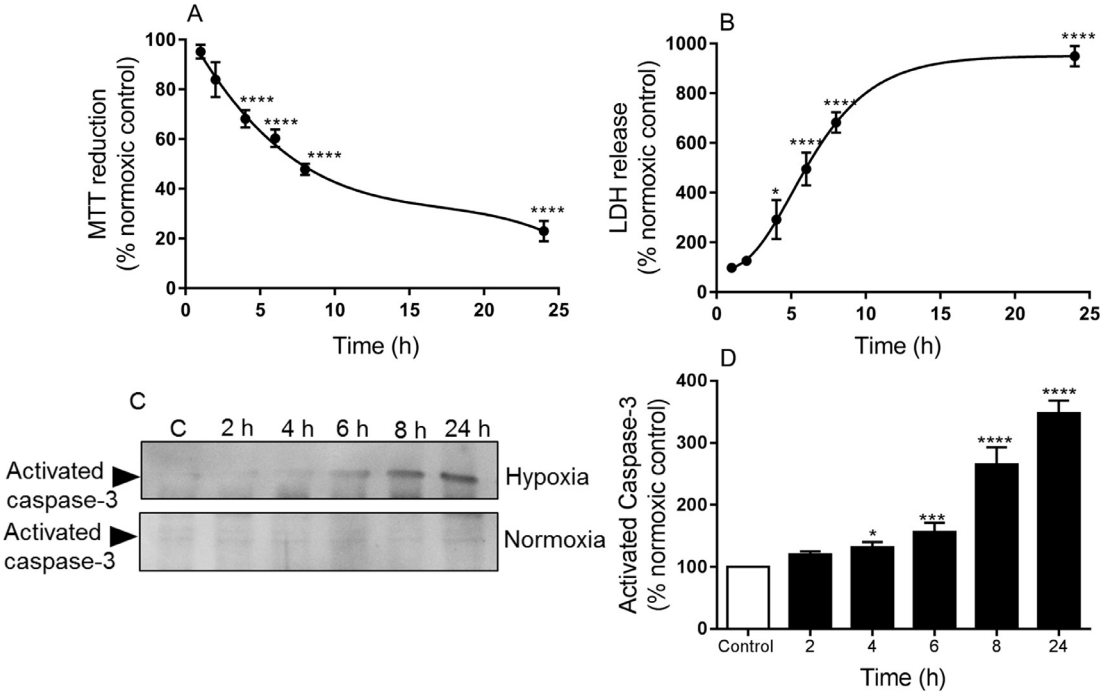

Fig. 12. Effect of simulated hypoxia on MTT reduction, LDH release and caspase 3 activity in differentiating N2a cells. Cells in glucose- and serum-free DMEM were exposed to hypoxia (1% O_2) for the indicated periods of time. Cell viability was assessed by measuring (A) the metabolic reduction of MTT by cellular dehydrogenases, (B) release of LDH into the culture medium and (C) caspase-3 activity via Western blot analysis using anti-active caspase 3 antibody. (D) Quantified caspase-3 activity data. Data are expressed as the percentage of the normoxic control (=100%) and represent the mean ± S.E.M. from four independent experiments, each performed in (A) quadruplicate or (B) sextuplicate. $^{*}P < 0.05$, $^{***}P < 0.0001$ and $^{****}p < 0.0001$ versus normoxic control.

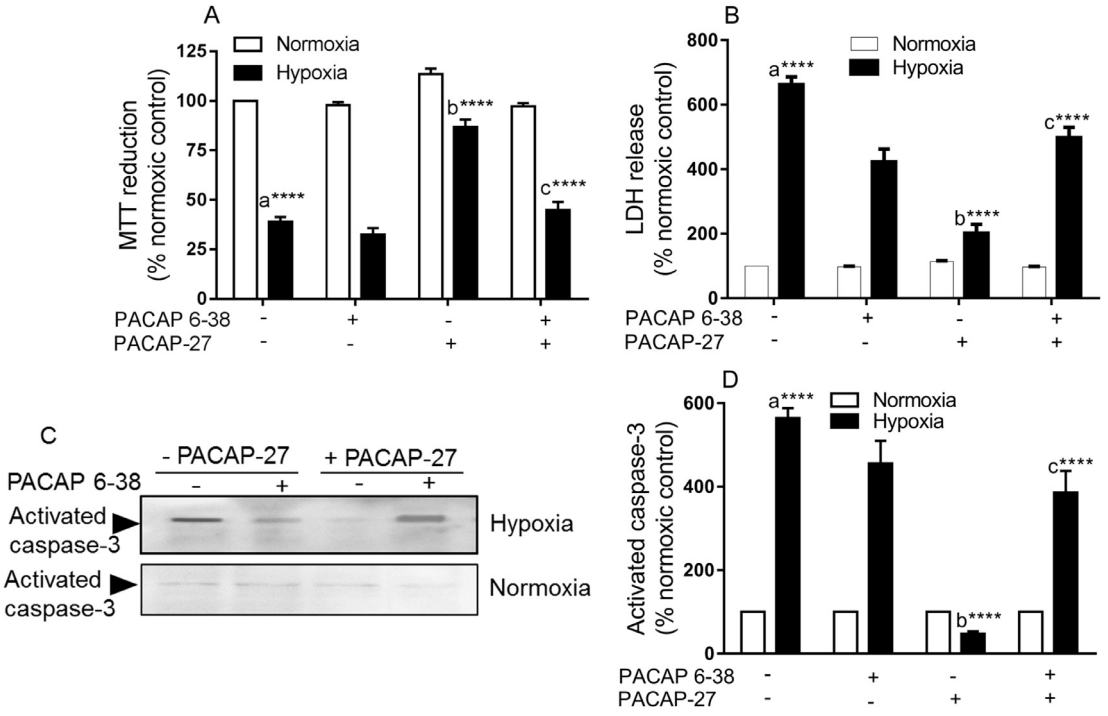

Fig. 13. The effect of PACAP-27 on hypoxia-induced cell death in N2a cells. Differentiating N2a cells were pre-treated with the PAC_1 receptor antagonist PACAP 6-38 (100 nM) for 30 min before the addition of PACAP-27 (100 nM) for 10 min prior to 8 h hypoxia (1% O_2) or 8 h normoxia. Cell viability was assessed by measuring (A) the metabolic reduction of MTT by cellular dehydrogenases, (B) release of LDH into the culture medium and (C) caspase-3 activity via Western blot analysis using anti-active caspase 3 antibody. (D) Quantified caspase-3 activity data. Data are expressed as a percentage of normoxia control cell values (=100%) and represent the mean ± S.E.M. from four independent experiments, each performed in (A) quadruplicate or (B) sextuplicate. $^{****}P < 0.0001$, (a) versus normoxia control, (b) versus hypoxia control (c) versus 100 nM PACAP-27 in the presence of hypoxia.

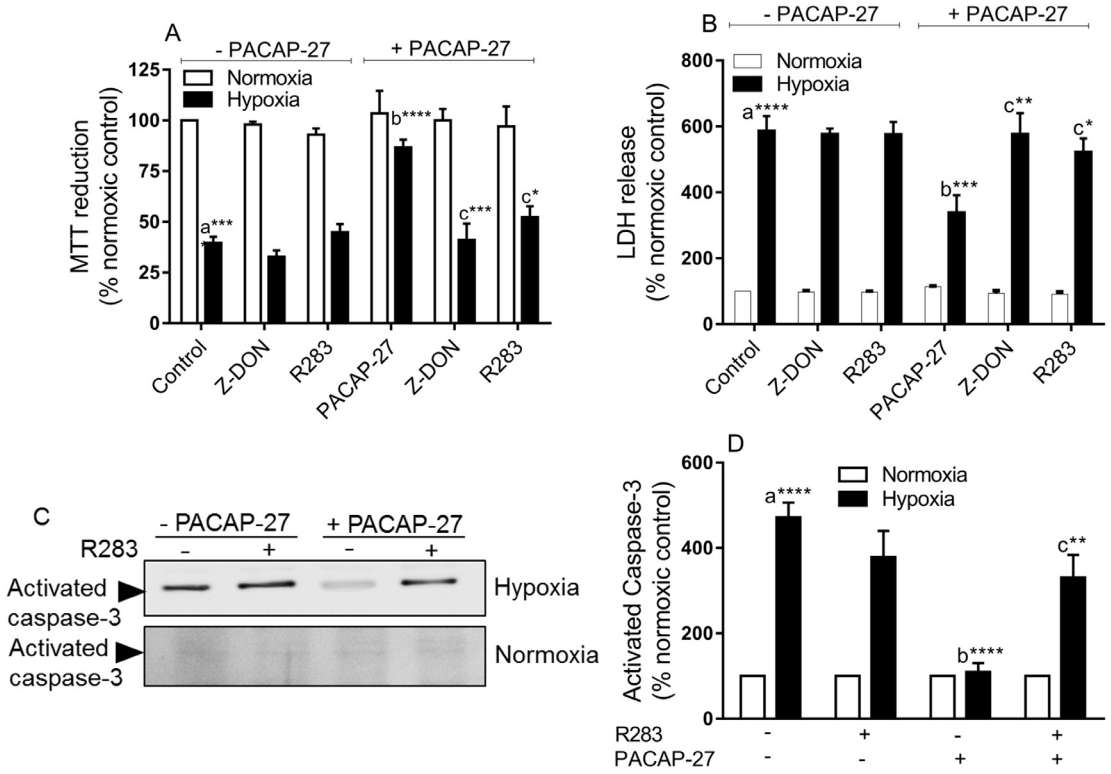

Fig. 14. The effects of the TG2 inhibitors Z-DON and R283 on PACAP-27 induced cell survival in N2a cells. Differentiating N2a cells were pre-treated for 1 h with the TG2 inhibitors Z-DON (150 μM) or R283 (200 μM) before the addition of PACAP-27 (100 nM) for 10 min prior to 8 h hypoxia (1% O_2) or 8 h normoxia. Cell viability was assessed by measuring (A) the metabolic reduction of MTT by cellular dehydrogenases, (B) release of LDH into the culture medium and (C) caspase-3 activity via Western blot analysis using anti-active caspase 3 antibody. (D) Quantified caspase-3 activity data. Data are expressed as a percentage of normoxia control cell values (=100%) and represent the mean ± S.E.M. from four independent experiments each performed in (A) quadruplicate and (B) sextuplicate. $^{*}P < 0.05$, $^{**}P < 0.01$, $^{***}P < 0.0001$ and $^{****}P < 0.0001$, (a) versus normoxia control, (b) versus hypoxia control (c) versus 100 nM PACAP-27 in the presence of hypoxia.

PACAP-27 induced cell survival (Fig. 14). To validate these observations in another cell model the role of TG2 in PAC_1 receptor-induced cell survival in human SH-SY5Y neuroblastoma cells was also investigated. Initial experiments demonstrated that PACAP-27 treatment produced transient increases in TG2 catalysed biotin-cadaverine incorporation and protein cross-linking activity, peaking at 30 min (Fig. 15A and C). Furthermore, as shown in Fig. 15, PACAP-27 stimulated concentration-dependent increases in biotin-amine incorporation activity (EC_{50} = 2.2 ± 1.0 nM; p[EC_{50}] = 8.9 ± 0.4; n = 3) and protein cross-linking activity (EC_{50} = 1.3 ± 0.5 nM; p[EC_{50}] = 9.0 ± 0.2; n = 3). Exposure of SH-SY5Y cells to simulated hypoxia (1% O_2) resulted in a time dependent decrease in MTT reduction, an increase in LDH release and activation of caspase 3 (data not shown), with 8 h used in subsequent experiments. As shown in Fig. 16, pre-treatment with PACAP-27 (100 nM; 10 min) significantly attenuated hypoxia-induced decrease in MTT reduction, release of LDH and activation of caspase-3 in SH-SY5Y cells (Fig. 16). Furthermore, PACAP 6-38 (100 nM; 30 min) reversed PACAP-27 induced protection confirming the role of the PAC_1 receptor in human SH-SY5Y cells (Fig. 16A–D). Finally, the TG2 inhibitors R283 and Z-DON attenuated PACAP-27 induced cell survival (Fig. 16E–G). Overall, these results demonstrate a role of TG2 in PAC_1 receptor-induced cell survival in both mouse N2a and human SH-SY5Y cells.

The role of TG2 in PAC_1 receptor induced neurite outgrowth was assessed by monitoring the outgrowth of axon-like processes following 24 and 48 h treatment with PACAP-27 (100 nM). The TG2 inhibitors Z-DON (150 μM) and R283 (200 μM) attenuated outgrowth of axon-like processes following 24 h (data not shown) and 48 h treatment with PACAP-27, confirming the involvement of TG2 (Fig. 17). These data confirm a role for TG2 in PAC_1 receptor mediated neurite outgrowth.

4. Discussion

The data in this report collectively suggest that PAC_1 receptor-mediated cell survival and neurite outgrowth are mediated by TG2, consistent with the view that TG2-mediated amine incorporation and protein cross-linking play important roles in these events.

4.1. In vitro modulation of TG2 transamidation activity by the PAC_1 receptor

Although the PAC_1 receptor is expressed in mitotic N2a cells [39,50] its functional expression in differentiating N2a cells has to our knowledge not been reported. Hence, this study has demonstrated for the first time functional expression of the PAC_1 receptor in N2a cells induced to differentiate with retinoic acid. The neuropeptide PACAP mediates neurite outgrowth and neuroprotection; however, it is not known if these events involve PAC_1 receptor-induced TG2 activation [51,42,29]. TG2 can catalyse two types of transamidation, namely (i) intra-, and/or inter-molecular covalent cross-links between protein-bound glutamine and protein-bound lysine residues, and (ii) cross-links between primary amines and protein-bound glutamine [54]. In this study the PAC_1 receptor agonist PACAP-27 triggered time- and concentration-dependent increases in TG2-mediated biotin-cadaverine incorporation and protein cross-linking activity in differentiating N2a cells. The EC_{50} values for PACAP-27 mediated

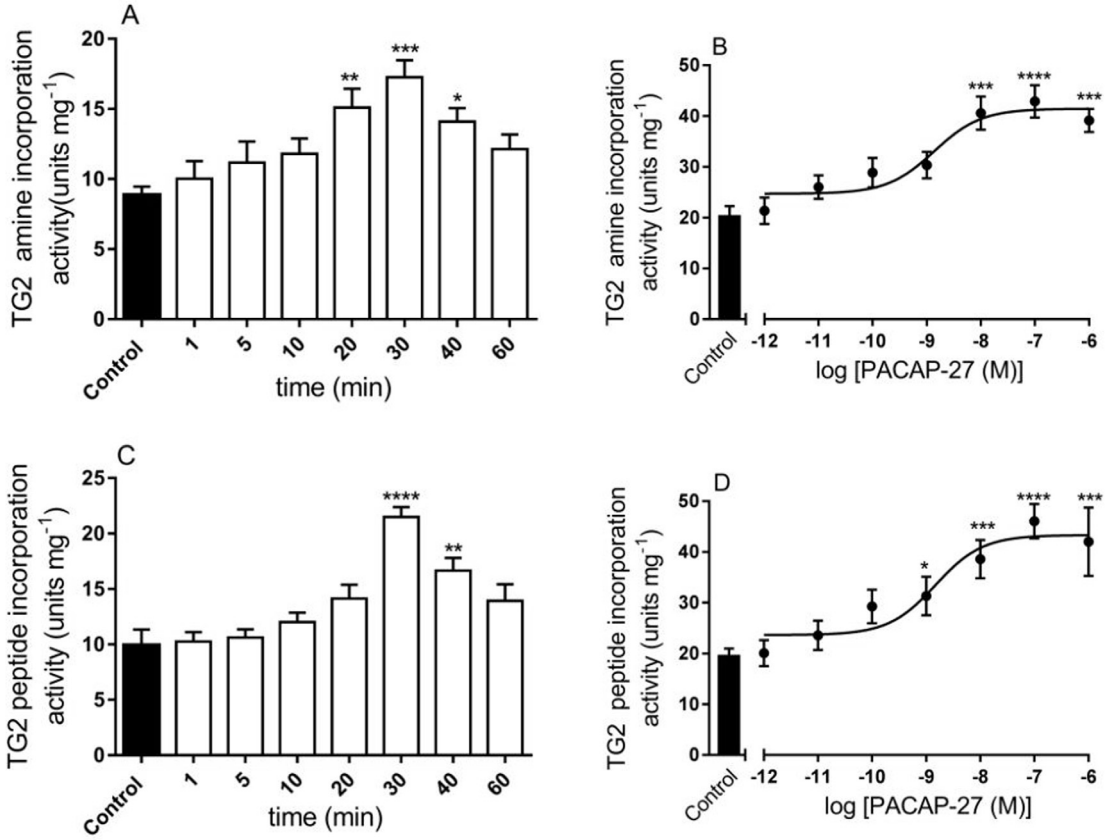

Fig. 15. Effect of PACAP-27 on transglutaminase activity in human SH-SY5Y neuroblastoma cells. Differentiating SH-SY5Y cells were either incubated with 100 nM PACAP-27 for the indicated time periods or for 30 min with the indicated concentrations of PACAP-27. Cell lysates were then subjected to the biotin-cadaverine incorporation (A and B) or protein cross-linking assay (C and D). Data points represent the mean TG specific activity ± S.E.M. from four (A and C) or three (B and D) independent experiments. $^{*}P < 0.05$, $^{**}P < 0.01$, $^{***}P < 0.001$, and $^{****}P < 0.0001$ versus control response.

transglutaminase-catalysed amine incorporation (0.08 nM) and protein cross-linking activity (0.4 nM) are in-line with the affinity of PACAP-27 for the PAC_1 receptor [17,18,28]. Furthermore, PACAP-27-induced TG2 activity was blocked by the PAC_1 receptor antagonist PACAP 6-38 [58]. Overall these data suggest that activation of TG2 by PACAP-27 is mediated via the PAC_1 receptor. It is important to note that PACAP 6-38 also displays high affinity for the $VPAC_2$ receptor [16]; however, since the $VPAC_2$ agonist Bay 55-9837 did not trigger TG2 activity the effects of PACAP 6-38 are mediated entirely via the PAC_1 receptor. Finally, the PAC_1 receptor-induced increases in TG activity were inhibited by R283 and Z-DON, confirming that the observed increases in TG activity were via TG2.

At present, very little is known regarding the regulation of TG2 enzymic activity by GPCRs. Examples in the literature include muscarinic receptor-mediated increases in TG2 activity in SH-SY5Y cells [78] and 5-HT_{2A} receptor-mediated transamidation (TG-catalysed) of the small G-protein Rac1 in the rat cortical cell line A1A1v [13]. The study by Zhang et al. [78] measured *in situ* TG2 activity (polyamine incorporation) triggered by the non-selective muscarinic agonist carbachol, whereas, Dai et al. [13] reported TG2 catalysed incorporation of 5-hydroxytryptamine into Rac1. 5-HT_{2A} receptor-mediated incorporation of 5-HT into the small GTPases RhoA and Rab4 has also been observed in platelets [75]. It was suggested that 5-HT_{2A} and muscarinic receptor-mediated release of Ca^{2+} from intracellular Ca^{2+} stores may be responsible for triggering TG transamidating activity [78,75]. Our recent studies have shown that the $G_{i/o}$-protein coupled A_1 adenosine receptor stimulates TG2 activation in H9c2 cardiomyocyte-like cells [74]. Since TG2 transamidase activity modulates protein function by cross-linking and incorporation of small molecule mono- and polyamines into protein substrates, it is likely that activation of TG2 by GPCRs plays a major role in the regulation of cellular function [54,20].

4.2. Role of Ca^{2+} in PAC_1 receptor-mediated TG2 activation

The transamidating activity of TG2 is dependent upon Ca^{2+}, which promotes the "open" form of TG2 and negates the inhibitory actions of the nucleotides GTP, GDP and ATP [34]. Previous studies have shown that release of Ca^{2+} from intracellular Ca^{2+} stores or influx of extracellular Ca^{2+} is linked to TG activation in response to GPCR stimulation [78,75,74]. The data presented in the current work indicate that PAC_1 receptor-induced transamidase activity is dependent upon extracellular Ca^{2+}. Previous studies have shown that the PAC_1 receptor promotes Ca^{2+} mobilization from intracellular stores and Ca^{2+} influx via N-type calcium channels [3] in rat cerebellar granule cells. In this study, PACAP-27-triggered Ca^{2+} responses were abolished in the absence of extracellular Ca^{2+}, which is indicative of Ca^{2+} influx. Clearly, further studies are required to determine the mechanism(s) of PAC_1 receptor-induced Ca^{2+} influx in differentiated N2a cells and its role in TG2 activation. It is interesting to note that changes in intracellular [Ca^{2+}] required for TG2 transamidating activity are typically in the order 3–100 μM [34]. However, there is growing evidence that intracellular [Ca^{2+}] can reach levels sufficient to activate TG2, for example in calcium microdomains that occur near the cell membrane following the opening of voltage gated Ca^{2+} channels or near internal stores [6,34]. Alternatively, the role of Ca^{2+} in PAC_1 receptor-induced TG2 activation may require the sensitization of

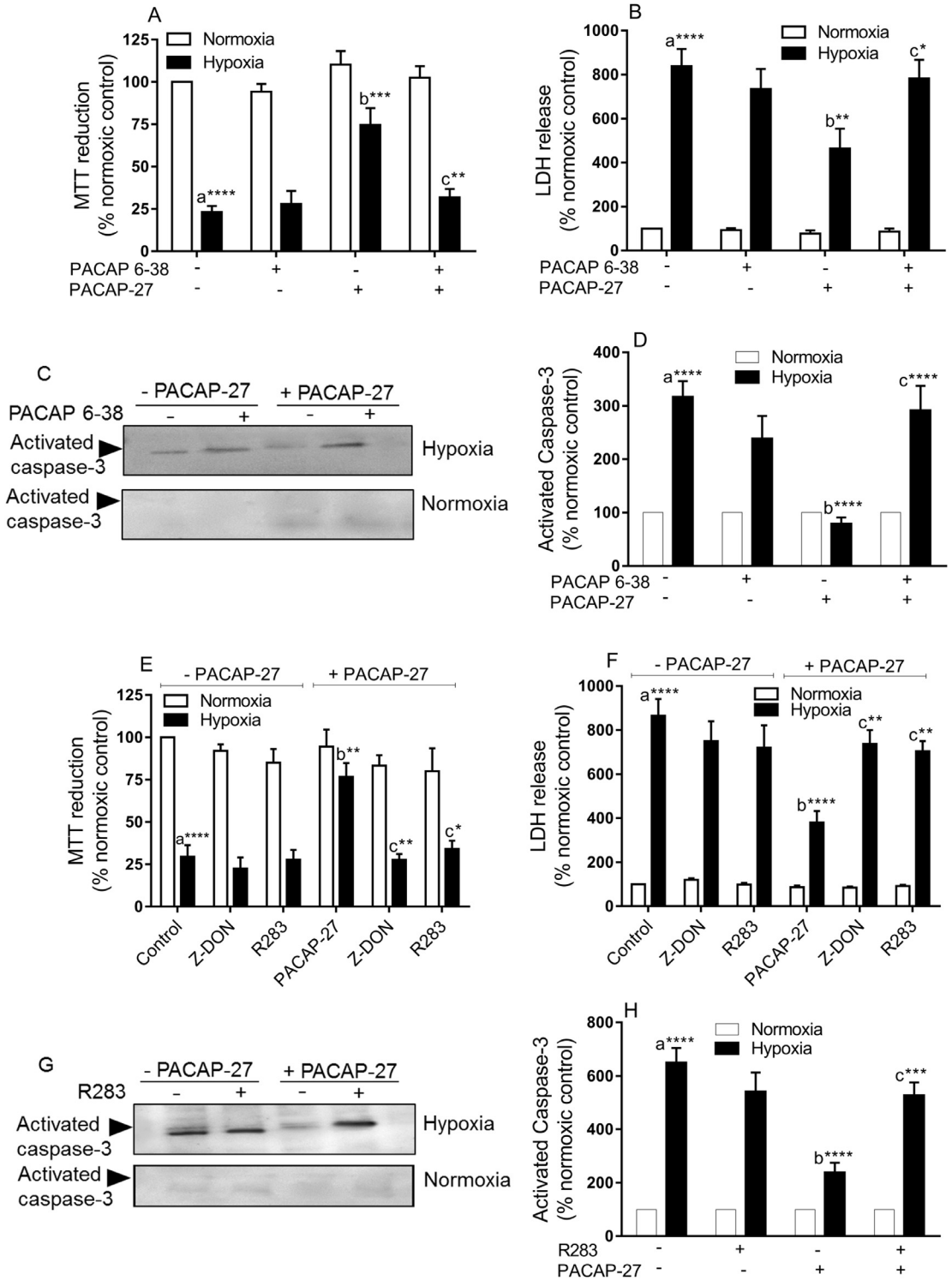

Fig. 16. The effect of PACAP-27 on hypoxia-induced cell death in human SH-SY5Y cells. Differentiating SH-SY5Y cells were pre-treated either with the PAC_1 receptor antagonist PACAP 6-38 (100 nM) for 30 min (panels A–D) or with the TG2 inhibitors Z-DON (150 μM) or R283 (200 μM) for 1 h (panels E–H) before the addition of PACAP-27 (100 nM) for 10 min prior to 8 h hypoxia (1% O_2) or 8 h normoxia. Cell viability was assessed by measuring the metabolic reduction of MTT by cellular dehydrogenases (panels A,E), release of LDH into the culture medium (panels B,F) and caspase-3 activity via Western blot analysis using anti-active caspase 3 antibody (panels C,G). Quantified caspase-3 activity data are shown in panels D and H. Data are expressed as a percentage of normoxia control cell values (=100%) and represent the mean ± S.E.M. from four independent experiments each performed in (A,E) quadruplicate and (B,F) sextuplicate. $^{*}P < 0.05$, $^{**}P < 0.01$, $^{***}P < 0.0001$ and $^{****}P < 0.0001$, (a) versus normoxia control, (b) versus hypoxia control (c) versus 100 nM PACAP-27 in the presence of hypoxia.

TG2 to low levels of intracellular [Ca^{2+}]. For example, interaction of TG2 with protein binding partners and/or membrane lipids have been proposed to induce a conformational change that promotes activation at low levels of intracellular [Ca^{2+}] [34].

4.3. Role of protein kinases in PAC_1 receptor-mediated TG2 activation

The phosphorylation of TG2 by PKA inhibits its transamidating activity but augments its kinase activity [49]. These contrasting

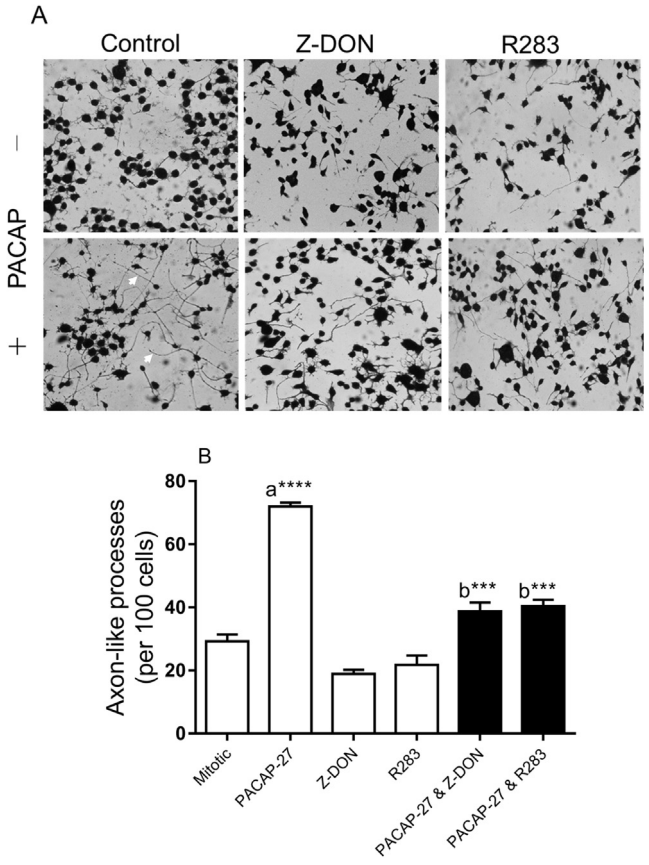

Fig. 17. The effect of TG2 inhibitors on PACAP-27 induced outgrowth of axon-like processes in differentiating N2a cells. (A) N2a cells were incubated for 1 h with the TG2 inhibitors Z-DON (150 μM) or R283 (200 μM) before treatment with PACAP-27 (100 nM) in serum-free DMEM for 48 h. Following stimulation the cells were fixed and stained with Coomassie blue. (B) Quantified data points represent the number of axon-like processes determined as described in Materials and Methods. Shown are the mean number of axons/100 cells ± S.E.M. from four independent experiments each performed in quadruplicate. White arrows indicate typical axon-like processes. $^{***}P < 0.0001$ and $^{****}P < 0.0001$, (a) versus mitotic control, (b) versus 100 nM PACAP-27 alone.

effects on TG2 activity were obtained using histidine-tagged TG2 immobilized on nickel-agarose and incubated with the catalytic subunit of PKA. In this study the PKA inhibitors KT 5720 and *Rp*-cAMPs completely blocked PACAP-27-induced TG2 transamidating activity, which reflects PAC_1 receptor signalling via cAMP/PKA. The PAC_1 receptor also activates PLC/DAG/PKC (via G_q-protein coupling) signalling and hence we determined the role of PKC. The broad spectrum PKC inhibitor Ro 318220 inhibited PACAP-27-induced TG2 activity, indicating that G_q-protein coupling is involved in PAC_1 receptor-mediated TG2 activation. The PAC_1 receptor also activates ERK1/2, JNK1/2, p38 MAPK and PKB [51,44,8]. In this study we observed PACAP-27-induced activation of ERK1/2, JNK1/2, and PKB but not p38 MAPK. The MEK1/2 (upstream activator of ERK1/2) inhibitor PD 98059 blocked PACAP-27-induced TG2 activity, suggesting a prominent role for ERK1/2. These observations are comparable to A_1 adenosine receptor-mediated activation of TG2 in H9c2 cells, which was also sensitive to PKC and ERK1/2 inhibition [74]. In transfected HEK293 cells, PAC_1 receptor-induced ERK1/2 is dependent upon calcium influx and PLC/DAG/PKC [45] and hence the inhibition of PACAP-27-induced TG2 by removal of extracellular Ca^{2+} and inhibition of PKC may reflect their up-stream role(s) in ERK1/2 activation. In the current study, PAC_1 receptor-induced ERK1/2 activation is independent of Ca^{2+} influx and partially sensitive to PKC inhibition. Similarly, PKA can activate ERK1/2 [65] and therefore the effect of PKA inhibitors on PAC_1 receptor TG2 activation may also reflect the up-stream role of PKA in ERK1/2 activation. In SH-SY5Y cells PAC_1 receptor-induced ERK1/2 activation is cAMP-dependent but PKA-independent [51]. However, in guinea-pig cardiac neurons [11] and N2a cells (the current study) PAC_1 receptor-induced ERK1/2 signalling is PKA-dependent. Hence, PKA-mediated inhibition of TG2 activation may indeed reflect the up-stream role of PKA in ERK1/2 activation. Finally, PACAP-27-induced TG2 activation was also sensitive to inhibition of PKB and JNK1/2, suggesting a role for these kinases in PAC_1 receptor-induced TG2 activation.

We have previously shown that TG2 is phosphorylated following activation of the A_1 adenosine receptor in H9c2 cells [74]. The current data demonstrate that TG2 is also phosphorylated following PAC_1 receptor activation. Furthermore, PAC_1 receptor-induced TG2 phosphorylation was attenuated by pharmacological inhibition of MEK1/2, PKA and removal of extracellular Ca^{2+}. It is not clear how the absence of extracellular Ca^{2+} blocks TG2 phosphorylation since PAC_1 receptor-induced ERK1/2 activation is independent of Ca^{2+} influx. One possible explanation is that changes in $[Ca^{2+}]_i$ promote conformational changes in TG2 that facilitate its phosphorylation by protein kinase(s). Alternatively, Ca^{2+} influx may play a role in augmenting PAC_1 receptor-induced PLC/PKC signalling. However, the fact that the PKC inhibitor Ro 31-8220 did not block TG2 phosphorylation, suggests that PKC may regulate other targets involved in TG2 activation. The next logical step would be to identify the specific site(s) of TG2-associated serine and threonine phosphorylation. Previous studies have shown that TG2 is phosphorylated by PKA at Ser^{215} and Ser^{216} [48] and at an unknown site(s) by PTEN-induced putative kinase 1 (PINK1; [47]). At present the precise role of PAC_1 receptor-induced TG2 phosphorylation is not known. However, PKA-mediated phosphorylation of TG2 enhances its interaction with the scaffolding protein 14-3-3 and increases TG2 kinase activity, whereas PINK1-mediated phosphorylation of TG2 blocks its proteasomal degradation [48,49,47]. It is also conceivable that TG2 phosphorylation sensitizes TG2 to low levels of intracellular $[Ca^{2+}]$ or alters its subcellular location. Work underway will determine the functional consequences of PAC_1 receptor-induced TG2 phosphorylation.

4.4. In situ visualisation of TG2 activity

Fluorescence microscopy was used to visualise *in situ* TG2 activity following PAC_1 receptor activation. The results were comparable to PAC_1 receptor-induced amine incorporation activity observed *in vitro*. However, given the covalent nature of biotin-X-cadaverine incorporation into protein substrates, it was surprising to observe that *in situ* TG2 activity returned to basal levels after 40 min. Possible explanations for this include reversal of amine incorporation by TG [64], targeting of modified proteins for degradation or their rapid removal from the cell. Our previous studies have reported the rapid expulsion of biotinylated proteins from H9c2 cells following treatment with PMA or forskolin [1]. It could be that the rapid expulsion of biotinylated proteins from N2a cells occurs via exosomes [30]. Since N2a cells secrete exosomes it will be of interest to determine whether amine-labeled proteins can be detected in exosomes purified from cell culture supernatants obtained from these cells following PACAP-27 treatment [9].

4.5. Role of TG2 in PAC_1 receptor-induced cytoprotection

Previous studies have shown that TG2 protects human SH-SY5Y neuroblastoma cells against heat shock-induced cell death [69]. Similarly, TG2 mediates protection of neuronal cells against hypoxia and oxygen/glucose deprivation-induced cell death by attenuating the HIF hypoxic response pathway [21]. Likewise, PACAP is widely recognized as a neuroprotective peptide and

potential therapeutic agent for the treatment of cerebral ischaemia and various neurodegenerative disorders [57,36]. The mechanisms of PACAP/PAC_1 receptor-induced neuroprotection are complex and involve multiple signalling pathways that include PKA, PKB, ERK1/2, NF-κB and Ca^{2+} mobilization [44,4,42]. In this study we have shown for the first time a role for TG2 in PAC_1 receptor-induced cytoprotection in differentiating mouse N2a and human SH-SY5Y neuroblastoma cells. However, whilst it is not clear how PAC_1 receptor-induced TG2 activation mediates cell survival, TG2 is known to regulate pathways associated with PACAP neuroprotection. For example, TG2 activates adenylyl cyclase and enhances cAMP/PKA dependent CRE-reporter gene activity in SH-SY5Y neuroblastoma cells [68] and promotes NF-κB signalling via cross-linking of IκBα [20]. In the current study inhibition of TG2 blocked PACAP-27 mediated attenuation of hypoxia-induced activation of caspase-3. Recent studies have shown that TG2 inhibits apoptosis via the down-regulation of the Bax expression and inhibition of caspase 3 and 9 [10]. Further work is required to determine the role of TG2 in PAC_1 receptor-induced cell survival.

4.6. Role of TG2 in PAC_1 receptor-induced neurite outgrowth

Previous studies have shown that TG2 is essential for differentiation/neurite outgrowth in human neuroblastoma SHSY5Y cells [69,61]. Mechanisms associated with TG2-induced neurite outgrowth include transamidation of RhoA and subsequent activation of ERK1/2 and p38 MAPK [61]. Similarly, PACAP triggers neuronal differentiation of human SH-SY5Y cells via a cAMP-dependent but PKA-independent pathway requiring activation of ERK1/2 and p38 MAPK [51]. The data presented in this study suggest that pharmacological inhibition of TG2 blocks PACAP-27-induced outgrowth of axon-like processes, suggesting the involvement of TG2 in PAC_1 receptor neurite outgrowth. However, further studies are required to identify the downstream substrates of TG2 and signalling pathways associated with the role of TG2 in PAC_1 receptor neuronal differentiation.

In conclusion, our data show for the first time that TG2 activity is regulated by the PAC_1 receptor in differentiating N2a and SH-SY5Y cells. Work is currently underway to understand more fully the role of TG2 in PAC_1 receptor signalling and modulation of neuronal cell function.

Conflicts of interest

The authors state no conflict of interest.

Acknowledgements

This work was supported by a PhD studentship from the Saudi Arabian Government (UMU473). We would like to thank Gordon Arnott for help with confocal imaging.

References

[1] I. Almami, J.M. Dickenson, A.J. Hargreaves, P.L.R. Bonner, Modulation of transglutaminase 2 activity in H9c2 cells by PKC and PKA signalling: a role for transglutaminase 2 in cytoprotection, Br. J. Pharmacol. 171 (2014) 3946–3960.
[2] V. Barve, F. Ahmed, S. Adsule, S. Banerjee, S. Kulkarni, P. Katiyar, et al., Synthesis, molecular characterization, and biological activity of novel synthetic derivatives of chromen-4-one in human cancer cells, J. Med. Chem. 49 (2006) 3800–3808.
[3] M. Basille-Dugay, H. Vaudry, A. Fournier, B. Gonzalez, D. Vaudry, Activation of PAC1 receptors in rat cerebellar granule cells stimulates both calcium mobilization from intracellular stores and calcium influx through N-type calcium channels, Front Endocrinol. 4 (2013) 56.
[4] P.S. Baxter, M.-A. Martel, A. McMahon, P.C. Kind, G.E. Hardingham, Pituitary adenylate cyclase-activating peptide induces long-lasting neuroprotection through the induction of activity-dependent signaling via the cyclic AMP response element-binding protein-regulated transcription co-activator 1, J. Neurochem. 118 (2011) 365–378.
[5] B.L. Bennett, D.T. Sasaki, B.W. Murray, E.C. O'Leary, S.T. Sakata, W. Xu, et al., SP 600125, an anthrapyrazolone inhibitor of Jun N-terminal kinase, Proc. Natl. Acad. Sci. U.S.A. 98 (2001) 13681–13686.
[6] M.J. Berridge, Calcium microdomains: organization and function, Cell Calcium 40 (2006) 405–412.
[7] W.B. Bollag, X. Zhong, E.M. Dodd, D.M. Hardy, X. Zheng, W.T. Allred, Phospholipase D signaling and extracellular signal-regulated kinase-1 and -2 phosphorylation (activation) are required for maximal phorbol-ester-induced transglutaminase activity, a marker of keratinocyte differentiation, J. Pharmacol. Exp. Ther. 312 (2005) 1223–1231.
[8] A. Castorina, S. Scuderi, A.G. D'Amico, F. Drago, V. D'Agata, PACAP and VIP increase the expression of myelin-related proteins in rat schwannoma cells: involvement of PAC1/VPAC2 receptor-mediated activation of PI3K/Akt signaling pathways, Exp. Cell Res. 322 (2014) 108–121.
[9] M. Chivet, C. Javalet, K. Laulagnier, B. Blot, F.J. Hemming, R. Sadoul, Exosomes secreted by cortical neurons upon glutamatergic synapse activation specifically interact with neurons, J. Extracell. Vesicles 3 (2014) 24722, http://dx.doi.org/10.3402/jev.v3.24722.
[10] S.Y. Cho, J.H. Lee, H.D. Bae, E.M. Jeong, G.Y. Jang, C.W. Kim, D.M. Shin, J.H. Jeon, I.G. Kim, Transglutaminase 2 inhibits apoptosis induced by calcium-overload through down-regulation of Bax, Exp. Mol. Med. 42 (2010) 639–650.
[11] T.A. Clason, B.M. Girard, V. May, R.L. Parsons, Activation of MEK/ERK signaling by PACAP in guinea pig cardiac neurons, J. Mol. Neurosci. 59 (2016) 309–316.
[12] S. Condello, D. Caccamo, M. Currò, N. Ferlazzo, G. Parisi, R. Ientile, Transglutaminase 2 and NF-κB interplay during NGF-induced differentiation of neuroblastoma cells, Brain Res. 1207 (2008) 1–8.
[13] Y. Dai, N.L. Dudek, T.B. Patel, N.A. Muma, Transglutaminase-catalysed transmidation: a novel mechanism for Rac1 activation by 5-hydroxytryptamine$_{2A}$ receptor stimulation, J. Pharmacol. Exp. Ther. 326 (2008) 153–162.
[14] P.D. Davis, C.H. Hill, E. Keech, G. Lawton, J.S. Nixon, A.D. Sedgwick, et al., Potent selective inhibitors of protein kinase C, FEBS Lett. 259 (1989) 61–63.
[15] R.J. de Wit, D. Hekstra, B. Jastorff, W.J. Stec, J. Baraniak, R. Van Driel, P.J. Van Haastert, Inhibitory action of certain cyclophosphate derivatives of cAMP on cAMP-dependent protein kinases, Eur. J. Biochem. 142 (1984) 255–260.
[16] T. Dickinson, S.S. Fleetwood-Walker, R. Mitchell, E.M. Lutz, Evidence for roles of vasoactive intestinal polypeptide (VIP) and pituitary adenylate cyclase activating polypeptide (PACAP) receptors in modulating the responses of rat dorsal horn neurons to sensory inputs, Neuropeptides 31 (1997) 175–185.
[17] L. Dickson, I. Aramori, J. McCulloch, J. Sharkey, K. Finlayson, A systematic comparison of intracellular cyclic AMP and calcium signalling highlights complexities in human VPAC/PAC receptor pharmacology, Neuropharmacol 51 (2006) 1086–1098.
[18] L. Dickson, K. Finlayson, VPAC and PAC receptors: from ligands to function, Pharmacol. Ther. 121 (2009) 294–316.
[19] D.T. Dudley, L. Pang, S.J. Decker, A.J. Bridges, A.R. Saltiel, A synthetic inhibitor of the mitogen-activated protein kinase cascade, Proc. Natl. Acad. Sci. U.S.A. 92 (1995) 7686–7689.
[20] R.L. Eckert, M.T. Kaartinen, M. Nurminskaya, A.M. Belkin, G. Colak, G.V.W. Johnson, K. Mehta, Transglutaminase regulation of cell function, Physiol. Rev. 94 (2014) 383–417.
[21] A.J. Filiano, C.D.C. Bailey, J. Tucholski, S. Gundemir, G.V.W. Johnson, Transglutaminase 2 protects against ischemic insult, interacts with HIF1β, and attenuates HIF1 signaling, FASEB J. 22 (2008) 2662–2675.
[22] A.J. Filiano, J. Tucholski, P.J. Dolan, G. Colak, G.V.W. Johnson, Transglutaminase 2 protects against ischemic stroke, Neurobiol. Dis. 39 (2010) 334–343.
[23] G. Frampton, P. Invernizzi, F. Bernuzzi, H.Y. Pae, M. Quinn, D. Horvat, C. Galindo, L. Huang, M. McMillin, B. Cooper, L. Rimassa, S. DeMorrow, Interleukin-6-driven progranulin expression increases cholangiocarcinoma growth by an Akt-dependent mechanism, Gut 61 (2012) 268–277.
[24] K.F. Freund, K.P. Doshi, S.L. Gaul, D.A. Claremon, D.C. Remy, J.J. Baldwin, et al., Transglutaminase inhibition by 2-[(2-oxopropyl)thio]imidazolium derivatives: mechanism of factor XIIIa inactivation, Biochemistry 33 (1994) 10109–10119.
[25] S. Gundemir, G. Colak, J. Tucholski, G.V.W. Johnson, Transglutaminase 2: a molecular Swiss army knife, Biochim. Biophys. Acta 1823 (2012) 406–419.
[26] Y.S. Hah, H.G. Kang, H.Y. Cho, S.H. Shin, U.K. Kim, B.W. Park, S.I. Lee, G.J. Rho, J. R. Kim, J.H. Byun, JNK signaling plays an important role in the effects of TNF-α and IL-1β on in vitro osteoblastic differentiation of cultured human periosteal-derived cells, Mol. Biol. Rep. 40 (2013) 4869–4881.
[27] A.J. Hargreaves, M.J. Fowler, M. Sachana, J. Flaskos, M. Bountouri, I.C. Coutts, et al., Inhibition of neurite outgrowth in differentiating mouse N2a neuroblastoma cells by phenyl saligenin phosphate: effects on MAP kinase (ERK 1/2) activation, neurofilament heavy chain phosphorylation and neuropathy target esterase activity, Biochem. Pharmacol. 71 (2006) 1240–1247.
[28] A.J. Harmar, J. Fahrenkrug, I. Gozes, M. Laburthe, V. May, J.R. Pisegna, D. Vaudry, H. Vaudry, J.A. Waschek, S.I. Said, Pharmacology and functions of receptors for vasoactive intestinal peptide and pituitary adenylate-activating polypeptide: IUPHAR Review 1, Br. J. Pharmacol. 166 (2012) 4–17.
[29] M. Jóźwiak-Bębenista, E. Kowalczyt, J.Z. Nowak, The cyclic AMP effects and neuroprotective activities of PACAP and VIP in cultured astrocytes and neurons exposed to oxygen-glucose deprivation, Pharmacol. Rep. 67 (2015) 332–338.
[30] A. Kalani, A. Tyagi, N. Tyagi, Exosomes: mediators of neurodegeneration, neuroprotection and therapeutics, Mol. Neurobiol. 49 (2014) 590–600.

[31] H. Kase, K. Iwahashi, S. Nakanishi, Y. Matsuda, K. Yamada, M. Takahashi, et al., K-252 compounds, novel and potent inhibitors of protein kinase C and cyclic nucleotide-dependent protein kinases, Biochem. Biophys. Res. Commun. 142 (1987) 436–440.

[32] J.H. Kim, S.C. Lee, J. Ro, H.S. Kang, H.S.Y.S. Kim, Jnk signaling pathway-mediated regulation of Stat3 activation is linked to the development of doxorubicin resistance in cancer cell lines, Biochem. Pharmacol. 79 (2010) 373–380.

[33] Y.H. Kim, D.H. Lee, J.H. Jeong, Z.S. Guo, Y.J. Lee, Quercetin augments TRAIL-induced apoptotic death: involvement of the ERK signal transduction pathway, Biochem. Pharmacol. 75 (2008) 1946–1958.

[34] R. Király, M.A. Demény, L. Fésüs, Protein transamidation by transglutaminase 2 in cells: a disputed Ca^{2+}-dependent action of a multifunctional protein, FEBS J. 278 (2011) 4717–4739.

[35] S.A. Keilbaugh, W.H. Prusoff, M.V. Simpson, The PC12 cell as a model for studies of the mechanism of induction of peripheral neuropathy by anti-HIV-I dideoxynucleoside analogs, Biochem. Pharmacol. 42 (1991) R5–R8.

[36] E.H. Lee, S.R. Seo, Neuroprotective role of pituitary adenylate cyclase-activating polypeptide in neurodegenerative diseases, BMB Rep. 47 (2014) 369–375.

[37] I.T. Lee, C.C. Lin, C.H. Wang, W.J. Cherng, J.S. Wang, C.M. Yang, ATP stimulates PGE_2/cyclin D1-dependent VSMCs proliferation via STAT3 activation: role of PKCs-dependent NADPH oxidase/ROS generation, Biochem. Pharmacol. 85 (2013) 954–964.

[38] K.N. Lee, S.A. Arnold, P.J. Birkbichler, M.K. Patterson Jr, B.M. Fraij, Y. Takeuchi, H.A. Carter, Site-directed mutagenesis of human tissue transglutaminase: Cys-277 is essential for transglutaminase activity but not for GTPase activity, Biochim. Biophys. Acta 1202 (1993) 1–6.

[39] V. Leliévre, N. Pineau, J. Du, C.-H. Wen, T. Nguyen, T. Janet, et al., Differential effects of peptide histidine isoleucine (PHI) and related peptides on stimulation and suppression of neuroblastoma cell proliferation, J. Biol. Chem. 273 (1998) 19685–19690.

[40] G.R. Lilley, J. Skill, M. Griffin, P.L.R. Bonner, Detection of Ca^{2+}-dependent transglutaminase activity in root and leaf tissue of monocotyledonous and dicotyledonous plants, Plant Physiol. 117 (1998) 1115–1123.

[41] T. Manabe, K. Tatsumi, M. Inoue, H. Matsuyoshi, M. Makinodan, S. Yokoyama, A. Wanaka, L3/Lhx8 is involved in the determination of cholinergic or GABAergic fate, J. Neurochem. 94 (2005) 723–730.

[42] D.-L. Manecka, S.F. Mahmood, L. Grumolato, I. Lihrmann, Y. Anouar, Pituitary adenylate cyclase-activating polypeptide (PACAP) promotes both survival and neuritogenesis in PC12 cells through activation of nuclear factor κB (NF-κB) pathway, J. Biol. Chem. 288 (2013) 14936–14948.

[43] S. Manngiavacchi, M.E. Wolf, D1 dopamine receptor stimulation increases the rate of AMPA receptor insertion onto the surface of cultured nucleus accumbens neurons through a pathway dependent on protein kinase A, J. Neurochem. 88 (2004) 1261–1271.

[44] V. May, E. Lutz, C. Mackenzie, K.C. Schutz, K. Dozark, K.M. Braas, Pituitary adenylate cyclase-activating polypeptide (PACAP)/PAC_1HOP1 receptor activation co-ordinates multiple neurotrophic signaling pathways, J. Biol. Chem. 285 (2010) 9749–9761.

[45] V. May, T.A. Clason, T.R. Buttolph, B.M. Girard, R.L. Parsons, Calcium influx, but not intracellular calcium release, supports PACAP-mediated ERK activation in HEK PAC1 receptor cells, J. Mol. Neurosci. 54 (2014) 342–350.

[46] S. Mhaouty-Kodja, Ghα/tissue transglutaminase 2: an emerging G protein in signal transduction, Biol. Cell 96 (2004) 363–367.

[47] B. Min, Y.C. Kwon, K.M. Choe, K.C. Chung, PINK1 phosphorylates transglutaminase 2 and blocks its proteasomal degradation, J. Neurosci. Res. 93 (2015) 722–735.

[48] S. Mishra, L.J. Murphy, Phosphorylation of transglutaminase 2 by PKA at Ser216 creates 14.3.3 binding sites, Biochem. Biophys. Res. Commun. 347 (2006) 1166–1170.

[49] S. Mishra, G. Melino, L.J. Murphy, Transglutaminase 2 kinase activity facilitates protein kinase A-induced phosphorylation of retinoblastoma protein, J. Biol. Chem. 282 (2007) 18108–18115.

[50] A. Miura, Y. Kambe, K. Inoue, H. Tatsukawa, T. Kurihara, M. Griffin, S. Kojima, A. Miyata, Pituitary adenylate cyclase-activating polypeptide Type 1 receptor (*PAC1*) gene is suppressed by transglutaminase 2 activation, J. Biol. Chem. 288 (2013) 32720–32730.

[51] T.K. Monaghan, C.J. MacKenzie, R. Plevin, E.M. Lutz, PACAP-38 induces neuronal differentiation of human SH-SY5Y neuroblastoma cells via cAMP-mediated activation of ERK and p38 MAP kinases, J. Neurochem. 104 (2008) 74–88.

[52] W. Montejo-López, N. Rivera-Ramírez, J. Escamilla-Sánchez, U. García-Hernández, J.A. Arias-Montaño, Heterologous, PKC-mediated desensitization of human histamine H_3 receptors expressed in CHO-K1 cells, Neurochem. Res. 41 (2016) 2415–2424.

[53] T. Mosmann, Rapid colorimetric assay for cellular growth and survival: application to proliferation and cytotoxicity assays, J. Immunol. Methods 65 (1983) 55–63.

[54] M.V. Nurminskaya, A.M. Belkin, Cellular functions of tissue transglutaminase, Int. Rev. Cell Mol. Biol. 294 (2012) 1–97.

[55] M.J. Perry, S.A. Mahoney, L.W. Haynes, Transglutaminase C in cerebellar granule neurons: regulation and localization of substrate cross-linking, Neuroscience 65 (1995) 1063–1076.

[56] E.P.S. Pratt, A.E. Salyer, M.L. Guerra, G.H. Hockerman, Ca^{2+} influx through L-type Ca^{2+} channels and Ca^{2+}-induced Ca^{2+} release regulate cAMP accumulation and Epac1-dependent ERK1/2 activation in INS-1 cells, Mol. Cell. Endocrinol. 419 (2016) 60–71.

[57] D. Reglodi, P. Kiss, A. Lubics, A. Tamas, Review on the protective effects of PACAP in models of neurodegenerative diseases *in vitro* and *in vivo*, Curr. Pharm. Des. 17 (2011) 962–972.

[58] P. Robberecht, P. Gourlet, P. De Neef, M.C. Woussen-Colle, M.C. Vandermeers-Piret, A. Vandermeers, J. Christophe, Structural requirements for the occupancy of pituitary adenylate cyclase activating polypeptide (PACAP) receptors and adenylate cyclase activation in human neuroblastoma NB-OK-1 cell membranes. Discovery of PACAP(6–38) as a potent antagonist, Eur. J. Biochem. 207 (1992) 239–246.

[59] M.S. Rybchyn, M. Slater, A.D. Conlgrave, M.S. Mason, An Akt-dependent increase in canonical Wnt signaling and a decrease in sclerostin protein levels are involved in strontium ranelate-induced osteogenic effects in human osteoblasts, J. Biol. Chem. 286 (2011) 23771–23779.

[60] S. Schaertl, M. Prime, J. Wityak, C. Dominguez, I. Munoz-Sanjuan, R.E. Pacifici, et al., A profiling platform for the characterization of transglutaminase 2 (TG2) inhibitors, J. Biomol. Screen. 15 (2010) 478–487.

[61] U.S. Singh, J. Pan, Y.-L. Kao, S. Joshi, K.L. Young, K.M. Baker, Tissue transglutaminase mediates activation of RhoA and MAP kinase pathways during retinoic acid-induced neuronal differentiation of SH-SY5Y cells, J. Biol. Chem. 278 (2003) 391–399.

[62] T.F. Slaughter, K.E. Achyuthan, T.S. Lai, C.S. Greenberg, A microtiter plate transglutaminase assay utilizing 5-(biotinamido) pentylamine as substrate, Anal. Biochem. 205 (1992) 166–171.

[63] P.K. Smith, R.I. Krohn, G.T. Hermanson, A.K. Mallia, F.H. Gartner, M.D. Provenzano, et al., Measurement of protein using bicinchoninic acid, Anal. Biochem. 150 (1985) 76–85.

[64] J. Stamnaes, B. Fleckenstein, L.M. Sollid, The propensity for deamidation and transamidation of peptides by transglutaminase 2 is dependent on substrate affinity and reaction conditions, Biochim. Biophys. Acta 1784 (2008) 1804–1811.

[65] P.J.S. Stork, J.M. Schmitt, Crosstalk between cAMP an MAP kinase signalling in the regulation of cell proliferation, Trends Cell Biol. 12 (2002) 258–266.

[66] A.P. Sutter, K. Maaser, B. Gerst, A. Krahn, Scherübl H. Zeitz, Enhancement of peripheral benzodiazepine receptor ligand-induced apoptosis and cell cycle arrest of esophageal cancer cells by simultaneous inhibition of MAPK/ERK kinase, Biochem. Pharmacol. 67 (2004) 1701–1710.

[67] R.G. Tremblay, M. Sikorska, J.K. Sandhu, P. Lanthier, M. Riecco-Lutkiewiz, M. Bani-Yaghoub, Differentiation of mouse neuro 2A cells into dopamine neurons, J. Neurosci. Methods 186 (2010) 60–67.

[68] J. Tucholski, G.V.W. Johnson, Tissue transglutaminase directly regulates adenylyl cyclase resulting in enhanced cAMP-response element-binding protein (CREB) activation, J. Biol. Chem. 278 (2003) 26838–26843.

[69] J. Tucholski, M. Lesort, G.V.W. Johnson, Tissue transglutaminase is essential for neurite outgrowth in human neuroblastoma SH-SY5Ycells, Neuroscience 102 (2001) 481–491.

[70] S.M. Trigwell, P.T. Lynch, M. Griffin, A.J. Hargreaves, P.L. Bonner, An improved colorimetric assay for the measurement of transglutaminase (type II)-(γ-glutamyl) lysine cross-linking activity, Anal. Biochem. 330 (2004) 164–166.

[71] I. Vallejo, M. Vallejo, Pituitary adenylate cyclase-activating polypeptide induces astrocyte differentiation of precursor cells from developing cerebral cortex, Mol. Cell. Neurosci. 21 (2002) 671–683.

[72] L. Vanella, G. Raciti, I. Barbagallo, R. Bonfanti, N. Abraham, A. Campisi, Tissue transglutaminase expression during neuronal differentiation of human mesenchymal stem cells, CNS Neurol. Disord.: Drug Targets 14 (2015) 24–32.

[73] D. Vaudry, A. Falluel-Morel, S. Bourgault, M. Basille, D. Burel, O. Wurtz, A. Fournier, B.K.C. Chow, H. Hashimoto, L. Galas, H. Vaudry, Pituitary adenylate cyclase-activating polypeptide and its receptors: 20 years after the discovery, Pharmacol. Rev. 61 (2009) 283–357.

[74] F.S. Vyas, A.J. Hargreaves, P.L.R. Bonner, D.J. Boocock, C. Coveney, J.M. Dickenson, A_1 adenosine receptor-induced phosphorylation and modulation of transglutaminase 2 activity in H9c2 cells: a role in cell survival, Biochem. Pharmacol. 107 (2016) 41–58.

[75] D.J. Walther, J.-U. Peter, S. Winter, M. Höltje, N. Paulmann, M. Grohmann, et al., Serotonylation of small GTPases is a signal transduction pathway that triggers platelet α-granule release, Cell 115 (2003) 851–862.

[76] H. Wang, Y. Chen, H. Zhu, S. Wang, X. Zhang, D. Xu, K. Cao, J. Zou, Increased response to β_2-adrenoreceptor stimulation augments inhibition of Ikr in heart failure ventricular myocytes, PLoS ONE 8 (2012) e46186.

[77] K. Werner, D. Neumann, R. Seifert, Analysis of the histamine H_2-receptor in human monocytes, Biochem. Pharmacol. 92 (2014) 369–379.

[78] J. Zhang, M. Lesort, R.P. Guttmann, G.V.W. Johnson, Modulation of the *in situ* activity of tissue transglutaminase by calcium and GTP, J. Biol. Chem. 273 (1998) 2288–2295.